STUDYING THE BIOLOGY OF AQUATIC ANIMALS THROUGH CALCIFIED STRUCTURES

EDITED BY: Esteban Avigliano, Alejandra Vanina Volpedo and Benjamin D. Walther

PUBLISHED IN: Frontiers in Marine Science

frontiers Research Topics

Frontiers eBook Copyright Statement

The copyright in the text of individual articles in this eBook is the property of their respective authors or their respective institutions or funders. The copyright in graphics and images within each article may be subject to copyright of other parties. In both cases this is subject to a license granted to Frontiers.

The compilation of articles constituting this eBook is the property of Frontiers.

Each article within this eBook, and the eBook itself, are published under the most recent version of the Creative Commons CC-BY licence. The version current at the date of publication of this eBook is CC-BY 4.0. If the CC-BY licence is updated, the licence granted by Frontiers is automatically updated to the new version.

When exercising any right under the CC-BY licence, Frontiers must be attributed as the original publisher of the article or eBook, as applicable.

Authors have the responsibility of ensuring that any graphics or other materials which are the property of others may be included in the CC-BY licence, but this should be checked before relying on the CC-BY licence to reproduce those materials. Any copyright notices relating to those materials must be complied with.

Copyright and source acknowledgement notices may not be removed and must be displayed in any copy, derivative work or partial copy which includes the elements in question.

All copyright, and all rights therein, are protected by national and international copyright laws. The above represents a summary only. For further information please read Frontiers' Conditions for Website Use and Copyright Statement, and the applicable CC-BY licence.

ISSN 1664-8714
ISBN 978-2-88966-112-1
DOI 10.3389/978-2-88966-112-1

About Frontiers

Frontiers is more than just an open-access publisher of scholarly articles: it is a pioneering approach to the world of academia, radically improving the way scholarly research is managed. The grand vision of Frontiers is a world where all people have an equal opportunity to seek, share and generate knowledge. Frontiers provides immediate and permanent online open access to all its publications, but this alone is not enough to realize our grand goals.

Frontiers Journal Series

The Frontiers Journal Series is a multi-tier and interdisciplinary set of open-access, online journals, promising a paradigm shift from the current review, selection and dissemination processes in academic publishing. All Frontiers journals are driven by researchers for researchers; therefore, they constitute a service to the scholarly community. At the same time, the Frontiers Journal Series operates on a revolutionary invention, the tiered publishing system, initially addressing specific communities of scholars, and gradually climbing up to broader public understanding, thus serving the interests of the lay society, too.

Dedication to Quality

Each Frontiers article is a landmark of the highest quality, thanks to genuinely collaborative interactions between authors and review editors, who include some of the world's best academicians. Research must be certified by peers before entering a stream of knowledge that may eventually reach the public - and shape society; therefore, Frontiers only applies the most rigorous and unbiased reviews.
Frontiers revolutionizes research publishing by freely delivering the most outstanding research, evaluated with no bias from both the academic and social point of view. By applying the most advanced information technologies, Frontiers is catapulting scholarly publishing into a new generation.

What are Frontiers Research Topics?

Frontiers Research Topics are very popular trademarks of the Frontiers Journals Series: they are collections of at least ten articles, all centered on a particular subject. With their unique mix of varied contributions from Original Research to Review Articles, Frontiers Research Topics unify the most influential researchers, the latest key findings and historical advances in a hot research area! Find out more on how to host your own Frontiers Research Topic or contribute to one as an author by contacting the Frontiers Editorial Office: researchtopics@frontiersin.org

STUDYING THE BIOLOGY OF AQUATIC ANIMALS THROUGH CALCIFIED STRUCTURES

Topic Editors:
Esteban Avigliano, Consejo Nacional de Investigaciones Científicas y Técnicas (CONICET), Argentina
Alejandra Vanina Volpedo, University of Buenos Aires, Argentina
Benjamin D. Walther, Texas A&M University Corpus Christi, United States

Citation: Avigliano, E., Volpedo, A. V., Walther, B. D., eds. (2020). Studying the Biology of Aquatic Animals through Calcified Structures. Lausanne: Frontiers Media SA. doi: 10.3389/978-2-88966-112-1

Table of Contents

05 ***Editorial: Studying the Biology of Aquatic Animals Through Calcified Structures***
Esteban Avigliano, Alejandra Vanina Volpedo and Benjamin D. Walther

08 ***Fresh Submarine Groundwater Discharge Augments Growth in a Reef Fish***
Julian Lilkendey, Timo Pisternick, Sarah I. Neumann, Danishta Dumur Neelayya, Stefanie Bröhl, Yashvin Neehaul and Nils Moosdorf

19 ***Peeling the Otolith of Fish: Optimal Parameterization for Micro-CT Scanning***
Jonas E. Vasconcelos-Filho, Felix S. L. Thomsen, Borko Stosic, Antonio C. D. Antonino, Daniel A. Duarte, Richard J. Heck, Rosangela P. T. Lessa, Francisco M. Santana, Beatrice P. Ferreira and Paulo J. Duarte-Neto

30 ***Discriminating Natal Source Populations of a Temperate Marine Fish Using Larval Otolith Chemistry***
Troy A. Rogers, Anthony J. Fowler, Michael A. Steer and Bronwyn M. Gillanders

47 ***Elemental Ratios in Cuttlebone Indicate Growth Rates in the Cuttlefish* Sepia pharaonis**
Ming-Tsung Chung, Kuo-Fang Huang, Chen-Feng You, Chuan-Chin Chiao and Chia-Hui Wang

59 ***Habitat Use Patterns and Identification of Essential Habitat for an Endangered Coastal Shark With Vertebrae Microchemistry: The Case Study of* Carcharhinus porosus**
Leonardo Manir Feitosa, Valderi Dressler and Rosangela Paula Lessa

71 ***Do the Fish Scales Shape of* Mugil curema *Reflect the Genetic Structure Using Microsatellites Markers and the Mexican Marine Ecoregions Classification?***
Eloísa Pacheco-Almanzar, Nadia Loza-Estrada and Ana L. Ibáñez

81 ***Annual Bands in Vertebrae Validated by Bomb Radiocarbon Assays Provide Estimates of Age and Growth of Whale Sharks***
Joyce J. L. Ong, Mark G. Meekan, Hua Hsun Hsu, L. Paul Fanning and Steven E. Campana

88 ***Fish Species Identification Using the Rhombic Squamation Pattern***
Ana L. Ibáñez, Ebenezer Guerra and Eloísa Pacheco-Almanzar

96 ***Fish and Sclerochronology Research in the Mediterranean: Challenges and Opportunities for Reconstructing Environmental Changes***
Sanja Matić-Skoko, Melita Peharda, Dario Vrdoljak, Hana Uvanović and Krešimir Markulin

108 ***Port Jackson Shark Growth is Sensitive to Temperature Change***
Christopher Izzo and Bronwyn May Gillanders

115 ***Seasonal Movement Patterns of the Bigfin Reef Squid* Sepioteuthis lessoniana *Predicted Using Statolith* $\delta^{18}O$ *Values***
Chun-I Chiang, Ming-Tsung Chung, Jen-Chieh Shiao, Pei-Ling Wang, Tin-Yam Chan, Atsuko Yamaguchi and Chia-Hui Wang

129 ***Northern Benguela* Merluccius paradoxus *Annual Growth From Otolith Chronologies Used for Age Verification and as Indicators of Fisheries-Induced and Environmental Changes***
Margit R. Wilhelm, Bryan A. Black, Tarron Lamont, Sarah C. Paulus, Chris Bartholomae and Deon C. Louw

147 ***Growing Up Down South: Spatial and Temporal Variability in Early Growth of Fuegian Sprat* Sprattus fuegensis *From the Southwest Atlantic Ocean***
Virginia A. García Alonso, Daniel R. Brown, Marcelo Pájaro and Fabiana L. Capitanio

163 ***Polymorphism in Conservative Structures? The Scapulocoracoids in Skates Genus* Psammobatis *(Chondrichthyes, Arhynchobatidae) and the Validity of* P. parvacauda**
E. Mabragaña, M. González-Castro, V. Gabbanelli, D. M. Vazquez and J. M. Díaz de Astarloa

172 ***Otolith Chemistry Reveals Natal Region of Larval Capelin in Coastal Newfoundland, Canada***
Ashley Tripp, Hannah M. Murphy and Gail K. Davoren

183 ***Water and Otolith Chemistry: Implications for Discerning Estuarine Nursery Habitat Use of a Juvenile Flatfish***
Filipe Martinho, Beatriz Pina, Margarida Nunes, Rita P. Vasconcelos, Vanessa F. Fonseca, Daniel Crespo, Ana Lígia Primo, Ana Vaz, Miguel A. Pardal, Bronwyn M. Gillanders, Susanne E. Tanner and Patrick Reis-Santos

195 ***Growth Rate, Ration, and Temperature Effects on Otolith Elemental Incorporation***
Jessica A. Miller and Thomas P. Hurst

211 ***First Insights Into the Growth and Population Structure of* Cottoperca trigloides *(Perciformes, Bovichtidae) From the Southwestern Atlantic Ocean***
María Eugenia Lattuca, Facundo Llompart, Esteban Avigliano, Marta Renzi, Ileana De Leva, Claudia Clementina Boy, Fabián Alberto Vanella, María Eugenia Barrantes, Daniel Alfredo Fernández and Cristiano Queiroz de Albuquerque

225 ***Cryptic Lives of Conspicuous Animals: Otolith Chemistry Chronicles Life Histories of Coastal Lagoon Fishes***
Frederick Feyrer, Matthew Young, Darren Fong, Karin Limburg and Rachel Johnson

234 ***Comparison of Otolith Microstructure of Herring Larvae and Sibling Adults Reared Under Identical Early Life Conditions***
Susanne Tonheim, Aril Slotte, Leif Andersson, Arild Folkvord and Florian Berg

frontiers in Marine Science

EDITORIAL
published: 31 August 2020
doi: 10.3389/fmars.2020.00687

Editorial: Studying the Biology of Aquatic Animals Through Calcified Structures

Esteban Avigliano[1,2]*, *Alejandra Vanina Volpedo*[1,2] *and Benjamin D. Walther*[3]

[1] Facultad de Ciencias Veterinarias, Universidad de Buenos Aires, Buenos Aires, Argentina, [2] CONICET-Universidad de Buenos Aires, Instituto de Investigaciones en Producción Animal, Buenos Aires, Argentina, [3] Department of Life Sciences, Texas A&M University - Corpus Christi, Corpus Christi, TX, United States

Keywords: calcified structures, otolith, fish, marine resource, calcium carbonate, fisheries

OPEN ACCESS

Edited and reviewed by:
Angel Borja,
Technological Center Expert in Marine and Food Innovation (AZTI), Spain

Correspondence:
Esteban Avigliano
estebanavigliano@conicet.gov.ar

Specialty section:
This article was submitted to Marine Ecosystem Ecology, a section of the journal Frontiers in Marine Science

Received: *23 July 2020*
Accepted: *28 July 2020*
Published: *31 August 2020*

Citation:
Avigliano E, Volpedo AV and Walther BD (2020) Editorial: Studying the Biology of Aquatic Animals Through Calcified Structures. Front. Mar. Sci. 7:687. doi: 10.3389/fmars.2020.00687

Editorial on the Research Topic

Studying the Biology of Aquatic Animals Through Calcified Structures

Calcified structures of aquatic animals can be classified according to their biological function (equilibrium, hearing, structure, etc.), composition (hydroxyapatite, calcium carbonate), and crystallography (aragonite, vaterite, calcite) (Tzadik et al., 2017; Thomas and Swearer, 2019). The chemistry and morphometry of structures such as otoliths, statoliths, spines, scales, bones, cuttlebone, and shells among others, have been widely used to reconstruct organism movement and water properties in many different environments (Walther et al., 2014; Tzadik et al., 2017; Thomas and Swearer, 2019; Avigliano et al., 2020a). Trace and majority elements (e.g., strontium, barium, manganese, magnesium, zinc, lithium, copper, etc.) deposited into the calcified structures can provide insights about habitats experienced during the life histories of fish and other organisms, as well as endogenous processes including growth and metabolism (Hüssy et al., 2020). A robust knowledge about drivers that have an impact on chemistry and shape, and the potential interaction between them, is required to accurately interpret chemical and morphometric patterns. Many studies have implicitly assumed that the water chemical composition is the main driver about composition of these structures. However, in the last decade, field and experimental studies have revealed a complex network of endogenous and exogenous factors that can interact with each other and control uptake and incorporation of elements into (Hüssy et al., 2020). Among the known important endogenous factors are genetics, physiological processes (e.g., reproduction, metamorphosis), growth rate, ontogeny, and biomineralization (Campana, 1999; Loewen et al., 2016; Thomas and Swearer, 2019; Hüssy et al., 2020). The environment to which organisms are exposed throughout their lives is one of the main exogenous drivers, where variables such as temperature, pH, salinity, depth, and dissolved oxygen, can modify the chemical composition of the water directly as well as alter organisms physiology and uptake and incorporation dynamics (Limburg et al., 2015; Loewen et al., 2016; Crichton, 2018; Thomas and Swearer, 2019; Hüssy et al., 2020). Secondarily, diet and even differential fishing pressure (which directly impacts growth parameters) can also play an important role in chemical composition (Ranaldi and Gagnon, 2009; Catalán et al., 2018). Likewise, the factors that affect the shape of these structures are complex (Lombarte and Lleonart, 1993; Vignon and Morat, 2010).

The objective of this Research Topic was to encourage the use of calcified structures (lethal and non-lethal) to study the biology of aquatic animals, not only otoliths of bony fishes, but also structures of cartilaginous fishes and mollusks, among others. The aim was also to highlight

multiple analytical approaches including chemistry, morphology and morphometry that were synthesized with biological or environmental data, field observations or experimental tests, that paid special attention to the potential variables that affect the incorporation of trace elements. Several articles of this Research Topic were presented at "II Latin American Workshop on otoliths and other calcified structures" (Buenos Aires-Argentina on August 28–30, 2019). In total, 20 manuscripts compose this Research Topic, covering a variety of themes, revised below.

CHEMICALLY UNALTERABLE STRUCTURES

Structures that are chemically unalterable are primarily composed of calcium carbonate, continually accrete, and are not subsequently resorbed or otherwise metabolically active (Thomas and Swearer, 2019). Depending on both endogenous and exogenous factors, calcium carbonate is accreted in the form of vaterite, calcite, or aragonite, the latter being the most abundant in most inert calcified structures (Oliveira et al., 1996; Crichton, 2018). Among these structures are the otoliths (teleost fishes), statoliths (mollusks like cephalopods), statocysts (cnidarians), and the calcified portion of the mollusk shells. These structures are acellular and while primarily composed of calcium carbonate, they are formed on a proteinaceous matrix (Thomas and Swearer, 2019).

A variety of included papers employed unalterable structures. Lilkendey et al. used otoliths to study the somatic growth rates of reef fish, and their relationship with fresh submarine groundwater discharge. Other authors used sclerochronological techniques in Mediterranean fishes to reconstruct environmental changes (Matić-Skoko et al.) and quantify temporal variability in growth of fishes from the Southwest and North Atlantic Ocean (Garcia Alonso et al.; Lattuca et al.,; Tonheim et al.; Wilhelm et al.). Otolith chemistry was used to identify natal sources, delineate stock structure and investigate life histories of marine fishes from many regions including the South and North Pacific (Feyrer et al.; Rogers et al.), and Southwestern Atlantic (Lattuca et al.) and North Atlantic (Tripp et al.) oceans. In addition, Vasconcelos-Filho et al. described a non-destructive micro-computed tomography scan protocol to explore the eco-densitometry of otoliths which could be used in a wide range of species to study age and growth. Matić-Skoko et al. have also done a review on otolith chemistry and sclerochronology research in the Mediterranean.

Studies using controlled laboratory assays were also contributed that develop our understanding of the mechanisms regulating elemental incorporation into otoliths, including growth rate, water composition, salinity, and temperature (Miller and Hurst; Martinho et al.). Moreover, Tonheim et al., identified the influence and importance of environmental and genetic factors for *Clupea harengus* otolith chemistry throughout the life of a fish, along with assessments of genetic contributions to phenotypic variability on the otolith microstructure. Finally, stable oxygen isotopes of statoliths from the squid *Sepioteuthis lessoniana* were used to predict seasonal movement patterns (Chiang et al.), while the cuttlebone chemistry ratio was a promising growth rate proxy for evaluating differences among wild populations of cuttlefish (Chung et al.).

CHEMICALLY ALTERABLE STRUCTURES

Among the most chemically alterable structures used for the biological studies of aquatic organisms are the scales and the skeletal system (spines, fin rays, bones, etc.) (Avigliano et al., 2019). These structures, unlike the inert ones, are formed by living tissue immersed in a hydroxyapatite matrix, which may be subject to resorption (Tzadik et al., 2017). The resorption phenomenon can limit the use of these structures to, for example, trace life history using chemical markers. On the other hand, the resorption of growth *annuli* in scales and bones can lead to underestimation of the age of the organisms studied.

Nevertheless, since the extraction of some structures such as scales or fin rays turns out to be non-lethal, it may offer a viable alternative way to study vulnerable fishes provided comparable chemical signatures to otoliths are found in these structures (Woodcock et al., 2013; Avigliano et al., 2019). In addition, structures like vertebrae provide an opportunity to study cartilaginous fishes that lack otoliths. Non-lethal methods using spines and scales have been employed to study lifetime movement patterns and assess stock structure in many species (Rude et al., 2014; Seeley et al., 2015; Seeley and Walther, 2018; Avigliano et al., 2019). Although scale and fin spine resorption through life is well-documented, chemical stability in the marginal area has been observed, making it a suitable tool for stock identification in some fishes (e.g., Avigliano et al., 2020b).

This collection brings together an interesting diversity of articles on calcified structures such as vertebrae and scales. Researchers applied vertebrae microchemistry to investigate habitat use of an endangered coastal shark (Feitosa et al.), while vertebrae increment patterns were also used as a proxy of somatic growth of a philopatric and demersal shark (Izzo and Gillanders). Vertebrate were also used to provide the first validation of the annual formation of growth bands in the whale shark using bomb radiocarbon assays (Ong et al.). Moreover, intra and interspecific morphometric variation of scapula-coracoids of three skate species were analyzed to assess its utility as a diagnostic characteristic (Mabragaña et al.). Finally, geometric morphometric approaches were used in scales to delimit fish species and assess how fish scale shape varies with genetic structure or with marine ecoregions (Ibáñez et al.; Pacheco-Almanzar et al.).

FINAL REMARKS

In summary, this Research Topic includes 20 papers that gathered 148 authors of several universities and research centers from 20 countries (Argentina, Australia, Brazil, Canada, Croatia, Germany, Iceland, Japan, Mauritius, Mexico, Namibia, New Zealand, Norway, Pakistan, Portugal, Saudi Arabia, South Africa, Sweden, Taiwan, USA). Most of the studies were developed in an interdisciplinary and inter-institutional framework, reflecting the

importance of collaborative research development and bringing new knowledge to the study of calcified structures.

AUTHOR CONTRIBUTIONS

EA conceived the Research Topic and wrote the manuscript. AV and BW wrote the manuscript. All authors contributed to the article and approved the submitted version.

ACKNOWLEDGMENTS

This collection of articles was possible thanks to the collaboration of the reviewers (approximately 50 reviewers), who selflessly invested their time. We thank the 148 authors who entrusted us with their manuscript submissions. We also thank Red Interdisciplinaria de Otolitometría Latino Americana (RIO-LA), whose members have contributed as authors and reviewers.

REFERENCES

Avigliano, E., Carvalho, B. M., Miller, N., Gironde, S. C., Tombari, A., Limburg, K. E., et al. (2019). Fin spine chemistry as a non-lethal alternative to otoliths for stock discrimination in an endangered catfish. *Mar. Ecol. Prog. Ser.* 614, 147–157. doi: 10.3354/meps12895

Avigliano, E., Ivanovic, M., Prandoni, N., Méndez, A., Pisonero, J., and Volpedo, A. V. (2020a). Statolith chemistry as a stock tag in the Argentine shortfin squid Illex argentinus. *Reg. Stud. Mar. Sci.* 38:101355. doi: 10.1016/j.rsma.2020.101355

Avigliano, E., Miller, N., Maichak de Carvalho, B., Gironde, S. C., Tombari, A., and Volpedo, A. V. (2020b). Fin spine metals by LA-ICP-MS as a method for fish stock discrimination of Genidens barbus in anthropized estuaries Fisheries Research Fin spine metals by LA-ICP-MS as a method for fi sh stock discrimination of Genidens barbus in anthropized estuaries. *Fish. Res.* 230:105625. doi: 10.1016/j.fishres.2020.105625

Campana, S. E. (1999). Chemistry and composition of fish otoliths: pathways, mechanisms and applications. *Mar. Ecol. Prog. Ser.* 188, 263–297. doi: 10.3354/meps188263

Catalán, I. A., Alós, J., Díaz-Gil, C., Pérez-Mayol, S., Basterretxea, G., Morales-Nin, B., et al. (2018). Potential fishing-related effects on fish life history revealed by otolith microchemistry. *Fish. Res.* 199, 186–195. doi: 10.1016/j.fishres.2017.11.008

Crichton, R. (2018). Chapter 19 - biomineralization. In: *Biological Inorganic Chemistry*, 3rd edn, ed R. Crichton (Cambridge, MA: Academic Press), 517–544.

Hüssy, K., Limburg, K. E., de Pontual, H., Thomas, O. R. B., Cook, P. K., Heimbrand, Y., et al. (2020). Element patterns in otoliths: the role of biomineralization. *Rev. Fish Sci. Aquac.* 1–33. doi: 10.1080/23308249.2020.1760204

Limburg, K. E., Walther, B. D., Lu, Z., Jackman, G., Mohan, J., Walther, Y., et al. (2015). In search of the dead zone: use of otoliths for tracking fish exposure to hypoxia. *J. Mar. Syst.* 141, 167–178. doi: 10.1016/j.jmarsys.2014.02.014

Loewen, T. N., Carriere, B., Reist, J. D., Halden, N. M., and Anderson, W. G. (2016). Linking physiology and biomineralization processes to ecological inferences on the life history of fishes. *Comp. Biochem. Physiol. Part A Mol. Integr. Physiol.* 202, 123–140. doi: 10.1016/j.cbpa.2016.06.017

Lombarte, A., and Lleonart, J. (1993). Otolith size changes related with body growth, habitat depth and temperature. *Environ. Biol. Fishes* 37, 297–306. doi: 10.1007/BF00004637

Oliveira, A. M., Farina, M., Ludka, I. P., and Kachar, B. (1996). Vaterite, calcite, and aragonite in the otoliths of three species of piranha. *Naturwissenschaften* 83, 133–135. doi: 10.1007/s001140050262

Ranaldi, M. M., and Gagnon, M. M. (2009). Accumulation of cadmium in the otoliths and tissues of juvenile pink snapper (*Pagrus auratus* Forster) following dietary and waterborne exposure. *Comp. Biochem. Physiol. C Toxicol. Pharmacol.* 150, 421–427. doi: 10.1016/j.cbpc.2009.06.007

Rude, N. P., Smith, K. T., and Whitledge, G. W. (2014). Identification of stocked muskellunge and potential for distinguishing hatchery-origin and wild fish using pelvic fin ray microchemistry. *Fish Manage. Ecol.* 21, 312–321. doi: 10.1111/fme.12081

Seeley, M., Miller, N., and Walther, B. (2015). High resolution profiles of elements in Atlantic tarpon (*Megalops atlanticus*) scales obtained via cross-sectioning and laser ablation ICP-MS: a literature survey and novel approach for scale analyses. *Environ. Biol. Fishes* 98, 2223–2238. doi: 10.1007/s10641-015-0443-z

Seeley, M. E., and Walther, B. D. (2018). Facultative oligohaline habitat use in a mobile fish inferred from scale chemistry. *Mar. Ecol. Prog. Ser.* 598, 233–245. doi: 10.3354/meps12223

Thomas, O. R. B., and Swearer, S. E. (2019). Otolith biochemistry—A review. *Rev. Fish Sci. Aquac.* 27, 458–489. doi: 10.1080/23308249.2019.1627285

Tzadik, O. E., Curtis, J. S., Granneman, J. E., Kurth, B. N., Pusack, T. J., Wallace, A. A., et al. (2017). Chemical archives in fishes beyond otoliths: a review on the use of other body parts as chronological recorders of microchemical constituents for expanding interpretations of environmental, ecological, and life-history changes. *Limnol. Oceanogr. Methods* 15, 238–263. doi: 10.1002/lom3.10153

Vignon, M., and Morat, F. (2010). Environmental and genetic determinant of otolith shape revealed by a non-indigenous tropical fish. *Mar. Ecol. Prog. Ser.* 411, 231–241. doi: 10.3354/meps08651

Walther, B. D., Thorrold, S. R., and Olney, J. E. (2014). Geochemical signatures in otoliths record natal origins of american shad. *Trans. Am. Fish. Soc.* 137, 57–69. doi: 10.1577/T07-029.1

Woodcock, S. H., Grieshaber, C. A., and Walther, B. D. (2013). Dietary transfer of enriched stable isotopes to mark otoliths, fin rays, and scales. *Can. J. Fish. Aquat. Sci.* 70, 1–4. doi: 10.1139/cjfas-2012-0389

Conflict of Interest: The authors declare that the research was conducted in the absence of any commercial or financial relationships that could be construed as a potential conflict of interest.

Copyright © 2020 Avigliano, Volpedo and Walther. This is an open-access article distributed under the terms of the Creative Commons Attribution License (CC BY). The use, distribution or reproduction in other forums is permitted, provided the original author(s) and the copyright owner(s) are credited and that the original publication in this journal is cited, in accordance with accepted academic practice. No use, distribution or reproduction is permitted which does not comply with these terms.

frontiers in Marine Science

ORIGINAL RESEARCH
published: 11 October 2019
doi: 10.3389/fmars.2019.00613

Fresh Submarine Groundwater Discharge Augments Growth in a Reef Fish

Julian Lilkendey[1,2†], Timo Pisternick[1,3], Sarah I. Neumann[1], Danishta Dumur Neelayya[3], Stefanie Bröhl[1], Yashvin Neehaul[3] and Nils Moosdorf[1,4†]*

[1] Leibniz Centre for Tropical Marine Research (ZMT), Bremen, Germany, [2] School of Science, Auckland University of Technology, Auckland, New Zealand, [3] Mauritius Oceanography Institute (MOI), Albion, Mauritius, [4] Institute of Geosciences, University of Kiel, Kiel, Germany

Fresh submarine groundwater discharge (fresh SGD), the efflux of terrestrial groundwater directly into the ocean, is a ubiquitous pathway for nutrient-rich freshwater to coastal ecosystems, altering their hydrography, hydrochemistry, and primary productivity. Yet only little is known about the effects of fresh SGD on the fitness of higher trophic levels such as teleost fish. Otolith analysis revealed that somatic growth rates were significantly higher and settlement to reef habitat took place significantly earlier in juvenile gray demoiselle *Chrysiptera glauca* exposed to fresh SGD as compared to strictly marine conditions. Contrary to expectations, feeding conditions were comparable in both habitats. We propose that physiologically beneficial environmental conditions brought about by the submarine influx of cold acidic freshwater enabled juvenile fish to exhibit elevated growth rates, thereby increasing their survival potential. This effect would directly link changes in groundwater on land to variations in marine primary and secondary consumer biomass at the coast.

Keywords: coral reef, submarine groundwater discharge, damselfish, fitness, survival potential, feeding habits, otolith age reading, growth effect

OPEN ACCESS

Edited by:
Esteban Avigliano, National Council for Scientific and Technical Research (CONICET), Argentina

Reviewed by:
Ana Laura Ibañez, Universidad Autónoma Metropolitana, Mexico
Marcelo Soeth, Federal University of Paraná, Brazil

****Correspondence:***
Julian Lilkendey
julian.lilkendey@icloud.com

†ORCID:
Julian Lilkendey
orcid.org/0000-0003-3165-1079
Nils Moosdorf
orcid.org/0000-0003-2822-8261

Specialty section:
This article was submitted to Marine Ecosystem Ecology, a section of the journal Frontiers in Marine Science

Received: *20 July 2019*
Accepted: *18 September 2019*
Published: *11 October 2019*

Citation:
Lilkendey J, Pisternick T, Neumann SI, Dumur Neelayya D, Bröhl S, Neehaul Y and Moosdorf N (2019) Fresh Submarine Groundwater Discharge Augments Growth in a Reef Fish. Front. Mar. Sci. 6:613. doi: 10.3389/fmars.2019.00613

INTRODUCTION

Submarine groundwater discharge (SGD) is an important, albeit subtle pathway for nutrient rich freshwater to coastal ecosystems (Johannes and Hearn, 1985; Lapointe and O'Connell, 1989; Slomp and Van Cappellen, 2004; Luo et al., 2018). The phenomenon referred to as SGD entails the recirculation of seawater as well as the influx of fresh terrestrial groundwater (fresh SGD) (Burnett et al., 2003; Moore, 2010) and occurs nearly ubiquitously at the shorelines (Moosdorf et al., 2015). Here we will focus on fresh SGD, since its ramifications on coastal ecology are far more incisive: globally, fresh SGD amounts to up to 10% of the gross river discharge (Taniguchi et al., 2002). The process is responsible for habitat modifications and niche partitioning in benthic communities via local changes in water temperature, salinity, and pH (Amato et al., 2016; Foley, 2018). Fresh SGD can drive a coastal ecosystem's primary production via nutrient enrichment, which in turn leads to elevated primary and secondary consumer biomass (Dale and Miller, 2008; Waska and Kim, 2011; Encarnação et al., 2014; Hata et al., 2016; Utsunomiya et al., 2017; Lecher and Mackey, 2018; Piló et al., 2018). The assessment of factors influencing the abundance and growth of these consumers, in particular teleost fishes, is of ever-growing concern since this information is vital to predict consequences of anthropogenic actions on ecosystem functioning and productivity (Burnett et al., 2018; Shoji and Tominaga, 2018).

In marine fish early life stages rapid growth generally decreases predation mortality (Anderson, 1988; Houde, 1989). Improved feeding conditions are proposed to have positive effects on the condition and growth of teleost fishes (Jones, 1986). On settlement, juvenile reef fish suffer high rates of mortality which signifies this life history stage as an especially critical bottleneck for a fish cohort (Almany and Webster, 2006). Enhanced somatic condition, augmented growth, and earlier settlement are consequently indicators of elevated survival potential and confer higher fitness to reef fish (Booth, 1995; Suthers, 1998; Hoey and McCormick, 2004). Water temperatures, pH levels, dissolved oxygen content, and salinity divergent from the marine conditions a fish is adapted to may pose as physiological stressors, potentially negatively affecting condition and growth (Pauly, 1998; Choat and Roberson, 2002). Altered growth rates caused by the influx of fresh SGD to a coastal marine ecosystem are, therefore, highly likely to modify individual fitness and thereby population sizes in fishes.

Damselfishes are a widespread and abundant component of coastal fish communities around the world. Members of the family frequently serve as model organisms since they share life-history traits with the majority of benthic and coastal fishes and invertebrates (Simpson et al., 2016). Demersal, territorial adults produce pelagic larvae which are dispersed throughout the intertidal zone by tides and currents (Sale, 2002). Juveniles settle at first in small upper littoral rock or tide pools before dispersal onto the upper reef flat takes place (Gopinadha Pillai and Mohan, 1990).

We hypothesize that fresh SGD alters the fitness of primary and secondary consumers through changes in water quality characteristics and enhanced primary productivity in coastal marine ecosystems. We consequently aim at investigating the small-scale effects of fresh SGD on the growth rates of juvenile gray demoiselle *Chrysiptera glauca* in two contrasting tide pools in Mauritius to predict meso-and large-scale impacts of the process on secondary consumer biomass in coastal ecosystems. Semi-enclosed tide pools influenced by fresh groundwater seepage constitute a valuable field laboratory since these environments exhibit markedly lowered water temperatures, pH, and salinities combined with elevated nutrient loadings due to high water residence times at low tide (Foley, 2018).

MATERIALS AND METHODS

Study Sites

The intertidal zone of Mauritius is characterized by volcanic rock (Montaggioni, 1982) and serves as a habitat to early life stages of various reef fishes (Sato et al., 2008). Mauritius' lagoons are highly impacted by dissolved nutrient input from SGD (Burnett et al., 2006; Ramessur et al., 2012). The main source of anthropogenic derived nutrients in fresh SGD in Mauritius are domestic and industrial sewage as well as agricultural activities such as sugar cane farming (Ramessur, 2002). Sampling took place in two tide pools situated at the West coast of Mauritius: one characterized by visible fresh submarine groundwater seepage in Albion (375 m^2, 20°12′59.5″S, 57°23′48.2″E) and another strictly marine one in Flic-en-Flac (350 m^2, 20°16′17.7″S, 57°22′13.9″E) (**Figure 1**). Both tide pools were located in lagoons of fringing reefs and sheltered from waves by reef crests. Even though post-larvae of *C. glauca* are usually recruited to tidal pools all year round, there is a profusion of them during November–December (Gopinadha Pillai and Mohan, 1990). Sampling from October 2017 to January 2018 also allowed for investigating a period with high precipitation rates and strong expected effects from fresh SGD (Oehler et al., 2018) (see **Supplementary Table S1**).

Environmental Parameters, Substrate Compositions, and Fish Densities

Local influx of fresh SGD is known to significantly alter the water quality characteristics of coastal ecosystems (Moosdorf et al., 2015). We used *in situ* measurements of physico-chemical parameters to characterize the hydrography and hydrochemistry of the two study tide pools. Water temperature, pH level, oxygen content, and salinity were recorded at both locations during rising tide conditions at mid tide cycle once per month using a WTW multiprobe. Further, hobo loggers were deployed for 24 h inside both tide pools in November 2017. This allowed for the assessment of water depth, temperature, and salinity fluctuations along a full tidal cycle (see **Supplementary Figure S1**). Water samples for subsequent nutrient measurements were collected in replicates once per month. Per sample 50 ml of seawater were filtered (Sterile Syringe Filter, Corning, CA 0.2 μm), transferred to pre-rinsed centrifuge tubes (with a headspace remaining) and stored frozen (–20°C) in the laboratory. Nutrient analyses of water samples were performed in the laboratory of the Mauritius Oceanography Institute in Albion, Mauritius. Nitrite, nitrate, silicate, and phosphate concentrations were determined using standard methods with a discrete analyser (Systea Easychem Plus) equipped with a 5 cm reading cell.

To evaluate substrate composition, a 50 × 50 cm rectangle containing a grid of 25 10 cm × 10 cm squares was placed randomly 10 times inside each tide pool. Relative substrate cover was assessed visually for each placement. Since visual counts are a common methodology to quantify organism densities in reef environments (Halford and Thompson, 1994), we counted juveniles while wading in transects through each tide pool once per month. We tracked the waded distance via the global positioning system (Garmin GPSMAP 64s) and counted *C. glauca* individuals in a range of 50 cm to each side. Every sampling month we covered ca. 60 m × 1 m, equivalent to an area of ca. 60 m^2. Identification from on top the water surface was possible since juveniles of *C. glauca* are easily distinguishable from other damselfish species by their gray color and the fluorescent V on the dorsal side of the head (Allen and Steene, 1987). The total number of individuals was set in relation to tide pool area and pooled across sampling months.

Feeding Conditions

Fish were caught with hand nets, stored in ambient seawater for 1–2 h before being euthanized by transfer to a 30% ethanol/seawater solution. In the laboratory, fish were gradually transferred to 50 and 70% ethanol/freshwater

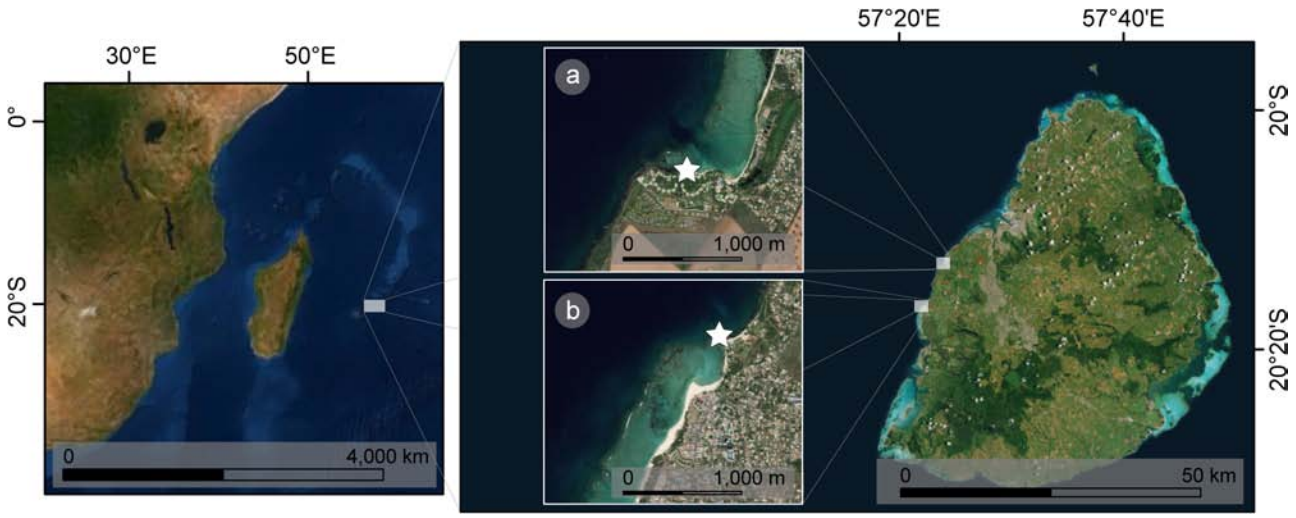

FIGURE 1 | The island of Mauritius in the South-West Indian Ocean with the two sampling tide pools at its West coast: Stars mark the locations of (A) a tide pool influenced by submarine groundwater discharge at Albion, (B) a strictly marine tide pool at Flic-en-Flac.

solution (Döring et al., 2018). Specimens of *C. glauca* were measured by standard length (distance between the tip of the snout and the posterior end of the last vertebra, SL, nearest mm), eviscerated, and weighed (EM, ±0.001 g). We identified food organisms to class level. As plants (macrophytes) were among the principal food components in the stomachs of juvenile *C. glauca*, numerical counts were regarded as not suitable. We, therefore, followed the recommendations from literature and used the frequency of occurrence method for stomach content analysis (Hyslop, 1980). Further, a condition index (CI) was calculated for each individual by using b of the length-weight relationship (Suthers, 1998) (Eq. 1):

$$CI = EM \times SL^{-b} \times 100 \quad (1)$$

Chlorophyll *a* concentrations were recorded once at the end of the sampling period in January 2018 using a MANTA water quality multi-probe (Eureka Environmental Engineering).

Otolith Preparation and Reading

The lapilli otoliths were dissected under a stereomicroscope, cleaned with deionized water, and stored dry in FEMA-cells (26 × 76 mm). Otoliths were fixed on glass slides using 2-component adhesive (Araldite 2020/A and Araldite 2020/B) and ground sequentially on glass plates by silicon carbide (SiC) powder with grit sizes of 400 and 800. After polishing with waterproof SiC grinding paper (grain size of 5 μm), otoliths in immersion oil were examined with a digital microscope (Keyence VHX-5000) using transmitted light at a magnification of 400×–800×. With the digital microscope it was possible to compose depth-stitchings of different focus levels. Daily deposition of increments on the lapillus otolith has been validated in a number of species from this family (Pitcher, 1988; Thresher et al., 1989; Wellington and Victor, 1989; Thorrold and Milicich, 1990) and we therefore assumed that increments on the lapilli of *C. glauca* were deposited daily (Wellington and Victor, 1992). The increment closest to the core of the otolith was assumed to be formed at the day of hatching, as is the case in many other species from the family Pomacentridae (Wellington and Victor, 1989). The number of increments was determined from 3 replicate increment counts. The mean count was accepted if the counts deviated by less than 10%, otherwise the otolith was rejected (n = 7) (Wilson and Meekan, 2002). Increment counts were conducted and otolith radius (OR) was measured using ImageJ 1.49 (Rasband, WS, US National Institutes of Health, Bethesda, MD)[1]. Peripheral otolith growth is a valuable condition index in juvenile reef fishes since it is correlated with RNA/DNA ratios, an indicator for protein biosynthesis in teleost fishes (Clemmesen and Doan, 1996; Suthers, 1998). We, therefore, digitally measured the widths of the last two complete peripheral increments of the otolith. The settlement mark was identified as the first increment of a transition zone, characterized by a rapid narrowing in increment width (Wilson and McCormick, 1997; Retzel et al., 2007) (**Supplementary Figure S2**).

Growth Model

The relationship between SL and juvenile age (in days) was modeled using the Gompertz growth curve (Stevenson and Campana, 1992) (Eq. 2):

$$SL_t = SL_0 \times e^{k\,(1-e^{(G\times t)})} \quad (2)$$

Daily somatic growth rates thus are described with first derivate of Eq. 2 (Döring et al., 2018) (Eq. 3):

$$dSL_t/dt = SL_0 \times k \times Ge^{k\left(1-e^{-G\times t}\right)-G\times t} \quad (3)$$

[1]http://imagej.nih.gov/ij/

where SL_t is the larval length at a given time t, SL_0 is the fish length on the day of hatching, and k the specific growth rate. G characterizes the exponential decline of the specific growth rate.

Statistical Analyses

Inter tide pool differences in the linear relationships between the log-transformed data on SL and EM, as well as between SL and OR were tested. The assumption of parallel lines was met for the relationship between SL and EM, intercepts were consequently compared using analysis of covariance. Since no significant differences were found, the relationship between SL and EM of all sampled juveniles was described using a single power function. Further, since the assumption of parallel lines was not met, linear regression analysis was performed to describe the relationship between SL and OR for each tide pool individually (Villegas-Hernández et al., 2007). For all data the assumptions of normal distribution (Shapiro–Wilk-test, $p > 0.05$) and homogenous variances (Bartlett-test, $p > 0.05$) were tested (Howell, 2007). One-way analysis of variance (ANOVA) was employed to compare the monthly pooled density and age at settlement values between tide pools. Since data did not meet the assumption of equal variances a nonparametric Mann-Whitney-U-test was used to test for inter tide pool differences in chlorophyll a concentrations. Factorial ANOVA was employed to explore the effects of the categorical predictors tide pool and sampling month on the explanatory variables CI, mean peripheral otolith increment width, and somatic growth rates. To achieve normal distribution and variance homogeneity, data on somatic growth rates were log-transformed. All statistical analyses were carried out in JMP Pro 14.0.0 (SAS Institute Inc., Cary, NC)[2]. Sample sizes for all conducted statistical analyses are listed in **Table 1**.

RESULTS

Tide Pool Hydrography and Hydrochemistry

Water temperature and pH in the tide pool at Albion steadily increased from October 2017 to January 2018 and were usually markedly lower than in the tide pool at Flic-en-Flac (**Figures 2A,B**). Water in both tide pools was generally supersaturated with oxygen and dissolved oxygen content was higher in the tide pool at Flic-en-Flac as opposed to the one at Albion in all months except November (**Figure 2C**). Salinity in the tide pool at Flic-en-Flac continuously ranged around 35 while in the tide pool at Albion salinity was below 20 in most months (**Figure 2D**). Nitrite, Nitrate, and Silicate concentrations were generally substantially higher in the tide pool at Albion than in the one at Flic-en-Flac. All three parameters exhibited increasing trends inside both tide pools throughout the sampling period (**Figures 2E–G**). Phosphate concentrations, on the other hand, were very similar and exhibited decreasing trends from October to January (**Figure 2H**).

In November environmental parameters were, as an exception, sampled closer to high tide, explaining the divergent salinity, oxygen, and pH levels for this month (**Supplementary Figure S1**). All these observations suggest a strong influx of fresh SGD into the Albion tide pool hence this tide pool will be referred to as influenced by fresh "SGD." Contrary, the Flic-en-Flac tide pool provided strictly marine environmental conditions for the study species and this tide pool is henceforth called "marine."

Benthic Cover and Juvenile Densities

Relative benthic cover compositions were quite different between both tide pools. While no sessile algae were recorded in the tide pool influenced by fresh SGD, the bottom of the marine tide pool was to a great extant covered by macroalgae and turfalgae (**Table 2**). We also found that *C. glauca* densities were not significantly different in the two study tide pools (ANOVA, $F_{(1,\ 8)} = 0.2497$, $p = 0.6326$) (**Table 2**).

Feeding Conditions

Almost all juveniles examined for the present study fed on a mix of filamentous green algae, crustacean copepods, moluscs, and plant detritus. Moreover, the diet occasionally included calcifying corals, gastropods, insects/arachnids of terrestrial origin, and ichthyoplankton. Plastic particles or fibers were found in the stomachs

[2]www.jmp.com

TABLE 1 | Number of juvenile *Chrysiptera glauca* used for the respective analysis.

	SGD				Marine				
	Oct 17	Nov 17	Dec 17	Jan 18	Oct 17	Nov 17	Dec 17	Jan 18	Total
Stomach content	10	14	16	14	15	12	10	15	96
Condition index	10	14	16	14	16	12	10	15	107
Lapillus radius	10	12	13	14	15	9	8	15	96
Otolith reading	8	9	10	11	13	9	8	13	81
Age at settlement	5	8	10	10	9	3	7	10	62
Peripheral otolith growth	10	11	12	11	14	9	8	13	88

Specimens were sampled in a tide pool affected by fresh submarine groundwater seepage (SGD) and in a strictly marine one (marine) from October 2017 to January 2018.

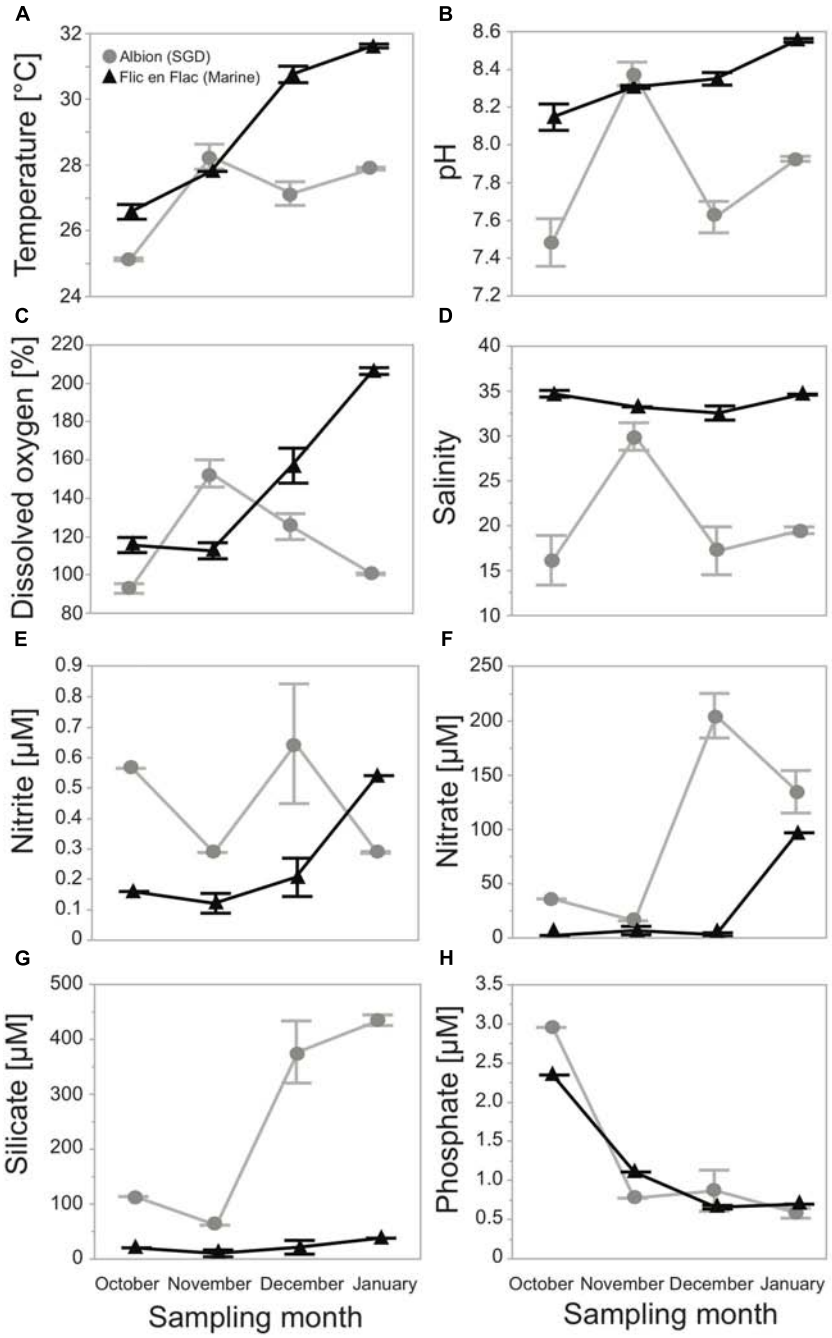

FIGURE 2 | Monthly time series of physico-chemical parameters recorded inside a tide pool influenced by fresh SGD at Albion (SGD, gray dots) and inside a strictly marine tide pool at Flic-en-Flac (Marine, black triangles): **(A)** Water temperature, **(B)** water pH, **(C)** water dissolved oxygen content, **(D)** salinity, **(E)** nitrite, **(F)** nitrate, **(G)** silicate, and **(H)** phosphate concentrations.

of 16% of all fish (**Table 3**). Two factorial ANOVA revealed no significant differences in juvenile CI throughout tide pools and months ($F_{(7,\ 104)} = 1.70$, $p = 0.12$). Mean chlorophyll *a* concentrations [± standard deviation (SD)] were significantly higher in the strictly marine tide pool (0.50 ± 0.20 µg/l) when compared to the tide pool influenced by SGD (0.39 ± 0.07 µg/l) (Mann–Whitney-*U*-test, $Z = -2.23$, $n1 = 86$ and $n2 = 156$, $p < 0.05$).

Otolith Growth, Somatic Growth, and Settlement

Since there was no observable spatial difference in the relationship between juvenile standard length (**Figure 3**) and

TABLE 2 | Mean benthic cover composition (% ±SD) and juvenile *Chrysiptera glauca* densities (individuals 100 m^{-2} ±SD) in a tide pool affected by fresh submarine groundwater seepage (SGD) and in a strictly marine one (marine).

	Macroalgae	Turfalgae	Sand	Rubble	Rock	Fish density
SGD	0	0	27 ± 41	36 ± 35	37 ± 41	10 ± 4
Marine	22 ± 32	21 ± 17	2 ± 3	1 ± 4	54 ± 28	9 ± 3

eviscerated mass (EM), a common power function is given as follows: $EM = 0.0019 \times SL^{3.4507}$, $r^2 = 0.99$.

Two factorial ANOVA showed no significant differences in juvenile peripheral otolith growth throughout tide pools and months ($F_{(7,\ 87)} = 1.00$, $p = 0.44$). The linear relationships between SL and OR showed a proportionality between otolith growth and fish somatic growth (inside the fresh SGD influenced tide pool: $OR = 87.140321 + 9.9018163 \times SL$, $r^2 = 0.95$, and inside the strictly marine tide pool: $OR = 42.1809 + 12.571021 \times SL$, $r^2 = 0.95$) (**Figure 3**).

For each sampling location we computed a distinctive Gompertz growth function (**Figure 4**): SGD tide pool: $SL_t = 7.26 \times e^{2.85\ (1-e^{(0.0099\times t)})}$, $r^2 = 0.89$; marine tide pool: $SL_t = 7.21 \times e^{2.78\ (1-e^{(0.0083\times t)})}$, $r^2 = 0.91$. The first derivative of the Gompertz growth models gave us the daily somatic growth rates, which served to back-calculate the amount of somatic tissue individuals were able to accumulate in both tide pools per day. For all months, somatic growth rates were significantly higher in juveniles sampled in the fresh SGD influenced tide pool when compared to their conspecifics sampled in the marine tide pool. Also, in both tide pools juvenile somatic growth rates were significantly higher in November and January than in October (ANOVA, $F_{(7,\ 78)} = 32.2585$, $p < 0.0001$, Tukey HSD, $p < 0.05$).

Chrysiptera glauca individuals sampled in the SGD influenced tide pool settled at a significantly younger age (19.9 ± 2.8 days, $n = 33$) than their counterparts taken from the strictly marine tide pool (22.1 ± 2.7 days, $n = 29$) (ANOVA, $F_{(1,\ 61)} = 9.67$, $p < 0.01$).

DISCUSSION

While the impact of fresh SGD on benthic and pelagic primary producer community structuring is rather well studied, little is known about the process' effects on the fitness of consumers in higher trophic levels such as teleost fish (Lecher and Mackey, 2018). Determination of factors influencing the fitness of fish in coastal environments is, however, of consistently high concern to make predictions about anthropogenic impacts on marine ecosystems and, ultimately, on fisheries' productivity. We show that somatic growth rates were significantly higher and settlement to reef habitat took place significantly earlier in juvenile gray demoiselle *C. glauca* exposed to fresh SGD when compared to strictly marine conditions. Since feeding conditions were comparable among tide pools, we propose that physiologically beneficial environmental conditions rather than food availability elevate the survival potential of marine fish exposed to fresh SGD.

The encountered cold, acidic, nutrient-rich fresh SGD is known to condition benthic marine macro faunal communities (Amato et al., 2016; Foley, 2018; Piló et al., 2018). The interactions between substrate for algae cultivation, macrophytic food abundance, and damselfish densities can be manifold (Wellington and Victor, 1985; Ceccarelli et al., 2005; Ceccarelli, 2007; Hoey and Bellwood, 2010) and intraspecific density dependent effects were additionally shown to modify growth in damselfish (Booth, 1995). We followed up on this relationship by visually assessing substrate cover composition and *C. glauca* densities within each tide pool. The strictly marine tide pool was to a great extant covered with macroalgae, while these benthic primary producers were completely absent from the tide pool influenced by SGD. Due to similar values in shelter providing rocks and in juvenile densities, it can be suspected that density dependent mortality as well as predator induced stress are comparable in both tide pools (Schmitt and Holbrook, 1999; Holbrook and Schmitt, 2002).

Feeding conditions are proposed to be directly related to somatic wealth and growth in fishes (Jones, 1986), and are thus expected to have important ramifications for juvenile survival and recruitment (Hoey and McCormick, 2004). Further, nutrient rich fresh SGD has the potential to elevate chlorophyll *a* levels and macrophyte abundances in coastal marine ecosystems (Machado and Imberger, 2014; Welti et al., 2015; Amato et al., 2016; Honda et al., 2018). To test for inter tide pool differences in feeding conditions, we investigated juvenile stomach contents and nutritional condition as well as chlorophyll *a* concentrations. In juvenile reef fishes, otolith growth rates as condition indices are regarded as superior to morphometric (e.g., length to mass)

TABLE 3 | Frequency of occurrence of food organisms (to phylogenetic class level) and particles in the stomachs of *Chrysiptera glauca* (as percentage of all juveniles) sampled in either a tide pool influenced by fresh submarine groundwater discharge (SGD), in a strictly marine tide pool (marine), as well as in both tide pools combined (total).

	Chlorophyceae	Plant detritus	Anthozoa	Arachnida/ Insecta	Bivalvia	Gastropoda	Ichthyoplankton	Maxillopoda	Plastic particles
SGD	75.9	100	33.3	31.5	1.9	3.7	11.1	64.8	16.7
Marine	46.2	100	46.2	6.0	4.0	5.8	0	92.3	15.4
Total	61.3	100	39.6	18.9	2.8	4.7	5.7	78.3	16.0

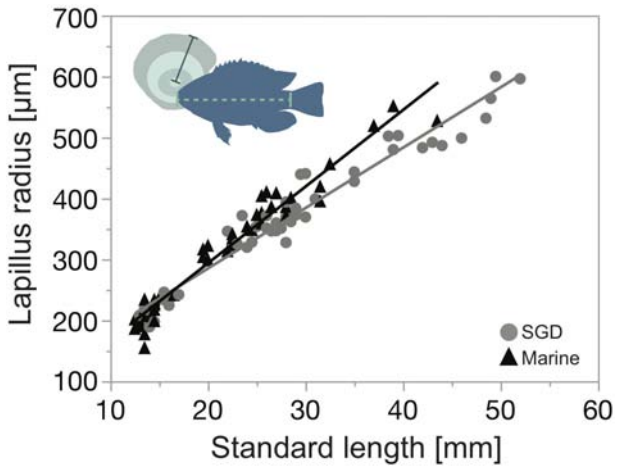

FIGURE 3 | Relationship between lapillus (green) radius (dark green solid line) and juvenile *Chrysiptera glauca* (blue silhouette) standard length (light green dashed line) inside a tide pool influenced by fresh submarine groundwater seepage (SGD, gray circles), and in a strictly marine tide pool (marine, black triangles).

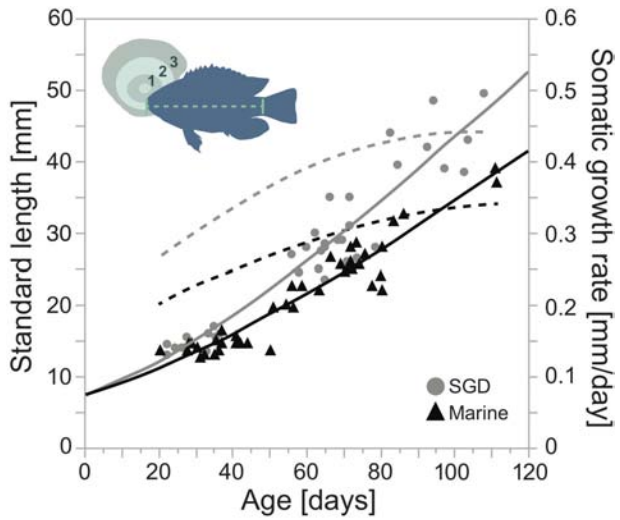

FIGURE 4 | Relationship between standard length (light green dashed line, mm), somatic growth rates (mm per day), and age (days) as deducted from otolith (green) increment counts (dark green numbers) in juvenile *Chrysiptera glauca* (blue silhouette). Gray and black solid lines represent Gompertz growth curves (GGC), gray and black dashed lines represent growth rates (mm per day) calculated from first derivative of the GGC. Gray circles indicate individuals sampled inside a tide pool influenced by fresh submarine groundwater seepage (SGD), and black triangles those sampled in a strictly marine tide pool (marine).

relationships (Suthers, 1998). We, therefore, analyzed somatic energy storage (i.e., CI) combined with peripheral otolith growth to assess the nutritional wealth of *C. glauca* individuals in the two study tide pools. Both indices showed neither significant spatial nor temporal differences. *C. glauca* is omnivorous and demonstrably able to utilize a variety of food sources (Hiatt and Strasburg, 1960; Gopinadha Pillai and Mohan, 1990). Stomach contents analysis showed that *C. glauca*'s diet is highly dependent on green algae and plant detritus. Taking into account the markedly higher benthic algae abundance and chlorophyll *a* levels in the marine tide pool, and that nutritional condition (CI and peripheral otolith growth) was temporally and spatially constant, feeding conditions for *C. glauca* could not be assumed to be more favorable in the SGD tide pool.

Back-calculation of size from otoliths assumes that there is proportionality between otolith and somatic growth rates (Vigliola et al., 2000). We verified this assumption by calculating a regression relationship between otolith radius and SL for each tide pool. Because of a lower slope inside the tide pool influenced by fresh SGD, a significant interaction between somatic growth and site was detected. An otolith growth uncoupled from somatic growth in acidic waters was previously described in juvenile ocellated wrasse *Symphodus ocellatus* and attributed to the "growth effect" (Di Franco et al., 2019): slower-growing individuals have a tendency to have larger otoliths than their faster-growing counterparts at the same length (Campana, 1990).

In reef fishes it is likely that linkages between early life stages occur when there is selection for a cumulative trait, e.g., body size. They can be effective not only between life history stages of the same individual, but also between generations through maternal effects, e.g., size at hatching (Leis and McCormick, 2002). In brown demoiselle *Neopomacentrus filamentosus* individuals that survived intense selective mortality 1–3 months after settlement were those fish that were larger at hatching and the ones that grew faster during planktonic life (Vigliola and Meekan, 2002). In our case a strong carry over effect of larval fitness at hatching on juvenile growth cannot be expected since length at hatching did not differ markedly between both sampled populations (SGD tide pool: 7.26 mm; marine tide pool: 7.21 mm).

Predatory mortality severely affects population sizes and is often highest for the youngest recruits (Hixon, 1991; Almany and Webster, 2006). A rapid increase in body length, however, generally enhances the survival chances in marine fish early life stages [growth-mortality hypothesis (Anderson, 1988; Houde, 1989)]. Somatic growth rates at a given age were in the range of previously published values for the species (Gopinadha Pillai and Mohan, 1990) and consistently higher in juveniles sampled in the SGD influenced tide pool than in juveniles taken from the marine tide pool. Previous studies in damselfish have shown that faster growing larvae settle at a younger age (Thorrold and Milicich, 1990). Settlement in *C. glauca* occurred inside a time frame frequently observed in damselfishes (Wellington and Victor, 1989). Further, the faster growing *C. glauca* individuals sampled in the SGD influenced tide pool indeed settled at a significantly younger age when compared to their slower growing counterparts taken from the strictly marine tide pool. Earlier settlement decreases the planktonic larval duration, a life history stage particularly prone to high mortality rates (Leis, 1991). Thus, the observed elevated somatic growth rates and earlier settlement can be expected to elevate survival potential and ultimately confer higher fitness to individuals sampled in the fresh SGD influenced tide pool as compared to the strictly marine tide pool (Houde, 1989; Thorrold and Milicich, 1990; Hoey and McCormick, 2004).

The interplay between food levels, metabolism, and somatic growth may be complex (Auer et al., 2015), but direct effects of environmental parameters on growth and survival in marine fish are generally regarded as stronger than the indirect ones exhibited by enhanced food availability (Houde, 2008). Additionally, we show that feeding conditions were comparable in both study tide pools. Our results, therefore, lead us to conclude that physiologically beneficial environmental conditions brought about by the submarine influx of cold acidic freshwater enabled juvenile fish to exhibit elevated growth rates in the SGD influenced tide pool.

Even in waters well saturated with oxygen, increased temperatures caused by climate change will act as stressors on low-latitude fishes, hampering growth via metabolic constraints (Rodgers et al., 2018). The submarine influx of cold freshwater, on the other hand, may act as a buffer against elevated water temperatures, thereby enhancing growth in ectothermic organisms. Further, teleost fishes almost always exhibit better growth rates in intermediary salinity conditions (Boeuf and Payan, 2001). This has been correlated with a lower standard metabolic rate and explained by a salinity dependent food conversion efficiency (Kinne, 1960; Imsland et al., 2001). Lowered pH also tends to increase the growth rates in marine fish (Di Franco et al., 2019; Jarrold and Munday, 2019). This could potentially be explained by either increased energy intake or reduced energy expenditure in acidified waters (Munday et al., 2009). First evidence of enhanced growth in temperate juvenile marbled sole *Pseudopleuronectes yokohamae* caused by the influx of nutrient rich fresh SGD was presented only recently by Fujita et al. (2019). The authors proposed a positive relationship between fish growth, SGD derived nutrient loadings, and elevated primary producer as well as primary consumer (i.e., prey) abundances but were unable to conclusively substantiate a connection between these trophic levels. We, on the other hand, propose that elevated somatic growth rates in juvenile fish subjected to fresh SGD are caused by a combination of the aforementioned physiological effects and not necessarily food availability.

Past studies have shown that small-scale field experiments are suitable to estimate fitness of reef fishes at large scales (Steele and Forrester, 2005). Still, it remains to be determined how much the local variations in water quality caused by fresh SGD affect the biomass of marine secondary consumers on larger geographical scales. Investigations combining otolith microchemistry (e.g., oxygen isotopy) and age reading are warranted to further assess whether even non-territorial fishes exposed to fresh SGD exhibit signs of increased survival potential (Thorrold et al., 1997; Kim and Lee, 2003). Due to elevated primary productivity, food is not necessarily a limited resource in coastal ecosystems influenced by fresh SGD (Jones, 1986; Lecher and Mackey, 2018). Thus, even small changes in ambient hydrography and hydrochemistry caused by the influx of fresh groundwater will lead to differences in growth, which - over time - will translate into significant differences in population sizes (Retzel et al., 2007), elevating the biomass available to a fishery.

A range of stressors increasingly threatens coastal marine ecosystems, yet these habitats provide livelihoods through fisheries to 260 million people (Teh and Sumaila, 2013). Anthropogenic modifications to the hydrography and hydrochemistry of coastal marine ecosystems through altered groundwater fluxes will have significant implications for a system's carrying capacity and fisheries productivity (Burnett et al., 2018). Given the ubiquitous nature of fresh SGD (Taniguchi et al., 2002) our work highlights the need for groundwater fluxes to be included in environmental management plans. It furthermore illuminates future challenges such as balancing anthropogenic freshwater use and coastal fisheries' productivity, particularly given the potential for climate change to aggravate freshwater scarcity.

DATA AVAILABILITY STATEMENT

Biological data that support the findings of this study have been deposited in PANGAEA and are accessible at https://doi.pangaea.de/10.1594/PANGAEA.897645.

ETHICS STATEMENT

Research was carried out in accordance to Mauritian laws and regulations and under direct supervision of scientist of the Mauritius Oceanography Institute (MOI). The animal study was reviewed and approved by the MOI Board. The employed sampling strategy ensured that the fish stock at those study sites was not depleted – therefore, as a conservation effort and to minimize the impact on the fish population, the monthly sample size was kept relatively small. No non-target or by-catch specimens were collected during the study.

AUTHOR CONTRIBUTIONS

JL and NM conceived the research and prepared the initial manuscript. JL and TP designed the sampling. JL, TP, DD, and YN conducted the field work. TP and YN measured the physico-chemical parameters. SN and SB processed the fish and prepared the otoliths for reading. SB conducted the stomach content analysis. JL performed the otolith readings and statistically analyzed the data. All authors contributed to later revisions.

FUNDING

This study was funded by the German Federal Ministry of Education and Research (BMBF; Grant #01LN1307A awarded to NM).

ACKNOWLEDGMENTS

We would like to thank Elisabeth Myers, Gladys M. Okemwa, and Andreas Kunzmann for help in species identification; Anishta Audit-Manna, Chetanand Samyan, and Shane Sunassee for their help in sample collection and analytical procedures; Rebecca Gorniak for her help in fish dissection and otolith

preparation; Sebastian Flotow for his valuable support in otolith preparation and in digital imagery; and Werner Ekau for help regarding statistical applications. We would like to express our gratitude to Ruby M. Pillay for administrative support in conducting this study.

SUPPLEMENTARY MATERIAL

The Supplementary Material for this article can be found online at: https://www.frontiersin.org/articles/10.3389/fmars.2019.00613/full#supplementary-material

REFERENCES

Allen, G. R., and Steene, R. C. (1987). *Reef Fishes of the Indian Ocean*. Neptune City, NJ: T.F.H. Publications.

Almany, G. R., and Webster, M. S. (2006). The predation gauntlet: early post-settlement mortality in reef fishes. *Coral Reefs* 25, 19–22. doi: 10.1007/s00338-005-0044-y

Amato, D., Bishop, J. M., Glenn, C. R., Dulai, H., and Smith, C. M. (2016). Impact of submarine groundwater discharge on marine water quality and reef biota of Maui. *PLoS One* 11:e016582. doi: 10.1371/journal.pone.0165825

Anderson, J. T. (1988). A review of size dependant survival during pre-recruit stages of fishes in relation to recruitment. *J. Northwest Atl. Fish. Sci.* 8, 55–66. doi: 10.2960/j.v8.a6

Auer, S. K., Salin, K., Rudolf, A. M., Anderson, G. J., and Metcalfe, N. B. (2015). The optimal combination of standard metabolic rate and aerobic scope for somatic growth depends on food availability. *Funct. Ecol.* 29, 479–486. doi: 10.1111/1365-2435.12396

Boeuf, G., and Payan, P. (2001). How should salinity influence fish growth? *Comp. Biochem. Physiol. - C Toxicol. Pharmacol.* 130, 411–423. doi: 10.1016/S1532-0456(01)00268-X

Booth, D. J. (1995). Juvenile groups in a coral-reef damselfish: density-dependent effects on individual fitness and population demography. *Ecology* 76, 91–106. doi: 10.2307/1940634

Burnett, K. M., Wada, C. A., Taniguchi, M., Sugimoto, R., and Tahara, D. (2018). Evaluating the tradeoffs between groundwater pumping for snow-melting and nearshore fishery productivity in Obama City, Japan. *Water* 10:1556. doi: 10.3390/w10111556

Burnett, W. C., Aggarwal, P. K., Aureli, A., Bokuniewicz, H., Cable, J. E., Charette, M. A., et al. (2006). Quantifying submarine groundwater discharge in the coastal zone via multiple methods. *Sci. Total Environ.* 367, 498–543. doi: 10.1016/j.scitotenv.2006.05.009

Burnett, W. C., Bokuniewicz, H., Huettel, M., Moore, W. S., and Taniguchi, M. (2003). Groundwater and pore water inputs to the coastal zone. *Biogeochemistry* 66, 3–33. doi: 10.1023/b:biog.0000006066.21240.53

Campana, S. E. (1990). How reliable are growth back-calculations based on otoliths? *Can. J. Fish. Aquat. Sci.* 47, 2219–2227. doi: 10.1139/f90-246

Ceccarelli, D. M. (2007). Modification of benthic communities by territorial damselfish: a multi-species comparison. *Coral Reefs* 26, 853–866. doi: 10.1007/s00338-007-0275-1

Ceccarelli, D. M., Jones, G. P., and McCook, L. J. (2005). Effects of territorial damselfish on an algal-dominated coastal coral reef. *Coral Reefs* 24, 606–620. doi: 10.1007/s00338-005-0035-z

Choat, J., and Roberson, D. (2002). "Age-Based Studies," *in Coral reef fishes: dynamics and diversity in a complex ecosystem*. ed P. F Sale (San Diego, CA: Academic Press), 57–80. doi: 10.1016/b978-012615185-5/50005-0

Clemmesen, C., and Doan, T. (1996). Does otolith structure reflect the nutritional condition of a fish larva? Comparison of otolith structure and biochemical index (RNA/DNA ratio) determined on cod larvae. *Mar. Ecol. Prog. Ser.* 138, 33–39. doi: 10.3354/meps138033

Dale, R. K., and Miller, D. C. (2008). Hydrologic interactions of infaunal polychaetes and intertidal groundwater discharge. *Mar. Ecol. Prog. Ser.* 363, 205–215. doi: 10.3354/meps07455

Di Franco, A., Calo, A., Sdiri, K., Cattano, C., Milazzo, M., and Guidetti, P. (2019). Ocean acidification affects somatic and otolith growth relationship in fish: evidence from an *in situ* study. *Biol. Lett* 15:20180662. doi: 10.1098/rsbl.2018.0662

Döring, J., Neumann, S. I., Sloterdijk, H., and Ekau, W. (2018). Seasonal growth differences of larval *Hyporhamphus picarti* (Hemiramphidae) in the Sine Saloum estuary, Senegal. *J. Appl. Ichthyol* 34, 97–102. doi: 10.1111/jai.13528

Encarnação, J., Leitão, F., Range, P., Piló, D., Chícharo, M. A., and Chícharo, L. (2014). Local and temporal variations in near-shore macrobenthic communities associated with submarine groundwater discharges. *Mar. Ecol* 36, 926–941. doi: 10.1111/maec.12186

Foley, L. (2018). Karst-channelled intertidal submarine groundwater discharge (SGD) conditions the form of the rock pool sessile assemblage. *Estuar. Coast. Shelf Sci.* 213, 236–244. doi: 10.1016/J.ECSS.2018.08.014

Fujita, K., Shoji, J., Sugimoto, R., Nakajima, T., Honda, H., Takeuchi, M., et al. (2019). Increase in fish production through bottom-up trophic linkage in coastal waters induced by nutrients supplied via submarine groundwater. *Front. Environ. Sci.* 7:82. doi: 10.3389/fenvs.2019.00082

Gopinadha Pillai, C. S., and Mohan, M. (1990). Ecology and biology of *Abudefduf glaucus* (Cuvier) (Pomacentridae, Pisces) from minicoy atoll, Lakshadweep. *Indian J. Fish.* 37, 15–23.

Halford, A. R., and Thompson, A. A. (1994). "Visual census surveys of reef fish," in *Long-term Monitoring of the Great Barrier Reef - Standard Operational Procedure Number 3*, (Townsville: Australian Institute of Marine Science).

Hata, M., Sugimoto, R., Hori, M., Tomiyama, T., and Shoji, J. (2016). Occurrence, distribution and prey items of juvenile marbled sole *Pseudopleuronectes yokohamae* around a submarine groundwater seepage on a tidal flat in southwestern Japan. *J. Sea Res.* 111, 47–53. doi: 10.1016/j.seares.2016.01.009

Hiatt, R. W., and Strasburg, D. W. (1960). Ecological relationships of the fish fauna on coral reefs of the Marshall Islands. *Ecol. Monogr.* 30, 65–127. doi: 10.2307/1942181

Hixon, M. A. (1991). "Predation as a process structuring coral reef fish communities," in *The Ecology of Fishes on Coral Reefs*, ed. P. F. Sale (San Diego: Academic Press), 475–508. doi: 10.1016/b978-0-08-092551-6.50022-2

Hoey, A. S., and Bellwood, D. (2010). Damselfish territories as a refuge for macroalgae on coral reefs. *Coral Reefs* 29, 107–118. doi: 10.1007/s00338-009-0567-8

Hoey, A. S., and McCormick, M. I. (2004). Selective predation for low body condition at the larval-juvenile transition of a coral reef fish. *Oecologia* 139, 23–29. doi: 10.1007/s00442-004-1489-3

Holbrook, S. J., and Schmitt, R. J. (2002). Competition for shelter space causes density-dependent predation mortality in damselfishes. *Ecology* 83, 2855–2868. doi: 10.1890/0012-9658(2002)083%5B2855:cfsscd%5D2.0.co;2

Honda, H., Sugimoto, R., and Kobayashi, S. (2018). "Submarine groundwater discharge and its influence on primary production in japanese coasts: case study in Obama Bay," in *The Water-Energy-Food Nexus: Human-Environmental Security in the Asia-Pacific Ring of Fire*, eds A. Endo, and T. Oh (Singapore: Springer), 101–115. doi: 10.1007/978-981-10-7383-0_8

Houde, E. D. (1989). Comparative growth, mortality, and energetics of marine fish larvae: temperature and implied latitudinal effects. *Fish. Bull.* 87, 471–495.

Houde, E. D. (2008). Emerging from Hjort's shadow. *J. Northwest Atl. Fish. Sci.* 41, 53–70. doi: 10.2960/J.v41.m634

Howell, D. C. (2007). *Statistical Methods for Psychology*, 7th ed. Belmont, CA: Cengage Wadsworth.

Hyslop, E. J. (1980). Stomach contents analysis - a review of methods and their application. *J. Fish Biol.* 17, 411–429. doi: 10.1111/j.1095-8649.1980.tb02775.x

Imsland, A. K., Foss, A., Gunnarsson, S., Berntssen, M. H., FitzGerald, R., Bonga, S. W., et al. (2001). The interaction of temperature and salinity on growth and food conversion in juvenile turbot (*Scophthalmus*

maximus). *Aquaculture* 198, 353–367. doi: 10.1016/s0044-8486(01)00507-5

Jarrold, M. D., and Munday, P. L. (2019). Diel CO_2 cycles and parental effects have similar benefits to growth of a coral reef fish under ocean acidification. *Biol. Lett.* 15:20180724. doi: 10.1098/rsbl.2018.0724

Johannes, R. E., and Hearn, C. (1985). The effect of submarine groundwater discharge on nutrient and salinity regimes in a coastal lagoon off Perth. *Western Australia. Estuar. Coast. Shelf Sci.* 21, 789–800. doi: 10.1016/0272-7714(85)90073-3

Jones, G. P. (1986). Food availability affects growth in a coral reef fish. *Oecologia* 70, 136–139. doi: 10.1007/BF00377123

Kim, G., and Lee, K.-K. (2003). Large submarine groundwater discharge (SGD) from a volcanic island. *Geophys. Res. Lett.* 30, 1–4. doi: 10.1029/2003gl018378

Kinne, O. (1960). Growth, food intake, and food conversion in a euryplastic fish exposed to different temperatures and salinities. *Physiol. Zool.* 33, 288–317. doi: 10.1086/664584

Lapointe, B. E., and O'Connell, J. (1989). Nutrient-enhanced growth of *Cladophora prolifera* in Harrington Sound, Bermuda: eutrophication of a confined, phosphorus-limited marine ecosystem. *Estuar. Coast. Shelf Sci.* 28, 347–360. doi: 10.1016/0272-7714(89)90084-X

Lecher, A. L., and Mackey, K. R. M. (2018). Synthesizing the effects of submarine groundwater discharge on marine biota. *Hydrobiologia* 5:60. doi: 10.3390/hydrology5040060

Leis, J. M. (1991). "The pelagic stage of reef fishes: the larval biology of coral fishes," in *The Ecology of Fishes on Coral Reefs*, ed. P. F. Sale (San Diego: Academic Press), 277–278.

Leis, J. M., and McCormick, M. I. (2002). "The biology, behavior, and ecology of the pelagic, larval stage of coral reef fishes," in *Coral Reef Fishes: Dynamic and Diversity in a Complex Ecosystem*, ed. P. F. Sale (San Diego, CA: Elsevier), 171–199. doi: 10.1016/b978-012615185-5/50011-6

Luo, X., Jiao, J. J., Liu, Y., Zhang, X., Liang, W., and Tang, D. (2018). Evaluation of water residence time, submarine groundwater discharge, and maximum new production supported by groundwater borne nutrients in a coastal upwelling shelf system. *J. Geophys. Res. Ocean.* 123, 631–655. doi: 10.1002/2017JC013398

Machado, D. A., and Imberger, J. (2014). Modeling the impact of natural and anthropogenic nutrient sources on phytoplankton dynamics in a shallow coastal domain. *Western Australia. Environ. Fluid Mech.* 14, 87–111. doi: 10.1007/s10652-013-9296-1

Montaggioni, L. F. (1982). Pleistocene marine depositional environments from Mauritius island, Indian Ocean. *Geobios* 15, 161–179. doi: 10.1016/s0016-6995(82)80018-1

Moore, W. S. (2010). The effect of submarine groundwater discharge on the ocean. *Ann. Rev. Mar. Sci.* 2, 59–88. doi: 10.1146/annurev-marine-120308

Moosdorf, N., Stieglitz, T., Waska, H., Dürr, H. H., and Hartmann, J. (2015). Submarine groundwater discharge from tropical islands: a review. *Grundwasser* 20, 53–67. doi: 10.1007/s00767-014-0275-3

Munday, P. L., Crawley, N. E., and Nilsson, G. E. (2009). Interacting effects of elevated temperature and ocean acidification on the aerobic performance of coral reef fishes. *Mar. Ecol. Prog. Ser.* 388, 235–242. doi: 10.3354/meps08137

Oehler, T., Eiche, E., Putra, D., Adyasari, D., Hennig, H., Mallast, U., et al. (2018). Timing of land-ocean groundwater nutrient fluxes from a tropical karstic region (southern Java, Indonesia). *J. Hydrol.* 565, 662–671. doi: 10.5194/hess-2017-621

Pauly, D. (1998). Tropical fishes: patterns and propensities. *J. Fish Biol.* 53, 1–17. doi: 10.1006/jfbi.1998.0810

Piló, D., Barbosa, A. B., Teodósio, M. A., Encarnação, J., Leitão, F., Range, P., et al. (2018). Are submarine groundwater discharges affecting the structure and physiological status of rocky intertidal communities? *Mar. Environ. Res.* 136, 158–173. doi: 10.1016/j.marenvres.2018.02.013

Pitcher, C. R. (1988). Validation of a technique for reconstructing daily patterns in the recruitment of coral reef damselfish. *Coral Reefs* 7, 105–111. doi: 10.1007/BF00300969

Ramessur, R. T. (2002). Anthropogenic-driven changes with focus on the coastal zone of Mauritius, south-western Indian Ocean. *J. Mater. Cycles Waste Manag.* 3, 99–106. doi: 10.1007/s10113-002-0045-0

Ramessur, R. T., Boodhoo, K., Balgobin, J., Povinec, P., and Burnett, W. C. (2012). Dissolved nutrients from submarine groundwater in Flic en Flac lagoon, Mauritius. *West. Indian Ocean J. Mar. Sci.* 10, 121–127.

Retzel, A., Hansen, A. D., and Grønkjær, P. (2007). Otolith growth of Springer's demoiselle, *Chrysiptera springeri* (Pomacentridae, Allen & Lubbock), on a protected and non-protected coral reef. *J. Appl. Ichthyol.* 23, 568–572. doi: 10.1111/j.1439-0426.2007.00865.x

Rodgers, G., Rummer, J., Johnson, L., and McCormick, M. (2018). Impacts of increased ocean temperatures on a low-latitude coral reef fish – Processes related to oxygen uptake and delivery. *J. Therm. Biol* 79, 95–102. doi: 10.1016/j.jtherbio.2018.12.008

Sale, P. F. (ed.) (2002). *Coral Reef Fishes - Dynamics and Diversity in a Complex Ecosystem*. Amsterdam: Academic Press.

Sato, N., Asahida, T., Terashima, H., Hurbungs, M. D., and Ida, H. (2008). Species composition and dynamics of larval and juvenile fishes in the surf zone of Mauritius. *Environ. Biol. Fish.* 81, 229–238. doi: 10.1007/s10641-007-9194-9

Schmitt, R. J., and Holbrook, S. J. (1999). Mortality of juvenile damselfish: implications for assessing processes that determine abundance. *Ecology* 80, 35–50. doi: 10.1890/0012-9658(1999)080[0035:MOJDIF]2.0.CO;2

Shoji, J., and Tominaga, O. (2018). "Relationships between submarine groundwater discharge and coastal fisheries as a water-food nexus," in *The Water-Energy-Food Nexus*, eds A. Endo, and T. Oh (Singapore: Springer Nature), 117–131. doi: 10.1007/978-981-10-7383-0_9

Simpson, S. D., Radford, A. N., Nedelec, S. L., Ferrari, M. C. O., Chivers, D. P., McCormick, M. I., et al. (2016). Anthropogenic noise increases fish mortality by predation. *Nat. Commun.* 7, 1–7. doi: 10.1038/ncomms10544

Slomp, C. P., and Van Cappellen, P. (2004). Nutrient inputs to the coastal ocean through submarine groundwater discharge: controls and potential impact. *J. Hydrol.* 295, 64–86. doi: 10.1016/j.jhydrol.2004.02.018

Steele, M. A., and Forrester, G. E. (2005). Small-scale field experiments accurately scale up to predict density dependence in reef fish populations at large scales. *PNAS* 102, 13513–13516. doi: 10.1073/pnas.0504306102

Stevenson, D. K., and Campana, S. E. (1992). "Analysis of otolith microstructure data," in *Otolith Microstructure Examination and Analysis*, eds D. Stevenson, and S. Campana (Ottawa: Canada Communication Group - Publishing), 126.

Suthers, I. M. (1998). Bigger? Fatter? Or is faster growth better? Considerations on condition in larval and juvenile coral-reef fish. *Aust. J. Ecol.* 23, 265–273. doi: 10.1111/j.1442-9993.1998.tb00730.x

Taniguchi, M., Burnett, W. C., Cable, J. E., and Turner, J. V. (2002). Investigation of submarine groundwater discharge. *Hydrol. Process.* 16, 2115–2129. doi: 10.1002/hyp.1145

Teh, L. C. L., and Sumaila, U. R. (2013). Contribution of marine fisheries to worldwide employment. *Fish Fish.* 14, 77–88. doi: 10.1111/j.1467-2979.2011.00450.x

Thorrold, S. R., Campana, S. E., Jones, C. M., and Swart, P. K. (1997). Factors determining δ^{13} C and δ^{18} O fractionation in aragonitic otoliths of marine fish. *Geochim. Cosmochim. Acta* 61, 2909–2919. doi: 10.1016/S0016-7037(97)00141-5

Thorrold, S. R., and Milicich, M. J. (1990). Comparison of larval duration and pre- and post-settlement growth in two species of damselfish, *Chromis atripectoralis* and *Pomacentrus coelestis* (Pisces: Pomacentridae), from the Great Barrier Reef. *Mar. Biol.* 105, 375–384. doi: 10.1007/BF01316308

Thresher, R. E., Colin, P. L., and Bell, L. J. (1989). Planktonic duration, distribution and population structure of Western and Central Pacific damselfishes (*Pomacentridae*). *Copeia* 2, 420–434.

Utsunomiya, T., Hata, M., Sugimoto, R., Honda, H., Kobayashi, S., Miyata, Y., et al. (2017). Higher species richness and abundance of fish and benthic invertebrates around submarine groundwater discharge in Obama Bay, Japan. *J. Hydrol. Reg. Stud.* 11, 139–146. doi: 10.1016/j.ejrh.2015.11.012

Vigliola, L., Harmelin-Vivien, M., and Meekan, M. G. (2000). Comparison of techniques of back-calculation of growth and settlement marks from the otoliths of three species of *Diplodus* from the Mediterranean Sea. *Can. J. Fish. Aquat. Sci.* 1299, 1291–1299. doi: 10.1139/f00-055

Vigliola, L., and Meekan, M. G. (2002). Size at hatching and planktonic growth determine post-settlement survivorship of a coral reef fish. *Oecologia* 131, 89–93. doi: 10.1007/s00442-001-0866-4

Villegas-Hernández, H., González-Salas, C., Aguilar-Perera, A., and López-Gómez, M. J. (2007). Settlement dynamics of the coral reef fish *Stegastes partitus*, inferred from otolith shape and microstructure analysis. *Aquat. Biol.* 1, 249–258. doi: 10.3354/ab00026

Waska, H., and Kim, G. (2011). Submarine groundwater discharge (SGD) as a main nutrient source for benthic and water-column primary production in a large intertidal environment of the Yellow Sea. *J. Sea Res.* 65, 103–113. doi: 10.1016/j.seares.2010.08.001

Wellington, G. M., and Victor, B. C. (1985). El Niño mass coral mortality: a test of resource limitation in a coral reef damselfish population. *Oecologia* 68, 15–19. doi: 10.1007/BF00379466

Wellington, G. M., and Victor, B. C. (1989). Planktonic larval duration of one hundred species of Pacific and Atlantic damselfishes (Pomacentridae). *Mar. Biol.* 101, 557–567. doi: 10.1007/BF00541659

Wellington, G. M., and Victor, B. C. (1992). Regional differences in duration of the planktonic larval stage of reef fishes in the eastern Pacific Ocean. *Mar. Biol.* 113, 491–498. doi: 10.1007/bf00349176

Welti, N., Gale, D., Hayes, M., Kumar, A., Gasparon, M., Gibbes, B., et al. (2015). Intertidal diatom communities reflect patchiness in groundwater discharge. *Estuar. Coast. Shelf Sci.* 163, 116–124. doi: 10.1016/j.ecss.2015.06.006

Wilson, D. T., and McCormick, M. I. (1997). Spatial and temporal validation of settlement marks in the otoliths of tropical reef fishes. *Mar. Ecol. Prog. Ser.* 153, 259–271. doi: 10.3354/meps153259

Wilson, D. T., and Meekan, M. G. (2002). Growth-related advantages for survival to the point of replenishment in the coral reef fish *Stegastes partitus* (Pomacentridae). *Mar. Ecol. Prog. Ser.* 231, 247–260. doi: 10.3354/meps231247 doi: 10.3354/meps231247

Conflict of Interest: The authors declare that the research was conducted in the absence of any commercial or financial relationships that could be construed as a potential conflict of interest.

Copyright © 2019 Lilkendey, Pisternick, Neumann, Dumur Neelayya, Bröhl, Neehaul and Moosdorf. This is an open-access article distributed under the terms of the Creative Commons Attribution License (CC BY). The use, distribution or reproduction in other forums is permitted, provided the original author(s) and the copyright owner(s) are credited and that the original publication in this journal is cited, in accordance with accepted academic practice. No use, distribution or reproduction is permitted which does not comply with these terms.

frontiers in Marine Science

ORIGINAL RESEARCH
published: 26 November 2019
doi: 10.3389/fmars.2019.00728

Peeling the Otolith of Fish: Optimal Parameterization for Micro-CT Scanning

*Jonas E. Vasconcelos-Filho[1,2], Felix S. L. Thomsen[3], Borko Stosic[1,4], Antonio C. D. Antonino[5], Daniel A. Duarte[5], Richard J. Heck[6], Rosangela P. T. Lessa[7], Francisco M. Santana[8], Beatrice P. Ferreira[2] and Paulo J. Duarte-Neto[1,4]**

[1] Graduate Program in Biometry and Applied Statistics, Federal Rural University of Pernambuco, Recife, Brazil, [2] Department of Oceanography, Federal University of Pernambuco, Recife, Brazil, [3] Department of Electrical and Computer Engineering, National University of the South, Buenos Aires, Argentina, [4] Department of Statistics and Informatics, Federal Rural University of Pernambuco, Recife, Brazil, [5] Department of Nuclear Energy, Federal University of Pernambuco, Recife, Brazil, [6] School of Environmental Sciences, University of Guelph, Guelph, ON, Canada, [7] Department of Fisheries and Aquaculture, Federal Rural University of Pernambuco, Recife, Brazil, [8] Academic Unit of Serra Talhada, Federal Rural University of Pernambuco, Recife, Brazil

OPEN ACCESS

Edited by:
Alejandra Vanina Volpedo, University of Buenos Aires, Argentina

Reviewed by:
Tanja Schulz-Mirbach, Ludwig Maximilian University of Munich, Germany
Ralf Anken, Institute of Aerospace Medicine, German Aerospace Center (DLR), Germany

***Correspondence:**
Paulo J. Duarte-Neto
pjduarteneto@gmail.com

Specialty section:
This article was submitted to Marine Ecosystem Ecology, a section of the journal Frontiers in Marine Science

Received: 16 August 2019
Accepted: 08 November 2019
Published: 26 November 2019

Citation:
Vasconcelos-Filho JE, Thomsen FSL, Stosic B, Antonino ACD, Duarte DA, Heck RJ, Lessa RPT, Santana FM, Ferreira BP and Duarte-Neto PJ (2019) Peeling the Otolith of Fish: Optimal Parameterization for Micro-CT Scanning. Front. Mar. Sci. 6:728. doi: 10.3389/fmars.2019.00728

In this paper, we aim to provide optimal parameters for micro-computed tomography scans of fish otoliths. We tested fifteen different combinations to *sagittae*. The images were scaled to Hounsfield units, and segmented in two distinct volumes-of-interest (external and internal). The strategy we applied, for identifying optimum scan settings for otoliths, included analyses of the sinogram, the distribution of the Hounsfield units and the signal-to-noise ratio. Based on these tests, the optimum sets of parameters for the acquisition of tomographic images of sagittal otoilths were 80 kV, 220 μA, and 0.5 mm aluminum filter. The method allowed 3D shape analysis, internal and external density distribution, layer-by-layer density segmentation, and a potential objective method to count growth rings in otoliths. It was possible to compare mean densities between species, and we observed a significant difference among them. In addition, there are ontogenic changes, which could be increasing or decreasing the density. In this study, we applied tomography for several otolith analysis, that could be of great interest for future studies in diverse areas that use otoliths as the basic structure of analysis, or represents a new research line called eco-densitometry of otoliths, where tomography could be applied to explore the density within an ecological perspective.

Keywords: eco-densitometry, fishery biology, Hounsfield units, Meshlab, radiodensity, 3D otoliths

1. INTRODUCTION

Over recent years, x-ray computed tomography (CT) has evolved from an exclusive tool of medicine into a widely accepted technique for analyzing the internal structure of objects in a non-destructive way (Schoepf and Costello, 2004; Budoff and Shinbane, 2016; Jalaguier-Coudray et al., 2016). The ability to quantify the distribution of the internal radiodensity of samples has found applications in many fields, including material engineering (Velichko et al., 2007), biology (including *in vivo* research) (Postnov et al., 2002, 2003; Fürst et al., 2008; Lowe et al., 2013), soil science (Taina et al., 2008), and archeology (Noever et al., 2015).

A micro-computed tomography (micro-CT) scan involves digitally reconstructing a set of projections formed by the transmitted x-ray beam through the sample (Kak and Slaney, 2001). These projections are two-dimensional images with micrometric pixel resolution, and the gray-scale of the pixels reflects the mean of the attenuation coefficient of the material, caused by the scattering and/or absorption of photons due to interactions with the object (Grodstein, 1957). Therefore, materials with greater density generally present greater attenuation and the representative pixel is closer to white, by convention.

The instrumental parameters, notably x-ray tube voltage (kV), current (μA) and beam filtering are fundamental for proper image acquisition. In conventional tomography, during the photons production, the X-ray beam contains different energy values. This spectrum of values is called poly-energetic beam and this energy variation leads to an error in the attenuation coefficients. Then, filters are used to reduce this error, blocking the emission of photons of less energy. Low voltages generate low energy photons, which may not penetrate the object, while high voltages result in images with low contrast. Electric current controls the number of photons produced, while an increased number of photons produces an enormous amount of information catches by a detector. Thus, finding an optimal combination of these parameters is a process required for each type of structure (Kak and Slaney, 2001; Hsieh, 2009).

Computed tomography is one of the emerging techniques with perhaps the greatest potential for the study of fish otoliths (Starrs et al., 2014), which are calcified structures found in the inner ear of bony fish, responsible for hearing and balance (Popper and Fay, 1993). These structures are used in studies regarding age, migration, population structure, phylogeny, feeding ecology, and life histories, constituting an important tool in diverse fields of ichthyology and fishery science (Panfili et al., 2002; Duarte-Neto et al., 2008; Green et al., 2009). The pioneering approach presented three-dimensional (3D) images of the otoliths from the Atlantic Cod (*Gadus morhua*), by Hamrin et al. (1999), demonstrating the promising use of such images in the identification of stocks based on otolith shape. Subsequently, the Fish Ageing by Otolith Shape Analysis (FAbOSA) group have tried to improve the procedure using prolonged exposure, ionic solution and different organic solvents (Arneri et al., 2002), however, they have not found any internal structures.

Several possibilities arised from the potential use of micro-CT analysis for otoliths. Yan et al. (2009) tried to relate otolith CT values to different water pollution degrees. Browning et al. (2012) also used CT to analyze morphology changes as consequence of a stressful condition in Red Drum (*Sciaenops ocellatus*) and Bignami et al. (2013) to see how ocean acidification influence on Cobia (*Rachycentron canadum*) otoliths. More recently, Mapp et al. (2016) used a non-conventional tomography, the synchrotron radiation, to render an otolith of Plaice (*Pleuronectes platessa*) and shown growth rings.

Although the use of CT on otoliths dated back from the late 1990s, general advances in this field are more recent. Those were due to advances in instrumentation, which resulted in a significant improvement in spatial resolution and the capability of generating images with voxel sizes of three μm. This allows observing tiny details, such as annual growth structures with a thickness of about 20 μm (Jenkins, 1990; Waldron and Kerstan, 2001; Santana et al., 2006; Lessa et al., 2008).

Though many of these studies (except for FAbOSA) have succeeded in their objectives, they do not present the methodological aspects behind this new experimental procedure, which may be considered a relatively costly time and expensive technique, mainly the one used by Mapp et al. (2016). In the present work, we describe a protocol developed for the optimal acquisition of conventional micro-CT images of sagittal otoliths, considering different species and a spectrum of CT parameters. We then explored several applicabilities of this new procedure and discuss their advantages.

TABLE 1 | Lengths and observed ages of the individuals used in the present study.

Images	Species	Length (cm)	Age (years)	HU	Voxel (μm)
AS02	*A. solandri*	159 TL	5.53*	6770.03 ± 910.66	8
AS11	*A. solandri*	139.7 TL	2.89*	6667.82 ± 950.87	7
AS12	*A. solandri*	142.3 TL	3.13*	6854.89 ± 937.57	7
AS1294	*A. solandri*	155 TL	4.73*	6735.74 ± 972.63	8
AS17	*A. solandri*	131 TL	2.23*	6810.47 ± 1030.96	7
AS28	*A. solandri*	151 TL	4.11*	6743.12 ± 930.96	7
AS35	*A. solandri*	118 TL	1.47*	6752.87 ± 1053.92	6
AC36	*A. coeruleus*	10.9 TL	1	8584.08 ± 954.49	3
AC37	*A. coeruleus*	24 TL	5	7817.11 ± 982.37	3
AC38	*A. coeruleus*	22 TL	4	7830.75 ± 984.98	3
AC39	*A. coeruleus*	24.9 TL	4	7850.02 ± 1006.73	3
AC40	*A. coeruleus*	26.2 TL	4	7747.89 ± 1003.95	3
AC41	*A. coeruleus*	25.8 TL	6	7615.58 ± 965.14	3
AC42	*A. coeruleus*	32 TL	15	7441.57 ± 1026.62	5
AC43	*A. coeruleus*	30.1 TL	8	7593.43 ± 959.9	5
HP09	*H. plumierii*	32.5 TL	20	8287.79 ± 1016.93	8
HP118	*H. plumierii*	26.6 TL	14	8149.19 ± 1008.72	6
HP150	*H. plumierii*	18.3 TL	8	7914.35 ± 875.31	3
OO132	*O. oglinum*	18.9 SL	0.73*	8609.35 ± 923.45	3
OO134	*O. oglinum*	14.8 SL	0.52*	8534.63 ± 971.38	3
OO279	*O. oglinum*	18 SL	0.68*	8551.46 ± 933.31	3
TA22	*T. albacares*	119 FL	3*	8555.16 ± 1455.08	11
TA119	*T. albacares*	120 FL	3*	8460.58 ± 1272.79	13
TO55	*T. obesus*	105.8 FL	3.22*	6686.81 ± 951.39	10
TO70	*T. obesus*	142.7 FL	5.59*	6659.76 ± 863.66	10
TO77	*T. obesus*	127.3 FL	4.49*	6536.35 ± 882.73	10
TO78	*T. obesus*	157.3 FL	6.85*	6438.39 ± 879.18	11
TO79	*T. obesus*	128.7 FL	4.58*	6517.55 ± 933.39	10
TO83	*T. obesus*	138.7 FL	5.29*	6497.41 ± 879.96	10
TO89	*T. obesus*	105.6 FL	3.21*	6780.36 ± 958.21	9

**Estimated ages from the already published growth curves (Stéquert et al., 1996; Lessa et al., 2008; McBride et al., 2008; Duarte-Neto et al., 2012). TL, Total length; FL, Fork length; SL, Standard length; HU, Hounsfield units (mean ± standard deviation).*

2. MATERIALS AND METHODS

2.1. Imaging

Thirty left *sagittae* from six species were investigated: seven from *Acanthocybium solandri* (Cuvier, 1829); eight from *Acanthurus coeruleus* (Bloch and Schneider, 1801); three from *Haemulon plumierii* (Lacepéde, 1801); three from *Opisthonema oglinum* (Lesueur, 1818); two from *Thunnus albacares* (Bonnaterre, 1788); and seven from *T. obesus* (Lowe, 1839) (**Table 1**). We choose these species to include a wide range of patterns of habitats, biological parameters, taxonomic groups and age-class.

The otoliths were embedded in a styrofoam cube (**Figures 1A,B**) and scanned vertically in a Nikon Metrology model XT H 225 ST scanner (**Figure 1C**), maintained by the X-ray Computed Tomography Laboratory of the Department of Nuclear Energy, Federal University of Pernambuco, Brazil. The larger axis was placed perpendicular to the support base (**Figure 1A**) to minimize the Feret diameter and consequently to maximize the resolution of the resulting volume, yielding an isotropic image resolution. This procedure is important to increase the richness of detail and information and, consequently, each image has a voxel size that optimizes the acquisition, respecting the size of the otolith.

We varied the voltage from 60 to 100 kV in steps of 10 kV, with maximum electrical current based on the voltage vs. current relationship that always reaches 50,000 detected photons in 500 ms (**Figure 1D**). We executed this process with three aluminum filters of 0.5, 1.0, and 1.5 mm thickness, generating fifteen different scans.

2.2. Calibration, Segmentation, and Analysis

An otolith scanned with different parameter settings, will result in imagery with different apparent attenuation coefficient values. We converted these coefficients to an arbitrary scale called the Hounsfield scale, where its measure is the Hounsfield unit (HU), where the air is zero HU, and distilled water is 1000 HU, according to the linear equation:

$$HU = \frac{\mu_x - \mu_{water}}{\mu_{water}} * 1000 \quad (1)$$

where μ_x and μ_{water} are the linear attenuation coefficients of the material and water, respectively. This transformation is necessary to represent the radiodensity in a dimensionless scale for purposes of comparisons with other studies (Buzug, 2008).

Four specific analyses were performed to diagnose the parameters. First, histograms of the sinograms were computed. The sinogram is a graph that compiles of all projections, taken at different angles in a single image. Thus, the distribution of the detected photons allows to analyze the saturation of the CT detector; only values in the interval of 0.2 and 0.8 were considered as appropriate. Second, the reconstructed volumes have been segmented into two volumes-of-interest. We labeled the voxels as the inner region and exterior shell. We then smoothed and removed disconnected regions from the initial volumes-of-interest using 3D morphological operations and registered the smoothed volumes-of-interest to all remaining scans of the same otolith. At the end of this process, the histograms of the interior and exterior volumes of interest have been computed to analyze the possible overlap between them. Third, we computed statistical measures: the contrast of the signal as the standard deviation of the inner region σ_{in} and the magnitude of the noise as the standard deviation on a homogenous void region outside the otolith σ_{out}, composed by air or the styrofoam fixture. The signal-to-noise ratio (SNR) compares the object signal to the background noise within an image and reads SNR = σ_{in} / σ_{out}. A final *post-hoc* analysis was performed after finding the optimum parameter set and was conducted to determine the feasibility of detecting the expected yearly growth rings.

For the 3D visualization, an R script was first written to extract the contour pixel of the otolith from each 2D projection. Based on these x, y and z coordinates of each pixel, the color scaled reconstruction and iterative 3D visualization of otolith images was carried out using MeshLab software (Cignoni et al., 2008). Descriptive statistics of the image density were estimated and five lines were drawn starting from the nucleus toward the edge, following the reading axes indicated in previous age and growth studies of each species using R language (R Core Team, 2018). Each row was smoothed using a five-point moving average. After the smoothing, the means of these lines were plotted to verify the alternation of densities relative to the formation of the growth rings.

We evaluated the possible correlation between the mean radiodensity of each otolith and the respective fish length, using simple linear correlation analysis, in order to detect ontogenetic trends for each species. The mean values of HU among species were also compared using the Kruskal-Wallis test followed by Dunn's *post-hoc*. All statistical analyses were performed in R, with a significance level of 0.05.

3. RESULTS AND DISCUSSION

3.1. Protocol for the Optimal Acquisition

All sets of parameters resulted in high-quality external imagery with varying tonalities. It was possible to discern external structures such as the *sulcus acusticus*, *ostium*, *rostrum*, *cauda* and *excisura*, as well as the fluctuations of the margins and the depth of the *sulcus acusticus* (**Figures 2**, **3**). Finally, 3D imagery enables analysis of the whole otolith surface, curvature between faces and the deepness of *sulcus acusticus*.

In **Figure 4A**, the black curves represent the exterior volume and the gray curves represent the interior volume. These curves overlapped in the scans with voltages of 60 kV, 100 kV and filter of 1.5 mm aluminum. Therefore, these parameters were not considered suitable from this point of view. However, analysis of the signal-to-noise ratio showed that the combination of 60 kV and 0.5 mm aluminum filter yields a better relationship between real signal and noise, in contrast with higher voltages or thicker filters (**Table 2**). Thus, we did not discard the possible use of 60 kV, however, 70 and 80 kV with 0.5 mm filter were considered the most appropriate parameters since they presented good results in all analysis. Both satisfy the Rose criterion (Rose, 1948), that classifies images with SNR > 5 as adequate. The sinogram analysis confirms the quality of the choice of parameters (**Figure 4B**), i.e., the detector did not saturate for any

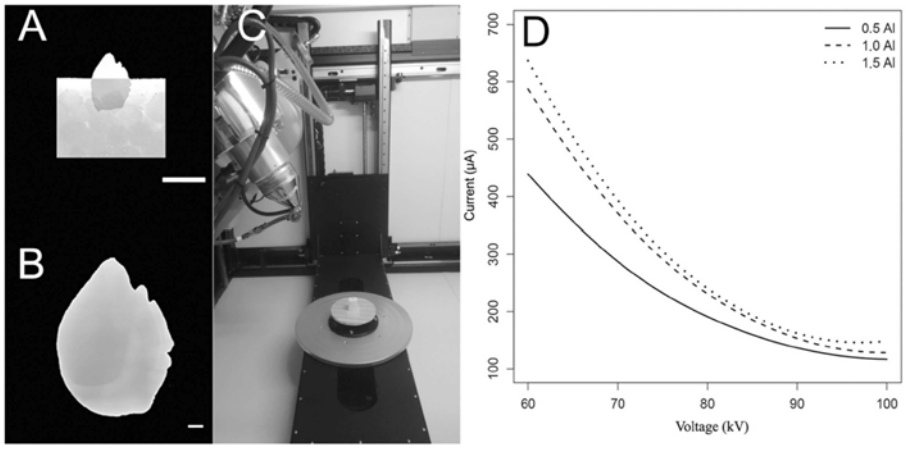

FIGURE 1 | Procedure of tomographic images acquisition of *sagittae*. **(A)** *Sagittal* otolith of *Haemulon plumierii* vertically positioned in a styrofoam cube. Scalebar = 10 mm. **(B)** Tomographic image of respective otolith in grayscale after acquisition. Scale bar = 1 mm. **(C)** Otolith on base support previous scanning. **(D)** Relationship of voltage and current supported by machine for three filters used (0.5, 1.0, 1.5 mm).

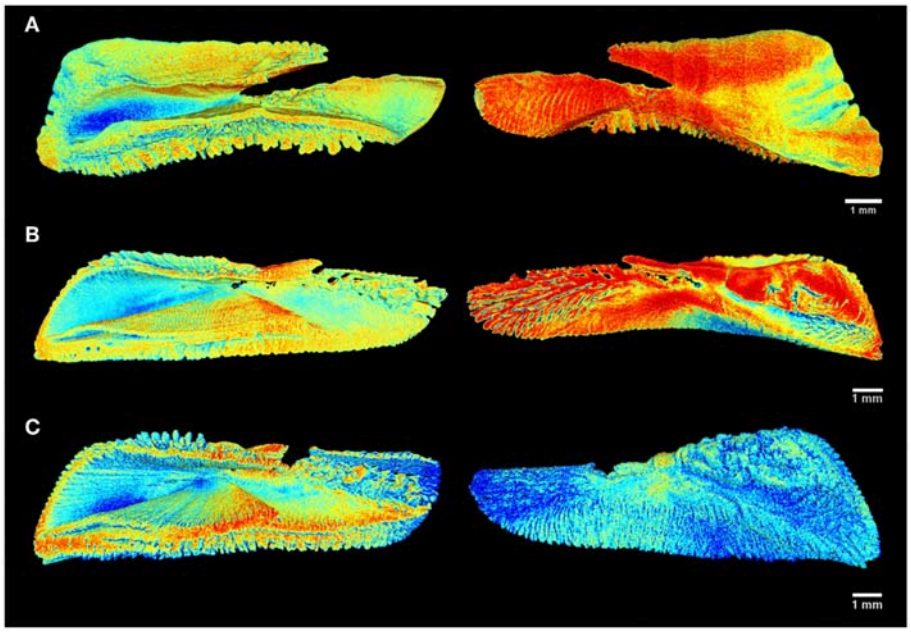

FIGURE 2 | Tomographic imagery of the external and inner face of the sagittal otoliths of **(A)** *Acanthocybium solandri*, **(B)** *Thunnus albacares*, and **(C)** *Thunnus obesus* using Meshlab, where in red are denser regions and in blue the surfaces of lower density values.

of the configurations. More precisely, lower voltage yields lower density contrast.

Combining these factors, the best images were achieved with medium voltages (70 and 80 kV) and a 0.5 mm aluminum filter. The worst images were achieved when using a 1.5 mm aluminum filter, as it was either not possible to capture information on density or artifacts were formed. The term artifact here refers to any systematic discrepancy between CT numbers in a reconstructed image, and the true attenuation coefficients of the object (Barrett and Keat, 2004).

FAbOSA group, in 2000, also used 80 kV and aluminum filter, but they obtained lower resolution and noisier images, possibly due to an outdated machine and lack of necessary computational power. Consequently, it was not possible to observe the growth rings. More recently, Yan et al. (2009) used a high voltage (130 kV) and low current (30 μA), where higher photon energies penetrated the otolith and no information on density was captured. Mapp et al. (2016) using monochromatic X-ray with 53 kV and no filter, rendered 3D imagery highlighting the growth rings. Although those

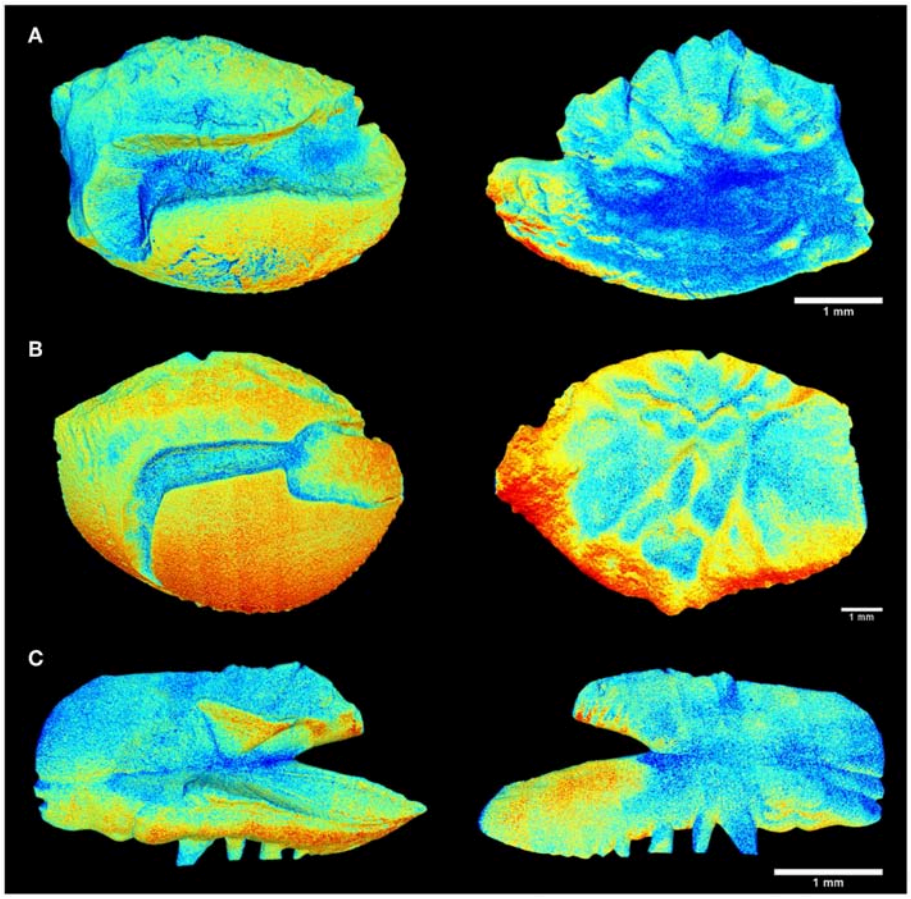

FIGURE 3 | Tomographic imagery of the external and inner face of the sagittal otoliths of **(A)** *Acanthurus coeruleus*, **(B)** *Haemulon plumierii*, and **(C)** *Opisthonema oglinum* using Meshlab, where in red are denser regions and in blue the surfaces of lower density values.

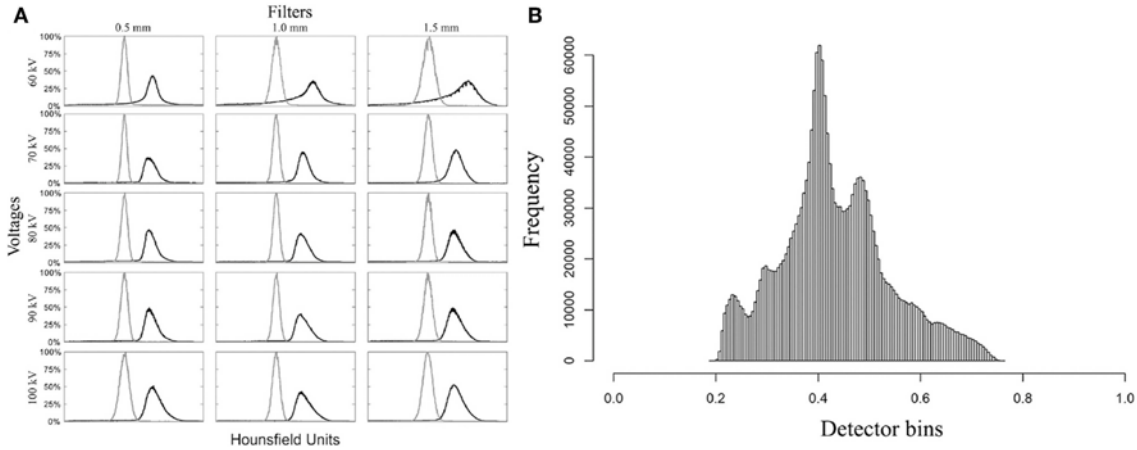

FIGURE 4 | Diagnostic graphs of optimum set micro-CT parameters evaluation. **(A)** Mosaic of histograms used to segment inner part (gray curve) from external part (black curve). **(B)** Example of detector response for the parameter set 80 kV with 0.5 mm aluminum filter for *Haemulon plumierii*.

authors considered that the objective proposed was reached, they reported some artifacts and did not experiment with other tomography settings. To reduce artifacts and improve SNR, therefore, our results suggested inner structures as a function of density are better visualized using the following parameters: 80 kV, 220 μA and 0.5 mm aluminum filter. From this, all the

following procedures were conducted on samples imaged using only this configuration. It is important to emphasize that these set parameters are optimal for this micro-CT device model. The current would be unique to our configuration and the voltage and filtering are critical, and would be relevant to any instrument. Also, after calibration to Hounsfield unit scale, it is perfectly possible to compare values between machines, samples material or parameters.

TABLE 2 | Signal-to-noise ratio (mean ± standard deviation) of sagittal otoliths.

	Filters (mm)		
Voltages (kV)	**0.5**	**1**	**1.5**
60	9.50 ± 3.80	7.59 ± 2.65	6.44 ± 2.35
70	8.11 ± 3.39	7.13 ± 2.70	5.80 ± 2.04
80	7.46 ± 4.55	6.25 ± 2.47	5.17 ± 1.84
90	6.54 ± 3.80	5.47 ± 2.08	4.33 ± 1.78
100	5.43 ± 3.60	4.70 ± 1.78	4.01 ± 1.71

3.2. Exploring Otolith Density Variation

Micro-CT imagery can provide shape, density distribution and structures of the otolith. The present investigation is the first study to present tomography images of entire otoliths with a discernible of internal and external density distributions using a conventional micro-CT. Using the correct set of parameters and appropriate voxel size (resolution), one can correctly represent the mean attenuation coefficient of the otolith material and obtain rich details regarding density.

The linear attenuation coefficients were converted in Hounsfield units (HU), with the minimum value of 2,941.94 for *T. obesus* and the maximum of 11,839 for *T. albacares*, but the highest mean radiodensity was 8,609.35 HU for *O. oglinum* (**Table 1**). Yan et al. (2009) found an HU between 2,500 and 4,600 for *asteriscus* and *lapillus* of the carp otolith, respectively. Mapp et al. (2016) and FAbOSA group (2002) did not present HU values. Nevertheless, other calcified structures are out of this range, e.g., scallop shells (744 HU) (Diez et al., 2013) and ureteral stone (1,350 HU) (Hameed et al., 2013).

The density is one of the relevant properties to the functional role of otoliths, and it is defined by the modifications of

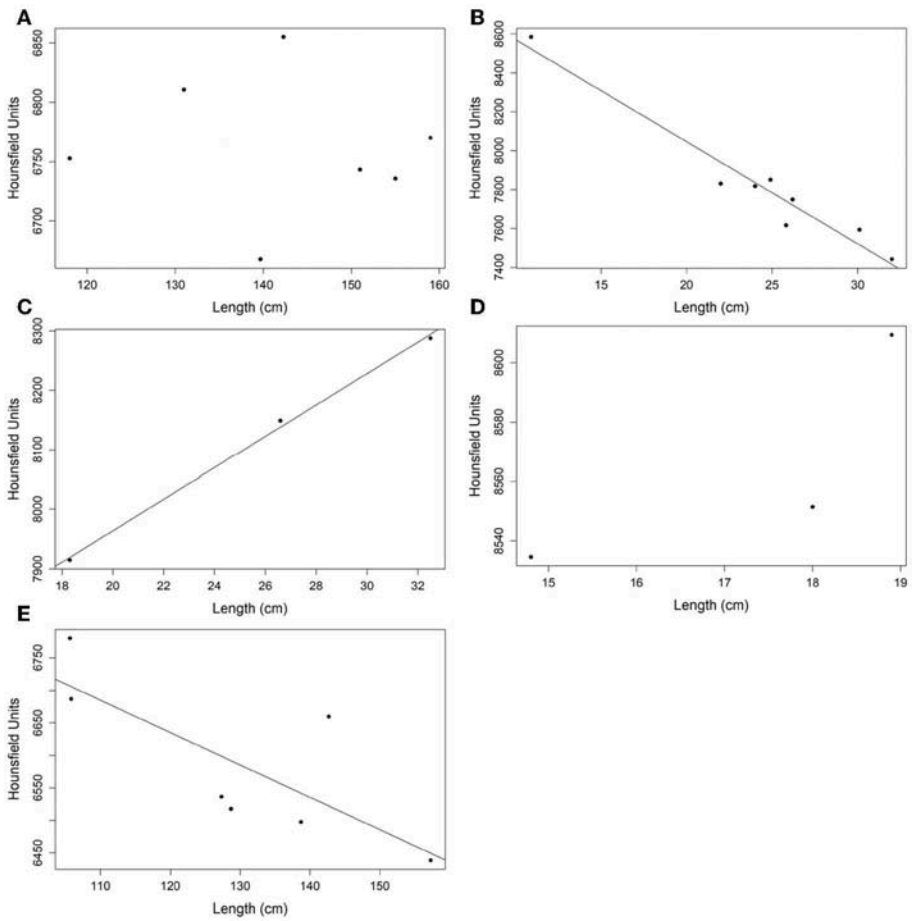

FIGURE 5 | Correlation analysis between the mean radiodensity of otoliths and fish length. **(A)** *Acanthocybium solandri*; **(B)** *Acanthurus coeruleus*; **(C)** *Haemulon plumierii*; **(D)** *Opisthonema oglinum*; and **(E)** *Thunnus obesus*.

TABLE 3 | Paired comparison of radiodensities of otoliths by species using Kruskal-Wallis (Kruskal-Wallis = 25,403, df = 5, *p*-value < 0.05) followed by *post-hoc* Dunn test.

Comparison	*Z*	*p*-valor
AC - AS	2.03	0.04
AC - HP	−0.61	0.54
AS - HP	−2.12	0.03
AC - OO	−1.39	0.16
AS - OO	−2.88	0.00
HP - OO	−0.65	0.52
AC - TA	−1.02	0.31
AS - TA	−2.32	0.02
HP - TA	−0.44	0.66
OO - TA	0.15	0.88
AC - TO	3.19	0.00
AS - TO	1.12	0.26
HP - TO	2.99	0.00
OO - TO	3.75	0.00
TA - TO	3.07	0.00

AS, A. solandri; AC, A. coeruleus; HP, H. plumierii; OO, O. oglinum; TA, T. albacares; TO, T. obesus. Z, Dunn's test statistic and its respective p-value.

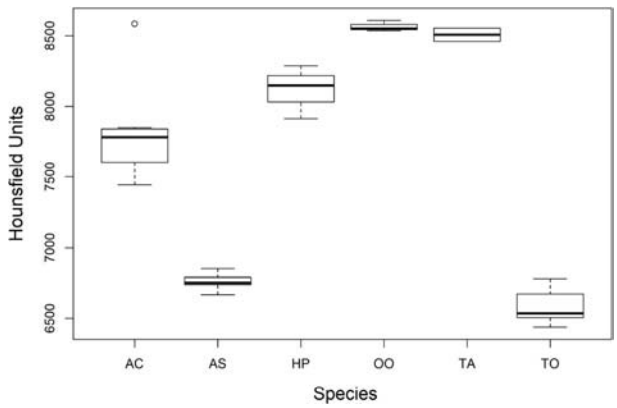

FIGURE 6 | Comparison of the average radiodensities of the otoliths of the studied species. AS, *A. solandri*; AC, *A. coeruleus*; HP, *H. plumierii*; OO, *O. oglinum*; TA, *T. albacares*; TO, *T. obesus*. The elements of the box plot correspond to median, interquartile range (IQR) and upper and lower extremes (± 1.5*IQR*).

the crystalline forms of calcium carbonate ($CaCO_3$) (Schulz-Mirbach et al., 2019). Saccular otoliths are composed by aragonite (Carlström, 1963; Schulz-Mirbach et al., 2019), with a density equal to 2.93 g/cm^3. There are other forms with different densities and as well could be found in otolith: calcite, with rhombohedral crystals, which characterizes its density (2.71 g/cm^3) and higher stability (Lippmann, 1973); and vaterite (2.56 g/cm^3), which presents a hexagonal crystal, less stable and, consequently, more scarce in nature (Northwood and Lewis, 1968). Thus, the chemical proportion between those polymorphs could lead to distinct Hounsfield units, and, then, different values for *asteriscus* and *lapillus*. However, the values presented by Yan et al. (2009) seems to be reasonable and consistent for these structures.

The distribution of otolith radiodensity can be visualized using the linear conversion of the attenuation coefficient on RGB scale, in which blue corresponds to lowest density regions and red corresponds to regions of higher density (**Figures 2**, **3**). Externally, the deeper region of the *sulcus acusticus* exhibits the lowest densities, increasing toward the surface in all species. Gauldie and Nelson (1990) also describe this pattern for other species, suggesting that contact with hair cells and the macula causes a reduction in the calcium deposition rate in this region.

A strong correlation between radiodensity and fish length was observed (**Figure 5**). However, there is not a unique pattern: a linear and positive correlation for *H. plumierii* and *O. oglinum*, a linear and negative correlation for *A. coeruleus* and *T. obesus*, and non-linear correlation for *O. oglinum*, which is considered a fast-growing and short-lived species (Lessa et al., 2008). No correlation was observed for *A. solandri*. This could be related to the fact that all individuals in this sample have reached the stationary growth phase, or two linear patterns could exist related to different sexes. McBride et al. (2008) suggested a difference in growth between males and females for this species. Unfortunately, we do not have information on sex definition to evaluate the second hypothesis.

There was a significant difference among mean radiodensities of studied species (**Table 3**), Dunn's *post-hoc* pointed out that *T. obesus* and *A. solandri* had Hounsfield units different from the other species (**Figure 6**). Both belong to the Scombridae family but from a different genus. Further, although they also belonged to the same genus *Thunnus*, the *T. albacares* otoliths had radiodensities greater than *T. obesus*, which in turn showed to be very similar to *A. solandri* (same family). Since these two tuna species are very close species, including their behaviors, we were expecting to find very similar results. Perhaps, the radiodensity of otoliths is not a phylogenetic response. An outlier was observed for *A. coeruleus* which can be explained by the age difference between this individual (AC36, 1-year-old) and the others (> 4 years).

Internally, empty cavities were observed for tuna otoliths (both species) (**Figure 7**). In some cases, it seems like a tunnel with an entrance but no exit and in other cases, there is no connection to the surface. These empty spaces are likely encased during the calcification process and, probably, are filled by endolymph. In addition, they reduce the otolith mass. However, whether their occurrence represents just a random process, or there is any related functional, or ecological reason needs to be clarified.

It was possible to extract a cross-section of the otolith (as usually done in age and growth studies using a metallographic saw) and observe the variation in density from the core toward the edges (**Figure 8**). The otolith formation consists of an alternation of the concentric bands of L- and D-zones, for mineral- and matrix-rich layers, respectively, which appear light and dark when viewed under transmitted light (Wainwrigth, 1963). Green et al. (2009) defined that the mineral-rich zone is denser than the mineral-deficient region. Thus, in **Figure 8** case, as we use transmitted light, the

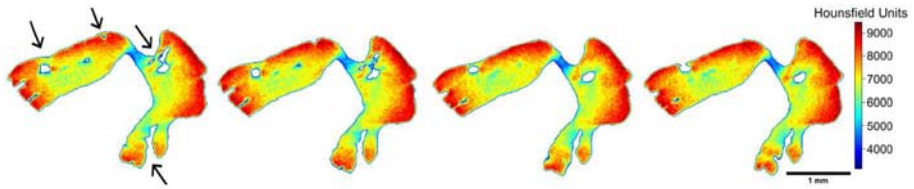

FIGURE 7 | A sequence of images along the *z*-axis, illustrating the opening and closing of internal spaces found in individuals of *Thunnus albacares* and *T. obesus*. The black arrows indicate the regions where these processes occurred.

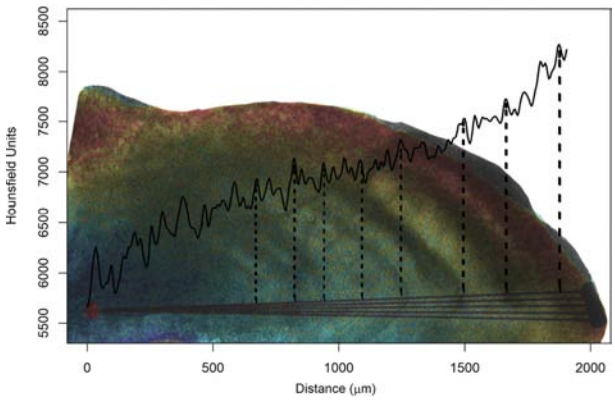

FIGURE 8 | Medium radiodensity (continuous black line) of the five lines drawn from the nucleus (red point) to the edge of the otolith, simulating the reading axis of *Acanthurus coeruleus*. The figure is composed by overlapping the photograph of the sectioned blade with a metallographic saw and its respective digital representation made by micro-computed tomography, where the highest values of radiodensity are represented in red and the smallest in blue. The vertical and dashed lines correspond to the observed growth rings and indicate their respective Hounsfield unit valleys. This image correspond to individual AC43 (see **Table 1**) with eight rings counted using a microscope and transmitted light.

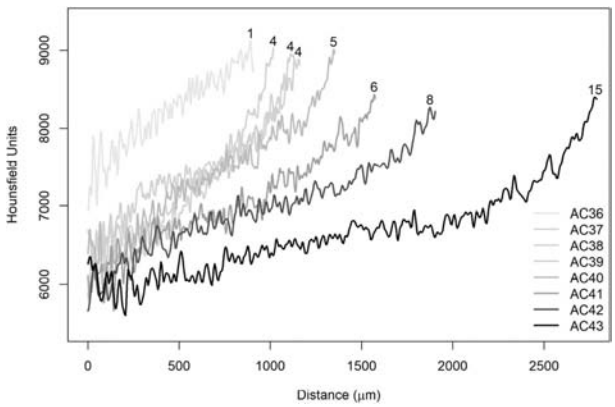

FIGURE 9 | Average radiodensities of the five lines, simulating the reading axis of *Acanthurus coeruleus*. The numbers at the end of the curves refer to the observed ages (years).

dashed lines indicate the end of dark bands (D-zones), where protein is more abundant and, consequently, less dense (valley).

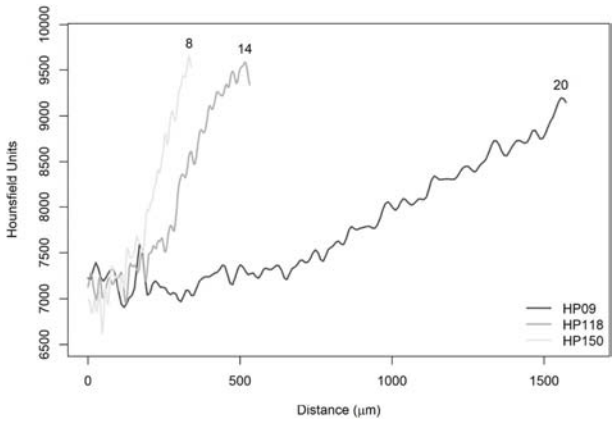

FIGURE 10 | Average radiodensities of the five lines, simulating the reading axis of *Haemulon plumierii*. The numbers at the end of the curves refer to the observed ages (years).

The sections closest to the nucleus were selected, where five lines were traced from the nucleus to the edge of the otolith simulating reading axes used in age and growth studies (**Figure 8**). The same procedure was replicated for all otoliths and, in particular, *A. coeruleus* (**Figure 9**) and *H. plumierii* (**Figure 10**) showed a decrease in HU values with the aging of the animals. In addition, the three samples AC38, AC39, and AC40, which are the same age, exhibited similar behavior among themselves (**Figure 9**). The same was found for the two samples of *T. obesus* (3 years old) and the specimens of *T. albacares* (3 years old).

In **Figure 10**, it was observed that the curves showed the same behavior in the initial phase between 0 and 200 μm. In this specific section, it is possible to observe the effect of voxel size differences. The HP09 sample had a resolution equal to 8 μm and, therefore, could not capture the variation on the same scale as the other images (HP118 and HP150). Furthermore, it has been found that there is no effect of voxel size on the displacement of the curves since six images of *A. coeruleus* that have a resolution equal to 3 μm showed the same pattern, as well as those with resolution equal to 5 μm (**Figure 9**). Actually, the reason for the displacements is attributed to ontogenetic variations.

The three *O. oglinum* specimens presented the same pattern (**Figure 11**) with coincident peaks and valleys since their estimated ages were less than 1 year. In addition, the region between 0 and 150 μm showed great variation. This corroborates

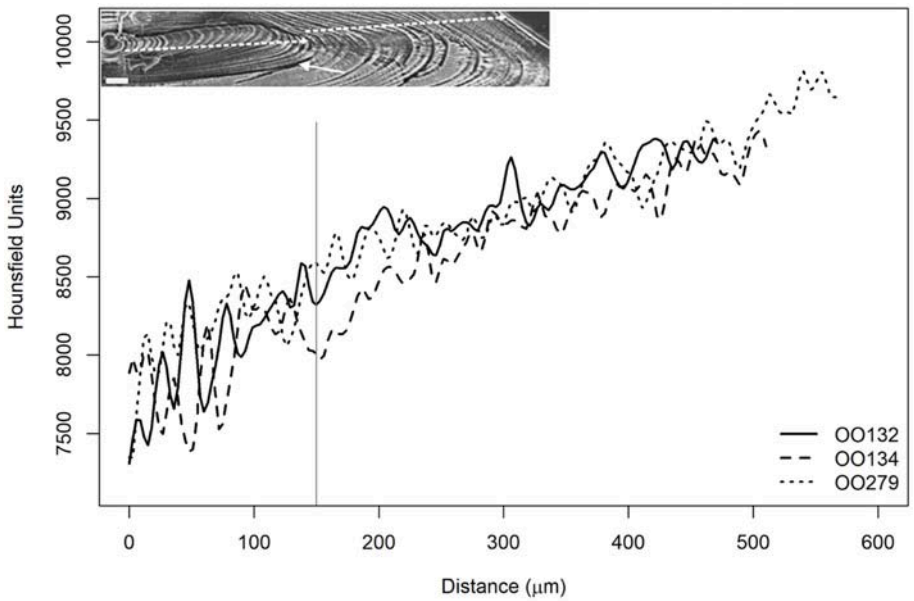

FIGURE 11 | Average radiodensities of the five lines, simulating the reading axis of *O. oglinum*. The estimated ages for the three samples were less than 1 year and similar behavior was observed for both curves of mean Hounsfield units. The vertical, gray and continuous line indicates the core distance of 150 μm, where the authors of the present study related to the change in growth phase explained by Lessa et al. (2008). The inset depicts a sectioned otolith of *O. oglinum* photographed with a scanning electron microscope, showing the growth rings. The two dashed lines indicate the two phases described by Lessa et al. (2008).

the study by Lessa et al. (2008), where it was possible to measure the thickness of the micro-increments (daily) and observed the occurrence of two zones with distinct patterns, as shown in **Figure 11**. In the paper, the authors associated the first zone to marks of life history events at beginning of fish life, such as the opening of the mouth, migration, and settlement. It reinforces the idea that the radiodensity fluctuations observed in the present work could also be associated with the occurrence of growth marks represented by these events.

These results indicate that the number of peaks and valleys is related to the micro or macrostructures, which could be related to age or life history events. Besides, it is important to emphasize that, in the future, this procedure could be made automatic, removing the inter-rater error omnipresent in the conventional approach. Using the difference between them, we could segment layer-by-layer reconstructing thus the previous form, therefore "peeling" the otolith. In addition, Limburg and Elfman (2017) mapped the trace elements and they found composition variations due to differences in crystallization, growth or other factors. Such heterogeneity influence the radiodensity. So, the combination of these methods would provide a better ecological inference of otolith density variations.

During otolith formation, the core (otolith *nucleus*) is the first part to be formed and has the lowest density due to its chemical composition made primarily by glycoproteins (Sasagawa and Mugiya, 1996) and other organic material (Fermin et al., 1998; Borelli et al., 2001; Pisam et al., 2002). In age and growth studies, knowing the position of the otolith nucleus and type of cut used (cross-sectional or longitudinal) is fundamental.

In the current work, we described a protocol that can be applied for otoliths of a wide range of species, with a detailed yet non-destructive procedure that fully preserves samples for other uses. The determination of voxel size and machine resolution are important first steps that were achieved in our study. With high-resolution instrumentation, it will be truly possible to distinguish features such as overlapping growth bands in the edge of otoliths of older individuals, which often result in longevity underestimation. Finally, in extreme cases, where a unique sample is available, as deep-sea fishes and critically endangered species, non-destructive methods are the best alternative.

DATA AVAILABILITY STATEMENT

The datasets generated for this study are available on request to the corresponding author.

ETHICS STATEMENT

Ethical review and approval was not required for the animal study because the samples used in the present study were obtained from existing otoliths collections in laboratories.

AUTHOR CONTRIBUTIONS

All authors contributed equally to the development of the research project, sections of the text, editing, feedback, and

discussion throughout the development of this manuscript. JV-F and DD conducted experimental procedures. JV-F, FT, and PD-N performed the analysis.

FUNDING

The Brazilian authors were supported by the Brazilian fostering agencies FACEPE (APQ-0178 - 1.08/14), FINEP (0798/10), CAPES (174/2012), and CNPq (312218/2013-3 and 457387/2014-9 MCTI/CNPQ/Universal 14/2014). FT acknowledges the Argentine National Agency for promotion of science and technology ANPCyT (PICT 2017-1731).

ACKNOWLEDGMENTS

The authors are grateful to Dr. Guelson Batista for the otolith samples from Thunnus albacares, all staff members of the Computed Tomography Laboratory of the Federal University of Pernambuco. The present manuscript is a part of the following Ph.D. thesis (Vasconcelos, 2019).

REFERENCES

Arneri, E., Bergström, N., Cardinale, M., Claes, E., Clevestam, P., de Clerck, N., et al. (2002). *Fish Ageing by Otolith Shape Analysis (FAbOSA): Final Report to the European Commission*. FAIR CT97 3402 report.

Barrett, J. F., and Keat, N. (2004). Artifacts in CT: recognition and avoidance 1. *Radiographics* 24, 1679–1691. doi: 10.1148/rg.246045065

Bignami, S., Enochs, I. C., Manzello, D. P., Sponaugle, S., and Cowen, R. K. (2013). Ocean acidification alters the otoliths of a pantropical fish species with implications for sensory function. *Proc. Natl. Acad. Sci. U.S.A.* 110, 7366–7370. doi: 10.1073/pnas.1301365110

Borelli, G., Mayer-Gostan, N., De Pontual, H., Boeuf, G., and Payan, P. (2001). Biochemical relationships between endolymph and otolith matrix in the trout (*Oncorhynchus mykiss*) and turbot (*Psetta maxima*). *Calcif. Tissue Int.* 69, 356–364. doi: 10.1007/s00223-001-2016-8

Browning, Z. S., Wilkes, A. A., Moore, E. J., Lancon, T. W., and Clubb, F. J. (2012). The effect of otolith malformation on behavior and cortisol levels in juvenile red drum fish (*Sciaenops ocellatus*). *Comparat. Med.* 62, 251–256.

Budoff, M. J., and Shinbane, J. S. (2016). *Cardiac CT Imaging: Diagnosis of Cardiovascular Disease*. London: Springer International Publishing.

Buzug, T. M. (2008). *Computed Tomography: From Photon Statistics to Modern Cone-Beam CT*. Berlin: Springer Science & Business Media.

Carlström, D. (1963). A crystallographic study of vertebrate otoliths. *Biol. Bull.* 125, 441–463. doi: 10.2307/1539358

Cignoni, P., Callieri, M., Corsini, M., Dellepiane, M., Ganovelli, F., and Ranzuglia, G. (2008). "MeshLab: an open-source mesh processing tool," in *Eurographics Italian Chapter Conference*, eds V. Scarano, R. De Chiara, and U. Erra (Salerno: The Eurographics Association).

Diez, M. E., Orensanz, J. M., Márquez, F., and Cremonte, F. (2013). Shell damage in the tehuelche scallop aequipecten tehuelchus caused by *Polydora rickettsi* (polychaeta: Spionidae) infestation. *J. Inverteb. Pathol.* 114, 107–113. doi: 10.1016/j.jip.2013.07.001

Duarte-Neto, P., Higa, F. M., and Lessa, R. P. (2012). Age and growth estimation of bigeye tuna, *Thunnus obesus* (teleostei: Scombridae) in the Southwestern Atlantic. *Neotrop. Ichthyol.* 10, 148–158. doi: 10.1590/S1679-62252012000100014

Duarte-Neto, P., Lessa, R., Stosic, B., and Morize, E. (2008). The use of sagittal otoliths in discriminating stocks of common dolphinfish (*Coryphaena hippurus*) off Northeastern Brazil using multishape descriptors. *ICES J. Mar. Sci.* 65, 1144–1152. doi: 10.1093/icesjms/fsn090

Fermin, C., Lychakov, D., Campos, A., Hara, H., Sondag, E., Jones, T., et al. (1998). Otoconia biogenesis, phylogeny, composition and functional attributes. *Histol. Histopathol.* 13, 1103–1154.

Fürst, A., Meier, D., Michel, S., Schmidlin, A., Held, L., and Laib, A. (2008). Effect of age on bone mineral density and micro architecture in the radius and tibia of horses: an xtreme computed tomographic study. *BMC Vet. Res.* 4:3. doi: 10.1186/1746-6148-4-3

Gauldie, R., and Nelson, D. (1990). Otolith growth in fishes. *Comparat. Biochem. Physiol. A Physiol.* 97, 119–135. doi: 10.1016/0300-9629(90)90159-P

Green, B. S., Mapstone, B. D., Carlos, G., and Begg, G. A. (eds.). (2009). "Introduction to otoliths and fisheries in the tropics," in *Tropical Fish Otoliths: Information for Assessment, Management and Ecology* (Springer Science & Business Media), 1–22. doi: 10.1007/978-1-4020-5775-5_1

Grodstein, G. W. (1957). *X-ray Attenuation Coefficients From 10 kev to 100 mev*. Technical report, DTIC Document.

Hameed, D. A., Elgammal, M. A., ElGanainy, E. O., Hageb, A., Mohammed, K., El-Taher, A. M., et al. (2013). Comparing non contrast computerized tomography criteria versus dual x-ray absorptiometry as predictors of radio-opaque upper urinary tract stone fragmentation after electromagnetic shockwave lithotripsy. *Urolithiasis* 41, 511–515. doi: 10.1007/s00240-013-0596-1

Hamrin, S., Arneri, E., Doering-Arjes, P., Mosegaard, H., Patwardhan, A., Sasov, A., et al. (1999). A new method for three-dimensional otolith analysis. *J. Fish Biol.* 54, 223–225. doi: 10.1111/j.1095-8649.1999.tb00627.x

Hsieh, J. (2009). *Computed Tomography: Principles, Design, Artifacts, and Recent Advances*. Bellingham, WA: SPIE.

Jalaguier-Coudray, A., Delarbre, B., Brenot-Rossi, I., Houvenaeghel, G., Villard-Mahjoub, R., Viens, P., et al. (2016). Contribution of FDG PET/CT for the optimization of the management of additional lesions detected on local staging breast MRI. *Am. J. Roentgenol.* 206, 891–900. doi: 10.2214/AJR.15.14656

Jenkins, G. (1990). Age, growth rate, and growth trajectory determined from otolith microstructure of Southern bluefin tuna *Thunnus maccoyii* larvae. *Mar. Ecol. Prog. Ser.* 63, 93–104. doi: 10.3354/meps063093

Kak, A., and Slaney, M. (2001). *Principles of Computerized Tomographic Imaging*. Philadelphia, PA: Society for Industrial and Applied Mathematics.

Lessa, R., Duarte-Neto, P., Morize, E., and Maciel, R. (2008). Otolith microstructure analysis with OTC validation confirms age overestimation in Atlantic thread herring *Opisthonema oglinum* from North-Eastern Brazil. *J. Fish Biol.* 73, 1690–1700. doi: 10.1111/j.1095-8649.2008.02043.x

Limburg, K. E., and Elfman, M. (2017). Insights from two-dimensional mapping of otolith chemistry. *J. Fish Biol.* 90, 480–491. doi: 10.1111/jfb.13048

Lippmann, F. (ed.). (1973). "Crystal chemistry of sedimentary carbonate minerals," in *Sedimentary Carbonate Minerals* (Springer), 5–96.

Lowe, T., Garwood, R. J., Simonsen, T. J., Bradley, R. S., and Withers, P. J. (2013). Metamorphosis revealed: time-lapse three-dimensional imaging inside a living chrysalis. *J. R. Soc. Interf.* 10:20130304. doi: 10.1098/rsif.2013.0304

Mapp, J., Fisher, M., Atwood, R., Bell, G., Greco, M., Songer, S., et al. (2016). Three-dimensional rendering of otolith growth using phase contrast synchrotron tomography. *J. Fish Biol.* 88, 2075–2080. doi: 10.1111/jfb.12949

McBride, R. S., Richardson, A. K., and Maki, K. L. (2008). Age, growth, and mortality of wahoo, *Acanthocybium solandri*, from the Atlantic coast of Florida and the Bahamas. *Mar. Freshw. Res.* 59, 799–807. doi: 10.1071/MF08021

Noever, C., Keiler, J., and Glenner, H. (2015). First 3D reconstruction of the rhizocephalan root system using MicroCT. *J. Sea Res.* 113, 58–64. doi: 10.1016/j.seares.2015.08.002

Northwood, D. O., and Lewis, D. (1968). Transformation of vaterite to calcite during grinding. *Am. Mineral.* 53, 2089–2092.

Panfili, J., De Pontual, H., Troadec, H., and Wrigh, P. J. (2002). *Manual of Fish Sclerochronology*. Brest: IFREMER-IRD.

Pisam, M., Jammet, C., and Laurent, D. (2002). First steps of otolith formation of the zebrafish: role of glycogen? *Cell Tissue Res.* 310, 163–168. doi: 10.1007/s00441-002-0622-z

Popper, A. N., and Fay, R. R. (1993). Sound detection and processing by fish: critical review and major research questions (part 1 of 2). *Brain Behav. Evol.* 41, 14–25. doi: 10.1159/000113821

Postnov, A., De Clerck, N., Sasov, A., and Van Dyck, D. (2002). 3D *in-vivo* x-ray microtomography of living snails. *J. Microsc.* 205, 201–204. doi: 10.1046/j.0022-2720.2001.00986.x

Postnov, A., Vinogradov, A., Van Dyck, D., Saveliev, S., and De Clerck, N. (2003). Quantitative analysis of bone mineral content by x-ray microtomography. *Physiol. Meas.* 24:165. doi: 10.1088/0967-3334/24/1/312

R Core Team (2018). *R: A Language and Environment for Statistical Computing*. Vienna: R Foundation for Statistical Computing.

Rose, A. (1948). The sensitivity performance of the human eye on an absolute scale. *JOSA* 38, 196–208. doi: 10.1364/JOSA.38.000196

Santana, F., Morize, E., and Lessa, R. (2006). Age and growth of the spotted goatfish, *Pseudupeneus maculatus* (bloch, 1793) in Brazil, validated through marginal increment and oxytetracycline dyes in the sagittae. *J. Appl. Ichthyol.* 22, 132–137. doi: 10.1111/j.1439-0426.2006.00724.x

Sasagawa, T., and Mugiya, Y. (1996). Biochemical properties of water-soluble otolith proteins and the immunobiochemical detection of the proteins in serum and various tissues in the tilapia *Oreochromis niloticus*. *Fish. Sci.* 62, 970–976. doi: 10.2331/fishsci.62.970

Schoepf, U. J., and Costello, P. (2004). CT angiography for diagnosis of pulmonary embolism: state of the art 1. *Radiology* 230, 329–337. doi: 10.1148/radiol.2302021489

Schulz-Mirbach, T., Ladich, F., Plath, M., and Heß, M. (2019). Enigmatic ear stones: what we know about the functional role and evolution of fish otoliths. *Biol. Rev.* 94, 457–482. doi: 10.1111/brv.12463

Starrs, D., Ebner, B. C., and Fulton, C. J. (2014). All in the ears: unlocking the early life history biology and spatial ecology of fishes. *Biol. Rev*. 91, 86–105. doi: 10.1111/brv.12162

Stéquert, B., Panfili, J., and Dean, J. (1996). Age and growth of yellowfin tuna, Thunnus albacares, from the Western Indian Ocean, based on otolith microstructure. *Oceanogr. Literat. Rev*. 12:1275.

Taina, I. A., Heck, R. J., and Elliot, T. R. (2008). Application of x-ray computed tomography to soil science: a literature review. *Can. J. Soil Sci.* 88, 1–19. doi: 10.4141/CJSS06027

Vasconcelos, J. (2019). *Tomografia computadorizada aplicada a otólitos em 3D*. (Ph.D. thesis). Federal Rural University of Pernambuco, Recife, Brazil.

Velichko, A., Holzapfel, C., and Mücklich, F. (2007). 3d characterization of graphite morphologies in cast iron. *Adv. Eng. Mater.* 9, 39–45. doi: 10.1002/adem.200600175

Wainwrigth, S. A. (1963). Skeletal organization in the coral, *Pocillopora damicornis*. *J. Cell Sci.* 3, 169–183.

Waldron, M. E., and Kerstan, M. (2001). Age validation in horse mackerel (*Trachurus trachurus*) otoliths. *ICES J. Mar. Sci.* 58, 806–813. doi: 10.1006/jmsc.2001.1071

Yan, L.-n., Li, S.-r., Luo, J.-y., Du, F.-q., Ma, G.-l., Wang, Y.-l., et al. (2009). Tentative application of computed tomography to study of otoliths and their responses to environment variations. *Front. Mater. Sci. China* 3, 187–193. doi: 10.1007/s11706-009-0031-2

Conflict of Interest: The authors declare that the research was conducted in the absence of any commercial or financial relationships that could be construed as a potential conflict of interest.

Copyright © 2019 Vasconcelos-Filho, Thomsen, Stosic, Antonino, Duarte, Heck, Lessa, Santana, Ferreira and Duarte-Neto. This is an open-access article distributed under the terms of the Creative Commons Attribution License (CC BY). The use, distribution or reproduction in other forums is permitted, provided the original author(s) and the copyright owner(s) are credited and that the original publication in this journal is cited, in accordance with accepted academic practice. No use, distribution or reproduction is permitted which does not comply with these terms.

frontiers in Marine Science

ORIGINAL RESEARCH
published: 27 November 2019
doi: 10.3389/fmars.2019.00711

Discriminating Natal Source Populations of a Temperate Marine Fish Using Larval Otolith Chemistry

Troy A. Rogers[1,2], Anthony J. Fowler[2], Michael A. Steer[2] and Bronwyn M. Gillanders[1]*

[1] Southern Seas Ecology Laboratories, School of Biological Sciences, The University of Adelaide, Adelaide, SA, Australia,
[2] South Australian Research and Development Institute – Aquatic Sciences, Henley Beach, SA, Australia

The life cycles of many marine species depend on a dispersive larval stage that connects spatially segregated populations. However, quantifying larval movement among populations remains one of the greatest challenges in marine ecology. Such movement determines whether a population is essentially a self-recruiting stock, or if it forms part of a larger meta-population where recruits originate from multiple sources. Previous research has struggled to differentiate between such stock structure models for King George whiting (*Sillaginodes punctatus*; Perciformes) in southern Australia, largely due to difficulties in identifying the source populations of dispersing larvae. In this study, pelagic larvae were collected throughout the only recognized spawning area in South Australia in 2017 and 2018. First, we identified that the distribution of larvae was broadly divisible into two groups – those in southern Spencer Gulf and those in Investigator Strait. Then, the incremental structure and elemental composition of otoliths of larvae from the two regions were compared to determine if they had originated from a common source population. There were no spatial differences in the sizes (3.0–5.0 mm SL), ages (5–21 days), hatch dates (April 7–24) or average growth rates (0.09–0.21 mm d^{-1}) of larvae. However, multi-elemental (Li, Mg, Mn, Sr, and Ba) otolith signatures differed significantly between the two regions, primarily driven by differences in concentrations of Li and Ba. Although otolith signatures were year-specific, larvae were assigned to their region of capture with 70–82% accuracy. Larvae in each region hatched at the same time yet had significantly different otolith chemistry, providing strong evidence that those in southern Spencer Gulf and Investigator Strait originated from spatially segregated water masses. This study has demonstrated the ability of otolith chemistry to discriminate source populations of pelagic larvae in a fully marine environment, which provides a basis to quantify larval movement between fish populations.

Keywords: larvae, connectivity, otolith chemistry, microstructure, LA-ICP-MS, early life history, lithium, King George whiting

OPEN ACCESS

Edited by:
Alejandra Vanina Volpedo, University of Buenos Aires, Argentina

Reviewed by:
Audrey J. Geffen, University of Bergen, Norway
Guido Plaza, Pontificia Universidad Católica de Valparaíso, Chile

****Correspondence:***
Troy A. Rogers
troy.rogers@adelaide.edu.au

Specialty section:
This article was submitted to Marine Ecosystem Ecology, a section of the journal Frontiers in Marine Science

Received: *27 August 2019*
Accepted: *05 November 2019*
Published: *27 November 2019*

Citation:
Rogers TA, Fowler AJ, Steer MA and Gillanders BM (2019) Discriminating Natal Source Populations of a Temperate Marine Fish Using Larval Otolith Chemistry. Front. Mar. Sci. 6:711. doi: 10.3389/fmars.2019.00711

INTRODUCTION

Many marine species conform to a bipartite life cycle whereby spawning grounds and nursery areas are spatially segregated, and larval transport is an obligate process that connects life history stages (Cowen et al., 2000). The dispersal of larvae in marine environments is heavily influenced by physical oceanographic processes, which results in a high probability of mixing between larvae

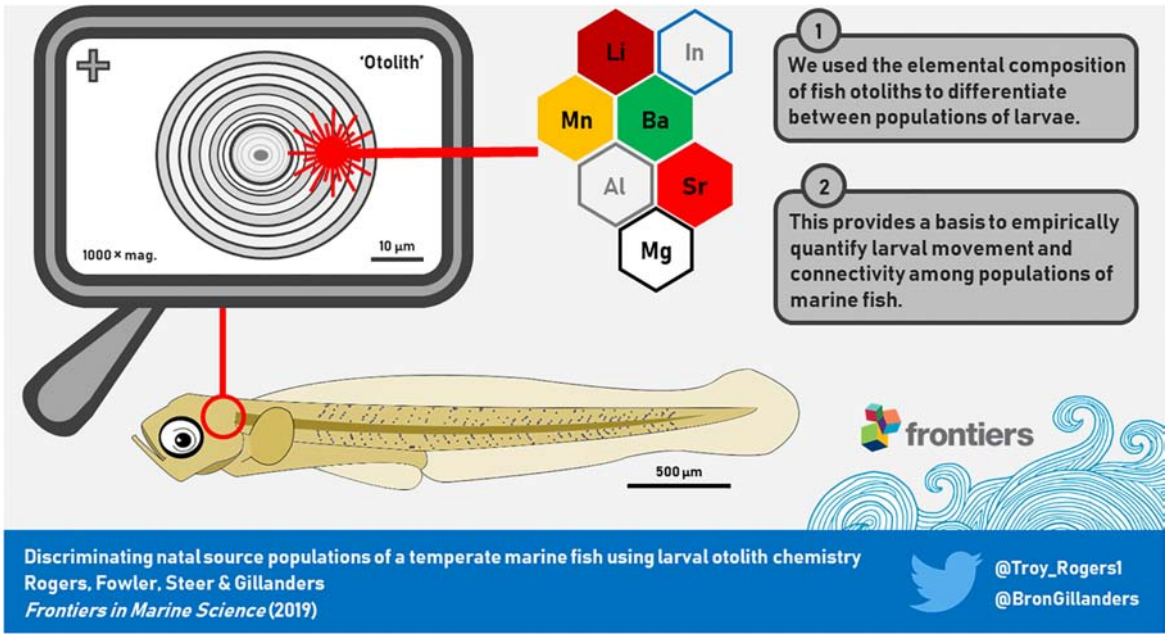

GRAPHICAL ABSTRACT | The elemental composition of microscopic otoliths of fish larvae were used as an environmental marker to differentiate between populations of larvae. The ability to discriminate between larvae that originated from different source populations provides a basis to quantify larval movement in marine ecosystems.

that originate from different source populations (Norcross and Shaw, 1984; Cowen and Sponaugle, 2009; Leis et al., 2011). Identifying the degree of larval exchange among populations is necessary to understand population dynamics and inform stock structure. However, quantifying larval movement among populations remains a significant challenge. On one hand, a population may be primarily maintained by larval production and dispersal from other populations, and is considered demographically open (Caley et al., 1996). Alternatively, larvae may recruit to the population to which they were born and the population is demographically closed as it is essentially self-recruiting (Swearer et al., 1999; Jones et al., 2005). It is likely that most marine populations are maintained by a combination of both processes – i.e., a proportion of self-recruitment that is supplemented by larval production from other populations (Swearer et al., 2002; Cowen and Sponaugle, 2009).

The most significant barrier to empirically quantifying larval movement has been the difficulty in differentiating between larvae from different source populations (Thorrold et al., 2002; Cowen and Sponaugle, 2009). This is largely associated with the logistical challenges involved in marking inherently small larvae that experience extremely high mortality rates. In recent years, natural environmental markers, such as the geochemical signatures in calcified structures, have become a leading approach to study the biology of even the smallest aquatic animals (Campana, 1999; Thorrold et al., 2007; Tzadik et al., 2017). The otoliths (ear stones) of teleost fishes are paired crystalline structures that form during embryonic development and record environmental information at a highly resolved temporal scale (Campana, 1999; Elsdon et al., 2008). They form increments at a daily periodicity which can be used to estimate age, and in turn, calculate hatch dates and larval growth rates (Campana and Neilson, 1985; Campana and Jones, 1992). The calcium carbonate generated during daily increment formation is derived from the surrounding aquatic environment, which contains elements in minor and trace quantities that can be incorporated into the otolith at the precipitating surface. Once incorporated, these elements are permanently retained and represent a chronological record of environmental history (Campana, 1999; Elsdon et al., 2008). The geochemical signatures in otoliths can be used as a tool to discriminate between fish populations, and have been successfully applied to assess stock structure (Campana et al., 1994; Tanner et al., 2016), reconstruct ontogenetic movement patterns (Elsdon and Gillanders, 2003; Fowler et al., 2005), and evaluate the contributions of source populations to nursery areas (Gillanders and Kingsford, 1996; Tanner et al., 2012).

The analysis of otolith chemistry has the potential to discriminate between source populations of larvae by comparing the elemental signatures of their otoliths prior to dispersal (Thorrold et al., 2002; Barbee and Swearer, 2007). Most studies of larval otolith chemistry have considered the otoliths of embryonic larvae from substrate-attached egg masses before the larvae have hatched (e.g., Warner et al., 2005; Ruttenberg and Warner, 2006; Barbee and Swearer, 2007; Standish et al., 2008). In such cases, the entire otolith relates to embryonic development at the single location where the eggs were collected. However, most commercially important marine fish species are broadcast spawners that produce large numbers of pelagic eggs and larvae (Sadovy, 2001; Murua and Saborido-Rey, 2003). Relatively few studies have considered pelagic larvae

(but see Ludsin et al., 2006; Lazartigues et al., 2014, 2017), and even fewer have considered pelagic larvae in marine environments (but see Brophy et al., 2003; Schaffler et al., 2009). This likely relates to a number of factors that include: the logistical challenges involved in collecting recently hatched larvae from open marine ecosystems; the limited amount of calcified material deposited at the natal origin because of the potential for dispersal immediately after spawning; and the analytical difficulties in detecting differences in elemental signatures where environmental gradients are potentially less pronounced (Barbee and Swearer, 2007; Standish et al., 2008).

King George whiting (*Sillaginodes punctatus*; Perciformes) is a demersal marine finfish species that is endemic to temperate coastal waters of southern Australia, where it supports important commercial and recreational fisheries (Kailola et al., 1993; Steer et al., 2018). South Australia is at the center of this geographic distribution and provides the highest State-based catches (Mobsby, 2018). However, in recent years, catches from two of the most productive fishery regions, Spencer Gulf and Gulf St. Vincent, have declined to record lows. In addition, there are differences in regional population characteristics that may be indicative of localized population processes (Steer et al., 2018). Despite extensive research of the life history of this species (Fowler and Short, 1996; Jenkins et al., 1997; Fowler et al., 1999, 2000a; Jenkins et al., 2000, 2016), there remains considerable uncertainty about the source populations that replenish nursery areas in different regions. Across south-eastern Australia, the only recognized spawning area for King George whiting is in southern Spencer Gulf and Investigator Strait, which is the region that connects the two gulf systems (**Figure 1**; Fowler et al., 1999, 2000b). Adults are multiple batch spawners that release pelagic eggs repeatedly between March and June (Fowler et al., 1999). The larvae undergo a prolonged dispersal phase of 3–5 months during the austral winter, from which the survivors eventually settle in protected bays between July and November (Fowler and Short, 1996; Jenkins et al., 1997; Fowler et al., 2000a; Rogers et al., 2019a). However, in South Australia, the relationships between the recognized spawning ground and nursery areas are poorly understood.

A recent study identified significant differences in the natal otolith chemistry of larvae that settled to nursery areas in Spencer Gulf and Gulf St. Vincent, suggesting that recruits in each gulf originated from different source populations (Rogers et al., 2019b). Because of the short distances between the nursery areas in these regions and the recognized spawning area, there are two primary hypotheses regarding the sources of larvae to nursery areas in Spencer Gulf and Gulf St. Vincent. The first hypothesis is that the recognized spawning area is comprised of multiple different source populations that replenish nursery areas in each region. Alternatively, larvae that recruit to one region may originate from the recognized spawning area, whilst the larvae that recruit to the other region may originate from a different spawning source elsewhere. The aim of this study was to determine if larval King George whiting in their natal waters of southern Spencer Gulf and Investigator Strait originated from a common source population. The specific objectives were to: (1) identify the distribution and abundance of recently hatched larvae throughout Southern Spencer Gulf and Investigator Strait; and (2) compare the early life history characteristics and otolith chemistry of larvae to assess the potential for different source populations. Otolith chemistry signatures could then be compared between larvae and recruits to evaluate hypotheses concerning population connectivity and stock structure.

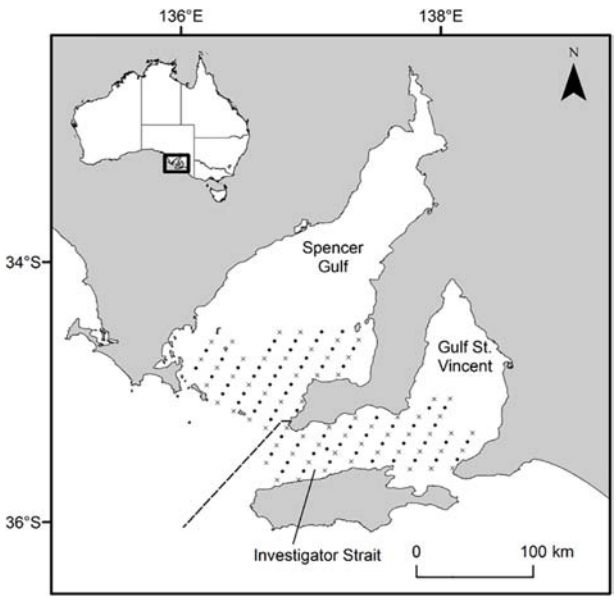

FIGURE 1 | Map of South Australia's gulf systems showing the geo-referenced stations where plankton samples were collected in 2017 and 2018. Oblique tows (•) were done at every station (n = 126) and vertical tows with CTD casts (×) at almost every second station (n = 62). The dashed line separates Southern Spencer Gulf and Investigator Strait stations. Inset, map of Australia showing the study area along the southern coastline.

MATERIALS AND METHODS

Study Area

This study focused on recently hatched King George whiting larvae in the recognized spawning area throughout southern Spencer Gulf and Investigator Strait, South Australia (**Figure 1**; Fowler et al., 1999, 2000b). This area connects the semi-enclosed seas of Spencer Gulf and Gulf St. Vincent, to the oceanic waters of the eastern Great Australian Bight. The region experiences significant seasonal changes in physical environmental characteristics and oceanographic regimes which largely relate to the formation of frontal systems at the mouths of Spencer Gulf and Investigator Strait (Petrusevics, 1993; Middleton and Bye, 2007; Petrusevics et al., 2011). Temperature and salinity increase in the gulfs during the austral summer, which leads to the formation of thermohaline fronts that inhibit shelf-gulf exchange. The frontal systems dissipate as gulf temperatures decrease in late autumn (May), and shelf/gulf exchange resumes as lower density shelf water is drawn into southern Spencer Gulf and Investigator Strait.

Sample Collection

Larvae were sampled on two research cruises from April 25 to May 1, 2017 and April 24–30, 2018 aboard the RV *Ngerin* at 126 geo-referenced stations arranged in a 4 × 2 nm grid pattern (**Figure 1**). Plankton samples were collected from a combination of oblique and vertical tows using paired bongo nets of 0.57 m diameter with 500 μm mesh. An oblique tow was done at every station (n = 126), whilst a vertical tow was done at almost every second station (n = 62). Each net was fitted with a flow-meter which was calibrated using factory coefficients to estimate the distance traveled by each net during each tow (General Oceanics, 2030; FL, United States). Plankton samples were preserved in 100% ethanol and refrigerated at 4°C prior to sorting. A SBE 19plus V2 SeaCAT Profiler CTD (SeaBird Scientific, WA, United States) was attached to the bottom of the vertical net frame and recorded temperature (°C) and salinity at 1 m intervals during each vertical net tow. King George whiting eggs are buoyant and the larvae remain near the surface until post-flexion (Bruce, 1995; Ham and Hutchinson, 2003). Therefore, we considered the mean CTD data from the surface to 5 m depth to best represent the environmental conditions experienced during early ontogeny. Maps were created in ArcGIS (v. 10.6; ESRI, CA, United States).

Sample Processing

Larval fish were sorted from the plankton using a modified Sedgwick-Rafter sorting tray under a dissecting microscope (Olympus SZX7; Tokyo, Japan). Larval King George whiting were identified following the morphological descriptions by Bruce (1995). The primary diagnostic characteristics were: shallow-bodied, elongate larvae with a small head; a single series of dorsal and ventral melanophores; and a moderate to long uncoiled gut (**Figure 2A**; Bruce, 1995). To aid identification, larvae were viewed at 20× magnification on a computer screen using an Olympus DP73 video camera attached to the microscope, and used Olympus Stream software (v. 1.9.1; Tokyo, Japan). Morphological identifications were verified using an *in situ* hybridization (ISH) molecular technique. This technique uses a horseradish peroxidase (HRP) enzyme conjugated oligonucleotide probe that binds specifically to mitochondrial 16S ribosomal RNA of King George whiting and generates a blue color through oxidization with a HRP reactive substrate (**Figure 3**; Oxley et al., 2017). The ISH probe was applied to a tissue sample from each larva after the head had been removed to prevent potential contamination of the otoliths. The identification of all King George whiting larvae used in otolith analyses (n = 134) was verified using the ISH molecular technique (**Table 1**).

At each station, the density of larvae per volume of water filtered was estimated by the equation:

$$D = \frac{n}{V} \quad (1)$$

where D is the density of larvae (ind. per m^3), n is the number of larvae in each sample, and V is the volume of water filtered (m^3). V was calculated as the area of the paired nets ($2 \times \pi r^2$) multiplied by the distance traveled according to the flowmeter readings. Each larva was measured for standard length (SL) to the nearest 0.1 mm. Larvae ranged in size from 1.6 to 9.3 mm SL. However, we constrained otolith analyses to larvae of ≤5 mm to minimize potential dispersion from their natal environment. In 2018, the abundance of larvae in Investigator Strait was considerably higher than elsewhere, and therefore a random sub-sample of larvae (n = 42) representative of the overall distribution was used for otolith analyses. The otoliths (sagittae and lapilli) were clearly visible in the heads of the larvae under a dissecting microscope at 60× magnification fitted with a polarizing filter (**Figure 2A**). Only the sagittal otoliths were used for analyses, which were extracted using stainless steel dissecting needles. Hereafter, a fine-tipped synthetic paintbrush was used for all otolith transfers to prevent contamination from metallic

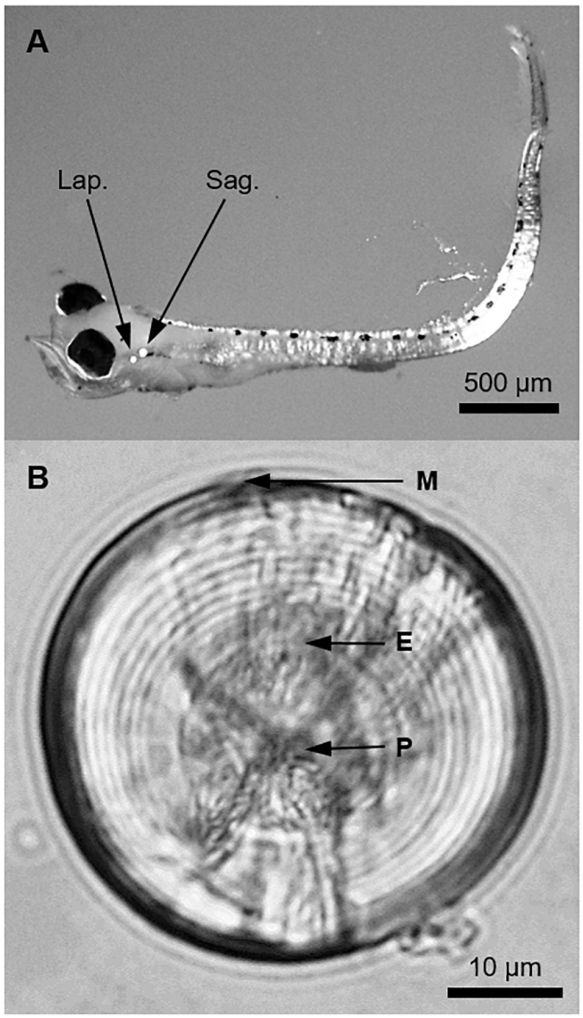

FIGURE 2 | (A) A pre-flexion larval King George whiting of 3.7 mm SL viewed at 20× magnification under a dissecting microscope. Polarized light was used to illuminate the otoliths (Lap., lapillus; Sag., sagitta). **(B)** Whole sagittal otolith of a larval King George whiting viewed from the proximal surface (sulcus upward) at 1,000× magnification using immersion oil (P, primordium; E, exogenous feeding check; M, posterior margin). Otolith diameter was 48.9 μm and the larva was 18 days old and 4.7 mm SL.

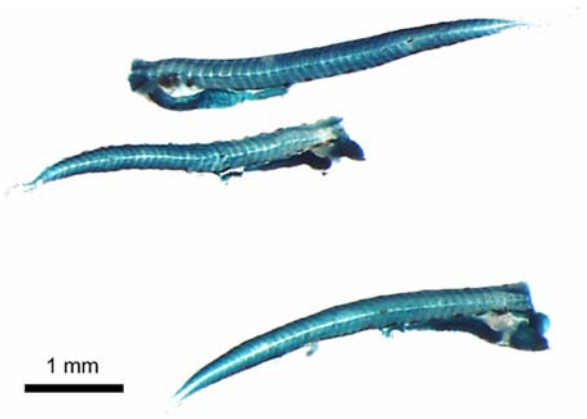

FIGURE 3 | Larval King George whiting following confirmation of identification using the *in situ* hybridization (ISH) molecular technique. Larvae were viewed at 20× magnification under a dissecting microscope. The head of each larva was removed to prevent potential contamination of the otoliths.

instruments. Otoliths were rinsed in a drop of ultrapure water, then transferred to a bath of ultrapure 15% H_2O_2 buffered with 0.1 N NaOH for 15 min to remove adhering organic material (Warner et al., 2005; Barbee and Swearer, 2007; Standish et al., 2011). Otoliths were then transferred through three drops of ultrapure water to remove residual cleaning solution and were then air dried under a laminar flow hood.

Otolith Microstructure

The sagittae from King George whiting larvae are hemispherical in shape, with a convex proximal surface (sulcus face) and almost flat distal surface. One otolith from each larva (n = 134) was randomly selected for microstructure analysis, and the other was used for trace element chemistry. The former was viewed whole, orientated sulcus face upward in immersion oil, at 1,000× magnification under a compound microscope (Olympus BX51; Tokyo, Japan). For interpretation, each otolith was viewed on a computer screen using an image analysis system (Olympus DP73 video camera, Olympus Stream v. 1.9.1; Tokyo, Japan). Otoliths were measured from the anterior to posterior margins to the nearest 0.1 μm. Daily increment formation for otoliths of King George whiting has been validated from reared larvae of known age (B. D. Bruce and D. A. Short, unpublished). Increments were counted from the primordium to the posterior margin (**Figure 2B**). Two counts were done for each otolith. If these counts differed, additional counts were done until an acceptable estimate of age was achieved. If not, the otolith was rejected (n = 3). After aging, each otolith was cleaned of oil and mounted in thermoplastic glue (CrystalBond 509; ProSciTech, QLD, Australia) for storage.

Larval growth rates were calculated in two ways. The "average growth rate" (mm d^{-1}) provided an estimate of mean daily growth rate from hatch to capture, and was calculated as:

$$\frac{L_c - L_o}{a} \tag{2}$$

where L_c is length at capture, L_o is length at hatch (2.1 mm; Bruce, 1995), and a is age (d). However, this method provides no information on daily variation in growth rate. As such, retrospective length at age and daily growth rates were calculated from otolith increment widths using the "back-calculation with biological intercept algorithm" (Campana, 1990; Campana and Jones, 1992). This technique depends on proportional somatic and otolith growth, for which there were strong linear relationships in each year (r^2 = 0.79 and 0.78 in 2017 and 2018, respectively; **Supplementary Figure S1**). Daily increments were measured from the primordium to posterior margin to the nearest 0.1 μm, and the size of each larva on successive days was estimated by the equation:

$$L_a = L_c + \left(\frac{(O_a - O_c)\,(L_c - L_o)}{(O_c - O_o)}\right) \tag{3}$$

where L_a is the length at age a, L_c is length at capture, L_o is length at hatch (2.1 mm; Bruce, 1995), O_a is the otolith radius at age a, O_c is the otolith radius at capture, and O_o is otolith radius at hatch. Here, O_o was defined as the distance from the closest increment to the primordium, and O_a was calculated from accumulating successive increments (Fowler and Short, 1996). The estimates of size at age and daily growth rate were averaged across larvae in each region and year.

Trace Element Chemistry

Otolith chemistry preparation and analytical processing were modified from Barbee and Swearer (2007). A gridded microscope slide was coated with a thin layer of thermoplastic glue (CrystalBond 509; ProSciTech, QLD, Australia), which was spiked with indium (^{115}In) at ∼200 ppm to aid discrimination during analysis (Reis-Santos et al., 2012). On each slide, up to 20 otoliths were orientated sulcus face upward on individual grid squares on top of the hardened thermoplastic glue. The slide was then heated on a hotplate for 3 s at 80°C to soften the glue, which

TABLE 1 | Summary of sample details used to compare otolith microstructure and elemental chemistry of larval King George whiting from Southern Spencer Gulf and Investigator Strait in 2017 and 2018.

Year	Region	*n*	Stations	Fish length (mm)	Otolith diameter (μm)	Age (*d*)	Ave. growth rate (mm d^{-1})	Temperature (°C)	Salinity (ppt)
2017	Spencer Gulf	19	13	4.0 (0.6)	40.6 (8.7)	13.3 (3.0)	0.140 (0.03)	19.2 (0.7)	37.0 (0.6)
	Investigator Strait	31	11	3.9 (0.6)	41.3 (9.1)	13.7 (3.5)	0.136 (0.03)	18.6 (0.2)	36.2 (0.1)
2018	Spencer Gulf	39	19	3.9 (0.4)	41.9 (7.9)	13.1 (2.6)	0.137 (0.02)	19.5 (0.5)	36.7 (0.6)
	Investigator Strait	42	17	3.8 (0.4)	37.4 (7.0)	11.8 (2.6)	0.140 (0.02)	19.2 (0.5)	36.4 (0.2)

n, number of larvae; stations, no. of stations larvae sourced from. All other values are in the form mean (SD).

caused the otoliths to "sink" into it using their own mass. This meant that each otolith was mounted in glue around its margin, but presented a largely exposed proximal surface for laser ablation (**Figure 4A**). A total of seven such slides were prepared and stored in resealable plastic bags prior to analysis.

Otoliths were analyzed for trace element chemistry by laser ablation-inductively coupled plasma-mass spectrometry (LA-ICP-MS). The system consisted of a Resonetics ASI (ACT, Australia) 193 nm excimer LA system coupled to an Agilent (Santa Clara, CA, United States) 7900 quadrupole ICP-MS, which was located at Adelaide Microscopy (Adelaide, SA, Australia). Up to four slides, each bearing 20 otoliths, were placed in the sealed chamber at one time and viewed remotely using a video camera. Otoliths were ablated using a 19 μm diameter laser "spot" at a pulse rate of 4 Hz and a beam density at the sample of ∼3.5 J cm^{-2}. Each otolith was sampled through the primordium from the proximal to distal surfaces. Due to the small diameter of larval otoliths (21.2–61.7 μm), no pre-ablation pass was done. Instead, the first 2 s of data were cropped to remove data that could have been affected by possible surface contamination. Ablation occurred in a ^{4}He flushed chamber that was mixed with ^{40}Ar for injection into the plasma. The elements quantified for analysis were ^{7}Li, ^{25}Mg, ^{55}Mn, ^{88}Sr, and ^{138}Ba, as well as ^{43}Ca that was used as the internal standard. The concentration of otolith ^{43}Ca was assumed to be constant at 38.8% (Yoshinaga et al., 2000). ^{115}In was also measured to aid discrimination between otolith material and thermoplastic glue during analysis (Reis-Santos et al., 2012), and ^{27}Al was measured as an indicator of metallic contamination (Lazartigues et al., 2016). Calibration was achieved against the National Institute of Standards (NIST) 612 glass standard (Lahaye et al., 1997). Background measurements were recorded for 30 s prior to each sample ablation, with a measurement of each element recorded every 0.17 s. Sample acquisition times ranged from ∼15 to 35 s due to the different sizes of otoliths. Data reduction, including background subtractions and calculation of minimum detection limits (MDL), was done offline in the Igor Pro workspace using Iolite software (v. 2.5; Paton et al., 2011). Data were converted to molar concentrations and standardized to calcium (element:Ca, μmol mol^{-1}). All analyses used the element:Ca data.

Internal precision and accuracy were assessed by analyzing the NIST 612 as an unknown sample against the known concentrations, and external precision was assessed by measurements of MACS-3 (United States Geological Survey; VA, United States) calcium carbonate reference material. NIST 612 and MACS-3 were analyzed twice at the beginning and end of each session, and after every 10 ablations to correct for instrumental drift (n = 18). Mean recovery for the NIST 612 was 99.99–100.05% for each element. Mean relative standard deviation (RSD) for NIST 612 was: 0.6% (Li), 1.1% (Mg), 0.3% (Mn), 0.3% (Sr), and 0.5% (Ba). External precision (RSD) assessed by measurements of MACS-3 was: 3.3% (Li), 3.9% (Mg), 2.0% (Mn), 3.7% (Sr) and 2.7% (Ba). Mean MDL (μmol mol^{-1}) based on three times the standard deviation of the blank gases adjusted for ablation yield (Lahaye et al., 1997) were: 0.39 (Li), 1.63 (Mg), 0.56 (Mn), 0.02 (Sr), and 0.02 (Ba).

Data Analysis

Environmental and Biological Characteristics

Environmental (temperature and salinity) and biological (length, age, otolith diameter and average growth rate) characteristics were compared between regions and years by two-way analysis of variance (ANOVA). Region and year were fixed factors in the full factorial model. Parametric assumptions of normality (Shapiro–Wilk) and equality of group variances (Levene's Test) were satisfied after square-root transformation. When significant differences were found, Tukey HSD *post hoc* comparisons were used to determine the source of differences between group means. Individual growth trajectories calculated from daily increment widths were compared between regions and years by repeated-measures analysis of variance (RM-ANOVA). Statistical analyses were done using SPSS Statistics (v. 26.0; IBM Corp., NY, United States).

Trace Element Chemistry

The concentration of Mn was used to separate the elemental data in two parts (Barbee and Swearer, 2007). Mn concentrations spiked at the primordium, which were consistent with larval otolith chemistry studies of other species (e.g., Brophy et al., 2004; Barbee and Swearer, 2007; Macdonald et al., 2008; Lazartigues et al., 2017). The two areas were: (1) "primordial area"– mean elemental concentrations of the 25 scans surrounding the peak count in Mn (**Figure 4B**). This incorporated the primordium and the immediately surrounding otolith material, and relates to the earliest stages of embryonic development and larval growth. It is representative of the "natal origin" of pelagic larvae (0 to ∼5 days post fertilization). (2) "Non-primordial area"– mean elemental concentrations from the proximal surface to the primordial area. This corresponds to larval development from the onset of exogenous feeding until the time of capture (∼5 to 20 days).

The elemental ratios of Li:Ca, Mg:Ca, Mn:Ca, Sr:Ca, and Ba:Ca exceeded the detection limits of the ICP-MS for all samples (100%). Parametric assumptions were violated for Li:Ca regardless of transformation type. Therefore, to apply a consistent statistical approach to all elements and enable them to be combined for multivariate analyses, non-parametric tests were used. For each area of the otolith, elemental chemistry was compared between regions and years using a two-factor PERMANOVA design for each element individually and all elements combined (Anderson, 2001). Region and year were fixed factors in the full factorial model. Element:Ca data were normalized prior to constructing resemblance matrices based on Euclidean distance dissimilarity, and analyzed using unrestricted permutation with 9999 random repeats. When significant differences were found, *post hoc* pair-wise comparisons were used to identify the source of differences between means. Multivariate data were reduced to two-dimensions and visualized using non-metric multidimensional scaling (nMDS) and canonical analysis of principal coordinates (CAP) (Anderson and Willis, 2003). Multi-elemental data were compared between spatial groups of larvae in each year, and then pooled together in a single analysis to evaluate variation between years. Vector diagrams in each canonical plot show the influence of individual

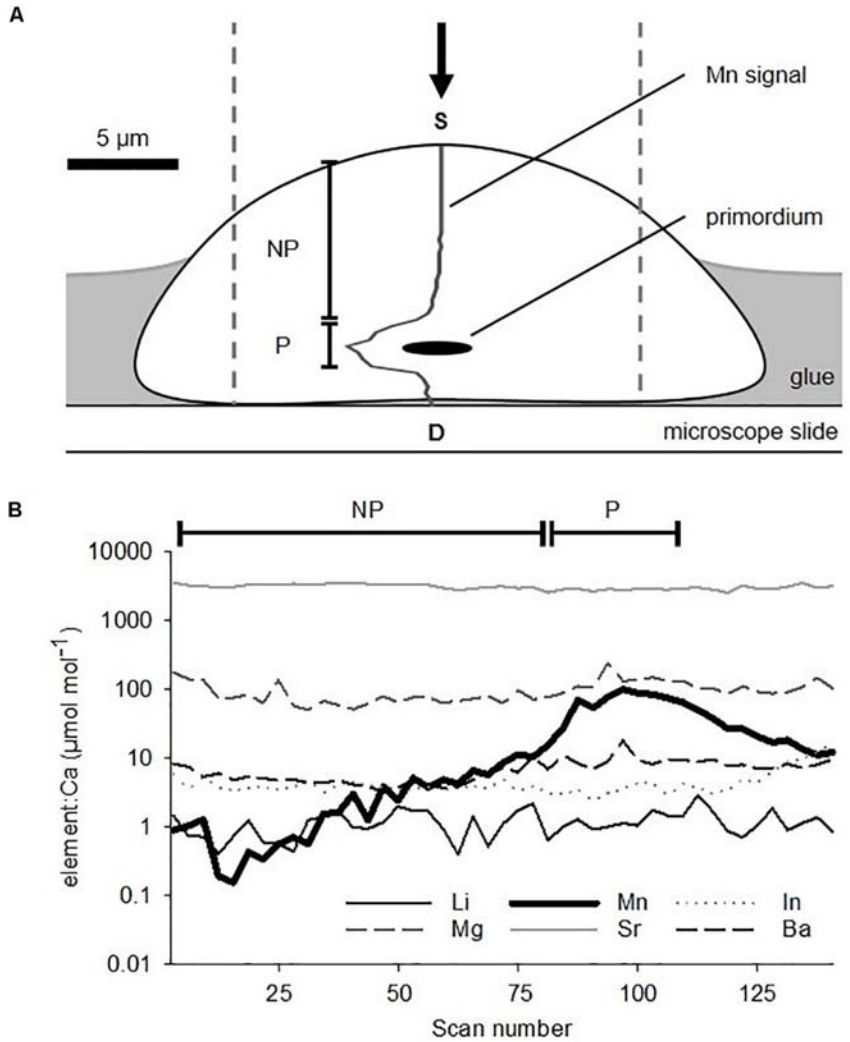

FIGURE 4 | (A) Schematic cross-section of a sagittal otolith from a larval King George whiting mounted sulcus face upward on a microscope slide in preparation for elemental analysis. Dashed lines show the area that the LA-ICP-MS ablation path encompassed. The arrow indicates the direction of laser ablation. ^{55}Mn signal is overlaid on the otolith. **(B)** Example of a time-resolved multi-elemental profile for a larval otolith ablated through the primordium from the proximal (S) to distal (D) surfaces. Note the logarithmic scale. NP, non-primordial area; P, primordial area.

elements to sample positioning in multivariate space. The relative length and direction of each vector correspond to its discriminatory ability. Leave-one-out cross validation was used to classify larvae to groups for each region and year based on the multi-elemental signals of the remaining samples. The performance of CAP to discriminate between groups was evaluated using Cohen's Kappa (κ) statistic, which is a method of calculating the chance-corrected percentage of agreement between actual and predicted group memberships. Values of κ range from 0 to 1, where 0 indicates that the CAP resulted in no improvement over chance, and 1 indicates perfect agreement (Titus et al., 1984). Statistical analyses were done using PRIMER (v. 7.0.13; Auckland, NZ) and figures were produced using SigmaPlot (v. 14.0; Systat Software Inc., San Jose, CA, United States).

RESULTS

Environmental Characteristics

In both 2017 and 2018, there were strong temperature and salinity gradients that increased northward in southern Spencer Gulf and eastward in Investigator Strait (**Figure 5**). In 2017, temperature ranged from 17.8 to 19.9°C in southern Spencer Gulf and 17.9 to 19.6°C in Investigator Strait. Despite within-region variation, southern Spencer Gulf was significantly warmer than Investigator Strait (**Supplementary Figure S2**). Water temperatures across the study area were 0.5–0.7°C warmer in 2018. Salinity also showed greater variation within than between regions. The largest variation in salinity was in southern Spencer Gulf in 2017 which increased from 35.6 to 37.5. In 2017, salinity was significantly higher in southern Spencer

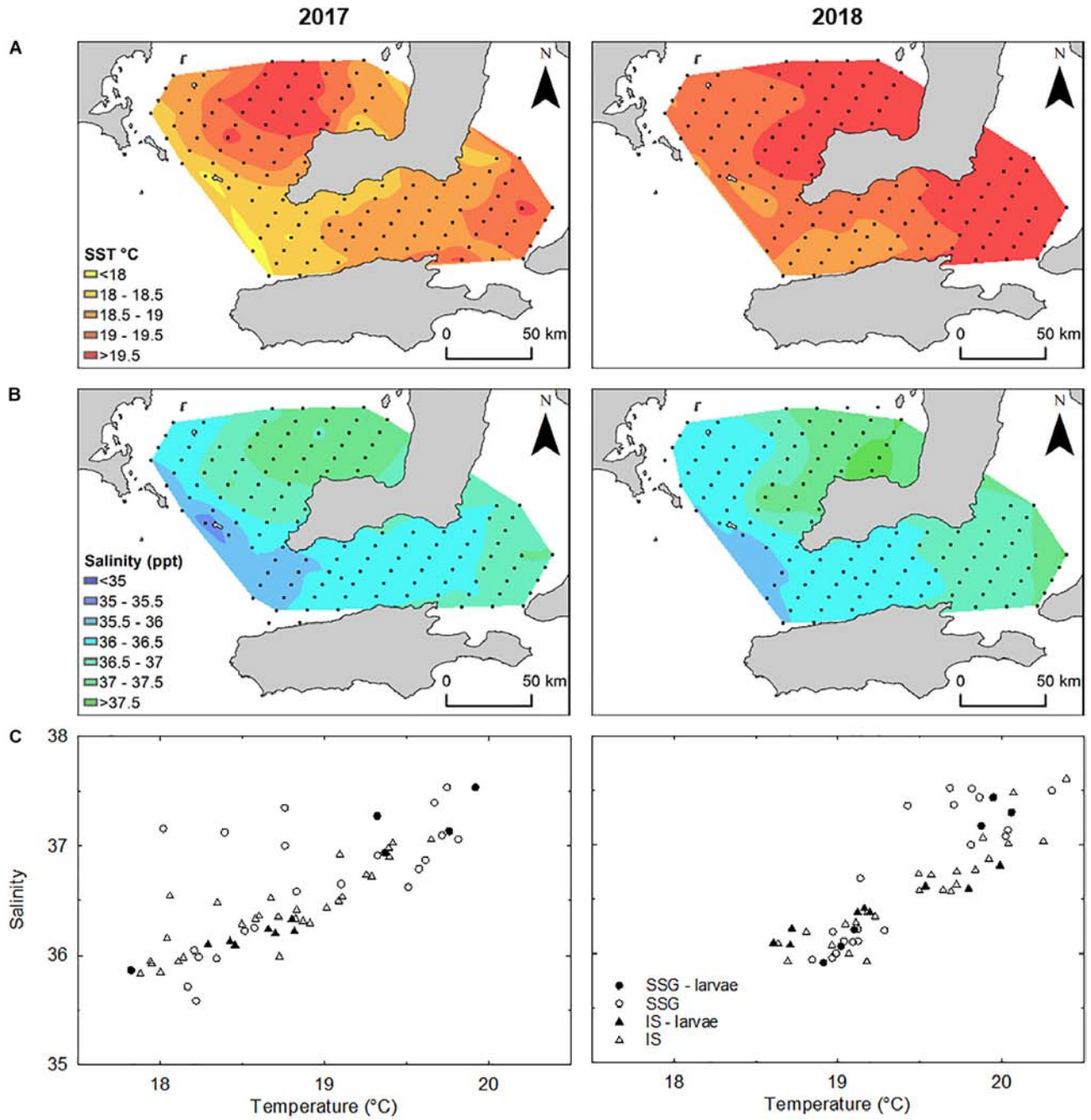

FIGURE 5 | (A) Interpolated mean temperature (°C) and **(B)** salinity to a depth of 5 m from the surface determined from CTD casts (n = 62) in 2017 and 2018. **(C)** Temperature-Salinity plots for sampling stations where CTD casts were done in each year. Stations where larvae were captured and used in otolith analyses are represented by closed symbols.

Gulf than Investigator Strait, but there were no differences in 2018 or between years. Although there were no regional differences for temperature and salinity in 2018, T–S plots separated the sampling stations into two clusters in each region (**Figure 5C**): (1) low temperature (18.6–19.3°C) and low salinity (35.8–36.5); and (2) high temperature (19.5–20.5°C) and high salinity (36.5–37.5).

Larval Distribution

In total, 360 larval King George whiting were captured throughout the study (n = 100 in 2017 and n = 260 in 2018). Larvae ranged in size from 1.6 to 7.6 mm SL in 2017, and 1.7 to 9.3 mm SL in 2018. The spatial distribution of larvae was similar in both years. Larvae in Investigator Strait were distributed as a single group at a high density,

whereas larvae in southern Spencer Gulf were distributed in small patches at lower densities (**Figure 6A**). In both years, larval abundance and density was higher in Investigator Strait than southern Spencer Gulf. There was a break in the distribution of larvae between the two regions. Based on the spatial distribution, larvae were separated into two groups: (1) southern Spencer Gulf and (2) Investigator Strait. The larvae considered for otolith analyses from these two groups were ≤5.0 mm SL to ensure that there had been minimal dispersion from the place where they had been spawned. The distribution of larvae of this size range was consistent with the overall distribution of larvae of mixed sizes (**Figure 6B**). The highest density of larvae ≤ 5.0 mm SL was in Investigator Strait in both years.

Early Life History Characteristics

The larvae used for otolith analyses ranged in size from 3.0 to 5.0 mm SL and in age from 5 to 21 days (**Figure 7**). There were no differences in the sizes and ages of larvae between regions or years (**Supplementary Table S1**). Otolith diameter for these larvae ranged from 21.2 to 61.7 μm and were strongly related to standard length and age (r^2 = 0.75 and r^2 = 0.78, respectively). Otoliths of larvae ≤ 3.0 mm SL were not large enough (≤20 μm diameter) for elemental analysis with LA-ICP-MS. In 2017 larvae hatched from April 8 to April 24, and in 2018 from April 7 to April 23. Mean hatch dates did not differ between regions or years. There was considerable variation in average growth rates which ranged from 0.09 to 0.21 mm d^{-1}. However, there were no differences between regions or years. Furthermore, there were no differences in average growth rates between larvae from the low and high temperature groups in 2018 (*t*-test; t = 0.44, df = 24, P = 0.667). Mean daily growth rates calculated from increment measurements showed a significant ontogenetic shift, although there were no differences between regions or years (**Supplementary Table S2**). The range was from 0.17 to 0.20 mm d^{-1} for age 0–4 days, then declined considerably on day 5 from 0.11 to 0.13 mm d^{-1} and then remained consistent from age 5 to 15 days (**Figure 8**).

Trace Element Chemistry

Individual Elements

There was considerable variation in the elemental concentrations in otoliths that resulted in numerous spatial and temporal differences (**Figure 9** and **Table 2**). For the primordial area, concentrations of Li and Ba differed between regions in 2017, being considerably higher for Investigator Strait than southern

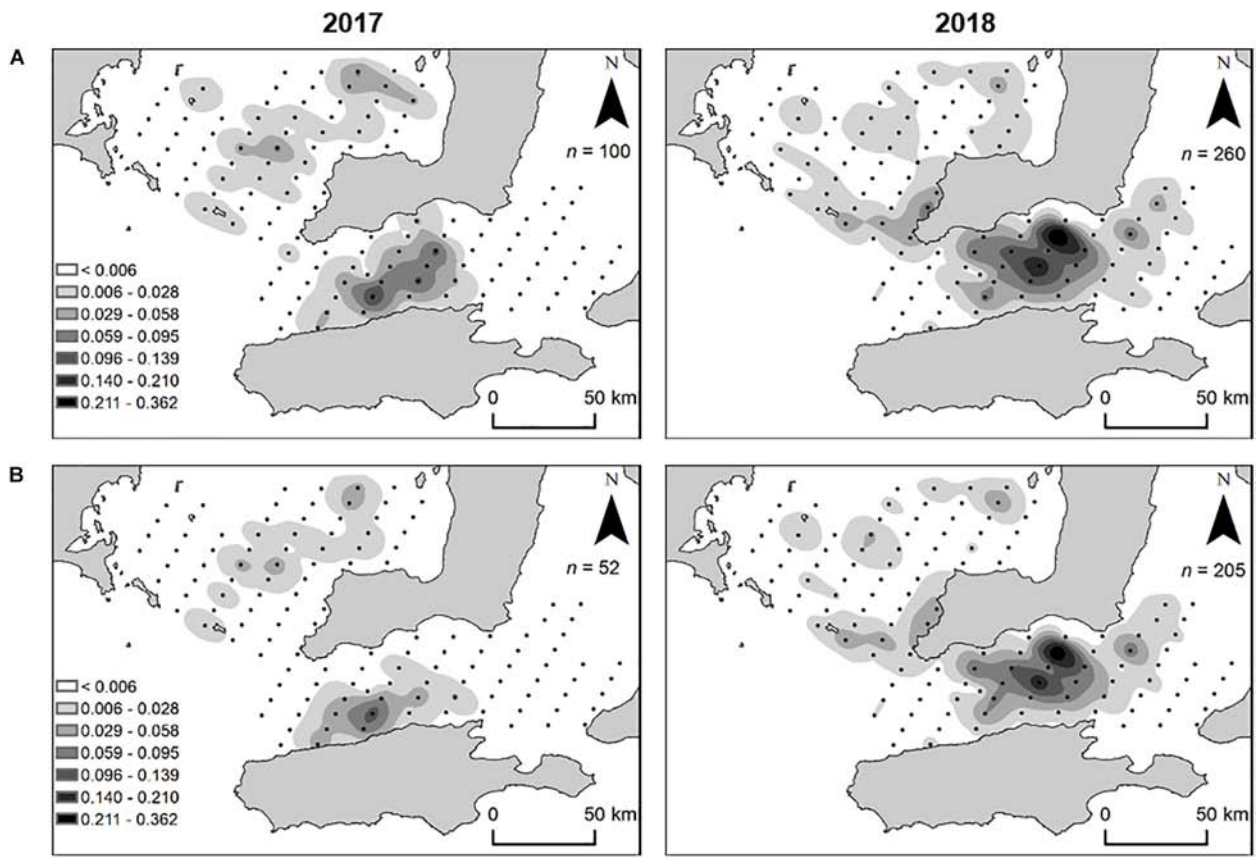

FIGURE 6 | Spatial distribution and density (larvae m^{-3}) of King George whiting larvae collected from Southern Spencer Gulf and Investigator Strait, South Australia, in 2017 and 2018. **(A)** All larvae captured; **(B)** larvae ≤ 5 mm SL. For clarity, maps show larval density from oblique tows which accounted for 89.7% of larvae captured (n = 323/360).

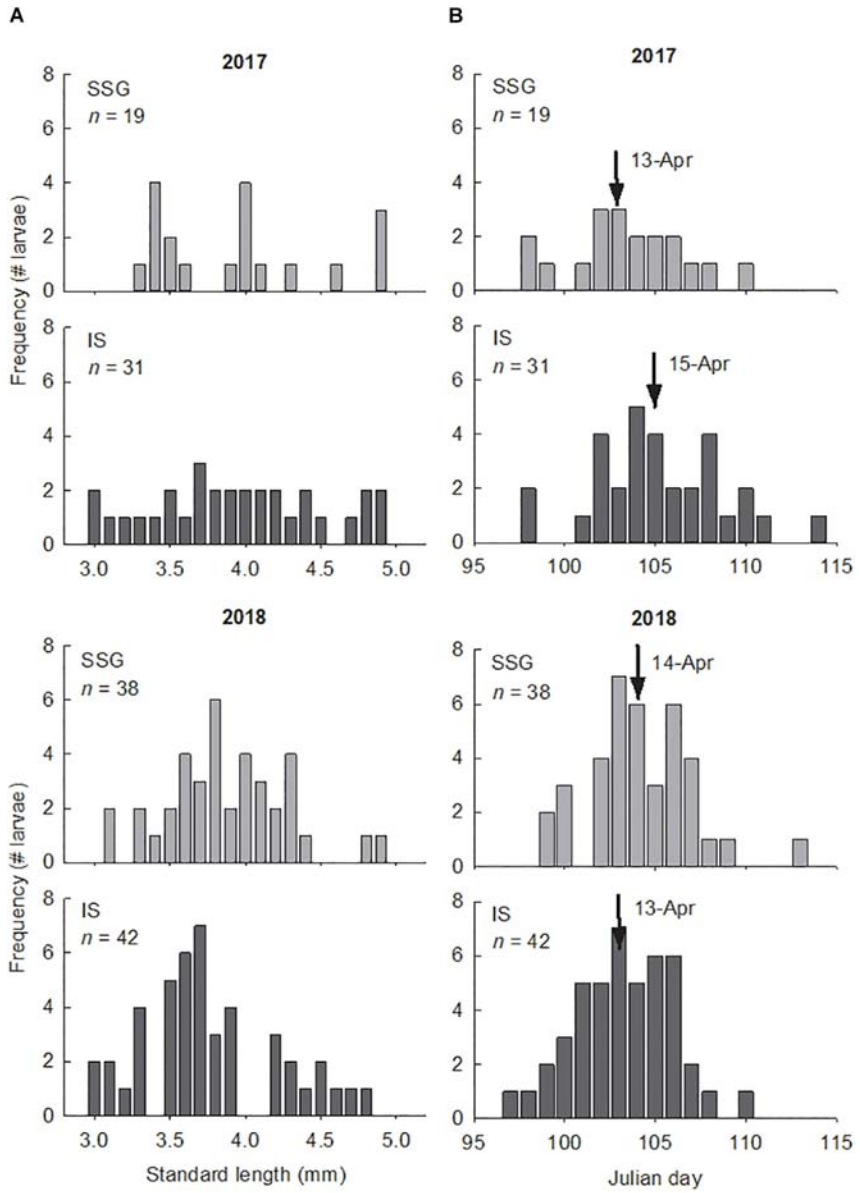

FIGURE 7 | (A) Length frequency distributions of King George whiting larvae from Southern Spencer Gulf (SSG) and Investigator Strait (IS) in 2017 and 2018. Size was constrained to larvae of ≤5 mm SL. **(B)** Frequency histograms showing the number of aged larvae that hatched on the nominated Julian day in 2017 and 2018. Arrows identify the mean hatch day.

Spencer Gulf (**Figure 9A**). Li concentrations were fourfold higher for Investigator Strait in 2017, but in 2018, there were no differences. Instead, regional differences were observed for Mg and Ba which were both higher for Investigator Strait. Ba was consistently higher for Investigator Strait than southern Spencer Gulf in each year. The concentrations of each element differed significantly between years. Concentrations of Li, Mn and Ba were higher in 2017, whilst Mg and Sr were higher in 2018. Concentrations of Mn were 10–20-fold higher for the primordial area compared to the remainder of the otolith.

For the non-primordial area, Li was the only element that differed between regions (**Table 2**). Concentrations of Li were higher for Investigator Strait than southern Spencer Gulf in each year, with the magnitude of difference considerably greater in 2017 (**Figure 9B**). There were significant between-year differences for the concentrations of Li, Mg, and Ba, which were consistent with the primordial area of the otolith. Concentrations of Sr were higher in Investigator Strait in 2017, but higher in southern Spencer Gulf in 2018.

Multi-Elemental Signatures

When individual elements were combined into a single matrix, significant differences were evident between regions in each year for the primordial area (**Table 2**). Regional differences were

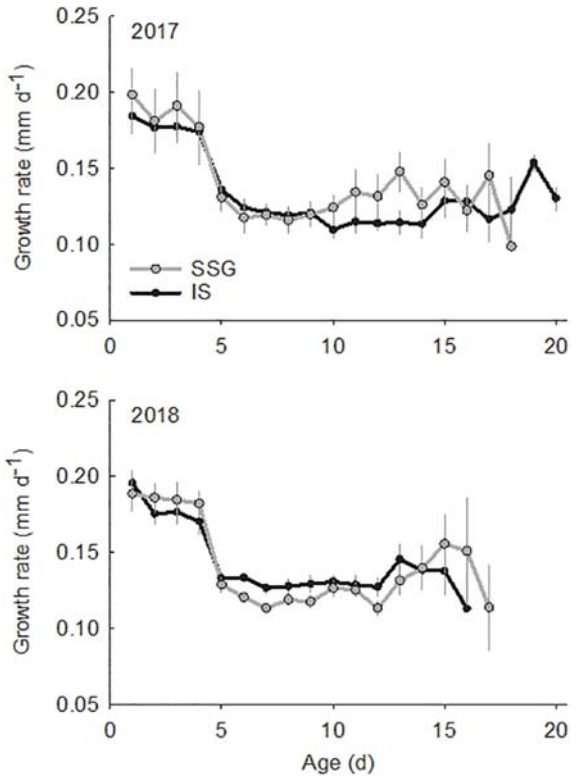

FIGURE 8 | Comparison of mean daily growth rates (mm d^{-1}) for King George whiting larvae from Southern Spencer Gulf (SSG; light) and Investigator Strait (IS; dark) in 2017 and 2018. Error bars are ±1 SE.

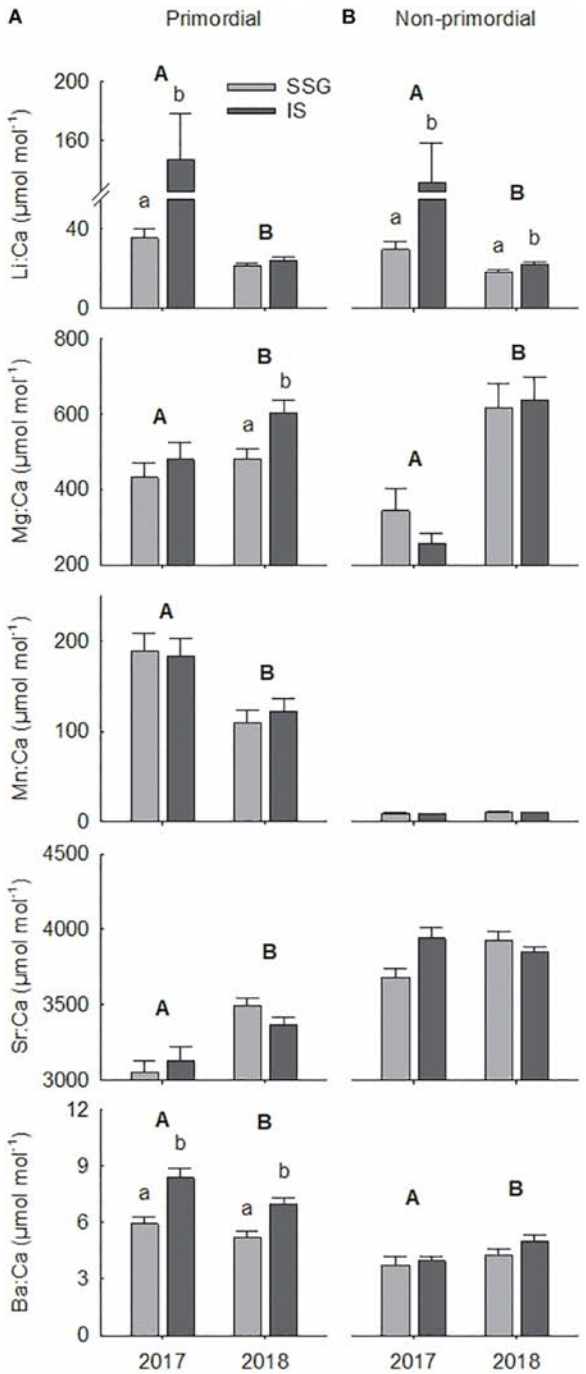

FIGURE 9 | Regional comparisons of mean element:Ca ratios (µmol mol^{-1}) for the **(A)** primordial area and **(B)** non-primordial area of larval King George whiting otoliths in 2017 and 2018. Letters identify significant differences ($P < 0.05$; capitals, between years; lower case, between regions). Error bars are +1 SE. SSG, Southern Spencer Gulf (light); IS, Investigator Strait (dark).

considerably greater in 2017 due to higher concentrations of Li for Investigator Strait. Regional differences in 2017 were driven by Li and Ba, and in 2018 by Ba (**Figure 10A**). Inter-annual differences in Li, Mn, and Sr were responsible for significant differences in regional multi-elemental signatures between years. Overall classification of larvae back to their region of capture was 82 and 70% in 2017 and 2018, respectively, and ranged from 66 to 94% for individual regions (**Table 3**).

For the non-primordial area, multi-elemental signatures differed between regions in 2017 but not 2018. Regional differences in 2017 were exclusively driven by higher concentrations of Li for Investigator Strait. Inter-annual variation in concentrations of Li, Mg, and Sr were responsible for differences in regional multi-elemental signatures between years (**Figure 10B**). Overall classification success was 80% in 2017, but was considerably lower in 2018 at 53% (**Table 3**). When both regions and years were combined in a single analysis, elemental signatures were most similar among regions within the same year (**Supplementary Table S3**).

DISCUSSION

The aim of this study was to determine whether larval King George whiting in their natal waters of southern Spencer Gulf and Investigator Strait originated from a common source population. Firstly, we described the distribution and abundance of larvae throughout the only recognized spawning area in southern Australia. We then used the incremental structure and

TABLE 2 | Summary of two-factor PERMANOVAs for the effect of year and region on individual and combined element: Ca ratios for the **(a)** primordial area and **(b)** non-primordial area of larval King George whiting otoliths.

		Li		Mg		Mn		Sr		Ba		All elements	
	df	MS	*F*	MS	*F*	MS	*F*	MS	*F*	MS	*F*	MS	*F*
(a) Primordial													
Year	1	22.35	35.08***	6.70	7.32**	12.48	13.65***	23.05	28.45***	5.76	7.43**	70.34	17.36***
Region	1	10.87	17.06***	3.64	3.97*	0.01	0.01	0.15	0.19	19.88	25.65***	34.55	8.53***
Year × Region	1	8.14	12.78***	0.99	1.08	0.36	0.40	1.61	1.99	0.08	0.11	11.18	2.76*
Residuals	127	0.64		0.92		0.91		0.81		0.78		4.05	
(b) Non-primordial													
Year	1	22.20	35.52***	30.48	41.48***	<0.01	<0.01	2.39	2.56	4.66	4.85*	59.73	13.95***
Region	1	13.03	20.85***	0.23	0.32	<0.01	<0.01	2.62	2.79	2.87	2.99	18.76	4.38**
Year × Region	1	7.57	12.11**	0.47	0.64	<0.01	<0.01	8.25	8.81**	0.01	0.01	16.31	3.81**
Residuals	127	0.62		0.73		1.03		0.94		0.96		4.28	

*Year and region were fixed factors. *P < 0.05; **P < 0.01; ***P < 0.001.*

multi-elemental signatures recorded in their otoliths to assess the potential for different source populations within the large spawning area.

Environmental Characteristics

The incremental structure and elemental composition of calcified structures is heavily influenced by the aquatic environment, and as such, geographic differences in environmental characteristics underpin the use of otolith-based techniques to discriminate between fish populations (Campana, 1999; Elsdon et al., 2008). Physical and chemical gradients in open marine environments are generally less pronounced compared to estuarine and freshwater systems (Standish et al., 2008). Even so, only small changes in environmental characteristics may be sufficient to be manifested as detectable differences in otolith elemental concentrations. For example, Atlantic croaker larvae collected from three water masses in the Mid-Atlantic Bight based on temperature and salinity showed significantly different otolith chemistry, suggesting that multiple source populations contributed to recruitment (Schaffler et al., 2009). In the present study, significant differences in temperature and salinity were evident between southern Spencer Gulf and Investigator Strait in 2017 that corresponded to distinct otolith

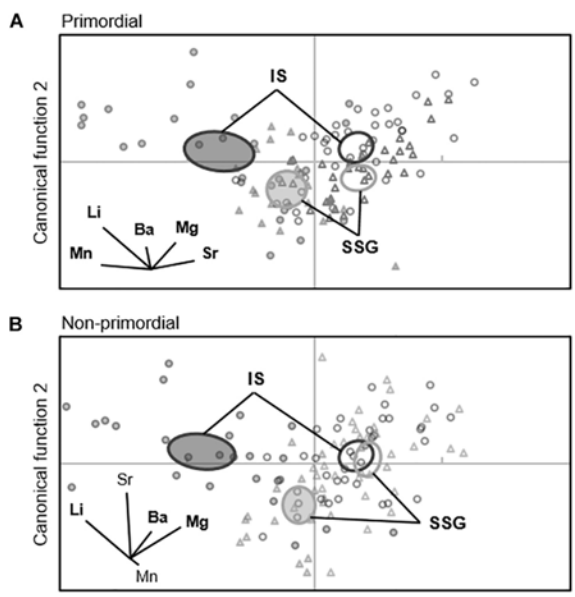

FIGURE 10 | Canonical variate plots of the multi-elemental chemistry for the **(A)** primordial area and **(B)** non-primordial area of larval King George whiting otoliths in 2017 (shaded) and 2018 (open). Ellipses show 95% confidence around group means. Vector diagrams show the direction and weight of individual elements to sample distribution. Elements in bold contribute most to group differences. SSG, Southern Spencer Gulf (▲, light); IS, Investigator Strait (●, dark).

TABLE 3 | Classification success for the spatial comparison of multi-elemental chemistry for the **(a)** primordial and **(b)** non-primordial areas of larval King George whiting otoliths in 2017 and 2018.

		SSG	IS
(a) Primordial			
2017	SSG	**94**	6
	IS	26	**74**
	Overall	**82**	
	κ	0.65	
2018	SSG	**66**	34
	IS	26	**74**
	Overall	**70**	
	κ	0.39	
(b) Non-primordial			
2017	SSG	**89**	11
	IS	26	**74**
	Overall	**80**	
	κ	0.60	
2018	SSG	**60**	40
	IS	53	**47**
	Overall	**53**	
	κ	0.07	

Data represent the percentage (%) of larvae from the region of capture (row) allocated to each region (column). Bold values are correctly assigned. SSG, Southern Spencer Gulf; IS, Investigator Strait.

signatures for larvae in each region. In 2018, environmental differences between regions were less prominent, which was reflected in greater similarity among regional otolith signatures. However, unlike Schaffler et al. (2009), we were unable to confidently discriminate between water masses based solely on environmental characteristics. Temperature and salinity demonstrated a similar gradient within each region in both years that increased away from the mouth into the two gulfs. These environmental gradients are characteristic of the seasonal thermohaline frontal systems that form at the entrance of Spencer Gulf and Investigator Strait (Bruce and Short, 1990; Petrusevics, 1993; Petrusevics et al., 2011).

Distribution and Abundance of Larvae

The spatial distribution and density of larvae differed considerably between southern Spencer Gulf and Investigator Strait. Larval abundance and density was higher for Investigator Strait in both 2017 and 2018, with larvae concentrated in the middle of the strait. In contrast, larvae in southern Spencer Gulf were distributed as a mosaic of small patches of low densities. For the latter region, in 2018, the highest densities of larvae were collected at the frontal zone across the mouth of the gulf. The patterns of larval distribution and areas of highest abundance in this study were consistent with those observed throughout the same study area in 1999 (Fowler, 2000). There was a discontinuity in the distribution of larvae between the two regions that corresponded to the environmental gradients at the entrances to Spencer Gulf and Investigator Strait. These observations provide further support to the findings of previous studies which have suggested that the frontal systems act as environmental barriers which inhibit water exchange, and subsequent plankton transport, during the austral summer and autumn (Bruce and Short, 1990; Petrusevics, 1993; Fowler, 2000; Petrusevics et al., 2011). Because the seasonality of the frontal systems coincides with the peak spawning period for King George whiting (Fowler et al., 1999, 2000b), it is possible that eggs and larvae in Spencer Gulf and Investigator Strait are separated until exchange between the gulfs and the waters of the continental shelf resumes after the fronts have dissipated.

Early Life History Characteristics

Otolith microstructure analysis is a useful tool for investigating the early life history characteristics of developing larvae, which can be used to discriminate between fish that have occupied different environments (Campana and Neilson, 1985; Campana and Jones, 1992; Watai et al., 2018). The discriminatory power of this technique largely depends on variation in somatic growth rates that manifest as differences in otolith increment widths. However, despite spatial differences in temperature, we found no differences in the sizes, ages, hatch dates or average growth rates of larvae between regions or years. Furthermore, there were no spatial differences in daily growth trajectories from the otolith increment widths. The only difference evident was an ontogenetic shift in the daily growth rates of all larvae at 5 days post hatch, that would be associated with the transition from endogenous to exogenous feeding (Bruce, 1995). Because of the similar environmental gradients in each region, it is possible that spatial differences were masked when samples were combined into regional groups. However, that appears unlikely because of the weak relationships between early life history (e.g., average growth rate) and environmental characteristics (e.g., temperature). Another possibility is that the spatial variation in temperature (∼2°C) and salinity (∼2 ppt) may have been insufficient to affect somatic growth, and therefore was not manifested in the otolith structure. Regardless, we were unable to discriminate between groups of larvae based on the characteristics derived from otolith microstructure analysis.

The primary interest of the analyses of otolith chemistry was to compare the multi-elemental signatures of larvae to determine if they had originated from a common source population. We identified significant differences in otolith chemistry between larvae from southern Spencer Gulf and Investigator Strait in each year, although the magnitude of difference was considerably greater in 2017. The differences suggest larvae from the two regions were hatched into, and subsequently developed in, water masses with different physical and/or chemical conditions that influenced otolith chemistry (Campana, 1999; Elsdon et al., 2008). There was considerable inter-annual variation in regional multi-elemental signatures, with the magnitude of difference between years greater than regional differences within years. Such inter-annual variation has implications for characterizing the geochemical signatures of larval populations, and also for studies that consider the natal signatures of otoliths from juvenile or adult fish (Gillanders, 2002; Reis-Santos et al., 2012).

In addition to differences among regions and years, there was considerable variation in elemental concentrations within otoliths. Spatial and temporal variation was considerably higher in the primordial area compared to the non-primordial area. The largest difference was a significant increase in Mn concentration at the primordium. Such elevated concentrations are unlikely to reflect environmental availability, but rather relate to physiological processes during embryonic development or crystallization of the otolith nucleus (Brophy et al., 2004; Ruttenberg et al., 2005). Barbee and Swearer (2007) separated larval otolith chemistry data in the same way, but found equally strong differences among populations for the primordial and non-primordial areas. The early life history of their species of interest involves substrate-attached egg masses, and therefore all the otolith material related to embryonic development at a single location. In contrast, the pelagic eggs and larvae of broadcast spawning species are subject to dispersal immediately after being released (Norcross and Shaw, 1984; Cowen and Sponaugle, 2009). The potential for transport is even greater for marine species that reproduce in exposed coastal or open waters. Because larvae of such species may only remain near their spawning ground for a short period of time, such as a few days, the amount of otolith material that corresponds to the natal environment is likely to be very limited (Barbee and Swearer, 2007; Standish et al., 2008). As such, for pelagic marine larvae the elemental composition of the otolith material that immediately surrounds the primordium may best reflect the natal environment. However, recent research suggests that otolith formation during embryonic development is considerably influenced by maternally derived chemical signatures, which could potentially mask environmentally driven variation (Hegg et al., 2018; Loeppky et al., 2018). Consequently, it is necessary

to separate the elemental data accordingly to account for such maternal effects.

Ecological Interpretation of Elemental Signatures

Larvae from southern Spencer Gulf and Investigator Strait hatched at the same time and developed at a similar rate, but had significantly different multi-elemental signatures relating to their natal origin. The differences in otolith chemistry indicate that larvae in the two regions occupied spatially segregated water masses, and suggest that each region supports its own spawning population (Campana, 1999; Elsdon et al., 2008). Evidence of two distinct spawning populations within the recognized spawning area has considerable implications for understanding the ontogenetic connectivity and stock structure of King George whiting. Spatial differences in multi-elemental signatures were primarily driven by concentrations of Ba and Li. Specifically, in both years, the otoliths of larvae from Investigator Strait showed significantly higher Ba concentrations compared to those from Spencer Gulf. Otolith Ba incorporation in marine fishes generally reflects ambient availability and shows a negative relationship with salinity (Elsdon and Gillanders, 2005; Walther and Thorrold, 2006; Izzo et al., 2018). A similar trend in otolith Ba concentration was identified for the natal signatures of settled King George whiting recruits, with those in Gulf St. Vincent having considerably higher Ba concentrations than Spencer Gulf (Rogers et al., 2019b). As such, the most parsimonious hypothesis is that each putative source population replenishes nursery areas in the adjacent gulf region, and as such, each gulf supports a largely closed population. That is, for Spencer Gulf, larvae are spawned in the south and disperse northward to the nursery areas, whilst larvae spawned in Investigator Strait disperse eastward and replenish nursery areas in Gulf St. Vincent. This scenario is consistent with the meta-population structure of King George whiting in South Australia hypothesized by Fowler et al. (2000a) and Rogers et al. (2019b). Because the two spawning grounds are separated by 50–100 km, only small-scale adult movement is required for exchange between populations to maintain genetic homogeneity (Kent et al., 2018).

Otolith Li concentrations for 10 of 25 larvae collected from Investigator Strait in 2017 were drastically higher than for larvae from elsewhere in either year. The mean Li concentration in the otoliths of these larvae was 287.4 μmol mol^{-1} (compared to 32.9 μmol mol^{-1} for the other larvae in the sample), which exceeded any published otolith Li concentrations (<50 μmol mol^{-1}). These larvae were collected at three consecutive sampling stations within 2 h of each other, and all larvae from these stations demonstrated exceedingly high Li values. We believe that sample contamination is unlikely because larvae were randomized at each stage of processing, were processed in a clean laboratory, and there were no systematic differences in the concentrations of the other elements measured from the same otoliths. One possible explanation is that the pronounced Li concentrations reflect a localized environmental phenomena that was directly manifested in otolith chemistry (Elsdon et al., 2008; Izzo et al., 2018). Lithium is only present in the salt fraction of endolymphatic fluid and is therefore unlikely to directly substitute for calcium at the precipitating surface (Thomas et al., 2017). As such, incorporation of Li into the otolith most likely occurs through random trapping in interstitial spaces of aragonite crystal during daily increment formation, and may reflect ambient concentrations (Izzo et al., 2016; Thomas et al., 2017). Lithium incorporation could also be facilitated by increased interstitial space following the substitution of calcium for elements with larger atomic radii, such as Sr or Ba (de Vries et al., 2005). However, there were no systematic changes in these elements with Li concentrations. Another possibility is that the elevated Li signature may have been maternally transferred, and in which case, the larvae were the progeny of a common spawning female (Thorrold et al., 2006; Starrs et al., 2013). Regardless of the source of Li, spatio-temporal differences in otolith chemistry remained similar when Li was excluded from multi-elemental analyses (see **Supplementary Appendix A**).

Implications and Future Directions

A common application of otolith chemistry is to analyze the natal signatures of juvenile or adult fish to estimate the number of source populations that contribute to recruitment (e.g., Gillanders and Kingsford, 1996; Standish et al., 2011; Tanner et al., 2012). Whilst such studies provide considerable insight into population connectivity and stock structure, they cannot identify the source populations from where larvae originated and the degree to which populations rely on larval production from elsewhere. This was the situation with King George whiting in South Australia. There was evidence to suggest that recruits in Spencer Gulf and Gulf St. Vincent originated from different source populations (Rogers et al., 2019b). In the present study, we determined that the recognized spawning area throughout southern Spencer Gulf and Investigator Strait constitutes two source populations based on the elemental composition of larval otoliths. The next step is to explore the relationships between the different spawning grounds and nursery areas to understand population dynamics and inform stock structure. One possible approach is to simulate larval dispersal using a biophysical model (Fowler et al., 2000a; Jenkins et al., 2000). This technique has been successfully applied to simulate larval transport of western king prawns in Spencer Gulf (McLeay et al., 2016), and has the capacity to be applied to King George whiting. Alternatively, otolith chemistry has the potential to empirically quantify larval movement between populations. This can be achieved by collecting larvae from all potential source populations, characterizing the elemental signatures of their otoliths, and then comparing them to the natal signatures of juveniles in different nursery areas. In this way, otolith chemistry can be used to address ecological questions not currently approachable using other techniques.

DATA AVAILABILITY STATEMENT

The datasets generated for this study are available on request to the corresponding author.

ETHICS STATEMENT

Sample collection and processing was reviewed and approved by The University of Adelaide Animal Ethics Committee (S2016-133).

AUTHOR CONTRIBUTIONS

TR, AF, MS, and BG conceived and designed the study. TR, AF, and MS assisted with sample collection. TR wrote the manuscript, performed the laboratory processing and sample preparation, operated the LA-ICP-MS, collected and analyzed the data, and applied the statistical analyses. AF, MS, and BG revised the manuscript.

FUNDING

Operating costs were largely funded by the Fisheries Research and Development Corporation (Project No. 2016-003). Larval otolith chemistry analysis (LA-ICP-MS) was funded by a Holsworth Wildlife Research Endowment Grant (Ecological Society of Australia), awarded to TR. This study was part of a Ph.D. by TR who was supported by an Australian Post-graduate Award (APA) and a Playford Memorial Trust Ph.D. Scholarship.

ACKNOWLEDGMENTS

We thank M. Drew, A. Hogg, D. Matthews, P. Rogers, and the crew of the RV *Ngerin* for assisting with sample collection. M. Drew and E. Westlake sorted mixed larvae from plankton samples. We thank S. Swearer (University of Melbourne, Australia) for discussions about larval otolith chemistry and providing an otolith processing protocol. S. Gilbert (Adelaide Microscopy, Australia) assisted with LA-ICP-MS operation. A. Oxley (SARDI) developed and applied the ISH technique to verify larval identifications. D. Matthews prepared the maps. Additional logistic support was provided by the South Australian Research and Development Institute (Aquatic Sciences). We thank the reviewers for comments that greatly improved the manuscript.

SUPPLEMENTARY MATERIAL

The Supplementary Material for this article can be found online at: https://www.frontiersin.org/articles/10.3389/fmars.2019.00711/full#supplementary-material

REFERENCES

Anderson, M. J. (2001). A new method for non-parametric multivariate analysis of variance. *Aust. Ecol.* 26, 32–46. doi: 10.1111/j.1442-9993.2001.01070.pp.x

Anderson, M. J., and Willis, T. J. (2003). Canonical analysis of principal coordinates: a useful method of constrained ordination for ecology. *Ecology* 84, 511–525. doi: 10.1890/0012-9658(2003)084%5B0511:caopca%5D2.0.co;2

Barbee, N. C., and Swearer, S. E. (2007). Characterizing natal source population signatures in the diadromous fish *Galaxias maculatus*, using embryonic otolith chemistry. *Mar. Ecol. Prog. Ser.* 343, 273–282. doi: 10.3354/meps06886

Brophy, D., Danilowicz, B., and Jeffries, T. (2003). The detection of elements in larval otoliths from Atlantic herring using laser ablation ICP-MS. *J. Fish Biol.* 63, 990–1007. doi: 10.1046/j.1095-8649.2003.00223.x

Brophy, D., Jeffries, T. E., and Danilowicz, B. S. (2004). Elevated manganese concentrations at the cores of clupeid otoliths: possible environmental, physiological, or structural origins. *Mar. Biol.* 144, 779–786. doi: 10.1007/s00227-003-1240-3

Bruce, B. D. (1995). Larval development of King George whiting, *Sillaginodes punctata*, school whiting, *Sillago bassensis*, and yellow fin whiting, *Sillago schomburgkii* (Percoidei: Sillaginidae), from South Australian waters. *Fish. Bull.* 93, 27–43.

Bruce, B. D., and Short, D. A. (1990). Observations on the distribution of larval fish in relation to a frontal zone at the mouth of Spencer Gulf, South Australia. *Bureau Rural Resour. Proc.* 15, 124–137.

Caley, M., Carr, M., Hixon, M., Hughes, T., Jones, G., and Menge, B. (1996). Recruitment and the local dynamics of open marine populations. *Annu. Rev. Ecol. Syst.* 27, 477–500. doi: 10.1146/annurev.ecolsys.27.1.477

Campana, S. E. (1990). How reliable are growth back-calculations based on otoliths? *Can. J. Fish. Aquat. Sci.* 47, 2219–2227. doi: 10.1139/f90-246

Campana, S. E. (1999). Chemistry and composition of fish otoliths: pathways, mechanisms and applications. *Mar. Ecol. Prog. Ser.* 188, 263–297. doi: 10.3354/meps188263

Campana, S. E., Fowler, A. J., and Jones, C. M. (1994). Otolith elemental fingerprinting for stock identification of Atlantic cod (*Gadus morhua*) using laser ablation ICPMS. *Can. J. Fish. Aquat. Sci.* 51, 1942–1950. doi: 10.1139/f94-196

Campana, S. E., and Jones, C. M. (1992). "Analysis of otolith microstructure data," in *Otolith Microstructure Examination and Analysis, Book 117. Canadian Special Publication of Fisheries and Aquatic Sciences*, eds D. K. Stevenson, and S. E. Campana, (Ottowa: Department of Fisheries and Oceans).

Campana, S. E., and Neilson, J. D. (1985). Microstructure of fish otoliths. *Can. J. Fish. Aquat. Sci.* 42, 1014–1032. doi: 10.1139/f85-127

Cowen, R. K., Lwiza, K. M., Sponaugle, S., Paris, C. B., and Olson, D. B. (2000). Connectivity of marine populations: open or closed? *Science* 287, 857–859. doi: 10.1126/science.287.5454.857

Cowen, R. K., and Sponaugle, S. (2009). Larval dispersal and marine population connectivity. *Annu. Rev. Mar. Sci.* 1, 443–466. doi: 10.1146/annurev.marine.010908.163757

de Vries, M. C., Gillanders, B. M., and Elsdon, T. S. (2005). Facilitation of barium uptake into fish otoliths: influence of strontium concentration and salinity. *Geochim. Cosmochim. Acta* 69, 4061–4072. doi: 10.1371/journal.pone.0218446

Elsdon, T., and Gillanders, B. (2005). Consistency of patterns between laboratory experiments and field collected fish in otolith chemistry: an example and applications for salinity reconstructions. *Mar. Freshw. Res.* 56, 609–617.

Elsdon, T. S., and Gillanders, B. M. (2003). Reconstructing migratory patterns of fish based on environmental influences on otolith chemistry. *Rev. Fish Biol. Fish.* 13, 217–235. doi: 10.1023/b:rfbf.0000033071.73952.40

Elsdon, T. S., Wells, B. K., Campana, S. E., Gillanders, B. M., Jones, C. M., Limburg, K. E., et al. (2008). Otolith chemistry to describe movements and life-history parameters of fishes: hypotheses, assumptions, limitations and inferences. *Oceanogr. Mar. Biol. Annu. Rev.* 46, 297–330.

Fowler, A. J. (2000). *Preliminary Assessment of the Application of the Daily egg Production Method for Estimating the Spawning Biomass of King George Whiting (Sillaginodes punctata) in South Australian Waters*. Adelaide, SA: South Australian Research and Development Institute.

Fowler, A. J., Black, K. P., and Jenkins, G. P. (2000a). Determination of spawning areas and larval advection pathways for King George whiting in southeastern

Australia using otolith microstructure and hydrodynamic modelling. II. South Australia. *Mar. Ecol. Prog. Ser.* 199, 243–254. doi: 10.3354/meps199243

Fowler, A. J., Gillanders, B., and Hall, K. (2005). Relationship between elemental concentration and age from otoliths of adult snapper (*Pagrus auratus*, Sparidae): implications for movement and stock structure. *Mar. Freshw. Res.* 56, 661–676.

Fowler, A. J., McLeay, L., and Short, D. (1999). Reproductive mode and spawning information based on gonad analysis for the King George whiting (Percoidei: Sillaginidae) from South Australia. *Mar. Freshw. Res.* 50, 1–14.

Fowler, A. J., McLeay, L., and Short, D. (2000b). Spatial variation in size and age structures and reproductive characteristics of the King George whiting (Percoidei: Sillaginidae) in South Australian waters. *Mar. Freshw. Res.* 51, 11–22.

Fowler, A. J., and Short, D. A. (1996). Temporal variation in the early life-history characteristics of the King George whiting (*Sillaginodes punctata*) from analysis of otolith microstructure. *Mar. Freshw. Res.* 47, 809–818.

Gillanders, B. M. (2002). Temporal and spatial variability in elemental composition of otoliths: implications for determining stock identity and connectivity of populations. *Can. J. Fish. Aquat. Sci.* 59, 669–679. doi: 10.1139/f02-040

Gillanders, B. M., and Kingsford, M. J. (1996). Elements in otoliths may elucidate the contribution of estuarine recruitment to sustaining coastal reef populations of a temperate reef fish. *Mar. Ecol. Prog. Ser.* 141, 13–20. doi: 10.3354/meps141013

Ham, J. M., and Hutchinson, W. G. (2003). *Spawning and Larval Rearing Research on King George Whiting (Sillaginodes punctata) Relevant to Aquaculture and Fisheries Biology*. Adelaide, SA: South Australian Research and Development Institute.

Hegg, J. C., Kennedy, B. P., and Chittaro, P. (2018). What did you say about my mother? The complexities of maternally derived chemical signatures in otoliths. *Can. J. Fish. Aquat. Sci.* 76, 81–94. doi: 10.1139/cjfas-2017-0341

Izzo, C., Doubleday, Z. A., and Gillanders, B. M. (2016). Where do elements bind within the otoliths of fish? *Mar. Freshw. Res.* 67, 1072–1076.

Izzo, C., Reis-Santos, P., and Gillanders, B. M. (2018). Otolith chemistry does not just reflect environmental conditions: a meta-analytic evaluation. *Fish Fish.* 19, 441–454. doi: 10.1111/faf.12264

Jenkins, G. P., Black, K. P., and Hamer, P. A. (2000). Determination of spawning areas and larval advection pathways for King George whiting in southeastern Australia using otolith microstructure and hydrodynamic modelling. I. Victoria. *Mar. Ecol. Prog. Ser.* 199, 231–242. doi: 10.3354/meps199231

Jenkins, G. P., Black, K. P., Wheatley, M. J., and Hatton, D. N. (1997). Temporal and spatial variability in recruitment of a temperate, seagrass-associated fish is largely determined by physical processes in the pre-and post-settlement phases. *Mar. Ecol. Prog. Ser.* 148, 23–35. doi: 10.3354/meps148023

Jenkins, G. P., Hamer, P. A., Kent, J. A., Kemp, J., Sherman, C., and Fowler, A. J. (2016). *Spawning Sources, Movement Patterns, and Nursery Area Replenishment of Spawning Populations of King George Whiting in South-Eastern Australia—Closing the Life History Loop*. Canberra: Fisheries Research and Development Corporation.

Jones, G. P., Planes, S., and Thorrold, S. R. (2005). Coral reef fish larvae settle close to home. *Curr. Biol.* 15, 1314–1318. doi: 10.1016/j.cub.2005.06.061

Kailola, P., Williams, M., Stewart, P., Reichelt, R., McNee, A., and Grieve, C. (1993). *Australian Fisheries Resources. Bureau of Resource Sciences and the Fisheries Research and Development Corporation Canberra, Australia*. Brisbane, QLD: Imprint Limited.

Kent, J., Jenkins, G., and Sherman, C. D. (2018). Low levels of genetic structuring in King George whiting *Sillaginodes punctatus* across two geographic regions. *J. Fish Biol.* 92, 523–531. doi: 10.1111/jfb.13510

Lahaye, Y., Lambert, D., and Walters, S. (1997). Ultraviolet laser sampling and high resolution inductively coupled plasma-mass spectrometry of NIST and BCR-2G glass reference materials. *Geostand. Newsletter* 21, 205–214. doi: 10.1111/j.1751-908x.1997.tb00671.x

Lazartigues, A., Girard, C., Brodeur, P., Lecomte, F., Mingelbier, M., and Sirois, P. (2017). Otolith microchemistry to identify sources of larval yellow perch in a fluvial lake: an approach towards freshwater fish management. *Can. J. Fish. Aquat. Sci.* 75, 474–487. doi: 10.1139/cjfas-2016-0289

Lazartigues, A. V., Plourde, S., Dodson, J. J., Morissette, O., Ouellet, P., and Sirois, P. (2016). Determining natal sources of capelin in a boreal marine park using otolith microchemistry. *ICES J. Mar. Sci.* 73, 2644–2652. doi: 10.1093/icesjms/fsw104

Lazartigues, A. V., Sirois, P., and Savard, D. (2014). LA-ICP-MS analysis of small samples: carbonate reference materials and larval fish otoliths. *Geostand. Geoanal. Res.* 38, 225–240.

Leis, J. M., Siebeck, U., and Dixson, D. L. (2011). How Nemo finds home: the neuroecology of dispersal and of population connectivity in larvae of marine fishes. *Integr. Comp. Biol.* 51, 826–843. doi: 10.1093/icb/icr004

Loeppky, A. R., Purchase, C. F., and Davoren, G. K. (2018). Chemical signatures in embryonic otoliths of capelin, *Mallotus villosus*: influence of family and environmental conditions. *J. Exp. Mar. Biol. Ecol.* 498, 25–31. doi: 10.1016/j.jembe.2017.10.007

Ludsin, S. A., Fryer, B. J., and Gagnon, J. E. (2006). Comparison of solution-based versus laser ablation inductively coupled plasma mass spectrometry for analysis of larval fish otolith microelemental composition. *Trans. Am. Fish. Soc.* 135, 218–231. doi: 10.1577/t04-165.1

Macdonald, J. I., Shelley, J. M. G., and Crook, D. A. (2008). A method for improving the estimation of natal chemical signatures in otoliths. *Trans. Am. Fish. Soc.* 137, 1674–1682. doi: 10.1577/t07-249.1

McLeay, L., Doubell, M., Roberts, S., Dixon, C., Andreacchio, L., James, C., et al. (2016). A biophysical model to assess the trade-off between larval recruitment and catch in southern Australia's largest prawn fishery. *Fish. Oceanogr.* 25, 164–182. doi: 10.1111/fog.12143

Middleton, J. F., and Bye, J. A. (2007). A review of the shelf-slope circulation along Australia's southern shelves: Cape Leeuwin to Portland. *Prog. Oceanogr.* 75, 1–41. doi: 10.1016/j.pocean.2007.07.001

Mobsby, D. (2018). *Australian Fisheries and Aquaculture Statistics 2017. Fisheries Research and Development Corporation Project 2018-134, Book 95*. Canberra: ABARES.

Murua, H., and Saborido-Rey, F. (2003). Female reproductive strategies of marine fish species of the North Atlantic. *J. Northwest Atlantic Fish. Sci.* 33, 23–31. doi: 10.2960/j.v33.a2

Norcross, B. L., and Shaw, R. F. (1984). Oceanic and estuarine transport of fish eggs and larvae: a review. *Trans. Am. Fish. Soc.* 113, 153–165. doi: 10.1577/1548-8659(1984)113<153:oaetof>2.0.co;2

Oxley, A. P., Catalano, S. R., Wos-Oxley, M. L., Westlake, E. L., Grammer, G. L., and Steer, M. A. (2017). Using in situ hybridization to expand the daily egg production method to new fish species. *Mol. Ecol. Resour.* 17, 1108–1121. doi: 10.1111/1755-0998.12707

Paton, C., Hellstrom, J., Paul, B., Woodhead, J., and Hergt, J. (2011). Iolite: freeware for the visualisation and processing of mass spectrometric data. *J. Anal. Atomic Spectr.* 26, 2508–2518.

Petrusevics, P. (1993). SST fronts in inverse estuaries, South Australia-indicators of reduced gulf-shelf exchange. *Mar. Freshw. Res.* 44, 305–323.

Petrusevics, P., Bye, J., Luick, J., and Teixeira, C. E. (2011). Summer sea surface temperature fronts and elevated chlorophyll-a in the entrance to Spencer Gulf, South Australia. *Cont. Shelf Res.* 31, 849–856. doi: 10.1016/j.csr.2011.02.009

Reis-Santos, P., Gillanders, B. M., Tanner, S. E., Vasconcelos, R. P., Elsdon, T. S., and Cabral, H. N. (2012). Temporal variability in estuarine fish otolith elemental fingerprints: implications for connectivity assessments. *Estuarine Coast. Shelf Sci.* 112, 216–224. doi: 10.1016/j.ecss.2012.07.027

Rogers, T. A., Fowler, A. J., Steer, M. A., and Gillanders, B. M. (2019a). Resolving the early life history of King George whiting (*Sillaginodes punctatus*: Perciformes) using otolith microstructure and trace element chemistry. *Mar. Freshw. Res.* 70:16.

Rogers, T. A., Fowler, A. J., Steer, M. A., and Gillanders, B. M. (2019b). Spatial connectivity during the early life history of a temperate marine fish inferred from otolith microstructure and geochemistry. *Estuarine Coast. Shelf Sci.* 227, 12.

Ruttenberg, B. I., Hamilton, S. L., Hickford, M. J., Paradis, G. L., Sheehy, M. S., Standish, J. D., et al. (2005). Elevated levels of trace elements in cores of otoliths and their potential for use as natural tags. *Mar. Ecol. Prog. Ser.* 297, 273–281. doi: 10.3354/meps297273

Ruttenberg, B. I., and Warner, R. R. (2006). Spatial variation in the chemical composition of natal otoliths from a reef fish in the Galapagos Islands. *Mar. Ecol. Prog. Ser.* 328, 225–236. doi: 10.3354/meps328225

Sadovy, Y. (2001). The threat of fishing to highly fecund fishes. *J. Fish Biol.* 59, 90–108. doi: 10.1006/jfbi.2001.1760

Schaffler, J. J., Reiss, C. S., and Jones, C. M. (2009). Spatial variation in otolith chemistry of Atlantic croaker larvae in the Mid-Atlantic Bight. *Mar. Ecol. Prog. Ser.* 382, 185–195.

Standish, J. D., Sheehy, M., and Warner, R. R. (2008). Use of otolith natal elemental signatures as natural tags to evaluate connectivity among open-coast fish populations. *Mar. Ecol. Prog. Ser.* 356, 259–268. doi: 10.3354/meps07244

Standish, J. D., White, J. W., and Warner, R. R. (2011). Spatial pattern of natal signatures in the otoliths of juvenile kelp rockfish along the Californian coast. *Mar. Ecol. Prog. Ser.* 437, 279–290. doi: 10.3354/meps09241

Starrs, D., Davis, J. T., Schlaefer, J., Ebner, B. C., Eggins, S. M., and Fulton, C. J. (2013). Maternally transmitted isotopes and their effects on larval fish: a validation of dual isotopic marks within a meta-analysis context. *Can. J. Fish. Aquat. Sci.* 71, 387–397. doi: 10.1139/cjfas-2013-0416

Steer, M., Fowler, A., McGarvey, R., Feenstra, J., Smart, J., Rogers, P., et al. (2018). *Assessment of the South Australian Marine Scalefish Fishery in 2016. Report to PIRSA Fisheries and Aquaculture, SARDI Publication no F2017/000427-1, SARDI Research Report Series no 974.* Adelaide, SA: South Australian Research and Development Institute.

Swearer, S. E., Caselle, J. E., Lea, D. W., and Warner, R. R. (1999). Larval retention and recruitment in an island population of a coral-reef fish. *Nature* 402, 799–803.

Swearer, S. E., Shima, J. S., Hellberg, M. E., Thorrold, S. R., Jones, G. P., Robertson, D. R., et al. (2002). Evidence of self-recruitment in demersal marine populations. *Bull. Mar. Sci.* 70, 251–271.

Tanner, S. E., Reis-Santos, P., and Cabral, H. N. (2016). Otolith chemistry in stock delineation: a brief overview, current challenges and future prospects. *Fish. Res.* 173, 206–213. doi: 10.1016/j.fishres.2015.07.019

Tanner, S. E., Vasconcelos, R. P., Cabral, H. N., and Thorrold, S. R. (2012). Testing an otolith geochemistry approach to determine population structure and movements of European hake in the northeast Atlantic Ocean and Mediterranean Sea. *Fish. Res.* 125, 198–205. doi: 10.1016/j.fishres.2012.02.013

Thomas, O. R., Ganio, K., Roberts, B. R., and Swearer, S. E. (2017). Trace element–protein interactions in endolymph from the inner ear of fish: implications for environmental reconstructions using fish otolith chemistry. *Metallomics* 9, 239–249. doi: 10.1039/c6mt00189k

Thorrold, S. R., Jones, G. P., Hellberg, M. E., Burton, R. S., Swearer, S. E., Neigel, J. E., et al. (2002). Quantifying larval retention and connectivity in marine populations with artificial and natural markers. *Bull. Mar. Sci.* 70, 291–308.

Thorrold, S. R., Jones, G. P., Planes, S., and Hare, J. A. (2006). Transgenerational marking of embryonic otoliths in marine fishes using barium stable isotopes. *Can. J. Fish. Aquat. Sci.* 63, 1193–1197. doi: 10.1139/f06-048

Thorrold, S. R., Zacherl, D. C., and Levin, L. A. (2007). Population connectivity and larval dispersal: using geochemical signatures in calcified structures. *Oceanography* 20, 80–89. doi: 10.5670/oceanog.2007.31

Titus, K., Mosher, J. A., and Williams, B. K. (1984). Chance-corrected classification for use in discriminant analysis: ecological applications. *Am. Midl. Nat.* 111, 1–7.

Tzadik, O. E., Curtis, J. S., Granneman, J. E., Kurth, B. N., Pusack, T. J., Wallace, A. A., et al. (2017). Chemical archives in fishes beyond otoliths: a review on the use of other body parts as chronological recorders of microchemical constituents for expanding interpretations of environmental, ecological, and life-history changes. *Limnol. Oceanogr. Methods* 15, 238–263. doi: 10.1002/lom3.10153

Walther, B. D., and Thorrold, S. R. (2006). Water, not food, contributes the majority of strontium and barium deposited in the otoliths of a marine fish. *Mar. Ecol. Prog. Ser.* 311, 125–130. doi: 10.3354/meps311125

Warner, R. R., Swearer, S. E., Caselle, J. E., Sheehy, M., and Paradis, G. (2005). Natal trace-elemental signatures in the otoliths of an open-coast fish. *Limnol. Oceanogr.* 50, 1529–1542. doi: 10.4319/lo.2005.50.5.1529

Watai, M., Hiraoka, Y., Ishihara, T., Yamasaki, I., Ota, T., Ohshimo, S., et al. (2018). Comparative analysis of the early growth history of Pacific bluefin tuna *Thunnus orientalis* from different spawning grounds. *Mar. Ecol. Prog. Ser.* 607, 207–220. doi: 10.3354/meps12807

Yoshinaga, J., Nakama, A., Morita, M., and Edmonds, J. S. (2000). Fish otolith reference material for quality assurance of chemical analyses. *Mar. Chem.* 69, 91–97. doi: 10.1016/s0304-4203(99)00098-5

Conflict of Interest: The authors declare that the research was conducted in the absence of any commercial or financial relationships that could be construed as a potential conflict of interest.

Copyright © 2019 Rogers, Fowler, Steer and Gillanders. This is an open-access article distributed under the terms of the Creative Commons Attribution License (CC BY). The use, distribution or reproduction in other forums is permitted, provided the original author(s) and the copyright owner(s) are credited and that the original publication in this journal is cited, in accordance with accepted academic practice. No use, distribution or reproduction is permitted which does not comply with these terms.

frontiers in Marine Science

ORIGINAL RESEARCH
published: 10 January 2020
doi: 10.3389/fmars.2019.00796

Elemental Ratios in Cuttlebone Indicate Growth Rates in the Cuttlefish *Sepia pharaonis*

Ming-Tsung Chung[1,2], Kuo-Fang Huang[3], Chen-Feng You[4,5], Chuan-Chin Chiao[6,7] and Chia-Hui Wang[1,8]*

[1] Department of Environmental Biology and Fisheries Science, National Taiwan Ocean University, Keelung, Taiwan, [2] Institute of Oceanography, National Taiwan University, Taipei, Taiwan, [3] Institute of Earth Sciences, Academia Sinica, Taipei, Taiwan, [4] Department of Earth Sciences, National Cheng Kung University, Tainan, Taiwan, [5] Earth Dynamic System Research Center, National Cheng Kung University, Tainan, Taiwan, [6] Department of Life Science, National Tsing Hua University, Hsinchu, Taiwan, [7] Institute of Systems Neuroscience, National Tsing Hua University, Hsinchu, Taiwan, [8] Center of Excellence for the Oceans, National Taiwan Ocean University, Keelung, Taiwan

OPEN ACCESS

Edited by:
Esteban Avigliano, National Council for Scientific and Technical Research (CONICET), Argentina

Reviewed by:
Roberta Callicó Fortunato, University of Buenos Aires, Argentina
Cristiano Albuquerque, Federal Rural University of the Semi-Arid Region, Brazil

****Correspondence:***
Chia-Hui Wang
chwang99@mail.ntou.edu.tw

Specialty section:
This article was submitted to Marine Ecosystem Ecology, a section of the journal Frontiers in Marine Science

Received: *16 August 2019*
Accepted: *10 December 2019*
Published: *10 January 2020*

Citation:
Chung M-T, Huang K-F, You C-F, Chiao C-C and Wang C-H (2020) Elemental Ratios in Cuttlebone Indicate Growth Rates in the Cuttlefish Sepia pharaonis. Front. Mar. Sci. 6:796. doi: 10.3389/fmars.2019.00796

Cuttlebone is a hard calcified structure that supports the cuttlefish body and aids in the regulation of buoyancy. The calcification rate of cuttlebone is high and is close to the growth rate of the cuttlefish mantle. The growth rate of the body mantle may strongly influence the incorporation of elements into the cuttlebone; however, the process has not been well studied. This is the first study to examine trace element incorporation into cuttlebone in detail. Controlled laboratory experiments and analyses of wild-caught cuttlefish revealed that both temperature and growth rate influence the elemental ratios of Li/Ca and Sr/Ca in cuttlebone. The variation in the elemental ratio was influenced the most by growth rates. After controlling for the minor influence of temperature, cuttlebone Li/Ca ratios appeared to be a potential proxy of cuttlefish growth. The relationship between growth rate and temperature-corrected Li/Ca ratios is positive and linear, and the trend does not vary between the sexes or across most of the life stages. In addition, the Li/Ca ratio is a promising growth rate proxy for evaluating differences among wild populations of cuttlefish, and the proxy could facilitate studies on cuttlefish biology and cuttlefish fisheries management.

Keywords: geochemistry, temperature, growth condition, trace elements, biogenic carbonate

INTRODUCTION

Elemental compositions of biogenic carbonate have been used extensively as environmental proxies for various factors, such as temperature, salinity, and water mass, and are usually applied in studies on foraminifera (Lea, 2003), coral (Lea, 2003; Corrège, 2006), fish otoliths (Bath et al., 2000), and mollusk shells (Schöne et al., 2011). It is now apparent that an vital effect is one of controlling factors of Me/Ca (Minor and trace metal element/Calcium) ratio, biasing Me/Ca ratio as an environmental proxy (Gillikin et al., 2005; Schöne et al., 2011; Sturrock et al., 2012; Chang and Geffen, 2013; Grammer et al., 2017; D'Olivo et al., 2018). Consequently, controlling for the biological factor would enable the calibration of carbonate Me/Ca ratios and facilitate the accurate determination

of environmental conditions, particularly temperature (Zhao et al., 2017). Conversely, carbonate Me/Ca ratios can also be a source of information on physiological conditions by acting as a proxy for biological characteristics, leading to an understanding of the influence of physiological factors on biokinetics (Sturrock et al., 2015).

Me/Ca ratios of biogenic carbonate often reflect salinity, environmental temperature, and water chemistry conditions (Bath et al., 2000; Lea, 2003; Corrège, 2006; Schöne et al., 2011) and have been reported to be highly related to carbonate growth rate. For example, growth rates of biogenic carbonates showed a positive relationship with Li/Ca ratio in mollusk shells (Thébault et al., 2009), Mg/Ca ratio in otoliths (Sturrock et al., 2015), and Sr/Ca ratio in mollusk shells (Gillikin et al., 2005), but a negative trend in the Sr/Ca ratio of otoliths (Sturrock et al., 2015). However, the trace element chemistry of cuttlebone carbonate, the inner shell of cuttlefish, has been relatively understudied, although a few research have reported population or geographic differences in cuttlebone trace element chemistry (Ikeda et al., 1999; Turan and Yaglioglu, 2010).

Cuttlefish possess an internal shell, the cuttlebone, which is embedded in a cuttlebone sac. The size of the cuttlebone corresponds to mantle length of cuttlefish for supporting the body structure and controlling their buoyancy (Birchall and Thomas, 1983; Sherrard, 2000). Structurally, the cuttlebone comprises inner and outer cones. The outer cone, or dorsal shield, is thick, non-porous, and calcified and acts as a cover to seal off the lamellae. Conversely, the inner cone consists of a number of lamellae (**Figure 1**), and each layer is comprised of a single septum with a number of vertical pillars. The components of lamellae are based on an organic framework filled with calcium carbonate in aragonite form (Florek et al., 2009). Previous studies on cuttlebone structure have focused on the number of lamellae, each of which is formed over approximately 1.75 days; thus, they offer a mechanism for estimating the age of cuttlefish (Bettencourt and Guerra, 2001; Chung and Wang, 2013). Cuttlebone growth during ontogenetic development is through continuous lamellar formation. Although one layer does not follow the 1-day rule (Bettencourt and Guerra, 2001; Chung and Wang, 2013), the cuttlebone still records environmental and internal physiological signals over its lifetime.

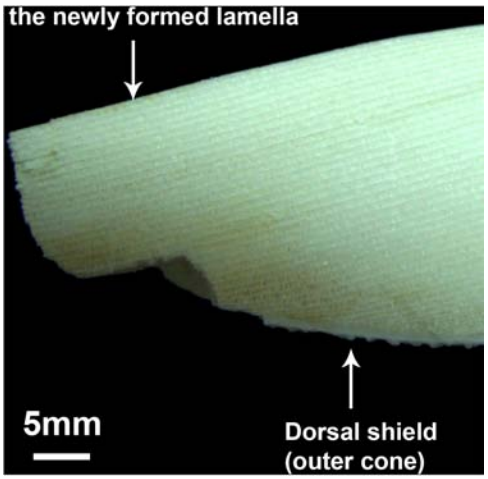

FIGURE 1 | Longitudinal transection of a cuttlebone. The layers represent the structural units, lamellae, of the inner cone of a cuttlebone.

The similar lengths of the cuttlebone and mantle imply a coupling of the calcification rate of the cuttlebone to the growth rate of the cuttlefish. This means that biological factors may influence the incorporation of elements into the cuttlebone. In addition, the rate of lamellar formation can be as high as 1.5 mm every 1.75 days in *Sepia pharaonis* (Chung and Wang, 2013), which is much more rapid in comparison with other biogenic aragonite carbonate observed for example, in statoliths, otoliths, corals, and bivalve shells. Therefore, further studies on Me/Ca ratios are required, particularly Li/Ca, Mg/Ca, and Sr/Ca ratios, with regard to the effects of growth rate on elemental incorporation in cuttlebone.

The pharaoh cuttlefish, *S. pharaonis*, is the species of interest in the present study. The species is widely distributed in the Indo-Pacific Ocean and harvested heavily by coastal fisheries. Overfishing in the region highlights the urgent need for the protection of their juveniles (Mehanna et al., 2014). In the coastal waters around Taiwan, the species is relatively larger than other cuttlefish species, implying that they have a more rapid growth rate (Lu and Chung, 2017). Although the species has a short lifespan and generally exhibits rapid growth, few studies have explored its growth rate, growth phases, and growth trends across life stages and among different populations (Minton, 2004), which potentially hampers fishery resource management efforts. If the elemental ratios observed in cuttlebone could be validated as a useful proxy, it could be a powerful tool for monitoring cuttlefish growth in the field and improve upon the traditional approach, lamellar measurement. Because lamellar formation rate is inconsistent under different environments, across different cuttlefish life stages, and between cuttlefish species (Chung and Wang, 2013), its use for measurement may bias the determination of growth rate in wild cuttlefish.

To evaluate elemental incorporation in *S. pharaonis* cuttlebone, we applied three strategies to investigate the relationship between cuttlebone Me/Ca ratios and growth rate and temperature. The first method was a controlled laboratory experiment in which cuttlefish hatchlings were reared for 1 month at three different temperatures (20, 25, and 30°C) to evaluate the relationships between cuttlebone elemental incorporation and temperature and cuttlebone growth rate. The second method involved evaluating the effect of growth rate and temperature on Me/Ca ratios in wild cuttlefish that were captured monthly in the course of a year. Then, maturity and sex were assessed as potential physiological factors influencing the results. The third method involved using relative growth condition factor (Kn) values, which were compared with the Me/Ca ratio to evaluate whether there is a relationship between cuttlefish size and cuttlebone chemistry in wild populations. The Kn value indicates the individual body mass above ($Kn > 1$) or below ($Kn < 1$) the population average at a given mantle length (Bello, 2006). The results of these three tests provided

information on cuttlebone chemistry and demonstrated potential for the application of Me/Ca ratios as a geochemical proxy.

MATERIALS AND METHODS

Laboratory-Controlled Experiment

The rearing experimental design is described in detail in Chung and Wang (2013), and cuttlebones used in the present study were from the previous study. In short, egg capsules and hatchlings of cuttlefish, *S. pharaonis,* were reared in a temperature-controlled environment at 20, 25, and 30°C. After hatching, the cuttlefish were immersed immediately in seawater containing alizarin complexone (25 ppm) for 3 h before being reared in controlled environments for 1 month. At 1-month, 10–11 individuals were selected at random from each of the three temperature treatments. Mantle length and body weight were recorded for each hatchling. The cuttlebone was dissected from each capsule, ultrasonically cleaned with 10% H_2O_2 to remove adherent tissues, and washed three times with MilliQ water. The samples were dried overnight in the oven at 40°C before being stored in acid-cleaned vials. Carbonate growth during the rearing period was estimated by measuring the alizarin complexone staining band to the end of the last septum, after which the growth rate was obtained by dividing the increase in length by 30 (the number of rearing days).

Rearing seawater was prepared by using a commercial product of sea salt. The rearing seawater was collected directly from the rearing tank with acid-washed syringes and immediately filtered using 0.22-μm filters, acidified through the addition of ultrapure concentrated HNO_3 (J. T. Baker) to maintain pH at 1, and then stored in a freezer. Rearing seawater was collected at least once a week during the rearing period. Samples were diluted in a series of concentrations up to 500-fold and analyzed using inductively coupled plasma optical emission spectrometry (ICP-OES, Thermo Fisher Scientific) at the Isotope Geochemistry Lab, Department of Earth Sciences, National Cheng Kung University, Taiwan. An in-house standard with multiple elements (Li, Mg, Ca, Sr) was prepared by using single element standards (HPS High-Purity Standards, United States) and measured in comparison with a reference material, NIST SRM 1640 (Trace Elements in Natural Water, National Institute of Standards and Technology, United States). The validation of in-house standard was through repeating measurements over 6 months, and the measurements for all elements showed a relative standard deviation lower than 3%. In addition, a percentage error for all element was lower than 3% with respect to NIST SRM 1640 (the difference between a measured and certified value, divided by the certified value and then multiplied by 100%). Then, the in-house standard was used to generate calibration curves for four selected elements. NIST SRM 1643e (Trace Elements in Water, National Institute of Standards and Technology, United States) was used in the samples analysis procedure to determine accuracy of analysis, which was observed to be lower than 2% of percentage error for all elements (Li: 1.9%; Mg: 0.8%; Ca: 0.5%; Sr: 1.2%). In addition, the matrix effect on elemental concentrations was monitored and calibrated by an in-house seawater standard. The limit of detection (LOD) and limit of quantification (LOQ) ranged from 5 to 15 μg/L for four elements in the analyses (see details in **Supplementary Material**). Me/Ca ratios were calculated and applied in the subsequent statistical analyses and discussions.

Cuttlebone growth patterns are discriminative, and the outermost portion of cuttlebone was obtained for chemical analyses. Organic matter in the lamellar microstructure (Florek et al., 2009), which cannot be degraded in the cleaning procedure using H_2O_2, may bias the chemical concentration of cuttlebone carbonate. Therefore, pieces of cuttlebone were immersed overnight in reagent grade 6% NaClO to degrade structural organic material. After removing the supernatant solution, the cuttlebone sample that remained in the vials was immersed in MilliQ water for ultrasonic cleaning for 1 min. The samples were washed in MilliQ water three times, and then the cuttlebone samples were transferred to a new acid-washed vial and subjected to three additional MilliQ cleanings of 1 min each using an ultrasonic cleaner. After cleaning, the cuttlebone was dissolved in 0.3 N HNO_3 and diluted to 100 ppm Ca. High-resolution inductively coupled plasma mass spectrometry (HR-ICP-MS; Thermo Fisher Scientific, Element 2) was used to analyze samples at the Isotope Geochemistry Lab, Department of Earth Sciences, National Cheng Kung University, Taiwan. The aragonite reference material, FEBS-1 (Otolith-certified reference material for trace metals, National Research Council, Canada) was used to determine the element concentrations in samples, and JCp-1 (coral standards) was measured every nine samples as an internal standard to monitor the instrument drift. The measured elemental concentration of JCp-1 was also checked against certified values to ensure that the analysis was accurate and precise. Four isotopes were analyzed in low-resolution mode: ^{7}Li, ^{25}Mg, ^{43}Ca, and ^{86}Sr. The LOD and LOQ ranged from 0.03 to 5 μg/L, depending on the element (see details in **Supplementary Material**). Precision of analyses (RSD) was Li/Ca: 5.2%, Mg/Ca: 4.0%, Sr/Ca: 3.8%, and accuracy (% error) was Li/Ca: 9.9%, Mg/Ca: -4.7%, Sr/Ca:4.6%.

The elemental partition coefficient was calculated as follows:

$$D_{Me/Ca} = \frac{Me/Ca_{cabonate}}{Me/Ca_{rearing\ seawater}}$$

An average value from each temperature-controlled tank was applied to the $Me/Ca_{rearing\ seawater}$ value to determine individual $D_{Me/Ca}$ values. First, we used the Shapiro–Wilk test to evaluate the normality of data and Levene's test to examine the equality of variances among temperature treatments. A one-way analysis of variance (ANOVA), a Welch's ANOVA (for heterogeneity), or a Kruskal–Wallis test (for non-normal distribution) was conducted to evaluate the effect of water temperature on rearing seawater Me/Ca, $D_{Me/Ca}$, and cuttlebone growth rate. A follow-up Pearson's correlation test was performed to examine the relationship between $D_{Me/Ca}$ and cuttlebone growth rate.

Wild Cuttlefish

Sepia pharaonis were collected predominantly at depths of between 30 and 60 m off Donggang, on Taiwan's southwestern coast (DG population) and between depths of 2 and 10 m

around the Penghu Islands in the Taiwan Strait (PH population) from September 2009 to December 2010. The samples were collected by trawling, and latitude, longitude, and depth data were recorded. The 208 captured cuttlefish were weighed, their mantle lengths measured, and their stage of maturity estimated based on the Workshop on Sexual Maturity Staging of Cephalopods (ICES, 2010) criteria. One hundred sixty-four specimens from the DG population were used for the evaluation of the effects of temperature and growth rates on Me/Ca ratios as well as for assessing relationships between male and female cuttlefish and between different maturity stages (1 to 3a; 1: immature, 2a: developing, 2b: maturing, and 3a: mature). In the case of the PH population, only individuals that had reached stage 3a (n = 40) were selected for comparison with the DG population on the basis of Me/Ca ratios. In both populations, growth condition was assessed after calculating Kn according to the following equation (Bello, 2006):

$$\mathrm{Kn} = \mathrm{W_i}/\alpha \mathrm{ML}^{\beta}$$

where W_i is the individual body mass (g), ML is the mantle length, and α and β are the parameters estimated from the weight–length relationships of different populations (DG population, α: 3.71×10^{-4} and β: 2.74; PH population: α: 5.66×10^{-4} and β: 2.65).

After dissection from the mantle, cuttlebones were cleaned using 10% H_2O_2 to remove clinging tissue and washed three times with MilliQ water. They were then dried in an oven at 40°C for 48 h before being cut longitudinally. The width of the final lamella of each cuttlebone was measured to assess the growth rate of cuttlebone carbonate at the time of capture, considering one lamella was consistently formed approximately every 1.75 days from the juvenile stage (Chung and Wang, 2013). The carbonate powder of the last increment was sampled using a dissecting needle. Powder samples were immersed in reagent grade 6% NaClO and maintained overnight to degrade structural organic matter, washed three times with MilliQ water, transferred to a new acid-washed vial, and washed three more times with MilliQ water. All procedures were similar to the steps applied for the reared cuttlefish. The cleaned powder was dissolved in 0.3 N HNO_3 and diluted to a concentration of 100 ppm Ca. Samples were analyzed using HR-ICP-MS (Thermo Fisher Scientific, Element XR) at the Institute of Earth Sciences, Academia Sinica, Taiwan. The Me/Ca ratios in the cuttlebone were measured using an in-house standard, the Me/Ca ratios of which had been certified. Repeated measurements of FEBS-1 indicated the precision and accuracy of the analysis. Four isotopes were analyzed in low-resolution mode: ^{7}Li, ^{25}Mg, ^{43}Ca, and ^{86}Sr. The LOD and LOQ ranged from 0.1 to 15 μg/L, depending on the element (see details in **Supplementary Material**). RSD values were 3.2, 7.2, and 2.1% for Li/Ca, Mg/Ca, and Sr/Ca, respectively, and accuracies (% error) were -3.1, -3.8, and -0.3%, respectively.

Natural seawater was collected regularly from October 2009 to November 2010 in the DG population area and from November 2009 to November 2010 in the PH population area. The daily sea surface temperature at the sampling locations was derived from the database of the Central Weather Bureau, Taiwan[1]. The collected water samples were filtered with acid wash syringes and 0.22-μm filters, acidified through the addition of ultrapure concentrated HNO_3 (J. T. Backer) to maintain the pH at 1, and then stored under freezing conditions. NASS-6 (Seawater reference material for trace metals, National Research Council Canada) was used to determine water elemental concentrations in a series of dilutions from 100 to 300-fold and measured after every nine samples to monitor instrumental drift. The measurement of 200-fold diluted CASS-4 (Nearshore seawater certified reference material for trace metals and other constituents, National Research Council Canada) provided the accuracy measurements of the elemental concentrations (% error: -8.3, 9.1, 4.6, and -1.4% for Li, Mg, Sr, and Ca, respectively. Samples were diluted 200-fold and analyzed using HR-ICP-MS (Thermo Fisher Scientific, Element XR) at the Institute of Earth Sciences, Academia Sinica, Taiwan. The LOD and LOQ ranged from 0.03 to 10 μg/L, depending on the element (see details in **Supplementary Material**).

We first evaluated the variation of Me/Ca in natural seawater in a time series using an ordinary least squares estimation. Where seawater Me/Ca ratio was demonstrated to not be significantly different in the course of the sampling period, cuttlebone Me/Ca ratios were used directly in subsequent statistical analyses instead of the elemental partition coefficient. Subsequently, the effect of temperature and growth rate, as well as growth rate nested in temperature, were assessed using a multiple linear regression model with backward selection. The model with the best fit was selected based on the lowest Akaike information criterion. The third step was to execute multiple linear regression models to examine the effect of sex and maturity on the relationship between cuttlebone Me/Ca and growth rate. All statistics were performed in R (R Core Team, 2018), and figures were made using the ggplot2 package in R (Wickham, 2009).

RESULTS

Laboratory-Controlled Experiment

The average temperatures recorded for the ideal range in an experimental design were 20.3 ± 0.2°C, 25.4 ± 0.3°C, and 30.6 ± 0.7°C (using a WTW COND 3310 Multi-Mode Water Meter, Kenelec Scientific). The influence of temperature on hatchling growth was significant, with mantle length and body weight both being larger at lower temperatures (one-way ANOVA. Mantle length: n = 31, df = 2, F-value = 116, $p < 0.01$. Body weight: n = 31, df = 2, F-value = 180, $p < 0.01$; **Table 1**). Similarly, cuttlebone grew significantly faster toward lower temperatures (one-way ANOVA, n = 31, df = 2, F-value = 76.7, $p < 0.01$; **Table 1**).

$Sr/Ca_{rearing\ seawater}$ and $Mg/Ca_{rearing\ seawater}$ values varied significantly between temperature treatments (Kruskal–Wallis test. $Sr/Ca_{rearing\ seawater}$: df = 2, chi-squared = 10.62, $p < 0.01$; $Mg/Ca_{rearing\ seawater}$: df = 2, chi-squared = 6.62, p = 0.03); however, no differences were observed for $Li/Ca_{rearing\ seawater}$ values (Kruskal–Wallis test: df = 2, chi-squared = 2.03, p = 0.36;

[1]https://e-service.cwb.gov.tw/wdps/

TABLE 1 | Results of laboratory-controlled experiments with three temperature treatments.

	Cuttlefish				Cuttlebone Me/Ca			Rearing seawater Me/Ca		
Group (°C)	Sample number	Mantle length (mm)	Body weight (g)	Cuttlebone growth rate (mm/day)	Li/Ca (umol/mol)	Mg/Ca (mmol/mol)	Sr/Ca (mmol/mol)	Li/Ca (mmol/mol)	Mg/Ca (mol/mol)	Sr/Ca (mmol/mol)
20	10	15.7 ± 0.86	0.72 ± 0.06	0.27 ± 0.03	7.36 ± 1.49	16.2 ± 4.84	0.41 ± 0.05	1.32 ± 0.16	4.96 ± 0.64	0.78 ± 0.06
25	10	11.6 ± 1.27	0.31 ± 0.09	0.11 ± 0.04	3.82 ± 0.64	5.87 ± 2.21	0.57 ± 0.07	1.47 ± 0.33	5.40 ± 1.10	0.90 ± 0.19
30	11	8.79 ± 0.89	0.15 ± 0.06	0.08 ± 0.04	3.21 ± 0.32	4.27 ± 1.51	0.44 ± 0.12	1.20 ± 0.014	5.57 ± 0.05	0.57 ± 0.06

details shown in **Table 1**). After $Me/Ca_{rearing\ seawater}$ had been calibrated and elemental partition coefficients had been determined, $D_{Li/Ca}$ and $D_{Mg/Ca}$ showed a decreasing trend with temperature increases (one-way Welch's ANOVA, $D_{Li/Ca}$: $df = 2$, F-value = 639, $p < 0.01$; $D_{Mg/Ca}$: $df = 2$, F-value = 59.6, $p < 0.01$; **Figure 2**). Contrariwise, $D_{Sr/Ca}$ showed a significantly increasing trend with an increase in temperature (one-way Welch's ANOVA, $df = 2$, F-value = 34.9, $p < 0.01$; **Figure 2**). Different growth rates were observed among temperature groups, and they were significantly correlated with the elemental partition coefficients, with a positive trend for $D_{Li/Ca}$ and $D_{Mg/Ca}$ and a negative trend for $D_{Sr/Ca}$ (Pearson's correlation, $D_{Li/Ca}$: $df = 23$, $t = 11.2$, $p < 0.01$, $r = 0.919$; $D_{Mg/Ca}$: $df = 26$, $t = 8.31$, $p < 0.01$, $r = 0.852$; $D_{Sr/Ca}$: $df = 27$, $t = -5.73$, $p < 0.01$, $r = -0.741$; **Figure 2**).

Wild Cuttlefish

The 168 individual cuttlefish captured in the DG population comprised 96 females and 72 males (**Table 2**). Few were immature (maturity stage 1), and the largest proportion of specimens for both sexes was at stage 3. Both mantle length and body mass were generally larger in females at every maturity stage.

Sea surface temperature during the sampling period ranged from 24 to 31°C, and seawater Me/Ca values were fairly

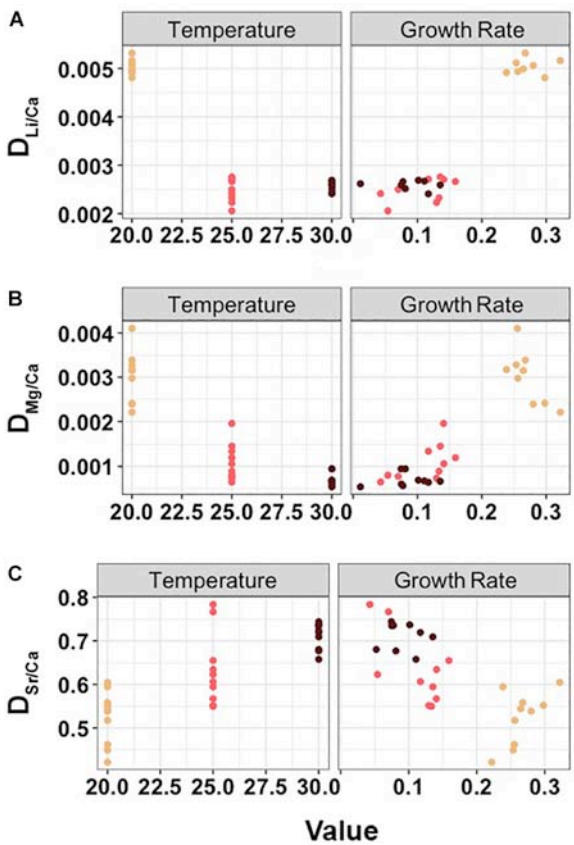

FIGURE 2 | Partition coefficients of Li/Ca **(A)**, Mg/Ca **(B)** and Sr/Ca **(C)** among temperature groups and in relation to cuttlebone growth rate.

TABLE 2 | Wild cuttlefish data used to evaluate cuttlebone Me/Ca (element/calcium) ratios (1, immature; 2a, developing; 2b, maturing; and 3a, mature).

Cuttlefish						Cuttlebone			
Population	**Gender**	**Maturity stage**	**Sample number**	**Mantle length (cm)**	**Body Weight (Kg)**	**Width of the last increment (mm)**	**Li/Ca (umol/mol)**	**Mg/Ca (mmol/mol)**	**Sr/Ca (mmol/mol)**
DG	F	1	8	12.91 ± 2.40	0.26 ± 0.13	0.48 ± 0.06	14.02 ± 2.01	1.74 ± 0.86	3.56 ± 0.13
		2a	34	15.93 ± 3.45	0.46 ± 0.27	0.45 ± 0.05	14.37 ± 1.69	1.66 ± 0.70	3.53 ± 0.24
		2b	10	17.24 ± 3.58	0.57 ± 0.36	0.44 ± 0.05	14.67 ± 1.26	2.13 ± 1.50	3.55 ± 0.28
		3a	44	23.51 ± 3.77	1.25 ± 0.50	0.36 ± 0.10	12.17 ± 2.15	2.07 ± 1.37	4.01 ± 0.52
	M	1	1	12.7	0.23	0.54	15.40	2.16	3.36
		2a	17	15.83 ± 2.90	0.44 ± 0.25	0.43 ± 0.05	14.36 ± 1.46	1.84 ± 0.69	3.60 ± 0.22
		2b	19	16.69 ± 4.23	0.51 ± 0.33	0.45 ± 0.05	14.87 ± 0.71	1.87 ± 0.87	3.40 ± 0.23
		3a	35	20.89 ± 5.87	0.96 ± 0.65	0.38 ± 0.08	13.60 ± 1.81	1.88 ± 0.77	3.79 ± 0.38
PH	F	3a	18	25.33 ± 3.20	1.41 ± 0.40	NA	11.13 ± 1.53	1.87 ± 0.42	4.05 ± 0.35
	M	3a	22	25.48 ± 6.01	1.55 ± 0.99	NA	12.85 ± 2.53	1.75 ± 0.55	3.69 ± 0.45

consistent and not significantly different across months and years, with the average values being 2.38 ± 0.08, 28.0 ± 5.61, and 7.57 ± 0.92 mmol/mol for Li/Ca, Mg/Ca, and Sr/Ca, respectively (**Table 3**). There was negligible variation in seawater Me/Ca with time; therefore, instead of an element partition coefficient, cuttlebone Me/Ca values in wild cuttlefish were used in the subsequent statistical analyses.

Multiple linear regression models with a backward selection method were applied to determine the best-fit model that described the levels of the effects of temperature and growth rate on Me/Ca ratios. For all three Me/Ca ratios, the best fit was explained by temperature and growth rate (increment width) with no interaction between the two factors, and the residuals in the best-fit model showed normality and homogeneity. Temperature and growth rate (increment width) explained 56% and 43% of the variation in cuttlebone Li/Ca and Sr/Ca ratios, respectively, but no significance of variables was observed in cuttlebone Mg/Ca. The model showed that growth rate contributed to more variation in the cuttlebone Li/Ca and Sr/Ca ratios than temperature. For example, a 1°C increase in temperature reduced the cuttlebone Li/Ca ratio by 0.11, and a 7°C difference in overall temperature records changed cuttlebone Li/Ca ratio by only 0.77. The difference was negligible when compared with the 7.6 to 18.4 cuttlebone Li/Ca ratio range. Similarly, temperature had a minor influence on cuttlebone Sr/Ca values, which fell by only 0.024 with each 1°C decrease in temperature. Therefore, we normalized the temperature at 24°C for both Li/Ca and Sr/Ca values and examined how Me/Ca and growth rate were related both between the sexes and at different maturity stages.

The temperature-corrected cuttlebone Li/Ca ratio increased linearly with an increase in growth rate, and there was no difference in slope between female and male cuttlefish. However, the intercept value was higher for the male cuttlefish (**Table 4** and **Figure 3**). The linear relationship was consistent at most of the maturity stages and in either sex, with the exception of females at stage 2a and males at stage 2b. Conversely, the temperature-corrected cuttlebone Sr/Ca ratio decreased exponentially with an increase of growth rate, and the Sr/Ca ratio trend was similar between both sexes and in the maturity stages, with the exception of females at stage 2a (**Table 4** and **Figure 3**).

TABLE 3 | Linear regression analysis (ordinary least squares) of natural seawater Me/Ca (element/calcium) in time series.

	df	Mean square	*F*-value	*p*-value
Li/Ca				
Year	1	5.44×10^{-4}	0.09	0.77
Month	8	1.08×10^{-2}	1.82	0.14
Residuals	19	5.94×10^{-3}		
Mg/Ca				
Year	1	31.45	0.79	0.39
Month	8	11.87	0.30	0.96
Residuals	19	39.71		
Sr/Ca				
Year	1	0.13	0.11	0.74
Month	8	0.27	0.24	0.98
Residuals	19	1.13		

Comparisons Between Two Populations From Different Areas

Forty cuttlefish at stage 3a were captured from the PH population, comprising 18 females and 22 males (**Table 2**). The females were smaller than the males, which was opposite to the trend observed in the cuttlefish from the DG population. Sea surface temperatures ranged from 19.5 to 26.3°C, and temperature correction of cuttlebone Li/Ca and Sr/Ca ratios followed the aforementioned approaches, where Li/Ca and Sr/Ca values were normalized at 24°C and calibrated as -0.11 and -0.024 per°C, respectively. We modeled temperature-corrected Me/Ca ratios with Kn between populations. **Table 5** summarizes the model output and displays a significant positive relationship between temperature-corrected Li/Ca ratios and Kn. However, the slope was different between populations of females from each of the study sites. A reverse trend for Kn was revealed in the temperature-corrected Sr/Ca ratio, and the significance was only observed in females.

TABLE 4 | Multiple linear regression analyses of temperature-corrected cuttlebone Me/Ca (element/calcium) between sexes and among maturity stages.

		Estimated	Std. error	*t*-value	*p*-value	R2
Temperature-corrected Li/Ca						
Gender	Intercept	7.09	0.53	13.31	<0.01*	0.56
	Increment	16.77	1.27	13.25	<0.01*	
	GenderM	0.58	0.21	2.76	<0.01*	
Female:	Intercept	6.61	0.75	8.76	<0.01*	0.62
Stage	Increment	16.90	2.02	8.36	<0.01*	
	Stage1	−0.30	4.68	−0.06	0.95	
	Stage2a	8.11	2.28	3.55	<0.01*	
	Stage2b	1.74	4.32	0.40	0.69	
	Increment: Stage1	1.49	9.84	0.15	0.88	
	Increment: Stage2a	−16.37	5.21	−3.15	<0.01*	
	Increment: Stage2b	−1.56	10.01	−0.16	0.88	
Male:	Intercept	6.76	0.94	7.17	<0.01*	0.58
Stage	Increment	19.10	2.42	7.89	<0.01*	
	Stage1	−1.35	1.10	−1.23	0.22	
	Stage2a	−0.10	2.67	−0.04	0.97	
	Stage2b	8.98	2.51	3.57	<0.01*	
	Increment: Stage1	NA	NA	NA	NA	
	Increment: Stage2a	0.38	6.23	0.06	0.95	
	Increment: Stage2b	−20.33	5.68	−3.58	<0.01*	
Temperature-corrected Sr/Ca						
Gender	Intercept	2.88	0.09	33.66	<0.01*	0.43
	Ln(Increment)	−0.95	0.10	−10.59	<0.01*	
	GenderM	−0.004	0.04	−0.11	0.92	
Female:	Intercept	2.99	0.14	20.90	<0.01*	0.50
Stage	Ln(Increment)	−0.91	0.13	−6.82	<0.01*	
	Stage1	0.14	0.65	0.22	0.83	
	Stage2a	0.54	0.34	1.61	0.11	
	Stage2b	0.19	0.61	0.32	0.75	
	Ln(Increment): Stage1	0.29	0.85	0.35	0.73	
	Ln(Increment): Stage2a	0.82	0.40	2.07	0.04*	
	Ln(Increment): Stage2b	0.38	0.72	0.53	0.60	
Male:	Intercept	2.89	0.20	14.61	<0.01*	0.40
Stage	Ln(Increment)	−0.98	0.20	−4.92	<0.01*	
	Stage1	−0.10	0.24	−0.42	0.68	
	Stage2a	0.59	0.50	1.18	0.24	
	Stage2b	0.63	0.51	1.24	0.22	
	Ln(Increment): Stage1	NA	NA	NA	NA	
	Ln(Increment): Stage2a	0.71	0.58	1.24	0.22	
	Ln(Increment): Stage2b	0.98	0.63	1.55	0.13	

*Significance: $p < 0.05$.

DISCUSSION

Elemental incorporation into inorganic carbonates should adhere to thermodynamic and kinetic laws, but elemental signals recorded in biogenic carbonates deviate from the scheme due to the influence of physiological factors. Me/Ca ratios in biogenic aragonite carbonate have been studied in bivalve shells, coral, and fish otoliths. However, relatively few studies have been conducted on cephalopod hard structures such as statoliths and cuttlebone. To the best of our knowledge, this represents the first study to assess Li/Ca, Mg/Ca, and Sr/Ca ratios in cuttlebone carbonate. Its functional structure makes cuttlebone unique among biogenic aragonite carbonates because growth or lamellar formation is closely correlated with an increase in mantle length. Our results show that both temperature and growth rates influence elemental incorporation, with some variations across the elements studied. We compared the results of controlled experiments in the laboratory with data obtained from wild cuttlefish in the field to comprehensively evaluate the factors influencing trace element incorporation.

Li/Ca

The relationship between Li/Ca and temperature is not consistent among all biogenic carbonates. Thermodynamics would predict an increase in carbonate Li/Ca with an increase in temperature (Hall and Chan, 2004), and that is the case in the shells of some bivalve species (Thébault et al., 2009). However, temperature has a negative effect on the Li/Ca ratio in corals, brachiopods, benthic foraminifera (Marriott et al., 2004b; Raddatz et al., 2013) and cuttlebone in the present study. According to the exponential curve of the temperature-dependent relationship demonstrated by Marriott et al. (2004a), cuttlebone $D_{Li/Ca}$ decreases 6.6% per°C, which is a higher rate than in inorganic calcite (4.6% per°C, Marriott et al., 2004a) and in *Porites* coral (4.9% per°C, Marriott et al., 2004a) but not as high as in cold water coral (*Lophelia pertusa*, 7.3% per°C, Raddatz et al., 2013). However, the effect of temperature on cuttlebone $D_{Li/Ca}$ values was not evaluated based on similar growth rate. Therefore, the effect could be overestimated when an increasing growth rate in the warmer environment increases the $D_{Li/Ca}$ values.

Growth rate and temperature are both important factors that contribute to the variation in cuttlebone Li/Ca ratios in wild cuttlefish. The range of temperature in natural habitats is 7°C, which is less than the laboratory test range of 10°C. In addition, wild specimens exhibit more variable growth rates. Therefore, we evaluated the growth rate in wild cuttlebone by correcting the influence of temperature on the wild cuttlebone Li/Ca ratio. After temperature correction, the Li/Ca ratio presented a convincing linear and positive relationship with cuttlebone growth rates (**Figure 3**). The positive relationship between carbonate Li/Ca values and calcification rates has been observed in synthetic aragonite (Gabitov et al., 2011) and mollusk shells (Thébault et al., 2009; Thébault and Chauvaud, 2013). In addition, the positive relationships further indicate that cuttlebone Li/Ca is a potential proxy for cuttlefish growth based on increases in cuttlebone Li/Ca values.

Before using cuttlebone Li/Ca as a proxy for growth rate, we evaluated the Li/Ca relationship between sexes and among maturity stages. There were no differences in the slopes between cuttlebone Li/Ca ratios and growth rates at maturity between females and males, excluding females at the 2a stages and males at the 2b stages (**Figure 3**). Uncoupling of cuttlebone Li/Ca and increased width may be due to a change in the frequency of lamellar formation, which could be associated with life stage (Chung and Wang, 2013), food availability (le Goff et al., 1998; Martínez et al., 2011), breeding (le Goff et al., 1998),

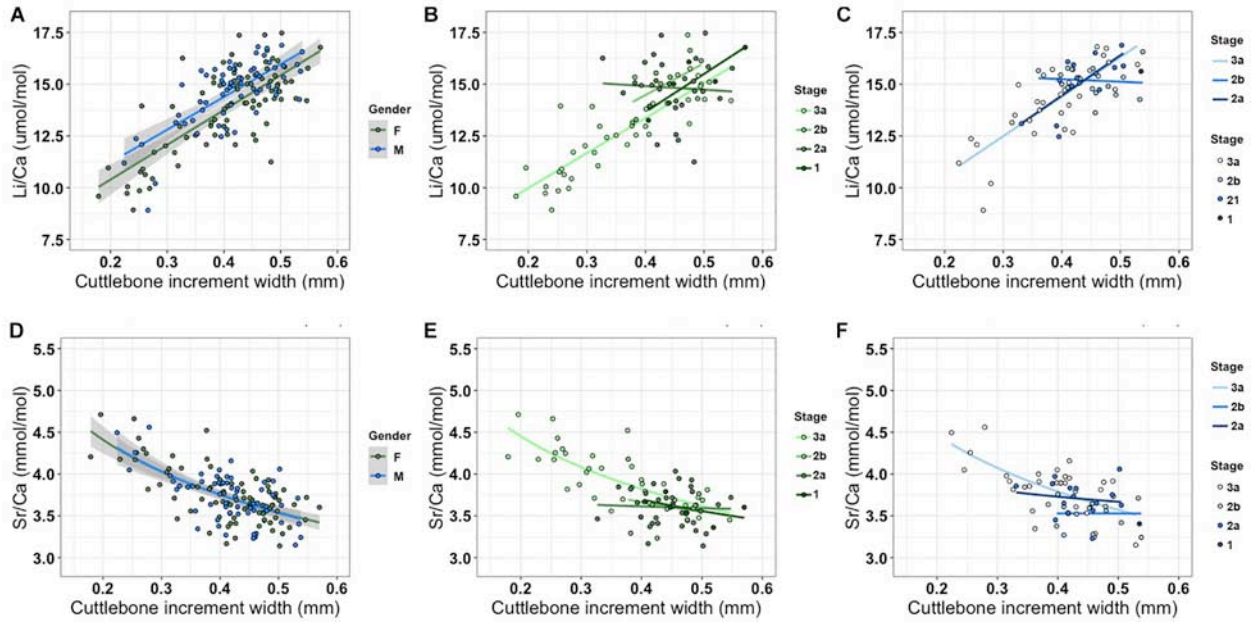

FIGURE 3 | Relationship between temperature-corrected Li/Ca **(A–C)** and Sr/Ca **(D–F)** and the width of last increment in cuttlebone. Increment width refers to the growth rate in wild cuttlefish. Comparisons among maturity stages are given for females **(B,E)** and males **(C,F)**. Results of multiple linear regression are presented in **Table 4** (1, immature; 2a, developing; 2b, maturing; and 3a, mature).

TABLE 5 | Multiple linear regression analyses of temperature-corrected cuttlebone Me/Ca (element/calcium) with Kn (relative growth condition) values between two populations (DG and PH).

	Estimated	Std. error	*t*-value	*p*-value	R2
Temperature-corrected Li/Ca: Female					
Intercept	−3.35	3.47	−0.97	0.34	0.32
Kn	15.74	3.43	4.58	<0.01*	
Location PH	13.94	5.04	2.77	<0.01*	
Kn: Population PH	−15.39	4.88	−3.15	<0.01*	
Temperature-corrected Li/Ca: Male					
Intercept	6.29	3.19	1.97	0.05	0.26
Kn	7.87	3.26	2.42	0.02*	
Location PH	−3.93	4.63	−0.85	0.40	
Kn: Population PH	2.35	4.64	0.51	0.61	
Temperature-corrected Sr/Ca: Female					
Intercept	6.54	0.89	7.32	<0.01*	0.15
Kn	−2.53	0.87	−2.90	<0.01*	
Location PH	−1.09	1.14	−0.96	0.34	
Kn: Population PH	1.15	1.10	1.05	0.30	
Temperature-corrected Sr/Ca: Male					
Intercept	4.68	0.67	7.02	<0.01*	0.12
Kn	−0.85	0.68	−1.26	0.22	
Location PH	0.45	0.95	0.47	0.64	
Kn: Population PH	−0.62	0.95	−0.65	0.52	

*Significance: $p < 0.05$.

or mechanical buoyancy control (Denton and Gilpin-Brown, 1961). Overall, the cuttlebone Li/Ca ratio could be applied as a growth proxy in most maturation stages; however, further investigations into the uncoupling trends observed in the present study are required.

Mg/Ca

There has been a lot of discussion on the application of carbonate Mg/Ca values in paleotemperature reconstructions. Abiotic aragonite obtained from a precipitation experiment showed that the $D_{Mg/Ca}$ values were negative and decreased exponentially with a decrease in temperature (Gaetani and Cohen, 2006). However, planktonic foraminifera (Lea, 2003), coral (Gagnon et al., 2007; Reynaud et al., 2007), and mollusk shell Mg/Ca (Klein et al., 1996; Freitas et al., 2006) exhibited a positive relationship with temperature, although the slope varies based on taxa and species. The physiological regulation associated with growth or calcification rate potentially alters the partition coefficient of Mg incorporated into biogenic carbonate. For example, Reynaud et al. (2007) reported a direct temperature effect, temperature-induced growth, and light-induced growth as the three major factors influencing coralline Mg/Ca. Our controlled laboratory experiment confirmed that cuttlebone $D_{Mg/Ca}$ varies based on temperature and growth rate. We observed a negative trend between Mg/Ca and temperature in cuttlebone, which is consistent with the observation in abiotic aragonite. However, our results also revealed a growth rate associated with the variation in cuttlebone Mg/Ca. The mechanical underpinning of the growth rate effect on Mg/Ca in biogenic carbonate is unclear. For example, the Mg/Ca value of biogenic carbonate is positively correlated with growth rate in corals (Reynaud et al., 2007), but negatively correlated with growth rate in otoliths (Martin and Thorrold, 2005). The effect of growth rate is even species

dependent in bivalve shells (Carré et al., 2006; Schöne et al., 2011). Furthermore, there is no clear cuttlebone Mg/Ca incorporation trend in wild cuttlefish, either in relation to temperature or in relation to growth rate. The complex mechanism of the incorporation of Mg into biogenic carbonates has recently been explained by a metabolic control (DiMaria et al., 2010; Schöne et al., 2011). However, our results are limited to explain the metabolic effect on Mg/Ca ratio in cuttlebone and do not suggest that cuttlebone Mg/Ca is a proxy for any environmental or physiological condition with regard to wild cuttlefish.

Sr/Ca

According to thermodynamics, Sr/Ca ratios exhibit a negative relationship with temperature in inorganic aragonite (Kinsman and Holland, 1969) as well as in biogenic aragonite, such as corals (Goodkin et al., 2005; Gagnon et al., 2007; Reynaud et al., 2007) and squid statolith (Ikeda et al., 1998; Arkhipkin et al., 2004). Nevertheless, temperature may not influence cuttlefish statoliths (Zumholz et al., 2007) or may exhibit reverse influences on cuttlefish statoliths between prehatching and posthatchling (Gillanders et al., 2013). We also observed a contrary effect of temperature on cuttlebone Sr/Ca values, which was positive for reared cuttlefish but negative for wild cuttlefish. The observation could indicate other factors beyond the effect of temperature on cuttlebone Sr/Ca ratio.

Several studies have reported a considerable influence of calcification rate on biogenic carbonate Sr/Ca; for example, in corals (Reynaud et al., 2007) and in bivalve shells (Gillikin et al., 2005; Carré et al., 2006; Schöne et al., 2011). The influence of calcification rate on biogenic carbonate Sr/Ca could suppress the influence of temperature. In our controlled laboratory experiment, the positive relationship between temperature and cuttlebone $D_{Sr/Ca}$ is inconsistent with what has been observed in other biogenic carbonates as well as with theoretical predictions. When growth rate is taken into account in the evaluation of wild cuttlefish using a multiple linear regression model, the influence exerted by temperature on cuttlebone Sr/Ca is negative (linear relationship, -24 μmol/mol per°C), which is comparable to the observation for inorganic aragonite (linear relationship, -44 μmol/mol per°C; Gagnon et al., 2007). The finding reinforces the view that Sr/Ca ratio evaluation should consider growth rate.

However, the effect of growth rate on carbonate Sr/Ca values is not equal across all taxa and species because the effect could be positive, negative, or have no effect on shells in different bivalve species (Gillikin et al., 2005; Carré et al., 2006; Reynaud et al., 2007; Schöne et al., 2011; Zhao et al., 2017). Our findings in *S. pharaonis* cuttlebone are consistent with the results obtained for the shell of *Arctica islandica* (Schöne et al., 2011) but are inconsistent with the results of a precipitation experiment on abiotic aragonite (Gaetani and Cohen, 2006). According to Sturrock et al. (2015), blood Sr/Ca values and related physiological characteristics explain the reduced fish otolith Sr/Ca values while otolith growth increases. In such cases, physiological processes and body fluid chemistry influence the relationship between carbonate Sr/Ca and calcification rate in a way that could explain differences between taxa and species. Therefore, it would be inappropriate to use cuttlebone Sr/Ca as a proxy for growth rate currently due to the inconsistent findings in the literature and because the mechanism by which Sr/Ca in biogenic carbonate is influenced physiologically remains unclear.

Cuttlebone Li/Ca as an Indicator of Growth Rate in Wild Cuttlefish Populations

The Kn value represents a relative growth condition in animals: values higher than 1 signify greater weight than other individuals of the same length in a population, and values lower than 1 signify the reverse (Bello, 2006). Comparing individuals at stage 3a in both the DG and PH populations, it revealed a positive correlation between Kn values and temperature-corrected Li/Ca, indicating that individuals with superior growth conditions had higher growth rates; moreover, sex and location influence the pattern. For example, female cuttlefish from the DG population exhibited an increasing Kn trend that was relatively sharp compared with the trend in the PH population. However, the Kn trend was similar in male cuttlefish between the two populations (**Table 5** and **Figure 4**).

These Li/Ca and Kn value trends between sexes and populations provide information that could facilitate fishery

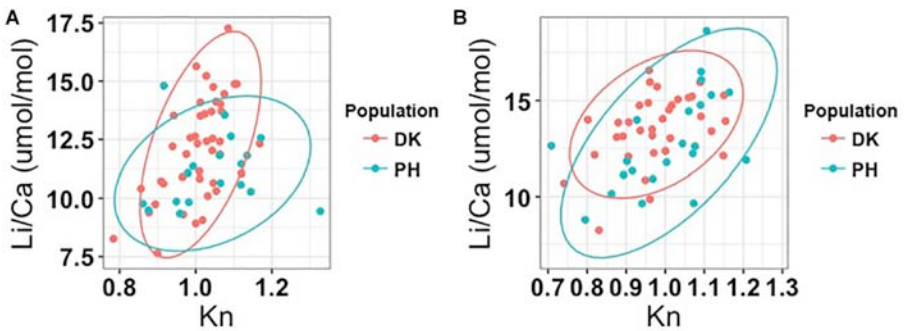

FIGURE 4 | Relationship between temperature-corrected Li/Ca and Kn (relative growth condition) values between two study populations. Only individuals at stage 3a were used in the analysis. Comparisons are given for females **(A)** and males **(B)**. Results of multiple linear regression are presented in **Table 5**.

management. For example, capturing cuttlefish with higher Kn values (better growth conditions) would imply removing bigger and heavier individuals from the ecosystem. At the same time, individuals with higher growth rates (higher Li/Ca values) are removed from the ecosystem. Such a strategy may exert a stronger effect on the females in the DG population than on the females in the PH population, because DG population has higher growth rates than PH population does at the same level of growth conditions. Consequently, low growth rate parents left in the ecosystem may produce low growth rate offspring. This phenomenon will be more obvious in the females of the DG population. Although, more investigations should be conducted on the relationships between elemental ratios and cuttlefish growth condition before a comprehensive tool for the management of cuttlefish fisheries can be developed, our results provide additional information for management and policy making to cuttlefish fisheries.

Implications

This study demonstrated that cuttlebone Li/Ca is a potential geochemical proxy that could enhance our understanding of cuttlefish growth and ecology. The proxy has a consistent relationship with cuttlebone growth rate in terms of mantle length growth rate. The use of a geochemical proxy has numerous benefits for cuttlefish ecology. First, it would be possible to reconstruct the growth rate history of an individual based on the results of the elemental analysis of cuttlebone carbonate formed at different life stages. Second, the elemental signals recorded in cuttlebone can be used to discriminate between populations and stocks (Ikeda et al., 1999; Turan and Yaglioglu, 2010). Integrating a growth rate proxy and other trace element signals would also facilitate the assessment of growth rates among identified population and stocks. Third, cuttlebone oxygen isotope values could reveal temperature regimes (Bettencourt and Guerra, 1999; Rexfort and Mutterlose, 2006). Applying a multiple geochemical approach along a cuttlebone growth transection enables the reconstruction of the life history of a cuttlefish and an understanding of its growth conditions at different temperatures. Finally, it could be possible to apply such proxies to ancient cephalopods such as belemnites (Ullmann et al., 2013; Immenhauser et al., 2016) through validation from modern cephalopod species such as cuttlefish in the study.

DATA AVAILABILITY STATEMENT

Publicly available datasets were analyzed in this study. All the data are presented in the manuscript.

ETHICS STATEMENT

Ethical review and approval was not required for the animal study because the study is using the biogenic carbonate structure, which was reserved by a previous published study.

AUTHOR CONTRIBUTIONS

C-HW led this work. C-HW and M-TC designed and conducted the experiments. M-TC and K-FH conducted the elemental analyses. C-FY assisted in the elemental analyses. C-CC assisted the wild cuttlefish collections. All authors contributed to the manuscript preparation.

FUNDING

This study was supported by the Ministry of Science and Technology, Taiwan (MOST 98-2628-B-007-001-MY3 and MOST 102-2621-B-019-006-MY3).

ACKNOWLEDGMENTS

We would like to thank Hui-Lun Chen and Lu-Peng Wang for assistance with cuttlefish collection, cuttlebone preparation, and measurement of lamellar widths, Dr. Hou-Chun Liu for assistance in water sample analyses, and Dr. Amy Featherstone for helpful suggestions for the manuscript. This manuscript was edited by Wallace Academic Editing.

SUPPLEMENTARY MATERIAL

The Supplementary Material for this article can be found online at: https://www.frontiersin.org/articles/10.3389/fmars.2019.00796/full#supplementary-material

REFERENCES

Arkhipkin, A. I., Campana, S. E., FitzGerald, J., and Thorrold, S. R. (2004). Spatial and temporal variation in elemental signatures of statoliths from the Patagonian longfin squid (*Loligo gahi*). *Can. J. Fish. Aquat. Sci.* 61, 1212–1224. doi: 10.1139/f04-075

Bath, G. E., Thorrold, S. R., Jones, C. M., Campana, S. E., McLaren, J. W., and Lam, J. W. H. (2000). Strontium and barium uptake in aragonitic otoliths of marine fish. *Geochim. Cosmochim. Acta* 64, 1705–1714. doi: 10.1016/S0016-7037(99)00419-6

Bello, G. (2006). Tentacle club length and body condition in the cuttlefishes *Sepia elegans* Blainville, 1827 and *Sepia orbignyana* Férussac, 1826 (Cephalopoda: Sepiidae). *Zool. Anz.* 244, 187–192. doi: 10.1016/j.jcz.2005.10.001

Bettencourt, V., and Guerra, A. (1999). Carbon- and oxygen-isotope composition of the cuttlebone of *Sepia officinalis*: a tool for predicting ecological information? *Mar. Biol.* 133, 651–657. doi: 10.1007/s002270050505

Bettencourt, V., and Guerra, A. (2001). Age studies based on daily growth increments in statoliths and growth lamellae in cuttlebone of cultured *Sepia officinalis*. *Mar. Biol.* 139, 327–334. doi: 10.1007/s002270100582

Birchall, J. D., and Thomas, N. L. (1983). On the architecture and function of cuttlefish bone. *J. Mater. Sci.* 18, 2081–2086. doi: 10.1007/BF00555001

Carré, M., Bentaleb, I., Bruguier, O., Ordinola, E., Barrett, N. T., and Fontugne, M. (2006). Calcification rate influence on trace element concentrations in aragonitic bivalve shells: evidences and mechanisms. *Geochim. Cosmochim. Acta* 70, 4906–4920. doi: 10.1016/j.gca.2006.07.019

Chang, M. Y., and Geffen, A. J. (2013). Taxonomic and geographic influences on fish otolith microchemistry. *Fish Fish.* 14, 458–492. doi: 10.1111/j.1467-2979.2012.00482.x

Chung, M.-T., and Wang, C.-H. (2013). Age validation of the growth lamellae in the cuttlebone from cultured *Sepia pharaonis* at different stages. *J. Exp. Mar. Biol. Ecol.* 447, 132–137. doi: 10.1016/j.jembe.2013.02.020

Corrège, T. (2006). Sea surface temperature and salinity reconstruction from coral geochemical tracers. *Palaeogeogr. Palaeoclimatol. Palaeoecol.* 232, 408–428. doi: 10.1016/j.palaeo.2005.10.014

Denton, E. J., and Gilpin-Brown, J. B. (1961). The distribution of gas and liquid within the cuttlebone. *J. Mar. Biol. Assoc. United Kingdom* 41, 365–381. doi: 10.1017/S0025315400023973

DiMaria, R. A., Miller, J. A., and Hurst, T. P. (2010). Temperature and growth effects on otolith elemental chemistry of larval Pacific cod, *Gadus macrocephalus*. *Environ. Biol. Fishes* 89, 453–462. doi: 10.1007/s10641-010-9665-2

D'Olivo, J. P., Sinclair, D. J., Rankenburg, K., and McCulloch, M. T. (2018). A universal multi-trace element calibration for reconstructing sea surface temperatures from long-lived *Porites* corals: removing "vital-effects.". *Geochim. Cosmochim. Acta* 239, 109–135. doi: 10.1016/j.gca.2018.07.035

Florek, M., Fornal, E., Gómez-Romero, P., Zieba, E., Paszkowicz, W., Lekki, J., et al. (2009). Complementary microstructural and chemical analyses of *Sepia officinalis* endoskeleton. *Mater. Sci. Eng. C* 29, 1220–1226. doi: 10.1016/j.msec.2008.09.040

Freitas, P. S., Clarke, L. J., Kennedy, H., Richardson, C. A., and Abrantes, F. (2006). Environmental and biological controls on elemental (Mg/Ca, Sr/Ca and Mn/Ca) ratios in shells of the king scallop *Pecten maximus*. *Geochim. Cosmochim. Acta* 70, 5119–5133. doi: 10.1016/j.gca.2006.07.029

Gabitov, R. I., Schmitt, A. K., Rosner, M., McKeegan, K. D., Gaetani, G. A., Cohen, A. L., et al. (2011). In situ δ7Li, Li/Ca, and Mg/Ca analyses of synthetic aragonites. *Geochem. Geophys. Geosyst.* 12:Q03001. doi: 10.1029/2010GC003322

Gaetani, G. A., and Cohen, A. L. (2006). Element partitioning during precipitation of aragonite from seawater: a framework for understanding paleoproxies. *Geochim. Cosmochim. Acta* 70, 4617–4634. doi: 10.1016/j.gca.2006.07.008

Gagnon, A. C., Adkins, J. F., Fernandez, D. P., and Robinson, L. F. (2007). Sr/Ca and Mg/Ca vital effects correlated with skeletal architecture in a scleractinian deep-sea coral and the role of Rayleigh fractionation. *Earth Planet. Sci. Lett.* 261, 280–295. doi: 10.1016/j.epsl.2007.07.013

Gillanders, B. M., Wilkinson, L. M., Munro, A. R., and de Vries, M. C. (2013). Statolith chemistry of two life history stages of cuttlefish: effects of temperature and seawater trace element concentration. *Geochim. Cosmochim. Acta* 101, 12–23. doi: 10.1016/j.gca.2012.10.005

Gillikin, D. P., Lorrain, A., Navez, J., Taylor, J. W., André, L., Keppens, E., et al. (2005). Strong biological controls on Sr/Ca ratios in aragonitic marine bivalve shells. *Geochem. Geophys. Geosyst.* 6:Q05009. doi: 10.1029/2004GC000874

Goodkin, N. F., Hughen, K. A., Cohen, A. L., and Smith, S. R. (2005). Record of little ice age sea surface temperatures at Bermuda using a growth-dependent calibration of coral Sr/Ca. *Paleoceanography* 20:A4016. doi: 10.1029/2005PA001140

Grammer, G. L., Morrongiello, J. R., Izzo, C., Hawthorne, P. J., Middleton, J. F., and Gillanders, B. M. (2017). Coupling biogeochemical tracers with fish growth reveals physiological and environmental controls on otolith chemistry. *Ecol. Monogr.* 87, 487–507. doi: 10.1002/ecm.1264

Hall, J. M., and Chan, L. H. (2004). Li/Ca in multiple species of benthic and planktonic foraminifera: thermocline, latitudinal, and glacial-interglacial variation. *Geochim. Cosmochim. Acta* 68, 529–545. doi: 10.1016/S0016-7037(03)00451-4

ICES (2010). *Report of the Workshop on Sexual Maturity Staging of Cephalopods (WKMSCEPH)*. Copenhagen: ICES.

Ikeda, Y., Arai, N., Sakamoto, W., Kodokoro, H., and Yoshida, K. (1998). Microchemistry of the Statoliths of the Japanese common squid *Todarodes pacificus* with special reference to its relation to the vertical temperature profiles of squid habitat. *Fish. Sci.* 64, 179–184. doi: 10.2331/fishsci.64.179

Ikeda, Y., Arai, N., Sakamoto, W., and Yoshida, K. (1999). Trace elements in cephalopod calcified tissue: cuttlebone as a possible tracer for life historical events of cuttlefish. *Int. J. PIXE* 09, 335–343. doi: 10.1142/S0129083599000437

Immenhauser, A., Schöne, B. R., Hoffmann, R., and Niedermayr, A. (2016). Mollusc and brachiopod skeletal hard parts: intricate archives of their marine environment. *Sedimentology* 63, 1–59. doi: 10.1111/sed.12231

Kinsman, D. J. J., and Holland, H. D. (1969). The co-precipitation of cations with CaCO3—IV. The co-precipitation of Sr2+ with aragonite between 16° and 96°C. *Geochim. Cosmochim. Acta* 33, 1–17. doi: 10.1016/0016-7037(69)90089-1

Klein, R. T., Lohmann, K. C., and Thayer, C. W. (1996). Bivalve skeletons record sea-surface temperature and δ18O via Mg/Ca and 18O/16O ratios. *Geology* 24, 415–418.

le Goff, R., Gauvrit, E., Pinczon Du Sel, G., and Daguzan, J. (1998). Age group determination by analysis of the cuttlebone of the cuttlefish *Sepia Officinalis* L. in reproduction in the bay of Biscay. *J. Mollus. Stud.* 64, 183–193. doi: 10.1093/mollus/64.2.183

Lea, D. W. (2003). "Elemental and isotopic proxies of past ocean temperatures," in *Treatise on Geochemistry*, eds H. Holland, and K. Turekian, (Amsterdam: Elsevier), 1–26. doi: 10.1016/B0-08-043751-6/06114-4

Lu, C. C., and Chung, W. S. (2017). *Guide to the Cephalopods of Taiwan*. Taichung: Huayu Nature Book Trade.

Marriott, C. S., Henderson, G. M., Belshaw, N. S., and Tudhope, A. W. (2004a). Temperature dependence of δ7Li, δ44Ca and Li/Ca during growth of calcium carbonate. *Earth Planet. Sci. Lett.* 222, 615–624. doi: 10.1016/j.epsl.2004.02.031

Marriott, C. S., Henderson, G. M., Crompton, R., Staubwasser, M., and Shaw, S. (2004b). Effect of mineralogy, salinity, and temperature on Li/Ca and Li isotope composition of calcium carbonate. *Chem. Geol.* 212, 5–15. doi: 10.1016/j.chemgeo.2004.08.002

Martin, G. B., and Thorrold, S. R. (2005). Temperature and salinity effects on magnesium, manganese, and barium incorporation in otoliths of larval and early juvenile spot *Leiostomus xanthurus*. *Mar. Ecol. Prog. Ser.* 293, 223–232. doi: 10.3354/meps293223

Martínez, P., Bettencourt, V., Guerra, A., and Moltschaniwskyj, N. A. (2011). How temperature influences muscle and cuttlebone growth in juvenile cuttlefish (*Sepia elliptica*) (Mollusca: Cephalopoda) under conditions of food stress. *Can. J. Zool.* 78, 1855–1861. doi: 10.1139/z00-115

Mehanna, S. F., Al-Kharusi, L., and Al-Habs, S. (2014). Population dynamics of the pharaoh cuttlefish *Sepia pharaonis* (Mollusca: Cephalopoda) in the Arabian Sea coast of Oman. *Indian J. Fish.* 61, 7–11.

Minton, J. W. (2004). The pattern of growth in the early life cycle of individual *Sepia pharaonis*. *Mar. Freshw. Res.* 55, 415–422.

R Core Team (2018). *R: A language and Environment for Statistical Computing*. Available at: http://www.r-project.org/ (accessed January 1, 2018).

Raddatz, J., Liebetrau, V., Rüggeberg, A., Hathorne, E., Krabbenhöft, A., Eisenhauer, A., et al. (2013). Stable Sr-isotope, Sr/Ca, Mg/Ca, Li/Ca and Mg/Li ratios in the scleractinian cold-water coral *Lophelia pertusa*. *Chem. Geol.* 352, 143–152. doi: 10.1016/j.chemgeo.2013.06.013

Rexfort, A., and Mutterlose, J. (2006). Stable isotope records from *Sepia officinalis*—a key to understanding the ecology of belemnites? *Earth Planet. Sci. Lett.* 247, 212–221. doi: 10.1016/j.epsl.2006.04.025

Reynaud, S., Ferrier-Pagès, C., Meibom, A., Mostefaoui, S., Mortlock, R., Fairbanks, R., et al. (2007). Light and temperature effects on Sr/Ca and Mg/Ca ratios in the scleractinian coral *Acropora* sp. *Geochim. Cosmochim. Acta* 71, 354–362. doi: 10.1016/j.gca.2006.09.009

Schöne, B. R., Zhang, Z., Radermacher, P., Thébault, J., Jacob, D. E., Nunn, E. V., et al. (2011). Sr/Ca and Mg/Ca ratios of ontogenetically old, long-lived bivalve shells (*Arctica islandica*) and their function as paleotemperature proxies. *Palaeogeogr. Palaeoclimatol. Palaeoecol.* 302, 52–64. doi: 10.1016/j.palaeo.2010.03.016

Sherrard, K. M. (2000). Cuttlebone morphology limits habitat depth in eleven species of *Sepia* (Cephalopoda: Sepiidae). *Biol. Bull.* 198, 404–414. doi: 10.2307/1542696

Sturrock, A. M., Hunter, E., Milton, J. A., Johnson, R. C., Waring, C. P., and Trueman, C. N. (2015). Quantifying physiological influences on otolith microchemistry. *Methods Ecol. Evol.* 6, 806–816. doi: 10.1111/2041-210X.12381

Sturrock, A. M., Trueman, C. N., Darnaude, A. M., and Hunter, E. (2012). Can otolith elemental chemistry retrospectively track migrations in fully marine fishes? *J. Fish Biol.* 81, 766–795. doi: 10.1111/j.1095-8649.2012.03372.x

Thébault, J., and Chauvaud, L. (2013). Li/Ca enrichments in great scallop shells (*Pecten maximus*) and their relationship with phytoplankton blooms. *Palaeogeogr. Palaeoclimatol. Palaeoecol.* 373, 108–122. doi: 10.1016/j.palaeo.2011.12.014

Thébault, J., Schöne, B. R., Hallmann, N., Barth, M., and Nunn, E. V. (2009). Investigation of Li/Ca variations in aragonitic shells of the ocean quahog *Arctica islandica*, northeast Iceland. *Geochem. Geophys. Geosyst.* 10:Q12008. doi: 10.1029/2009GC002789

Turan, C., and Yaglioglu, D. (2010). Population identification of common cuttlefish (*Sepia officinalis*) inferred from genetic, morphometric and cuttlebone chemistry data in the NE Mediterranean Sea. *Sci. Mar.* 74, 77–86. doi: 10.3989/scimar.2010.74n107

Ullmann, C. V., Campbell, H. J., Frei, R., Hesselbo, S. P., Pogge von Strandmann, P. A., and Korte, C. (2013). Partial diagenetic overprint of Late Jurassic belemnites from New Zealand: implications for the preservation potential of δ7Li values in calcite fossils. *Geochim. Cosmochim. Acta* 120, 80–96. doi: 10.1016/j.gca.2013.06.029

Wickham, H. (2009). *ggplot2: Elegant Graphics for Data Analysis*. Berlin: Springer Science & Business Media, 216.

Zhao, L., Schöne, B. R., and Mertz-Kraus, R. (2017). Controls on strontium and barium incorporation into freshwater bivalve shells (*Corbicula fluminea*). *Palaeogeogr. Palaeoclimatol. Palaeoecol.* 465, 386–394. doi: 10.1016/j.palaeo.2015.11.040

Zumholz, K., Hansteen, T. H., Piatkowski, U., and Croot, P. L. (2007). Influence of temperature and salinity on the trace element incorporation into statoliths of the common cuttlefish (*Sepia officinalis*). *Mar. Biol.* 151, 1321–1330. doi: 10.1007/s00227-006-0564-1

Conflict of Interest: The authors declare that the research was conducted in the absence of any commercial or financial relationships that could be construed as a potential conflict of interest.

Copyright © 2020 Chung, Huang, You, Chiao and Wang. This is an open-access article distributed under the terms of the Creative Commons Attribution License (CC BY). The use, distribution or reproduction in other forums is permitted, provided the original author(s) and the copyright owner(s) are credited and that the original publication in this journal is cited, in accordance with accepted academic practice. No use, distribution or reproduction is permitted which does not comply with these terms.

frontiers in Marine Science

ORIGINAL RESEARCH
published: 06 March 2020
doi: 10.3389/fmars.2020.00125

Habitat Use Patterns and Identification of Essential Habitat for an Endangered Coastal Shark With Vertebrae Microchemistry: The Case Study of *Carcharhinus porosus*

Leonardo Manir Feitosa[1,2]*, Valderi Dressler[3] and Rosangela Paula Lessa[1,2]

[1] Programa de Pós-Graduação em Biologia Animal, Departamento de Biologia, Universidade Federal de Pernambuco, Recife, Brazil, [2] Laboratório de Dinâmica de Populações Marinhas (DIMAR), Departamento de Pesca e Aquicultura, Universidade Federal Rural de Pernambuco, Recife, Brazil, [3] Laboratório de Espectrometria Atômica, Departamento de Química, Universidade Federal de Santa Maria, Santa Maria, Brazil

Sharks are among the most endangered and data poor vertebrates in the world. The lack of information regarding their habitat use is especially concerning since these are crucial for the establishment of priority areas for species conservation. Investigating the trace elements present in shark vertebrae has become an interesting tool to analyze species habitat use over individuals' lifetimes. Therefore, we applied vertebrae microchemistry to investigate habitat use of *Carcharhinus porosus* in Brazil's Northern Coast (BNC). We also discuss methodological issues that must be addressed in the future to make microchemistry studies with elasmobranchs at low latitudes more robust. Vertebrae from seventeen individuals sampled in the 1980s (n = 8), and in 2017 and 2018 (n = 9) were evaluated through laser ablation inductively coupled plasma mass spectrometry. We analyzed five elements known to reflect environmental characteristics (Ba, Ca, Mg, Mn, and Sr) by sex, seasons, decades of capture, and life stages. Since Ca is the most abundant element in the vertebrae, we calculated element:Ca ratios and employed these proportions for all statistical analysis. We also used fisheries-independent catch data from the 1980s to test if the BNC is a nursery area for *C. porosus*. We found significant differences in element concentrations between sexes in both multi and single-element analysis, while decades differed only in the multi-element and Sr:Ca. Furthermore, seasons differed in both multi-element and Mg:Ca and Ba:Ca ratios. We did not find differences between life stages. Neonate multi-element signatures yielded three major groups, thus suggesting that the species has at least three birthing grounds in the area. Despite the occurrence of individuals of all sizes, adults show a more distinct occurrence pattern. Our results point toward the hypothesis that the BNC is an essential habitat for this species since its whole life cycle occurs in this area. Therefore, the BNC is a critical area for its conservation. We reinforce that future studies with strictly tropical species should investigate the effects of metabolism, the species' growth rate, and the validation of other elements capable of demonstrating fine-scale changes in habitat to reduce the inherent noise in microchemistry studies.

Keywords: Carcharhinidae, Brazil's Northern Coast, movement ecology, vertebrae trace elements, tropical coastal shark

OPEN ACCESS

Edited by:
Alejandra Vanina Volpedo, University of Buenos Aires, Argentina

Reviewed by:
Oscar Sosa-Nishizaki, Ensenada Center for Scientific Research and Higher Education (CICESE), Mexico
Bree J. Tillett, The University of Queensland, Australia

***Correspondence:**
Leonardo Manir Feitosa
lmfeitos@gmail.com

Specialty section:
This article was submitted to Marine Ecosystem Ecology, a section of the journal Frontiers in Marine Science

Received: *28 September 2019*
Accepted: *17 February 2020*
Published: *06 March 2020*

Citation:
Feitosa LM, Dressler V and Lessa RP (2020) Habitat Use Patterns and Identification of Essential Habitat for an Endangered Coastal Shark With Vertebrae Microchemistry: The Case Study of Carcharhinus porosus. Front. Mar. Sci. 7:125. doi: 10.3389/fmars.2020.00125

INTRODUCTION

Basic biological data such as demographic parameters, life history traits, reproductive patterns, and habitat use are crucial for species management and conservation (Cochrane, 2002). However, sharks are among the taxonomic groups with less basic information available, thus hampering proper conservation actions in all geographical scales (Dulvy et al., 2014). Furthermore, most shark populations are subjected to overfishing and an overall decreasing habitat quality due to water pollution, which raises concern for their sustainability in the near future.

Sharks in Brazil are facing similar problems, and legislation aiming at mitigating them has not followed along (Barreto et al., 2017). In addition, several nationally and internationally endangered species are consistently caught as bycatch in the shrimp and teleost targeted fisheries (Palmeira et al., 2013; Almerón-Souza et al., 2018; Feitosa et al., 2018). Brazil's Northern Coast (BNC) is the main region in the country where sharks experience bycatch (Oliver et al., 2015). The region comprises Maranhão, Pará, and Amapá states, thus including the Amazon estuary, and is one of the main fishing grounds of the country, harboring a great diversity of sharks, including endemic species (Lessa et al., 1999b). Furthermore, it is considered a global conservation hotspot for these *taxa* and several portions are or should be protected areas (Dulvy et al., 2014; Davidson and Dulvy, 2017).

Nevertheless, artisanal and semi-industrial gillnet fisheries targeting large teleost species such as the Acoupa Weakfish *Cynoscion acoupa* and the Brazilian Spanish Mackerel *Scomberomorus brasiliensis* have caused severe population collapses in endemic shark species such as *Isogomphodon oxyrhynchus* in Brazil's northern coast (Lessa et al., 2016). These fisheries use drift gillnets soaked for up to 12 h with 170 mm meshes between knots, 4 to 6 m in height extending for at least 3 km for *Cynoscion acoupa* (de Almeida et al., 2014) and 60 mm meshes for *S. brasiliensis* reaching more than 5 km in extension (Mourão et al., 2014). The smalltail shark *Carcharhinus porosus* is another shark species that has suffered severe declines, but its collapse has been under documented. The only evidences of collapse are an 85% decrease in the biomass captured in 2004 in the BNC, which is considered its global center of abundance, and its extremely low genetic diversity in the same area (Lessa et al., 2006; Tavares et al., 2013).

Since this species corresponded to 43% of the sharks caught by gillnets in the region during the 1980s and 1990s (Lessa, 1997), this dramatic decline is of particular concern. Despite its small size (150 cm estimated maximum length), its life history traits make it easily susceptible to overfishing since its fecundity is low (average of 6 pups per gestation), the reproductive cycle is biannual, and both sexes reach sexual maturity with 6 years old (Lessa and Santana, 1998). It is highly associated to turbid and dynamic areas with mangrove rich coasts (Feitosa et al., 2020), and juveniles were consistently caught near estuaries in Maranhão state's coast (Menni and Lessa, 1998). Nevertheless, its habitat use patterns are still poorly understood.

Several techniques such as acoustic and satellite telemetry have been recently applied to study habitat use of several shark species (Hazin et al., 2013; Taylor et al., 2017). However, these methods are expensive, require the capture, tagging, and release of live specimens, and only gather data within a limited timeframe of the animal's life (Fraser et al., 2018). As a counterpart, the evaluation of trace element composition in fish hard parts provides a glimpse of how an animal uses its habitat during its whole lifetime (Walther, 2019). Therefore, it is a promising technique that has been widely used for teleost fishes (de Pontual and Geffen, 2002; Gillanders, 2005; Elsdon et al., 2008; Paillon et al., 2014), and is being increasingly applied on sharks and rays (Tillett et al., 2011; Izzo et al., 2016; McMillan et al., 2017, 2018). Several elements such as Strontium (Sr), Barium (Ba), Manganese (Mn), and Magnesium (Mg) have been considered to be reliable proxies for environmental tracers of species habitat use, since their concentration in the vertebrae has been shown to reflect their environmental concentrations (McMillan et al., 2017).

More specifically, Sr and Ba are related to changes in salinity, in which the former is more abundant in saltwater and the latter in freshwater (McMillan et al., 2017). On the other hand, both Mn and Mg are associated with large variations in water temperature, but Mn concentration changes are also believed to reflect proximity of mangrove areas (Paillon et al., 2014; Smith et al., 2016). Since these trace element concentrations are marked in the vertebrae and no evidence of element reabsorption by the body exists, evaluating their variations in hard parts enables the understanding of changes in trace element composition throughout an individual's lifetime. With these, key information on the type of habitat a species uses during each life stage (McMillan et al., 2017), and even potential nursery areas (Tillett et al., 2011; Lewis et al., 2016; Smith et al., 2016; Heupel et al., 2018) can be obtained. However, several aspects of this methodology need to be addressed to improve the robustness of conclusions, especially in areas with little environmental variation such as the BNC.

Unraveling the habitat use patterns of a species according to age, together with other biological information can provide enough information to establish key areas for a species conservation such as nurseries. Thus, this study aimed at investigating these patterns across life stages and between sexes for one of the most heavily fished shark species in the Brazilian northern coast through vertebrae trace elements. We also used the vertebrae microchemistry data to investigate eventual changes in habitat use when the species was abundant (1980s) and after population collapse (2010s), as well as investigating eventual chemical differences between seasons. Furthermore, we tested the data obtained to the criteria developed by Heupel et al. (2007), which define the assumptions for an area to be considered an elasmobranch nursery, and discuss the existence of an essential habitat for the species in the area. Finally, we briefly discuss knowledge gaps that need to be filled by future elasmobranch vertebrae microchemistry studies carried out with species inhabiting low latitude areas.

MATERIALS AND METHODS

Sampling Area

Brazil's northern coast (4°11′40.58″N to 2°18′45.53″S) is a highly indented area subjected to the Amazon River's estuary of which Maranhão state is part (**Figure 1**). Temperatures suffer little variation during the year (average water temperature 28°C), but the region experiences two marked seasonal pluviometry cycles. The rainy season extends from January to June and the dry season from August to December, with a transition period in July. In addition, daily tidal cycles pose a great level of dynamism to the coastal areas with spring tides reaching up to 7 m in amplitude from high to low. The vast amount of estuaries and the tropical climate grant the region the unique characteristics of its mangrove forests, with trees reaching 30 m in height and extending for over 5,000 km^2 (Souza-Filho, 2005). Due to its highly productive and turbid waters, diversity and endemism levels are high, thus making it one of the most important areas for shark conservation in the world.

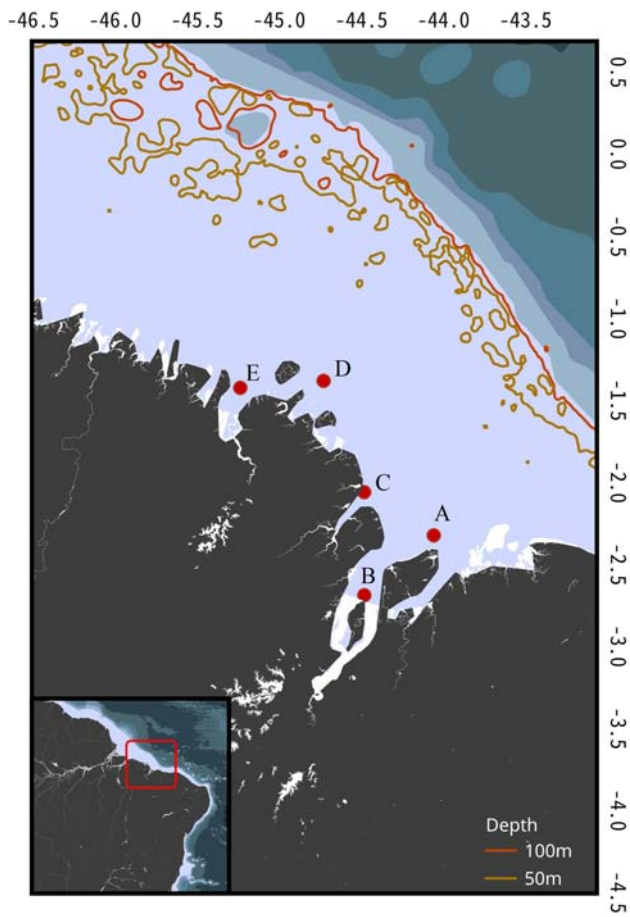

FIGURE 1 | Brazil's Northern Coast (area within the red square) with sampling locations, and 50 and 100 m depth isobaths. A, Canal do Navio; B, Ilha dos Caranguejos; C, Araoca; D, Farol São João; E, Turiaçu.

Sampling Design

Smalltail shark vertebrae were sampled from specimens landed in the Raposa municipality in Maranhão state (0°59′0.88″S to 2°18′45.53″S). Blocks of five vertebrae were retrieved from seventeen specimens. Since carcasses were already processed (headed and gutted), identification followed the field remarks pointed by Compagno (1984), such as the origin of the second dorsal fin over the midbase of a strongly notched anal fin. Samples were collected according to the Brazilian environmental laws under the license (License SISBIO, 49663-1). Since samples obtained in 2017 and 2018 were collected from dead specimens landed and traded in local markets, no ethics committee approval is necessary. For the samples collected in the 1980s, no ethics committee existed at the time.

For the vertebrae microchemistry analysis, frozen samples were thawed and two vertebrae from each block were retrieved. The connecting tissue was removed and vertebrae were air dried for 48 h (n = 9). Samples collected by R. Lessa and V. Batista in the 1980s were also included in the analysis (n = 8) (see Lessa and Santana, 1998 for sampling locations). Although these were subjected to formaldehyde 4% treatment, it does not impair our analysis since there is no evidence of this kind of procedure affecting microchemistry results – other than sodium concentration (Mohan et al., 2017). Furthermore, although we acknowledge that the sample size used was somewhat small, other studies using trace elements for habitat use, and even age and growth analysis, used smaller sample sizes for critically endangered, vulnerable, and near threatened shark and teleost species, including with a single hard part sample (Scharer et al., 2012; Hermann et al., 2016; Mohan et al., 2018). Indeed, collecting new vertebrae samples from the smalltail shark is difficult due to their rarity.

Vertebrae Processing

For processing, all vertebrae were embedded in polyester resin and air-dried for 48 h. Vertebrae were transversely sectioned with a low speed diamond Isomet^{TM} (Buehler) saw (**Figure 2**). Translucent and opaque ring pairs were considered to be formed

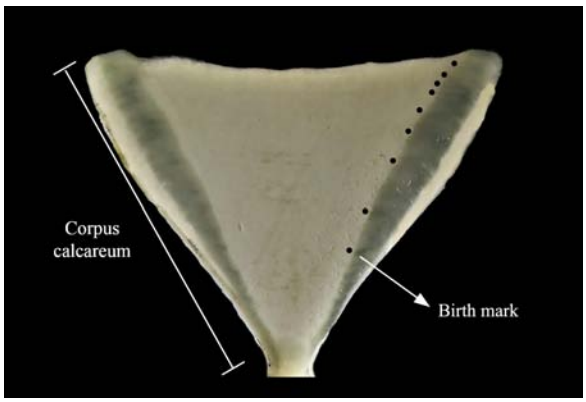

FIGURE 2 | *Carcharhinus porosus* vertebrae section. Black dots represent translucent bands counted as part of the ring pairs.

annually (Lessa and Santana, 1998). Prior to analysis by laser ablation inductively coupled plasma mass spectrometry (LA-ICP-MS), vertebrae sections were polished with silicon carbide paper (no 8000), washed ultrasonically with ultrapure water (Milli-Q, Millipore), and air-dried in sterilized plastic vials for 48 h before analysis. Cleaned samples were stored individually in hermetic plastic bags until laser ablation.

Analytical measurements were taken at the *Laboratório de Espectrometria Atômica - Departamento de Química* (UFSM) with a Q-switched pulse 213 nm Nd:YAG laser ablation system (NWR 213, ESI – New Wave Research) coupled to an Agilent 7500 inductively coupled plasma mass spectrometer. The laser was operated with a pulse frequency of 20 Hz, a scan speed of 30 $\mu m\ s^{-1}$, and an energy output of 0.2 to 0.3 mJ per pulse. Under these conditions, each crater width was approximately 25 μm. The ablated material was conducted through a Teflon-coated tube into the ICP-MS using Argon as a carrier gas (0.85 $dm^3\ min^{-1}$). The ICP was operated at 1,300 W nominal powers with outer and intermediate gas flows of 15.0 and 1.1 $dm^3\ min^{-1}$, respectively. Quantification was performed using element:Calcium ratios as internal standard for each element. The NIST 612 certified reference material was employed to obtain counts per second (CPS). The limit of detection (LOD) was calculated following Longerich et al. (1996) and elements that did not meet this standard were excluded from the analysis.

Experimental Fisheries Data

We also used the catch dataset from the specimens captured between 1984 and 1987 and that was the basis for the Lessa and Santana (1998) study. The inverted von Bertalanffy growth function was calculated to obtain an age estimate based on the total size of each individual. All specimens sampled (n = 930) were computed, together with the sampling location, month, year, total length, and depth. However, we only used the season, month, and depth information to evaluate eventual occurrence patterns based on such abiotic factors (**Table 1**).

Data Analysis

The distance for each growth band from the nucleus was measured to obtain the exact positioning of the element concentration counts provided by the LA-ICP-MS. This enabled the establishment of the profile for each element analyzed by year of life. Since specimens had different ages and the information on habitat use per life stage is much more meaningful than on an annual basis, life stages were chosen following the age and growth data for both sexes (Lessa and Santana, 1998). The neonate portion of vertebrae was considered to range from the birthmark to the end of the first year of life, followed by the juvenile phase between the start of the second year of life to the end of the third. The sub-adult stage was subdivided in two groups to avoid misrepresenting habitat use patterns of larger sub-adults: sub-adult1 ranging from the third year to the end of the fourth, and sub-adult2 ranging from the start of the fifth to the end of the sixth year of life. Adult reads were considered from the sixth year to the end of the vertebra.

Seventeen individuals (**Table 2**) were analyzed in a multi-element LA-ICP-MS for ^{24}Mg, ^{43}Ca, ^{55}Mn,^{86}Sr, ^{138}Ba,^{112}Cd,^{206}Pb, and ^{208}Pb. Element:Ca ratios were calculated for each element with raw concentration counts later transformed into concentrations (ppm) by the equation formulated by Longerich et al. (1996). A Ca concentration of 35% was considered in the present study to convert element reads from CPS to ppm. These data were then either log(x + 1) transformed (for the PERMANOVA and SIMPER analyses) or scaled with the Z transformation (for the cluster analysis) to obtain results on the same scale for all elements analyzed. Only elements that have already been validated to represent proxies for environmental features such as salinity and temperature changes, and that remained above the LOD were used in further analysis. Average reads for each life stage, element, and sample were calculated and used on the subsequent statistical analysis. We performed multi and single-element PERMANOVAs with an Euclidian distance resemblance matrix, a 1000 permutations, and a significance level of 0.05 to evaluate multi and single-elemental differences in habitat use for the species. Sexes, life stages, seasons, and decades of capture were considered fixed factors.

We also performed similarity percentages analysis (SIMPER) for each factor using Euclidian distance. This analysis aimed at evidencing which elements were most important for the chemical signature of the sexes, seasons, and decades. It is important to stress that SIMPER results are not related to the actual concentration of each element in the vertebrae, but to the percentage of contribution that each element has on explaining the total distance calculated through the distance matrix. Therefore, an element with high percentage in the SIMPER results is not necessarily present in high concentrations in the vertebrae. Finally, we did a cluster analysis with average distances to check if groups would be formed based on their multi-element chemical signature exclusively with the data from the neonate phase. All statistical analysis were performed in R version 3.5.1 (R Core Team, 2013) except for the SIMPER which was performed in PRIMER7 software.

RESULTS

Out of the elements analyzed, only Ca, Mg, Mn, Sr, and Ba were used for the habitat use analysis due to their reliability as proxies for environmental tracers in elasmobranchs. Cd and Pb isotopes were excluded from the final analysis because they were below the limit of detection (LOD). No significant statistical differences between life stages were found in any of the PERMANOVAs performed. However, significant differences were found between sexes, seasons, and decades in the multi-element analysis, as well as for sexes in all element:Ca analysis. Furthermore, significant differences were found in the single-element PERMANOVAs between decades for Sr:Ca, and between seasons for Mg:Ca and Ba:Ca (**Table 3**).

As expected based on the PERMANOVA results, SIMPER demonstrated that the chemical signatures were strongly different for sexes, with Sr being much more important in females than in males, and Ba following the inverse pattern in males (**Table 4**). Furthermore, SIMPER results demonstrate the clear signal of Ba in the rainy season and elevated percentage of Sr importance

TABLE 1 | Sex ratio (M:F) of catch data published by Lessa et al. (1999a) discriminated by season, month, and depth range.

Factor		Sex ratios (M:F)				
		Neonate	Juvenile	Subadult1	Subadult2	Adult
Season						
	Rainy	0.67	1.02	1.36	1.00	**0.54**
	Transition	0.75	2.13	0.88	**0.88**	1.00
	Dry	0.70	0.88	1.59	3.20	6.00
Month						
	January	0	0.88	1.00	0	**0.60**
	February	0	1.00	2.00	1.00	0
	March	0	0	3.00	**0.40**	**0.42**
	May	4.00	1.33	1.00	1.00	1.00
	June	0.29	0.76	6.00	0.13	2.00
	July	0.75	2.13	0.88	0.13	1.00
	August	1.30	0.84	1.10	**0.75**	**0.17**
	September	0.67	1.00	1.00	0	0
	October	0.29	0.94	0.75	13.00	6.50
	November	0	1.67	0.67	0	0
	December	0	0	0	0	1.00
Depth (m)						
	0 to 10	0.33	0.50	0.38	0	**0.50**
	10 to 20	0.88	0.98	1.10	3.00	2.67
	20 to 35	0	0	16.00	6.75	1.67

Bolded values correspond to female biased occurrence, while underlined values correspond to male biased occurrence.

TABLE 2 | Total length (TL), sex, location, date of capture, and source for each individual sampled and analyzed with LA-ICP-MS.

Sample	TL (cm)	Age (years)	Sex	Sampling station	Season	Month	Year	Source
CP A4 37	85.3	9	Male	Canal do Navio	Dry	October	1984	Lessa, 1986
CP A39 01	85.6	12	Male	Caranguejos	Rainy	March	1986	Lessa, 1986
CP A39 09	87.5	9	Female	Caranguejos	Rainy	March	1986	Lessa, 1986
CP A50 09	73	7	Female	Araoca	Dry	October	1987	Lessa, 1986
CP A50 12	80	7	Female	Araoca	Dry	October	1987	Lessa, 1986
CP A50 16	101	11	Female	Araoca	Dry	October	1987	Lessa, 1986
CP B4 02	90	15	Male	Farol São João	Rainy	March	1989	Stride et al., 1992
CP B4 06	97	12	Male	Farol São João	Rainy	March	1989	Stride et al., 1992
CP101	85.94	8	Male	Canal do Navio	Dry	October	2017	Present study
CP103	67.09	7	Male	Canal do Navio	Dry	October	2017	Present study
CP104	64.49	7	Male	Canal do Navio	Dry	October	2017	Present study
CP105	63.84	7	Male	Canal do Navio	Dry	October	2017	Present study
CP106	65.14	8	Male	Canal do Navio	Dry	October	2017	Present study
CP108	56.04	5	Male	Canal do Navio	Dry	October	2017	Present study
CP109	61.89	6	Female	Canal do Navio	Dry	October	2017	Present study
CP110	65.2	7	Female	Turiaçu	Rainy	April	2018	Present study
CP111	115	18	Female	Canal do Navio	Dry	October	2018	Present study

in the dry season (**Figure 3**). Regarding the decades of the samples analyzed, the major differences were found between Sr and Mn, with the former being much more significant in the 1980s and the latter being sharply more important in the 2010s. Overall, the element with the smallest variation in all factors evaluated was Mn (SIMPER whole Av. Value = 1.04; Standard Deviation = 0.102) (**Table 4**). Sr had the highest variation among factors (Av. Value = 2.47; Standard Deviation = 0.217), followed by Ba (Av. Value = 1.02; Standard Deviation = 0.157), and Mg (Av. Value = 2.94; Standard Deviation = 0.149). As demonstrated, Mg and Sr average values are two-fold higher than Mn and Ba.

Cluster results with the multi-element signatures for the neonate phase demonstrated that individuals have different birthplaces. Indeed, the cluster analysis evidenced at least three birthing grounds based on the average chemical similarities between individuals with a cophenetic distance of 0.952 (**Figure 4**). Furthermore, since the locations in **Figure 4** reflect the collection places of the adults instead of the actual birth

TABLE 3 | Results for the one-step PERMANOVAs calculated for the multi and single-element analysis with life stage, decade, season, and sex of individuals as factors.

Element	Life Stage			Decade			Season			Sex		
	df	MS	*p*	df	MS	*p*	df	MS	*p*	df	MS	*p*
Multi	4	0.1638	0.9930	1	2.9047	**0.0299**	1	3.8046	**0.0119**	1	12.4393	**0.0009**
Residuals	78	0.7473		81	0.7472		81	0.6807		81	0.5741	
Mg:Ca	4	0.0062	0.9950	1	0.2419	0.1748	1	1.2927	**0.0023**	1	2.3744	**0.0009**
Residuals	78	0.1326		81	0.1347		81	0.1217		81	0.1084	
Mn:Ca	4	0.1188	0.3916	1	0.0463	0.5495	1	0.0406	0.5924	1	1.9551	**0.0009**
Residuals	78	0.1091		81	0.1103		81	0.1104		81	0.0867	
Sr:Ca	4	0.0016	1.0000	1	2.1345	**0.0129**	1	0.8638	0.1339	1	5.9686	**0.0009**
Residuals	78	0.3665		81	0.3267		81	0.3424		81	0.2794	
Ba:Ca	4	0.0371	0.9001	1	0.4818	0.0519	1	1.6072	**0.0009**	1	2.1411	**0.0009**
Residuals	78	0.1289		81	0.1200		81	0.1061		81	0.0995	

Df, degrees of freedom; MS, mean square values; p, probability of results being due to random factors. Statistically significant measures are in bold.

TABLE 4 | SIMPER results for sexes, seasons, and decades evaluated. Av., average; SD, squared distance.

	Male		Female		Dry		Rainy		1980s		2010s	
Element	Av. Value	Av. SD	Av. Value	Av. SD	Av. Value	Av. SD	Av. Value	Av. SD	Av. Value	Av. SD	Av. Value	Av. SD
Mg	3.08	0.061	2.73	0.177	2.86	0.166	3.13	0.016	2.88	0.216	2.99	0.059
Sr	2.70	0.063	2.15	0.594	2.41	0.478	2.63	0.021	2.31	0.591	2.63	0.081
Mn	1.17	0.107	0.86	0.057	1.03	0.133	1.08	0.056	1.02	0.073	1.07	0.145
Ba	1.14	0.102	0.81	0.096	0.91	0.110	1.22	0.097	1.09	0.204	0.93	0.042

areas, and the localities are intermingled among the clusters, the birthing grounds seem to be specific, but adults use the same larger area. Finally, the cluster shows the use of the same birthing grounds across decades since reads from samples collected in the 1980s and in 2017 and 2018 were gathered in the clusters (**Table 2**). Sample CP105 has a different chemical signature than all the other samples and likely represents an individual born in a different area.

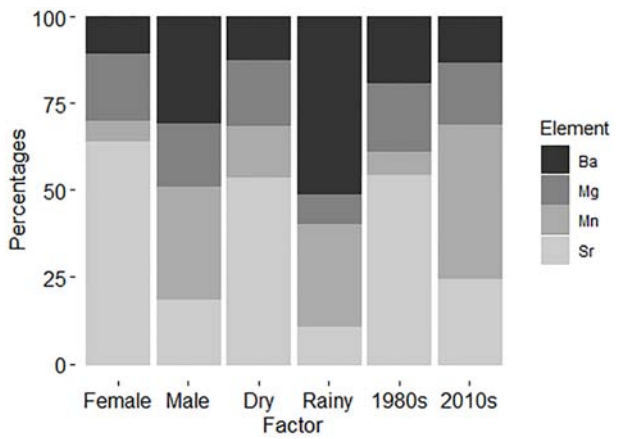

FIGURE 3 | Similarity percentages (SIMPER) demonstrating the chemical signatures for the factors analyzed. Total $n = 17$ (sex – female: $n = 7$; male: $n = 10$), (seasons – dry: $n = 12$; rainy: $n = 5$), (sampling decades – 1980: $n = 8$; 2010: $n = 9$).

DISCUSSION

Patterns of Habitat Use Inferred From Vertebrae Microchemistry Data

Results demonstrated that the smalltail shark likely does not undertake habitat partitioning throughout its ontogeny (**Table 3**). However, multi and single-element PERMANOVAs separately testing differences between seasons, sexes, and decades yielded statistically significant differences. Overall, the PERMANOVA results suggest that all life stages of the *C. porosus* population use the whole area in a constant manner. However, the differences obtained demonstrate that the smalltail shark likely presents sex segregation, which is a somewhat widespread behavior among shark species (Wearmouth and Sims, 2010). Nevertheless, it is not clear if the specimens move further away from the coast or to deeper areas where salinity is expected to be higher in the rainy seasons due to predominance of freshwater in the surface.

Seasonality in the region is strong and the sex differences in multi-element signatures shown by the SIMPER analysis (**Figure 3**) seem to reinforce this argument, since Ba is much more representative for males. Indeed, Ba is an element known as a surrogate for the proximity to freshwater runoff areas (Smith et al., 2013). However, experimental fisheries catch data point to a greater proportion of females near the coast on the rainy season instead of males. Indeed, Ba has a greater importance for designating the typical chemical pattern in males than in females, as it does in the rainy season when

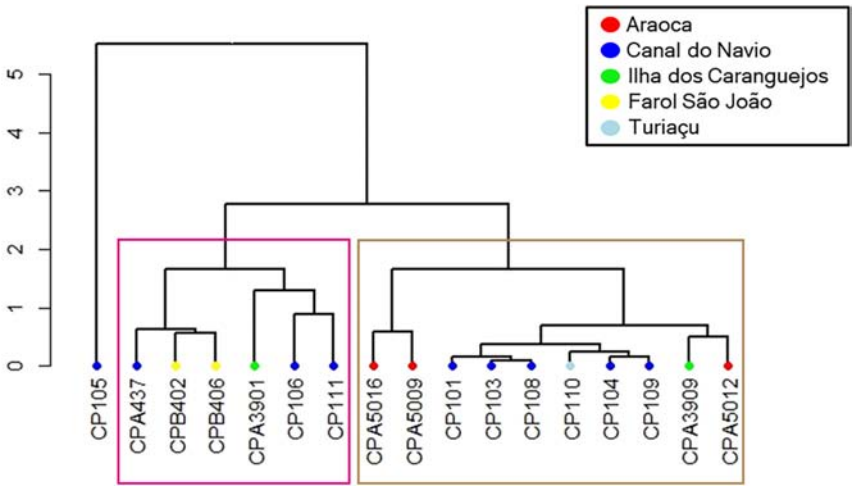

FIGURE 4 | Cluster analysis for neonate multi-element chemical signatures. Sample codes are in the *x*-axis. Sites are the sampling points where adults were captured. Each branch tip color represents a sampling location: red, Araoca, blue, Canal do Navio, light blue, Turiaçu, green, Ilha dos Caranguejos, yellow, Farol São João. The two major clusters found are highlighted by the pink and brown rectangles.

compared to the dry season (**Table 4**). It is important to notice that, despite this higher importance, Sr is more abundant than Ba in both sexes and seasons (**Table 4**). Regardless, no evidence was obtained that *C. porosus* enters freshwater systems. In fact, geochemical data from within the Amazon River point toward similar levels of Sr and Ba on the edge of the saltwater intrusion area near Óbidos (Seyler and Boaventura, 2003). Although we found no information on the geochemical characteristics of the rivers that compose the larger Gulf of Maranhão area from where the specimens were collected, they have similar physical characteristics to the Amazon River, are subjected to the same weather pattern, and could have similar trace element compositions. However, further research to describe such chemical patterns in both the rivers and their estuaries is necessary.

Even though the SIMPER results demonstrate a drastic change in Sr percentages of contribution between the dry (higher) and rainy (lower) seasons, its single-element results yielded no significant differences between them. In fact, the incongruence between analyses is likely related to the higher variance for Ba, which was indeed statistically significant in the single-element analysis between seasons (**Table 2**). On the other hand, Mg was also significantly different between seasons in the single-element analysis. Since its concentration is considered to be negatively affected by temperature variations (Smith et al., 2013), we tested it to investigate potential dives for deeper areas in which water temperature would be significantly lower than in coastal waters. This behavior has been shown for several shark species (Afonso and Hazin, 2015), but never for a small coastal one. Indeed, no evidence of such dives were obtained for *C. porosus*, which is in accordance with the known biology of the species, thus reinforcing that its distribution is likely restricted to the coastal waters within the continental platform (Lessa et al., 1999a). However, there is also evidence pointing that Mg may suffer biological influences from diet and physiology on a species-specific basis (McMillan et al., 2017). Therefore, its results must be taken cautiously and further laboratory validation needs to be done.

Results from the Mn single-element analysis likely indicate that the species remains near the coast subjected to influences from mangrove habitat, since Mn is considered to be more abundant in coastal areas with mangrove forests nearby and no differences were obtained between life stages (Paillon et al., 2014). This result is also in accordance with the average values computed for Mn in **Table 4**. Furthermore, we obtained statistically significant differences between sexes for the Mn:Ca ratios as for the other elements in both single and multi-element analysis. Although manganese is also known to be a physiologically active element participating on the activation of reproductive hormones, as well as protein production and cellular signals (Smith et al., 2013), no differences in growth and age at maturity exists between sexes for *C. porosus* (Lessa et al., 1999a). While the hypothesis that Mn results may be affected by physiological features requires further testing, its results presented herein are evaluated on a more comprehensive array, especially in the cluster analysis discussed below.

Evaluation of Nursery Criteria and Suggestions for Effective Species Management

Nurseries have long been considered as one of the most critical areas for elasmobranch conservation since they provide key habitat for neonates and juveniles to grow and thus guarantee recruitment for the next generations (Lessa et al., 1999b). However, there have been several attempts to define what would be considered as a nursery, since these areas should be preserved to guarantee population recruitment (Beck et al., 2001; Heupel et al., 2007, 2018). Therefore, Heupel et al. (2007) developed three testable criteria to designate a given area as a nursery, which

are: (1) newborns and young-of-year specimens must be more commonly found in the studied area than elsewhere, (2) must remain in that area for longer periods of time, and (3) the area must be repeatedly used across years. Furthermore, Heupel et al. (2018) have considered that the statement by Beck et al. (2001) that juveniles and adults should not coexist in a nursery to be true.

Recently, Heupel et al. (2018) revised the existing literature testing the criteria and stated that small-bodied coastal sharks tend not to have specific nursery areas. Indeed, applying those criteria to the gillnet capture and microchemistry data presented herein, the smalltail shark seems to follow this statement for four reasons. First, although the BNC has the highest occurrence of newborns and young-of-year specimens known in any other area along its geographical distribution (Lessa et al., 1999a, 2006), it is not the only area where they are found. In fact, other areas with known neonate and young-of-year captures in Brazil are Sergipe and São Paulo state's coasts (Sadowsky, 1967; Meneses et al., 2005), and other such areas are likely to exist throughout its distribution. However, their numbers are still proportionately much lower than in the BNC.

Second, they seem to stay in the same area until reaching sexual maturity as shown by the experimental fisheries data. Even though these data (**Table 1**) show a somewhat sex segregation behavior, the lack of differences between life stages shown by the microchemistry data reinforce the idea that individuals remain in the same area throughout their lives. Therefore, the species whole life cycle is likely fulfilled in the nearshore waters of the BNC. Regardless, adult females are more abundant during the rainy season, especially in March when they correspond to twice the number of adult males caught in the area. On the other hand, the sex ratio is skewed toward adult males in the dry season, especially October (**Table 1**). Interestingly, the sex ratio between adult males and females becomes less skewed during June and July when the transition between the rainy and dry seasons occur. We argue that these differences in occurrence between adult individuals, together with the microchemistry results, are strong evidence that a seasonal habitat partitioning between sexes likely occurs in the BNC population.

However, fishing gear might also be responsible for these catch patterns. Experimental fisheries surveys carried out in the BNC with different gillnet sizes during the 1980s and 1990s have conflicting results. Lessa et al. (1999a), using gillnets 900 m long (7.5 m in height and 80 mm mesh size between knots) caught 1,128 specimens between 1984 and 1987 from which ∼80% comprised neonates or juveniles. On the other hand, Stride et al. (1992) only caught adult individuals (N = 78) on the same areas using gillnets with larger mesh sizes (200 mm between knots, 400 m long, and 6 m height) than the ones used by Lessa et al. (1999a). Furthermore, increasing mesh sizes resulted in a decrease in capture of *C. porosus* from 14% in the 200 mm mesh to 0.8% in the 300 mm mesh size (Stride et al., 1992). Thus, gear selectivity is an important source of bias for the life stage occurrences observed. In addition, specimens were most commonly caught in areas where salinity tended to be higher, but no information on seasonal changes in captures are provided (Stride et al., 1992).

Regardless, Stride et al. (1992) caught a large number of pregnant females (n = 10). Among those samples, six were caught in May and most had near-term embryos (size at birth at 30 cm TL). This information, together with the existing reproductive, catch, and habitat use data for the species led us to argue that most *C. porosus* females likely give birth in the second trimester (rainy season), and copulation likely takes place in October with females that are resting from gestation from the previous year. Further evidence for that is the capture of an adult female used in the present study (individual CP111) with fresh mating scars in October 2018 (**Supplementary Figure S1**).

Third, the existence of at least two groups in the cluster analysis (**Figure 4**), as well as the grouping of samples captured in the 1980s and 2017/2018 point toward the existence of reused birthing grounds and possible philopatric behavior. Future research should focus on catching neonates and juveniles and evaluating the vertebral edge microchemistry signature to compare with the ones obtained in the present study to assign accurately each one to a specific birthing ground. Molecular studies through genotype reconstruction or long-term telemetry of adult females are also effective tools to prove this hypothesis. Furthermore, the coexistence of adults born in areas with diverging chemical signatures (**Figure 4**) reinforces the hypothesis that the BNC's smalltail sharks comprise a single population and thus should be managed as a single unit.

Fourth, young-of-year, juveniles, subadults, and adults coexist. Despite the neonates and juveniles being completely absent from areas deeper than 20 m, individuals from all life stages inhabit the shallow coastal waters of the BNC (Lessa and Santana, 1998). Therefore, we argue that the BNC, especially the eastern Amazon coast in Maranhão state, does not fulfill the elasmobranch nursery criteria. Additionally, the species likely spends its whole life cycle within the continental platform, but with a small degree of habitat partitioning between sexes and several different birthing grounds. Furthermore, recent analysis estimated that the Northern coast of South America (defined as the coastal extension between Guyana and Maranhão state) is actually the region with the smallest decline in catch probability along the species distribution (Feitosa et al., 2020). The last IUCN species assessment also considers this area as the center of abundance for this species (Lessa et al., 2006). Therefore, based on the evidence herein presented and the published information for this species, we argue that the BNC is actually an Essential Fish Habitat (EFH) area for *C. porosus*, especially the shallow coastal banks and estuarine areas of the BNC as noted by Lessa et al. (1999a).

While the BNC is likely not a nursery for the *C. porosus*, it seems to be a much more important area for this species. Knip et al. (2010) developed a hypothesis of how small-sized sharks, such as *C. porosus*, use their habitats. The authors argue that such species tend to be highly dependent on nearshore areas and typically do not roam very far, especially for the high abundance of prey. This was the case for *C. sorrah*, another small-sized tropical shark inhabiting nearshore waters off Australia, which showed some degree of site-fidelity but some individuals did roam to further areas (Knip et al., 2012a). Further evidence supporting this conclusion is that *C. porosus* is an opportunistic species that feeds mainly on small teleosts such as *Stellifer naso* and *Macrodon ancylodon*, which are highly abundant in the area regardless of season (Lessa and Almeida, 1997). Therefore,

C. porosus seems to fit the theoretical model for small-sized sharks developed by Knip et al. (2010).

Since *C. porosus* seems to have a restricted dispersion capacity due to its small size, it is reasonable to assume that individuals in the BNC are a single population, but connectivity with adjacent areas such as the Guyanas and Suriname need to be further investigated. Regardless, evidence points to a low genetic diversity scenario in the BNC population (Tavares et al., 2013), which is in agreement with both the critically endangered status in Brazil and the lack of connectivity between the BNC population and individuals from other areas. In fact, this pattern is likely a life history feature for this species, since several local extinctions have been reported throughout its range in Brazil (Lessa et al., 2018). Nevertheless, roaming capacity for this species needs to be further investigated. This is especially important due to the fisheries interactions that populations may experience. If individuals have little roaming behavior, localized populations are more likely to be severely impacted by fisheries in areas where fishing pressure is strong, such as the BNC (Knip et al., 2010, 2012b).

Improvement Suggestions for Future Microchemistry Studies at Low Latitudes

Although elasmobranch vertebrae microchemistry has proven to be a robust technique to evaluate habitat use patterns (McMillan et al., 2017), there is not enough information on the physiological processes involved in element uptake by the vertebrae. Indeed, few studies have been carried out in controlled environments evaluating the effects of biotic (diet, physiology) and abiotic factors (salinity, temperature, pH) on element concentrations (Smith et al., 2013; Pistevos et al., 2019). In addition, elasmobranch microchemistry studies are mostly carried out with temperate species subjected to a much more variable environment with strong seasonality. Therefore, the published literature is not always in accordance with the environmental characteristics of the tropics. Consequently, it is a lot harder for researchers studying tropical species to draw strong conclusions about their results based on literature specialized in species from regions subjected to temperate climate.

Regardless, it is clear that a lot more research in both tropical and temperate areas is necessary to fill the major elasmobranch microchemistry knowledge gaps pointed by McMillan et al. (2017). Therefore, we discuss what we consider the next frontiers for elasmobranch vertebrae microchemistry research carried out with tropical sharks and rays. We also raise two questions regarding the main knowledge gaps for elasmobranch microchemistry based on the published literature and our data.

First, which elements are capable of assessing finer-scale changes in habitat use for species subjected to little environmental variation? The smalltail shark might indeed have little variation in habitat use and, since the habitat environmental characteristics are generally stable over time, the trace elements we analyzed were not capable of detecting fine scale changes, such as salinity differences detected by Tillett et al. (2011). Therefore, we reinforce the need to study element uptake physiology in depth and to validate the environmental signal each element provides, especially for species occurring in low latitudes. A potential candidate might be sulfur, which could be a successful element to evaluate horizontal migrations and distance from the coast (see Rubenstein and Hobson, 2004; Doubleday et al., 2018 for further information), since it seems to reflect organic matter concentration in the water.

Second, what is the effect of metabolic rate on the time it takes for a given water chemical signature to be marked on the vertebrae? To our knowledge, the only study ever carried out investigating how growth and environmental history affected elemental concentration in the vertebrae was done by Smith et al. (2013). As expected, specimens in higher temperatures had a significantly higher growth rate when compared to those at lower temperatures, as well as the deposition rate. However, growth rates did not have a significant effect on elemental composition (Smith et al., 2013). Therefore, it is expected that specimens occurring in low latitudes have higher growth and vertebrae deposition rates. Nevertheless, few conclusions regarding the effects of temperature on vertebrae growth and element composition on adults can be drawn, since this experiment was performed with juvenile individuals of *Urobatis halleri*. Thus, the question of how much time is necessary for the chemistry of a given water mass to have a distinct signature on the vertebrae remains. In fact, this is such a difficult topic that the same question exists for otoliths, even though some data point to a timeframe between 25 and 40 days for a signature to be formed (Walsh and Gillanders, 2018).

Another important factor to consider is the difference in growth rate during ontogenetic development (Walther and Limburg, 2012). Indeed, *C. porosus* is expected to grow 7 $cm.year^{-1}$ on the first 4 years of life, and decreasing to 4 $cm.year^{-1}$ from then on (Lessa et al., 1999a). Therefore, it is likely that the chemical signals from the subadult2 phase and further are subjected to different metabolic and growth rates. Furthermore, this pattern is likely to be species-specific, since each has different growth rates and life histories. Perhaps a good alternative to overcome this problem would be to choose a model species of relatively easy rearing in controlled environments for each major taxonomic group of sharks (family Carcharhinidae, Lamnidae, etc.). Studying these models would potentially enable researchers to extrapolate the results obtained to the other species from the same group, thus obtaining stronger interpretations from the data.

CONCLUSION

In general, our vertebrae microchemistry results suggest that the smalltail shark population occurring in the BNC is a single stock with different birthing grounds. This was the first study employing vertebrae microchemistry on an elasmobranch in the Neotropical region, and we recommend a few methodological advancements based on both our data and knowledge gaps we identified in the published literature. Since *C. porosus* spends its whole life cycle in the coastal waters and abundances seem to be much higher in the BNC than any other area of its known distribution, the region is a crucial area for its conservation on a global scale. A short-term feasible conservation strategy to mitigate its bycatch in fisheries targeting two of the most important Brazilian fishing resources could be the release of

live specimens, especially those under 70 cm TL and hence sexually immature. It is worth noting that, even though their productivity has been declining quickly, it is impossible to ban the target fisheries, since several communities depend on them for subsistence. Therefore, managing the target fisheries will likely have a positive effect on *C. porosus* populations. However, since elasmobranchs have a longer life cycle, these management strategies would require a longer time to rebuild its stock. Another feasible and perhaps more crucial action would be to implement effectively the existing conservation areas throughout the BNC, notably in Maranhão state. Finally, the legal framework, especially to enable *in situ* inspections, adequate deterrent measures for prohibited catches, and the existence of fisheries statistic programs along the BNC are crucial to monitor trends in geographical occurrence and stock size.

DATA AVAILABILITY STATEMENT

The datasets generated for this study are available on request to the corresponding author.

ETHICS STATEMENT

Ethical review and approval was not required for the animal study because sampling involved only already fished specimens. Other animals used in this study were sampled between 1984 and 1989, when no Ethical standards existed in Brazil, thus no Ethics Committee approval exists for them.

AUTHOR CONTRIBUTIONS

LF participated on the study design, field sampling, vertebrae processing, aging, and preparation for the LA-ICP-MS analysis, as well as analyzed the data, and wrote the manuscript. VD participated on the LA-ICP-MS laboratory work, provided key insights on data analysis, and reviewed the manuscript. RL participated on the study design, sample preparation and analysis on the LA-ICP-MS, data analysis, provided the experimental fisheries catch data used, and reviewed the manuscript.

FUNDING

This study was financed in part by the Coordenação de Aperfeiçoamento de Pessoal de Nivel Superior – Brazil (CAPES) – Finance code 001. Comissão Interministerial para os Recursos do Mar (CIRM) funded the data collection along the Maranhão Coast (1984/1988) and Conselho Nacional de Desenvolvimento Científico e Tecnológico – CNPq provided Productivity Research Grants (306672/2015-4 and 302276/2017-3) to RL and VD, respectively. In addition, we acknowledge the help of Vinicius M. Neves in the LA-ICP-MS processing, and Mariana Bonfim in the data analysis.

ACKNOWLEDGMENTS

We thank FACEPE and CNPq under the projects APQ 10.11-2015 and 306672/15, respectively, for covering the costs of the LA-ICP-MS analysis, FACEPE for providing a scholarship to LF under the process IBPG 0089-2.05/17. We also thank Dr. Francisco Marcante Santana for the help with reading growth rings and aging specimens, and the thorough discussions about the results, Dr. Ana Paula Barbosa Martins for her thoughts on the contents of this manuscript. In addition, we acknowledge the help of Vinicius M. Neves in the LA-ICP-MS 1099 processing, and Mariana Bonfim and Dr. Jonas Vasconcelos in the data analysis. Furthermore, we thank Leandro Augusto de Souza Junior, Dr. Leandro Manzoni Vieira, Clarisse Éleres Figueiredo, and Rafael Antonio Brandão for helping with figure editing and elaboration, and Maylis Labonne (IRD, France) for critical readings. Finally, we thank Dr. Jorge Nunes, Dr. Getúlio Rincon, and the fishers from Raposa for the help with sample collection.

SUPPLEMENTARY MATERIAL

The Supplementary Material for this article can be found online at: https://www.frontiersin.org/articles/10.3389/fmars.2020.00125/full#supplementary-material

FIGURE S1 | Mating scars on the left pectoral fin of individual CP111.

REFERENCES

Afonso, A. S., and Hazin, F. H. V. (2015). Vertical movement patterns and ontogenetic niche expansion in the tiger shark, *Galeocerdo cuvier*. *PLoS One* 10:e0116720. doi: 10.1371/journal.pone.0116720

Almerón-Souza, F., Sperb, C., Castilho, C. L., Figueiredo, P. I. C. C., Gonçalves, L. T., Machado, R., et al. (2018). Molecular identification of shark meat from local markets in Southern Brazil based on DNA barcoding: evidence for mislabeling and trade of endangered species. *Front. Genet.* 9:138. doi: 10.3389/fgene.2018.00138

Barreto, R. R., Bornatowski, H., Motta, F. S., Santander-Neto, J., Vianna, G. M. S., and Lessa, R. (2017). Rethinking use and trade of pelagic sharks from Brazil. *Mar. Policy* 85, 114–122. doi: 10.1016/j.marpol.2017.08.016

Beck, M. W., Heck, K. L., Able, K. W., Childers, D. L., Eggleston, D. B., Gillanders, B. M., et al. (2001). The identification, conservation, and management of estuarine and marine nurseries for fish and invertebrates. *BioScience* 51, 633–641.

Compagno, L. J. V. (1984). *FAO Species Catalogue. Sharks of the World, Part 2 – Carcharhiniformes*, Vol. 4. Rome: Food and Agriculture Organization of the United Nations, 251–633.

Cochrane, K. L. (2002). *A Fishery Manager's Guidebook: Management Measures and Their Applications*, ed. K. L. Cochrane (Rome: Food and Agriculture Organization).

de Almeida, Z. S., de Santos, N. B., Carvalho-Neta, R. N. F., and de Pinheiro, A. L. R. (2014). "Análise multidisciplinar das pescarias de emalhe da pescada-amarela, de camarão de puçá de muruada e da catação de caranguejo uçá em três municípios costeiros do Maranhão," in *A Pesca Marinha e Estuarina no Brasil: Estudos de Caso Multidisciplinares*, eds M. Haimovici, J. M. Andriguetto Filho, and P. S. Sunye (Rio Grande: Editora da FURG), 161–170.

Davidson, L. N. K., and Dulvy, N. K. (2017). Global marine protected areas to prevent extinctions. *Nat. Ecol. Evol.* 1:0040. doi: 10.1038/s41559-016-0040

de Pontual, H., and Geffen, A. J. (2002). "Otolith microchemistry," in *Manual of Fish Sclerochronology*, eds J. Panfili, H. Pontual, H. Troadec, and P. J. Wright (Brest: Ifremer), 245–307. doi: 10.1643/OT-03-266

Doubleday, Z. A., Cliff, J., Izzo, C., and Gillanders, B. M. (2018). Untapping the potential of sulfur isotope analysis in biominerals. *Mar. Ecol. Prog. Ser.* 598, 159–166. doi: 10.3354/meps12605

Dulvy, N. K., Fowler, S. L., Musick, J. A., Cavanagh, R. D., Kyne, P. M., Harrison, L. R., et al. (2014). Extinction risk and conservation of the world's sharks and rays. *eLife* 3:e00590. doi: 10.7554/eLife.00590

Elsdon, T., Wells, B., Campana, S., Gillanders, B., Jones, C., Limburg, K., et al. (2008). "Otolith chemistry to describe movements and life-history parameters of fishes," in *Oceanography and Marine Biology: An Annual Review*, 46th Edn, eds R. N. Gibson, R. J. A. Atkinson, and J. D. M. Gordon (Boca Raton, FL: CRC Press), 297–330. doi: 10.1201/9781420065756.ch7

Feitosa, L. M., Martins, A. P. B., Giarrizzo, T., Macedo, W., Monteiro, I. L., Gemaque, R., et al. (2018). DNA-based identification reveals illegal trade of threatened shark species in a global elasmobranch conservation hotspot. *Sci. Rep.* 8:3347. doi: 10.1038/s41598-018-21683-5

Feitosa, L. M., Martins, L. P. M., de Souza-Junior, L. A., and Lessa, R. P. (2020). Potential distribution and population trends of the smalltail shark *Carcharhinus porosus* inferred from species distribution models and historical catch data. *Aquat. Conserv.* doi: 10.1002/aqc.3293

Fraser, K. C., Davies, K. T., Davy, C. M., Ford, A. T., Flockhart, D. T. T., and Martins, E. G. (2018). Tracking the conservation promise of movement ecology. *Front. Ecol. Evol.* 6:150. doi: 10.3389/FEVO.2018.00150

Gillanders, B. M. (2005). Otolith chemistry to determine movements of diadromous and freshwater fish. *Aquat. Living Resour.* 18, 291–300. doi: 10.1051/alr:2005033

Hazin, F. H. V., Afonso, A. S., De Castilho, P. C., Ferreira, L. C., and Rocha, B. C. L. M. (2013). Regional movements of the tiger shark, *Galeocerdo cuvier*, off Northeastern Brazil: inferences regarding shark attack hazard. *An. Acad. Bras. Ciênc.* 85, 1053–1062. doi: 10.1590/S0001-37652013005000055

Hermann, T. W., Stewart, D. J., Limburg, K. E., Castello, L., and Hermann, T. W. (2016). Unravelling the life history of Amazonian fishes through otolith microchemistry. *R. Soc. Open Sci.* 3:160206. doi: 10.1098/rsos.160206

Heupel, M. R., Carlson, J. K., and Simpfendorfer, C. A. (2007). Shark nursery areas: concepts, definition, characterization and assumptions. *Mar. Ecol. Prog. Ser.* 337 287–297. doi: 10.3354/meps337287

Heupel, M. R., Kanno, S., Martins, A. P. B., and Simpfendorfer, C. A. (2018). Advances in understanding the roles and benefits of nursery areas for elasmobranch populations. *Mar. Freshw. Res.* 70, 897–907. doi: 10.1071/MF18081

Izzo, C., Huveneers, C., Drew, M., Bradshaw, C. J. A., Donnellan, S. C., and Gillanders, B. M. (2016). Vertebral chemistry demonstrates movement and population structure of bronze whaler. *Mar. Ecol. Prog. Ser.* 556, 195–207. doi: 10.3354/meps11840

Knip, D. M., Heupel, M. R., and Simpfendorfer, C. A. (2010). Sharks in nearshore environments: models, importance, and consequences. *Mar. Ecol. Prog. Ser.* 402, 1–11. doi: 10.3354/meps08498

Knip, D. M., Heupel, M. R., and Simpfendorfer, C. A. (2012a). Evaluating marine protected areas for the conservation of tropical coastal sharks. *Biol. Conserv.* 148, 200–209. doi: 10.1016/j.biocon.2012.01.008

Knip, D. M., Heupel, M. R., and Simpfendorfer, C. A. (2012b). Habitat use and spatial segregation of adult spottail sharks *Carcharhinus sorrah* in tropical nearshore waters. *J. Fish Biol.* 80, 767–784. doi: 10.1111/j.1095-8649.2012.03223.x

Lessa, R., and Almeida, Z. (1997). Analysis of stomach contents of the smalltail shark *Carcharhinus porosus* from northern Brazil. *Cybium* 21, 123–133.

Lessa, R., Almeida, Z., Santana, F. M., Siu, S., and Perez, M. (2006). *Carcharhinus Porosus,* Smalltail Shark. The IUCN Red List of Threatened Species, 8235. Available online at: https://dx.doi.org/10.2305/IUCN.UK.2006.RLTS.T60220A12324372.en (accessed July 26, 2017).

Lessa, R., Batista, V. S., and Santana, F. M. (2016). Close to extinction? The collapse of the endemic daggernose shark (*Isogomphodon oxyrhynchus*) off Brazil. *Glob. Ecol. Conserv.* 7, 70–81. doi: 10.1016/j.gecco.2016.04.003

Lessa, R., and Santana, F. M. (1998). Age determination and growth of the smalltail shark, *Carcharhinus porosus*, from northern Brazil. *Mar. Freshw. Res.* 49, 705–711. doi: 10.1071/MF98019

Lessa, R., Santana, F., Menni, R., and Almeida, Z. (1999a). Population structure and reproductive biology of the smalltail shark (*Carcharhinus porosus*) off Maranhão (Brazil). *Mar. Freshw. Res.* 50, 383–388.

Lessa, R., Santana, F. M., Rincón, G., Gadig, O. B. F., and El-Deir, A. C. D. (1999b). *Biodiversidade de Elasmobrânquios do Brasil*. Recife: Ministério do Meio Ambiente.

Lessa, R. P. (1986). Contribuição ao conhecimento da biologia de carcharhinus porosus ranzani, 1839 das reentrâncias maranhenses. *Acta Amaz.* 16/17, 73–86.

Lessa, R. P. (1997). Sinopse dos estudos sobre elasmobrânquios da costa do Maranhão. *Bol. Lab. Hidrobiol.* 10, 19–36.

Lessa, R. P. T., Repinaldo-Filho, F. P. M., Moro, G., Charvet, P., and Santana, F. M. (2018). "Carcharhinus porosus," in *Livro Vermelho da Fauna Brasileira Ameaçada de Extinção*, Vol. 6, Peixes (Brasília: ICMBio), 950–953.

Lewis, J. P., Patterson, W. F., Carlson, J. K., and McLachlin, K. (2016). Do vertebral chemical signatures distinguish juvenile blacktip shark (*Carcharhinus limbatus*) nursery regions in the northern Gulf of Mexico? *Mar. Freshw. Res.* 67, 1014–1022. doi: 10.1071/MF15088

Longerich, H. P., Jackson, S. E., and Günther, D. (1996). Inter-laboratory note. Laser ablation inductively coupled plasma mass spectrometric transient signal data acquisition and analyte concentration calculation. *J. Anal. At. Spectrom.* 11, 899–904. doi: 10.1039/JA9961100899

McMillan, M. N., Huveneers, C., Semmens, J. M., and Gillanders, B. M. (2018). Natural tags reveal populations of conservation dependent school shark use different pupping areas. *Mar. Ecol. Prog. Ser.* 599, 147–156. doi: 10.3354/meps12626

McMillan, M. N., Izzo, C., Wade, B., and Gillanders, B. M. (2017). Elements and elasmobranchs: hypotheses, assumptions and limitations of elemental analysis. *J. Fish Biol.* 90, 559–594. doi: 10.1111/jfb.13189

Meneses, T. S., Santos, F. N., and Pereira, C. W. (2005). Fauna De Elasmobrânquios Do Litoral Do Estado De Sergipe, Brasil. *Arq. Ciênc. Mar.* 38, 79–83. doi: 10.2312/ActaFish.2017.5.1.33-42

Menni, R. C., and Lessa, R. P. (1998). The chondrichthyan community off Maranhão (northeastern Brazil) II. Biology of species. *Acta Zool. Lilloana* 44, 69–89.

Mohan, J. A., Miller, N. R., Herzka, S. Z., Sosa-nishizaki, O., Kohin, S., Dewar, H., et al. (2018). Elements of time and place: manganese and barium in shark vertebrae reflect age and upwelling histories. *Proc. R. Soc. B Biol. Sci.* 285:20181760. doi: 10.1098/rspb.2018.1760

Mohan, J. A., TinHan, T. C., Miller, N. R., and David Wells, R. J. (2017). Effects of sample cleaning and storage on the elemental composition of shark vertebrae. *Rapid Commun. Mass Spectrom.* 31, 2073–2080. doi: 10.1002/rcm.7998

Mourão, K. R. M., do Espírito-Santo, R. V., Silva, B. B., Almeida, M. C., Isaac, V. J., Frédou, T., et al. (2014). "A pesca de *scomberomorus brasiliensis* e alternativas para o seu manejo no litoral nordeste do Pará – Brasil," in *A Pesca Marinha e Estuarina no Brasil: Estudos de Caso Multidisciplinares*, eds M. Haimovici, J. M. Andriguetto, Filho, and P. S. Sunye (Rio Grande: Editora da FURG), 171–180.

Oliver, S., Braccini, M., Newman, S. J., and Harvey, E. S. (2015). Global patterns in the bycatch of sharks and rays. *Mar. Policy* 54, 86–97. doi: 10.1016/j.marpol.2014.12.017

Paillon, C., Wantiez, L., Kulbicki, M., Labonne, M., and Vigliola, L. (2014). Extent of mangrove nursery habitats determines the geographic distribution of a coral reef fish in a South-Pacific Archipelago. *PLoS One* 9:e105158. doi: 10.1371/journal.pone.0105158

Palmeira, C. A. M., da Rodrigues-Filho, L. F. S., de Sales, J. B. L., Vallinoto, M., Schneider, H., and Sampaio, I. (2013). Commercialization of a critically endangered species (largetooth sawfish, *Pristis perotteti*) in fish markets of northern Brazil: authenticity by DNA analysis. *Food Control* 34, 249–252. doi: 10.1016/j.foodcont.2013.04.017

Pistevos, J. C. A., Reis-Santos, P., Izzo, C., and Gillanders, B. M. (2019). Element composition of shark vertebrae shows promise as a natural tag. *Mar. Freshw. Res.* 70, 1722–1733. doi: 10.1071/MF18423

R Core Team (2013). *R: A Language and Environment for Statistical Computing*. Vienna: R Foundation for Statistical Computing.

Rubenstein, D. R., and Hobson, K. A. (2004). From birds to butterflies: animal movement patterns and stable isotopes. *Trends Ecol. Evol.* 19, 256–263. doi: 10.1016/j.tree.2004.03.017

Sadowsky, V. (1967). Selachier aus dem Litoral von Sao Paulo, Brasilien. *Beitr. Neotropischen Fauna* 5, 71–88. doi: 10.1080/01650526709360398

Scharer, R. M., Patterson, W. F., Carlson, J. K., and Poulakis, G. R. (2012). Age and growth of endangered smalltooth sawfish (*Pristis pectinata*) verified with LA-ICP-MS analysis of vertebrae. *PLoS One* 7:e47850. doi: 10.1371/journal.pone.0047850

Seyler, P. T., and Boaventura, G. R. (2003). Distribution and partition of trace metals in the Amazon basin. *Hydrol. Process.* 17, 1345–1361. doi: 10.1002/hyp.1288

Smith, W. D., Miller, J. A., and Heppell, S. S. (2013). Elemental markers in elasmobranchs: effects of environmental history and growth on vertebral chemistry. *PLoS One* 8:e62423. doi: 10.1371/journal.pone.0062423

Smith, W. D., Miller, J. A., Márquez-Farías, J. F., and Heppell, S. S. (2016). Elemental signatures reveal the geographic origins of a highly migratory shark: prospects for measuring population connectivity. *Mar. Ecol. Prog. Ser.* 556, 173–193. doi: 10.3354/meps11844

Souza-Filho, P. W. M. (2005). Costa de Manguezais de Macromaré da Amazônia: cenários morfológicos, mapeamento e quantificação de áreas usando dados de sensores remotos. *Rev. Bras. Geofís.* 23, 427–435. doi: 10.1590/s0102-261x2005000400006

Stride, R. K., da Batista, V. S., and Raposo, L. A. B. (1992). *Pesca Experimental de Tubarão com Redes de Emalhar no Litoral Maranhense*, 3rd Edn. São Luís: CORSUP/EDUFMA.

Tavares, W., da Silva Rodrigues-Filho, L. F., Sodré, D., Souza, R. F. C., Schneider, H., Sampaio, I., et al. (2013). Multiple substitutions and reduced genetic variability insharks. *Biochem. Syst. Ecol.* 49, 21–29. doi: 10.1016/j.bse.2013.02.004

Taylor, M. D., Babcock, R. C., Simpfendorfer, C. A., and Crook, D. A. (2017). Where technology meets ecology: acoustic telemetry in contemporary Australian aquatic research and management. *Mar. Freshw. Res.* 68, 1397–1402. doi: 10.1071/MF17054

Tillett, B. J., Meekan, M. G., Parry, D., Munksgaard, N., Field, I. C., Thorburn, D., et al. (2011). Decoding fingerprints: elemental composition of vertebrae correlates to age-related habitat use in two morphologically similar sharks. *Mar. Ecol. Prog. Ser.* 434, 133–142. doi: 10.3354/meps09222

Walsh, C. T., and Gillanders, B. M. (2018). Extrinsic factors affecting otolith chemistry – implications for interpreting migration patterns in a diadromous fish. *Environ. Biol. Fishes* 101, 905–916. doi: 10.1007/s10641-018-0746-y

Walther, B. D. (2019). The art of otolith chemistry: interpreting patterns by integrating perspectives. *Mar. Freshw. Res.* 70, 1643–1658. doi: 10.1071/MF18270

Walther, B. D., and Limburg, K. E. (2012). The use of otolith chemistry to characterize diadromous migrations. *J. Fish Biol.* 81, 796–825. doi: 10.1111/j.1095-8649.2012.03371.x

Wearmouth, V. J., and Sims, D. W. (2010). Sexual segregation in Elasmobranchs. *Biol. Mar. Mediterr.* 17, 236–239.

Conflict of Interest: The authors declare that the research was conducted in the absence of any commercial or financial relationships that could be construed as a potential conflict of interest.

Copyright © 2020 Feitosa, Dressler and Lessa. This is an open-access article distributed under the terms of the Creative Commons Attribution License (CC BY). The use, distribution or reproduction in other forums is permitted, provided the original author(s) and the copyright owner(s) are credited and that the original publication in this journal is cited, in accordance with accepted academic practice. No use, distribution or reproduction is permitted which does not comply with these terms.

frontiers in Marine Science

ORIGINAL RESEARCH
published: 31 March 2020
doi: 10.3389/fmars.2020.00166

Do the Fish Scales Shape of *Mugil curema* Reflect the Genetic Structure Using Microsatellites Markers and the Mexican Marine Ecoregions Classification?

Eloísa Pacheco-Almanzar, Nadia Loza-Estrada and Ana L. Ibáñez*†

Departamento de Hidrobiología, Universidad Autónoma Metropolitana-Iztapalapa, Mexico City, Mexico

OPEN ACCESS

Edited by:
Alejandra Vanina Volpedo, University of Buenos Aires, Argentina

Reviewed by:
Alfonso Aguilar-Perera, Universidad Autónoma de Yucatán, Mexico
Roberta Callicó Fortunato, University of Buenos Aires, Argentina

***Correspondence:**
Ana L. Ibáñez
ana@xanum.uam.mx

†ORCID:
Ana L. Ibáñez
orcid.org/0000-0002-6062-9172

Specialty section:
This article was submitted to Marine Ecosystem Ecology, a section of the journal Frontiers in Marine Science

Received: *09 December 2019*
Accepted: *03 March 2020*
Published: *31 March 2020*

Citation:
Pacheco-Almanzar E, Loza-Estrada N and Ibáñez AL (2020) Do the Fish Scales Shape of Mugil curema Reflect the Genetic Structure Using Microsatellites Markers and the Mexican Marine Ecoregions Classification? Front. Mar. Sci. 7:166. doi: 10.3389/fmars.2020.00166

Mugil curema is a teleost fish of economic importance that shows wide phenotypic variability in the coasts of Mexico. Intraspecific morphological variability might replicate either genetic dissimilarity between groups or environmental conditions according to phenotypic plasticity. Fish scales shape was used to discriminate location variants, genetic structure obtained by microsatellite markers, and marine ecoregions of Mexico. The present study uses landmarks and geometric morphometric statistical approaches to address the specific question: if and how fish scale shape varies with genetic structure or with marine ecoregions. This is assessed using seven landmarks by scale, the coordinates of which were subjected to a generalized Procrustes analysis, followed by a principal components analysis and quadratic discriminant analysis with cross-validation analysis on shape. Also, the significance of classifications was assessed by multivariate analysis of covariance (MANCOVA). The proportion of total shape variance explained by total length and by centroid size was 3.8 and 3.0%, respectively. Therefore, only shape (without size) was used for the analysis. MANCOVA was significant in all cases, with locations, genetic structure, and marine ecoregions. The cross-validated discriminant analysis by location correctly classified 42.2%, whereas with the genetic structure prearrangement and marine ecoregions, the identification rates were 58.3 and 57.0%, respectively. It was surprising that, as the same as in the genetic structure (microsatellite analysis), San Antonio Bay, Texas formed a group with Sabancuy, Campeche, Celestun, and Sisal, Yucatan (the Caribbean locations). Likewise, Huave Lagoon System, Oaxaca, located in the Pacific coast is more similar to the Caribbean sites unlike the other locations from the Pacific area, which are similar results depicted with microsatellite analysis. On the other hand, using the marine ecoregions arrangement, the findings indicate that the Mexican Tropical Pacific and the Chiapas-Nicaragua marine ecoregions were very different as opposed to the two marine ecoregions from the Gulf of Mexico more similar in fish scale shape. The Mexican

Tropical Pacific ecoregions show more identification rate (80.4%), whereas the rest of marine ecoregions discriminate less than 53.3%. Possibly, hydrographic features as currents or upwellings circumscribe boundaries between marine ecoregions, and this could produce inherent genetic structure.

Keywords: connectivity, white mullet, Gulf of Mexico, Central Pacific, geometric morphometrics

INTRODUCTION

Mugil curema (Valenciennes, 1836) is basically an American species found in both the Atlantic and Pacific oceans, with few populations in African waters (Durand et al., 2012). The species is economically important, with catches of 6,067 metric tons in Mexico during the year 2017, of which 88% were from the Gulf of Mexico coasts and 12% from the Pacific coasts (Secretaría de Medio Ambiente Recursos Naturales y Pesca (SEMARNAP), 2017). A great body morphometric variability has been recorded for this species in the Gulf of Mexico, indicating the presence of more than one population (Ibáñez-Aguirre et al., 2006). Variation in shape in *M. curema* has been considered to reliably trace fish populations by applying geometric morphometric methods to one fish scale per specimen. Results have shown that fish scale shape clearly separates specimens of different localities (Ibáñez et al., 2007; Ibáñez and O'Higgins, 2011; Ibáñez, 2015). In general, fish scale shape is to a significant extent species-specific and helps determine stock membership (Ibáñez et al., 2007; Garduño-Paz et al., 2010). Furthermore, fish scale shape was used to identify geographic variants among the Lutjanidae (*Lutjanus argentiventris*, *L. guttatus*, and *L. peru*) of three geographic areas along the Pacific coast (Ibáñez et al., 2012a), with results indicating that specimens of each species from the three geographic areas formed two local populations. The consistency of these results for the three species analyzed established that this coincidence does not happen by chance. The variability in hydrogeomorphology, water productivity, and abundance of fish stocks possibly accounted for the observed differences in scale morphology and clarified why scale shape may be used to discriminate among stocks (De Pontual and Prouzet, 1987; Watkinson and Gillis, 2005; Ibáñez et al., 2007). In this sense, it can be surmised that scale morphology is regulated by habitat variability and food availability and type, leading to a differentiation of phenotypic characteristics (Swain and Foote, 1999; Ibáñez et al., 2012b).

As far as we know, only two studies have analyzed the influence of genetics on the shape of fish scales, those of Staszny et al. (2013) and Albertson et al. (2018). The two articles agree that both genetic and environmental factors can significantly influence the formation of scales, and thus the shape of a scale may be used as a tool to explain and detect the potential variability of the environmental influences that affect groups of genetically homogeneous fish.

Mexico's geographic position, between the Central-Western Atlantic and the Central-Eastern Pacific, explains much of its enormous biological diversity, where fish make up the group of vertebrates with the largest number of species (2,763 species; Espinosa-Pérez, 2014). Marine ecoregions have been defined in order to have a better understanding of their resources and geographic distribution. These marine ecoregions are influenced by environmental factors, including the temperature and circulation of large currents and seawater masses (Lara-Lara et al., 2008). At present, there are no studies based on morphometry or on whether the shape of the scales reflects this division of marine ecoregions.

Mugil curema inhabits coastal lagoons, estuaries, and rivers. The adults migrate to the open sea to spawn, where both eggs and hatchlings are subject to surface currents that aid their transportation. Later, the juveniles migrate to estuaries and coastal lagoons where they live until adulthood (Ibáñez, 1993). The spawning period of *M. curema* in the Gulf of Mexico was reported by Ibáñez and Colín (2014). In the northern Gulf of Mexico, Madre Lagoon and Tamiahua Lagoon, the spawning period occurs from the end of winter to spring, while in the more southern localities where water is warmer, sexually mature females have been reported in autumn and winter, especially for Alvarado Lagoon, Veracruz and Mecoacán Lagoon, Tabasco (Ibáñez and Colín, 2014). In addition, female individuals collected in the estuaries of Sabancuy, Campeche and Celestun, Yucatan, have a long spawning period from November to April (Pacheco-Almanzar et al., 2017). Thus, different spawning seasons have been reported for this species throughout the Gulf of Mexico. Similarly, different spawning periods have been recorded for the Mexican Pacific (Viera-Muñoz, 1979; Villaseñor-Talavera, 1991; Lucano-Ramírez and Michel-Morfín, 1997; Cabral-Solís, 1999). It is believed that spawning differences may have resulted in differences in the genetic structure of *M. curema* in the Gulf of Mexico, where three groups have been identified using microsatellite markers (Pacheco-Almanzar et al., 2017; Pacheco-Almanzar, 2019). It is also possible that changes in ocean currents produce diverse environments that generate marine ecoregions that are part of other larger and superior geographical entities, but at the same time have their own characteristics and particular features.

In view of this, it is both possible that populations of nearby water bodies attain connectivity and that populations become separated by mainstream currents. Understanding patterns of connectivity among populations is critical for the advance of accurate, spatially clear descriptions of population dynamics. As was mentioned above, fish scale shape has been used to identify geographic variants, but does it reflect the structure observed along Mexico's coasts using microsatellite markers or marine ecoregions?

Thus, the objective of this work was to determine if the scale shape reflects the genetic structure observed along the coasts of Mexico using microsatellite markers and also to analyze if the scale shape is related to the marine ecoregions. Three approaches

were addressed here: by locality, by spatial empirical genetic patterns, and by marine ecoregions. This was assessed through a geometric morphometric analysis.

MATERIALS AND METHODS

Fish Scale Collection

Mugil curema specimens were collected from commercial fisheries in San Antonio Bay, Texas (SAB) Madre Lagoon, Tamaulipas (LM), Tamiahua Lagoon (TA), Cazones Estuary (CA) and Alvarado Lagoon, Veracruz (AL), Mecoacán Lagoon, Tabasco (ME), Sabancuy, Campeche (SA), and Celestun (CE) and Sisal, Yucatan (SI), along the Gulf of Mexico in 2009 and 2015. Specimens were also collected in Cuyutlán Lagoon, Colima (CU), the Balsas River, Michoacán (BA), and Huave Lagoon System, Oaxaca (HU), along the Pacific coast of Mexico from 2009 to 2014 (**Figure 1**).

The marine ecoregionalization of Spalding et al. (2007) was used as follows: the Northern Gulf of Mexico marine ecoregion (NGM) composed by SAB and LM; the Southern Gulf of Mexico marine ecoregion (SGM) comprises TA, CA, AL, ME, SA, CE, and SI; the Mexican Tropical Pacific marine ecoregion (MTP) includes CU and BA; and the Chiapas-Nicaragua marine ecoregion is formed by HU. The distribution of the marine ecoregions is presented in **Figure 1**.

The fish were measured to the nearest millimeter. The average total length (TL) of all specimens was 261.0 ± 76.8 mm. Fish scales were obtained from the same fish specimens used for the population genetic analysis of Pacheco-Almanzar et al. (2017) (**Table 1**). All individuals were adults except for Sisal location. One scale per fish was used for the analysis from the left side of the body, between the two dorsal fins. No distinction between sexes was made. They were washed with mild soap and running water, dried, and stained with methylene blue. A digital image of each scale was taken using a Zeiss stereomicroscope (Stemi 2000-C, Carl-Zeiss-Straße, Oberkochen Germany) and an integrated 4.0 MP Canon digital camera (Canon, Ota, Tokyo).

The genetic groups proposed by Pacheco-Almanzar et al. (2017) were as follows (**Figure 1**): the Northern Gulf group (NG) includes the localities of LM, TA, and CA; the Central Gulf group (CG) includes AL and ME; the Southern Gulf group (SG) includes individuals from the localities SAB, SA, CE, SI, and HU (on the Pacific coast); and the Central Pacific group (CP) is formed by BA and CU (**Figure 1**).

Morphometrics

Seven landmarks per scale were recorded using the tpsDig v2.09 program (Rohlf, 2019) and following the protocol of Ibáñez et al. (2007). The landmarks were located on key features of the ctenoid scale that are common to all scales of the species under study. This ensures that in subsequent interpretations of results, variations in particular landmarks can be related to sharing features of shape. The following landmarks were considered appropriate: landmarks 1 and 3 are the ventrolateral and dorsolateral tips of the anterior portion of the scale; landmark 2 lies at the middle of the anterior edge of the scale; landmarks 4 and 6 lie at the boundary between the anterior portion with circuli and the posterior area covered by cteni (spine-like ornamentations); landmark 5 is the focus of the scale, and landmark 7 is positioned at the tip of the posterior portion or the exposed part of the scale (**Figure 2**).

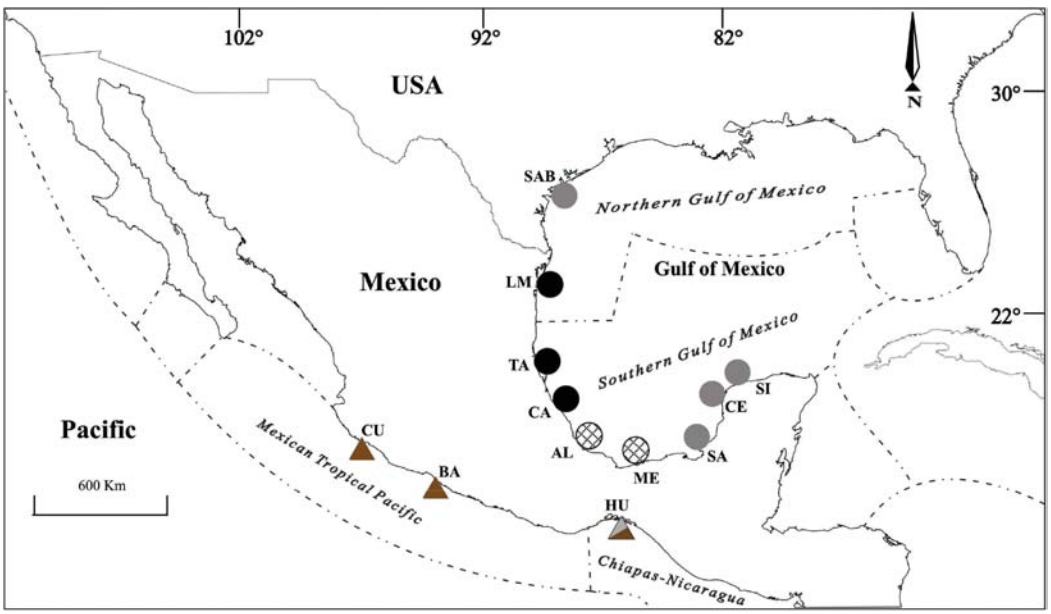

FIGURE 1 | Sampling locations in the Gulf of Mexico: San Antonio Bay, Texas (SAB); Madre Lagoon, Tamps. (LM); Tamiahua Lagoon (TA), Cazones (CA) y Alvarado Lagoon, Ver. (AL); Mecoacán, Tab. (ME); Sabancuy, Camp. (SA); Celestún (CE) and Sisal, Yucatán (SI); Mexican Pacific: Cuyutlán, Col. (CU); Balsas River, Mich. (BA); and Lagunar Huave System, Oax. (HU). In italic are the names of the marine ecoregions. Figures and their tonality form the microsatellite groups.

TABLE 1 | Collection sites, size of sample (N), size range (TL = total length in cm), and collection date of *M. curema*.

Area	Location	Group code	N	TL range	TL mean ± SD	Date
Gulf of Mexico	SAB	*Mcu*-GMSAB	24	9.2–14.3	11.77 ± 1.4	March 2015
	LM	*Mcu*-GMLM	49	24.9–31.2	28.6 ± 1.23	January 2009
	TA	*Mcu*-GMTA	42	26.7–35.0	30.15 ± 1.84	January 2009
	CA	*Mcu*-GMCA	50	24.5–34.7	30.67 ± 1.87	February 2009
	AL	*Mcu*-GMAL	52	24.6–35.7	29.77 ± 2.32	November 2009
	ME	*Mcu*-GMME	49	25.6–33.6	29.44 ± 1.82	November 2009
	SA	*Mcu*-GMSA	11	29.0–39.4	34.34 ± 3.88	November 2014
	CE	*Mcu*-GMCE	14	24.7–31.7	27.56 ± 2.07	April 2015
	SI	*Mcu*-GMSI	37	6.3–13.5	8.54 ± 1.52	April 2015
Mexico Pacific	CU	*Mcu*-PMCU	51	20.0–25.1	22.55 ± 1.01	July 2009
	BA	*Mcu*-PMBA	51	26.1–37.2	32.82 ± 2.27	July 2009
	HU	*Mcu*-PMHU	30	12.4–31.0	20.97 ± 7.16	June 2014

The configurations of the seven landmark coordinates were submitted to a generalized Procrustes analysis and, following a tangent projection (Dryden and Mardia, 1993, 1998), to a principal components (PCs) analysis (Dryden and Mardia, 1993, 1998; Kent, 1994). The scores of the specimens on all non-zero PCs from the analyses of the shape were regressed on the TL and the centroid size (CS) in order to see the extent to which fish scale size and shape variation is related to body size. The natural measure of size of a landmark configuration is the CS, the square root of the sum of squared distances of a set of landmarks from their centroid (Dryden and Mardia, 1998).

In order to examine the potential for differences in shape when classifying unknown specimens, the scores of the specimens on all non-zero PCs were submitted to a quadratic discriminant analysis to compute generalized Mahalanobis' distances and discriminant functions and to calculate the value of the latter in the classification. A cross-validated discriminant analysis was applied to assess and compare the efficacy of the shape in the classification by geographic variants (localities), genetic structure, and marine ecoregions.

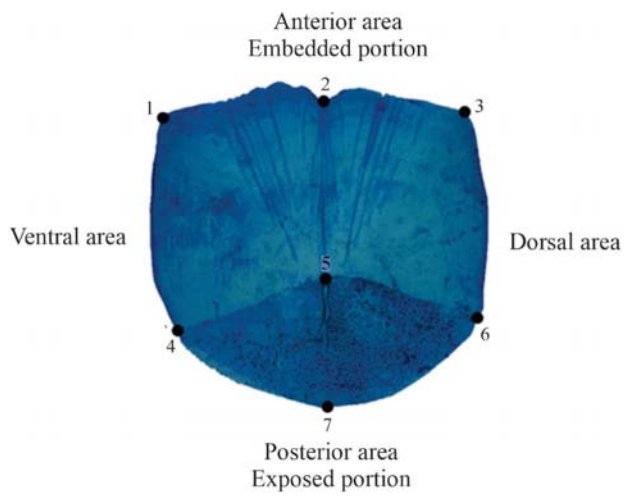

FIGURE 2 | Location of landmarks on scales of *Mugil curema*.

Finally, differences were assessed by a full multivariate analysis of covariance (MANCOVA) with the shape (all PC scores) as the dependent variable, total length as the covariate, and each of the three approaches addressed here: by locality, by spatial empirical genetic patterns, and by marine ecoregions as the grouping factors. The representation of scale shape by the different approaches was visualized using transformation grids (Bookstein, 1989; Marcus et al., 1996; Dryden and Mardia, 1998) computed with Morphologika2 v2.5 (O'Higgins and Jones, 2006). Statistical analyses were carried out using the Statistical Package for Social Sciences (SPSS v22.0, IBM Corporation, New York, NY, United States) and XLSTAT v2016.02 (XLSTAT Addinsoft Inc., New York, NY, United States) (Addinsoft, 2016).

RESULTS

The scale shape of the *M. curema* showed significant differences in the three approaches: localities, genetic structure, and ecoregions, according to the result of MANCOVA, which was significant in all cases ($p < 0.001$). Although the total length differed in all localities, genetic groups, and marine ecoregions, the proportions of shape variance by total length and centroid were 3.8 and 3.0%, respectively, for which reason only the shape (and not the size) was used in the analyses (**Table 2**).

The first canonical discriminant function for the 460 *M. curema* individuals classified by geographic variant explained 50.22% of the total variance among geographic variants, and the

TABLE 2 | MANCOVA test to assess the effect of locations, genetic structure, and marine ecoregions on scale shape.

Test	Wilks λ	*F*	*p*
Total length	0.920	3.784	<0.0001
Locations	0.177	7.780	<0.0001
Genetic structure	0.378	12.364	<0.0001
Marine ecoregions	0.533	10.453	<0.0001

p value of significance test.

second represented 20.49% (Wilks $\lambda = 0.144$, $p < 0.0001$). The original discriminant analysis correctly classified 47.6% of the fish scales in each locality, whereas the cross-validation analysis correctly classified 42.2% of the fish scales (**Table 3**). The best classification index (66.7%) was that of CU, followed by LM and SI with 65.3% and 59.5%, respectively. Most of the erroneous classifications occurred between CA-AL, SA-CE, and HU-SAB (**Table 3**). Three groups were defined in the graph of the first two discriminant functions, with the specimens of SAB, SI, SA, and CE separated mainly in the first discriminant function with respect to LM, ME, CA, AL, and TA with a considerable overlap of samples, whereas the BA and CU specimens with lower scores were separated in the second function (**Figure 3**). San Antonio Bay (SAB) is closer to the SA, CE, and SI localities in the Caribbean, while HU on the Pacific coast was more similar to the Gulf of Mexico localities than to the other Pacific localities.

The variations in shape among localities are presented in **Figure 3**, where the leftmost grid represents the mean shape of *M. curema* warped to a score of -2.0, basically for the localities in the north and center of the Gulf of Mexico (LM, TA, CA, ME, and AL) and the Huave system (HU) on the Pacific coast. This fish scale was characterized by a relatively shorter distance between the focus and landmark 7. Likewise, the rightmost grid represents the mean shape of *M. curema* warped to a score of 2.0, basically for the localities in the southern Gulf of Mexico (SI, SA, and CE) and SAB in the northwestern Gulf of Mexico. The downmost grid represents the localities along the Pacific (CU and BA). The key difference between the grids lies in the relative location of the focus, which is relatively more posterior in the Pacific localities. Further, the anterior edge of the scale was convex in the Pacific specimens but concave in the southern Gulf of Mexico specimens.

Regarding the discriminant analysis for the genetic groups, the first discriminant function explained 65.0% of the total variance, and the second represented 32.8% (Wilks $\lambda = 0.359$, $p < 0.0001$). The discriminant analysis correctly classified 62.0% of the original grouped cases, whereas the cross-validation resulted in a correct classification of 58.3% (**Table 4**). CP presented the best classification rate with 77.5% correctly classified after cross-validation and was followed by SG and NG with 62.9% and 52.5%, respectively. Misclassifications were common between NG and CG (**Table 4**). Three groups were defined in the graph of the first two discriminant functions of the analysis of the genetic groups. The SG specimens were separated mainly in the first discriminant function with respect to NG and CG with a considerable overlap of samples, whereas the CP specimens were separated by the second function (**Figure 4**).

With respect to the morphometrics arrangement of the marine ecoregions, the first discriminant function explained 61.5% of the total variance, and the second function represented 27.9% (Wilks $\lambda = 0.533$, $p < 0.0001$). The discriminant analysis correctly classified 58.7% of the original cases, whereas the cross-validation correctly classified 55.9% (**Table 5**). The best classification index was that of the MTP with 81.4%, followed by the NGM and the NC with 52.1% and 50.0%, respectively. The morphometrics results of the two discriminant functions indicate that the MTP was separated from the other marine ecoregions in the first function, compared with the other three marine ecoregions of the Gulf of Mexico (NGM and SGM) and the CN ecoregion of the Pacific coast (**Figure 5**).

DISCUSSION

There is currently a taxonomic problem still under discussion: if *M. curema* in the Pacific is the same species as that in the Atlantic. According to Durand et al. (2012), Durand and Borsa (2015), and Nirchio et al. (2017), the genetic distance between both coasts is from 3.2% to 5.4%, enough to be considered as cryptic species.

TABLE 3 | Classification results[a] in percentage of the discriminant analysis of the shape of the *M. curema* scale for the 12 geographic variants.

		Predicted group membership												
		Gulf of Mexico locations									Pacific locations			
	Location	SAB	LM	TA	CA	AL	ME	SA	CE	SI	CU	BA	HU	Total
Gulf of Mexico locations	SAB	**29.2**	0.0	0.0	0.0	4.2	4.2	4.2	8.3	16.7	8.3	4.2	20.8	100.0
	LM	2.0	**65.3**	4.1	0.0	2.0	8.2	0.0	0.0	0.0	8.2	8.2	2.0	100.0
	TA	2.3	11.4	**36.4**	2.3	6.8	11.4	0.0	2.3	0.0	11.4	9.1	6.8	100.0
	CA	0.0	14.0	4.0	**36.0**	18.0	10.0	0.0	0.0	0.0	4.0	2.0	12.0	100.0
	AL	3.8	9.6	13.5	23.1	**9.6**	15.4	1.9	1.9	1.9	7.7	9.6	1.9	100.0
	ME	0.0	24.5	16.3	8.2	4.1	**30.6**	0.0	2.0	2.0	6.1	2.0	4.1	100.0
	SA	0.0	0.0	9.1	9.1	0.0	0.0	**18.2**	45.5	9.1	0.0	0.0	9.1	100.0
	CE	7.1	0.0	7.1	0.0	0.0	0.0	28.6	**35.7**	14.3	7.1	0.0	0.0	100.0
	SI	5.4	0.0	0.0	5.4	5.4	2.7	5.4	8.1	**59.5**	8.1	0.0	0.0	100.0
Pac. location	CU	0.0	2.0	9.8	0.0	0.0	2.0	2.0	2.0	2.0	**66.7**	11.8	2.0	100.0
	BA	0.0	0.0	5.9	13.7	2.0	3.9	0.0	0.0	2.0	19.6	**52.9**	0.0	100.0
	HU	25.0	7.1	3.6	0.0	0.0	7.1	7.1	0.0	3.6	0.0	7.1	**39.3**	100.0

Total classification success for cross-validated predicted geographic variant. [a]Of cross-validated grouped cases, 42.2% were correctly classified. In bold the percentage of correct classification by locality.

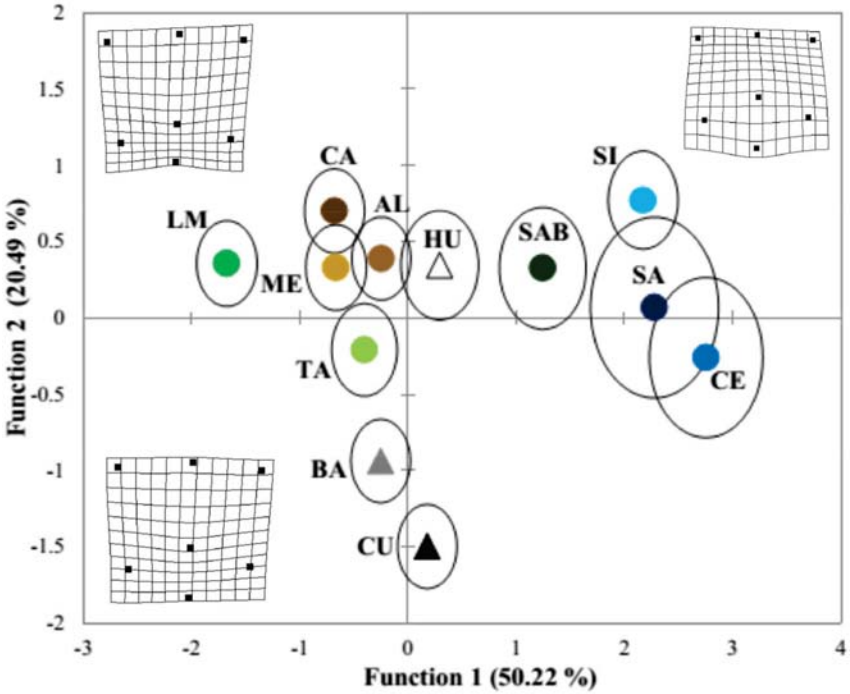

FIGURE 3 | Plot of the discriminant function scores from the analysis of geographic variants of *Mugil curema.* Circles, locations in Gulf of Mexico, and triangles, locations in the Mexican Pacific. The thin plate spline transformation grids represent the mean shape of *M. curema* for the localities: LM, TA, CA, ME, and AL (leftmost). The rightmost grid represents the mean shape for the SI, SA, CE, and SAB localities, and the downmost grid represents the localities along the Pacific (CU and BA).

The locations BA and CU from the Pacific (with exception of HU to be discussed later) showed more integrity within them in the canonical discrimination analysis (**Table 3**). In this sense, scale shape also agrees or reflects the difference between these two possible species.

The results obtained in this study indicate that the scale shape of the *M. curema* reflects the genetic patterns previously established by Pacheco-Almanzar et al. (2017) and Pacheco-Almanzar (2019). These could be assessed by the highest percentage of discrimination. This could be seen through the canonical discrimination results, the MANCOVA, and the Wilks λ values, as well as in the arrangements of the specimens in the discrimination figures, that is, the HU locality of the Pacific coast that is joined with the Gulf of Mexico localities (**Figure 3**) and the specimens of the Chiapas-Nicaragua ecoregion, represented only by the HU individuals, which take a position with the Gulf of Mexico localities (**Figure 5**). It was surprising that, as with the genetic structure (microsatellite analysis), San Antonio Bay formed a group with Sabancuy in Campeche, and Celestun and Sisal in Yucatan (the Caribbean localities).

Mugilid larvae are passively dispersed by currents, which enables the dispersion and flow of genes over long distances and across broad geographic scales (Whitfield et al., 2012). Current dynamics in each ocean may thus play an important role in defining both genetic and morphometric groups.

The California Current (CC) and the Costa Rica Coastal Current (CRCC) meet in the Mexican Pacific and are joined by part of the North Equatorial Current (NEC). The CRCC reaches only the Gulf of Tehuantepec where its surface waters return south due to an anticyclonic flow that forces the CRCC to leave the coast and feed the NEC. Consequently, the two groups found in the Pacific correspond to two marine ecoregions that may be seen as units of evolutionary isolation: the Mexican Tropical Pacific and the Chiapas-Nicaragua region according to Spalding et al. (2007). On the other hand, the Gulf of Mexico currents and river discharges divide this basin into two areas, the North where the Mississippi river (with a discharge of 18,400 m^3/s) is the primary source of watershed and discharge data for the Gulf of Mexico and the South that receives a great volume of Caribbean water. Also, different spawning seasons may result in different scale shapes and genetic structures of *M. curema* in the Gulf of Mexico (Ibáñez and Colín, 2014; Pacheco-Almanzar et al., 2017).

Ocean circulation acts as a barrier to the dispersal of larvae and leads to genetic structuring (Karlsson et al., 2009; Castillo-Olguín et al., 2012; Prieto-Ríos et al., 2014) and morphological differentiation (AnvariFar et al., 2013; Gkafas et al., 2013). The morphological variability recorded among different localities or geographic variants may be due to the genetic structure or to differences in the environmental conditions that prevail in each geographic area.

The causes of morphological differences among populations are often difficult to explain (Poulet et al., 2004; Silva et al., 2008). It has been suggested that the morphological

TABLE 4 | Classification results[a] for the cross-validation testing procedure for the four genetic groups: NG, North of GM; CG, Central of GM; SG, South of GM; CP, Central Pacific.

	Predicted group membership				
Genetic groups	**NG**	**CG**	**SG**	**CP**	**Total**
NG	**52.5**	26.2	5.0	16.3	100.0
CG	35.6	**41.6**	10.9	11.9	100.0
SG	4.3	19.8	**62.9**	12.9	100.0
CP	9.8	9.8	2.9	**77.5**	100.0

[a]*Of cross-validated grouped cases, 58.3% were correctly classified. In bold the percentage of correct classification by genetic groups.*

TABLE 5 | Classification results[a] for the cross-validation testing procedure for the four marine ecoregions: NGM, Northern Gulf of Mexico; SGM, Southern Gulf of Mexico; MTP, Mexican Tropical Pacific; CN, Chiapas-Nicaragua ecoregion.

Marine ecoregions	Predicted group membership				
	NGM	**SGM**	**MTP**	**CN**	**Total**
NGM	**52.1**	13.7	17.8	16.4	100.0
SGM	23.5	**47.5**	15.7	13.3	100.0
MTP	7.8	8.8	**81.4**	2.0	100.0
CN	26.7	10.0	13.3	**50.0**	100.0

[a]*Of cross-validated grouped cases, 55.9% were correctly classified. In bold the percentage of correct classification by marine ecoregions.*

characteristics of fish are determined by the interaction between genetic and environmental factors (Poulet et al., 2004; Salini et al., 2004; Pinheiro et al., 2005; AnvariFar et al., 2011, 2013). Studies such as that of Pinheiro et al. (2005) make clear that the environmental characteristics that prevail during the early stages of development, when individuals may be phenotypically affected by the environment, are particularly important regarding morphological results. For example, different environmental and habitat conditions, such as temperature, turbidity, food availability, and water depth and flow, in different rivers have been seen to cause morphological differentiation in *Capoeta* sp. specimens (Samaee et al., 2009; AnvariFar et al., 2011).

The genetic groups of *M. curema* previously differentiated through microsatellite markers (Pacheco-Almanzar et al., 2017; Pacheco-Almanzar, 2019) were successfully distinguished regarding the shape of their scales, indicating that both genetic and environmental factors can significantly influence the formation of the scale shape. Staszny et al. (2013) and Albertson et al. (2018) reported results similar to those of this study for other fish species. Finally, the integration of genetic data through phenotypic traits (the shape of the scale in this case) has the

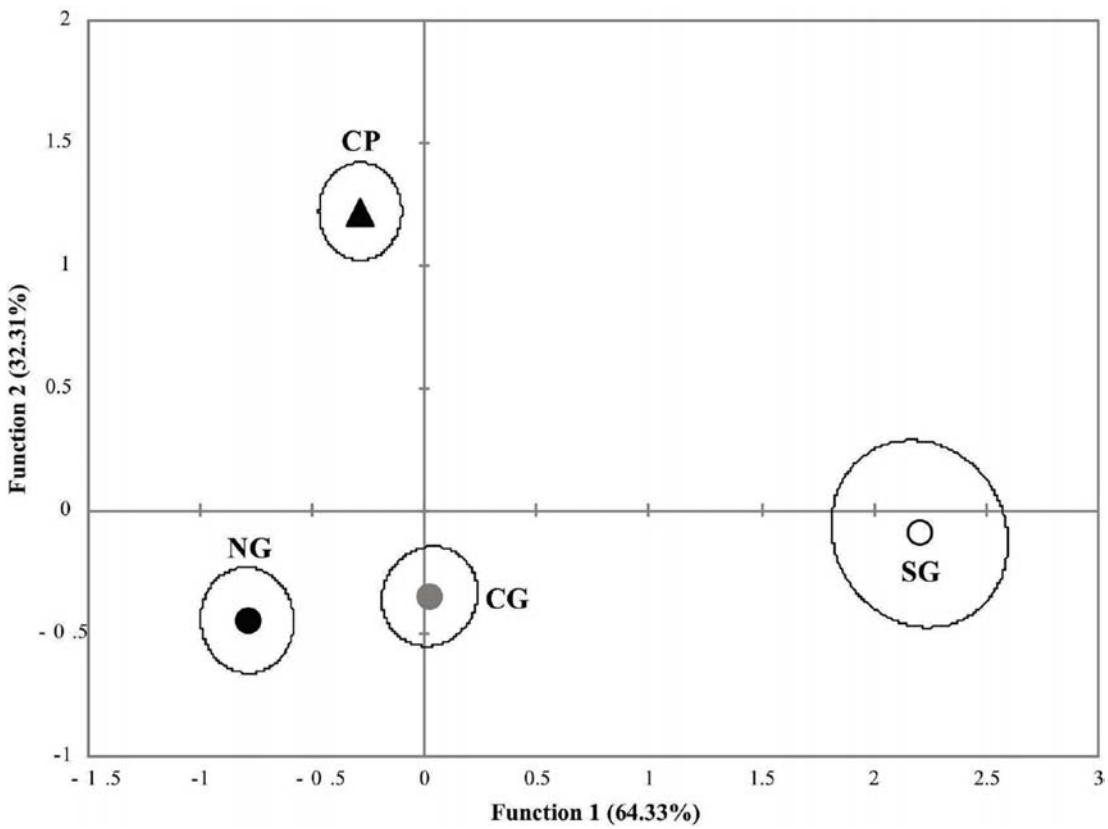

FIGURE 4 | Scatterplot of the discriminant function scores from the analysis of genetic groups of *Mugil curema*. Gulf of Mexico locations are circles, and Pacific are triangles. Genetic groups: NG, black; CG, gray; SG, white; CP, black.

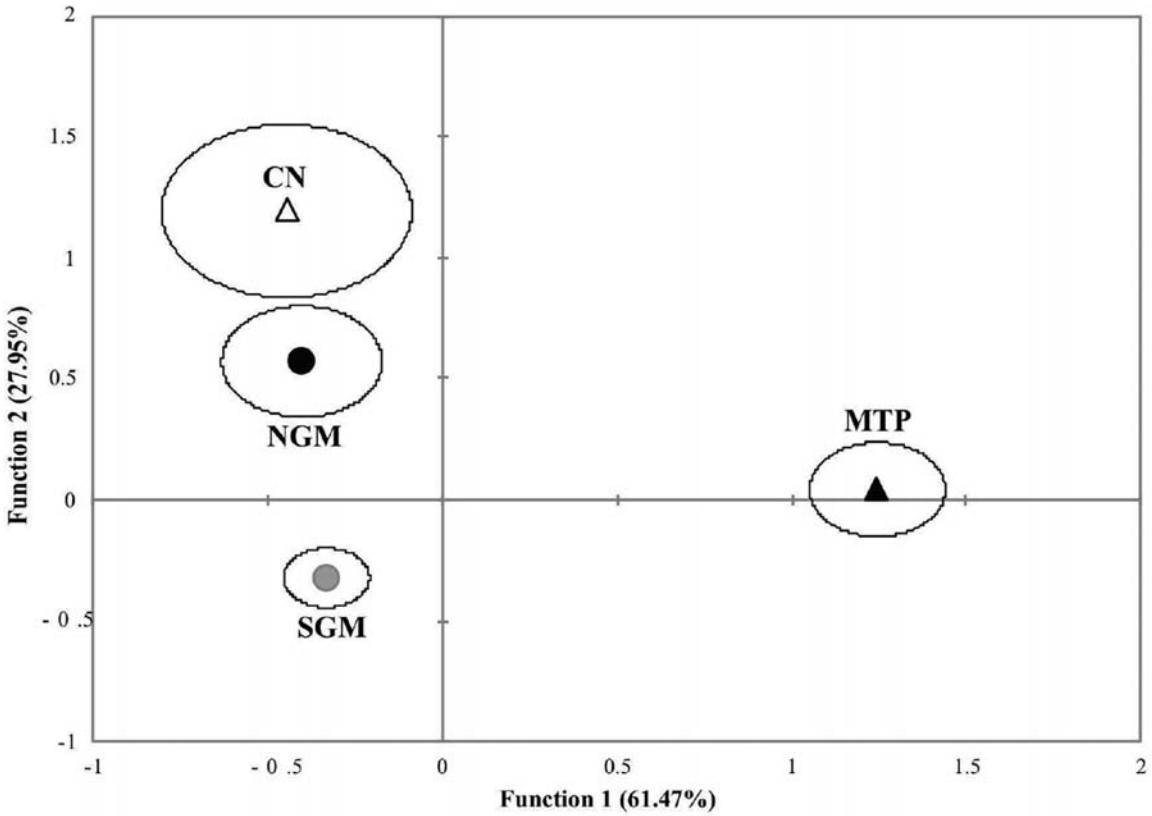

FIGURE 5 | Scatterplot of the discriminant function scores from the analysis of the marine ecoregions. Northern Gulf of Mexico (NGM), black circles; Southern Gulf of Mexico (SGM), gray circles; Mexican Tropical Pacific (MTP), black triangles; Chiapas-Nicaragua (CN), white triangles.

potential to provide a broad view of the roles of adaptation and evolution of phenotypes.

DATA AVAILABILITY STATEMENT

The datasets generated for this study are available on request to the corresponding author.

ETHICS STATEMENT

Research was carried out in accordance to Mexican laws and regulations. White mullet was collected under the Official Mexican Norm (NOM-016 PESC-1994) for commercial species. Fish were euthanized humanely by being placed directly into an ice water bath upon capture. No non-target or by-catch specimens were collected during the study.

AUTHOR CONTRIBUTIONS

EP-A and AI conceived the research and carried out the field work. NL-E processed and prepared the fish scales and performed the statistical analysis. EP-A reviewed the process and preparation of samples. EP-A prepared the initial manuscript. All authors contributed to later revisions.

FUNDING

This study was funded by the Universidad Autónoma Metropolitana and Consejo Nacional de Ciencia y Tecnología (CONACyT), project number 165569 under the Basic Science convening.

ACKNOWLEDGMENTS

The authors would like to thank Norman Boyd and James Simons for the sample of San Antonio Bay, Juan Carlos Pérez Jiménez for the sample of Sabancuy, Xavier Chiappa, Maribel Badillo, and Fernando Mex y Alfredo Gallardo for his help in sample collection of Sisal, Elaine Espino Barr from CRIP-Manzanillo for his help in sample collection of Colima, and Pedro Cervantes for the sample of Huave lagoon System. Many thanks to the Texas Parksand Wildlife Department, United States to Norman Boyd (San Antonio Bay Ecosystem Leader) and James Simons (A&M Texas University) who collected the samples from Texas.

REFERENCES

Addinsoft, (2016). *XLSTAT 2016: Data Analysis and Statistical Solution for Microsoft Excel*. Paris: Pentraeth.

Albertson, R. C., Kawasaki, K. C., Tetrault, E. R., and Powder, K. E. (2018). Genetic analyses in Lake Malawi cichlids identify new roles for Fgf signaling in scale shape variation. *Commun. Biol.* 1:55. doi: 10.1038/s42003-018-0060-4

AnvariFar, H., Farahmand, H., Silva, D. M., Bastos, R., Khyabani, A., and AnvariFar, H. (2013). Fourteen years after the Shahid-Rajaei dam construction: an evaluation of the morphometric and genetic differentiation between isolated up- and downstream populations of *Capoeta Capoeta gracilis* (Pisces: Cyprinidae) in the Tajan River of Iran. *Gen. Mol. Res.* 12, 3465–3478. doi: 10.4238/2013

AnvariFar, H., Khyabani, A., Farahmand, H., and Vatandoust, S. (2011). Detection of morphometric differentiation between isolated up- and downstream populations of Siah Mahi (*Capoeta capoeta gracilis*) (Pisces: Cyprinidae) in the Tajan river (Iran). *Hydrobiologia* 673, 41–52. doi: 10.1007/s10750-011-0748-7

Bookstein, F. L. (1989). Principal warps: thin-plate splines and the decomposition of deformations. *IEEE T. Pattern. Anal.* 11, 567–585. doi: 10.1109/34.24792

Cabral-Solís, E. G. (1999). *Estudio Sobre el Crecimiento y Aspectos Reproductivos de la Lebrancha Mugil curema* Cuvier y *Valenciennes, 1836, en la Laguna de Cuyutlán, Colima [Tesis de Maestría]*. Colima: Universidad de Colima.

Castillo-Olguín, E., Uribe-Alcocer, M., and Díaz-Jaimes, P. (2012). Assessment of the population genetic structure of *Sphyrna lewini* to identify conservation units in the Mexican Pacific. *Cienc. Mar.* 38, 635–652. doi: 10.7773/cm.v38i4.2110

De Pontual, H., and Prouzet, P. (1987). Atlantic salmon, *Salmo salar* L., stock discrimination by scale shape analysis. *Aquac. Fish. Manag.* 18, 277–289. doi: 10.1111/j.1365-2109.1987.tb00147.x

Dryden, I. L., and Mardia, K. V. (1993). Multivariate shape analysis. *Sankhya. Ser. A.* 55, 460–480.

Dryden, I. L., and Mardia, K. V. (1998). *Statistical Shape Analysis*. London: John Wiley and Sons.

Durand, J. D., and Borsa, P. (2015). Mitochondrial phylogeny of grey mullets (Acanthopterygii: Mugilidae) suggests high proportion of cryptic species. *C. R. Biol.* 338, 266–277. doi: 10.1016/j.crvi.2015.01.007

Durand, J. D., Shen, K. N., Chen, W. J., Jamandre, B. W., Blel, H., Diop, K., et al. (2012). Systematics of the grey mullets (Teleostei: Mugiliformes: Mugilic, dae): molecular phylogenetic evidence challenges two centuries of morphology-based taxonomy. *Mol. Phylogenet. Evol.* 64, 73–92. doi: 10.1016/j.ympev.2012.03.006

Espinosa-Pérez, H. (2014). Biodiversidad de peces en México. *Rev. Mex. Biodiv.* 85, 450–459. doi: 10.7550/rmb.32264

Garduño-Paz, M. V., Demetriou, M., and Adams, C. E. (2010). Variation in scale shape among alternative sympatric phenotypes of Arctic charr *Salvelinus alpinus* from two lakes in Scotland. *J. Fish. Biol.* 76, 1491–1497. doi: 10.1111/j.1095-8649.2010.02584.x

Gkafas, G. A., Tsigenopoulos, C., Magoulas, A., Panagiotaki, P., Vafidis, D., Mamuris, Z., et al. (2013). Population subdivision of saddled seabream *Oblada melanura* in the Aegean Sea revealed by genetic and morphometric analyses. *Aquat. Biol.* 18, 69–80. doi: 10.3354/ab00490

Ibáñez, A. L. (1993). Coexistence of *Mugil cephalus* and *M. curema* in a coastal lagoon in the Gulf of Mexico. *J. Fish. Biol.* 42, 959–961. doi: 10.1006/jfbi.1993.1101

Ibáñez, A. L. (2015). Fish traceability: guessing the origin of fish from a seafood market using fish scale shape. *Fish. Res.* 170, 82–88. doi: 10.1016/j.fishres.2015.05.016

Ibáñez, A. L., and Colín, A. (2014). Reproductive biology of *Mugil curema* and *Mugil cephalus* from western Gulf of Mexico waters. *Bull. Mar. Sci.* 90, 941–952. doi: 10.5343/bms.2014.1004

Ibáñez, A. L., Cowx, I. G., and O'Higgins, P. (2007). Geometric morphometric analysis of fish scales for identifying genera, species, and local populations within the Mugilidae. *Can. J. Fish. Aquat. Sci.* 64, 1091–1100. doi: 10.1139/F07-075

Ibáñez, A. L., Espino-Barr, E., and Gallardo-Cabello, M. (2012a). Population connectivity among geographic variants within the Lutjanidae through fish scales shape recognition. *Sci. Mar.* 76, 667–675. doi: 10.3989/scimar.03675.09C

Ibáñez, A. L., Pacheco-Almanzar, E., and Cowx, I. G. (2012b). Does compensatory growth modify fish scale shape. *Environ. Biol. Fish.* 94, 477–482. doi: 10.1007/s10641-011-9962-4

Ibáñez, A. L., and O'Higgins, P. (2011). Identifying fish scales: the influence of allometry on scale shape and classification. *Fish. Res.* 109, 54–60. doi: 10.1016/j.fishres.2011.01.016

Ibáñez-Aguirre, A. L., Cabral-Solís, E., Gallardo-Cabello, M., and Espino-Barr, E. (2006). Comparative morphometrics of two populations of *Mugil curema* (Pisces: Mugilidae) on the Atlantic and Mexican Pacific coasts. *Sci. Mar.* 70, 139–145. doi: 10.3989/scimar.2006.70n1139

Karlsson, S., Saillant, E., and Gold, J. R. (2009). Population structure and genetic variation of lane snapper (*Lutjanus synagris*) in the northern Gulf of Mexico. *Mar. Biol.* 156, 1841–1855. doi: 10.1007/s00227-009-1217-y

Kent, J. T. (1994). The complex Bingham distribution and shape analysis. *J. R. Stat. Soc. Ser. B Stat. Methodol.* 56, 285–299. doi: 10.1109/TPAMI.2008.234

Lara-Lara, J. R., Arenas, V., Bazán, C., Díaz, V., Escobar, E., García, M. C., et al. (2008). *Los Ecosistemas Marinos. Capital Natural de México. 1: Conocimiento actual de la biodiversidad*. México: CONABIO, 135–159.

Lucano-Ramírez, G., and Michel-Morfín, J. E. (1997). Ciclo reproductivo y aspectos poblacionales de *Mugil curema* (Valenciennes, 1836) (Pisces: Mugilidae) en la laguna costera Agua Dulce Jalisco, México. *Oceanología* 1, 105–115.

Marcus, L. F., Corti, M., Loy, A., Naylor, G. J. P., and Slice, D. (eds) (1996). *Advances in Morphometrics*. New York, NY: Nato ASI series Plenum Press.

Nirchio, M., Oliveira, C., Siccha-Ramirez, R., Sene, V. F., Sola, L., Milana, V., et al. (2017). The *Mugil curema* species complex (Pisces. Mugilidae): a new karyotype for the Pacific white mullet mitochondrial lineage. *Comp. Cytogenet.* 2, 225–237. doi: 10.3897/CompCytogen.v11i2.11579

O'Higgins, P., and Jones, N. (2006). *Tools for Statistical Shape Analysis*. Heslington: Hull York Medical School.

Pacheco-Almanzar, E. (2019). *Conectividad Entre Poblaciones de Mugil Curema (Pisces: Mugilidae) en el Golfo de México y Pacífico mexicano*. Ph.D Thesis, México: Universidad Autonoma Metropolitana.

Pacheco-Almanzar, E., Ramírez-Saad, H., Velázquez-Aragón, J. A., Serrato, A., and Ibáñez, A. L. (2017). Diversity and genetic structure of white mullet populations in the Gulf of Mexico analyzed by microsatellite markers. *Estuar. Coast. Shelf. S.* 198, 249–256. doi: 10.1016/j.ecss.2017.09.015

Pinheiro, A., Teixeira, C. M., Rego, A. L., Marques, J. F., and Cabral, H. C. (2005). Genetic and morphological variation of *Solea lascaris* (Risso, 1810) along the Portuguese coast. *Fish. Res.* 73, 67–78. doi: 10.1016/j.fishres.2005.01.004

Poulet, N., Berrebi, P., Crivelli, A. J., Lek, S., and Argillier, C. (2004). Genetic and morphometric variations in the pikeperch (*Sander lucioperca* L.) of a fragmented delta. *Arch. Hydrobiol.* 159, 531–554. doi: 10.1127/0003-9136/2004/0159-0531

Prieto-Ríos, E., Solís-Marín, F. A., Borrero-Pérez, G. H., and Díaz-Jaimes, P. (2014). Filogeografía de *Holothuria* (Halodeima) *inornata* Semper, 1868 (Echinodermata: Holothuroidea). *Rev. Peru. Biol.* 21, 155–162. doi: 10.15381/rpb.v21i2.9818

Rohlf, F. J. (2019). *Tps-dig. Freeware, Chaps*. Available at: https://life.bio.sunysb.edu/morph/soft-dataacq.html (accessed July 22, 2019).

Salini, J. P., Milton, D. A., Rahman, M. J., and Hussain, M. G. (2004). Allozyme and morphological variation throughout the geographic range of the tropical shad, hilsa *Tenualosa ilisha*. *Fish. Res.* 66, 53–69. doi: 10.1016/S0165-7836(03)00124-3

Samaee, S. M., Patzner, R. A., and Mansour, N. (2009). Morphological differentiation within the population of Siah Mahi, *Capoeta capoeta gracilis*, (Cyprinidae, Teleostei) in a river of the south Caspian Sea basin: a pilot study. *J. Appl. Ichthyol.* 25, 583–590. doi: 10.1111/j.1439-0426.2009.01256.x

Secretaría de Medio Ambiente, Recursos Naturales y Pesca (SEMARNAP), (2017). *Anuario estadístico. (de)Acuacultura y Pesca 2017*. México: Secretaría de Medio Ambiente, Recursos Naturales y Pesca, 300.

Silva, D. M., Da Cruz, A. D., Bastos, R. P., Telles, M. P. C., and Diniz-Filho, J. A. F. (2008). Morphometric and genetic differentiation among populations of *Eupemphix nattereri* (Amphibia, Anura, Leiuperidae) from central Brazil. *Iheringia, Sér. Zool.* 98, 493–500. doi: 10.1590/S0073-47212008000400013

Spalding, M. D., Fox, H. E., Allen, G. R., Davidson, N., Ferdaña, Z. A., Finlayson, F., et al. (2007). Marine ecoregions of the world: a bioregionalization of coastal and shelf Areas. *BioScience* 57, 573–583. doi: 10.1641/B570707

Staszny, Á, Havas, E., Kovács, R., Urbányi, B., Paulovits, G., Bencsik, D., et al. (2013). Impacts of environmental and genetic factors on

the scale shape of zebrafish, *Danio rerio* (Hamilton 1822): a geometric morphometrics study. *Acta. Biol. Hung.* 64, 462–475. doi: 10.1556/ABiol.64.2013.4.6

Swain, D. P., and Foote, C. J. (1999). Stocks and chameleons: the use of phenotypic variation in stock identification. *Fish. Res.* 43, 113–128. doi: 10.1016/S0165-7836(99)00069-7

Viera-Muñoz, A. (1979). *Proyecto Cultivo de Lisa (Mugil curema y Mugil cephalus) en el Estado de Jalisco*. Mexico City: Programa de inversiones públicas para el desarrollo rural. Departamento de Pesca, Mexico City, Mexico.

Villaseñor-Talavera, R. (1991). *Determinación de una Escala de Madurez Sexual Específica y Ovocitos de la Lisa Blanca Mugil Curema (Valenciennes, 1836) de la Región Litoral Central de Nayarit, México*. San Nicolás de los Garza, NL: Memorias del II Congreso Nacional de Ictiología.

Watkinson, D. A., and Gillis, D. M. (2005). Stock identification of Lake Winnipeg walleye based on fourier and wavelet description of scale outline signals. *Fish. Res.* 72, 193–203. doi: 10.1016/j.fishres.2004.11.002

Whitfield, A. K., Panfili, J., and Durand, J. D. (2012). A global review of the cosmopolitan flathead mullet *Mugil cephalus* Linnaeus 1758 (Teleostei: Mugilidae), with emphasis on the biology, genetics, ecology and fisheries aspects of this apparent species complex. *Rev. Fish. Biol. Fish.* 22, 641–681. doi: 10.1007/s11160-012-9263-9

Conflict of Interest: The authors declare that the research was conducted in the absence of any commercial or financial relationships that could be construed as a potential conflict of interest.

Copyright © 2020 Pacheco-Almanzar, Loza-Estrada and Ibáñez. This is an open-access article distributed under the terms of the Creative Commons Attribution License (CC BY). The use, distribution or reproduction in other forums is permitted, provided the original author(s) and the copyright owner(s) are credited and that the original publication in this journal is cited, in accordance with accepted academic practice. No use, distribution or reproduction is permitted which does not comply with these terms.

frontiers in Marine Science

BRIEF RESEARCH REPORT
published: 06 April 2020
doi: 10.3389/fmars.2020.00188

Annual Bands in Vertebrae Validated by Bomb Radiocarbon Assays Provide Estimates of Age and Growth of Whale Sharks

Joyce J. L. Ong[1], Mark G. Meekan[2], Hua Hsun Hsu[3], L. Paul Fanning[4] and Steven E. Campana[5]*

[1] Department of Ecology, Evolution and Natural Resources, Rutgers University, New Brunswick, NJ, United States, [2] Australian Institute of Marine Science, Crawley, WA, Australia, [3] Center for Environment and Water, King Fahd University of Petroleum and Minerals, Dhahran, Saudi Arabia, [4] Marine Fisheries Department, Food and Agriculture Organization of the United Nations, Karachi, Pakistan, [5] Life and Environmental Sciences, University of Iceland, Reykjavik, Iceland

OPEN ACCESS

Edited by:
Benjamin D. Walther,
Texas A&M University Corpus Christi,
United States

Reviewed by:
John R. Wallace,
Northwest Fisheries Science Center
(NOAA), United States
John Austin Mohan,
Texas A&M University, United States

***Correspondence:**
Joyce J. L. Ong
joyce.ong.jl@gmail.com

Specialty section:
This article was submitted to
Marine Ecosystem Ecology,
a section of the journal
Frontiers in Marine Science

Received: 12 December 2019
Accepted: 10 March 2020
Published: 06 April 2020

Citation:
Ong JJL, Meekan MG, Hsu HH,
Fanning LP and Campana SE (2020)
Annual Bands in Vertebrae Validated
by Bomb Radiocarbon Assays
Provide Estimates of Age and Growth
of Whale Sharks.
Front. Mar. Sci. 7:188.
doi: 10.3389/fmars.2020.00188

Conservation and management strategies for endangered and threatened species require accurate estimates of demographic parameters such as age and growth. The whale shark, *Rhincodon typus*, is the largest fish in the world and is highly valued in the eco-tourism sector. Despite conservation concerns and advances in our understanding of their life history, basic demographic parameters for growth, longevity and mortality are of questionable accuracy; previous growth studies could not agree whether the vertebral growth bands were formed annually or biannually. Here, we provide the first validation of the annual formation of growth bands within the vertebrae of the whale shark using bomb radiocarbon assays. Ages of up to 50 years were estimated from sectioned vertebrae of sharks collected in Taiwan and Pakistan. There was no cessation of the formation of growth bands in the vertebrae of older sharks and our study provides the oldest observed longevity for this species. Initial estimates of growth (k = 0.01–0.12) and natural mortality rates (M = 0.09–0.14) are consistent with those expected of long-lived sharks, which highlights their sensitivity to fishing pressure and conservation concerns.

Keywords: whale shark, vertebrae, age determination, radiocarbon, longevity, growth bands

INTRODUCTION

Accurate and reliable estimates of the age and growth of individuals in a population are central to effective strategies for the management and conservation of any species. For teleost marine fishes, estimates of age are usually obtained from counts of the annual growth bands formed within otoliths, which are calcified structures within the skull case (Campana, 2001). For elasmobranchs such as sharks, skates and rays, which lack otoliths, age estimates have been calculated from growth bands formed in the vertebrae (Cailliet, 1990).

It is critical that age estimates provided by otoliths and vertebrae are accurate, since uncertainty or underestimates surrounding these ages can lead to stock collapses

of exploited species (e.g., orange roughy *Hoplostethus atlanticus*; Smith et al., 1995), or compromise the effectiveness of recovery programs for species that are threatened or endangered. For this reason, many studies have sought to validate the timing of the production of growth bands (Campana, 2001). A common approach is to tag individuals with a chemical marker such as oxytetracycline (OTC) that is laid down within an otolith or vertebrae. Individuals are released and when recaptured at some time in the future, the tag acts as a time stamp that allows the rate of deposition of subsequent growth bands to be determined. For large fishes and sharks that are relatively long-lived and difficult to tag and recapture, validation of annual banding patterns can also be obtained through an analysis of bomb radiocarbon in vertebrae. Above-ground testing of thermonuclear weapons in the 1950s and 60s increased the ratio of carbon 14 isotopes in the atmosphere that were then mixed into the ocean, passed up food webs and incorporated into marine organisms. As a result, the timing of the deposition of bands can be validated by comparing carbon isotope values within vertebrae, with an isotope baseline chronology of known age (Campana, 2001; Campana et al., 2002; Goldman et al., 2012).

The whale shark, *Rhincodon typus*, is a huge (up to 18 m length; Mcclain et al., 2015), highly migratory, filter-feeding shark found in all tropical and warm temperate seas (Compagno, 2001; Chen et al., 2002; Stevens, 2007). It forms aggregations in productive coastal areas and is a highly valued target for marine eco-tourism (e.g., Huveneers et al., 2017). However, the whale shark has recently been classified as Endangered (IUCN Red List; Pierce and Norman, 2016) and there is now an urgent need for reliable and accurate information on age and growth of the species in order to develop effective conservation and management strategies. At present, there is relatively little demographic data available, especially for large or mature individuals. Using X-radiography, Wintner (2000) analyzed the growth bands in whole vertebrae of juveniles that had stranded on the coast of South Africa to develop an initial growth curve for the species. More recently, Hsu et al. (2014) provided growth and age estimates for individuals collected from a fishery in Taiwan and used marginal increment ratios and centrum edge analysis to conclude that growth bands were deposited biannually in both whole and sectioned vertebrae. The reliability of the age estimates of these studies remains unknown and is of concern, because other studies show that whole vertebrae are known to provide underestimates of age and longevity, and thus overestimates of growth rate in slow-growing sharks (Cailliet and Goldman, 2004; Harry, 2018; Natanson et al., 2018). To our knowledge, only one study has attempted to validate an aging method for whale sharks, which involved a captive immature shark reared in an aquarium after being fed OTC. When the animal died 2 years later, two growth bands were observed following the OTC mark (Wintner, 2000).

Here, we provide the first age validation of whale sharks using bomb radiocarbon assays. We then used sectioned vertebrae from a small sample of sharks to provide initial estimates of growth, longevity and mortality data that can be used in support of current conservation and management efforts.

METHODS

Sample Collection

A subset of vertebral samples were taken from 92 vertebral samples that were previously published in Hsu et al. (2014). These were dead individuals that had been landed by the Taiwanese fishery, before the whale shark fishery was closed in November 2007 (Hsu et al., 2012). The vertebral sample from Pakistan was obtained from a dead stranded whale shark.

Sample Preparation and Age Interpretation

The vertebral samples from Hsu et al. (2014) were sectioned with a single cut using paired blades separated by a spacer on an Isomet low-speed diamond-bladed saw. Sections were digitally photographed at 2048 × 1536 resolution using a digital color Leica camera DFC295 mounted on a stereo microscope Leica M205C (Leica Microsystems, Germany), while immersed in ethanol. Age interpretation was based on images enhanced for contrast using Adobe Photoshop CS6, following the interpretation criteria of Natanson et al. (2002). The precision of the age determinations was quantified with both average percent error (APE) and coefficient of variation (CV) (Campana, 2001).

Bomb Radiocarbon Analyses

Vertebrae used for bomb radiocarbon age validation were taken from two specimens that had died after becoming entangled in fishing gear. A 10 m total length (TL) female with an estimated weight of 7000 kg was landed in Karachi, Pakistan in February 2012. One of the cervical vertebrae was cleaned of tissue and then stored frozen. A second individual, a mature male weighing 8500 kg with TL of 9.9 m was landed in Taiwan in April 2005. A cervical vertebra over the gills was extracted and stored in ethanol until assay. Vertebral growth bands from both sharks were isolated from 1 mm thick longitudinal sections of the vertebrae. All sections were prepared using the same procedure outlined above. Sections were digitally photographed at 2048 × 2048 resolution under a binocular microscope at 16–40X magnification using reflected light while immersed in ethanol.

Multiple samples from each of the vertebral sections (N = 11 samples; 5–13 mg each) were extracted from growth bands visible in the corpus calcareum region while working at 16X magnification under a binocular microscope. For the shark landed in Taiwan, the first three growth bands were extracted as a single sample from the vertebral section. For the shark landed in Pakistan, the first-formed growth band (distal to the birth band) was extracted, as were individual growth bands corresponding to later growth. Extracted samples were isolated as solid pieces using a Gesswein high-speed hand tool fitted with steel bits < 1 mm in diameter. The presumed date of sample formation was calculated as the year of shark collection minus the annulus count from the birth band to the mid-point of the sample. After sonification in Super Q water and drying, the sample was weighed to the nearest 0.1 mg in preparation for ^{14}C assay with accelerator mass spectrometry (AMS). AMS assays also provided $\delta^{13}C$ (‰) values,

which were used to correct for isotopic fractionation effects. Radiocarbon values were subsequently reported as $\Delta^{14}C$, which is the per mil (‰) deviation of the sample from the radiocarbon concentration of 19th-century wood, corrected for sample decay prior to 1950 according to methods outlined by Stuiver and Polach (1977). The mean standard deviation of the individual radiocarbon assays was about 4‰.

To assign dates of formation to an unknown sample, it is necessary that the $\Delta^{14}C$ of the unknown sample be compared with a $\Delta^{14}C$ chronology based on known-age material (a reference chronology). Since whale sharks are surface planktivores, we assumed that a reference chronology for dissolved inorganic carbon (DIC) in surface waters was most appropriate for our analysis. Therefore, we used a reference chronology developed from young known-age otoliths (calcium carbonate) in the northwest Atlantic (Campana et al., 2008), which has a period of increasing bomb radiocarbon values nearly identical to that of surface waters off of both Pakistan and Taiwan (Andrews et al., 2011a). We also included another reference chronology based on corals from the Mentawai Islands in Sumatra, Indonesia (Grumet et al., 2004).

Growth Models

Preliminary growth estimates were obtained from length-at-age data using two types of growth model. The first was a conventional 3-parameter von Bertanlanffy growth function (Von Bertalanffy, 1938) and the second was a logistic growth function (Smart et al., 2013) with length-at-birth fixed at 60 cm (Chang et al., 1997).

3-parameter von Bertanlanffy growth function:

$$L_t = L_0 + (L_\infty - L_0)(1 - e^{-kt})$$

Logistic growth function with fixed length-at-birth:

$$L_t = \frac{L_\infty L_0 e^{kt}}{L_\infty + L_0(e^{kt} - 1)}$$

where L_t is length-at-age t, L_0 is length-at-age 0, L_∞ is asymptotic length and k is the growth coefficient.

Longevity estimates generally require either a precisely defined growth model or an estimate of mortality rate, neither of which were available here. Therefore, only the observed maximum age is reported here. Natural mortality was estimated from two equations. The first was based on the linear regression equation of observed maximum age (Hoenig, 1983):

$$\ln(M) = 1.44 - 0.982 \times \ln(t_{max})$$

The second natural mortality estimate was based on the non-linear least squares equation of observed maximum age, with a prediction error of 0.32 (Then et al., 2015):

$$M = 4.899 \times {t_{max}}^{-0.916}$$

where M is the estimated instantaneous rate of natural mortality and $t_{\max}$ is the observed maximum age.

RESULTS

Counts of Growth Bands in Vertebrae Samples

All vertebrae exhibited distinct growth band (annulus) patterns (**Figure 1**). The birth mark was identified as the most pronounced first band. Subsequent annuli consisted of a pair of alternating opaque and translucent bands that crossed the entire centrum, except in the oldest sharks. Band width decreased with age, narrowing substantially in the oldest individuals (**Figure 1**). Counts of growth bands in 20 sharks ranged from 15 to 50 (**Table 1**). Aging precision was acceptable across both readers, with an APE of 5.5% and CV of 8.2%.

Bomb Radiocarbon Assays and Age Validation

The date of formation of the vertebral samples was estimated in two ways: (1) through age determination of the shark based on growth band (annulus) counts; and (2) through comparison

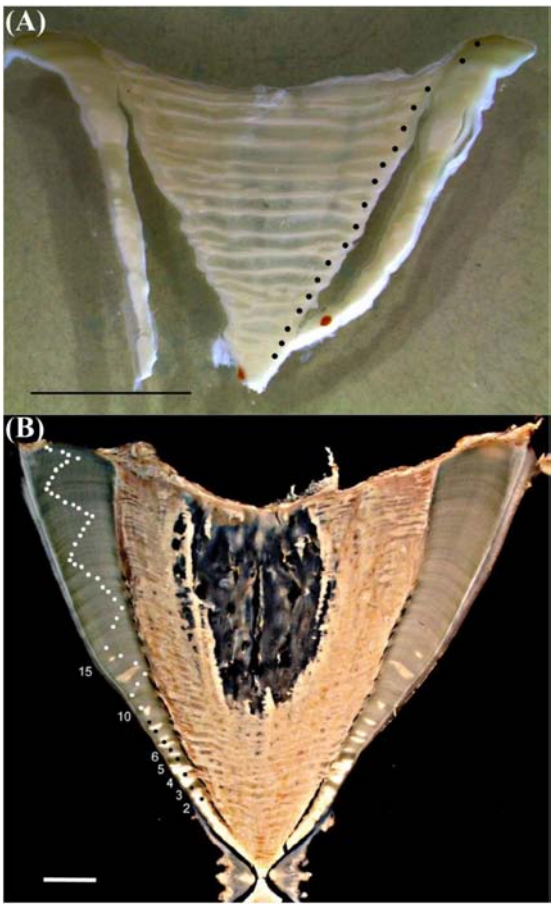

FIGURE 1 | Images of sectioned whale shark vertebrae with annotations of growth bands. **(A)** Vertebra from Taiwan (RT04) showing 18 growth bands. **(B)** Vertebra from Pakistan (RT20) used for bomb radiocarbon assay showing 50 growth bands. Scale bars – 1 cm.

TABLE 1 | Summary details for vertebral samples.

ID	Date of collection	Sex	TL (cm)	Weight (kg)	Growth bands
RT01	18 March 2001	F	425	760	23
RT02	26 May 2005	F	345	400	18
RT03	NA	M	596	2000	24
RT04	NA	NA	NA	NA	18
RT05	NA	M	423	750	18
RT06	NA	M	391	600	21
RT07	18 May 2005	M	421	700	25
RT08	30 September 2005	M	372	350	20
RT09	26 April 2005	M	358	360	16
RT10	3 July 2005	M	494	1100	16
RT11	6 October 2005	F	NA	NA	15
RT12	2 July 2005	M	503	905	18
RT13	13 September 2005	M	300	200	18
RT14	10 July 2005	M	430	450	19
RT15	18 June 2005	M	386	450	17
RT16	NA	NA	NA	NA	19
RT17	10 October 2005	M	526	NA	19
RT18	3 May 2005	M	268	123	17
RT19	April 2005	M	990	8500	35
RT20	February 2012	F	1000	7000	50

TL, total length (cm). RT19 and RT20 were samples used in the bomb radiocarbon analyses. All samples were collected in Taiwan except for RT20, which was collected in Pakistan.

TABLE 2 | Details for bomb radiocarbon assays.

ID	Growth bands sampled	Date of formation	$\delta^{13}C$ (‰)	$\Delta^{14}C$ (‰)
RT19	1–3	1972.0	−15.1	81.3
RT20	0–1	1962.5	−13.3	15.1
RT20	1	1962.5	−13.3	15.1
RT20	2	1963.5	−13.9	59.4
RT20	3	1964.5	−13.1	70.0
RT20	4	1965.5	−12.9	70.0
RT20	5	1966.5	−15.5	40.0
RT20	5	1966.5	−15.6	40.0
RT20	6	1967.5	−12.8	20.6
RT20	10	1971.5	−12.1	63.4
RT20	15	1976.5	−11.9	45.0

RT19 was collected in Taiwan and RT20 was collected in Pakistan. Each row is a separate assay, any replicates were from different assays.

of annulus $\Delta^{14}C$ values with the values known to be present in surface marine waters at the time (the NWA reference chronology). Agreement between the annulus- and $\Delta^{14}C$ -based dates would confirm that the annuli were interpreted correctly for age estimation, at least on average. Under- or over-aging of annuli would be apparent as a left or right phase-shifting of the reference curve relative to the assay values.

Eleven samples from two whale sharks, aged 35 and 50 years based on growth band counts, were analyzed for $\Delta^{14}C$ (**Table 2**). Assay values ranged between 15.1 and 70.0. Two of the samples, including one with the earliest date of formation (1962.5), were too depleted in $\Delta^{14}C$ (15.1 and 20.6) to have formed post-bomb (**Figure 2**), but no pre-bomb samples were identified. The remaining $\Delta^{14}C$ values all ranged between 40 and 70, which is consistent with a post-bomb year of formation. All samples were characterized by $\delta^{13}C$ values consistent with typical shark vertebrae of metabolic origin (mean = −13.6; SE = 0.4; **Table 2**).

All of the assay values aligned well with the reference chronologies (**Figure 2A**), with no obvious bias to one side or the other. Since errors in growth band counts would result in misalignment of the reference and assay values, the assay results indicate that the two sharks must have been aged correctly, at least on average. The 35-year old shark from Taiwan was least informative in this respect, since its post-bomb assay value indicated only that the shark could not have been over-aged by more than 10 years. Conversely, aging error of more than about 5 years would have been apparent as an obvious misalignment in the 50-year old Pakistan shark.

Preliminary Growth, Longevity and Mortality Estimates

Both sexes were combined for estimation of growth (**Figure 2B**). The von Bertanlanffy growth function produced an asymptotic length L_∞ = 2189 cm and a growth coefficient k = 0.014 year^{-1}. The logistic growth function with a fixed length-at-birth L_0 = 60 cm produced estimates of L_∞ = 1071 cm and k = 0.122 year^{-1}. We caution, however, that the estimates of asymptotic length and growth coefficients are uncertain because of low sample size. The maximum observed age was 50 years based on vertebral aging and bomb radiocarbon assays. The Hoenig (1983) estimated rate of instantaneous natural mortality was 0.09 year^{-1}, while the estimate from Then et al. (2015) was 0.14 year^{-1}.

DISCUSSION

Our study used bomb radiocarbon assays to provide the first validated age estimates for whale sharks. We showed that growth bands in sectioned vertebrae can provide accurate estimates of sharks aged up to 50 years old. These results confirm the use of sectioned vertebrae as age indicators for these sharks, as is also the case for other large species, such as white (Hamady et al., 2014), shortfin mako (Natanson et al., 2006), sandbar (Andrews et al., 2011b), and porbeagle (Natanson et al., 2002) sharks. We found no evidence that vertebral counts underestimated the age of older individuals, as can be the case for porbeagle and white sharks (Francis et al., 2007; Hamady et al., 2014), presumably because the much larger asymptotic body size means that there is no cessation of vertebral growth in the older sharks we sampled in our study.

Although our understanding of the movements, behavior, connectivity and distribution of whale sharks have improved dramatically over the last 10 years (Schmidt et al., 2009; Sequeira et al., 2012, 2013), basic life history traits such as age, longevity and mortality remain unknown and are frequently inferred (e.g., Bradshaw et al., 2007). This lack of basic demographic information has been consistently highlighted in multiple reviews

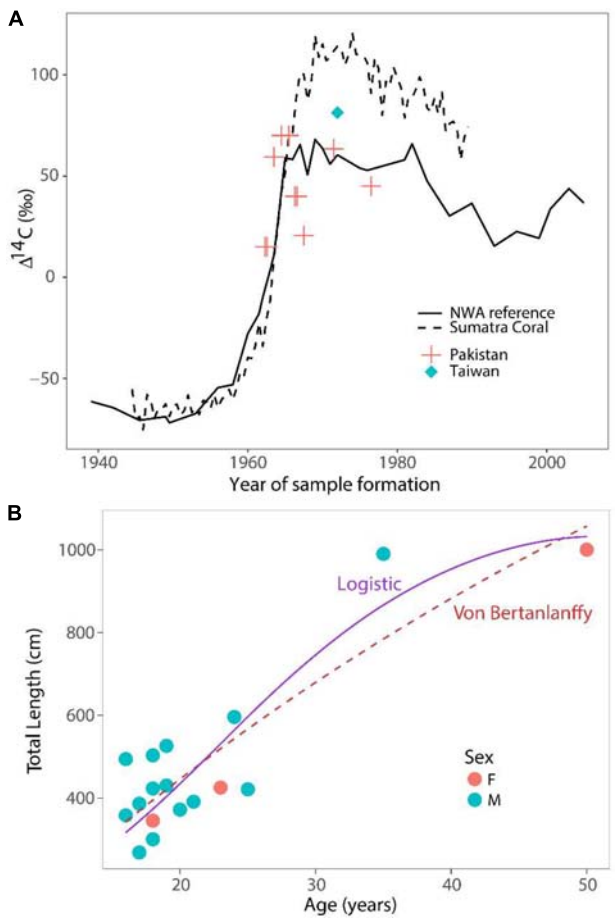

FIGURE 2 | Results of bomb radiocarbon assays and growth models. **(A)** Bomb radiocarbon ($\Delta^{14}C$) results of whale shark vertebrae from two locations (Pakistan – red crosses; Taiwan – blue diamond) compared to two reference chronologies (carbonate surface water reference from north west Atlantic – solid line; coral reference from Sumatra – dashed line). **(B)** Length-at-age data fitted with logistic (solid purple) and von Bertanlanffy (dashed red) growth models. Data pooled between sexes for both models.

of the biology and ecology of whale sharks (Colman, 1997; Stevens, 2007; Rowat and Brooks, 2012). Few studies have directly estimated age, growth and longevity from vertebral samples of wild populations, due to the lack of samples. To our knowledge, only two studies (Wintner, 2000; Hsu et al., 2014) have analyzed vertebral growth bands to provide age estimates. In the first of these, Wintner (2000) used x-radiography to count bands within the vertebral centra of 15 whale sharks from South Africa and assumed that these were formed annually. The oldest specimen was a male with 31 growth bands (770 cm precaudal length), but a von Bertanlanffy growth model could not be fitted to the data. A second, more recent study by Hsu et al. (2014) analyzed the vertebrae of 92 whale sharks collected by a fishery off the coast of Taiwan. Age validation was based on two forms of marginal increment analysis, which gave inconsistent results. This approach has been criticized as a problematic form of age validation, but is often the only technique available to researchers when mark-recapture studies are not feasible (Campana, 2001; Cailliet and Goldman, 2004). Based on this validation, Hsu et al. (2014) assumed that two growth bands were formed each year. In their study, the oldest specimen (a male, 988 cm total length) had 42 growth bands and was thus assumed to be 21 years old. Perhaps more importantly, counts of growth bands by Hsu et al. (2014) were made in the intermedialia region, which contrasts to most other studies that use the corpus calcareum region of shark vertebrae for age interpretation (e.g., Campana et al., 2002; Christiansen et al., 2016). Our results, based on growth bands visible in the corpus calcareum region of sectioned vertebrae and validated with bomb radiocarbon assays, confirmed that growth bands must have formed annually, suggesting that the study of Hsu et al. (2014) overestimated growth rates of the species.

Our estimate of k = 0.014 year^{-1} for whale sharks from the von Bertanlanffy growth model was lower than the estimates provided by both Wintner (2000) and Hsu et al. (2014). The study by Wintner (2000) reported linear growth for 15 individuals, all of which were less than 8 m in length and under 30 years old. To constrain the growth curve, Wintner (2000) added two theoretical data points (60 and 100 years with 14 m TL) to obtain k = 0.032 or 0.021 year^{-1}, respectively, with L_∞ of 13.7 m TL. The more recent study by Hsu et al. (2014) included the lengths of 3 full-term embryos and used a modified 2-parameter von Bertanlanffy growth model to obtain two growth curves that were based on either biannual or annual deposition of growth bands. For annual growth bands, they reported estimates of k = 0.021 year^{-1} with L_∞ of 15.3 m TL. In our study, the predicted L_∞ (21.9 m TL) was close to the largest maximum length ever recorded in the wild, estimated at 20 m from Taiwan in March 1987 (Chen et al., 2002) and close to maximum sizes recorded in other locations (Mcclain et al., 2015). This suggests that the growth models of both Wintner (2000) and Hsu et al., 2014 underestimated maximum sizes of whale sharks. We did, however, find a large difference between the growth coefficients of the von Bertanlanffy and the logistic growth models, with the latter having higher growth coefficients but seeming to underestimate L_∞. In this context, it is important to note that our dataset represents a small sample of individuals and only included two mature individuals, hence it is likely that the asymptotic length estimated in the von Bertanlanffy growth model was poorly constrained and thus unrealistic. Actual growth parameters are probably bracketed by the results of the two growth models. Given the closure of the fishery in Taiwan and the protection of whale sharks in the waters of many of the countries where they occur (Rowat and Brooks, 2012), increased sample sizes are likely to rely on unfortunate but opportunistic events such as stranding (Wintner, 2000; Speed et al., 2009) to provide new vertebrae for analysis. Alternatively, photo-identification and imagery techniques may now offer a means to estimate *in-situ* growth rates for whale sharks, for at least the individuals and size classes participating in nearshore aggregations (e.g., Perry et al., 2018).

Our estimates of natural mortality for whale sharks, ranging from 0.09 to 0.14 year^{-1} was close to those of other large species

of sharks, such as the filter-feeding basking shark (0.07 year^{-1}; Pauly, 2002; Campana et al., 2008), white (0.08 year^{-1}; Mollet and Cailliet, 2002), and scalloped hammerhead (0.10 year^{-1}; Cortés and Brooks, 2018) sharks. These estimates are generally considered low, however, for smaller whale sharks ($<$ 3 m TL), mortality rates may be higher, since the early juvenile stage is likely to be the most vulnerable to predators (Rowat and Brooks, 2012). Information on this life history stage is difficult to gather, because neonatal and very young whale sharks are only rarely encountered and are assumed to reside in the open ocean away from coasts (Rowat et al., 2008).

Our estimates of slower growth and greater observed longevity have important implications for conservation of whale sharks. Underestimation of longevity and overestimation of growth is a serious concern for management strategies for fisheries, because it has led to population crashes due to overharvesting (e.g., orange roughy; Smith et al., 1995). The case for whale sharks is somewhat different from other species that are targeted in fisheries, in part because they are protected across most of their distribution (Bradshaw et al., 2008; Hsu et al., 2012). This status reflects the continuing rise and value of eco-tourism in sites where they aggregate, such as Ningaloo Reef in Western Australia (Meekan et al., 2006). Although the harvesting of whale sharks has been reduced for over a decade, the sizes and abundances of populations have declined in multiple regions (Theberge and Dearden, 2006; Bradshaw et al., 2008), which is reflected in the recent upgrade of the species from Threatened to Endangered by the IUCN Red List (Pierce and Norman, 2016). Given the slow growth rates, extended longevity, late maturity and global connectivity of this species (Bradshaw et al., 2007; Graham and Roberts, 2007; Sequeira et al., 2013), this species is likely to be highly susceptible to sources of anthropogenic mortality such as ship-strike (Bradshaw et al., 2007; Speed et al., 2008). We are hopeful that the demographic data we have provided in this study will help to improve the accuracy of population models (e.g., persistence, survival) and hence, better inform management and conservation efforts for this iconic species.

DATA AVAILABILITY STATEMENT

All datasets generated for this study are included in the article/supplementary material.

ETHICS STATEMENT

This study was carried out in accordance with the guidelines of use of animal tissue/cadaver and the protocol was approved by the University of Western Australia Institutional Biosafety Committee.

AUTHOR CONTRIBUTIONS

MM and SC conceived of the idea, HH and LF provided the vertebral samples. JO did the sample preparation and analyses for vertebrae aging. SC contributed to bomb radiocarbon results and verified aging results. JO wrote the manuscript, with critical feedback and help from SC, MM, LF, and HH.

FUNDING

This work was supported by the Fisheries and Oceans Canada, US National Science Foundation Grant OCE-9985884, and the University of Iceland. Travel funding was provided by the Australian Institute of Marine Science.

ACKNOWLEDGMENTS

We are grateful to Warren Joyce for his help in the sectioning of the vertebral samples, and Prof. Shoou Jeng Joung at National Taiwan Ocean University for the use of his laboratory space to section and image the vertebral samples. We thank Brett Taylor for helping to improve the manuscript.

REFERENCES

Andrews, A. H., Kalish, J. M., Newman, S. J., and Johnston, J. M. (2011a). Bomb radiocarbon dating of three important reef-fish species using Indo-Pacific 14C chronologies. *Mar. Freshw. Res.* 62, 1259–1269.

Andrews, A. H., Natanson, L. J., Kerr, L. A., Burgess, G. H., and Cailliet, G. M. (2011b). Bomb radiocarbon and tag-recapture dating of sandbar shark (*Carcharhinus plumbeus*). *Fish. Bull.* 109, 454–465.

Bradshaw, C. J. A., Fitzpatrick, B. M., Steinberg, C. C., Brook, B. W., and Meekan, M. G. (2008). Decline in whale shark size and abundance at ningaloo reef over the past decade: the world's largest fish is getting smaller. *Biol. Conserv.* 141, 1894–1905. doi: 10.1016/j.biocon.2008.05.007

Bradshaw, C. J. A., Mollet, H. F., and Meekan, M. G. (2007). Inferring population trends for the world's largest fish from mark-recapture estimates of survival. *J. Anim. Ecol.* 76, 480–489. doi: 10.1111/j.1365-2656.2006.01201.x

Cailliet, G. M. (1990). *Elasmobranch Age Determination and Verification: an Updated Review*. Silver Spring, MA: NOAA.

Cailliet, G. M., and Goldman, K. J. (2004). "Age determination and validation in chondrichthyan fishes," in *Biology of Sharks and Their Relatives*, eds J. C. Carrier, J. A. Musick, and M. R. Heithaus, (Boca Raton, FL: CRC Press), 404–453.

Campana, S. E. (2001). Accuracy, precision and quality control in age determination, including a review of the use and abuse of age validation methods. *J. Fish Biol.* 59, 197–242. doi: 10.1111/j.1095-8649.2001.tb00127.x

Campana, S. E., Natanson, L. J., and Myklevoll, S. (2002). Bomb dating and age determination of large pelagic sharks. *Can. J. Fish. Aquat. Sci.* 59, 450–455. doi: 10.1139/f02-027

Campana, S. E., Shelton, P., Simpson, M., and Lawson, J. (2008). "Status of basking sharks in Atlantic Canada," in *Canadian Science Advisory Secretariat*, (Ottawa ON: Fisheries and Oceans Canada), 2008/004.

Chang, W.-B., Leu, M.-Y., and Fang, L.-S. (1997). Embryos of the Whale Shark, *Rhincodon typus*: early growth and size distribution. *Copeia* 1997, 444–446.

Chen, C. T., Liu, K. M., and Joung, S. J. (2002). "Preliminary report on Taiwan's whale shark fishery," in *Elasmobranch biodiversity, Conservation and Management: Proceedings of the International Seminar and Workshop, Sabah, Malaysia, July 1997*, eds S. L. Fowler, T. M. Reed, and F. A. Dipper, (Gland: IUCN SSC Shark Specialist Group), 162–167.

Christiansen, H. M., Campana, S. E., Fisk, A. T., Cliff, G., Wintner, S. P., Dudley, S. F. J., et al. (2016). Using bomb radiocarbon to estimate age and growth of the white shark, *Carcharodon carcharias*, from the southwestern Indian Ocean. *Mar. Biol.* 163:144.

Colman, J. G. (1997). A review of the biology and ecology of the whale shark. *J. Fish Biol.* 51, 1219–1234. doi: 10.1111/j.1095-8649.1997.tb01138.x

Compagno, L. J. V. (2001). "Sharks of the world: an annotated and illustrated catalogue of shark species known to date, vol2: Bullhead, mackerel and carpet sharks (Heterodontiformes, Lamniformes and Orectolobiformes)," in *FAO Species Catalogue for Fishery Purposes*, (Rome: FAO), 269.

Cortés, E., and Brooks, E. N. (2018). Stock status and reference points for sharks using data-limited methods and life history. *Fish Fish.* 19, 1110–1129. doi: 10.1111/faf.12315

Francis, M. P., Campana, S. E., and Jones, C. M. (2007). Age under-estimation in New Zealand porbeagle sharks (*Lamna nasus*): is there an upper limit to ages that can be determined from shark vertebrae? *Mar. Freshw. Res.* 58, 10–23.

Goldman, K. J., Cailliet, G. M., Andrews, A. H., and Natanson, L. J. (2012). "Assessing the age and growth of chondrichthyan fishes," in *Biology of Sharks and their Relatives*, eds J. C. Carrier, J. A. Musick, and M. R. Heithaus, (Boca Raton, FL: CRC Press), 423–452.

Graham, R. T., and Roberts, C. M. (2007). Assessing the size, growth rate and structure of a seasonal population of whale sharks (*Rhincodon typus* Smith 1828) using conventional tagging and photo identification. *Fish. Rese.*84, 71–80. doi: 10.1016/j.fishres.2006.11.026

Grumet, N. S., Abram, N. J., Beck, J. W., Dunbar, R. B., Gagan, M. K., Guilderson, T. P., et al. (2004). Coral radiocarbon records of Indian Ocean water mass mixing and wind-induced upwelling along the coast of Sumatra, Indonesia. *J. Geophys. Res.* 109:C05003.

Hamady, L. L., Natanson, L. J., Skomal, G. B., and Thorrold, S. R. (2014). Vertebral bomb radiocarbon suggests extreme longevity in white sharks. *PLoS One* 9:e84006. doi: 10.1371/journal.pone.0084006

Harry, A. V. (2018). Evidence for systemic age underestimation in shark and ray ageing studies. *Fish Fish.* 19, 185–200. doi: 10.1111/faf.12243

Hoenig, J. M. (1983). Empirical use of longevity data to estimate mortality rates. *Fish. Bull.* 82, 898–903.

Hsu, H. H., Joung, S. J., Hueter, R. E., and Liu, K. M. (2014). Age and growth of the whale shark (*Rhincodon typus*) in the north-western Pacific. *Mar. Freshw. Res.* 65, 1145–1154.

Hsu, H. H., Joung, S. J., and Liu, K. M. (2012). Fisheries, management and conservation of the whale shark *Rhincodon typus* in Taiwan. *J. Fish Biol.* 80, 1595–1607. doi: 10.1111/j.1095-8649.2012.03234.x

Huveneers, C., Meekan, M. G., Apps, K., Ferreira, L. C., Pannell, D., and Vianna, G. M. S. (2017). The economic value of shark-diving tourism in Australia. *Rev. Fish Biol. Fish.* 27, 665–680. doi: 10.1007/s11160-017-9486-x

Mcclain, C. R., Balk, M. A., Benfield, M. C., Branch, T. A., Chen, C., Cosgrove, J., et al. (2015). Sizing ocean giants: patterns of intraspecific size variation in marine megafauna. *PeerJ* 3, e715. doi: 10.7717/peerj.715

Meekan, M. G., Bradshaw, C. J. A., Press, M., Mclean, C., Richards, A., Quasnichka, S., et al. (2006). Population size and structure of whale sharks *Rhincodon typus* at Ningaloo Reef. *Western Australia. Mar. Ecol. Prog. Ser.* 319, 275–285. doi: 10.3354/meps319275

Mollet, H. F., and Cailliet, G. M. (2002). Comparative population demography of elasmobranchs using life history tables, Leslie matrices and stage-based matrix models. *Mar. Freshw. Res.* 53, 503–515.

Natanson, L. J., Kohler, N. E., Ardizzone, D., Cailliet, G. M., Wintner, S. P., and Mollet, H. F. (2006). ""Validated age and growth estimates for the shortfin mako, *Isurus oxyrinchus*," in *the North Atlantic Ocean," in Special Issue: Age and Growth of Chondrichthyan Fishes: New Methods, Techniques and Analysis*, eds J. K. Carlson, and K. J. Goldman, (Dordrecht: Springer Netherlands), 367–383. doi: 10.1007/978-1-4020-5570-6_16

Natanson, L. J., Mello, J. J., and Campana, S. E. (2002). Validated age and growth of the porbeagle shark (*Lamna nasus*) in the western North Atlantic Ocean. *Fish. Bull.* 100, 266–278.

Natanson, L. J., Skomal, G. B., Hoffmann, S. L., Porter, M. E., Goldman, K. J., and Serra, D. (2018). Age and growth of sharks: do vertebral band pairs record age? *Mar. Freshw. Res.* 69, 1440–1452.

Pauly, D. (2002). "Growth and mortality of the Basking Shark *Cetorhinus maximus* and their implications for management of Whale Sharks *Rhincodon typus*," in *Elasmobranch Biodiversity, Conservation and Management: Proceedings of the International Seminar and Workshop*, eds S. L. Fowler, T. M. Reed, and F. A. Dipper, (Gland: IUCN SSC Shark Specialist Group), 199–206.

Perry, C. T., Figueiredo, J., Vaudo, J. J., Hancock, J., Rees, R., and Shivji, M. (2018). Comparing length-measurement methods and estimating growth parameters of free-swimming whale sharks (*Rhincodon typus*) near the South Ari Atoll, Maldives. *Mar. Freshw. Res.* 69, 1487–1495.

Pierce, S. J., and Norman, B. (2016). "Rhincodon typus," in *The IUCN Red List of Threatened Species 2016, e.T19488A2365291* (Gland: International Union for Conservation of Nature and Natural Resources).

Rowat, D., and Brooks, K. S. (2012). A review of the biology, fisheries and conservation of the whale shark *Rhincodon typus*. *J. Fish Biol.* 80, 1019–1056. doi: 10.1111/j.1095-8649.2012.03252.x

Rowat, D., Gore, M. A., Baloch, B. B., Islam, Z., Ahmad, E., Ali, Q. M., et al. (2008). New records of neonatal and juvenile whale sharks (*Rhincodon typus*) from the Indian Ocean. *Environ. Biol. Fishes* 82, 215–219. doi: 10.1007/s10641-007-9280-z

Schmidt, J. V., Schmidt, C. L., Ozer, F., Ernst, R. E., Feldheim, K. A., Ashley, M. V., et al. (2009). Low genetic differentiation across three major ocean populations of the whale shark. Rhincodon typus. *PLoS One* 4:e4988. doi: 10.1371/journal.pone.0004988

Sequeira, A., Mellin, C., Rowat, D., Meekan, M. G., and Bradshaw, C. J. A. (2012). Ocean-scale prediction of whale shark distribution. *Divers. Distrib.* 18, 504–518. doi: 10.1111/j.1472-4642.2011.00853.x

Sequeira, A. M. M., Mellin, C., Meekan, M. G., Sims, D. W., and Bradshaw, C. J. A. (2013). Inferred global connectivity of whale shark *Rhincodon typus* populations. *J. Fish Biol.* 82, 367–389. doi: 10.1111/jfb.12017

Smart, J. J., Harry, A. V., Tobin, A. J., and Simpfendorfer, C. A. (2013). Overcoming the constraints of low sample sizes to produce age and growth data for rare or threatened sharks. *Aquat. Conserv.: Mar. Freshwat. Ecosyst.* 23, 124–134. doi: 10.1002/aqc.2274

Smith, D. C., Robertson, S. G., Fenton, G. E., and Short, S. A. (1995). Age determination and growth of orange roughy (*Hoplostethus atlanticus*): a comparison of annulus counts with radiometric ageing. *Can. J. Fish. Aquat. Sci.* 52, 391–401. doi: 10.1139/f95-041

Speed, C. W., Meekan, M. G., Rowat, D., Pierce, S. J., Marshall, A. D., and Bradshaw, C. J. A. (2008). Scarring patterns and relative mortality rates of Indian Ocean whale sharks. *J. Fish Biol.* 72, 1488–1503. doi: 10.1111/j.1095-8649.2008.01810.x

Speed, C. W., Meekan, M. G., Russell, B. C., and Bradshaw, C. J. A. (2009). Recent whale shark (*Rhincodon typus*) beach strandings in Australia. *Mar. Biodiv. Records* 2:E15.

Stevens, J. D. (2007). Whale shark (*Rhincodon typus*) biology and ecology: a review of the primary literature. *Fish. Res.* 84, 4–9. doi: 10.1016/j.fishres.2006.11.008

Stuiver, M., and Polach, H. A. (1977). Discussion reporting of 14C data. *Radiocarbon* 19, 355–363. doi: 10.1017/s0033822200003672

Theberge, M. M., and Dearden, P. (2006). Detecting a decline in whale shark *Rhincodon typus* sightings in the Andaman Sea, Thailand, using ecotourist operator-collected data. *Oryx* 40, 337–342. doi: 10.1017/s0030605306000998

Then, A. Y., Hoenig, J. M., Hall, N. G., and Hewitt, D. A. (2015). Evaluating the predictive performance of empirical estimators of natural mortality rate using information on over 200 fish species. *ICES J. Mar. Sci.* 72, 82–92. doi: 10.1093/icesjms/fsu136

Von Bertalanffy, L. (1938). A quantitative theory of organic growth (inquiries on growth laws. II). *Hum Biol* 10, 181–213.

Wintner, S. P. (2000). Preliminary study of vertebral growth rings in the whale shark, *Rhincodon typus*, from the East Coast of South Africa. *Environ. Biol. Fishes* 59, 441–451.

Conflict of Interest: The authors declare that the research was conducted in the absence of any commercial or financial relationships that could be construed as a potential conflict of interest.

Copyright © 2020 Ong, Meekan, Hsu, Fanning and Campana. This is an open-access article distributed under the terms of the Creative Commons Attribution License (CC BY). The use, distribution or reproduction in other forums is permitted, provided the original author(s) and the copyright owner(s) are credited and that the original publication in this journal is cited, in accordance with accepted academic practice. No use, distribution or reproduction is permitted which does not comply with these terms.

frontiers in Marine Science

ORIGINAL RESEARCH
published: 17 April 2020
doi: 10.3389/fmars.2020.00211

Fish Species Identification Using the Rhombic Squamation Pattern

Ana L. Ibáñez†, Ebenezer Guerra and Eloísa Pacheco-Almanzar*

Departamento de Hidrobiología, Universidad Autónoma Metropolitana Unidad Iztapalapa, Mexico City, Mexico

The shape of fish scales is, to a considerable degree, species-specific, making it possible to identify species using only one fish scale per specimen. However, to our knowledge, the shape of the rhombic lamination pattern has not been considered to identify species. This study used landmarks and geometric morphometric approaches to address two questions: (1) whether the rhombic lamination pattern of fish scales along the longitudinal axis varies within species and sex and (2) how many fish scales of the rhombic squamation pattern should be considered to obtain an adequate identification. These questions were assessed with a MANCOVA and a cross-validated quadratic discriminant analysis (DA) using the rhombus of one, three, and six scales, and 6, 14, and 26 landmarks, respectively, in order to discriminate between two co-generic species, *Mugil cephalus* and *Mugil curema*. Proportions of the total shape variance explained by the total length and the centroid size were 2.3, 11.8, and 10.5% and 4.2, 5.1, and 5.4% for one, three, and six scales, respectively. Thus, analyses were performed on the shape and the form (shape plus size). The MANCOVA and DA analyses were found to be effective in detecting differences in scale pattern shape between species (except in the case of three scales; $p = 0.079$ for the shape and $p = 0.065$ for the form), whereas no differences were recorded between size and sex in all cases. Findings indicate that a good identification of species is possible, with no significant differences when using shape or form. The DA provided values of 75.8, 75.0, and 73.4% based on the shape, and of 72.7, 75.8, and 75.0% based on the form, for 1, 3 and 6 scales, respectively. Thus, it is possible to obtain a rapid and reliable identification of species using the rhombus of one scale only without considering the size. This is a useful finding in practical terms since scaling requires data on length. The finding of a suitable discrimination using only the rhombus of one scale raises the possibility of using an ocular adaptor on a camera or mobile phone, allowing many individuals to be easily screened without having to collect scales.

Keywords: geometric morphometrics, landmarks, teleost fish, elasmoid scales, fish mullet, *Mugil cephalus*, *Mugil curema*

OPEN ACCESS

Edited by:
Benjamin D. Walther,
Texas A&M University Corpus Christi,
United States

Reviewed by:
Fernanda Gabriela Biolé,
University of Buenos Aires, Argentina
Monica Vanessa Garduno Paz,
Universidad Autónoma del Estado
de México, Mexico
Ryan Taylor,
Environment Agency, United Kingdom

***Correspondence:**
Ana L. Ibáñez
ana@xanum.uam.mx

†ORCID:
Ana L. Ibáñez
orcid.org/0000-0002-6062-9172

Specialty section:
This article was submitted to
Marine Ecosystem Ecology,
a section of the journal
Frontiers in Marine Science

Received: *02 December 2019*
Accepted: *17 March 2020*
Published: *17 April 2020*

Citation:
Ibáñez AL, Guerra E and
Pacheco-Almanzar E (2020) Fish
Species Identification Using
the Rhombic Squamation Pattern.
Front. Mar. Sci. 7:211.
doi: 10.3389/fmars.2020.00211

INTRODUCTION

Scales of most teleost fish are of the elasmoid type. Elasmoid scales are thought to derive from the surface "dental" tissues that covered rhombic scales in ancestral osteichthyan fish (Sire and Huysseune, 2003). Scale morphology has been used to identify inland fish of North America (Daniels, 1996), as well as to design taxonomic keys for species of freshwater ecosystems of various

areas including California (Casteel, 1972), Britain, and Ireland (Maitland, 2004). Also, an atlas of scales of common Mediterranean teleost fish has recently been published (Bräger and Moritz, 2016). In the last years, fish scales have been used to discriminate among species and populations. The Fourier analysis of fish scales was initially used to discriminate populations (e.g., Jarvis et al., 1978; Richards and Esteves, 1997) and, later, different methods of shape analysis based on landmark data and geometric morphometric methods (GMM) were developed to discriminate among species and populations, as well as among sympatric phenotypes (Ibáñez et al., 2007, 2012a; Garduño-Paz et al., 2010; Staszny et al., 2012). All these studies collected only one fish scale per specimen. Fish scale shape is, to a significant degree, species-specific and is thus useful when defining stock membership.

According to Sire and Akimenko (2004), no reports exist on gene expression during skin development (Le Guellec et al., 2004); however, morphological data suggest that the skin is already pre-patterned at the onset of scale initiation. To date, there are no clear explanations on what factors determine the patterning of squamation in the regular development of scales in a chessboard order. It is known that morphogenesis such as apolipoprotein E, sonic hedgehog, and ectodysplasin A (Monnot et al., 1999; Kondo et al., 2001; Sire and Akimenko, 2004; Harris et al., 2008) are involved in the initiation and morphogenesis of scales (Levin, 2011).

For 12 years now, we have been studying the use of fish scale shape to identify genera, species and local populations of the Mugilidae and Lutjanidae (Ibáñez et al., 2007, 2012a, 2016) in order to determine the influence of allometry on scale shape and classification (Ibáñez and O'Higgins, 2011), to analyze variations in elasmoid fish scale patterns with regard to taxon and swimming mode (Ibáñez et al., 2009), to see whether compensatory growth modifies fish scale shape (Ibáñez et al., 2012b), to use fish scale shape to determine the origin of fish in fish traceability studies (Ibáñez, 2015) and to compare the discrimination of phenotypic stocks using fish otolith and scale shape (Ibáñez et al., 2017). In most of these studies, we have used as a model two co-generic species of fishery importance, *Mugil cephalus* (Linnaeus, 1758) and *Mugil curema* (Valenciennes, 1836), striped and white mullet, respectively.

Fish mullet are euryhaline species that play a significant role in small-scale coastal fisheries in numerous areas of the world. In Mexico, they constitute 1 of the 10 most important coastal fisheries, exceeding 28,000 tons annually. Most of the catches take place in the Gulf of Mexico, off the coasts of the states of Veracruz and Tamaulipas. According to Eschmeyer and Fong (2019), the family Mugilidae includes 25 genera and 74 species that live in coastal lagoons and estuaries at all latitudes, except for the polar regions. *Liza* and *Mugil* are the genera with the most species, with 12 and 16, respectively. The external morphology of this family is extremely conservative, which increases uncertainty in the discriminations. The effectiveness of species classification following easy, non-destructive, quick, and less costly methods that allow many specimens to be screened without collecting scales is thus highly relevant.

To our knowledge, no studies have compared the effectiveness of species discrimination based on the shape of the rhombic lamination pattern without collecting scales and using only a camera to photograph fish bodies. Therefore, the aim of this study was to evaluate a rapid assessment tool for species discrimination. Accordingly, this study compared the success of discrimination of two co-generic species of fish mullets, *M. cephalus* and *M. curema*, collected in Alvarado Lagoon near the Gulf of Mexico. Two specific questions were addressed: (1) does the rhombic lamination pattern of fish scales discriminate two similar co-generic species? and (2) how many fish scales of the rhombic squamation pattern are necessary to obtain an adequate identification? This was assessed by applying GMM to the rhombic pattern of one, three, and six scales (6, 14, and 26 landmarks, respectively) of the longitudinal series on the left flank of the fish. These two Mugilidae species were selected for this study since they are abundant along Mexico's coasts, they are important economically as a source of roe, and, as the rhombic lamination pattern has not been previously studied, we can use previous studies based on the one scale discrimination as comparison.

MATERIALS AND METHODS

Fish Scale Collection

Specimens were collected from one same area in order to minimize potential phenotypic differences due to the environment, as Ibáñez et al. (2007) specified. Specimens of *M. cephalus* (n = 64) and *M. curema* (n = 64) were collected from Alvarado Lagoon (N18°46′ and W95°46′), and were sexed, measured, and weighed. Most were adult specimens (87.5 and 89.1%) with average total lengths of 51.25 ± 6.46 and 41.30 ± 4.34 cm for females and males, respectively, for *M. cephalus* and 31.23 ± 2.52 and 29.67 ± 2.21 cm for females and males, respectively, for *M. curema* (**Table 1**). A piece of skin (with fish scales) was extracted from the left flank of the fish between the beginning of the first and second dorsal fins. Six landmarks per scale were considered following the TPSdig software (Rohlf, 2017). The landmarks were located on key structures of the ctenoid scale that are common to all scales of the species under study. The following landmarks were considered appropriate (**Figure 1**): landmarks 1 and 2 are the anterior points connected to the previous scale, landmarks 3 and 4 are the tips of the dorso-ventral portion of the scale, and landmarks 5 and 6 lie at the boundary between the marked and the posterior scale. Three analyses were run, the first was to describe the shape of one scale using 6 landmarks, the second to describe the shape of a configuration of three adjacent scales with 14 landmarks, and the third analysis described the shape of a configuration of six adjacent scale utilizing 26 landmarks. Since the total length was significantly different in the two species ($p < 0.05$), analyses were carried out for the shape and form (shape plus size).

Morphometrics

The configurations of the landmark coordinates for the sampled scales were scaled, translated and rotated using a generalized

TABLE 1 | Sample characteristics of fish mullets.

Species	Key	Sex	No. of fish	Total length range (cm)	Total length mean ± STD	Sample collection period
Mugil curema	Mcu	Female	28	27.4–36.5	31.23 ± 2.52	July–December 2018
		Male	29	27.0–34.4	29.67 ± 2.21	July–December 2018
		Und.	7	26.5–30.1	28.43 ± 1.31	August–October 2018
Mugil cephalus	Mce	Female	32	40.5–63.4	51.25 ± 6.46	June–December 2018
		Male	24	31.5–50.0	41.30 ± 4.34	June–December 2018
		Und.	8	30.0–41.5	35.46 ± 6.21	June–August 2018

Und. = Undetermined.

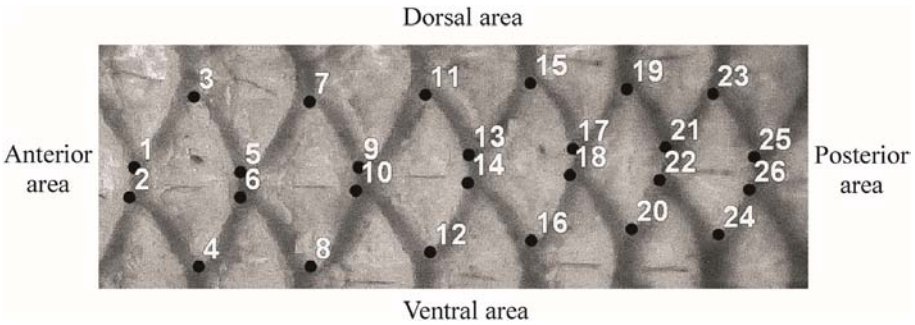

FIGURE 1 | Location of landmark used for the analysis to describe the shape of scales of Mugilidae fishes. For one scale, 6 landmarks were used (from landmark 1 to 6), as well 14 and 26 landmarks were used for three (from landmark 1 to 14) and six scales (from 1 to 26 landmarks).

Procrustes analysis (GPA). They were then submitted to a tangent projection (Dryden and Mardia, 1993) and later to a principal components analysis (PCA; Dryden and Mardia, 1993; Kent, 1994). The extremes of each PC were then used to recreate the expected shapes of the landmark configurations with those particular scores by adding to the mean tangent coordinates the products of these PC scores (PCs) and the eigenvectors for those PCs before projecting back from the tangent to the configuration space (O'Higgins et al., 2001). The variations in shape between the mean and the shapes represented by the extremes of the PCs of interest were pictured using transformation grids (Bookstein, 1989; Marcus et al., 1996; Dryden and Mardia, 1998) computed with morphologika2 (O'Higgins and Jones, 2006). In order to examine the potential for differences in shape when classifying unknown specimens, the scores of the specimens on all non-zero PCs were submitted to a quadratic discriminant analysis (SPSS ver. 25.0) to compute generalized Mahalanobis' distances and discriminant functions and to calculate the value of the latter in the classification. This was accomplished with a cross-validation in which multiple repeated analyses were carried out, leaving out one individual in the construction of the discriminant function before classifying this individual according to the function. This reduced the likelihood of overestimating the efficacy of the discriminant functions by using them to classify the specimens employed in their construction. Also, a cross-validated discriminant analysis was used to evaluate and compare the efficacy of the shape and the relative warp in the size–shape space in the discrimination of each species. The percentage of correct classification rates was documented. The analyses were run with 6, 14, and 26 landmarks using one, three, and six fish scales as mentioned above. Also, multivariate regressions of all PCs on species confirmed these general trends. Finally, differences were assessed by a full MANCOVA with all PC scores of shape and form (shape plus size) as dependent variables, total length as the covariate, and species and sex as grouping factors.

RESULTS

The GPA/PCA resulted in a set of PCs that describe the patterns of form and shape variability of the three scales of the rhombic lamination pattern. Specifically, we were concerned to know the extent to which scale form and shape variability relates to species. This was assessed directly by a quadratic discriminant analysis (see below), and was explored initially by an examination of the PCs. The first PC explained 41.2, 64.8, and 79.5% of the total variance, while the second accounted for 25.6, 9.5, and 3.8% in the GPA/PCA analysis of one, three, and six scales of the rhombic lamination pattern examined for the form analysis (79.4, 80.9, and 86.5% for the first three PCs, respectively). The first PC explained 43.7, 35.5, and 26.6% of the total variance while the second accounted for 21.1, 17.3, and 14.1% in the GPA/PCA analysis of one, three, and six scales of the rhombic lamination pattern examined for the shape analysis (79.2, 61.7, and 51.5% for the first three PCs, respectively) (**Table 2**).

The variation in shape between species is represented in **Figure 2** where the leftmost grids are the mean shape of *M. curema*, the rightmost grids are that of *M. cephalus*, and the reference shape is in the central grid for one, three, and six scales

TABLE 2 | Explained variance of PCs for each landmark configuration analysis.

Landmark configuration analysis	PC1	PC2	PC3	Accumulative variance (%)
Form analysis				
One scale	41.2	25.6	12.6	79.4
Three scales	64.8	9.5	6.6	80.9
Six scales	79.5	3.8	3.2	86.5
Shape analysis				
One scale	43.7	21.1	14.4	79.2
Three scales	35.5	17.3	8.9	61.7
Six scales	26.6	14.1	10.8	51.5

TABLE 3 | Cross-validated predicted species membership using form (indicated as treatment; see text) from the rhombic lamination pattern of one, three, and six fish scales.

	Predicted group membership						
	One scale		Three scales		Six scales		Total
Species	***M. cu***	***M. ce***	***M. cu***	***M. ce***	***M. cu***	***M. ce***	
Percent							
M. cu	73.4	26.6					100.0*
M. ce	28.1	71.9					100.0*
M. cu			78.1	21.9			100.0†
M. ce			26.6	73.4			100.0†
M. cu					73.4	26.6	100.0‡
M. ce					23.4	76.6	100.0‡

*M. cu = Mugil curema; M. ce = Mugil cephalus. *Of cross-validated grouped cases, 72.7% were correctly classified (Wilk's lambda = 0.676, $p < 0.001$) for the rhombic lamination pattern of one scale. †Of cross-validated grouped cases, 75.8% were correctly classified (Wilk's lambda = 0.467, $p < 0.001$) for the rhombic lamination pattern of three scales. ‡Of cross-validated grouped cases, 75.0% were correctly classified (Wilk's lambda = 0.313, $p < 0.001$) for the rhombic lamination pattern of six scales.*

of the rhombic lamination pattern under study (**Figures 2A–C**). The one scale pattern (**Figure 2A**) was characterized by a relative bending to the right of landmarks 1, 2, 5, and 6 for *M. curema*, and a similar bending to the left of the same landmarks for *M. cephalus*. An analogous trend was observed for the three and six scales of the rhombic lamination pattern (**Figures 2B,C**). The key difference was the relative location of the central landmarks which bent more to the right for *M. curema* than for *M. cephalus*. Furthermore, the anterior–posterior edge was concave in *M. curema* and convex in *M. cephalus*.

In the discriminant analyses, similar cross-validated classification rates were obtained using the shape and the combined scale size and shape (form space; **Tables 3**, **4**). Furthermore, the shape alone performed slightly better than the form when using the rhombic lamination pattern of one fish scale (**Table 4**). The cross-validated quadratic discriminant analysis using the form (**Table 3**) correctly classified 72.7, 75.8, and 75% for the rhombic lamination pattern of one, three, and six scales, respectively (Wilks' $\lambda = 0.676$, $p < 0.001$; Wilks'

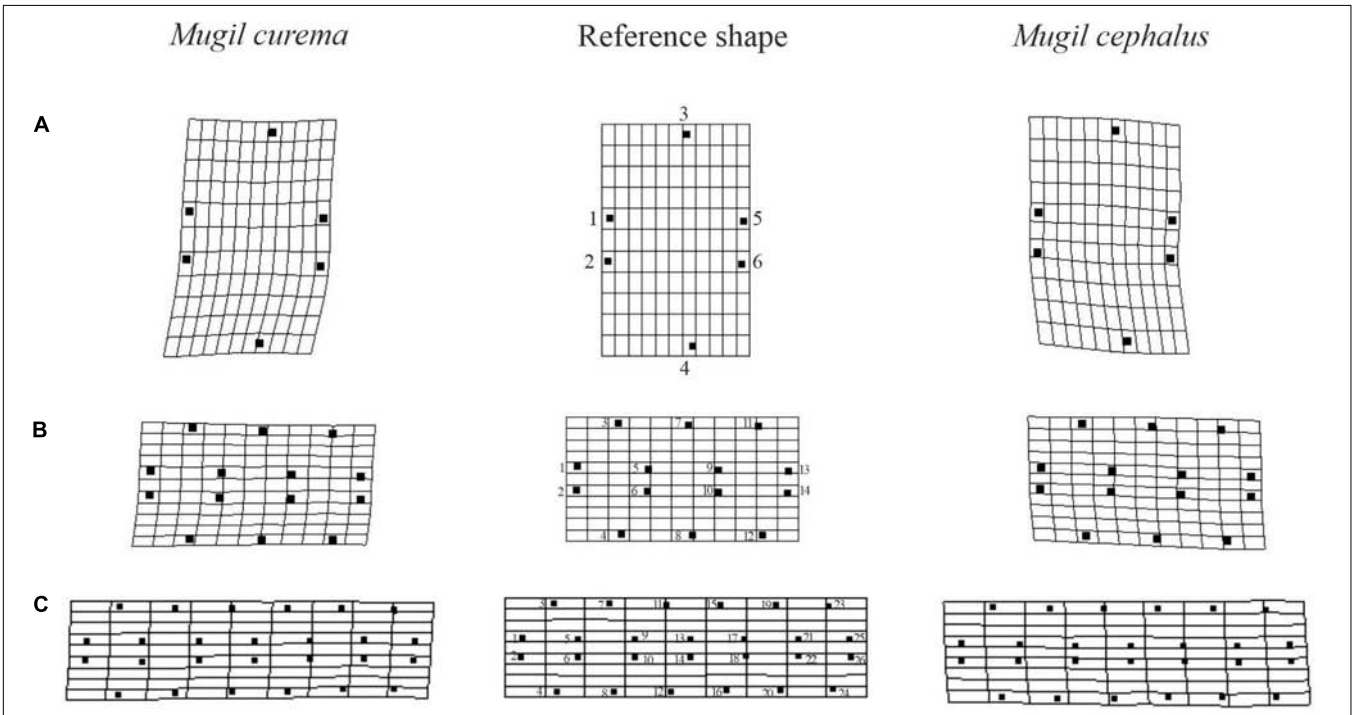

FIGURE 2 | Shape variation in each species visualized using transformation grids. Middle grid shows the regular reference grid in each rhombic squamation pattern showing the landmark utilized for the Procrustes analysis for one **(A)**, three **(B)**, and six **(C)** scales. Left, deformed grid drawn over the estimated shape for *Mugil curema* individuals; right, deformed grid drawn over the estimated shape for *M. cephalus*. Scales orientation are the same as in **Figure 1**.

TABLE 4 | Cross-validated predicted species membership using shape (indicated as treatment; see text) from the rhombic lamination pattern of one, three, and six fish scales.

	Predicted group membership						
	One scale		Three scales		Six scales		Total
Species	***M. cu***	***M. ce***	***M. cu***	***M. ce***	***M. cu***	***M. ce***	
Percent							
M. cu	75.0	25.0					100.0*
M. ce	23.4	76.6					100.0*
M. cu			76.6	23.4			100.0†
M. ce			26.6	73.4			100.0†
M. cu					73.4	26.6	100.0‡
M. ce					26.6	73.4	100.0‡

*M. cu = Mugil curema; M. ce = Mugil cephalus. *Of cross-validated grouped cases, 75.8% were correctly classified (Wilk's lambda = 0.680, p < 0.001) for the rhombic lamination pattern of one scale. †Of cross-validated grouped cases, 75.0% were correctly classified (Wilk's lambda = 0.482, p < 0.001) for the rhombic lamination pattern of three scales. ‡Of cross-validated grouped cases, 73.4% were correctly classified (Wilk's lambda = 0.327, p < 0.001) for the rhombic lamination pattern of six scales.*

$\lambda = 0.467$, $p < 0.001$ and Wilks' $\lambda = 0.313$, $p < 0.001$ for 1, 3, and 6 scales, respectively). The cross-validated quadratic discriminant analysis using the shape (**Table 4**) correctly classified 75.8, 75.0, and 73.4% for the rhombic lamination pattern of one, three, and six scales, respectively (Wilks' $\lambda = 0.680$, $p < 0.001$; Wilks' $\lambda = 0.482$, $p < 0.001$ and Wilks' $\lambda = 0.327$, $p < 0.001$ for one, three, and six scales, respectively). The *M. curema* data performed slightly better than those of *M. cephalus*. The graphic results of the previous analysis showed the combined histogram for the canonical scores (**Figures 3A–C**). The two species can be identified from the two distinct modes, particularly for one and six fish scales of the rhombic lamination pattern (**Figures 2A,C**), with the left one (gray) for *M. cephalus* having a slightly more leptokurtic distribution. The three fish scales of the rhombic lamination pattern (**Figure 2B**) showed the less normal distribution for *M. cephalus*.

MANCOVA analyses were found to be effective in detecting differences in the rhombic lamination pattern of scales between species (except for the case of three scales; $p = 0.079$ and $p = 0.065$ for shape and form, respectively), while no differences were found between size and sex in all cases (**Table 5**). The proportion of the total shape variance explained by the total length was 4.2, 5.1, and 5.4% for the rhombic lamination pattern of scales of one, three, and six scales, respectively.

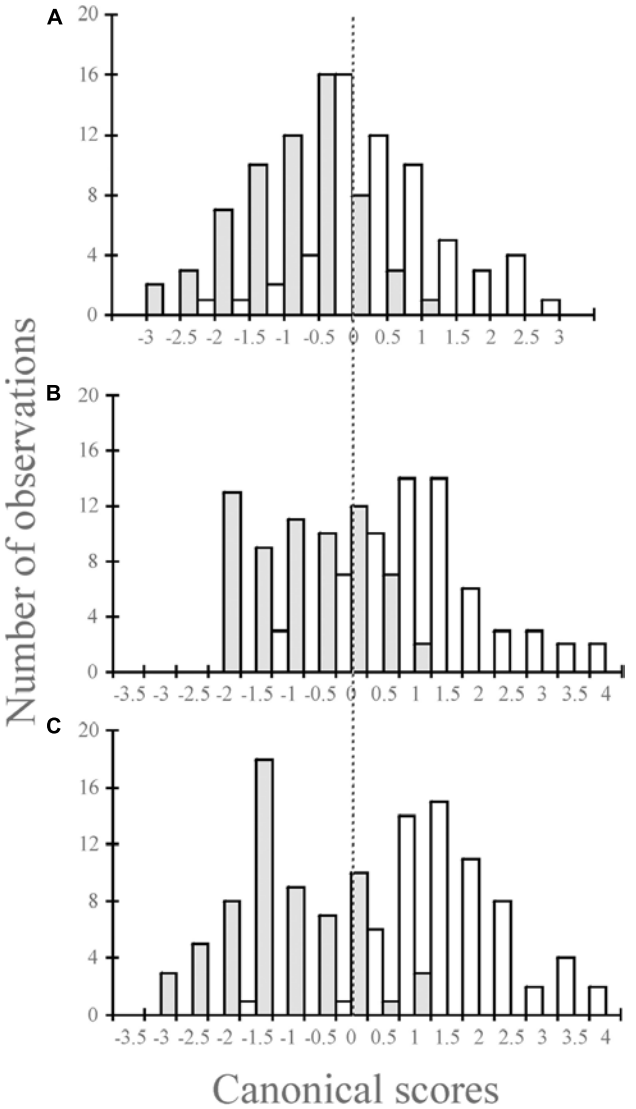

FIGURE 3 | Combined histogram for the canonical scores for *Mugil cephalus* (gray) and *M. curema* (white) species using 6, 14, and 26 landmarks for one **(A)**, three **(B)**, and six **(C)** scales of the rhombic squamation pattern.

DISCUSSION

Our results show that the rhombic lamination pattern of one, three, and six scales can be used to reliably identify species using GMM. In order to use this approach successfully in fisheries management, it is fundamental to comprehend the extent to which differences in the number of scales and fish size might have an effect on species identification.

The size of the fish (total length) did not change the shape significantly (**Table 5**) or improve species discrimination, as well as the number of scales scanned (**Tables 3**, **4**). This means that one may use one single rhombic lamination pattern for species discrimination without having to consider the size. This is a useful finding in practical terms since the form (shape plus size) requires data on body length. Accordingly, it also raises the possibility of using an ocular adaptor on a camera or cell phone allowing many specimens to be easily screened without having to collect a fish scale. This approach may also prove useful in a situation where it is not possible to quantify the size of the specimens. Nevertheless, the non-normality of the canonical scores of the rhombic lamination pattern for the three scales certainly reduced the effect of the MANCOVA analysis.

TABLE 5 | MANCOVA test to assess the effect of total length (Tl) on scale form and shape among species and sex by number of fish scales. *p*-Value of significance test.

		Form			Shape		
# Fish scales of the rhombic lamination pattern	**Test**	**Wilks' λ**	***F***	***p***	**Wilks' λ**	***F***	***p***
One	TL	0.925	0.929	0.509	0.943	0.887	0.530
	Species	0.857	1.917	**0.050**	0.877	2.059	**0.045**
	Sex	0.900	1.282	0.249	0.905	1.531	0.154
Three	TL	0.844	0.706	0.845	0.864	0.661	0.878
	Species	0.711	1.549	0.065	0.735	1.516	0.079
	Sex	0.758	1.218	0.242	0.760	1.325	0.168
Six	TL	0.592	1.034	0.442	0.614	1.007	0.482
	Species	0.471	1.684	**0.020**	0.493	1.652	**0.024**
	Sex	0.589	1.048	0.421	0.591	1.112	0.334

Significant values are in boldface.

Ibáñez et al. (2009), in a study that did not take into account fish size, verified the efficacy of the identification of scales from nine regions along the flank of teleost fish, and obtained the highest rates of correct identification using scales from the central–dorsal region of mature fish and scales from the same body region (Ibáñez et al., 2007, 2009; Garduño-Paz et al., 2010). Correct classification rates were as high as 98% for some species. In the present study, the scales analyzed for the rhombic lamination pattern were collected from the same body area belonging to the lateral series, and most were of sexually mature individuals. Although the rate of correct identification is reduced under some conditions, it compares reasonably with the rate of over 80% recorded in studies using otoliths to categorize co-generic species (Torres et al., 2000; Stransky and MacLellan, 2005). Variations among different species are regularly greater than those within a species; however, it has been suggested that *M. curema* and *M. cephalus* are not a single species but a species complex (Durand and Borsa, 2015). In this sense, a wide phenotypic variability is present (Ibáñez et al., 2006, 2007), which could reduce discrimination.

In order to explain the squamation pattern, Sire and Arnulf (1990) proposed that the tension transmitted to the skin during swimming may induce scale development as a means of resisting excessive bending. The rhombic lamination pattern of the scales may also be functionally related to the swimming mode. Both mullet species look similar and present a subcarangiform swimming mode (Breder, 1926). In this sense, the rhombic lamination pattern is also similar. Other similarities are present in these two mullets, such as the number of lateral scales, which is 36–40 in *M. cephalus* and 35–40 in *M. curema*, with modes 38 and 37, respectively (Harrison, 2002). Thus, differences in the rhombic lamination pattern could be due to the shape of the fish, with *M. cephalus* being a more robust species with a projectile shape and *M. curema* having a slimmer body. These differences were recognized by Jordan and Evermann (1896) in the specific description of these species from Central America and North America. Also, the *ctenii* of the scales are different in these species and have been used to discriminate them (Ibáñez and Gallardo-Cabello, 2005). Likewise, the roughness of the scale surface has been studied from the point of view of hydrodynamics (Sudo et al., 2002). Thus, the variations in shape of the scale lamination pattern could arise from adaptations to fluctuating hydrodynamic conditions. Supplementary studies that include biomechanical evaluations will offer a possibility to study the function–form relationship.

Scale morphology and squamation have been used to study scale morphology in different parts of the body (Chen et al., 2012; Mondéjar-Fernández and Clément, 2012), to describe the squamation pattern of osteichthyans providing new insights into the early evolution of osteichthyan scales, to understand the early osteichthyan body plan (Cui et al., 2019), and to study the morphology and articulated squamations of extinct species (Žigaite and Goujet, 2012). However, to our knowledge, no other analysis has used the rhombic lamination pattern to discriminate between species as is presented in this study.

Species identification is vital in the conservation of biodiversity and fisheries management, particularly considering the urgent need of correct species identification experienced by a fisheries control officer on the high seas (Fischer, 2013). Thus, this method is useful and non-destructive; it makes it possible to screen rare, museum specimens and endangered species, it allows many individuals in a community to be screened quickly, and it is an inexpensive method to discriminate species. In order to use such an approach effectively in fisheries management, it is important to have described and made available the rhombic lamination pattern of each species.

DATA AVAILABILITY STATEMENT

The datasets generated for this study are available on request to the corresponding author.

ETHICS STATEMENT

Research was carried out in accordance to Mexican laws and regulations. Striped and white mullet was collected under the Official Mexican Norm (NOM-016 PESC-1994) for commercial species. Fish were euthanized humanely by being placed directly into an ice water bath upon capture. No non-target or by-catch specimens were collected during the study.

AUTHOR CONTRIBUTIONS

AI and EP-A conceived the research. AI conducted the field work. EG processed and prepared the fish and performed the statistically analysis. EP-A reviewed the process and preparation of samples. AI prepared the initial manuscript and all authors contributed to later revisions.

FUNDING

This study was funded by the Universidad Autónoma Metropolitana.

ACKNOWLEDGMENTS

The authors would like to thank Manuel Castellanos for his help in sample collection and fish dissection.

REFERENCES

Bookstein, F. L. (1989). Principal warps: thin-plate splines and the decomposition of deformations. *IEEE T. Pattern Anal.* 11, 567–585. doi: 10.1109/34.24792

Bräger, Z., and Moritz, T. (2016). A scale atlas for common Mediterranean teleost fishes. *Vertebr. Zool.* 66, 275–386.

Breder, C. M. (1926). The locomotion of fishes. *Zool. N. Y.* 4, 159–297.

Casteel, R. W. (1972). A key based on scales, to the families of native California freshwater fishes. *Proc. Calif. Acad. Sci.* 39, 75–86.

Chen, D., Janvier, P., Ahlberg, P. E., and Blom, H. (2012). Scale morphology and squamation of the Late Silurian osteichthyan *Andreolepis* from gotland. *Sweden. Hist. Biol.* 24, 411–423. doi: 10.1080/08912963.2012.668187

Cui, X., Qiao, T., and Zhul, M. (2019). Scale morphology and squamation pattern of Guiyu oneiros provide new insights into early osteichthyan body plan. *Sci. Rep.* 9:4411. doi: 10.1038/s41598-019-40845-7

Daniels, R. A. (1996). "Guide to The Identification Of Scales Of The Inland Fishes of Northeastern North America," in *New York State Museum Bulletin* 498 (Albany, NY: The University of the State of New York).

Dryden, I. L., and Mardia, K. V. (1993). Multivariate shape analysis. *Sankhya Ser. A.* 55, 460–480.

Dryden, I. L., and Mardia, K. V. (1998). *Statistical Shape Analysis*. London: John Wiley & Sons.

Durand, J. D., and Borsa, P. (2015). Mitochondrial phylogeny of grey mullets (*Acanthopterygii*: Mugilidae) suggests high proportion of cryptic species. *C. R. Biol.* 338, 266–277. doi: 10.1016/j.crvi.2015.01.007

Eschmeyer, W. N., and Fong, J. D. (eds) (2019). *Catalog of Fishes: Species by Family/Subfamily. Electronic Version*. Available online at: http://researcharchive.calacademy.org/research/ichthyology/catalog/SpeciesByFamily.asp (accessed November 04, 2019).

Fischer, J. (Ed) (2013). *Fish. (Identification)Tools for Biodiversity and Fisheries Assessment: Review and Guidance for Decision-Makers*, ed. J. Fischer (Rome: *FAO*).

Garduño-Paz, M. V., Demetriou, M., and Adams, C. E. (2010). Variation in scale shape among alternative sympatric phenotypes of Arctic charr *Salvelinus alpinus* from two lakes in Scotland. *J. Fish Biol.* 76, 1491–1497. doi: 10.1111/j.1095-8649.2010.02584.x

Harris, M. P., Rohner, N., Schwarz, H., Perathoner, S., and Nüsslein-Volhard, C. (2008). Zebrafish eda and edar mutants reveal conserved and ancestral roles of ectodysplasin signaling in vertebrates. *PLoS Genet.* 4:10. doi: 10.1371/journal.pgen.1000206

Harrison, I. J. (2002). "Mugilidae," in *FAO Species Identification Guide for Fisheries Purposes. The Living Marine Resources of the Western Central Atlantic, Vol. 2. Bony Fishes part 1 (Acipenseridae to Grammatidae)*, ed. K. Carpenter (Rome: FAO), 1071–1085.

Ibáñez, A. L. (2015). Fish traceability: guessing the origin of fish from a seafood market using fish scale shape. *Fish. Res.* 170, 82–88. doi: 10.1016/j.fishres.2015.05.016

Ibáñez, A. L., Cabral-Solís, E., Gallardo-Cabello, M., and Espino-Barr, E. (2006). Comparative morphometrics of two population of Mugil curema in the Atlantic and Pacific coasts. *Sci. Mar.* 70, 139–145. doi: 10.3989/scimar.2006.70n1139

Ibáñez, A. L., Cowx, I. G., and O'Higgins, P. (2007). Geometric morphometric analysis of fish scales for identifying genera, species and local populations within the Mugilidae. *Can. J. Fish. Aquat. Sci.* 64, 1091–1100. doi: 10.1139/f07-075

Ibáñez, A. L., Cowx, I. G., and O'Higgins, P. (2009). Variation in elasmoid fish scale patterns is informative with regard to taxon and swimming mode. *Zool. J. Linn. Soc. Lond.* 155, 834–844. doi: 10.1111/j.1096-3642.2008.00465.x

Ibáñez, A. L., Espino-Barr, E., and Gallardo-Cabello, M. (2012a). Population connectivity among geographic variants within the Lutjanidae through fish scales shape recognition. *Sci. Mar* 76, 667–675. doi: 10.3989/scimar.03675.09C

Ibáñez, A. L., Pacheco-Almanzar, E., and Cowx, I. G. (2012b). Does compensatory growth modify fish scale shape? *Environ. Biol. Fish.* 94, 477–482. doi: 10.1007/s10641-011-9962-4

Ibáñez, A. L., and Gallardo-Cabello, M. (2005). Identification of two mugilidae species, Mugil cephalus and *M. curema* (*Pisces*:*Mugilidae*), using the ctenii of their scales. *B. Mar. Sci.* 77, 305–307.

Ibáñez, A. L., Hernández-Fraga, K., and Álvarez-Hernández, S. H. (2017). Discrimination analysis of phenotypic stocks comparing fish otolith and scale shapes. *Fish. Res.* 185, 6–13. doi: 10.1016/j.fishres.2016.09.025

Ibáñez, A. L., Jawad, L. A., and Sadighzadeh, Z. (2016). Morphometric variation of fish scales among some species of the family Lutjanidae from Iranian waters. *Cah. Biol. Mar.* 57, 289–295. doi: 10.21411/CBM.A.211AE0D1

Ibáñez, A. L., and O'Higgins, P. (2011). Identifying fish scales: the influence of allometry on scale shape and classification. *Fish. Res.* 109, 54–60. doi: 10.1016/j.fishres.2011.01.016

Jarvis, R. S., Klodowski, H. F., and Sheldon, S. P. (1978). New method of quantifying scale shape and an application to stock identification in Walleye (*Stizostedion vitreum* vitreum). *T. Am. Fish. Soc.* 107, 528–534. doi: 10.1577/1548-8659(1978)107<528:nmoqss>2.0.co;2

Jordan, D. S., and Evermann, E. (1896). The fishes of north and middle America: a descriptive catalogue of the species of fish like vertebrates found in the waters of North America north of the Isthmus of Panama. *Bull. U.S. Nat. Mus.* 47, 1–3313.

Kent, J. T. (1994). The complex bingham distribution and shape analysis. *J. Roy. Stat. Soc. B Met.* 56, 285–299. doi: 10.1111/j.2517-6161.1994.tb01978.x

Kondo, S., Kuwahara, Y., Kondo, M., Naruse, K., and Mitani, H. (2001). The medaka rs-3 locus required for scale development encodes ectodysplasin-A receptor. *Curr. Biol.* 11, 1202–1206. doi: 10.1016/S0960-9822(01)00324-4

Le Guellec, D., Morvan-Dubois, G., and Sire, J. Y. (2004). Skin development in bony fish with particular emphasis on collagen deposition in the dermis of the zebrafish (*Danio rerio*). *Int. J. Dev. Biol.* 48, 217–231. doi: 10.1387/ijdb.15272388

Levin, B. A. (2011). Ontogenetic causes and mechanisms for formation of differences in number of fish scales. *Russ. J. Dev. Biol.* 42, 186–191. doi: 10.1134/S1062360411030106

Maitland, P. S. (2004). *Keys to the Freshwater Fish of Britain and Ireland, With Notes on Their Distribution and Ecology*. Ambleside: Freshwater Biological Association.

Marcus, L. F., Corti, M., Loy, A., Naylor, G. J. P., and Slice, D. (eds) (1996). *Advances in Morphometrics*. New York, NY: Nato ASI series Plenum Press.

Mondéjar-Fernández, J., and Clément, G. (2012). Squamation and scale microstructure evolution in the porolepiformes (*Sarcopterygii*, *Dipnomorpha*) based on Heimenia ensis from the devonian of spitsbergen. *J. Vertebr. Paleontol.* 32, 267–284. doi: 10.1080/02724634.2012.646836

Monnot, M. J., Babin, P. J., Poleo, G., et al. (1999). Epidermal expression of apolipoprotein E Gene during Fin and Scale development and Fin regeneration in Zebrafish. *Dev. Dynam.* 214, 207–215. doi: 10.1002/(sici)1097-0177(199903)214:3<207::aid-aja4>3.0.co;2-5

O'Higgins, P., Chadfield, P., and Jones, N. (2001). Facial growth and the ontogeny of morphological variation within and between the primates *Cebus apella* and *Cercocebus torquatus*. *J. Zool. Lond.* 254, 337–357. doi: 10.1017/s095283690100084x

O'Higgins, P., and Jones, N. (2006). *Morphologika2: Tools for Statistical Shape Analysis. Version 2.5. Hull: Hull York Medical School*. Available online at: http://life.bio.sunysb.edu/morph/index.html (accessed April 18, 2019).

Richards, R. A., and Esteves, C. (1997). Use of scale morphology for discriminating wild stocks of Atlantic striped bass. *T. Am. Fish. Soc.* 126, 919–925. doi: 10.1577/1548-8659(1997)126<0919:uosmfd>2.3.co;2

Rohlf, J. F. (2017). *Tps Dig 2. Version 2.31. Ecology & Evolution and Anthropology*. Stony Brook, NY: Stony Brook University.

Sire, J. Y., and Akimenko, M. A. (2004). Scale development in fish: a review, with description of sonic hedgehog expression in the zebrafish (*Danio rerio*). *Int. J. Dev. Biol.* 48, 233–247. doi: 10.1387/ijdb.15272389

Sire, J. Y., and Arnulf, I. (1990). The development of squamation in four teleostean fishes with a survey of the literature. *Jpn. J. Ichthyol.* 37, 137–143. doi: 10.1007/BF02905381

Sire, J. Y., and Huysseune, A. (2003). Formation of skeletal and dental tissues in fish: a comparative and evolutionary approach. *Biol. Rev.* 78, 219–249. doi: 10.1017/s1464793102006073

Staszny, Á, Ferincz, Á, Weiperth, A., Havas, E., Urbányi, B., and Paulovits, G. (2012). Scale-morphometry study to discriminate Gibel carp (*Carassius gibelio*) populations in the balaton-catchment (Hungary). *Acta Zool. Acad. Sci. H.* 58, 19–27.

Stransky, C., and MacLellan, S. E. (2005). Species separation and zoogeography of redfish and rockfish (genus *Sebastes*) by otolith shape analysis. *Can. J. Fish. Aquat. Sci.* 62, 2265–2276. doi: 10.1139/f05-143

Sudo, S., Tsuyuki, K., Ito, Y., and Ikohagi, T. (2002). A study on the surface shape of fish scales. *JSME Int. J. C-Mech. Syst.* 45, 1100–1105. doi: 10.1299/jsmec.45.1100

Torres, G. J., Lombarte, A., and Morales-Nin, B. (2000). Sagittal otolith size and shape variability to identify geographical intraspecific differences in three species of the genus Merluccius. *J. Mar. Biol. Assoc. U.K.* 80, 333–342. doi: 10.1017/S0025315499001915

Žigaite, Ž, and Goujet, D. (2012). New observations on the squamation patterns of articulated specimens of Loganellia scotica (Traquair, 1898) (*Vertebrata*: *Thelodonti*) from the lower silurian of Scotland. *Geodiversitas* 34, 253–270. doi: 10.5252/g2012n2a1

Conflict of Interest: The authors declare that the research was conducted in the absence of any commercial or financial relationships that could be construed as a potential conflict of interest.

Copyright © 2020 Ibáñez, Guerra and Pacheco-Almanzar. This is an open-access article distributed under the terms of the Creative Commons Attribution License (CC BY). The use, distribution or reproduction in other forums is permitted, provided the original author(s) and the copyright owner(s) are credited and that the original publication in this journal is cited, in accordance with accepted academic practice. No use, distribution or reproduction is permitted which does not comply with these terms.

frontiers in Marine Science

REVIEW
published: 17 April 2020
doi: 10.3389/fmars.2020.00195

Fish and Sclerochronology Research in the Mediterranean: Challenges and Opportunities for Reconstructing Environmental Changes

Sanja Matić-Skoko[1], Melita Peharda[2], Dario Vrdoljak[1], Hana Uvanović[2] and Krešimir Markulin[3]*

[1] Laboratory of Ichthyology and Coastal Fisheries, Institute of Oceanography and Fisheries, Split, Croatia, [2] Laboratory of Fisheries Science and Management of Pelagic and Demersal Resources, Institute of Oceanography and Fisheries, Split, Croatia, [3] Laboratory of Chemical Oceanography and Sedimentology of the Sea, Institute of Oceanography and Fisheries, Split, Croatia

OPEN ACCESS

Edited by:
Alejandra Vanina Volpedo, University of Buenos Aires, Argentina

Reviewed by:
Audrey J. Geffen, University of Bergen, Norway
Beatriz Morales-Nin, Instituto Mediterráneo de Estudios Avanzados (IMEDEA), Spain

***Correspondence:**
Sanja Matić-Skoko
sanja@izor.hr

Specialty section:
This article was submitted to Marine Ecosystem Ecology, a section of the journal Frontiers in Marine Science

Received: 07 January 2020
Accepted: 12 March 2020
Published: 17 April 2020

Citation:
Matić-Skoko S, Peharda M, Vrdoljak D, Uvanović H and Markulin K (2020) Fish and Sclerochronology Research in the Mediterranean: Challenges and Opportunities for Reconstructing Environmental Changes. Front. Mar. Sci. 7:195. doi: 10.3389/fmars.2020.00195

Over the past two decades, the field of sclerochronology has been rapidly developing, with scientists devoting significant efforts to studying the physical and chemical variations in hard tissues of aquatic organisms. Most of this research has been limited to certain taxa and geographic areas. Although growth increments in fish otoliths are used for sclerochronology purposes, relatively little has been done in the Mediterranean Sea. According to the literature, the chemical composition of otoliths from Mediterranean fish species has primarily been used for analyzing migration patterns, habitat use, and population structure of commercially important fish species. To the best of our knowledge, there are no studies on fish growth chronology construction conducted in the Mediterranean Sea. In order to identify the opportunities for sclerochronology research on fish from the Mediterranean, we used FishBase to identify potential candidate species with a sufficiently long lifespan and clearly defined growth increments for growth chronology construction and otolith chemistry research. We also present the challenges and limitations for sclerochronology research, including: (i) very few fish species in the Mediterranean Sea have a longevity of several decades; (ii) issues associated with reliable age determination for certain long-lived fish species; (iii) a general lack of understanding and effort to constructed and manage otolith collections; and (iv) limitations imposed by the availability of funding, expertise, and instrumentation. Despite these challenges, fish sclerochronology research has strong potential in the Mediterranean and adjacent seas. Recent studies in the Adriatic Sea have resulted in the construction of bivalve chronologies and the geochemical analysis of shells, providing important time-series data for comparative analysis and a multispecies approach. Furthermore, studies conducted in other parts of the world have demonstrated great potential for the use of fish otoliths in monitoring environmental variability and the effects of pollutants and disturbance.

Keywords: otolith, sclerochronology, growth increments, geochemical fingerprints, stable isotopes, longevity, Mediterranean Sea

INTRODUCTION

Hard structures of aquatic organisms, including mollusk shells, fish otoliths, corals, and coralline algae, are deposited continuously during the life of the organism, and thereby contain environmental information collected over the organism's life cycle (e.g., Hudson et al., 1976; Jones, 1983; Black et al., 2008). The field of sclerochronology utilizes these data archives by investigating their morphological (i.e., increment width) and geochemical composition to deduce organismal life history traits as well as to reconstruct records of environmental and climatic change through space and time (Oschmann, 2009). Although many sclerochronology studies have been conducted on sedentary organisms, primarily the bivalve *Arctica islandica* (e.g., Schöne, 2013; Marali et al., 2017; Reynolds et al., 2018), fish also present a very interesting target taxon for sclerochronology research (e.g., Panfili et al., 2002; Black et al., 2005; Grønkjaer et al., 2013). The objective of this review was to focus primarily on papers that analyzed otoliths in relation to environmental and climatic changes. There are numerous studies in the review that analyzed fish growth and age from growth increment structures in the otoliths (e.g., Gutiérrez and Morales-Nin, 1986; Morales-Nin and Moranta, 1997; Reñones et al., 2007), but they did not directly relate them to the environmental conditions and a detailed review of such studies is beyond the scope of a present paper.

One of the challenges in evaluating the status of sclerochronology research lies within the fact that this term is not always used in publications addressing the morphological and/or geochemical properties of hard structures in aquatic organisms (Gillikin et al., 2019). This is especially the case for research conducted on fish, despite the publication of the very comprehensive *Manual of Fish Sclerochronology* (Panfili et al., 2002).

Fish possess several hard structures interesting for sclerochronology analysis, including scales, the skeleton, and otoliths (e.g., Chilton and Beamish, 1982; Panfili et al., 2002). Of these, otoliths—calcium carbonate structures located in the inner ear of the fish—are considered the most reliable, as they are metabolically inert, hindering re-absorption (Campana and Neilson, 1985), unlike other structures, such as scales (Simkiss, 1974). Otoliths contain periodically deposited growth increments, from daily to annual, and can thereby provide high temporal resolution data (e.g., Campana, 1999; Morales-Nin, 2000; Black et al., 2008; Elsdon et al., 2008). As fish can attain a maximal life span of several decades, otolith analysis can provide an important window into the past (e.g., Campana, 1999; Black et al., 2008).

Chemical research on otoliths includes analysis of elemental and/or isotopic composition. In 1999, Campana published a review paper on the chemistry and composition of otoliths, presenting in detail the state of the art on this subject at that time and the applications and assumptions of this type of research. The applications of otolith chemistry for describing movements and life-history parameters of fish were comprehensively presented by Elsdon et al. (2008). Numerous publications followed, clearly demonstrating the potential for otolith chemistry as a natural tag of fish stocks (e.g., Trueman et al., 2012; Darnaude and Hunter, 2018; Izzo et al., 2018; Wright et al., 2018). Although most studies focus on stock identification and migration history, the elemental composition of otoliths can also be applied for identifying bioavailable contaminants and establishing long-term trends (e.g., Søndergaard et al., 2015; Andronis et al., 2017; Mounicou et al., 2019). Furthermore, as oxygen isotopes ($\delta^{18}O$) are considered a proxy of water temperatures, analysis of otolith isotopic composition can enable reconstruction of environmental conditions (e.g., West et al., 2012; Willmes et al., 2019).

Use of otolith growth increments to construct fish growth chronology and establishing the relationship with environmental conditions have received increasing attention over the past decade. The methodology for this research has been derived from dendrochronology—the study of growth rings in trees (Black et al., 2005). Primary target organisms are long-living fish species, such as yelloweye rockfish (*Sebastes ruberrimus*, >70 years; Black et al., 2008), and northern rockfish (*Sebastes polyspinis*, ∼40 years; Matta et al., 2018). However, development of statistical methods and sample archives have also enabled growth chronology construction for shorter living species. For example, Tanner et al. (2019) constructed half a century chronology for a small, relatively short-lived (<16 years) pelagic fish (Atlantic horse mackerel, *Trachurus trachurus*).

The main objective of this paper is to present an overview of the sclerochronology related research in the Mediterranean Sea and to present its opportunities and challenges.

OVERVIEW OF PREVIOUS SCLEROCHRONOLOGY RELATED RESEARCH IN THE MEDITERRANEAN

In order to identify relevant publications on fish sclerochronology research in the Mediterranean Sea, we conducted a literature search through the Web of Science database. The keywords "Mediterranean" and "otolith" were used in combination with words "isotope," "element," "microchemistry," "chemistry," and "chronology." All publications obtained through this search were read in detail, and only those relating to otolith analysis were included (**Table 1** and **Supplementary Table S1**). Other structures, such as scales and vertebrae, were not considered for the purposes of this review.

Chemical analysis of otoliths has been conducted on over 41 fish species from the Mediterranean, and the most studied species are from the family Sparidae (**Table 1**). Published studies include data for the entire otolith (e.g., Iacumin et al., 1992; Gillanders et al., 2001; Marini et al., 2006; Arechavala-Lopez et al., 2016), data for a specific area of the otolith (e.g., Tanner et al., 2012; Mirasole et al., 2017; Rooker et al., 2019), and time series data (e.g., Correia et al., 2012; Mercier et al., 2012; Bouchoucha et al., 2018). In most reports, only a single species was analyzed, while Papadopoulou and Moraitopoulou-Kassimati (1977), Iacumin et al. (1992), Marini et al. (2006), Swan et al. (2006), Khemiri et al. (2014), Arechavala-Lopez et al. (2016), Mirasole et al. (2017), Bouchoucha et al. (2018), and Demirci et al. (2018) presented data for 2 to 24 different species.

TABLE 1 | List of Mediterranean fish species targeted in the otolith microchemistry research.

Family	Species	References
Anguillidae	*Anguilla anguilla*	Panfili et al., 2012; Capoccioni et al., 2014
Carangidae	*Trachurus mediterraneus*	Turan, 2006
	Trachurus trachurus	Iacumin et al., 1992
Centracanthidae	*Spicara maena*	Iacumin et al., 1992
Champsodontidae	*Chamsodon nudivittis*	Demirci et al., 2018
Clupeidae	*Sardina pilchardus*	Iacumin et al., 1992; Khemiri et al., 2014
Congridae	*Conger conger*	Papadopoulou and Moraitopoulou-Kassimati, 1977; Correia et al., 2011, 2012
Engraulidae	*Engraulis encrasicolus*	Iacumin et al., 1992; Marini et al., 2006; Guidetti et al., 2013; Khemiri et al., 2014
Gadidae	*Merlangus merlangus*	Papadopoulou and Moraitopoulou-Kassimati, 1977; Iacumin et al., 1992
	Trisopterus minutus	Iacumin et al., 1992
Gobiidae	*Gobius bucchichi*	Mirasole et al., 2017
	Gobius niger	Papadopoulou and Moraitopoulou-Kassimati, 1977
Labridae	*Coris julis*	Mirasole et al., 2017
	Symphodus ocellatus	Mirasole et al., 2017
Macrouridae	*Nezumia aequalis*	Swan et al., 2003, 2006
Moronidae	*Dicentrarchus labrax*	Iacumin et al., 1992; Traina et al., 2015; Arechavala-Lopez et al., 2016
Merlucciidae	*Merluccius merluccius*	Iacumin et al., 1992; Morales-Nin et al., 2005a; Swan et al., 2006; Tomas et al., 2006; Hidalgo et al., 2008; Tanner et al., 2012; Chang et al., 2012; Morales-Nin et al., 2014; Tanner et al., 2014; Vitale et al., 2016
Mugilidae	*Mugil cephalus*	Iacumin et al., 1992; Fortunato et al., 2017a,b
Mullidae	*Mullus barbatus*	Marini et al., 2006
Nemipteridae	*Nemipterus randalli*	Demirci et al., 2018
Pomacentridae	*Chromis chromis*	Mirasole et al., 2017
Sciaenidae	*Sciaena umbra*	Iacumin et al., 1992; Marini et al., 2006
	Umbrina cirrhosa	Marini et al., 2006
Scombridae	*Scomber japonicus*	Papadopoulou et al., 1978, 1980
	Thunnus alalunga	Davies et al., 2011
	Thunnus thynnus	Secor and Zdanowicz, 1998; Rooker et al., 2002, 2003, 2008a,b, 2014, 2019; Secor et al., 2002; Fraile et al., 2016
Sebastidae	*Helicolenus dactylopterus*	Swan et al., 2006
Serranidae	*Serranus scriba*	Iacumin et al., 1992
Sparidae	*Boops boops*	Iacumin et al., 1992
	Diplodus annularis	Papadopoulou and Moraitopoulou-Kassimati, 1977; Iacumin et al., 1992; Catalán et al., 2018
	Diplodus puntazzo	Iacumin et al., 1992
	Diplodus sargus	Iacumin et al., 1992; Di Franco et al., 2011, 2012, 2015b; Bouchoucha et al., 2018
	Diplodus vulgaris	Iacumin et al., 1992; Gillanders et al., 2001; Di Franco et al., 2014, 2015a; Mirasole et al., 2017; Bouchoucha et al., 2018
	Dentex dentex	Iacumin et al., 1992
	Lithognatus mormyrus	Iacumin et al., 1992
	Oblada melanura	Iacumin et al., 1992; Calò et al., 2016
	Pagellus erythrinus	Iacumin et al., 1992; Marini et al., 2006
	Sarpa salpa	Iacumin et al., 1992; Mirasole et al., 2017
	Sparus aurata	Iacumin et al., 1992; Mercier et al., 2012; Tournois et al., 2013; Arechavala-Lopez et al., 2016; Niklitschek and Darnaude, 2016
	Spondyliosoma cantharus	Iacumin et al., 1992
Soleidae	*Solea solea*	Dierking et al., 2012; Morat et al., 2012, 2013, 2014a,b

Species names listed as valid species according to World Register of Marine Species. More detail on these studies is available in ***Supplementary Table S1****.*

Recently, Chang and Geffen (2013) summarized taxonomic and geographic influences on fish otolith microchemistry based on a number-published paper worldwide and all those related to the Mediterranean are also included in this study.

In total, 12 species from the family Sparidae are listed in **Table 1**, and most were addressed only by Iacumin et al. (1992). This study analyzed the oxygen and carbon isotope composition of aragonite in fish otoliths with regard to their possible suitability in paleoenvironmental and paleobiological work. This was the first attempt to apply stable isotope analysis to fish otoliths from the Mediterranean Sea. The mostly analyzed species are those from Diplodus genus, particularly *D. sargus*, and *D. puntazzo*, regarding possible environmental interpretation of otolith fingerprints related to spatial patterns of population connectivity and dispersal of marine fishes (Di Franco et al., 2011, 2015b), dispersal scales of fish at various life history stages, which is critical for successful design of networks of marine protected areas (Di Franco et al., 2012, 2015a), within-otolith variability enabling its usage as a marker for fish exposure to stressful conditions (Di Franco et al., 2014).

The majority of research on otolith chemical composition has been conducted on commercially important species. Atlantic Bluefin tuna (*Thunnus thynnus*) was the target of several studies on the element (Secor and Zdanowicz, 1998; Rooker et al., 2003) and isotope composition (Secor et al., 2002; Rooker et al., 2008a,b, 2014, 2019), aiming to reconstruct movement and population exchange. Fraile et al. (2016) observed the depletion in $\delta^{13}C$ in *T. thynnus* otoliths over time, associating this with the oceanic uptake of anthropogenically derived CO_2 from the Mediterranean Sea over the past two decades. These studies

primarily focused on material deposited in the otolith core or during the first year of life.

The European hake (*Mercuccius merluccius*) is also an important target species for the analysis of otolith element and isotope composition, and different methodologies have been applied. Morales-Nin et al. (2005a) studied elements in different parts of the otoliths using laser ablation–spot analysis, while in a study from 2014, the same authors used the line scan approach. Laser ablation, as opposed to otolith dissolution that is applied in the analysis of the whole otolith, enables the collection of more data points that can be placed in time (e.g., Elsdon et al., 2008). Tomas et al. (2006) studied composition of the opaque and translucent bands with wavelength dispersive spectrometry (WDS) revealing that annual marks (translucent) were significantly richer in Sr and Ca and significantly poorer in Na than opaque bands. Swan et al. (2006) applied two methods—solution-based inductively coupled plasma mass spectrometry of the whole otolith and laser ablation analysis of the otolith nucleus on hake and bluemonth (*Helicolenus dactylopterus*). Chang et al. (2012) used hake otoliths to test different widths of ablation lines and evaluate the temporal resolution of data. Hidalgo et al. (2008) and Tanner et al. (2012) applied analysis of $\delta^{18}O$ and $\delta^{13}C$ to certain sections of the otolith, specifically the core and the edge zone, in determining hake movement and ecology. It is interesting that Tanner et al. (2012) combined stable isotope analysis with analysis of otolith element composition to obtain more comprehensive data. These studies on hake analyzed the migration, population structure, and ecology of this commercially important species. In recent papers, Tanner et al. (2014) accompanied genotype with otolith data to increase the classification accuracy of individuals to their potential natal origins, while Vitale et al. (2016) estimated longevity of 25 years of female hake by applying bomb radiocarbon dating.

Element and isotope composition of otoliths of the common sole (*Solea solea*) have been analyzed in a series of studies conducted in the Gulf of Lions, in the northwest Mediterranean (Dierking et al., 2012; Morat et al., 2012, 2013, 2014a,b). These studies analyzed dispersion between populations and the use of different habitats.

The chemical composition of otoliths as a proxy of environmental conditions has been analyzed in only a few studies in the Mediterranean Sea, including Traina et al. (2015). They investigated the metal content of European sea bass (*Dicentrarchus labrax*) otoliths from two fish aquaculture sites. Their results indicated variations in the concentrations of certain metals between locations that were likely due to industrial effluents.

To the best of our knowledge, there is no research in the Mediterranean Sea related to fish growth chronologies constructed from growth increment analysis. The literature search conducted through the Web of Science returned just one publication for the keyword combination "Mediterranean" and "fish" and "sclerochronology": a report by Prendergast and Schöne (2017) as the preface to the *Special Issue on Sclerochronology* containing research from different parts of the world including the Mediterranean, but not specifically on fish in the Mediterranean.

OPPORTUNITIES FOR FISH GROWTH CHRONOLOGY CONSTRUCTION

Over the past two decades, techniques developed in dendrochronology research have been applied for the construction of fish growth chronologies (Black et al., 2005, 2008). They clearly demonstrated the potential for obtaining long term data from growth patterns in otoliths and for identifying environmental drivers (Morrongiello et al., 2012; Rountrey et al., 2014). In a recent review, Black et al. (2019) presented a global list of fish species that have been the subject of sclerochronology studies that included growth chronology construction and applied cross-dating techniques. Their list includes 21 species, none of which were from the Mediterranean Sea. The most studied on the list are cold-water species, such as kelp greenling (*Hexagrammos decagrammus*) and black rockfish (*Sebastes melanops*) and other species from the genus *Sebastes* (*S. alutus*, *S. aurora*, *S. diploproa*, and *S. ruberrimus*). Other species were from the families: Girellidae, Labridae, Lethrinidae, Lutjanidae, Platycephalidae Pleuronectidae, Polyprionidae, Sciaenidae, and Scombridae. All of these are long-lived, non-migratory, nearshore residents with generalist diets that can be caught easily throughout a wide geographic range (Whitfield and Elliott, 2002).

Identifying target fish species with a sufficiently long life span and clearly defined growth increments is a prerequisite for statistically robust chronology construction. Unlike bivalves and trees that can live for several centuries (e.g., *A. islandica*, 507 years; Butler et al., 2013) or even millennia (e.g., *Pinus longaeva*, 4,900 years; Currey, 1965), fish have a shorter lifespan and present a greater challenge for constructing statistically robust chronologies. Another prerequisite for chronology construction is the availability of samples, which needs to take the conservation status of species into account. Although it is scientifically interesting to obtain data from endangered species, sampling such species should be clearly justified and ethically sound. Replication is essential for proper cross-dating that can yield annually resolved chronologies sensitive to environmental stressors (Hudson et al., 1976).

In order to identify possible candidates for fish growth chronology research in the Mediterranean Sea, we conducted a search of the FishBase database. This is a global, scientifically guided, biodiversity information system on fishes that provides a wide range of information (taxonomy, biology, trophic ecology, and life history) on all species currently known in the world, as well as historical data reaching back 250 years[1]. According to this database, a total of 755 fish species from 174 families inhabit the Mediterranean Sea. We made several reductions to obtain a reasonable pool of potentially interesting target species. Since the database provides data for maximal recorded total length (TL), maximal reported age, trophic level, and habitat p'nces (demersal, pelagic-neritic, benthopelagic, bathypelagic, bathydemersal, pelagic-oceanic, and reef-associated) and status (endemic, introduced, and native or questionable), we first removed all short-lived (<2 years) and

[1] fishbase.org

small fishes (TL < 30 cm). This resulted in the removal of species belonging to the families Apogonidae, Atherinidae, Blenniidae, Bregmacerotidae, Callionymidae, and Carapidae. Given their conservation status, Chondrichthyes and the primitive fishes (Myxinidae, Petromyzontidae, Chimaeridae, and Halosauridae) were also excluded. Furthermore, rare or poorly investigated species without any commercial interest or benthopelagic, bathypelagic, and bathydemersal fishes for which no age- related data were provided in FishBase were also excluded.

Finally, a pool of 263 fish species inhabiting Mediterranean Sea was obtained and used in the analysis. The estimated or determined maximum age of 31 fish species from 20 families was over 30 years. However, it is important to note that age was determined by age reading methods on specimens from the Mediterranean Sea for only 12 species (**Table 2**), while the age of other species was estimated based on growth equation parameters available for that specific species or closely related species from the same family, or age was reported for an area other than the Mediterranean Sea.

From these reports, the longest-living species in the Mediterranean Sea is the wreckfish, *Polyprion americanus* (see Peres and Haimovici, 2004). However, its maximum age of 76 years was reported for specimens from the continental shelf and slope off southern Brazil. Thus, its availability for sclerochronology studies in the Mediterranean is questionable, particularly since this species has been listed as Critically Endangered (CR) on the IUCN Red List (IUCN, 2017). The same is true for the red bream *Beryx decadactylus,* since the reported maximum age of 61 years was for specimens collected off the southeastern coast of the United States. To the best of our knowledge, there are no relevant data for the maximum age of either species in the Mediterranean.

The dusky grouper, *Epinephelus marginatus*, lives throughout the Mediterranean Sea and its maximum age of 60 years was reported for specimens from the Balearic Islands (Reñones et al., 2010). Most groupers are solitary, resident fishes. The Mediterranean is the upper limit of their northward distribution, and their growth in the Mediterranean is significantly slower than for groupers in tropical waters (Gracia_López and Castelló-Orway, 2003). Site specificity, a relatively slow growth rate (some species may not be mature until the age of 8 to 10 years) and spawning strategy (synchronic or protogynous hermaphrodites; Sadovy and Shapiro, 1987; Heemstra and Randall, 1993) make them particularly vulnerable (CITES/UNEP-WCMC, 2017). Although the long-life span and resident behavior makes *E. marginatus* an interesting candidate for construction of growth chronologies, its low abundance and protected status throughout the Mediterranean requires a strategic approach to sample collection extending over time, rather than single on-site sampling action.

Three families listed in **Table 2**—Sebastidae, Lutjanidae, and Sciaenidae—were identified earlier within the list of globally important fish taxa for sclerochronology research (Black et al., 2019). However, just two species from the Sebastidae family are listed in the Mediterranean Sea, and only *H. dactylopterus* can attain an age of over 40 years. Certain caution is needed, as this data was reported for individuals caught in the Northeast Atlantic and not in the Mediterranean Sea. According to the available data, *H. dactylopterus* grows faster and lives longer in the Northeast Atlantic than in the Mediterranean (Ragonese, 1989; Allain and Lorance, 2000; D'Onghia et al., 2004; Consoli et al., 2010). The maximum age reported for *H. dactylopterus* from the Mediterranean is 21 years (Consoli et al., 2010), questioning the availability of Mediterranean samples for growth analysis for this species.

Two species of Sciaenidae family are listed in **Table 2**. The maximum reported age for the meagre, *Argyrosomus regius,* in the Gulf of Cádiz (SW Iberian Peninsula) is 42 years (González-Quirós et al., 2011), while the brown meagre, *Sciaena umbra,* reached 31 years in the Gulf of Tunis (Chater et al., 2018). The dense calcium carbonate deposition of the large and very thick otoliths in Sciaenids reduces light transmission, making it almost impossible to distinguish hyaline and opaque zones (Arneri et al., 1998; Chater et al., 2018). According to Arneri et al. (1998), growth increments in otoliths of these taxa are more readable in cross-sections. Both species are commercially important and there is the potential for collection of representative otolith samples. However, further development of otolith reading techniques is needed to facilitate identification of growth increment boundaries and enable statistically robust chronology construction.

Two non-native species, yellowbar angelfish (*Pomacanthus maculosus*) and mangrove red snapper (*Lutjanus argentimaculatus*), have a lifespan of over 30 years (Grandcourt et al., 2004; Fry et al., 2006) and are interesting candidates for growth chronology construction. Both species entered the Mediterranean via the Suez channel and in recent years have established their populations in the eastern Mediterranean, along the coasts of Israel and Lebanon (Bariche, 2010; Sonin et al., 2019). The maximum reported age for *P. maculosus* is for specimens from the southern Arabian Gulf, while for *L. argentimaculatus* the maximum age data is reported for its native range—Papua New Guinea. These two species belong to long-living families (Grandcourt et al., 2004; Piddocke et al., 2015), and although determination of otolith growth patterns present certain challenges for the oldest specimens (Rezende and Ferreira, 2004; Steward et al., 2009), in the context of climate change they are interesting taxa for growth chronology research.

The remaining species listed in **Table 2** belong to the families Sparidae and Moronidae. There are total of 31 sparid species in the Mediterranean Sea, which are known to be slow-growing and long-lived (Hanel and Tsigenopoulos, 2011) and susceptible to over-exploitation due to their commercial importance (Comeros-Raynal et al., 2016). Sparid fishes generally have relatively large and easily readable sagittal otoliths, and despite the wealth of literature denouncing the use of whole, unsectioned otoliths in growth studies on sparid fishes (see Winkler et al., 2019), age determination using whole otoliths is still common. According to the information available in Fish Base, the maximum age reported for sparids in the Mediterranean ranges from 5 to 36 years (**Table 2**). Species with the greatest potential are common dentex *Dentex dentex* and zebra seabream *Diplodus cervinus.* Due to its commercial importance, wide distribution, clear growth patterns in otoliths, and lifespan of over 20 years (Kraljević et al., 1998), the gilt head seabream *Sparus aurata* is also an interesting candidate for sclerochronology research. From the Moronidae family, sea

TABLE 2 | The list of long-lived fish species in the Mediterranean Sea according to FishBase. Data sorted by descending maximum reported age.

Family	Species	Length (cm)	Maximum age (year)	Trophic level	Habitat	References
Serranidae	*Epinephelus marginatus*	150.0	60	4.1	Reef-associated	Reñones et al., 2010
Carangidae	*Pseudocaranx dentex*	122.0	49	3.9	Reef-associated	Kailola et al., 1993
Sebastidae	*Helicolenus dactylopterus*	50.0	43*	4.0	Bathydemersal	Allain and Lorance, 2000
Sciaenidae	*Argyrosomus regius*	230.0	42	4.3	Benthopelagic	González-Quirós et al., 2011
Moridae	*Mora moro*	80.0	39	3.8	Bathypelagic	Sutton et al., 2010
Pomacanthidae	*Pomacanthus maculosus*	61.0	36*	2.7	Reef-associated	Grandcourt et al., 2004
Sparidae	*Dentex dentex*	100.0	36	4.5	Benthopelagic	Baudouin et al., 2016
Sparidae	*Diplodus cervinus*	55.0	35	3.0	Reef-associated	Jarzhombek, 2007
Lutjanidae	*Lutjanus argentimaculatus*	150.0	31*	3.6	Reef-associated	Fry et al., 2006
Sciaenidae	*Sciaena umbra*	70.0	31	3.8	Demersal	Chater et al., 2018
Caproidae	*Capros aper*	30.0	30	3.1	Demersal	Hüssy et al., 2012
Moronidae	*Dicentrarchus labrax*	103.0	30	3.5	Demersal	Kottelat and Freyhof, 2007

**Data for specimens for locations other than Mediterranean Sea.*

bass, *Dicentrarchus labrax* can attain age of 30 years (Kottelat and Freyhof, 2007). The species mentioned in this paragraph are economically interesting, and EU Mediterranean countries collect relevant landing and biological data for them [data collection framework (DCF); Regulation (EU), 2017]. It is highly likely, either within monitoring programs or scientific research projects, that otoliths of these species are archived during several years or even decades by different institutions and could be used to extend time series data beyond the maximal reported age.

According to the data presented above, the availability of otoliths for long living species from the Mediterranean is quite limited, as there are only several species reaching a maximum reported age of over 30 years. However, development of statistical techniques enables construction of growth chronologies for shorter living fish species (<15 years) when samples are collected over several years or decades (Coulson et al., 2014). It is possible that, for certain fish species, adequate replicates for chronology construction can be obtained through archive collections.

OPPORTUNITIES FOR OTOLITH CHEMISTRY RESEARCH

Clarity of growth rings in otoliths is one of the main factors contributing to sclerochronology research, both for growth increment measurements and for otolith chemical analysis (Campana, 1999). Problems related to interpretation of increments in otolith, including age estimation and validation of periodicity, has been pointed out in number of studies in different parts of the world (e.g., Morales-Nin et al., 2005b; Stransky et al., 2005; Hüssy et al., 2016). This problem should not be underestimated, and interpretation of otolith increments needs to be carefully checked and validated. One of the most appreciated characteristics of otoliths is their lack of resorption. This means that once the material has been deposited, the organism will not use these minerals again, even in periods of starvation. Lack of resorption is not shared with other calcified structure (like scales and bones) in fishes or other vertebrates (Bilton, 1974; cited by Campana and Thorrold, 2001). Another special characteristic of otoliths is that they grow continuously throughout the lifetime of the fish (Campana, 1999).

In order to assign relevant chemistry data to a specific calendar year, it is crucial to distinguish growth increment boundaries (Black et al., 2005; Martino et al., 2019). However, many the most commercially important fish species living in the Mediterranean Sea do not have clearly distinguished growth patterns in their otoliths, which presents a challenge for this type of research. For example, it is still difficult to determine the growth boundaries for the first growth increments in otoliths of *Mullus barbatus* due slow growth and number of false-growth increments laid down before the annulus (Carbonara et al., 2018) and of *Merluccius merluccius* due to the fast growth (de Pontual et al., 2003; Piñeiro et al., 2007; Mellon-Duval et al., 2010) and long spawning period of the species (Morales-Nin and Aldebert, 1997) although a number of direct methods to validate age assessment were used, like mark-recapture (de Pontual et al., 2003; Mellon-Duval et al., 2010), first ring appearance (Belcari et al., 2006), or bomb radiocarbon dating (Vitale et al., 2016).

Species from the families Sparidae and Lutjanidae have annual growth rings, that although thin, are clearly visible (Piddocke et al., 2015; Winkler et al., 2019), and represent the most promising target taxa for sclerochronology studies. Interesting target species of Sparidae include *Dentex dentex*, *Diplodus cervinus*, and *Sparus aurata*. The latter species, together with *Dicentrarchus labrax* (Moronidae), are particularly interesting, as these are the most important fish aquaculture species throughout the Mediterranean region (Lacoue-Labarthe et al., 2016). In addition to these species and those listed in **Table 1**, another interesting taxon for chemical research of otoliths is *Seriola dumerili* (Carangidae), a species with a circumglobal distribution (Smith, 1997).

Instrumental restrictions, related to the quantity of material required for the analysis of stable isotopes in otoliths, has been the main limitation for the development of isotope related research in otoliths (Sreemany et al., 2017). Due to the small size of the otolith, this resulted in time averaging of data, and analyses were limited to whole otoliths (e.g., Rooker et al., 2008a), or certain parts of otoliths, e.g., the core (Siskey et al., 2016;

Rooker et al., 2019) or edge (Hidalgo et al., 2008; Tanner et al., 2012), without the possibility of obtaining time series data. Development of instruments and methods, including high-resolution laser ablation systems (e.g., Sreemany et al., 2017) and continuous flow isotope ratio mass spectrometry system for ultra-microvolume carbonate samples (Kitagawa et al., 2013; Sakamoto et al., 2017), have opened new opportunities for obtaining time series data from otoliths. Although significant progress was made in instrument development, many are still available only to a limited number of scientists. Therefore, new opportunities for collaborations and research directions related to the Mediterranean are required.

CHALLENGES AND LIMITATIONS FOR FISH SCLEROCHRONOLOGY RESEARCH IN THE MEDITERRANEAN SEA

Alongside the constraints imposed by the biological characteristics of species, there are other challenges to conducting sclerochronology research in the Mediterranean region. Although otoliths are small structures that are easily archived, there still appears to be a general lack of understanding and effort to construct and manage otolith collections. Panfili et al. (2002) clearly indicated the importance of archiving otoliths, highlighting the need to evaluate, catalog, and conserve otolith collections in a way that will make both the otolith and corresponding fish life history information more accessible to all researchers. The Instituto de Ciencias del Mar-CSIC (Spain) maintains an otolith reference collection that includes samples from different parts of the world, including the Western Mediterranean Sea[2]. One example of an online searchable database of otolith collections from other parts of the world is the otolith collection database housed at the Burke Museum[3]. Although English is generally accepted as a global scientific language, the Mediterranean is highly politically, economically, cultural, and linguistically diverse region, which impacts sample, data, and knowledge storage and sharing. While online searchable otolith collections are not currently possible for a number of reasons, efforts should be made by different institutions or even scientists themselves to archive otoliths together with relevant collection and biology data. It is highly recommended that collections contain samples for different species, not only commercially most important ones, and that special efforts are made to archive otoliths of rare species. Furthermore, Disspain et al. (2016) pointed out the potential to use otoliths from archeological sites to analyze changes in the environment occurring through human history. Linking archeologists with fish biologist and environmental scientists can provide great potential for sclerochronology research.

In addition to the issues related to the availability of otolith collections, continuous sampling over several decades is also a challenge given the limited availability of funding for long-term studies and the logistics associated with field sampling. Long-term time series data are needed to estimate the real status of exploited resources and their evolution over time (Battaglia et al., 2010) and to analyze climate change effects on marine species and communities (Azzurro et al., 2019). Today, most scientific research projects are short in duration, resulting in difficulties related to securing funds needed for maintaining a longer data time series (Lleonart and Maynou, 2003; Rochet and Trenkel, 2003). Even when data collection takes place over longer periods, it often suffers from inconsistencies in sampling design or sampling methods (Rochet and Trenkel, 2003; Rochet et al., 2005). Sampling designs often tend to be incomplete, lacking either randomization or replication, and as such can never conclusively demonstrate the causes of the observed changes. Sampling and storage protocols are often specific to the institution or project. It is, however, encouraging that all the EU Member States bordering the Mediterranean Sea, eight in total, are required to collect fisheries data using unified methodology [Regulation (EU), 2017].

Human resources present another important segment in the development of all marine-related research in the Mediterranean, including sclerochronology. Although otoliths have been analyzed in relation to age and growth, very few attempts have been made to link the data derived from otoliths with environmental data. Education in methods associated with growth increments analysis, chemical composition of otoliths, and statistical methods related to sclerochronology research is strongly needed, either through personal or workshop-based interactions, to stimulate the involvement of fisheries scientists in sclerochronology studies. Furthermore, sclerochronology includes biological, chemical, and physical aspects, requiring an interdisciplinary research team.

Different types of instrumentation are required for sclerochronology analysis. Some instruments need to be readily and continuously available, such as saws and grinding and polishing machines, while those for chemical analysis of otoliths can be offsite. For example, the Laser Ablation System coupled with a High-Resolution Inductively Coupled Plasma Mass Spectrometer (HR-ICPMS) is a sophisticated tool for analysis of elemental composition that is both very expensive and requires specially trained personnel. Careful sample preparation and establishing collaboration with institutions possessing such an instrument can enable the processing of otolith samples at a reasonable cost. Efforts should be made to develop human and research capacities within the framework of different international projects, thereby promoting scientific collaboration and the education of young researchers.

CONCLUSION

The Mediterranean Sea is a hotspot of marine biodiversity and is also one of the most impacted ecoregions globally (Halpern et al., 2008; Costello et al., 2010), due to increasing levels of human threats that affect all levels of biodiversity (Mouillot et al., 2011; Coll et al., 2012; Micheli et al., 2013) and due to severe impacts from climate change (Lejeusne et al., 2010) and biological invasions (Katsanevakis et al., 2012).

[2] ipt.vliz.be/eurobis

[3] www.burkemuseum.org

Determining historical changes in marine communities and consequently fisheries (Pauly and Zeller, 2016) allows us to better understand the present, in order to anticipate the future. This is particularly important in relation to the decline of marine resources (Bell et al., 2017). Thus, it is necessary to develop methods to document long-term trends and detect potential stressors. However, establishing causal relationships between a wide range of stressors and effects at the individual, species, or community level in marine ecosystems is a difficult task that requires the use of multiple lines of evidence (Adams, 2005). Fish are excellent candidates for the study of the effects of climate variability (Pörtner and Peck, 2010). In the Mediterranean Sea, besides the phenomenon of a northward shift in population distribution by native Mediterranean species, the arrival of alien species is also playing an important role in carving the faunal assemblages of the Mediterranean Sea. It is presumed that the coldest parts of the Mediterranean Sea (Gulf of Lyon and North Adriatic) could initially serve as a sanctuary for cold-temperate species, though continued warming of these areas could turn them into a cul-de-sac for such species. This is especially important for endemic species that could become extinct due to the trapping effect (Ben Rais Lasram et al., 2010).

Sclerochronology research has the potential to provide insight into environmental changes in the Mediterranean, both at the local and regional scales (Peharda et al., 2019a). Recent research conducted on bivalves in the Adriatic Sea resulted in a construction of bivalve chronologies (Peharda et al., 2018, 2019a) and geochemical analysis of shells (Markulin et al., 2019; Peharda et al., 2019b), providing important time-series data for comparative analysis and a multispecies approach. Such a multispecies approach has been very promising in other parts of the world, including the work by Black (2009), who analyzed growth increments in trees, bivalves and fish to identify climate variability signals. Further development of fish sclerochronology research in the Mediterranean could facilitate a multi-taxa approach, enabling us to gain a better understanding of environmental drivers in marine habitats.

AUTHOR CONTRIBUTIONS

SM-S and MP analyzed the data and existing literature in collaboration with DV, HU, and KM. SM-S and MP wrote the draft of the manuscript. All authors conceived the research, and participated in the improvement and revision of the document.

FUNDING

This study was fully supported by the Croatian Science Foundation (HRZZ) under project IP-2016-06-9884 (NurseFish).

SUPPLEMENTARY MATERIAL

The Supplementary Material for this article can be found online at: https://www.frontiersin.org/articles/10.3389/fmars.2020.00195/full#supplementary-material

TABLE S1 | Published sclerochronology research relating to otolith analysis in the Mediterranean Sea.

REFERENCES

Adams, S. M. (2005). Assessing cause and effect of multiple stressors on marine systems. *Mar. Poll. Bull.* 51, 649–657. doi: 10.1016/j.marpolbul.2004.11.040

Allain, V., and Lorance, P. (2000). Age estimation and growth of some deep-sea fish from the Northeast Atlantic Ocean. *Cybium* 24, 7–16.

Andronis, C., Evans, N. J., McDonald, B. J., Nice, H. E., and Gagnon, M. M. (2017). Otolith microchemistry: insights into bioavailable pollutants in a man-made, urban inlet. *Mar. Pollut. Bull.* 118, 382–387. doi: 10.1016/j.marpolbul.2017.02.037

Arechavala-Lopez, P., Milošević-González, M., and Sanchez-Jerez, P. (2016). Using trace elements in otoliths to discriminate between wild and farmed European sea bass (*Dicentrarchus labrax* L.) and Gilthead sea bream (*Sparus aurata* L.). *Int. Aquat. Res.* 8, 263–273. doi: 10.1007/s40071-016-0142-1

Arneri, E., Colella, S., and Giannetti, G. (1998). A method for the age determination of two Mediterranean sciaenids, *Sciaena umbra* (Linnaeus, 1758) and *Umbrina cirrhosa* (Linnaeus, 1758). *Rapp. Comm. Int. Mer Médit.* 35, 366–367.

Azzurro, E., Sbragaglia, V., Cerri, J., Bariche, M., Bolognini, L., Souissi, J. B., et al. (2019). Climate change, biological invasions, and the shifting distribution of Mediterranean fishes: a large-scale survey based on local ecological knowledge. *Glob. Change Biol.* 2019, 2779–2792. doi: 10.1111/gcb.14670

Bariche, M. (2010). First record of the angelfish Pomacanthus maculosus (Teleostei: Pomacanthidae) in the Mediterranean. *Aqua* 16, 31–33.

Battaglia, P., Romeo, T., Consoli, P., Scotti, G., and Andaloro, F. (2010). Characterization of the artisanal fishery and its socio-economic aspects in the central Mediterranean Sea (Aeolian Islands. Italy. *Fish. Res.* 102, 87–97. doi: 10.1016/j.fishres.2009.10.013

Baudouin, M., Marengo, M., Pere, A., Culioli, J. M., Santoni, M. C., Marchand, B., et al. (2016). Comparison of otolith and scale readings for age and growth estimation of common dentex *Dentex dentex*. *J. Fish Biol.* 88, 760–766. doi: 10.1111/jfb.12816

Belcari, P., Ligas, A., and Viva, C. (2006). Age determination and growth of juveniles of the European hake, *Merluccius merluccius* (L., 1758), in the northern Tyrrhenian Sea (NW Mediterranean). *Fish. Res.* 78, 211–217. doi: 10.1016/j.fishres.2006.01.006

Bell, J. D., Watson, R. A., and Ye, Y. (2017). Global fishing capacity and fishing effort from 1950 to 2012. *Fish Fish.* 18, 489–505. doi: 10.1111/faf.12187

Ben Rais Lasram, F., Guilhaumon, F., Albouy, C., Somot, S., Thuiller, W., and Mouillot, D. (2010). The Mediterranean Sea as a 'cul-de-sac' for endemic fishes facing climate change. *Glob. Change Biol.* 16, 3233–3245. doi: 10.1111/j.1365-2486.2010.02224.x

Bilton, H. (1974). "Effects of starvation and feeding on circulus formation on scales of young sockeye salmon of four racial origins, and of one race of young kokanee, coho and chinook salmon," in *The Ageing of Fish*, ed. T. B. Bagenal (Surrey: Unwin Brothers Ltd), 40–70.

Black, B. A. (2009). Climate-driven synchrony across tree, bivalve, and rockfish growth-increment chronologies of the northeast Pacific. *Mar. Ecol. Prog. Ser.* 378, 37–46. doi: 10.3354/meps07854

Black, B. A., Andersson, C., Butler, P. G., Carroll, M. L., DeLong, K. L., Reynolds, D. J., et al. (2019). The revolution of crossdating in marine palaeoecology and palaeoclimatology. *Biol. Lett.* 15:20180665. doi: 10.1098/rsbl.2018.0665

Black, B. A., Boehlert, G. W., and Yoklavich, M. M. (2005). Using tree-ring crossdating techniques to validate annual growth increments in long-lived fishes. *Can. J. Fish. Aquat. Sci.* 62, 2277–2284. doi: 10.1139/f05-142

Black, B. A., Boehlert, G. W., and Yoklavich, M. M. (2008). Establishing climate-growth relationships for yelloweye rockfish (*Sebastes ruberrimus*) in the northeast Pacific using a dendrochronological approach. *Fish. Oceanogr.* 17, 368–379. doi: 10.1111/j.1365-2419.2008.00484.x

Bouchoucha, M., Pécheyran, C., Gonzalez, J. L., Lenfant, P., and Darnaude, A. M. (2018). Otolith fingerprints as natural tags to identify juvenile fish life in ports. *Estuar. Coast. Shelf Sci.* 212, 210–218. doi: 10.1016/j.ecss.2018.07.008

Butler, P. G., Wanamaker, A. D., Scourse, J. D., Richardson, C. A., and Reynolds, D. J. (2013). Variability of marine climate on the North Icelandic Shelf in a 1357-year proxy archive based on growth increments in the bivalve *Arctica islandica*. *Palaeogeogr. Palaeoclimatol. Palaeoecol.* 373, 141–151. doi: 10.1016/j.palaeo.2012.01.016

Calò, A., Di Franco, A., De Benedetto, G. E., Pennetta, A., Pérez-Ruzafa, Á, and García-Charton, J. A. (2016). Propagule dispersal and larval patch cohesiveness in a Mediterranean coastal fish. *Mar. Ecol. Prog. Ser.* 544, 213–224. doi: 10.3354/meps11609

Campana, S. E. (1999). Chemistry and composition of fish otoliths: pathways, mechanisms and applications. *Mar. Ecol. Prog. Ser.* 188, 263–297. doi: 10.3354/meps188263

Campana, S. E., and Neilson, J. D. (1985). Microstructure of fish otoliths. *Can. J. Fish. Aquat. Sci.* 42, 1014–1032. doi: 10.1139/f85-127

Campana, S. E., and Thorrold, S. R. (2001). Otoliths, increments, and elements: keys to a comprehensive understanding of fish populations? *Can. J. Fish. Aquat. Sci.* 58, 30–38. doi: 10.1139/f00-177

Capoccioni, F., Lin, D.-Y., Iizuka, Y., Tzeng, W. N., and Ciccotti, E. (2014). Phenotypic plasticity in habitat use and growth of the European eel (*Anguilla anguilla*) in transitional waters in the Mediterranean area. *Ecol. Freshw. Fish* 23, 65–76. doi: 10.1111/eff.12049

Carbonara, P., Intini, S., Kolitari, J., Joksimović, A., Milone, N., Lembo, G., et al. (2018). A holistic approach to the age validation of *Mullus barbatus* L., 1758 in the Southern Adriatic Sea (Central Mediterranean). *Sci. Rep.* 8:13219. doi: 10.1038/s41598-018-30872-1

Catalán, I. A., Alós, J., Díaz-Gil, C., Pérez-Mayol, S., Basterretxea, G., Morales-Nin, B., et al. (2018). Potential fishing-related effects on fish life history revealed by otolith microchemistry. *Fish. Res.* 199, 186–195. doi: 10.1016/j.fishres.2017.11.008

Chang, M. Y., and Geffen, A. J. (2013). Taxonomic and geographic influences on fish otolith microchemistry. *Fish Fish.*14, 458–492. doi: 10.1111/j.1467-2979.2012.00482.x

Chang, M. Y., Geffen, A. J., Kosler, J., Dundas, S. H., and Maes, G. E. (2012). The effect of ablation pattern on LA-ICPMS analysis of otolith element composition in hake *Merluccius merluccius*. *Environ. Biol. Fish.* 95, 509–520. doi: 10.1007/s10641-012-0065-7

Chater, I., Romdhani-Dhahri, A., Dufour, J. L., Mahé, K., and Chakroun-Marzouk, N. (2018). Age, growth and mortality of *Sciaena umbra* (Sciaenidae) in the Gulf of Tunis. *Sci. Mar.* 82, 17–25. doi: 10.3989/scimar.04679.21a

Chilton, D. E., and Beamish, R. J. (1982). Age determination methods for fishes studied by the groundfish program at the Pacific Biological Station. *Can. Spec. Publ. Fish. Aquat. Sci.* 60:102.

Coll, M., Piroddi, C., Albouy, C., Ben Rais Lasram, F., Cheung, W. W. L., Christensen, V., et al. (2012). The Mediterranean under siege: spatial overlap between marine biodiversity, cumulative threats and marine reserves. *Glob. Ecol. Biogeogr.* 21, 465–481.

Comeros-Raynal, M. T., Polidoro, B., Broatch, J., Mann, B. Q., Gorman, C., Buxton, C., et al. (2016). Key predictors of extinction risk in sea breams and porgies (Family: Sparidae). *Biol. Conserv.* 202, 88–98. doi: 10.1016/j.biocon.2016.08.027

Consoli, P., Battaglia, P., Castriota, L., Esposito, V., Romeo, T., and Andaloro, F. (2010). Age, growth and feeding habits of the bluemouth rockfish, *Helicolenus dactylopterus dactylopterus* (Delaroche 1809) in the central Mediterranean (southern Tyrrhenian Sea). *J. Appl. Ichthyol.* 26, 583–591. doi: 10.1111/j.1439-0426.2010.01467.x

Correia, A. T., Barros, F., and Sial, A. N. (2011). Stock discrimination of European conger eel (*Conger conger* L.) using otolith stable isotope ratios. *Fish. Res.* 108, 88–94. doi: 10.1016/j.fishres.2010.12.002

Correia, A. T., Ramos, A. A., Barros, F., Silva, G., Hamer, P., Morais, P., et al. (2012). Population structure and connectivity of the European conger eel (*Conger conger*) across the north-eastern Atlantic and western Mediterranean: integrating molecular and otolith elemental approaches. *Mar. Biol.* 159, 1509–1525. doi: 10.1007/s00227-012-1936-3

Costello, M. J., Coll, M., Danovaro, R., Halpin, P., Ojaveer, H., and Miloslavich, P. (2010). A census of marine biodiversity knowledge, resources and future challenges. *PLoS One* 5:e12110. doi: 10.1371/journal.pone.0012110

Coulson, P. G., Black, B. A., Potter, I. C., and Hall, N. G. (2014). Sclerochronological studies reveal that patterns of otolith growth of adults of two co-occurring species of Platycephalidae are synchronised by water temperature variations. *Mar. Biol.* 161, 383–393. doi: 10.1007/s00227-013-2343-0

Currey, D. R. (1965). An ancient bristlecone pine stand in eastern Nevada. *Ecology* 46, 564–566. doi: 10.2307/1934900

Darnaude, A. M., and Hunter, E. (2018). Validation of otolith d18O values as effective natural tags for shelf-scale geolocation of migrating fish. *Mar. Ecol. Prog. Ser.* 598, 167–185. doi: 10.3354/meps12302

Davies, C. A., Brophy, D., Jeffries, T., and Gosling, E. (2011). Trace elements in the otoliths and dorsal spines of albacore tuna (*Thunnus alalunga*, Bonnaterre, 1788): an assessment of the effectiveness of cleaning procedures at removing post mortem contamination. *J. Exp. Mar. Bio. Ecol.* 396, 162–170. doi: 10.1016/j.jembe.2010.10.016

de Pontual, H., Bertignac, M., Battaglia, A., Bavouzet, G., Moguedet, P., and Groison, A.-L. (2003). A pilot tagging experiment on European hake (*Merluccius merluccius*): methodology and preliminary results. *ICES J. Mar. Sci.* 60, 1318–1327. doi: 10.1016/S1054-3139(03)00149-8

Demirci, S., Özyılmaz, A., Öksüz, A., Nadir, R. S., and Şimşek, E. (2018). Otolith chemistry of *Champsodon nudivittis* (Ogilby, 1895) and *Nemipterus randalli* (Russell, 1986) in Iskenderun Bay, Turkey. *J. Appl. Ichthyol.* 34, 1131–1135. doi: 10.1111/jai.13761

Di Franco, A, Bulleri, F., Pennetta, A., De, Benedetto G, Clarke, K. R., and Guidetti, P. (2014). Within-otolith variability in chemical fingerprints: implications for sampling designs and possible environmental interpretation. *PLoS One* 9:e101701. doi: 10.1371/journal.pone.0101701

Di Franco, A., de Benedetto, G., de Rinaldis, G., Raventos, N., Sahyoun, R., and Guidetti, P. (2011). Large scale-variability in otolith microstructure and microchemistry: the case study of *Diplodus sargus sargus* (Pisces: Sparidae) in the Mediterranean Sea. *Ital. J. Zool.* 78, 182–192. doi: 10.1080/11250003.2011.566227

Di Franco, A., Calò, A., Pennetta, A., De Benedetto, G., Planes, S., and Guidetti, P. (2015a). Dispersal of larval and juvenile seabream: implications for Mediterranean marine protected areas. *Biol. Conserv.* 192, 361–368. doi: 10.1016/j.biocon.2015.10.015

Di Franco, A., Gianni, F., and Guidetti, P. (2015b). Mismatch in early life traits between settlers and recruits in a Mediterranean fish: clue of the relevance of the settlement tail? *Acta Ichthyol. Piscat.* 45, 153–159. doi: 10.3750/AIP2015.45.2.05

Di Franco, A., Gillanders, B. M., De Benedetto, G., Pennetta, A., De Leo, G. A., and Guidetti, P. (2012). Dispersal patterns of coastal fish: implications for designing networks of marine protected areas. *PLoS One* 7:e31681. doi: 10.1371/journal.pone.0031681

Dierking, J., Morat, F., Letourneur, Y., and Harmelin-Vivien, M. (2012). Fingerprints of lagoonal life: migration of the marine flatfish Solea solea assessed by stable isotopes and otolith microchemistry. *Estuar. Coast. Shelf Sci.* 10, 23–32. doi: 10.1016/j.ecss.2011.03.018

Disspain, M. C. F., Ulm, S., and Gillanders, B. M. (2016). Otoliths in archaeology: methods, applications and future prospects. *J. Archaeol. Sci. Rep.* 6, 623–632. doi: 10.1016/j.jasrep.2015.05.012

D'Onghia, G., Lloris, D., Politou, C.-Y., Sion, L., and Dokos, J. (2004). New records of deep-water teleost fishes in the Balearic Sea and Ionian Sea (Mediterranean Sea). *Sci. Mar.* 68, 171–183. doi: 10.3989/scimar.2004.68s3171

Elsdon, T. S., Wells, B., Campana, S., Gillanders, B., Jones, C., Limburg, K., et al. (2008). *Otolith chemistry to describe movements and life-history parameters of fishes: hypotheses, assumptions, limitations and inferences in Oceanography and marine biology: an annual review*, Vol. 46. Boca Raton: CRC Press-Taylor & Francis Group, 297–330.

Fortunato, C. R., Durà, B. V., and Volpedo, A. (2017a). Otolith morphometry and microchemistry as habitat markers for juvenile Mugil cephalus Linnaeus 1758 in nursery grounds in the Valencian community, Spain. *J. Appl. Ichthyol.* 33, 163–167. doi: 10.1111/jai.13291

Fortunato, C. R., Galán, A. R., Alonso, G. I., Volpedo, A., and Durà, B. V. (2017b). Environmental migratory patterns and stock identification of *Mugil cephalus* in the Spanish Mediterranean Sea, by means of otolith microchemistry. *Estuar. Coast. Shelf Sci.* 188, 174–180. doi: 10.1016/j.ecss.2017.02.018

Fraile, I., Arrizabalaga, H., Groeneveld, J., Kölling, M., Santos, M. N., Macías, D., et al. (2016). The imprint of anthropogenic CO2 emissions on Atlantic bluefin tuna otoliths. *J. Mar. Syst.* 158, 26–33. doi: 10.1016/j.jmarsys.2015.12.012

Fry, G. C., Brewer, D. T., and Venables, W. N. (2006). Vulnerability of deepwater demersal fishes to commercial fishing: evidence from a study around a tropical volcanic seamount in Papua New Guinea. *Fish. Res.* 81, 126–141. doi: 10.1016/j.fishres.2006.08.002

Gillanders, B. M., Sanchez-Jerez, P., Bayle-Sempere, J., and Ramos-Espla, A. (2001). Trace elements in otoliths of the two-banded bream from a coastal region in the south-west Mediterranean: are there differences among locations? *J. Fish Biol.* 59, 350–363. doi: 10.1006/jfbi.2001.1643

Gillikin, D. P., Wanamaker, A. D., and Andrus, C. F. T. (2019). Chemical sclerochronology. *Chem. Geol.* 526, 1–6. doi: 10.1016/j.chemgeo.2019.06.016

González-Quirós, R., Del Árbol, J., García-Pacheco, M. del M, Silva-García, A. J., Naranjo, J. M., Nin, B. M., et al. (2011). Life-history of the meagre *Argyrosomus regius* in the Gulf of Cádiz (SW *Iberian Peninsula*). *Fish. Res.* 109, 140–149. doi: 10.1016/j.fishres.2011.01.031

Gracia_López, V., and Castelló-Orway, F. (2003). Preliminary data on the culture of juveniles of the dusky grouper, *Epinephelus marginatus* (Lowe, 1834). *Hidrobiológica* 13, 321–327.

Grandcourt, E. M., Al Abdessalaam, T. Z., Francis, F., and Al Shamsi, A. T. (2004). Biology and stock assessment of the Sparids, *Acanthopagrus bifasciatus* and *Argyrops spinifer* (Forsskål, 1775), in the Southern Arabian Gulf. *Fish. Res.* 69, 7–20. doi: 10.1016/j.fishres.2004.04.006

Grønkjaer, P., Pedersen, J. B., Ankjaerø, T. T., Kjeldsen, H., Heinemeier, J., Steingrund, P., et al. (2013). Stable N and C isotopes in the organic matrix of fish otoliths: validation of a new approach for studying spatial and temporal changes in the trophic structure of aquatic ecosystems. *Can. J. Fish. Aquat. Sci.* 70, 143–146. doi: 10.1139/cjfas-2012-0386

Guidetti, P., Petrillo, M., De Benedetto, G., and Albertelli, G. (2013). The use of otolith microchemistry to investigate spawning patterns of European anchovy: a case study in the eastern Ligurian Sea (NW Mediterranean). *Fish. Res.* 139, 1–4. doi: 10.1016/j.fishres.2012.10.015

Gutiérrez, E., and Morales-Nin, B. (1986). Time series analysis of daily growth in *Dicentrarchuslabrax* L. otoliths. *J. Exp. Mar. Biol. Ecol.* 103, 163–179. doi: 10.1016/0022-0981(86)90139-5

Halpern, B. S., Walbridge, S., Selkoe, K. A., Kappel, C. V., Micheli, F., D'Agrosa, C., et al. (2008). A global map of human impact on marine ecosystems. *Science* 319, 948–952. doi: 10.1126/science.1149345

Hanel, R., and Tsigenopoulos, C. S. (2011). "Phylogeny, Evolution and Taxonomy of sparids with some notes on their Ecology and Biology in Sea bream," in *Biology & Aquaculture of Sparidaen*, eds M. Pavlidis and C. C. Mylonas (Hoboken, NJ: Wiley-Blackwell), 51–74.

Heemstra, P. C., and Randall, J. E. (1993). *FAO Species Catalogue Cephalopods. An Annotated and Illustrated Catalogue of the Grouper, Rockcod, Hind, Coral, Grouper, and Lyretail Species Known to Date*. Rome: FAO Fish.

Hidalgo, M., Tomás, J., Høie, H., Morales-Nin, B., and Ninnemann, U. S. (2008). Environmental influences on the recruitment process inferred from otolith stable isotopes in Merluccius merluccius off the Balearic Islands. *Aquat. Biol.* 3, 195–207. doi: 10.3354/ab00081

Hudson, J. H., Shinn, E. A., Halley, R. B., and Lidz, B. (1976). Sclerochronology: a tool for interpreting past environments. *Geology* 4, 361–364. doi: 10.1130/0091-761319764<361:SATFIP<2.0.CO;2

Hüssy, K., Coad, J. O., Farrell, E. D., Clausen, L. W., and Clarke, M. W. (2012). Sexual dimorphism in size, age, maturation, and growth characteristics of boarfish (*Capros aper*) in the Northeast Atlantic. *ICES J. Mar. Sci.* 69, 1729–1735. doi: 10.1093/icesjms/fss156

Hüssy, K., Radtke, K., Plikshs, M., Oeberst, R., Baranova, T., Krumme, U., et al. (2016). Challenging ICES age estimation protocols: lessons learned from the eastern Baltic cod stock. *ICES J. Mar. Sci.* 73, 2138–2149. doi: 10.1093/icesjms/fsw107

Iacumin, P., Bianucci, G., and Longinelli, A. (1992). Oxygen and carbon isotopic composition of fish otoliths. *Mar. Biol.* 113, 537–542. doi: 10.1007/BF00349696

IUCN (2017). *IUCN Red List of Threatened Species. Version 2017–2.* Available online at: www.iucnredlist.org (accessed December 17, 2019).

Izzo, C., Reis-Santos, P., and Gillanders, B. M. (2018). Otolith chemistry does not just reflect environmental conditions: a meta-analytic evaluation. *Fish Fish.* 19, 441–454. doi: 10.1111/faf.12264

Jarzhombek, A. A. (2007). Compilation of studies on the growth of Acanthopterygii. *Russian Federal Res. Ins. Fish. Oceanogr. (VNIRO)*. 86.

Jones, D. S. (1983). Sclerochronology: reading the record of the molluscan shell. *Am. Sci.* 71, 384–391.

Kailola, P. J., Williams, M. J., Stewart, P. C., Reichelt, R. E., McNee, A., and Grieve, C. (1993). *Australian Fisheries Resources*. Canberra: Bureau of Resource Sciences, 422.

Katsanevakis, S., Bogucarskis, K., Gatto, F., Vandekerkhove, J., Deriu, I., and Cardoso, A. C. (2012). Building the European Alien Species Information Network (EASIN): a novel approach for the exploration of distributed alien species data. *Bioinvasions Rec* 1, 235–245. doi: 10.3391/bir.2012.1.4.01

Khemiri, S., Labonne, M., Gaamour, A., Munaron, J. M., and Morize, E. (2014). The use of otolith chemistry to determine stock structure of *Sardina pilchardus* and *Engraulis encrasicolus* in Tunisian Coasts. *Cah. Biol. Mar.* 55, 21–29.

Kitagawa, T., Ishimura, T., Uozato, R., Shirai, K., Amano, Y., Shinoda, A., et al. (2013). Otolith δ18O of Pacific bluefin tuna *Thunnus orientalis* as an indicator of ambient water temperature. *Mar. Ecol. Prog. Ser.* 481, 199–209. doi: 10.3354/meps10202

Kottelat, M., and Freyhof, J. (2007). *Handbook of European Freshwater Fishes*. Berlin: Publications Kottelat, Cornol and Freyhof.

Kraljević, M., Dulčić, J., and Tudor, M. (1998). Growth parameters of the gilt-head sea bream *Sparus aurata* L. in the eastern Adriatic (Croatian waters). *Period. Biol.* 100, 87–91.

Lacoue-Labarthe, T., Nunes, P. A. L. D., Ziveri, P., Cinar, M., Gazeau, F., Hall-Spencer, J. M., et al. (2016). Impacts of ocean acidification in a warming Mediterranean Sea: an overview. *Reg. Stud. Mar. Sci.* 5, 1–11. doi: 10.1016/j.rsma.2015.12.005

Lejeusne, C., Chevaldonne, P., Pergent-Martini, C., Boudouresque, C. F., and Perez, T. (2010). Climate change effects on a miniature ocean: the highly diverse, highly impacted Mediterranean Sea. *Trends Ecol.Evol.* 25, 250–260. doi: 10.1016/j.tree.2009.10.009

Lleonart, J., and Maynou, F. (2003). Fish stock assessment in Mediterranean: state of the art. *Sci. Mar.* 67, 37–49. doi: 10.3989/scimar.2003.67s137

Marali, S., Schöne, B. R., Mertz-Kraus, R., Griffin, S. M., Wanamaker, A. D., Matras, U., et al. (2017). Ba/Ca ratios in shells of *Arctica islandica* - Potential environmental proxy and crossdating tool. *Palaeogeogr. Palaeoclimatol. Palaeoecol.* 465, 347–361. doi: 10.1016/j.palaeo.2015.12.018

Marini, M., Campanelli, A., and Abballe, F. (2006). Measurement of alkaline and earthy ions in fish otolith and sea water using a high performance ion chromatography. *Mar. Chem.* 99, 24–30. doi: 10.1016/j.marchem.2005.01.009

Markulin, K., Peharda, M., Mertz-Kraus, R., Schöne, B. R., Uvanović, H., Kovač, Ž, et al. (2019). Trace and minor element records in aragonitic bivalve shells as environmental proxies. *Chem. Geol.* 507, 120–133. doi: 10.1016/j.chemgeo.2019.01.008

Martino, J. C., Fowler, A. J., Doubleday, Z. A., Grammer, G. L., and Gillanders, B. M. (2019). Using otolith chronologies to understand long-term trends and extrinsic drivers of growth in fisheries. *Ecosphere* 10:e02553. doi: 10.1002/ecs2.2553

Matta, M. E., Helser, T. E., and Black, B. A. (2018). Intrinsic and environmental drivers of growth in an Alaskan rockfish: an otolith biochronology approach. *Environ. Biol. Fish.* 101, 1571–1587. doi: 10.1007/s10641-018-0801-8

Mellon-Duval, C., De Pontual, H., Metral, L., and Quemener, L. (2010). Growth of European hake (*Merluccius merluccius*) in the Gulf of Lions based on conventional tagging. *ICES J. Mar. Sci.* 67, 62–70. doi: 10.1093/icesjms/fsp215

Mercier, L., Mouillot, D., Bruguier, O., Vigliola, L., and Darnaude, A. M. (2012). Multi-element otolith fingerprints unravel sea-lagoon lifetime migrations of gilthead sea bream *Sparus aurata*. *Mar. Ecol. Prog. Ser.* 444, 175–194. doi: 10.3354/meps09444

Micheli, F., Halpern, B. S., Walbridge, S., Ciriaco, S., Ferretti, F., Fraschetti, S., et al. (2013). Cumulative human impacts on Mediterranean and Black Sea marine ecosystems: assessing current pressures and opportunities. *PLoS One* 8:e79889. doi: 10.1371/journal.pone.0079889

Mirasole, A., Gillanders, B. M., Reis-Santos, P., Grassa, F., Capasso, G., Scopelliti, G., et al. (2017). The influence of high pCO2 on otolith shape, chemical and carbon isotope composition of six coastal fish species in a Mediterranean shallow CO2 vent. *Mar. Biol.* 164, 1–15. doi: 10.1007/s00227-017-3221-y

Morales-Nin, B. (2000). "Daily increments in otoliths: endogenous versus exogenous growth regulation," in *Proceedings of the Second International Symposium on Fish Otolith Research and Application* (Norway: Fisheries Research Special Publication), 53–68.

Morales-Nin, B., and Aldebert, Y. (1997). Growth of juvenile Merluccius merluccius in the Gulf of Lions (NW Medterranean) based on otolith microstructure and length-frequency analysis. *Fish. Res.* 30, 77–85. doi: 10.1016/s0165-7836(96)00553-x

Morales-Nin, B., and Moranta, J. (1997). Life history and fishery of the common dentex (*Dentex dentex*) in Mallorca (Balearic Islands, western

Mediterranean). *Fish. Res.* 30, 67–76. doi: 10.1016/s0165-7836(96)00560-7

Morales-Nin, B., Pérez-Mayol, S., Palmer, M., and Geffen, A. J. (2014). Coping with connectivity between populations of *Merluccius merluccius*: an elusive topic. *J. Mar. Syst.* 138, 211–219. doi: 10.1016/j.jmarsys.2014.04.009

Morales-Nin, B., Swan, S. C., Gordon, J. D. M., Palmer, M., Geffen, A. J., Shimmield, T., et al. (2005a). Age-related trends in otolith chemistry of *Merluccius merluccius* from the north-eastern Atlantic Ocean and the western Mediterranean Sea. *Mar. Freshw. Res.* 56, 599–607. doi: 10.1071/MF04151

Morales-Nin, B., Tores, G. J., Lombarte, A., and Recasens, L. (2005b). Otolith growth and age estimation in the European hake. *J. Fish Biol.* 53, 1155–1168. doi: 10.1111/j.1095-8649.1998.tb00239.x

Morat, F., Blamart, D., Candaudap, F., and Letourneur, Y. (2013). Differences in elemental chemistry and c-o stable isotope composition between left and right otoliths of a flatfish, the common sole Solea solea. *Vie Milieu* 63, 169–179.

Morat, F., Lecomte-Finiger, R., Blamart, D., Robert, M., and Letourneur, Y. (2012). Indicios preliminares de variaciones ontogenéticas y espaciales en las señales isotópicas y elementales de otolitos de Solea solea del Golfo de León (Mediterráneo noroccidental). *Sci. Mar.* 76, 647–657. doi: 10.3648/scimar.03648.09B

Morat, F., Letourneur, Y., Blamart, D., Pécheyran, C., Darnaude, A. M., and Harmelin-Vivien, M. (2014a). Offshore-onshore linkages in the larval life history of sole in the Gulf of Lions (NW-Mediterranean). *Estuar. Coast. Shelf Sci.* 149, 194–202. doi: 10.1016/j.ecss.2014.08.023

Morat, F., Letourneur, Y., Dierking, J., Pećheyran, C., Bareille, G., Blamart, D., et al. (2014b). The great melting pot. Common sole population connectivity assessed by otolith and water fingerprints. *PLoS One* 9:e0086585. doi: 10.1371/journal.pone.0086585

Morrongiello, J., Thresher, R., and Smith, D. (2012). Aquatic biochronologies and climate change. *Nat. Clim. Change* 2, 849–857. doi: 10.1038/nclimate1616

Mouillot, D., Albouy, C., Guilhaumon, F., Ben Rais Lasram, F., Coll, M., Devictor, V., et al. (2011). Protected and threatened components of fish biodiversity in the Mediterranean Sea. *Curr. Biol.* 21, 1044–1050. doi: 10.1016/j.cub.2011.05.005

Mounicou, S., Frelon, S., Le Guernic, A., Eb-Levadoux, Y., Camilleri, V., Février, L., et al. (2019). Use of fish otoliths as a temporal biomarker of field uranium exposure. *Sci. Total Environ.* 690, 511–521. doi: 10.1016/j.scitotenv.2019.06.534

Niklitschek, E. J., and Darnaude, A. M. (2016). Performance of maximum likelihood mixture models to estimate nursery habitat contributions to fish stocks: a case study on sea bream *Sparus aurata*. *Peer J.* 4:e2415. doi: 10.7717/peerj.2415

Oschmann, W. (2009). Sclerochronology: editorial. *Int. J. Earth Sci.* 98, 1–2. doi: 10.1007/s00531-008-0403-3

Panfili, J., Darnaude, A. M., Lin, Y. J., Chevalley, M., Iizuka, Y., Tzeng, W. N., et al. (2012). Habitat residence during continental life of the European eel *Anguilla anguilla* investigated using linear discriminant analysis applied to otolith Sr:Ca ratios. *Aquat. Biol.* 15, 175–185. doi: 10.3354/ab00414

Panfili, J., Meunier, F. J., Mosegaard, H., Troadec, H., Wright, P. J., and Geffen, A. J. (2002). *Manual of Fish Sclerochronology*. Brest: Ifremer-Ird coedition.

Papadopoulou, C., Kanias, G. D., and Moraitopoulou Kassimati, E. (1978). Zinc content in otoliths of mackerel from the Aegean. *Mar. Pollut. Bull.* 9, 106–108. doi: 10.1016/0025-326x(78)90482-4

Papadopoulou, C., Kanias, G. D., and Moraitopoulou-Kassimati, E. (1980). Trace element content in fish otoliths in relation to age and size. *Mar. Pollut. Bull.* 11, 68–72. doi: 10.1016/0025-326X(80)90546-9

Papadopoulou, C., and Moraitopoulou-Kassimati, E. (1977). Stable elements in skeletal formations of fish species from Greek waters. *Thalassia Jugoslavica* 13, 187–192.

Pauly, D., and Zeller, D. (2016). Catch reconstructions reveal that global marine fisheries catches are higher than reported and declining. *Nat. Commun.* 7:10244. doi: 10.1038/ncomms10244

Peharda, M., Vilibić, I., Black, B., Uvanović, H., Markulin, K., and Mihanović, H. (2019a). A network of bivalve chronologies from semi-enclosed seas. *PLoS One* 14:e0220520. doi: 10.1371/journal.pone.0220520

Peharda, M., Walliser, E. O., Markulin, K., Purroy, A., Uvanović, H., Janeković, I., et al. (2019b). *Glycymeris pilosa* (Bivalvia) – A high-potential geochemical archive of the environmental variability in the Adriatic Sea. *Mar. Env. Res.* 150:104759. doi: 10.1016/j.marenvres.2019.104759

Peharda, M., Vilibić, I., Black, B. A., Markulin, K., Dunić, N., Džoić, T., et al. (2018). Using bivalve chronologies for quantifying environmental drivers in a semi-enclosed temperate sea. *Sci. Rep.* 8:5559. doi: 10.1038/s41598-018-23773-w

Peres, M. B., and Haimovici, M. (2004). Age and growth of southwestern Atlantic wreckfish *Polyprion americanus*. *Fish. Res.* 66, 157–169. doi: 10.1016/s0165-7836(03)00207-8

Piddocke, T. P., Butler, G. L., Butcher, P. A., Purcell, S. W., Butcher, J. D., and Christidis, L. L. (2015). Age validation in the Lutjanidae: a review. *Fish. Res.* 167, 48–63. doi: 10.1016/j.fishres.2015.01.016

Piñeiro, C., Rey, J., de Pontual, H., and Goñi, R. (2007). Tag and recapture of European hake (*Merluccius merluccius* L.) off the Northwest Iberian Peninsula: first results support fast growth hypothesis. *Fish. Res.* 88, 150–154. doi: 10.1016/j.fishres.2007.08.015

Pörtner, H. O., and Peck, M. A. (2010). Climate change effects on fishes and fisheries: towards a cause-and-effect understanding. *J. Fish Biol.* 77, 1745–1779. doi: 10.1111/j.1095-8649.2010.02783.x

Prendergast, A. L., and Schöne, B. R. (2017). Oxygen isotopes from limpet shells: implications for palaeothermometry and seasonal shellfish foraging studies in the Mediterranean. *Palaeogeogr. Palaeoclimatol. Palaeoecol.* 484, 33–47. doi: 10.1016/j.palaeo.2017.03.007

Ragonese, S. (1989). *L'Applicazione dell'equazione di von Bertalanffy generale: il caso di Helicolenus dactylopterus (Delar.) (Pisces: Scorpaenidae) del Tirreno Settentrionale*. *Oebalia* 15, 753–762.

Regulation (EU) (2017). *2017/1004 of the European Parliament and of the Council of 17 May 2017 on the establishment of a Union framework for the Collection, Management and Use of Data in the Fisheries Sector and Support for Scientific Advice Regarding the Common Fisheries Policy and Repealing Council Regulation (EC) No 199/2008*. Brussels: EU.

Reñones, O., Grau, A., Mas, X., Riera, F., and Saborido-Rey, F. (2010). Reproductive pattern of an exploited dusky grouper *Epinephelus marginatus* (Lowe 1834) (Pisces: Serranidae) population in the western Mediterranean. *Sci. Mar.* 74, 523–537. doi: 10.3989/scimar.2010.74n3523

Reñones, O., Pineiro, C., Mas, X., and Goni, R. (2007). Age and growth of the dusky grouper *Epinephelus marginatus* (Lowe 1834) in an exploited population of the western Mediterranean Sea. *J. Fish Biol.* 71, 346–362. doi: 10.1111/j.1095-8649.2007.01482.x

Reynolds, D. J., Hall, I. R., Slater, S. M., Mette, M. J., Wanamaker, A. D., Scourse, J. D., et al. (2018). Isolating and reconstructing key components of North Atlantic Ocean variability from a sclerochronological spatial network. *Paleoceanogr. Paleoclimatol.* 33, 1086–1098. doi: 10.1029/2018PA003366

Rezende, S. M., and Ferreira, B. P. (2004). Age, growth and mortality of dog snapper *Lutjanus jocu* (Bloch & Schneider, 1801) in the northeast coast of Brazil. *Braz. J. Oceanogr.* 52, 107–121. doi: 10.1590/S1679-87592004000200003

Rochet, M. J., and Trenkel, V. M. (2003). Which community indicators can measure the impact of fishing? A review and proposals. *Can. J. Fish Aquat. Sci.* 60, 86–99. doi: 10.1139/f02-164

Rochet, M.-J., Trenkel, V. M., Bellail, R., Coppin, F., Le Pape, O., Mahé, J. C., et al. (2005). Combining indicator trends to assess ongoing changes in exploited fish communities: diagnostic of communities off the coasts of France. *ICES J. Mar. Sci.* 62:1647e1664. doi: 10.1016/j.icesjms.2005.06.009

Rooker, J. R., Arrizabalaga, H., Fraile, I., Secor, D. H., Dettman, D. L., Abid, N., et al. (2014). Crossing the line: migratory and homing behaviors of Atlantic bluefin tuna. *Mar. Ecol. Prog. Ser.* 504, 265–276. doi: 10.3354/meps10781

Rooker, J. R., Fraile, I., Liu, H., Abid, N., Dance, M. A., Itoh, T., et al. (2019). Wide-ranging temporal variation in transoceanic movement and population mixing of bluefin tuna in the North Atlantic Ocean. *Front. Mar. Sci.* 6:398. doi: 10.3389/fmars.2019.00398

Rooker, J. R., Secor, D. H., DeMetrio, G., Kaufman, A. J., Ríos, A. B., and Tičina, V. (2008a). Evidence of trans-Atlantic movement and natal homing of bluefin tuna from stable isotopes in otoliths. *Mar. Ecol. Prog. Ser.* 368, 231–239. doi: 10.3354/meps07602

Rooker, J. R., Secor, D. H., De Metrio, G., Schloesser, R., Block, B. A., and Neilson, J. D. (2008b). Natal homing and connectivity in Atlantic Bluefin Tuna populations. *Science* 322, 742–744. doi: 10.1126/science.1161473

Rooker, J. R., Secor, D. H., DeMetrio, G., Kaufman, A. J., Ríos, A. B., and Tičina, V. (2008a). Evidence of trans-Atlantic movement and natal homing of bluefin tuna from stable isotopes in otoliths. *Mar. Ecol. Prog. Ser.* 368, 231–239. doi: 10.3354/meps07602

Rooker, J. R., Secor, D. H., Zdanowicz, V. S., De Metrio, G., and Relini, L. O. (2003). Identification of Atlantic bluefin tuna (*Thunnus thynnus*) stocks from

putative nurseries using otolith chemistry. *Fish. Oceanogr.* 12, 75–84. doi: 10.1046/j.1365-2419.2003.00223.x

Rooker, J. R., Secor, D. H., Zdanowicz, V. S., Relini, L. O., Santamaria, N., Deflorio, M., et al. (2002). Otolith elemental fingerprints of Atlantic bluefin tuna from eastern and western nurseries. *ICCAT Collect. Vol. Sci. Papers* 54, 498–506.

Rountrey, A. N., Coulson, P. G., Meeuwig, J. J., and Meekan, M. (2014). Water temperature and fish growth: otoliths predict growth patterns of a marine fish in a changing climate. *Glob. Chang. Biol.* 20, 2450–2458. doi: 10.1111/gcb.12617

Sadovy, Y., and Shapiro, D. Y. (1987). Criteria for the diagnosis of hermaphroditism in fishes. *Copeia* 1987, 136–156.

Sakamoto, T., Komatsu, K., Yoneda, M., Ishimura, T., Higuchi, T., Shirai, K., et al. (2017). Temperature dependence of δ18O in otolith of juvenile Japanese sardine: laboratory rearing experiment with micro-scale analysis. *Fish. Res.* 194, 55–59. doi: 10.1016/j.fishres.2017.05.004

Schöne, B. R. (2013). *Arctica islandica* (Bivalvia): a unique paleoenvironmental archive of the northern North Atlantic Ocean. *Glob. Planet. Change* 111, 199–225. doi: 10.1016/j.gloplacha.2013.09.013

Secor, D. H., Campana, S. E., Zdanowicz, V. S., Lam, J. W. H., Yang, L., and Rooker, J. R. (2002). Inter-laboratory comparison of Atlantic and Mediterranean bluefin tuna otolith microconstituents. *ICES J. Mar. Sci.* 59, 1294–1304. doi: 10.1006/jmsc.2002.1311

Secor, D. H., and Zdanowicz, V. S. (1998). Otolith microconstituent analysis of juvenile bluefin tuna (*Thunnus thynnus*) from the Mediterranean Sea and Pacific Ocean. *Fish. Res.* 36, 251–256. doi: 10.1016/S0165-7836(98)00103-9

Simkiss, K. (1974). "Calcium metabolism of fish in relation to aging," in *The Ageing of Fish*, ed. T. B. Bagenal (London: Unwin Brothers Ltd), 1–12.

Siskey, M. R., Wilberg, M. J., Allman, R. J., Barnett, B. K., and Secor, D. H. (2016). Forty years of fishing: changes in age structure and stock mixing in northwestern Atlantic bluefin tuna (*Thunnus thynnus*) associated with size-selective and long-term exploitation. *ICES J. Mar. Sci. J. du Cons.* 73, 2518–2528. doi: 10.1093/icesjms/fsw115

Smith, C. L. (1997). *National Audubon Society field guide to tropical marine fishes of the Caribbean, the Gulf of Mexico, Florida, the Bahamas, and Bermuda*. New York, NY: Alfred A. Knopf, Inc, 720.

Søndergaard, J., Halden, N., Bach, L., Gustavson, K., Sonne, C., and Mosbech, A. (2015). Otolith chemistry of common sculpins (*Myoxocephalus scorpius*) in a mining polluted Greenlandic fiord (Black Angel Lead-Zinc Mine. West Greenland). *Water. Air Soil Pollut.* 226:336. doi: 10.1007/s11270-015-2605-1

Sonin, O., Edelist, D., and Golani, D. (2019). The occurrence of the Lessepsian migrant *Lutjanus argentimaculatus* in the Mediterranean, (Actinopterygii: Perciformes: Lutjanidae) first record from the coast of Israel. *Acta Adriat.* 60, 99–102. doi: 10.32582/aa.60.1.11

Sreemany, A., Kumar Bera, M., and Sarkar, A. (2017). Rapid and high-resolution stable isotopic measurement of biogenic accretionary carbonate using an online CO2 laser ablation system: standardization of the analytical protocol. *Rapid Commun. Mass Spec.* 31, 2109–2117. doi: 10.1002/rcm.7992

Steward, C. A., De Maria, K. D., and Shenker, J. M. (2009). Using otolith morphometrics to quickly and inexpensively predict age in the gray angelfish (*Pomacanthus arcuatus*). *Fish. Res.* 99, 123–129. doi: 10.1016/j.fishres.2009.05.011

Stransky, C., Gudmundsdóttir, S., Sigurdsson, T., Lemvig, S., Nedreaas, K., and Saborido-Rey, F. (2005). Age determination and growth of Atlantic redfish (*Sebastes marinus* and *S. mentella*): bias and precision of age readers and otolith preparation methods. *ICES J. Mar. Sci.* 62, 655–670. doi: 10.1016/j.icesjms.2005.01.018

Sutton, C. P., Tracey, D. M., Andrews, A. H., Hart, A. C., and MacGibbon, D. J. (2010). *Validated age and growth of ribaldo (Mora moro). New Zealand Fisheries Assessesment Report 2010/24.* Available online at: M:\SCIPOL\FARs\Electronic copies of Published FARs\2010 FARs\10_24_FAR.pdf (accessed August 19, 2010).

Swan, S. C., Geffen, A. J., Morales-Nin, B., Gordon, J. D. M., Shimmield, T., Sawyer, T., et al. (2006). Otolith chemistry: an aid to stock separation of *Helicolenus dactylopterus* (bluemouth) and *Merluccius merluccius* (European hake) in the Northeast Atlantic and Mediterranean. *ICES J. Mar. Sci.* 63, 504–513. doi: 10.1016/j.icesjms.2005.08.012

Swan, S. C., Gordon, J. D. M., Morales-Nin, B., Shimmield, T., Sawyer, T., and Geffen, A. J. (2003). Otolith microchemistry of *Nezumia aequalis* (Pisces: Macrouridae) from widely different habitats in the Atlantic and Mediterranean. *J. Mar. Biol. Assoc. U. K.* 83, 883–886. doi: 10.1017/S0025315403007987h

Tanner, S. E., Perez, M., Presa, P., Thorrold, S. R., and Cabral, H. N. (2014). Integrating microsatellite DNA markers and otolith geochemistry to assess population structure of European hake (*Merluccius merluccius*). *Estuar. Coast. Shelf Sci.* 142, 68–75. doi: 10.1016/j.ecss.2014.03.010

Tanner, S. E., Vasconcelos, R. P., Cabral, H. N., and Thorrold, S. R. (2012). Testing an otolith geochemistry approach to determine population structure and movements of European hake in the northeast Atlantic Ocean and Mediterranean Sea. *Fish. Res.* 12, 198–205. doi: 10.1016/j.fishres.2012.02.013

Tanner, S. E., Vieira, A. R., Vasconcelos, R. P., Dores, S., Azevedo, M., Cabral, H. N., et al. (2019). Regional climate, primary productivity and fish biomass drive growth variation and population resilience in a small pelagic fish. *Ecol. Indic.* 103, 530–541. doi: 10.1016/j.ecolind.2019.04.056

Tomas, J., Geffen, A. J., Millner, R. S., Pineiro, C. G., and Tserpes, G. (2006). Elemental composition of otolith growth marks in three geographically separated populations of European hake (*Merluccius merluccius*). *Mar. Biol.* 148, 1399–1413. doi: 10.1007/s00227-005-0171-6

Tournois, J., Ferraton, F., Velez, L., McKenzie, D. J., Aliaume, C., Mercier, L., et al. (2013). Temporal stability of otolith elemental fingerprints discriminates among lagoon nursery habitats. *Estuar. Coast. Shelf Sci.* 131, 182–193. doi: 10.1016/j.ecss.2013.07.006

Traina, A., Oliveri, E., Salvagio Manta, D., Barra, M., Mazzola, S., and Cuttitta, A. (2015). Metals content in otoliths of *Dicentrarchus labrax* from two fish farms of Sicily. *Environ. Monit. Assess.* 187:360. doi: 10.1007/s10661-015-4434-5

Trueman, C. N., Mackenzie, K. M., and Palmer, M. R. (2012). Identifying migrations in marine fishes through stable-isotope analysis. *J. Fish Biol.* 81, 826–847. doi: 10.1111/j.1095-8649.2012.03361.x

Turan, C. (2006). The use of otolith shape and chemistry to determine stock structure of Mediterranean horse mackerel *Trachurus mediterraneus* (Steindachner). *J. Fish Biol.* 69, 165–180. doi: 10.1111/j.1095-8649.2006.01266.x

Vitale, S., Andrews, A. H., Rizzo, P., Gancitano, S., and Fiorentino, F. (2016). Twenty-five-year longevity of European hake (Merluccius merluccius) from novel use of bomb radiocarbon dating in the Mediterranean Sea. *Mar. Freshw. Res.* 67, 1077–1080. doi: 10.1071/MF15376

West, C. F., Wischniowski, S., and Johnston, C. (2012). Pacific cod (*Gadus macrocephalus*) as a paleothermometer: Otolith oxygen isotope reconstruction. *J. Archaeol. Sci.* 39, 3277–3283. doi: 10.1016/j.jas.2012.05.009

Whitfield, A. K., and Elliott, M. (2002). Fishes as indicators of environmental and ecological changes within estuaries: a review of progress and some suggestions for the future. *J. Fish Biol.* 61, 229–250. doi: 10.1111/j.1095-8649.2002.tb01773.x

Willmes, M., Lewis, L. S., Davis, B. E., Loiselle, L., James, H. F., Denny, C., et al. (2019). Calibrating temperature reconstructions from fish otolith oxygen isotope analysis for California's critically endangered Delta Smelt. *Rapid Commun. Mass Spectrom.* 33, 1207–1220. doi: 10.1002/rcm.8464

Winkler, A. C., Duncan, M. I., Farthing, M. W., and Potts, W. M. (2019). Sectioned or whole otoliths? A global review of hard structure preparation techniques used in ageing sparid fishes. *Rev. Fish Biol. Fisheries* 29, 605–661. doi: 10.1007/s11160-019-09571-1

Wright, P. J., Régnier, T., Gibb, F. M., Augley, J., and Devalla, S. (2018). Assessing the role of ontogenetic movement in maintaining population structure in fish using otolith microchemistry. *Int. J. Bus. Innov. Res.* 17, 7907–7920. doi: 10.1002/ece3.4186

Conflict of Interest: The authors declare that the research was conducted in the absence of any commercial or financial relationships that could be construed as a potential conflict of interest.

Copyright © 2020 Matić-Skoko, Peharda, Vrdoljak, Uvanović and Markulin. This is an open-access article distributed under the terms of the Creative Commons Attribution License (CC BY). The use, distribution or reproduction in other forums is permitted, provided the original author(s) and the copyright owner(s) are credited and that the original publication in this journal is cited, in accordance with accepted academic practice. No use, distribution or reproduction is permitted which does not comply with these terms.

frontiers in Marine Science

ORIGINAL RESEARCH
published: 21 April 2020
doi: 10.3389/fmars.2020.00240

Port Jackson Shark Growth Is Sensitive to Temperature Change

Christopher Izzo† and Bronwyn May Gillanders*

Southern Seas Ecology Laboratories and the Environment Institute, School of Biological Sciences, The University of Adelaide, Adelaide, SA, Australia

Climatic effects on the growth of apex marine predators – such as sharks – are poorly understood; moreover, shifts in shark growth are primarily attributed to fishing pressure. This paucity of information impedes management and conservation planning for these taxa. Using vertebral increment patterning as a proxy of somatic growth, this study reconstructed mean growth of the philopatric and demersal *Heterodontus portusjacksoni* population from Gulf St Vincent (South Australia). A biochronology of shark growth spanning a 15 year period (1996–2010) was developed using mixed effects models. The biochronology showed considerable year-to-year deviations in growth that were significantly and negatively correlated with mean sea surface temperatures during the species' breeding season (July to November). These findings are consistent with mesocosm experiments and support the influence of changing climates on shark growth; particularly in an inshore, demersal, and highly philopatric shark species. It is likely that the effects of environmental variation occur in a species-specific manner, governed by life history strategies and ecological requirements. In this manner, life history traits might aid in estimating species vulnerability to climate change.

Keywords: climate change, growth, mixed effects modeling, phenology, Port Jackson shark

OPEN ACCESS

Edited by:
Esteban Avigliano, National Council for Scientific and Technical Research (CONICET), Argentina

Reviewed by:
André Martins Vaz-dos-Santos, Federal University of Paraná, Brazil
Gustavo Enrique Chiaramonte, Museo Argentino de Ciencias Naturales "Bernardino Rivadavia", Argentina

***Correspondence:**
Christopher Izzo
christopher.izzo@frdc.com.au

†Present address:
Christopher Izzo, Fisheries Research and Development Corporation, Adelaide, SA, Australia

Specialty section:
This article was submitted to Marine Ecosystem Ecology, a section of the journal Frontiers in Marine Science

Received: *08 December 2019*
Accepted: *27 March 2020*
Published: *21 April 2020*

Citation:
Izzo C and Gillanders BM (2020) Port Jackson Shark Growth Is Sensitive to Temperature Change. Front. Mar. Sci. 7:240. doi: 10.3389/fmars.2020.00240

INTRODUCTION

Environmental controls on the phenology and biology of terrestrial and aquatic taxa are well established (Parmesan, 2006). Key biological processes, such as growth, have been linked to temperature, with fluctuations in external conditions correlated to variations in growth. This is well-established in teleosts; with particular interest in climate change effects (Morrongiello et al., 2012). However, in top order predators such as sharks and marine mammals, there is little investigation of environmental controls on growth due to logistical constraints of controlled experimental studies and long-term observational work (Wittmann et al., 2016). Moreover, shifts in shark growth are primarily attributed to fishing effects (Walker et al., 1998), resulting in a paucity of information on the environmental correlates of growth in top order aquatic taxa.

Biochronologies provide a means of measuring growth deviations though time, using the incremental patterns of calcified structures as proxies of somatic growth (Morrongiello et al., 2012). For example, biochronologies of growth, based on tooth incremental patterns, have demonstrated growth-temperature relationships in New Zealand fur seals (Wittmann et al., 2016). Shark vertebrae, possess analogous incremental growth patterns and are widely used to estimate

chronological age (Cailliet and Goldman, 2004), with vertebral increments potentially providing suitable proxies of somatic shark growth when allometry is validated.

Biochronologies developed using mixed effects models allows assessment of the simultaneous effects of biological, environmental and temporal factors on population growth (Morrongiello et al., 2012). This approach enables quantification of growth responses to environmental fluctuation and/or management action (reduced fishing effort); while accounting for biological effects (age-/sex-based growth). This is advantageous compared to previous approaches for assessing temporal variation in shark growth, which are largely limited to comparisons of growth (von Bertalanffy) functions (Parsons, 1993) or length-at-age dynamics (Walker et al., 1998) across multiple sampling periods; thus prone to study-level confounding factors and failing to account for potentially influential covariates.

This study develops a biochronology of growth deviations of the Port Jackson shark subpopulation from Gulf St Vincent, using mixed effects models of vertebrae growth. Port Jackson sharks (*Heterodontus portusjacksoni*) provide an excellent shark species for biochronology development. This oviparous species is highly philopatric within its temperate southern Australian distribution, returning to natal sites to breed in the austral winter after migrating (Powter and Gladstone, 2008a; Powter and Gladstone, 2009). The extreme site fidelity of the species ensures that it does not alter its distribution even when exposed to unfavorable environmental conditions, and thus climate variation should be reflected in population growth. Moreover, there is no direct fishing for Port Jackson sharks and negligible fishing mortality as most sharks caught are discarded (Powter and Gladstone, 2008a; Tovar-Ávila et al., 2010); therefore, we assume that observed deviations in growth are primarily influenced by environmental processes. To test this assumption, we related year-to-year growth deviations to ecologically relevant periods of sea surface temperature data to explore the influence of climatic variation on growth *in situ*.

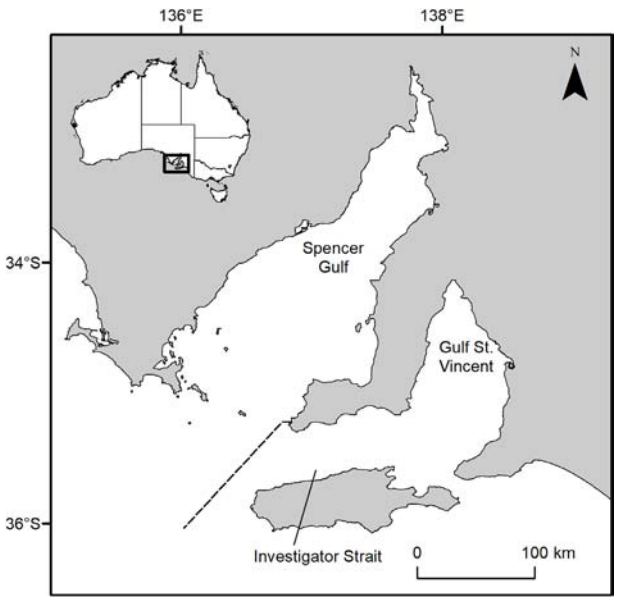

FIGURE 1 | Map of South Australia's gulf systems. The dashed line separates Spencer Gulf and Gulf St Vincent. Inset, map of Australia showing the study area along the southern coastline.

MATERIALS AND METHODS

Sharks (n = 50) were collected from the bycatch of commercial prawn trawlers operating in Gulf St Vincent (South Australia) between 2006 and 2011 (**Figure 1**). Gulf St Vincent is an inverse estuary that is largely sheltered from oceanic waves. Demographic data and tagging indicates that Port Jackson sharks inhabiting Gulf St Vincent and the adjacent Spencer Gulf form discrete subpopulations (Rodda and Svane, 2007; Izzo and Rodda, 2012).

Shark total length (in mm) and sex were recorded, and a section (n = 8–12) of vertebrae collected from under the first dorsal fin, were prepared for age determination using standard protocols (Izzo and Rodda, 2012). Vertebral centrum diameter was measured (in mm). Briefly, individual vertebra were cleaned of adhering tissue, dried and then embedded in epoxy resin to enable a transverse section (thickness = ∼500 μm) to be cut.

Growth increments (paired opaque and translucent bands) were counted, and widths measured under a dissecting microscope with transmitted light and image analysis software. Port Jackson shark vertebrae possess clear growth increments, and chemical marking has been used to verify that growth increments form annually (Tovar-Ávila et al., 2009; Izzo and Rodda, 2012), enabling the temporal resolution of shark growth to be validated.

Growth increments were assigned a year relative to the date of capture. Marginal increment and pre-natal vertebral growth were excluded from biochronology development as they may not represent a complete annual growth cycle, defined as January to December, based on a January hatch date (Rodda and Seymour, 2008).

Biochronologies, quantifying year-to-year growth deviations, were developed using linear mixed effects models (following Weisberg et al., 2010; Morrongiello and Thresher, 2015). Increment widths were log-transformed to meet model assumptions, with all continuous parameters mean centered to facilitate model convergence (Morrongiello and Thresher, 2015). Model fitting was undertaken in R (R Core Team, 2018), using the *lme4* package (Bates et al., 2013).

The random effects model structure was optimized by comparing a series of models with all combinations of the random terms that included: *Year*, *Cohort*, and *SharkID* (see **Table 1** for a description of the model terms). In all models, the *SharkID* term was fit with a random *Age* slope, enabling each shark to have its own age correction term, negating potential inter-individual differences that may arise from examining different centra in the vertebral column. Models were ranked using Akaike's Information Criterion corrected for small sample sizes (AICc) (Burnham and Anderson, 2004), using the *MuMIn* package (Bartoń, 2013; **Supplementary Table S1**).

TABLE 1 | Descriptions of the mixed effects model terms.

(i) Random model structure			
Model terms	**Description**	**Variance (± *SD*)**	**Correlation**
SharkID	Unique identifier for each shark: assesses correlation among repeated increment measures within an individual	0.030 (0.173)	
Age| SharkID	Random *Age* slope allows each shark to have a unique growth trajectory	0.002 (0.050)	0.530
Year	Year of increment formation: assesses correlation among growth years	0.010 (0.097)	
Cohort	Year that a shark hatched: assesses correlation within cohorts of sharks that share birth years	Na	
Residual		0.059 (0.242)	
(ii) Fixed model structure			
Model terms	**Description**	**Estimate (± SE)**	**t-statistic**
Age	Age when each annual increment was deposited (in years)	–0.115 (0.015)	–7.414
Age-at-capture	Age of shark at the time of capture (in years): assesses age-based growth	Na	
Sex	An individual's sex: assesses sex-based growth	Na	
Intercept		–1.026 (0.048)	–21.396

Model (i) variance components and (ii) parameter estimates for the growth biochronology of the Port Jackson shark. "Age\| SharkID" denotes fitting a random Age slope to the SharkID term. "na" indicates that the model term was excluded from the optimized growth model structure.

Model parameters were estimated using restricted maximum likelihood (REML).

The fixed effects structure was optimized by comparing a series of models that contained the optimized random effects structure (see above) and all combinations of the fixed covariates that included: *Sex* and *Age-at-capture* (see **Table 1**). All models contained a fixed *Age* term to account for ontogenetic variation in increment widths. Models were ranked using AICc (**Supplementary Table S1**). Comparisons among models with differing fixed effects terms were fitted using maximum likelihood, with the best ranked model re-fitted using REML (Zuur et al., 2009). Random *Year* effects representing the year-to-year deviations in population growth (the biochronology) were extracted from the model containing the optimized random and fixed effects structure.

The influence of sea surface temperature (SST in°C) on shark growth was assessed by relating temperature over three ecological periods: (i) annual growth cycle (January–December); (ii) austral winter to spring (July–November), coinciding with the breeding season (Powter and Gladstone, 2008b); and (iii) austral summer (December–February), coinciding with the timing of neonate hatching (Rodda and Seymour, 2008). Daily SST data (from –34.234, 138.078: see **Supplementary Table S2**) were averaged over the three ecological time periods. Temperature data for the three periods were correlated against the random *Year* effects (the year-to-year growth deviations) from the growth biochronology.

RESULTS

Increments were measured on vertebrae of 50 sharks (female = 24; male = 26) ranging from 2 to 14 years of age (**Figure 2A**) and 207 to 794 mm TL (**Figure 2B**). In total, 185 increments were measured (**Figure 2C**). Centrum diameter was significantly correlated to total length (**Figure 3**), confirming that Port Jackson shark vertebrae provide suitable proxies of somatic growth, developing in proportion to total length (**Figure 3**).

The shark biochronology spanned a 15 year period, between 1996 and 2010 (**Figure 4**) and showed considerable deviations in year-to-year growth based on the *Year* term (**Table 1**), with an extended period of above average growth between 2001 and 2004. The *SharkID* term suggested a large degree of inter-individual growth differences; with the correlation statistic indicating increasing shark growth with increasing age (**Table 1**). Neither specimen *Sex* nor *Age-at-capture* influenced shark growth (**Supplementary Table S1**).

Mean SST for the breeding season (austral winter to spring) was significantly and negatively correlated to shark growth (p = 0.020, r = –0.59) (**Table 2**). Mean annual SST had a similar negative influence on shark growth (r = –0.50). Water temperature had a negative effect on shark growth over the temperature conditions experienced. Conversely, mean summer SST had a weak positive correlation with growth (r = 0.18) (**Table 2**).

DISCUSSION

This study demonstrates that in the absence of targeted fishing pressure, shark growth fluctuates through time; with Port Jackson shark population growth negatively correlated with sea surface temperature over a 15 year period (between 1996 and 2010). This temperature effect was most prevalent in the species' winter/spring breeding period, whereby the species undergoes extended periods of residency on natal sites and are unlikely to actively regulate their external environment (i.e., through migration) (O'Gower, 1995; Powter and Gladstone, 2009). This study focused on an inshore, demersal and highly philopatric shark species, traits that while assumed to make the Port Jackson sharks conducive to developing biochronologies; likely render the species highly susceptible to localized climatic change. Conversely highly mobile, pelagic species may be better suited to actively mitigate the impacts of environmental fluctuation by undertaking range shifts to habitats with preferable environmental conditions (Last et al., 2011). It is likely that the effects of environmental variation on sharks (and elasmobranchs more generally) occur in a species-specific manner, governed

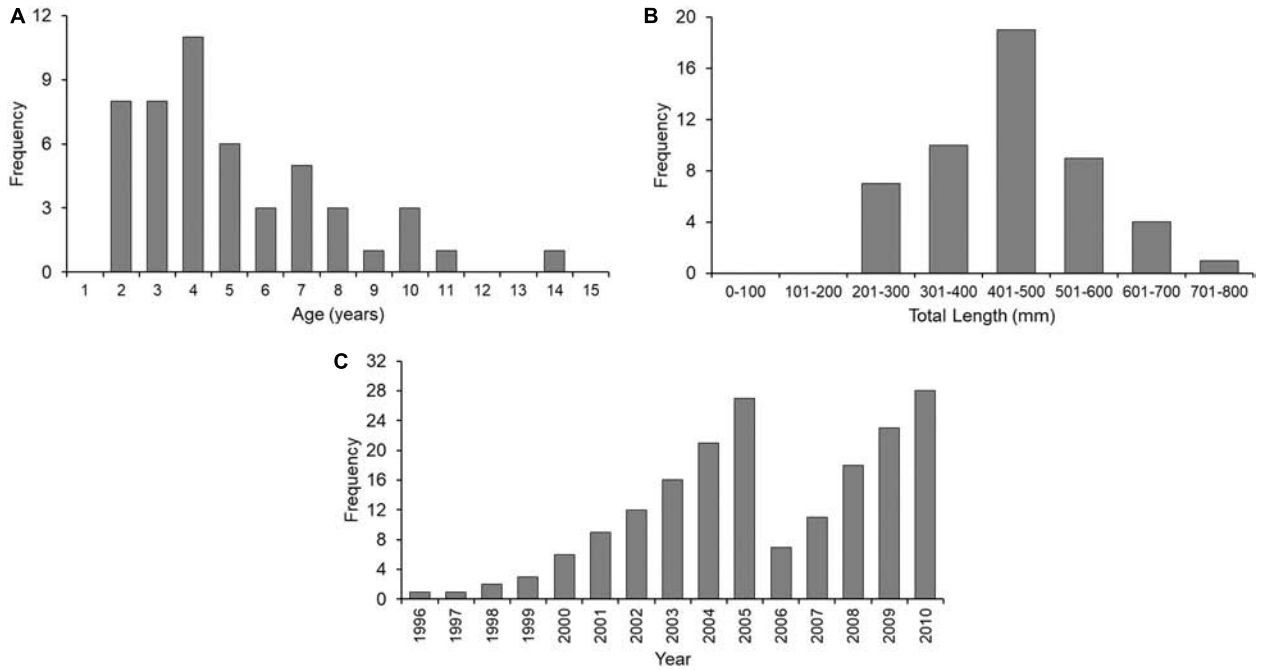

FIGURE 2 | Absolute frequency plots of **(A)** age (in years), **(B)** total length (in mm), and **(C)** increment measurements (per year), of Port Jackson shark samples examined in this study (n = 50 sharks).

by individual life history strategies and ecological requirements (Izzo et al., 2016). Thus, species life history traits might aid in assessing the vulnerability of elasmobranchs to climate change (Chin et al., 2010). However, intraspecific differences in growth (and metabolic performance) of subpopulations exposed to different local environmental conditions suggest elasmobranchs have the potential to demonstrate local adaptation to climatic stressors (Frisk and Miller, 2006; Di Santo, 2016).

Temperature was significantly and negatively related to Port Jackson shark growth. These findings are consistent with decreased growth reported for juvenile Port Jackson sharks held in laboratory and mesocosm experiments (Rodda, 2000; Pistevos et al., 2015) and empirical studies of global marine fish growth trends (Cheung et al., 2012) whereby, when faced with increasing water temperature, growth is reduced and fish attain smaller maximum sizes. The observed negative correlation between temperature and growth aligns with patterns of increasing growth with increasing latitudes reported in elasmobranch species (e.g., Lombari-Carlson et al., 2003; Frisk and Miller, 2006; Winton et al., 2014). This potentially reflects the species need to increase growth rates to account for shorter periods of optimal environmental conditions (Lombari-Carlson et al., 2003) consistent with a counter-gradient

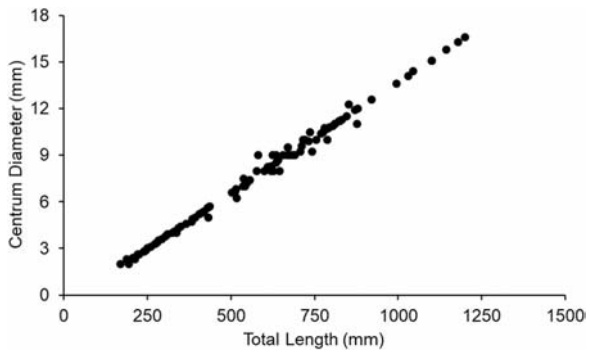

FIGURE 3 | Linear relationship between Port Jackson shark vertebral centrum diameter and total length (r = 0.99).

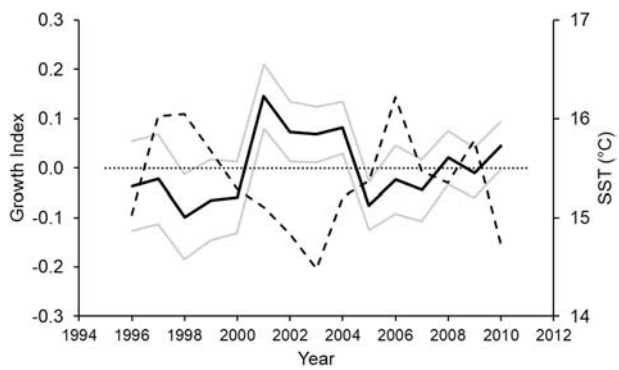

FIGURE 4 | Biochronology of Port Jackson shark growth variation (a unitless index; solid black line) around the population mean (dotted line) for the duration of the period studied (model intercept). Standard errors are shown as solid gray lines. The dashed line is the mean sea surface temperature (in°C) over the breeding season (austral winter to spring) of the species.

TABLE 2 | Correlation among Port Jackson shark *Growth* (the extracted random *Year* effects from the mixed effects growth model) and sea surface temperature over three ecological periods: (i) *Annual* growth cycle (January–December); (ii) *Breeding* season (July–November); and (iii) *Summer* (December–February).

	Correlation coefficient				*p*-value		
	Annual	**Breeding**	**Summer**		**Annual**	**Breeding**	**Summer**
Breeding	0.86			Breeding	0.001		
Summer	0.52	0.26		Summer	0.047	0.357	
Growth	−0.50	−0.59	0.18	Growth	0.056	0.020	0.511

Daily sea surface temperature data were averaged over the three time periods, and came from -34.234, 138.078 (IMOS[a]). [a]IMOS (2017) Australian Ocean Data Network, https://portal.aodn.org.au/, data accessed 4th December 2017.

variation of growth rates (Conover and Present, 1990). It is anticipated that under forecast climate scenarios, species are likely to be increasingly exposed to periods of suboptimal local environmental conditions, which in turn exacerbates the frequency and magnitude of variability in population growth (Neuheimer et al., 2011; Martino et al., 2019). More broadly, these findings provide indirect support of Bergmann's Rule in poikilotherms (Conover, 1990; Meiri, 2011), and suggest that in the absence of genetic variability within the Gulf St Vincent Port Jackson shark subpopulation (Izzo, unpublished data), population growth is primarily influenced by local environmental factors (Lombari-Carlson et al., 2003).

While this study explored the relationship between temperature and shark growth in isolation, experiments demonstrate that multiple parameters interact to affect shark growth; e.g., temperature and ocean acidification (Di Santo, 2015; Pistevos et al., 2015). Therefore, as species approach physiological temperature thresholds, growth will likely also be influenced by synergistic ocean acidification effects (Pistevos et al., 2015) and shifts in other biological and phenotypic processes; e.g., metabolism, reproductive timing, and/or juvenile survival (e.g., Rosa et al., 2014; Di Santo, 2015, 2016; Rosa et al., 2017). Given the logistical challenges of working with elasmobranchs *in situ*, few of these biological parameters are captured and thus, linkages between changing environmental conditions and biological processes are not well understood. Extrinsic influences on shark growth are highly complex, and when considered in conjunction with the effects of fishing (which may alter a population's phenotypic and/or genotypic composition: Walker et al., 1998), it is likely that a myriad of simultaneous factors may act upon the population to alter resilience through time.

The growth modeling did not identify an age cohort effect on population growth, suggesting rates of growth among year classes of Port Jackson sharks did not differ considerably. However, juvenile survival in oviparous (egg-laying) or viviparous (live-bearing) elasmobranch species has been shown to be adversely impacted under increased water temperatures and, or acidified ocean conditions (Rosa et al., 2014; Di Santo, 2015; Johnson et al., 2016). Nevertheless, the influence of external factors on year class strength may be explored using the approach employed in this study.

Port Jackson sharks are commonly encountered as a bycatch species throughout their southern Australian distribution (Powter and Gladstone, 2008a; Jones et al., 2008; Tovar-Ávila et al., 2010; Izzo and Rodda, 2012), however, the species is seldom retained, is highly robust, and not prone to post-capture mortality (Frick et al., 2010). This study assumed negligible fishing induced mortality in the Port Jackson shark population in Gulf St Vincent, and hence deviations in population growth were primarily attributed to environmental factors. However, targeted fishing pressure has been attributed to shifts in shark population growth (Lombari-Carlson et al., 2003) and length-at-age dynamics (Walker et al., 1998), as well as other broader ecological processes (Stevens et al., 2000). Biochronologies provide a means to explore the influence of fishing on population growth (e.g., Martino et al., 2019).

The model optimization process indicated that the age at capture term was not an important explanatory growth term, inferring the absence of an age trend in the growth data. We also interpreted this as confirmation of the absence of an age-bias in the sample data (Morrongiello and Thresher, 2015). Yet we acknowledge that the samples were predominately small to medium (juvenile/immature) individuals, as large adults are infrequently encountered in Gulf St Vincent (Izzo and Rodda, 2012). This impeded our ability to explore relative growth responses across all Port Jackson shark life history stages through the omission of potential growth phenotypes; and therefore, future studies should seek to access all life stages to assess the potential for differing growth responses throughout development (Morrongiello et al., 2012). Nevertheless, the biochronology approach employed here is advantageous, as it facilitates the examination of sharks from all life stages without requiring logistically challenging controlled experiments on large animals to be undertaken.

This study has demonstrated that in a demersal shark that encounters indirect fishing pressure and negligible fishing mortality, population growth is negatively related to sea surface temperature, consistent with mesocosm experiments. The direct consequences of this relationship are unknown, however, it is expected to result in a shift in the species phenology. Further studies are required to explore growth-temperature relationships in elasmobranch species with varying life history strategies and exposed to varying degrees of fishing pressure to understand the generality of the trends seen here. The mixed effects modeling approach used here provides a means of exploring elasmobranch growth time series, and might be expanded upon to explore how multiple environmental and, or biological parameters interact to influence shark growth. While this study explored the relationship between temperature and Port Jackson shark growth in isolation, future studies that include synergistic

relationships among a suite of simultaneously interacting factors will better reflect natural conditions.

DATA AVAILABILITY STATEMENT

The datasets generated for this study are available on request to the corresponding author.

ETHICS STATEMENT

Sample collection and processing was reviewed and approved by The University of Adelaide Animal Ethics Committee (S-022-2006).

AUTHOR CONTRIBUTIONS

CI and BG conceived, designed the study, and wrote the manuscript. CI collected and prepared the samples, collected and analyzed the data, and applied the statistical analyses.

FUNDING

Funding provided by the Sea World Research and Rescue Foundation Inc. (SWR/8/2007), awarded to CI.

ACKNOWLEDGMENTS

We thank J. Queiroz for assistance with sample preparation and D. Matthews for providing the map. We thank the crews of the numerous prawn trawlers that assisted in sample collection. We also thank the two reviewers for providing insightful comments which improved the manuscript.

SUPPLEMENTARY MATERIAL

The Supplementary Material for this article can be found online at: https://www.frontiersin.org/articles/10.3389/fmars.2020.00240/full#supplementary-material

REFERENCES

Bartoń, K. (2013). *MuMIn: Multi-Model Inference. R Package Version 1.9.13*. Avaliable at: http://CRAN.R-project.org/package=MuMIn/.(accessed December20, 2018)

Bates, D., Maechler, M., Bolker, B., and Walker, S. (2013). *lme4: Linear Mixed-Effects Models Using Eigen and s4*. Vienna: The R Foundation for Statistical Computing.

Burnham, K. P., and Anderson, D. R. (2004). Multimodel inference: understanding AIC and BIC in model selection. *Sociol. Methods Res.* 33, 261–304. doi: 10.1177/0049124104268644

Cailliet, G. M., and Goldman, K. J. (2004). "Age determination and validation in chondrichthyan fishes," in *Biology of Sharks and their Relatives*, eds J. Carrier, J. A. Musick, and M. Heithaus (San Diego, CA: CRC Press), 399–439.

Cheung, W. W. L., Sarmiento, J. L., Dunne, J., Frölicher, T. L., Lam, V. W. Y., Deng Palomares, M. L., et al. (2012). Shrinking of fishes exacerbates impacts of global ocean changes on marine ecosystems. *Nat. Clim. Change* 3, 254–258. doi: 10.1038/nclimate1691

Chin, A., Kyne, P. M., Walker, T. I., and McAuley, R. B. (2010). An integrated risk assessment for climate change: analysing the vulnerability of sharks and rays on Australia's Great Barrier Reef. *Global Change Biol.* 16, 1936–1953. doi: 10.1111/j.1365-2486.2009.02128.x

Conover, D. O. (1990). The relation between capacity for growth and length of growing season: evidence for and implications of countergradient variation. *Trans. Am. Fish. Soc.* 119, 416–430. doi: 10.1577/1548-8659(1990)119<0416:trbcfg>2.3.co;2

Conover, D. O., and Present, T. M. C. (1990). Countergradient variation in growth rate: compensation for length of the growing season among Atlantic silversides from different latitudes. *Oecologia* 83, 316–324. doi: 10.1007/BF00317554

Di Santo, V. (2015). Ocean acidification exacerbates the impacts of global warming on embryonic little skate, *Leucoraja erinacea* (Mitchill). *J. Exp. Mar. Biol. Ecol.* 463, 72–78. doi: 10.1016/j.jembe.2014.11.006

Di Santo, V. (2016). Intraspecific variation in physiological performance of a benthic elasmobranch challenged by ocean acidification and warming. *J. Exp. Biol.* 219, 1725–1733. doi: 10.1242/jeb.139204

Frick, L. H., Reina, R. D., and Walker, T. I. (2010). Stress related physiological changes and post-release survival of Port Jackson sharks (*Heterodontus portusjacksoni*) and gummy sharks (*Mustelus antarcticus*) following gill-net and longline capture in captivity. *J. Exp. Mar. Biol. Ecol.* 385, 29–37. doi: 10.1016/j.jembe.2010.01.013

Frisk, M. G., and Miller, T. J. (2006). Age, growth, and latitudinal patterns of two Rajidae species in the northwestern Atlantic: little skate (*Leucoraja erinacea*) and winter skate (*Leucoraja ocellata*). *Can. J. Fish. Aqu. Sci.* 63, 1078–1091. doi: 10.1139/f06-005

Izzo, C., Doubleday, Z. A., Grammer, G. L., Barnes, T. C., Delean, S., Ferguson, G. J., et al. (2016). Multi-species response to rapid environmental change in a large estuary system: a biochronological approach. *Ecol. Indic.* 69, 739–748. doi: 10.1016/j.ecolind.2016.05.019

Izzo, C., and Rodda, K. R. (2012). Comparative rates of growth of the Port Jackson shark throughout its southern Australian range. *Mar. Freshw. Res.* 63, 687–694.

Johnson, M. S., Kraver, D. W., Renshaw, G. M. C., and Rummer, J. L. (2016). Will ocean acidification affect the early ontogeny of a tropical oviparous elasmobranch (*Hemiscyllium ocellatum*)? *Conserv. Physiol.* 4:cow003. doi: 10.1093/conphys/cow003

Jones, A. A., Hall, N. G., and Potter, I. C. (2008). Size compositions and reproductive biology of an important bycatch shark species (*Heterodontus portusjacksoni*) in south-western Australian waters. *J. Mar. Biol. Assoc. U. K.* 88, 189–197. doi: 10.1017/s0025315408000209

Last, P. R., White, W. T., Gledhill, D. C., Hobday, A. J., Brown, R., Edgar, G. J., et al. (2011). Long-term shifts in abundance and distribution of a temperate fish fauna: a response to climate change and fishing practices. *Global Ecol. Biogeogr.* 20, 58–72. doi: 10.1111/j.1466-8238.2010.00575.x

Lombari-Carlson, L. A., Cortés, E., Parsons, G. R., and Manire, C. A. (2003). Latitudinal variation in life-history traits of bonnethead sharks, *Sphyrna tiburo*, (Carcharhiniformes: Sphyrnide) from the eastern Gulf of Mexico. *Mar. Freshw. Res.* 54, 875–883.

Martino, J. C., Fowler, A. J., Doubleday, Z. A., Grammer, G. L., and Gillanders, B. M. (2019). Using otolith chronologies to understand long-term trends and extrinsic drivers of growth in fisheries. *Ecosphere* 10:e02553.

Meiri, S. (2011). Bergmann's Rule – what's in a name? *Global Ecol. Biogeog.* 20, 203–207.

Morrongiello, J. R., and Thresher, R. E. (2015). A statistical framework to explore ontogenetic growth variation among individuals and populations: a marine fish example. *Ecol. Monogr.* 85, 93–115. doi: 10.1890/13-2355.1

Morrongiello, J. R., Thresher, R. E., and Smith, D. C. (2012). Aquatic biochronologies and climate change. *Nat. Clim. Change* 2, 849–857. doi: 10.1038/nclimate1616

Neuheimer, A., Thresher, R., Lyle, J., and Semmens, J. (2011). Tolerance limit for fish growth exceeded by warming waters. *Nat. Clim. Change* 1, 110–113. doi: 10.1038/nclimate1084

O'Gower, A. K. (1995). Speculations on a spatial memory for the Port Jackson shark (*Heterodontus portusjacksoni*) (Meyer) (Heterodontidae). *Mar. Freshw. Res.* 46, 861–871.

Parmesan, C. (2006). Ecological and evolutionary responses to recent climate change. *Annu. Rev. Ecol. Evol. Syst.* 37, 637–669. doi: 10.1146/annurev.ecolsys.37.091305.110100

Parsons, G. R. (1993). Age determination and growth of the bonnethead shark *Sphyrna tiburo*: a comparison of two populations. *Mar. Biol.* 117, 23–31. doi: 10.1007/bf00346422

Pistevos, J. C. A., Nagelkerken, I., Rossi, T., Olmos, M., and Connell, S. D. (2015). Ocean acidification and global warming impair shark hunting behaviour and growth. *Sci. Rep.* 5:16293. doi: 10.1038/srep16293

Powter, D. M., and Gladstone, W. (2008a). Demographic analysis of the Port Jackson shark *Heterodontus portusjacksoni* in the coastal waters of eastern Australia. *Mar. Freshw. Res.* 59, 444–455.

Powter, D., and Gladstone, W. (2008b). Embryonic mortality and predation on egg capsules of the port jackson shark *Heterodontus portusjacksoni* (Meyer). *J. Fish Biol.* 72, 573–584. doi: 10.1111/j.1095-8649.2007.01721.x

Powter, D. M., and Gladstone, W. (2009). Habitat-mediated use of space by juvenile and mating adult Port Jackson sharks. Heterodontus portusjacksoni, in Eastern Australia. *Pacific Sci.* 63, 1–14. doi: 10.2984/1534-6188(2009)63%5B1:huosbj%5D2.0.co;2

R Core Team, (2018). *R: A Language and Environment for Statistical Computing, v3.5*, 1st Edn. Vienna: R Foundation for Statistical Computing.

Rodda, K. (2000). *Development in the Port Jackson Shark Embryo*. Adelaide, SA: University of Adelaide.

Rodda, K., and Svane, I. (2007). "Tagging and movement in spencer gulf," in *Prawn Fishery By-Catch and Discards: Marine Ecosystem Analysis - Population Effects. FRDC Project No. 2003/023*, eds I. Svane, K. Rodda, and P. Thomas (Adelaide: SARDI Aquatic Sciences Research Report Series; no. 199), 89–111.

Rodda, K. R., and Seymour, R. S. (2008). Functional morphology of embryonic development in the Port Jackson shark *Heterodontus portusjacksoni* (Meyer). *J. Fish Biol.* 72, 961–984. doi: 10.1111/j.1095-8649.2007.01777.x

Rosa, R., Baptista, M., Lopes Vanessa, M., Pegado Maria, R., Ricardo Paula, J., Trübenbach, K., et al. (2014). Early-life exposure to climate change impairs tropical shark survival. *Proc. R. Soc. B Biol. Sci.* 281, 20141738. doi: 10.1098/rspb.2014.1738

Rosa, R., Rummer, J. L., and Munday, P. L. (2017). Biological responses of sharks to ocean acidification. *Biol. Lett.* 13:20160796. doi: 10.1098/rsbl.2016.0796

Stevens, J. D., Bonfil, R., Dulvy, N. K., and Walker, P. A. (2000). The effects of fishing on sharks, rays, and chimaeras (chondrichthyans), and the implications for marine ecosystems. *J. Mar. Sci.* 57, 476–494. doi: 10.1006/jmsc.2000.0724

Tovar-Ávila, J., Day, R. W., and Walker, T. I. (2010). Using rapid assessment and demographic methods to evaluate the effects of fishing on *Heterodontus portusjacksoni* off far-eastern Victoria. *Austr. J. Fish Biol.* 77, 1564–1578. doi: 10.1111/j.1095-8649.2010.02788.x

Tovar-Ávila, J., Izzo, C., Walker, T. I., Braccini, J. M., and Day, R. W. (2009). Assessing growth band counts from vertebrae and dorsal-fin spines for ageing sharks: comparison of four methods applied to *Heterodontus portusjacksoni*. *Mar. Freshw. Res.* 60, 898–903.

Walker, T. I., Taylor, B. L., Hudson, R. J., and Cottier, J. P. (1998). The phenomenon of apparent change of growth rate in gummy shark (*Mustelus antarcticus*) harvested off southern Australia. *Fish. Res.* 39, 139–163. doi: 10.1016/s0165-7836(98)00180-5

Weisberg, S., Spangler, G., and Richmond, L. S. (2010). Mixed effects models for fish growth. *Can. J. Fish. Aqu. Sci.* 67, 269–277. doi: 10.1139/f09-181

Winton, M. V., Natanson, L. J., Kneebone, J., Cailliet, G. M., and Ebert, D. A. (2014). Life history of *Bathyraja trachura* from the eastern Bering Sea, with evidence of latitudinal variation in a deep-sea skate species. *Mar. Biol. Assoc. U. K. J. Mar. Biol. Assoc. U. K.* 94, 411. doi: 10.1017/s0025315413001525

Wittmann, T. A., Izzo, C., Doubleday, Z. A., McKenzie, J., Delean, S., and Gillanders, B. M. (2016). Reconstructing climate–growth relations from the teeth of a marine mammal. *Mar. Biol.* 163, 1–11.

Zuur, A., Ieno, E. N., Walker, N., Saveliev, A. A., and Smith, G. M. (2009). *Mixed Effects Models and Extensions in Ecology With R*. New York, NY: Springer.

Conflict of Interest: The authors declare that the research was conducted in the absence of any commercial or financial relationships that could be construed as a potential conflict of interest.

Copyright © 2020 Izzo and Gillanders. This is an open-access article distributed under the terms of the Creative Commons Attribution License (CC BY). The use, distribution or reproduction in other forums is permitted, provided the original author(s) and the copyright owner(s) are credited and that the original publication in this journal is cited, in accordance with accepted academic practice. No use, distribution or reproduction is permitted which does not comply with these terms.

frontiers in Marine Science

ORIGINAL RESEARCH
published: 22 April 2020
doi: 10.3389/fmars.2020.00249

Seasonal Movement Patterns of the Bigfin Reef Squid *Sepioteuthis lessoniana* Predicted Using Statolith $\delta^{18}O$ Values

Chun-I Chiang[1,2], Ming-Tsung Chung[3], Jen-Chieh Shiao[3], Pei-Ling Wang[3], Tin-Yam Chan[1,4], Atsuko Yamaguchi[2] and Chia-Hui Wang[4,5]*

[1] Institute of Marine Biology, National Taiwan Ocean University, Keelung, Taiwan, [2] Graduate School of Fisheries and Environmental Sciences, Nagasaki University, Nagasaki, Japan, [3] Institute of Oceanography, National Taiwan University, Taipei, Taiwan, [4] Center of Excellence for the Oceans, National Taiwan Ocean University, Keelung, Taiwan, [5] Department of Environmental Biology and Fisheries Science, National Taiwan Ocean University, Keelung, Taiwan

Sepioteuthis lessoniana is a widely distributed neritic squid in the Indo-Pacific Ocean. It is an important species in fisheries, but species management is difficult because of inadequate information regarding its life history. The daily growth and $\delta^{18}O$ values from the core to the edge of statoliths of *S. lessoniana* collected in northern Taiwan were analyzed to predict the experienced temperature history along with ontogenetic stages. The probability of occurrence in a given area at each life stage in three seasonal groups was determined using salinity values, deduced and measured temperatures, and the known ecology of *S. lessoniana*. The results showed that ontogenetic variation in the statolith $\delta^{18}O$ values in *S. lessoniana* reflected the seasonal temperature fluctuation observed in Taiwanese waters, which indicated the reliability of the prediction method. Complex and diverse distribution and movement patterns were observed in the three seasonal groups. The results also indicated the importance of the waters near the coast of northeastern Taiwan as a spawning ground. Based on a model prediction, the distribution of *S. lessoniana* is likely associated with water temperature and current. A potential migration route from the Penghu Islands to northeastern Taiwan suggests a high level of population connectivity in *S. lessoniana* in Taiwan. This study provides information on the spatial and vertical distribution of *S. lessoniana* at various ontogenetic stages, which is essential for resource management and conservation of this commercial species.

Keywords: ***Sepioteuthis lessoniana*, statolith oxygen isotopes, temperature, geographic distribution, ontogenetic movement**

OPEN ACCESS

Edited by:
Alejandra Vanina Volpedo, University of Buenos Aires, Argentina

Reviewed by:
Bilin Liu, Shanghai Ocean University, China
Kolliyil S. Mohamed, Central Marine Fisheries Research Institute (ICAR), India

***Correspondence:**
Chia-Hui Wang
chwang99@mail.ntou.edu.tw

Specialty section:
This article was submitted to Marine Ecosystem Ecology, a section of the journal Frontiers in Marine Science

Received: *14 December 2019*
Accepted: *30 March 2020*
Published: *22 April 2020*

Citation:
Chiang C-I, Chung M-T, Shiao J-C, Wang P-L, Chan T-Y, Yamaguchi A and Wang C-H (2020) Seasonal Movement Patterns of the Bigfin Reef Squid Sepioteuthis lessoniana Predicted Using Statolith $\delta^{18}O$ Values. Front. Mar. Sci. 7:249. doi: 10.3389/fmars.2020.00249

INTRODUCTION

Planktonic paralarvae of loliginid squids are distributed widely after hatching by coastal trends and ocean currents (Young and Harman, 1988; Zeidberg and Hamner, 2002). By contrast, juveniles and adults live in coastal and inshore waters and are commonly aggregated in schools for spawning (Jereb and Roper, 2005). The distribution range of paralarvae is a critical parameter

for recruitment success and gene flow in cephalopod populations (O'dor, 1998; Moreno et al., 2008), and understanding movement patterns is crucial for studies on population structure, fishery management, and marine protected area evaluation (O'dor, 1992; Semmens et al., 2007). Temperature is one of the major factors affecting the movements of squids because squids are highly vulnerable to drastic changes in temperature. Direct data of the thermal movement patterns of squids have been collected primarily through external tagging (e.g., Ueta and Jo, 1990; Jackson et al., 2005; Gilly et al., 2006; Kanamaru et al., 2007; Bazzino et al., 2010). Low recapture rates and the size of the electronic device usually limit the success of squid tagging experiments (Semmens et al., 2007). Alternatively, elemental signatures (e.g., Sr:Ca ratio) of the hard structures of squid provide a potential source of information regarding the ambient temperatures that they have been exposed to (Ikeda et al., 2003; Yamaguchi et al., 2015, 2018; Liu et al., 2016). However, studies on the relationship between the Sr:Ca ratio and temperature have provided inconsistent results in different species (Elsdon and Gillanders, 2002, 2003; Gillanders et al., 2013). A technique that is more commonly applied to teleosts should be considered as a supplementary method for improving the accuracy and reliability of predictions.

In recent years, stable oxygen isotopic ratios (expressed as $\delta^{18}O$) in biogenic carbonates have been used to examine the spatial distribution and movement patterns of teleosts (e.g., Steer et al., 2010; Currey et al., 2014; Shiao et al., 2017). The $\delta^{18}O$ value in fish otoliths is in equilibrium with that in the ambient water, and $\delta^{18}O$ value uniformly increases with a decrease in seawater temperature in various species of fish (Elsdon and Gillanders, 2002; Høie et al., 2004a). Squid statoliths are composed of calcium carbonate, and the relationships between statolith and ambient water chemistry are similar to that of fish otoliths (Arkhipkin et al., 2004; Arkhipkin, 2005; Gillanders et al., 2013). Therefore, statolith $\delta^{18}O$ value can be analogously used as a temperature proxy for reconstructing the ontogenetic preferences of squids (Radtke, 1983; Landman et al., 2004; Trasviña-Carrillo et al., 2018). For example, Trasviña-Carrillo et al. (2018) analyzed the $\delta^{18}O$ value in the entire statolith of the jumbo squid *Dosidicus gigas* and found that temperature preference did not differ between sexes but did among ontogenetic stages because of differences in living depth. Landman et al. (2004) also predicated the experienced temperature of the giant squid *Architeuthis sanctipauli* to be in the range of 10.5–12.9°C and average living depths to be 125–250 m by analyzing the $\delta^{18}O$ values in one entire statolith, which are considered to provide lifelong average temperature data. However, micromill sampling for higher temporal resolution of $\delta^{18}O$ information (Høie et al., 2004b), which was used on fish otoliths, has never been used on squid statoliths to increase the temporal resolution of their ontogenetic thermal migration history.

The bigfin reef squid, *S. lessoniana*, is widely distributed in the neritic waters of the Indo-Pacific Ocean, which include the waters surrounding Taiwan (Roper et al., 1984; Okutani, 2015). Field observations have revealed that adults migrate from offshore areas to shallow inshore areas for spawning (Segawa, 1987). In the waters off the northern coast of Taiwan, *S. lessoniana* hatching occurs almost throughout the entire year; hatching peaks in May and August–September (Chen et al., 2015). Hatching can be divided into at least two seasonal groups (spring and autumn) on the basis of hatching date and life history traits of individuals (Ching et al., 2017). This species of squid is important to fisheries because of its high economic value, however, empirical evidence concerning the movement and distribution during the ontogenetic stages is scarce. Ueta and Jo (1990) studied the migration of subadult–adult individuals of *S. lessoniana* around Tokushima Prefecture, Japan, by using the tag–recapture method and fishery data. Their results suggested that this species stays in inshore waters and migrates to offshore waters for overwintering. Kanamaru et al. (2007) evaluated past tagging studies for *S. lessoniana* migration in Japan and reported that individuals released in autumn moved farther than those released in spring. However, additional empirical evidence to support these hypotheses is required because conventional tagging studies did not provide complete information on movement patterns throughout the life history of squids. In addition, high-resolution data of seasonal and geological movement patterns of *S. lessoniana* populations are required for species management.

The present study investigated the ontogenetic movement patterns of different seasonal groups of *S. lessoniana* in northern Taiwan through statolith $\delta^{18}O$ analyses. This study is the first attempt to generate a 3D habitat preference model, including spatial and depth preferences, and it is expected to provide new comprehensive spatial and temporal insights into migration patterns of cephalopods.

MATERIALS AND METHODS

Squid Collection and Age Estimation

Twenty-two adult *S. lessoniana* individuals were collected by jigging from the inshore waters of northeastern Taiwan (**Figure 1**) between November 2017 and March 2018. The mantle length (ML; in mm) of each individual was measured. Statoliths were extracted, cleaned ultrasonically using 70% hydrogen peroxide, rinsed, oven-dried, and embedded in Epofix resin (Struers, Denmark). The left statolith of each squid was ground and polished along the posterior side to approximately 50–100 μm above the core by using a metallographic grinding and polishing machine (P20FR-HA; Top Tech Machines co. Ltd., Taiwan). This thickness ensured that a sufficient volume of milling powder was available for isotopic analysis (>40 μg per sample). Alternative formation of translucent and opaque growth zones has been previously validated as occurring on a daily basis (Jackson, 1990); thus, the growth increment at the lateral dome region of statolith was examined from the photographs recorded under a compound microscope (400×, DM-2500, Leica Microsystems GmbH, Germany) by using a digital camera (DFC-450, Leica Microsystems Lt., Switzerland) to estimate age. The growth increments were counted twice, and an average value was used as daily age. If the difference between two counts was >5%, a third count was recorded to minimize measurement error (Arkhipkin and Shcherbich, 2012). The hatching date of

each individual was back-calculated from the deduced age (in days) and the date of collection. Each individual was further categorized into the nearest seasonal group according to its hatching month, namely spring (March–May), summer (June–August) and autumn (September–November). Based on the morphological and ecological changes in accordance with growth and age (Segawa, 1987), we defined four stages in *S. lessoniana* corresponding to age, namely the embryonic-paralarval (age: 0–20 days), juvenile (age: 20–60 days), juvenile–subadult (age: 60–110 days) and subadult–adult (age: >110 days) stages.

Isotopic Analysis

After age counting, statolith slides were drilled using an ESI New Wave Research Micromill and carbonate powders were collected sequentially from the edge to the core at the lateral dome region at intervals of 150–190 μm (**Figure 2**). The tip of the drill was approximately 200 μm in diameter (H23RS, Comet, Germany), and milling depth was set at approximately 150 μm. Most statoliths involved four drilling paths (except a smaller statolith, K180313003, which had three paths only), and each path was recorded to estimate covered daily growth.

The powder samples of each drilling path were transferred to glass vials and reacted with 100% orthophosphoric acid at 70°C in an automated online system (Kiel Carbonate IV, Thermo Electron Corporation, Germany) to produce CO_2. The values of $\delta^{18}O$ were determined by analyzing the released CO_2 gas by using a mass spectrometer (Finnigan MAT 253, Thermo Electron Corporation, Germany) at National Taiwan University. The long-term reproducibility of the Finnigan MAT 253 is higher than ±0.08% (one standard deviation [SD]) for $\delta^{18}O$, based on repeat samples of international reference standards (NBS-19, approximately 40–50 μg). The values of $\delta^{18}O$ (%) were reported in standard notation relative to standards Vienna Pee Dee Belemnite (VPDB) after calibration against the NBS-19 standard:

$$\delta^{18}\text{O values} = \left(\frac{^{18}\text{O}:^{16}\text{O}_{\text{sample}} - ^{18}\text{O}:^{16}\text{O}_{\text{standard}}}{^{18}\text{O}:^{16}\text{O}_{\text{standard}}}\right) \times 100(‰)$$

The temperature-dependent relationship of $\delta^{18}O$ values in biogenic aragonites is taxonomic and species specific (Shirai et al., 2018). However, no equation has been established for statoliths in *S. lessoniana*; hence, we applied the equation established for statoliths in another cephalopod species, *Sepia pharaonis* (Chung et al., unpublished data), to deduce experienced temperature in *S. lessoniana*.

$$\delta^{18}\text{O}_{\text{statolith,VPDB}} - \delta^{18}\text{O}_{\text{water,VSMOW}} = 2.88(\pm 0.14) - 0.20(\pm 5.40 \times 10^{-3}) \times \text{T}(^{\circ}\text{C})$$

where $\delta^{18}O_{statolith,VPDB}$ represents the statolith $\delta^{18}O$ values on a VPDB scale, and $\delta^{18}O_{water,VSMOW}$ represents the water $\delta^{18}O$ values on a VSMOW (Vienna Standard Mean Ocean Water) scale. The $\delta^{18}O_{water,VSMOW}$ values were derived using the relationship with salinity (S) in Taiwan Strait (Chang, 2000):

$$\delta^{18}\text{O}_{\text{water,VSMOW}} = 0.28 \times \text{S} - 9.38$$

To evaluate the feasibility of the equation, the relationship of measured and deduced temperature derived from the edge of statoliths in 22 crossed-season captured individuals were analyzed to understand if it followed the 1:1 correspondence. The duration (days) which statolith $\delta^{18}O$ values represented was considered, and the measured temperature was averaged based on the duration at the depth of 50 m.

Prediction of Movement Patterns

To accurately predict the experienced temperature and corresponding living areas of *S. lessoniana*, individual differences in living period and temporal and spatial variations in seawater temperature were considered in the evaluation. The individual living period and season corresponding to each data point of statolith $\delta^{18}O$ values were established through the examination of microstructure. During the defined period, water temperature and salinity were obtained from the HYbrid Coordinate Ocean Model website (HYCOM)[1] and are presented in a spatial resolution of 0.08° × 0.08° at the depths of 0, 30, 50, and 100 m, according to the living depth of this species (Roper et al., 1984; Tomano et al., 2016; Ammar and Maaroof, 2019). Next, we set the unit of the spatial grid at 0.4° × 0.4° to establish the movement pattern because this spatial grid covers the minimum range of squids captured in the adult stage in the present study (**Figure 1**). For setting units, the average values of temperature and salinity in each grid at each depths (0, 30, 50, and 100 m) was used to produce $\delta^{18}O_{water,VSMOW}$ values based on the equation established by Chang (2000).

The deduced temperature depended on the estimated statolith $\delta^{18}O$ value and the variation in water $\delta^{18}O$ values among grids at different depths. Therefore, each data point of statolith

[1]http://ncss.hycom.org/thredds/catalog.html

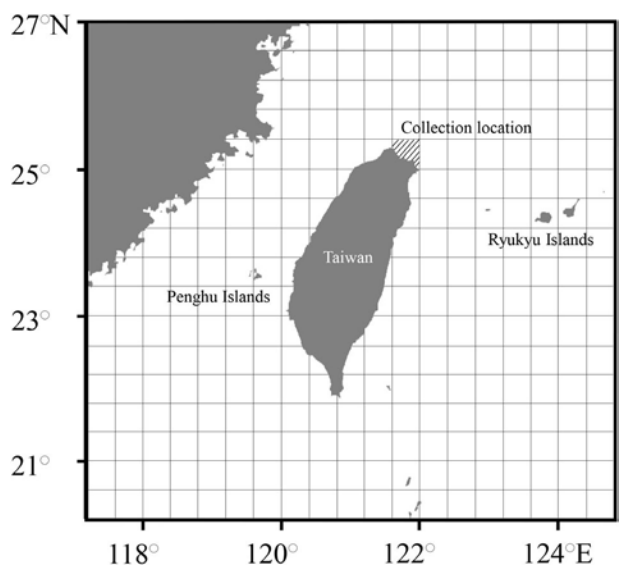

FIGURE 1 | Map showing the collection locations (slanted lines). The unit of spatial grids was 0.4° × 0.4° for the establishment of occurrence probability.

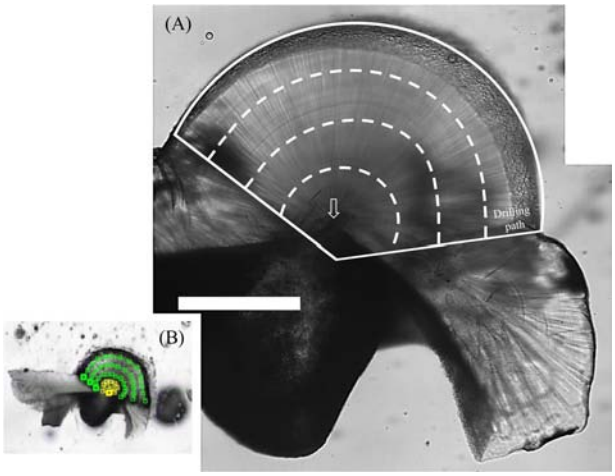

FIGURE 2 | Polished *S. lessoniana* statolith (K180116012) with the drilling paths for powder collection. **(A)** White solid lines indicate the entire powder collection area at the lateral dome region and dashed lines indicate approximate boundaries of the drilling path. Arrow indicates the statolith core. Scale bar = 400 μm. **(B)** The setting of the drilling path. Yellow and green lines indicate the paths of drill tip at the core and the outers of the core, respectively, square as a turning point. The intervals between lines are 150–190 μm.

δ^{18}O values was used to deduce the experienced temperature in every grid at various depths, each of which had their specific water δ^{18}O values. When the deduced temperature matched with the measured temperature (from the HYCOM), the grid thus obtained was considered the possible living area of the squid during a specific period; this period was estimated using the growth rings in the milling area for the statolith δ^{18}O measurement. The extent of match between the deduced and measured temperature was based on the comparison of probability distributions between these two values determined using Student's *t* test (**Figure 3**). The probability distribution of deduced temperature was modeled using a known living period (days) as well as an average and the uncertainty (SD) associated with the deduced temperature. The uncertainties were estimated by running Monte Carlo simulations 1,000 times and included variations in salinity, instrumental measurements, and parameters of the temperature-dependent equation. Similarly, the probability distribution of measured temperature was modeled using known living periods (days) and average values of measured temperature and associated SDs. Once the *t* test resulted in a *p* value larger than 0.05, we accepted that the two temperatures did not differ significantly and inferred a possibility of the occurrence of a living area in the grid (**Figure 3**). We repeated modeling to determine the matched area and depth of each statolith δ^{18}O value from individuals at each life stage.

Furthermore, we considered the collection location, spawning site, and movement ability of *S. lessoniana* to determine the possible living areas. The δ^{18}O value in the outermost portion of statoliths reflected the occurrence of *S. lessoniana* near the collection location. If this value represented the 10-day average of the signal, the maximum movement of *S. lessoniana* was calculated to be approximately 50 km away from the collection location because the mean swimming speed of adult *S. lessoniana* individuals is 5 km per day, according to a study by Kanamaru et al. (2007). Consequently, grids located farther than 50 km from the collection site were eliminated. In addition to this "backward" evaluation, based on the collection location, a "forward" method was also used to evaluate the living area at the embryonic-paralarval stage. We excluded the matched areas that were not adjacent to the coast because the egg capsules of *S. lessoniana* are always found in inshore waters (Segawa, 1987). Combining the results of forward and backward calculations and mobility, the possible occurrence of four life stages of individuals were further selected from the matched areas found based on the statolith δ^{18}O value.

After examining the living area at an individual level, we calculated the probability of occurrence in each setting area for

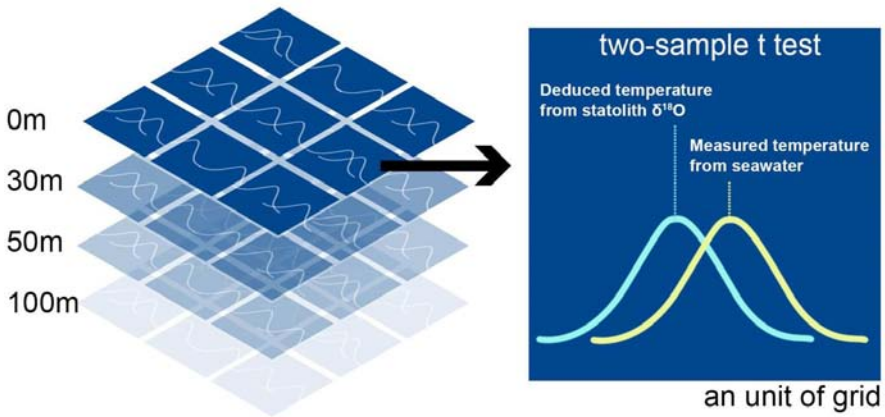

FIGURE 3 | Determination of the extent of matching between deduced and measured temperature by using the two-sample *t* test. The deduced temperature was based on the statolith δ^{18}O values, and measured temperature was the data extracted from the HYbrid Coordinate Ocean Model website. The test was conducted in each spatial grid (0.4° × 0.4°) at depths corresponding to each specific life stage of *S. lessoniana*. The criteria of matching were set at the *p* value of 0.05.

each seasonal group. The probability was calculated using the following equation:

$$P_j = \frac{C_{1j} + C_{2j} + \ldots + C_{kj}}{k_j}$$

where C_{kj} represents the occurrence of kth squid in area j, and k_j is the total number of individuals in grid j. If squid sample number 1 exists in grid 1 at a specific life stage, the C_{kj} value is 1; otherwise, the C_{kj} value is 0. Furthermore, the P_j value indicates the probability of occurrence in grid j. If the P_j value is 1, all squid samples at the same ontogenetic stage occur in grid j. If an area with a probability (p value) of >0.5 is identified, it would be considered a major residential area for *S. lessoniana* seasonal groups around Taiwan.

Statistical Analysis

To identify the effects of ontogenetic stage and hatching season on $\delta^{18}O_{statolith}$ value, differences in $\delta^{18}O_{statolith}$ values among all ontogenetic stages over the seasonal groups (spring, summer, and autumn) were examined using a non-parametric Scheirer–Ray–Hare extension of the Kruskal–Wallis test followed by *post hoc* multiple comparisons tests (Dunn's tests). A linear regression and an Analysis of Covariance (ANCOVA) were used to test if the experienced temperature deduced by the equation (Chung et al., unpublished data) was reasonable and close to 1:1 correspondence between measured and deduced temperature. All statistical tests were conducted using SPSS (ver. 20, IBM Corp., Armonk, NY, United States). The t test used to evaluate the extent of matching between deduced and measured temperatures and the Monte Carlo simulations were used for uncertainty determination were performed using R (R Core Team, 2018).

RESULTS

After statolith age determination, seven individuals were found to belong to the spring group with a mean (±SD) ML of 264 ± 49 mm and an age ranging from 150 to 167 days. Six individuals were found to belong to the summer group with a mean ML of 260 ± 24 mm and an age ranging from 146 to 192 days. Nine individuals were found to belong to the autumn group with a mean ML of 298 ± 45 mm and an age ranging from 140 to 177 days (**Table 1**). No significant difference in ML was observed between the seasonal groups [analysis of variance (ANOVA), $F = 1.944$, $p = 0.171$]. For statolith carbonate sampling, the drilling paths were averaged (±SD): 17.5 ± 8.4, 42.5 ± 7.8, 49.8 ± 7.0, and 53.3 ± 5.9 days from the core to the edge presenting the embryonic–paralarval, juvenile, juvenile–subadult, and subadult–adult stages, respectively.

Oxygen Isotopic Composition of the Statolith

Overall, $\delta^{18}O_{statolith}$ values ranged from −2.93 to −0.12‰ with a mean of −1.86 ± 0.79‰. Variations in the $\delta^{18}O_{statolith}$ values were not consistent among seasonal groups (**Figure 4A**). Larger variations were observed in the summer and autumn groups than in the spring group, however, the $\delta^{18}O_{statolith}$ values were not significantly different among the seasonal groups (Kruskal–Wallis test, $H = 1.506$, $p = 0.471$, **Table 2**). Ontogenetic stage differences were observed in $\delta^{18}O_{statolith}$ values (Kruskal–Wallis test, $H = 39.941$, $p < 0.001$, **Table 2**). The values decreased slightly from embryonic–paralarval stage to the juvenile stage and then increased until the subadult–adult stage (**Figure 4B**). The values of $\delta^{18}O_{statolith}$ in embryonic–paralarval stage were significantly lower than those in the subadult–adult stage (Dunn's tests, $Z = -4.078$, $p < 0.001$). In addition, the values in the juvenile stage were significantly different from those in the juvenile–subadult and subadult–adult stages. No interaction was observed between the seasonal group and ontogenetic stages in $\delta^{18}O_{statolith}$ values (**Table 2**).

Individual ontogenetic trends showed that the $\delta^{18}O_{statolith}$ values in the spring group ranged between −2.87 and −1.61‰ and were relatively stable until the statolith edge (**Figures 5A,B**). In the summer group, the $\delta^{18}O_{statolith}$ values in the statolith core

TABLE 1 | Sampling date, mantle length, age estimation, and back-calculated hatching date and season for each *S. lessoniana* individual used in statolith oxygen isotopic analysis.

Sample code	Mantle length (mm)	Age (day)	Sampling date	Hatching date	Seasonal group
K171102001	323	166	2 November 2017	20 May 2017	Spring
K171102003	285	167	2 November 2017	19 May 2017	Spring
K171102004	279	153	2 November 2017	2 June 2017	Spring
K171102006	313	152	2 November 2017	3 June 2017	Spring
K171102010	239	159	2 November 2017	27 May 2017	Spring
K171102011	215	167	2 November 2017	19 May 2017	Spring
K171102012	194	150	2 November 2017	5 June 2017	Spring
K180116002	256	148	16 January 2018	21 August 2017	Summer
K180116003	231	147	16 January 2018	22 August 2017	Summer
K180116005	261	146	16 January 2018	23 August 2017	Summer
K180116007	244	153	16 January 2018	16 August 2017	Summer
K180116012	264	160	16 January 2018	9 August 2017	Summer
K180313003	302	192	13 March 2018	2 September 2017	Summer
K180313001	339	176	13 March 2018	18 September 2017	Autumn
K180313002	302	172	13 March 2018	22 September 2017	Autumn
K180313004	271	163	13 March 2018	1 October 2017	Autumn
K180313007	253	140	13 March 2018	24 October 2017	Autumn
K180313008	234	143	13 March 2018	21 October 2017	Autumn
K180329001	354	177	29 March 2018	3 October 2017	Autumn
K180329002	360	164	29 March 2018	16 October 2017	Autumn
K180329003	285	176	29 March 2018	4 October 2017	Autumn
K180329004	281	174	29 March 2018	6 October 2017	Autumn

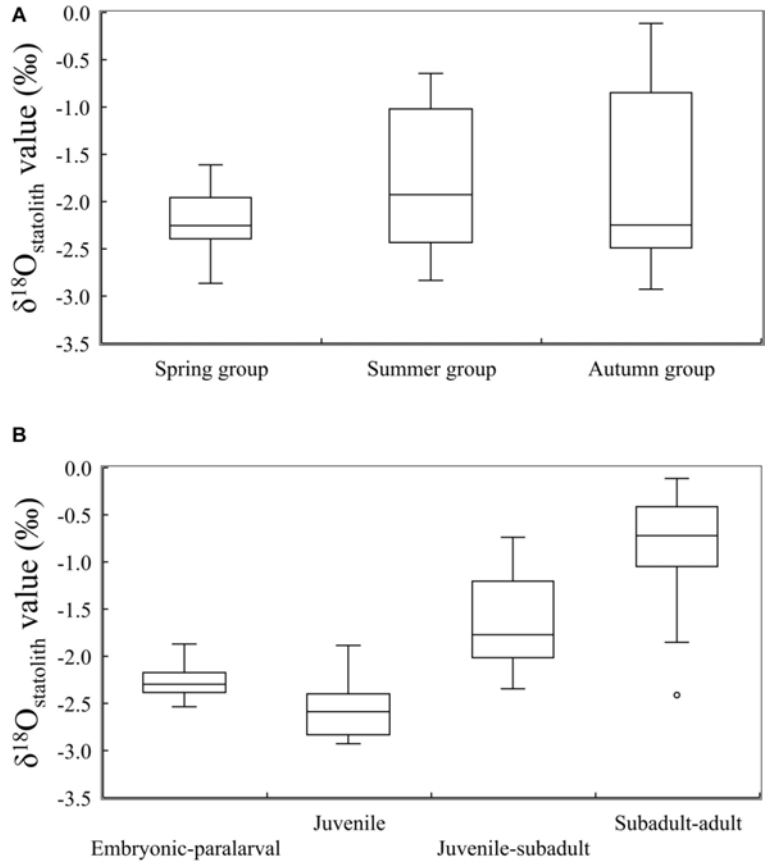

FIGURE 4 | $\delta^{18}O_{statolith}$ values in *S. lessoniana* **(A)** in three seasonal groups and **(B)** at four ontogenetic stages. The box plots show the interquartile range, with the median value indicated by the horizontal line; whiskers show the range. Circles indicate outliers.

varied from −2.54 to −1.87‰; they decreased to the lowest levels, between −2.32 and −2.83‰, at the juvenile stage and then increased to the highest levels, between −1.06 and −0.65‰, in the statolith edge (**Figures 5C,D**). The $\delta^{18}O_{statolith}$ values in the autumn group showed a pattern similar to that of the summer group (**Figures 5E–G**), but the $\delta^{18}O_{statolith}$ values were higher at the juvenile–subadult stage (−2.23 to −0.97‰) and subadult–adult stage (−0.50 to −0.12‰) than those in the summer group.

TABLE 2 | Results of non-parametric analysis of variance to test the differences in *S. lessoniana* statolith oxygen isotopes ratios among seasonal groups (spring, summer, and autumn) and ontogenetic (embryonic–paralarval, juvenile, juvenile–subadult, and subadult–adult) stages.

	df	SS	MS	H	*p*
Seasonal group	2	696.40		1.506	0.471
Ontogenetic stage	3	18472.92		39.941	**<0.001**
Seasonal group × Ontogenetic stage	6	4558.88		9.857	0.131
Total	73	33762.50	462.50		

Boldface indicates significant p values.

Predicted Occurrence Area and Movement Pattern

Individual values of deduced and measured temperature were close and the linear regression showed a well correspondent (**Figure 6**, $p < 0.001$). The slope was not significantly different from the line of 1:1 ($F_{1,34} = 0.83$, $p = 0.37$) indicating that the deduced temperature could reflect reasonably the experienced temperature of S. *lessoniana*.

Figures 7–9 present the distribution of occurrence probability of seasonal groups at different depths by comparing deduced and measured temperatures while considering collection location, spawning site, and movement ability. The probability of occurrence results indicated that the three seasonal groups of *S. lessoniana* in northeastern Taiwan have diverse distributions and movement patterns. The individuals in the spring group had the highest possibility of hatching in neritic waters (approximate depth: 0–50 m) near the coast, extending from northeastern to eastern Taiwan and the Ryukyu Islands (**Figure 7**). After hatching and reaching the paralarval stage, individuals were widely distributed in the inshore waters of northeastern Taiwan, possibly from the sea surface to an approximate depth of 50 m; these individuals may have subsequently migrated to relatively deeper waters near the coast of northeastern Taiwan or to the

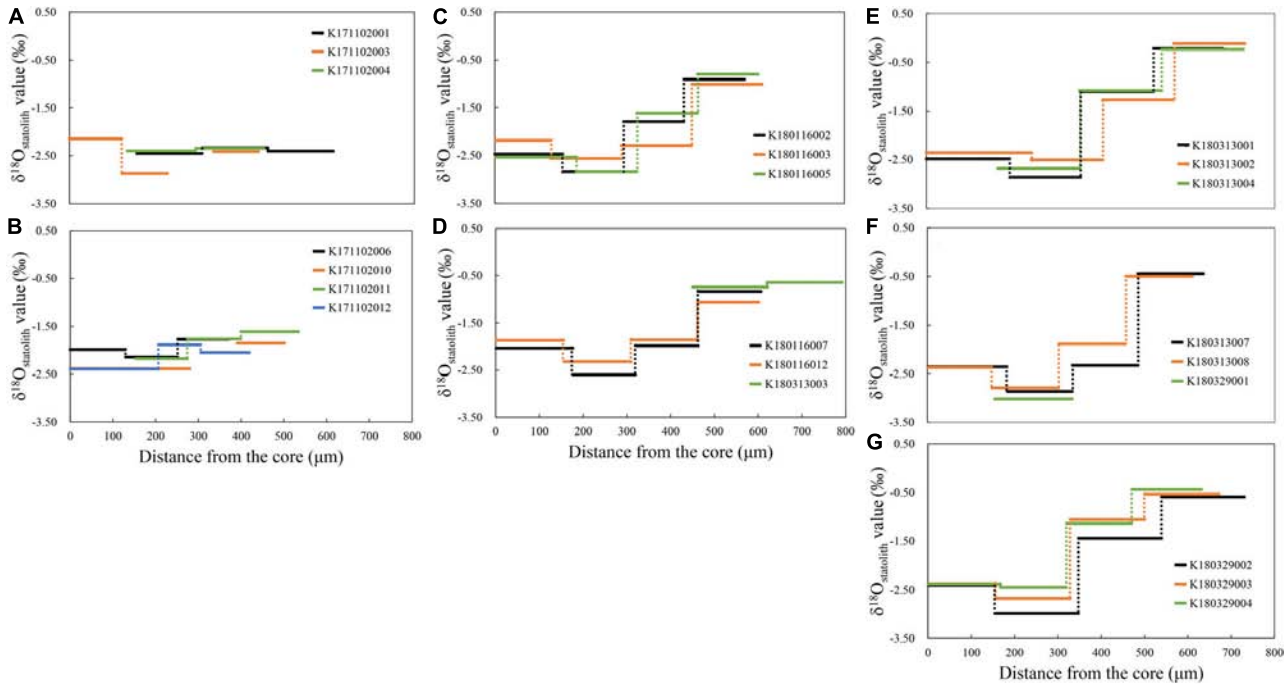

FIGURE 5 | $\delta^{18}O_{statolith}$ profiles of *S. lessoniana* from the statolith core to the edge of each individual in the spring group **(A,B)**, summer group **(C,D)**, and autumn group **(E–G)**.

offshore waters of eastern Taiwan. In addition, the waters at a depth of 30–50 m along southern Taiwan were also potential hatchling grounds, and the hatched individuals moved northward as the growth proceeded. Finally, they mainly remained in the northeastern waters during the subadult–adult stages (**Figure 7**).

The summer group was most likely to hatch in the areas near northeastern Taiwan, extending southward to the Penghu Islands (**Figure 8**). However, the predicted distribution at the juvenile stage covered a wide area, owing to constant seawater temperatures in summer. Similarly, a wide and deep living area (approximate depth: 100 m), including the inshore waters of northern Taiwan and the waters near the Ryukyu Islands (approximate depth: 100 m), was observed in the last two stages, and it differed from the pattern of the spring group.

In the autumn group, the predicted hatching sites were similar to those in the summer group (**Figure 9**). However, juvenile individuals might have been distributed in the southern waters (**Figure 9**), but they were not detected in the waters, with the probability >0.5, because the deduced temperature at this stage did not completely match the water temperature in the study area. The autumn group then spent their subadult and adult stage (approximately 3–4 months) in the inshore waters of northern Taiwan at depths between 0 and 100 m before capture.

DISCUSSION

Stable oxygen isotope ratios recorded in statoliths provide information regarding diverse movement patterns of *S. lessoniana*; differences in ontogenetic distributions were observed among the three seasonal groups. Although the approach for investigating the movement of animals by using $\delta^{18}O$ values in biogenic carbonates has been widely applied in studies on fish (Trueman et al., 2012; Currey et al., 2014; Shiao et al., 2017; Darnaude and Hunter, 2018), thus far, studies have not adapted this method to determine the movement history of cephalopods. We demonstrated the potential of using this approach in studies on cephalopod ecology. Because of the significant effects of larval dispersal and demographic population connectivity on cephalopod resources (O'dor, 1992; Boyle and Boletzky, 1996; Semmens et al., 2007), the results of the present study may improve the fishery management and conservation for the bigfin reef squid.

Variation in Statolith $\delta^{18}O$ Values in Relation to Experienced Temperature

The variation in statolith $\delta^{18}O$ values among individuals has been observed in several squid species and is associated with differences in experienced temperature (Radtke, 1983; Landman et al., 2004; Trasviña-Carrillo et al., 2018). The general trend of statolith $\delta^{18}O$ values is to decrease with an increase in temperature; this trend follows the theoretical predictions and observations from other biogenic carbonates (Rexfort and Mutterlose, 2006; Trueman et al., 2012; Kitagawa et al., 2013; Linzmeier et al., 2016). However, assessing the reliability of using statolith $\delta^{18}O$ values to reconstruct experienced temperature in cephalopods is challenging because previous studies have analyzed $\delta^{18}O$ value from an entire statolith, which indicates the mean experienced

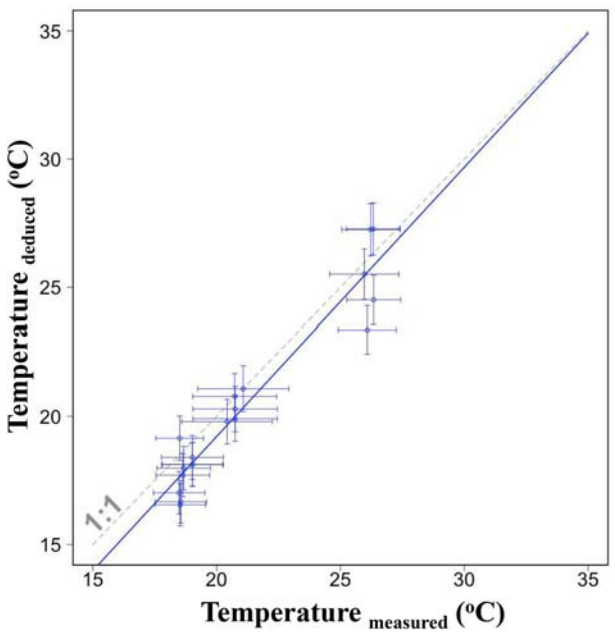

FIGURE 6 | The linear relationship between deduced temperatures from $\delta^{18}O$ values of individual statolith edges and corresponding measured temperatures in the same period. Horizontal error bars indicate one standard deviation of measured temperature; vertical error bars indicate one standard deviation evaluated by using Monte Carlo Simulations and considering uncertainty caused from salinity and parameter variation in the equation. Dashed line indicates the 1:1 correspondence.

temperature throughout its lifespan. Thus, in our study, we evaluated the deduced temperature compared with the seawater temperature and temperature preference of *S. lessoniana* at different life stages.

The deduced temperature of the embryonic stage and an approximate 20-day paralarval stage from the statolith core ranged from 22 to 28°C, regardless of seasonal group. This finding was consistent with those of other studies that found that *S. lessoniana* hatches in a warm environment of approximately 20 to 30°C (Segawa, 1987; Walsh et al., 2002; Ikeda et al., 2009). Each squid species has its optimum living temperature, which supports its growth and survival, particularly in its early life stages (Jackson and Choat, 1992; Forsythe et al., 2001). This suggests that the population of *S. lessoniana* in northern Taiwan shows a preference for this temperature at hatch.

The statolith $\delta^{18}O$ values exhibited variation after the paralarval stage among seasonal groups because of seawater temperature varying with the seasons. For example, the spring group experienced warmer (summer) temperatures at the juvenile and adult stages than at the hatching stage in spring. By contrast, the summer and autumn groups reached their juvenile and adult stages in autumn and winter, respectively hence, they experienced lower temperatures in their juvenile and adult stages than in their hatching stage. The summer and autumn groups exhibited more positive $\delta^{18}O$ values than the spring group at the juvenile and adult stages because of lower temperatures. Thus, the ontogenetic variation in statolith $\delta^{18}O$ values in the spring group was less obvious than in the summer and autumn groups (**Figure 4**). The statolith $\delta^{18}O$ values of *S. lessoniana* ontogenetic variation mirrored the seasonal temperature fluctuation off Taiwan waters, thus indicating the reliability of the prediction method used in the present study.

Prediction of Ontogenetic Movement and Geographical Distribution

The seasonal and vertical migration of squid species has been described in the literatures (Bazzino et al., 2010; Argüelles et al., 2012; Yamaguchi et al., 2019); this behavior was also observed in our study. Interpreting time-series data in squids is generally more difficult than interpreting data obtained from bivalves (e.g., Nakashima et al., 2004; Owen et al., 2008; Nishida et al., 2015) because the squid species move freely, unlike bivalves. We converted the measured statolith $\delta^{18}O$ values to the deduced temperature and cross-matched them with the seasonal and depth changes in the seawater temperatures to estimate the probability of the geographical distribution of *S. lessoniana* by using a procedure derived from a widely used method to study fish migration (involving the use of otolith $\delta^{18}O$ values; Thorrold et al., 1997; Weidel et al., 2007; Shiao et al., 2014). In our case, the movement patterns of *S. lessoniana* in four life stages exhibited diversity among the seasonal groups (**Figures 7–9**). These findings are comparable to the known ecology of *S. lessoniana*, including spawning (Segawa, 1987), migration (Ueta and Jo, 1990; Kanamaru et al., 2007) and depth distribution (Roper et al., 1984; Tomano et al., 2016).

According to statolith $\delta^{18}O$ values, most probably the individuals of the spring and summer groups hatched near the coasts of northeastern Taiwan, with an occurrence probability of 1; these findings support empirical evidence that the waters near the coast of northeastern Taiwan are one of main spawning grounds for *S. lessoniana* (Chen et al., 2015; Ching et al., 2017). The dominant topography in northern Taiwan is that of an eroded coastline with complicated topographical features and structures (Song et al., 1997), forming macroalgae-rich and coral-rich environments for spawning. In addition, the quantity of nutrients supplied by the year-round upwelling of the Kuroshio Current off northeastern Taiwan supports high primary production and sustains sequential consumers in the waters (Liu et al., 1992; Chen, 1997; Gong et al., 2003). Therefore, this biomass could be a crucial factor sustaining the abundance of *S. lessoniana* near Taiwan (e.g., Otero et al., 2008; Rodhouse et al., 2014). However, the individuals of the autumn group had a high probability (>0.8) of hatching in the waters of southern and southwestern Taiwan (i.e., the Penghu Islands). The paralarvae were transported northward by the Kuroshio Current or the South China Warm Current into the Taiwan Strait during September and October (Tang et al., 2000; Jan et al., 2002, 2006). Although the results suggest that waters at a depth of 100 m near the coast of southern Taiwan are also potential hatching grounds, adult females are unlikely to have laid eggs at a depth of down to 100 m because the environment is unsuitable for planktonic paralarvae and

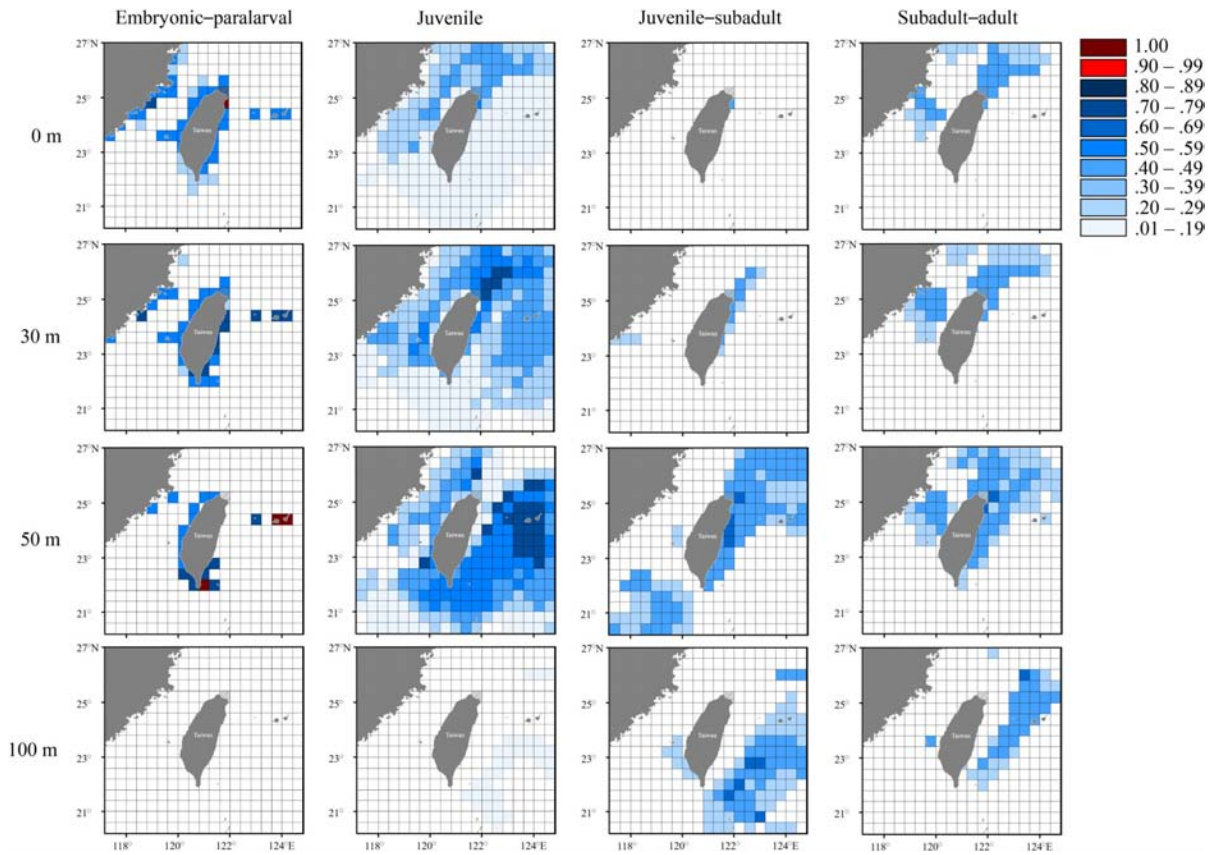

FIGURE 7 | Probability distribution based on experienced temperatures in *S. lessoniana* individuals in the spring group at each life stages. The legend indicates the probability value of occurrence.

no egg capsules have been observed on the seabed at the aforementioned depth.

Distribution of juvenile individuals appeared to be widespread around Taiwan, both horizontally and vertically. This distribution pattern has two possible explanations. First, the juvenile squids were passively shifted by ocean currents, thus reflecting the seawater temperatures of a larger region. Second, the consistent seawater temperatures around Taiwan in summer and autumn reduced the precision of distribution prediction. In particular, the estimated probabilities of juvenile distribution in autumn group were all less than 50%. Compared with the juvenile stage, the subadult–adult stages showed a narrower area of predicted distribution. In the spring group, the subadult individuals remained at a depth of approximately 50 m near the coast of northeastern Taiwan or at a depth of approximately 100 m in the inshore waters of eastern Taiwan. Subsequently, adult individuals migrated to the coasts of northeastern for mating and spawning. To our knowledge, larger individuals are rarely captured in the eastern waters, which suggests that the eastern waters are not a principal habitat for *S. lessoniana* individuals in the spring group. Nevertheless, the occurrence of *S. lessoniana* in the eastern water needs to be understood through additional surveys using systematic fishery records. By contrast, individuals in the juvenile–subadult stage in the summer group were mostly found in the areas between the coastal waters of China to northeastern Taiwan; furthermore, individuals in this stage in the autumn group might remain in the waters in northeastern Taiwan or around the Penghu Islands. Both the summer and autumn groups used the northern waters as their main habitat during the adult stage in winter. In addition, adult individuals in the autumn group appeared to move to further offshore waters (about 100 km). During winter months, drastic reductions in temperature occur in northern Taiwan primarily during strong northeasterly monsoon and cold surge events (Chen and Huang, 1999; Chen et al., 2002). In such a turbulent state, the individuals move offshore for overwintering and return to inshore areas for feeding and spawning when the environment becomes relatively stable. This explanation is consistent with the findings of Ueta and Jo (1990), who studied the migration of *S. lessoniana* subadult–adult individuals around Tokushima Prefecture.

The individuals in the seasonal groups in the present study exhibited a possible migration route from the Penghu Islands to northeastern Taiwan and considerable habitat overlap. In general, loliginid squids spawn throughout the year and consequently exhibit multicohort formation along with highly diverse dispersion patterns; hence, high levels of genetic diversity are achieved in the populations of these cephalopods (O'dor, 1998). A study reported that the elemental signatures in

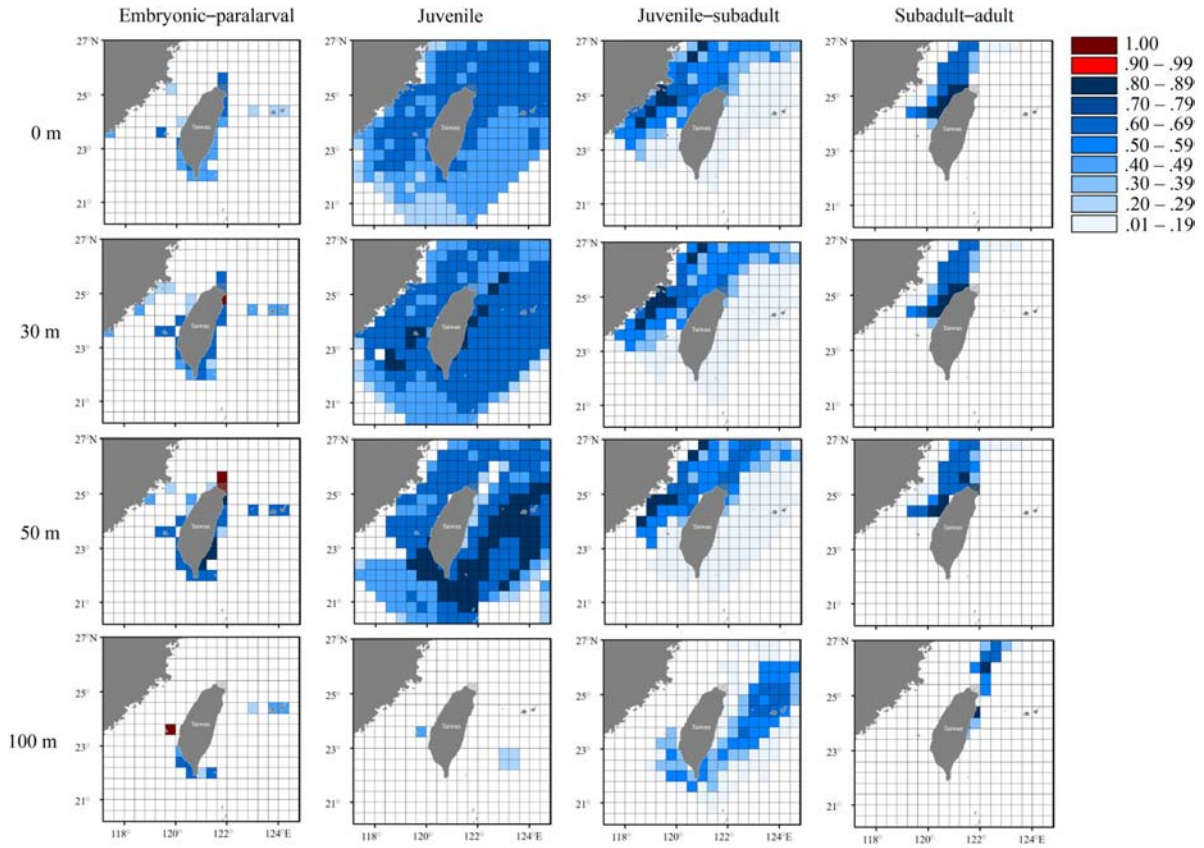

FIGURE 8 | Probability distribution based on experienced temperatures in *S. lessoniana* individuals in the summer group at each life stage. The legend indicates the probability value of occurrence.

the entire statolith exhibited less variation between *S. lessoniana* samples from northern Taiwan and the Penghu Islands for the same season (Ching et al., 2017). This finding suggests a high level of population connectivity in *S. lessoniana* in Taiwan. In recent years, the coexistence of three cryptic lineages of *S. lessoniana* has been reported in the Indo-Pacific Ocean (Cheng et al., 2014; Tomano et al., 2016). These cryptic lineages of *S. lessoniana* exhibit similar morphology but are genetically distinct (Akasaki et al., 2006; Hsiao et al., 2016; Shen et al., 2016). Although the extent of cryptic diversity within the *S. lessoniana* species complex in Taiwan remains unclear, a single cryptic lineage may be predominant in northern Taiwan and the Penghu Islands, based on the migration pattern prediction. Additional studies with larger areas of geographic sampling and using a combination of molecular methods are needed to provide more knowledge regarding the population structure of the bigfin reef squid over its distribution range.

Method Improvement and Applications in Future

As the first study to determine the ontogenetic movement of squid by using statolith $\delta^{18}O$ values, we provided information on the life history of *S. lessoniana*, but we acknowledge that our method can be improved considerably in the future. First, the $\delta^{18}O$ values in the juvenile statoliths of the autumn group suggested high experienced temperatures (approximately 25–29°C), and this does not satisfactorily accord with the observed water temperature range from the sea surface to a depth of 100 m depth in autumn. We emphasize that the mechanisms of isotopic fractionation in statoliths [such as the results of fish otolith by Thorrold et al. (1997) and Høie et al. (2004a)] and other potential sources of variability (e.g., Høie et al., 2004b; Darnaude and Hunter, 2018; Linzmeier, 2019) should be carefully considered. Second, the seawater $\delta^{18}O$ values vary by <1% across the surface in the present study area and by approximately 1% with depth (LeGrande and Schmidt, 2006), slightly biasing the prediction of experienced temperature. We used salinity to predict seawater $\delta^{18}O$ values, based on the equation established from the waters in Taiwan Strait (Chang, 2000). The development of location-specific relationships between salinity and seawater $\delta^{18}O$ values can minimize the bias of reconstructed temperature. Third, reducing the amount of sample powder from statolith can increase the temporal sampling resolution and enhance the precision of reconstructed temperature (Leder et al., 1996; Høie et al., 2004b). As reported by Sakamoto et al. (2019) in their otolith study, the weight of drilling powder can be as low as 0.3–11.4 μg, representing a temporal resolution of 10–30 days,

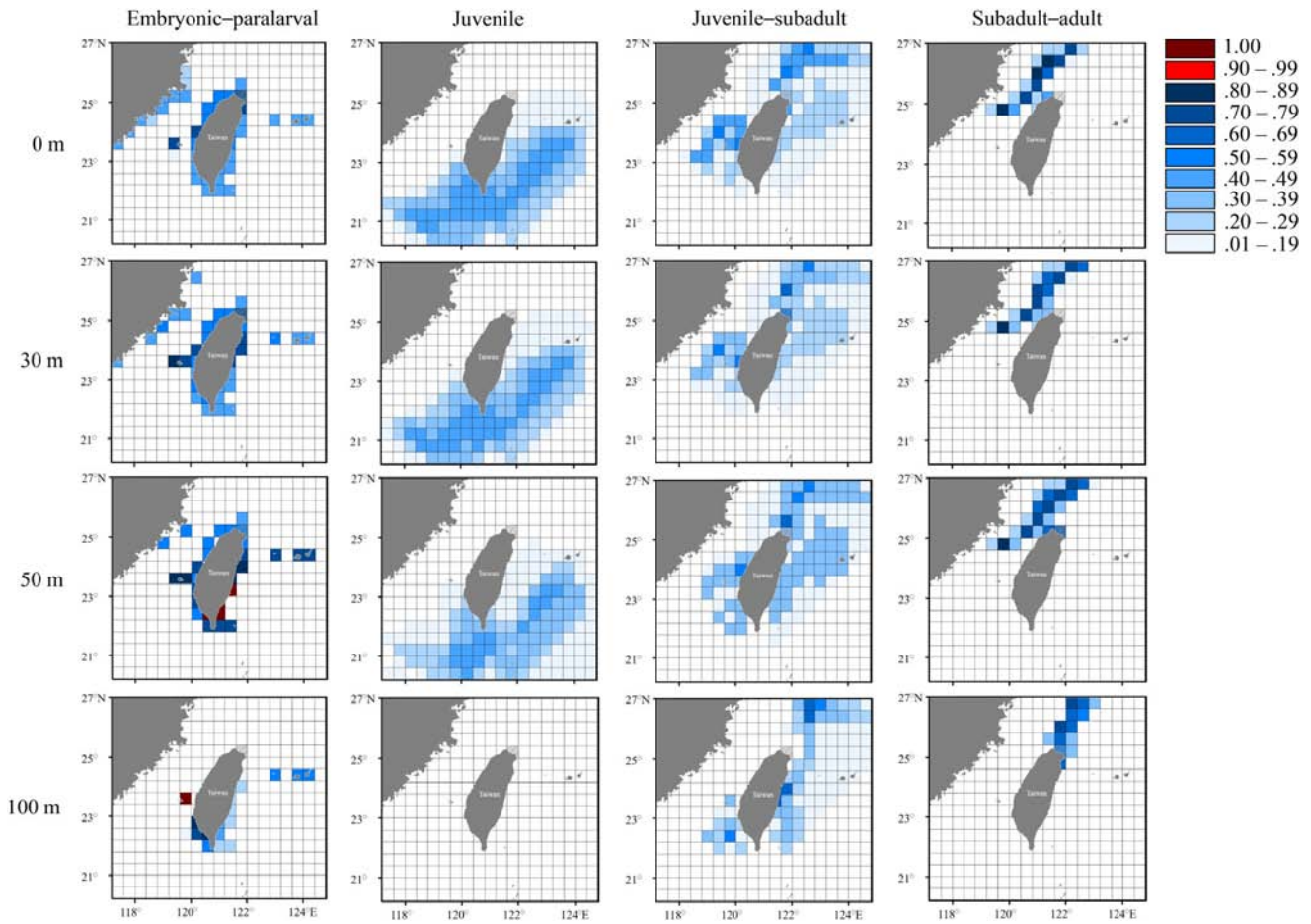

FIGURE 9 | Probability distribution based on experienced temperatures in *S. lessoniana* individuals of the autumn group at each life stage. The legend indicates the probability value of occurrence.

which is considerably higher than that in our study (>40 μg and approximately 30–50 days). A statolith analysis with higher temporal resolution can significantly benefit the studies on stock discrimination and individual migration. Fourth, defining minimum and maximum probabilities that can indicate the existence of *S. lessoniana* populations requires additional statistical support. In addition, the size of the spatial grid can be reduced to match the movement behavior of *S. lessoniana* for a higher precision of habitat determination.

Seawater temperature directly and strongly affects cephalopod ecology and fisheries (Jackson and Moltschaniwskyj, 2002; Forsythe, 2004). Statolith $\delta^{18}O$ is a crucial parameter that provides evidence of general patterns of distributional extent and movement. Statolith, which are involved in orientation and balance, are found in all cephalopod species; hence, they can be widely used for ecological research on cephalopods (Clarke, 1978; Arkhipkin, 2005). For example, the predicted geographical distributions based on statolith $\delta^{18}O$ signatures are comparable to the estimated stock boundaries determined using fishery data or tagging methods. Precise geographic boundary and habitat use (e.g., spawning ground) allow managers to implement suitable management measures to conserve targeted species (Gislason et al., 2000; Hobday et al., 2010). In recent years, in response to varaitions in the behavior of oceans and difficulties in managing resources, scientists have highlighted the importance of technological improvements through use of finer spatial and temporal scales for near real-time animal tracking (Maxwell et al., 2015; Dunn et al., 2016). This study combined the deduced temperatures of the individuals over ontogenetic stages to describe continuous movement patterns of *S. lessoniana* lifespan. The intra- and inter-annual movement patterns also support the decisions pertaining to the establishment of fishing grounds, forecasting of catches, and dynamic fishery management for cephalopods (e.g., Yamaguchi et al., 2019). However, the extent of geographic distribution resolution using statolith $\delta^{18}O$ may be species specific. Our results showed that accurately predicting residence waters during the periods when variations in water temperature of the region are not obvious (from summer to early autumn in Taiwan) is difficult. Thus, statolith $\delta^{18}O$ is unlikely to serve as the main indicator of distribution for tropical cephalopod species. Species with a large diel vertical migration (e.g., Young, 1978; Hunt and Seibel, 2000) also probably biases

the prediction of experienced temperature, thus increasing the risk of misinterpretation when this method is applied to a species. Establishing a temperature-dependent relationship of $\delta^{18}O$ for specific cephalopod species is also necessary for improving the approach in the future.

CONCLUSION

All wild squids possess natural isotopic signatures that are incorporated into their statoliths and reflect the environmental temperature or isotopes composition. Migration between waters may produce shifts in isotopic composition. This study applied sequential isotopic sampling to statoliths, and the findings suggest the ecological features of seasonal movement strategies and population connectivity in *S. lessoniana* in Taiwan. As a result, the waters off northeastern Taiwan have proven to be an important spawning ground for *S. lessoniana*. Implementing fishery management by restrictions or closed fishing zone during spawning seasons will ensure the recruitment of *S. lessoniana* population in Taiwan sustainable. Flexible life history traits and a large distribution range are critical for cephalopods and support a high level of genetic diversity and ensure population abundance. These findings extend the limited knowledge about the life history of *S. lessoniana* within a year. Future developments can reduce the uncertainty associated with this approach and provide more accurate species-specific interpretations of the variations of statolith $\delta^{18}O$ values within individuals and stocks of free-moving cephalopods.

DATA AVAILABILITY STATEMENT

The datasets generated for this study are available on request to the corresponding author.

ETHICS STATEMENT

Ethical review and approval was not required for the animal study because we collected the squid samples from the commercial fishery and did not conduct a control or treatment experiment.

AUTHOR CONTRIBUTIONS

C-HW led this project. C-HW, T-YC, and AY coordinated the experiment. T-YC and AY assisted in wild squid collections. C-IC wrote the manuscript and prepared the samples. C-IC and M-TC were responsible for data analysis. J-CS and P-LW contributed the isotopic analyses. All authors revised, reviewed, and finally approved the manuscript.

FUNDING

This study was funded by a project from the Ministry of Science and Technology, Taiwan (MOST 106-2611-M-019-004) to C-HW.

ACKNOWLEDGMENTS

The authors thank Bor-Neng Jenq and Pi-Hang Hung for their help with squid specimen collection. The authors also thank Ling-Wen Liu, Ching-Chun Cheng, and Ting-Hung Lin from National Taiwan University for assisting with statolith sample analysis and Dr. Yi-Chen Wang and Sheng-Yuan Teng from the National Taiwan Ocean University for their guidance on the temperature and salinity data capture. Comments by the two reviewers significantly improved the manuscript. This manuscript was edited by Wallace Academic Editing.

REFERENCES

Akasaki, T., Nikaido, M., Tsuchiya, K., Segawa, S., Hasegawa, M., and Okada, N. (2006). Extensive mitochondrial gene arrangements in coleoid Cephalopoda and their phylogenetic implications. *Mol. Phylogen. Evol.* 38, 648–658. doi: 10.1016/j.ympev.2005.10.018

Ammar, I., and Maaroof, R. (2019). First record of the squid *Sepioteuthis lessoniana* Férussac, 1831 in the Syrian coastal water. *SSRG Int. J. Agric. Env. Sci.* 6, 52–55. doi: 10.14445/23942568/ijaes-v6i1p108

Argüelles, J., Lorrain, A., Cherel, Y., Graco, M., Tafur, R., Alegre, A., et al. (2012). Tracking habitat and resource use for the jumbo squid *Dosidicus gigas*: a stable isotope analysis in the Northern Humboldt current system. *Mar. Biol.* 159, 2105–2116. doi: 10.1007/s00227-012-1998-2

Arkhipkin, A. I. (2005). Statoliths as black boxes (life recorders) in squid. *Mar. Freshwater Res.* 56, 573–583.

Arkhipkin, A. I., Campana, S. E., FitzGerald, J., and Thorrold, S. R. (2004). Spatial and temporal variation in elemental signatures of statoliths from the Patagonian longfin squid (*Loligo gahi*). *Can. J. Fish. Aquat. Sci.* 61, 1212–1224. doi: 10.1139/f04-075

Arkhipkin, A. I., and Shcherbich, Z. N. (2012). Thirty years' progress in age determination of squid using statoliths. *J. Mar. Biol. Assoc. U.K.* 92, 1389–1398. doi: 10.1017/s0025315411001585

Bazzino, G., Gilly, W. F., Markaida, U., Salinas-Zavala, C. A., and Ramos-Castillejos, J. (2010). Horizontal movements, vertical-habitat utilization and diet of the jumbo squid (*Dosidicus gigas*) in the Pacific Ocean off Baja California Sur. *Mexico Prog. Oceanogr.* 86, 59–71. doi: 10.1016/j.pocean.2010.04.017

Boyle, P., and Boletzky, S. (1996). Cephalopod populations: definition and dynamics. *Phil. Trans. R. Soc. Lond. B* 351, 985–1002. doi: 10.1111/1365-2656.12218

Chang, C. C. (2000). *Spatial and Temporal Variation of ^{18}O in the Sea Water from the Taiwan Strait*. Ph.D. thesis, National Sun Yat-sen University, Taiwan.

Chen, C. S., Chen, J. Y., and Lin, C. W. (2015). Variation in life-history traits for micro-cohorts of *Sepioteuthis lessoniana* in the waters off northern Taiwan. *Fish. Sci.* 81, 53–64. doi: 10.1007/s12562-014-0831-x

Chen, C. S., and Huang, J. M. (1999). A numerical study of precipitation characteristics over Taiwan island during the winter season. *Meteorol. Atmos. Phys.* 70, 167–183. doi: 10.1007/s007030050032

Chen, C. T. (1997). The Kuroshio intermediate water is the major source of nutrients on the East China Sea continental shelf. *Oceanogr. Lit. Rev.* 44, 531.

Chen, T. C., Yen, M. C., Huang, W. R., and Gallus, W. A. Jr. (2002). An east Asian cold surge: case study. *Mon. Weather Rev.* 130, 2271–2290. doi: 10.1175/1520-0493(2002)130<2271:aeacsc>2.0.co;2

Cheng, S., Anderson, F. E., Bergman, A., Mahardika, G., Muchlisin, Z., Dang, B., et al. (2014). Molecular evidence for co-occurring cryptic lineages within the *Sepioteuthis* cf. *lessoniana* species complex in the Indian and Indo-West Pacific Oceans. *Hydrobiologia* 725, 165–188. doi: 10.1007/s10750-013-1778-0

Ching, T. Y., Chen, C. S., and Wang, C. H. (2017). Spatiotemporal variations in life-history traits and statolith trace elements of *Sepioteuthis lessoniana* populations

around northern Taiwan. *J. Mar. Biol. Assoc. U.K* 99, 203–213. doi: 10.1017/s0025315417001801

Clarke, M. R. (1978). The cephalopod statolithan-introduction to its form. *J. Mar. Biol. Assoc. U.K.* 58, 701–712. doi: 10.1017/s0025315400041345

Currey, L. M., Heupel, M. R., Simpfendorfer, C. A., and Williams, A. J. (2014). Inferring movement patterns of a coral reef fish using oxygen and carbon isotopes in otolith carbonate. *J. Exp. Mar. Biol. Ecol.* 456, 18–25. doi: 10.1016/j.jembe.2014.03.004

Darnaude, A. M., and Hunter, E. (2018). Validation of otolith $\delta^{18}O$ values as effective natural tags for shelf-scale geolocation of migrating fish. *Mar. Ecol. Prog. Ser.* 598, 167–185. doi: 10.3354/meps12302

Dunn, D. C., Maxwell, S. M., Boustany, A. M., and Halpin, P. N. (2016). Dynamic ocean management increases the efficiency and efficacy of fisheries management. *Proc. Natl. Acad. Sci. U.S.A.* 113, 668–673. doi: 10.1073/pnas.1513626113

Elsdon, T. S., and Gillanders, B. M. (2002). Interactive effects of temperature and salinity on otolith chemistry: challenges for determining environmental histories of fish. *Can. J. Fish. Aquat. Sci.* 59, 1796–1808. doi: 10.1139/f02-154

Elsdon, T. S., and Gillanders, B. M. (2003). Reconstructing migratory patterns of fish based on environmental influences on otolith chemistry. *Rev. Fish Biol. Fish.* 13, 217–235. doi: 10.1023/b:rfbf.0000033071.73952.40

Forsythe, J. (2004). Accounting for the effect of temperature on squid growth in nature: from hypothesis to practice. *Mar. Freshwater Res.* 55, 331–339.

Forsythe, J., Walsh, L., Turk, P., and Lee, P. (2001). Impact of temperature on juvenile growth and age at first egg-laying of the Pacific reef squid *Sepioteuthis lessoniana* reared in captivity. *Mar. Biol.* 138, 103–112. doi: 10.1007/s002270000450

Gillanders, B. M., Wilkinson, L. M., Munro, A. R., and de Vries, M. C. (2013). Statolith chemistry of two life history stages of cuttlefish: effects of temperature and seawater trace element concentration. *Geochim. Cosmochim. Acta* 101, 12–23. doi: 10.1016/j.gca.2012.10.005

Gilly, W., Markaida, U., Baxter, C., Block, B., Boustany, A., Zeidberg, L., et al. (2006). Vertical and horizontal migrations by the jumbo squid *Dosidicus gigas* revealed by electronic tagging. *Mar. Ecol. Prog. Ser.* 324, 1–17. doi: 10.3354/meps324001

Gislason, H., Sinclair, M., Sainsbury, K., and O'boyle, R. (2000). Symposium overview: incorporating ecosystem objectives within fisheries management. *ICES J. Mar. Sci.* 57, 468–475. doi: 10.1006/jmsc.2000.0741

Gong, G. C., Wen, Y. H., Wang, B. W., and Liu, G. J. (2003). Seasonal variation of chlorophyll a concentration, primary production and environmental conditions in the subtropical East China Sea. *Deep Sea Res. II Top. Stud. Oceanogr.* 50, 1219–1236. doi: 10.1016/s0967-0645(03)00019-5

Hobday, A. J., Hartog, J. R., Timmiss, T., and Fielding, J. (2010). Dynamic spatial zoning to manage southern bluefin tuna (*Thunnus maccoyii*) capture in a multi−species longline fishery. *Fish. Oceanogr.* 19, 243–253. doi: 10.1111/j.1365-2419.2010.00540.x

Høie, H., Andersson, C., Folkvord, A., and Karlsen, Ø (2004b). Precision and accuracy of stable isotope signals in otoliths of pen-reared cod (*Gadus morhua*) when sampled with a high-resolution micromill. *Mar. Biol.* 144, 1039–1049. doi: 10.1007/s00227-003-1275-5

Høie, H., Otterlei, E., and Folkvord, A. (2004a). Temperature-dependent fractionation of stable oxygen isotopes in otoliths of juvenile cod (*Gadus morhua* L.). *ICES J. Mar. Sci.* 61, 243–251. doi: 10.1016/j.icesjms.2003.11.006

Hsiao, C. D., Shen, K. N., Ching, T. Y., Wang, Y. H., Ye, J. J., Tsai, S. Y., et al. (2016). The complete mitochondrial genome of the cryptic "lineage A" big-fin reef squid, *Sepioteuthis lessoniana* (Cephalopoda: Loliginidae) in Indo-West Pacific. *Mitochondrial DNA A* 27, 2433–2434.

Hunt, J., and Seibel, B. (2000). Life history of *Gonatus onyx* (Cephalopoda: Teuthoidea): ontogenetic changes in habitat, behavior and physiology. *Mar. Biol.* 136, 543–552. doi: 10.1007/s002270050714

Ikeda, Y., Arai, N., Kidokoro, H., and Sakamoto, W. (2003). Strontium: calcium ratios in statoliths of Japanese common squid *Todarodes pacificus* (Cephalopoda: Ommastrephidae) as indicators of migratory behavior. *Mar. Ecol. Prog. Ser.* 251, 169–179. doi: 10.3354/meps251169

Ikeda, Y., Ueta, Y., Anderson, F., and Matsumoto, G. (2009). Reproduction and life span of the oval squid *Sepioteuthis lessoniana* (Cephalopoda: Loliginidae): comparison between laboratory-cultured and wild-caught squid. *Mar. Biodivers. Rec.* 2:E50. doi: 10.1017/S175526720900061X

Jackson, G., and Moltschaniwskyj, N. (2002). Spatial and temporal variation in growth rates and maturity in the Indo-Pacific squid *Sepioteuthis lessoniana* (Cephalopoda: Loliginidae). *Mar. Biol.* 140, 747–754. doi: 10.1007/s00227-001-0746-9

Jackson, G. D. (1990). Age and growth of the tropical nearshore loliginid squid *Sepioteuthis lessoniana* determined from statolith growth-ring analysis. *Fish. Bull.* 88, 113–118.

Jackson, G. D., and Choat, J. H. (1992). Growth in tropical cephalopods: an analysis based on statolith microstructure. *Can. J. Fish. Aquat. Sci.* 49, 218–228. doi: 10.1139/f92-026

Jackson, G. D., O'Dor, R. K., and Andrade, Y. (2005). First tests of hybrid acoustic/archival tags on squid and cuttlefish. *Mar. Freshwater Res.* 56, 425–430.

Jan, S., Sheu, D. D., and Kuo, H. M. (2006). Water mass and through flow transport variability in the Taiwan Strait. *J. Geophys. Res. Oceans* 111:C12. doi: 10.1029/2006JC003656

Jan, S., Wang, J., Chern, C. S., and Chao, S. Y. (2002). Seasonal variation of the circulation in the Taiwan Strait. *J. Mar. Syst.* 35, 249–268. doi: 10.1007/s11356-018-3093-9

Jereb, P., and Roper, C. F. (2005). "*Sepioteuthis lessoniana* Férussac in Lesson, 1831," in *Cephalopods of the World: An Annotated and Illustrated Catalogue of Cephalopod Species Known to Date, Volume 2, Myopisd and Oegopsid Squids*, eds P. Jereb, and C. F. E. Roper (Rome: FAO), 95–97.

Kanamaru, H., Umeda, T., and Morikawa, A. (2007). Migration of the oval squid, *Sepioteuthis lessoniana* in northern and western waters of the Kyushu. *Bull. Saga Genkai Fish. Res. Dev. Cent.* 4, 51–57.

Kitagawa, T., Ishimura, T., Uozato, R., Shirai, K., Amano, Y., Shinoda, A., et al. (2013). Otolith $\delta^{18}O$ of Pacific bluefin tuna *Thunnus orientalis* as an indicator of ambient water temperature. *Mar. Ecol. Prog. Ser.* 481, 199–209. doi: 10.3354/meps10202

Landman, N., Cochran, J., Cerrato, R., Mak, J., Roper, C., and Lu, C. (2004). Habitat and age of the giant squid (*Architeuthis sanctipauli*) inferred from isotopic analyses. *Mar. Biol.* 144, 685–691. doi: 10.1007/s00227-003-1245-y

Leder, J., Swart, P. K., Szmant, A., and Dodge, R. (1996). The origin of variations in the isotopic record of scleractinian corals: I. *Oxygen Geochim. Cosmochim. Acta* 60, 2857–2870. doi: 10.1016/0016-7037(96)00118-4

LeGrande, A. N., and Schmidt, G. A. (2006). Global gridded data set of the oxygen isotopic composition in seawater. *Geophys. Res. Lett.* 33, L12604. doi: 10.1029/2006GL026011

Linzmeier, B. J. (2019). Refining the interpretation of oxygen isotope variability in free-swimming organisms. *Swiss J. Palaeontol.* 138, 109–121. doi: 10.1007/s13358-019-00187-3

Linzmeier, B. J., Kozdon, R., Peters, S. E., and Valley, J. W. (2016). Oxygen isotope variability within Nautilus shell growth bands. *PLoS One* 11:e0153890. doi: 10.1371/journal.pone.0153890

Liu, B. L., Cao, J., Truesdell, S. B., Chen, Y., Chen, X. J., and Tian, S. Q. (2016). Reconstructing cephalopod migration with statolith elemental signatures: a case study using *Dosidicus gigas*. *Fish. Sci.* 82, 425–433. doi: 10.1007/s12562-016-0978-8

Liu, K. K., Gong, G. C., Lin, S., Yang, C. Y., Wei, C. L., Pai, S. C., et al. (1992). The year-round upwelling at the shelf break near the northern tip of Taiwan as evidenced by chemical hydrography. *Terr. Atmos. Ocean Sci.* 3, 243–275.

Maxwell, S. M., Hazen, E. L., Lewison, R. L., Dunn, D. C., Bailey, H., Bograd, S. J., et al. (2015). Dynamic ocean management: defining and conceptualizing real-time management of the ocean. *Mar. Policy* 58, 42–50. doi: 10.1016/j.marpol.2015.03.014

Moreno, A., Dos Santos, A., Piatkowski, U., Santos, A. M. P., and Cabral, H. (2008). Distribution of cephalopod paralarvae in relation to the regional oceanography of the western Iberia. *J. Plankton Res.* 31, 73–91. doi: 10.1093/plankt/fbn103

Nakashima, R., Suzuki, A., and Watanabe, T. (2004). Life history of the Pliocene scallop Fortipecten, based on oxygen and carbon isotope profiles. *Palaeogeogr. Palaeoclimatol. Palaeoecol.* 211, 299–307. doi: 10.1016/j.palaeo.2004.05.011

Nishida, K., Suzuki, A., Isono, R., Hayashi, M., Watanabe, Y., Yamamoto, Y., et al. (2015). Thermal dependency of shell growth, microstructure, and stable isotopes in laboratory-reared *Scapharca broughtonii* (Mollusca: Bivalvia). *Geochem. Geophy. Geosy* 16, 2395–2408. doi: 10.1002/2014gc005634

O'dor, R. (1992). Big squid in big currents. *S. Afr. J. Mar. Sci.* 12, 225–235. doi: 10.2989/02577619209504705

O'dor, R. (1998). Can understanding squid life-history strategies and recruitment improve management? *S. Afr. J. Mar. Sci.* 20, 193–206. doi: 10.2989/025776198784126188

Okutani, T. (2015). "*Sepioteuthis Lessoniana* Férussac in Lesson, 1832," in Cuttlefishes and Squids of the World. Tokyo, Japan: Tokai University Press, 97.

Otero, J., Álvarez-Salgado, X. A., González, ÁF., Miranda, A., Groom, S. B., Cabanas, J. M., et al. (2008). Bottom-up control of common octopus *Octopus vulgaris* in the Galician upwelling system, northeast Atlantic Ocean. *Mar. Ecol. Prog. Ser.* 362, 181–192. doi: 10.3354/meps07437

Owen, E. F., Wanamaker, A. D., Feindel, S. C., Schöne, B. R., and Rawson, P. D. (2008). Stable carbon and oxygen isotope fractionation in bivalve (*Placopecten magellanicus*) larval aragonite. *Geochim. Cosmochim. Acta* 72, 4687–4698. doi: 10.1016/j.gca.2008.06.029

R Core Team, (2018). *R: A Language and Environment for Statistical Computing*. Available online at: http://www.r-project.org/ (accessed January 1, 2018)

Radtke, R. (1983). Chemical and structural characteristics of statoliths from the short-finned squid *Illex illecebrosus*. *Mar. Biol.* 76, 47–54. doi: 10.1007/bf00393054

Rexfort, A., and Mutterlose, J. (2006). Stable isotope records from *Sepia officinalis*—a key to understanding the ecology of belemnites? *Earth Planet Sci. Lett.* 247, 212–221. doi: 10.1016/j.epsl.2006.04.025

Rodhouse, P. G., Pierce, G. J., Nichols, O. C., Sauer, W. H., Arkhipkin, A. I., Laptikhovsky, V. V., et al. (2014). "Environmental effects on cephalopod population dynamics: implications for management of fisheries," in *the Advances in Marine Biology*, ed. E. A. G. Vidal (London, UK: Elsevier), 99–233. doi: 10.1016/b978-0-12-800287-2.00002-0

Roper, C. F. E., Sweeney, M. J., and Nauen, C. E. (1984). Cephalopods of the world: an annotated and illustrated catalogue of species of interest to fisheries. *FAO Fish. Synop.* 125, 1–277.

Sakamoto, T., Komatsu, K., Shirai, K., Higuchi, T., Ishimura, T., Setou, T., et al. (2019). Combining microvolume isotope analysis and numerical simulation to reproduce fish migration history. *Methods Ecol. Evol.* 10, 59–69. doi: 10.1111/2041-210x.13098

Segawa, S. (1987). Life history of the oval squid, *Sepioteuthis lessoniana*, in Kominato and adjacent waters central Honshu, Japan. *J. Tokyo Univ. Fish* 74, 67–105.

Semmens, J. M., Pecl, G. T., Gillanders, B. M., Waluda, C. M., Shea, E. K., Jouffre, D., et al. (2007). Approaches to resolving cephalopod movement and migration patterns. *Rev. Fish Biol. Fish.* 17, 401–423. doi: 10.1007/s11160-007-9048-8

Shen, K. N., Yen, T. C., Chen, C. H., Ye, J. J., and Hsiao, C. D. (2016). The complete mitochondrial genome of the cryptic "lineage B" big-fin reef squid, *Sepioteuthis lessoniana* (Cephalopoda: Loliginidae) in Indo-West Pacific. *Mitochondrial DNA A* 27, 2100–2101.

Shiao, J. C., Itoh, S., Yurimoto, H., Iizuka, Y., and Liao, Y. C. (2014). Oxygen isotopic distribution along the otolith growth axis by secondary ion mass spectrometry: applications for studying ontogenetic change in the depth inhabited by deep-sea fishes. *Deep Sea Res. I Oceanogr. Res. Pap.* 84, 50–58. doi: 10.1016/j.dsr.2013.10.006

Shiao, J. C., Sui, T. D., Chang, N. N., and Chang, C. W. (2017). Remarkable vertical shift in residence depth links pelagic larval and demersal adult jellynose fish. *Deep Sea Res. I Oceanogr. Res. Pap.* 121, 160–168. doi: 10.1016/j.dsr.2017.01.011

Shirai, K., Otake, T., Amano, Y., Kuroki, M., Ushikubo, T., Kita, N. T., et al. (2018). Temperature and depth distribution of Japanese eel eggs estimated using otolith oxygen stable isotopes. *Geochim. Cosmochim. Acta* 236, 373–383. doi: 10.1016/j.gca.2018.03.006

Song, G. S., Chang, Y. C., and Ma, C. P. (1997). Characteristics of submarine topography off northern Taiwan. *Terr. Atmos. Ocean Sci.* 8, 461–480.

Steer, M. A., Halverson, G. P., Fowler, A. J., and Gillanders, B. M. (2010). Stock discrimination of Southern Garfish (*Hyporhamphus melanochir*) by stable isotope ratio analysis of otolith aragonite. *Environ. Biol. Fishes* 89, 369–381. doi: 10.1007/s10641-010-9670-5

Tang, T., Tai, J., and Yang, Y. (2000). The flow pattern north of Taiwan and the migration of the Kuroshio. *Cont. Shelf Res.* 20, 349–371. doi: 10.1016/s0278-4343(99)00076-x

Thorrold, S. R., Campana, S. E., Jones, C. M., and Swart, P. K. (1997). Factors determining $\delta^{13}C$ and $\delta^{18}O$ fractionation in aragonitic otoliths of marine fish. *Geochim. Cosmochim. Acta* 61, 2909–2919. doi: 10.1016/s0016-7037(97)00141-5

Tomano, S., Sanchez, G., Kawai, K., Kasaoka, N., Ueta, Y., and Umino, T. (2016). Contribution of *Sepioteuthis* sp. 1 and Sepioteuthis sp. 2 to oval squid fishery stocks in western Japan. *Fish. Sci.* 82, 585–596. doi: 10.1007/s12562-016-0988-6

Trasviña-Carrillo, L. D., Hernández-Herrera, A., Torres-Rojas, Y. E., Galván-Magaña, F., Sánchez-González, A., and Aguíñiga-García, S. (2018). Spatial and trophic preferences of jumbo squid *Dosidicus giga*s (D'Orbigny, 1835) in the central Gulf of California: ecological inferences using stable isotopes. *Rapid Commun. Mass Spectrom.* 32, 1225–1236. doi: 10.1002/rcm.8147

Trueman, C. N., MacKenzie, K., and Palmer, M. (2012). Identifying migrations in marine fishes through stable−isotope analysis. *J. Fish Biol.* 81, 826–847. doi: 10.1111/j.1095-8649.2012.03361.x

Ueta, Y., and Jo, Y. (1990). Migration of the oval squid, *Sepioteuthis lessoniana* around Tokushima prefecture. *Suisanzoshoku* 38, 221–226.

Walsh, L., Turk, P., Forsythe, J., and Lee, P. (2002). Mariculture of the loliginid squid *Sepioteuthis lessoniana* through seven successive generations. *Aquaculture* 212, 245–262. doi: 10.1016/s0044-8486(02)00126-6

Weidel, B. C., Ushikubo, T., Carpenter, S. R., Kita, N. T., Cole, J. J., Kitchell, J. F., et al. (2007). Diary of a bluegill (*Lepomis macrochirus*): daily $\delta^{13}C$ and $\delta^{18}O$ records in otoliths by ion microprobe. *Can. J. Fish. Aquat. Sci.* 64, 1641–1645. doi: 10.1139/f07-157

Yamaguchi, T., Aketagawa, T., Takayama, K., Hirose, N., and Matsuyama, M. (2019). Migratory routes of different sized swordtip squid (*Uroteuthis edulis*) caught in the Tsushima Strait. *Fish. Res.* 209, 24–31. doi: 10.1016/j.fishres.2018.08.008

Yamaguchi, T., Kawakami, Y., and Matsuyama, M. (2015). Migratory routes of the swordtip squid *Uroteuthis edulis* inferred from statolith analysis. *Aquat. Biol.* 24, 53–60. doi: 10.3354/ab00635

Yamaguchi, T., Kawakami, Y., and Matsuyama, M. (2018). Analysis of the hatching site and migratory behaviour of the swordtip squid (*Uroteuthis edulis*) caught in the Japan Sea and Tsushima Strait in autumn estimated by statolith analysis. *Mar. Biol. Res.* 14, 105–112. doi: 10.1080/17451000.2017.1351616

Young, R. E. (1978). Vertical distribution and photosensitive vesicles of pelagic cephalopods from Hawaiian waters. *Fish. Bull.* 76, 583–615.

Young, R. E., and Harman, R. F. (1988). " Larva"," paralarva" and" subadult" in cephalopod terminology. *Malacologia* 29, 201–208.

Zeidberg, L., and Hamner, W. (2002). Distribution of squid paralarvae, *Loligo opalescens* (Cephalopoda: Myopsida), in the Southern California Bight in the three years following the 1997–1998 El Niño. *Mar. Biol.* 141, 111–122. doi: 10.1007/s00227-002-0813-x

Conflict of Interest: The authors declare that the research was conducted in the absence of any commercial or financial relationships that could be construed as a potential conflict of interest.

Copyright © 2020 Chiang, Chung, Shiao, Wang, Chan, Yamaguchi and Wang. This is an open-access article distributed under the terms of the Creative Commons Attribution License (CC BY). The use, distribution or reproduction in other forums is permitted, provided the original author(s) and the copyright owner(s) are credited and that the original publication in this journal is cited, in accordance with accepted academic practice. No use, distribution or reproduction is permitted which does not comply with these terms.

frontiers in Marine Science

ORIGINAL RESEARCH
published: 08 May 2020
doi: 10.3389/fmars.2020.00315

Northern Benguela *Merluccius paradoxus* Annual Growth From Otolith Chronologies Used for Age Verification and as Indicators of Fisheries-Induced and Environmental Changes

Margit R. Wilhelm[1,2]*, Bryan A. Black[2,3], Tarron Lamont[4,5], Sarah C. Paulus[6], Chris Bartholomae[6] and Deon C. Louw[6]

[1] Department of Fisheries and Aquatic Sciences, University of Namibia, Henties Bay, Namibia, [2] Marine Science Institute, The University of Texas at Austin, Port Aransas, TX, United States, [3] Laboratory of Tree-Ring Research, University of Arizona, Tucson, AZ, United States, [4] Oceans and Coasts Research Branch, Department of Environmental Affairs, Cape Town, South Africa, [5] Department of Oceanography, Marine Research Institute, University of Cape Town, Cape Town, South Africa, [6] National Marine Information and Research Centre, Ministry of Fisheries and Marine Resources, Swakopmund, Namibia

OPEN ACCESS

Edited by:
Esteban Avigliano,
Consejo Nacional de Investigaciones Científicas y Técnicas (CONICET), Argentina

Reviewed by:
Barbara Maichak de Carvalho,
Federal University of Paraná, Brazil
Guido Plaza,
Pontificia Universidad Católica de Valparaíso, Chile

***Correspondence:**
Margit R. Wilhelm
mwilhelm@unam.na

Specialty section:
This article was submitted to Marine Ecosystem Ecology, a section of the journal Frontiers in Marine Science

Received: 31 January 2020
Accepted: 17 April 2020
Published: 08 May 2020

Citation:
Wilhelm MR, Black BA, Lamont T, Paulus SC, Bartholomae C and Louw DC (2020) Northern Benguela Merluccius paradoxus Annual Growth From Otolith Chronologies Used for Age Verification and as Indicators of Fisheries-Induced and Environmental Changes. Front. Mar. Sci. 7:315. doi: 10.3389/fmars.2020.00315

In this study we develop a 32-year (1982–2013) otolith biochronology of the commercially important deepwater hake *Merluccius paradoxus* in the northern Benguela, Namibia. Mean annual growth (mm) calculated from 140 thin-sectioned *M. paradoxus* otoliths were compared with change in mean length at age 3 to age 4 determined from Namibian whole-otolith-read age-length keys (ALKs). Annual growth rates calculated from the two methods (overlapping 2000–2013) were strongly positively correlated ($\rho = 0.730$, $n = 14$, $p < 0.01$). This indirectly validated annual age determination of *M. paradoxus*, the accuracy of otolith chronologies, and the ability of ALKs to capture annual variability in fish growth. Annual *M. paradoxus* growth rates were significantly positively correlated with the July–September upwelling index 1982–2013 at 30°S, ($\rho = 0.414$, $n = 32$, $p < 0.05$) and positively correlated with August mean chlorophyll-a concentrations (as indicator for primary production) 2002–2013 in the 28–30°S area ($\rho = 0.734$, $n = 12$, $p < 0.01$). Annual *M. paradoxus* growth rates significantly negatively correlated with October (austral spring) sea surface temperatures in the 24–28°S area ($\rho = -0.381$, $n = 32$, $p < 0.05$). This Orange-River Namaqua upwelling cell corresponds to the area where juvenile and young adult *M. paradoxus* live, suggesting growth rate strongly responds to local forcing. We also determined that mean length-at-age 3 calculated from ALKs (current and literature) significantly increased from 1977 through 2016 at 0.075 cm.year^{-1} ($t = 3.04$, df = 41, $p = 0.004$), while length-at-age 8 significantly decreased at 0.25 cm.year^{-1} ($t = -3.59$, df = 30, $p = 0.001$). Both trends may indicate fisheries-induced adaptive changes. *M. paradoxus* occurring at >300 m bottom depth, are thus strongly influenced by fisheries. As an upper-level demersal predator, this species integrates signals throughout

the food web to provide a unique "view from the top" of long-term changes in the northern Benguela upwelling system. These results provide background ranges of growth variability and context for what will likely be negative impacts of predicted decreases in future upwelling.

Keywords: climate change, deepwater hake, fishery-induced adaptive change, inter-annual variability, sclerochronology, upwelling

INTRODUCTION

As one of the four major Eastern Boundary Upwelling Systems of the world, the Benguela Upwelling System, located along the west coast of southern Africa, supports a productive environment typified by a complex ecosystem structure that supports numerous species of substantial commercial value (Hutchings et al., 2009; Verheye et al., 2016). The deepwater hake, *Merluccius paradoxus*, form an important component of these commercially valued species, with the total stocks in the Benguela system representing more than 33% of the global hake biomass (Kathena et al., 2016). The Benguela system is commonly described as two sub-systems separated by the Lüderitz upwelling cell (Duncombe Rae, 2005), with the northern Benguela characterized by perennial upwelling, and the southern Benguela characterized by strongly seasonal upwelling (Hardman-Mountford et al., 2003; Lamont et al., 2018a). Recent studies have revealed that upwelling ecosystems globally are undergoing long-term change, marked by a poleward shift in upwelling, linked with poleward shifts in the atmospheric high pressure systems that drive upwelling-favorable winds (Rykaczewski et al., 2015; Wang et al., 2015). Similar changes have been observed in the Benguela system, with substantially less upwelling-favorable wind in the northern Benguela in recent years (Lamont et al., 2018a), accompanied by positive trends in Sea Surface Temperatures (SSTs) (Jarre et al., 2015). In contrast, coastal cooling of about 0.5°C per decade has been identified in the southern Benguela, though this cooling has been less pronounced farther south on the Agulhas Bank (Rouault et al., 2010). These cooling trends appear to be linked to an increase in upwelling-favorable south-easterly and easterly winds (Rouault et al., 2010; Lamont et al., 2018a).

Water temperature is one of the main factors influencing the biology, distribution and life history of fishes, along with other aquatic organisms, especially in high latitude freshwater systems (e.g., Magnuson et al., 1997; Casselman et al., 2002; Vieira et al., 2020). In temperate areas, too, fish growth increased due to a disproportionate lengthening of the growing season with climate change (e.g., Morrongiello et al., 2011). In the northern part of the northern Benguela (Angola-Benguela Front), a temperate marine system, increasing inshore temperatures in an ocean-warming hot-spot resulted in species mixing and even hybridization of two Sciaenid *Argyrosomus* species (Potts et al., 2014). Changing water temperatures thus have consequences for processes such as growth rates, timing of seasonal events (phenology), species distributions, species interactions, and overall levels of productivity (e.g., Carey and Zimmerman, 2014; Morrongiello et al., 2014; Tanner et al., 2019).

Apart from changes in the life history strategies and productivity of fish populations due to climate, changes in life history strategies can also occur as a result of selective fishing. For example, Morrongiello et al. (2019) determined, using a biochronology approach on a recently exploited temperate marine reef fish in Tasmania, that fishing not only increased adult growth rates, but it also changed thermal reaction norms to increased sensitivity of these fish to temperature, over the relatively short time period of 10 years. Fisheries-induced changes in growth rates due to density-dependent processes or selection for investment into pre-mature growth and reproduction of fish, were discussed by Lorenzen and Enberg (2002), and Enberg et al. (2012), respectively.

In the northern Benguela, the hakes, consisting of the shallow-water hake *Merluccius capensis* and deepwater hake *M. paradoxus* make up Namibia's most valuable fishery, and are a research priority at the Ministry of Fisheries and Marine Resources (MFMR). Exploitation of hakes (demersal trawl-fishing) in Namibia started in 1964 with catches peaking at 800,000 tons in 1972, with open access fishing by many foreign fleets. This resulted in an initial drastic decline in the stock biomass (Kirchner et al., 2012). From 1976 to 1989 the fishery was controlled by the International Commission for Southeast Atlantic Fisheries (ICSEAF), implementing a legal mesh size limit and member country quotas or total allowable catch (TAC) limits. Despite this, the stock biomass continued to decline to only 170,000 t by 1980. In 1990 Namibia became independent and the Ministry of Fisheries and Marine Resources (MFMR) took over management of the fishery on a heavily depleted resource. More stringent management measures were immediately implemented including closure of fishing to all foreign vessels, enforcement of a 200-mile exclusive economic zone and immediately reducing the TAC to 60,000 tons in 1990-1991. From 1992 to current, between 88,000 and 190,000 t (mean of 148,000 t) of hake have been caught annually (Wilhelm et al., 2015a). The Namibian hake resource is currently assessed (two stocks combined) using a Statistical Catch-at-Age Analysis (SCAA, since 1998) at between 14 and 26% of the pristine spawning stock biomass (SSB) and at 95–120% at best case scenario of SSB values of 1990 (Kirchner et al., 2012; Kathena et al., 2016). Climate-induced as well as fisheries-induced changes in growth, are expected to be evident in these stocks over the last few decades.

Merluccius paradoxus are believed to spawn on the western Agulhas Bank between 32 and 34°S in the southern Benguela (Strømme et al., 2016). The smallest juveniles caught in bottom trawls (<5 cm total length), are usually found between 31 and 32°S off the West coast of South Africa. As these fish grow, they move northwards and southwards, and fish between 15 and 65 cm

total length are most frequently caught off Namibia (Strømme et al., 2016). *M. paradoxus* grow to about 100 cm in length and to about 12 years of age. Length at 50% maturity (L50) is 41–54 cm and age at 50% maturity (A50) 4–6 years (Durholtz et al., 2015; Wilhelm et al., 2019).

Growth rates and age information of fishes are imperative to understanding population dynamics and life history strategies, and ultimately to improve methods for sustainable exploitation. Such information can be obtained through analyzing annual growth increments in fish otoliths. There are two ways to use annual otolith increments to describe fish growth rates. Counting annual increments to determine the age of individual fish is a relatively simple method to calculate population-level growth rates using, e.g., von Bertalanffy growth parameters. This is mostly applied to incorporate individual or cohort-level growth rate effects (e.g., Pilling et al., 2002), but also to explore environmental and temporal trends using time-series data (e.g., Baudron et al., 2014). This approach is usually used at a population-level and time-invariant analysis, and misses the complexity of the drivers of growth at individual level (Morrongiello and Thresher, 2015).

The second approach is using annual otolith growth as a proxy of fish growth and relies on the fact that fish somatic growth (fish length) and otolith growth (otolith length) are strongly related. The width of each annual increment can be measured to estimate the annual growth of an individual fish over their life span. An annual growth increment on a fish otolith usually consists of one zone pair, one translucent and one opaque zone. The translucent zone is thought to form during a period of slow somatic growth and the opaque zone is thought to form during a period of fast somatic growth, which often coincides with the productive period. The width of the annual increment thus generally reflects the annual fast growth period of the fish. Consequently, otolith chronologies have been used to describe annual growth rate variability of fish and explore its environmental drivers. For example, Boehlert et al. (1989) and Dorn (1992) showed that increment width chronologies of Pacific whiting, splitnose rockfish and canary rockfish caught off the coast of California were significantly correlated to sea surface temperature and upwelling, amongst other environmental variables. In this study we used both approaches to describe changes in *M. paradoxus* growth over time.

Black et al. (2005) described how the dendrochronology (tree ring analysis) technique of crossdating could be applied to sclerochronology (analysis of growth increments in hard structures) using a long-lived rockfish species caught off the Californian coast. The technique assumes that climate limits growth variation over time, causing synchronous growth increment widths of individuals from the same species and climate regime. Crossdating is then the process of matching these synchronous growth patterns among individuals beginning at the known year of capture and working back through time. Resulting biochronologies are therefore annually resolved and can be readily integrated with climate data. In the California Current Ecosystem of the northeast Pacific, Black et al. (2011) demonstrated that Pacific rockfish otolith chronologies strongly reflect inter-annual variability in winter upwelling. Moreover, these rockfish chronologies strongly correlated with other biological indicators including time series of seabird reproductive success, corroborating their ability to capture climate variables associated with bottom-up forcing (Black et al., 2014). Whenever possible, all growth increment data should be crossdated prior to developing biochronologies.

Morrongiello et al. (2014) and Morrongiello and Thresher (2015) use mixed effect modeling (MEM) (Weisberg et al., 2010) to analyze growth-increment widths. MEM efficiently represents the hierarchy of otolith biochronology data (Morrongiello et al., 2014) and captures both extrinsic (time, temperature, fishery activity, and spatial structure) and intrinsic (individual, age, sex, and cohort) effects. The MEM method makes use of all available information to partition the relative impact of intrinsic and extrinsic effects on growth variability (Morrongiello and Thresher, 2015). Morrongiello and Thresher (2015) demonstrate that temporal growth rate variability in Australian tiger flathead *Platycephalus richardsoni* was driven by two main factors, namely annual fluctuations in environmental conditions (extrinsic) and an intrinsic cohort-specific factor that reflects density dependence and/or juvenile experience. The biochronology approach thus demonstrates important applications in broad-scale ecological connectivity and hind-casting (Black et al., 2011, 2014) as well as disentangling fisheries, environmental, and genetic effects (Morrongiello et al., 2014; Morrongiello and Thresher, 2015) and in this way enables forecasting expected responses, which is necessary for Ecosystem Approach to Fisheries (EAF) management strategies. Otolith archives and their associated data also exist for the main commercial fish species in Namibia since 1991.

This study thus aims to make use of these archived otolith resources of the heavily exploited deepwater hake, *M. paradoxus*, in Namibia. Of the two hake species in the Benguela *M. capensis* has relatively fast growth rates and considerable dating uncertainties that result in age over-estimates when enumerating otolith translucent zones (Wilhelm et al., 2013, 2015b, 2017, 2018, 2019). We therefore used *M. paradoxus*, given that otolith growth and zonation is less variable, likely due to the stability of their deeper habitat relative to *M. capensis* (Wilhelm et al., 2019). Accordingly, ages from their otoliths are generally more readily identifiable due to fewer "false zones" or "checks" on their otoliths (BCC, 2015).

The aim of this study was, first, to develop an otolith biochronology of the commercially important deepwater hake, *M. paradoxus* caught in the northern Benguela off Namibia using otoliths collected from 1991 to 2014. We aimed to subsequently correlate the predicted growth estimated from the biochronology with years 3–4 growth rate changes of the fish from age-length keys, and fish condition indices to validate *M. paradoxus* annual age determination. We additionally aimed to test the relationships between predicted annual growth form the biochronology and selected environmental/climatic factors. Lastly, we aimed to describe the long-term changes in length-at-age of *M. paradoxus* using the first approach to age determination with current and historical data (from which otoliths had not been archived).

MATERIALS AND METHODS

The Study Species and Sample Collection

Merluccius paradoxus were collected during routine biomass surveys conducted by the Ministry of Fisheries and Marine Resources, Namibia (MFMR) covering the Namibian coast from 17 to 29°S (**Figure 1** and **Table 1**). Otoliths were available from surveys conducted since 1991 and ±30 otoliths were randomly selected from fish ≥35 cm, within ±5-year intervals from 1991 through 2013, totalling an initial 258 otoliths. Because of the truncated stock structure and distribution of *M. paradoxus* as described by Strømme et al. (2016) not many >65 cm *M. paradoxus* were available from survey catches in Namibia (**Table 1**).

Merluccius paradoxus were assumed to spawn in austral spring to summer (September to February) (Jansen et al., 2015). Thus the translucent zones on the otoliths of *M. paradoxus* were assumed to form mainly in spring (September–October), which has been validated with edge analysis (ICSEAF, 1983a; BCC, 2015; MW, unpublished data). In addition, most of the fish were caught January-February (**Table 1**), and most of them had translucent zones near or on the edge of the otolith, indicating that they had just completed these in spring or early summer or were still completing them in late summer. One increment was designated as the couplet of the relatively wide opaque zone and the relatively narrow translucent zone. Measurement of the last increment, if complete, was thus assumed to be from the austral spring-early summer (near the end of the previous year) to the summer of the year before, and thus reflected growth of mostly that calendar year (over austral autumn, winter and spring). For example, if a fish was caught in February 2014, the last complete increment was assumed to reflect growth from October 2012 to October 2013, and the second-last from October 2011 to October 2012, continuing backward in time. If incomplete, the last increment was omitted from the analysis.

Otolith Chronologies

In the laboratory, the otoliths were embedded in epoxy resin and transversally sectioned through the nucleus at 0.5 mm thickness using a low-speed double-bladed saw. The sections were mounted onto glass slides using Crystalbond™ adhesive. After drying, otoliths were polished with 10 μm lapping film to improve the clarity of the macrostructures. Each otolith was digitally photographed using Image-Pro® Plus Version 6.0 (Media Cybernetics, Inc.) software under a Leica dissecting microscope at 3.2× magnification.

Once imaged, the width of each annual otolith growth increment was measured using ImageJ 1.49d[1] (Abramoff et al., 2004) and the macro ObjectJ plugin Version 1.03p.[2] ImageJ was used here because of free access and accessibility for multiple

[1]http://imagej.nih.gov/ij/

[2]https://sils.fnwi.uva.nl/bcb/objectj/examples/TreeRings/TreeRings-9.htm

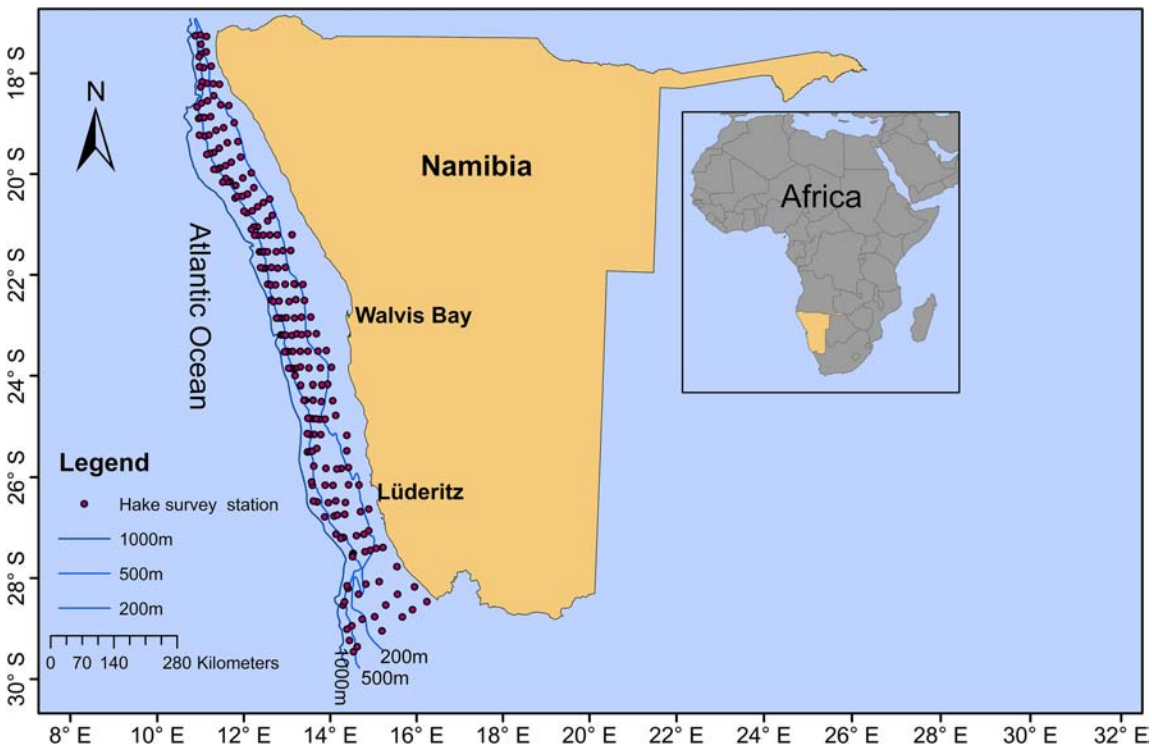

FIGURE 1 | Sampling area and demersal (hake) summer survey stations (red dots) from which samples were selected for the *Merluccius paradoxus* otolith chronology along the Namibian coast. Bottom depth contours (200, 500, and 1,000 m) are indicated by blue lines.

TABLE 1 | Sample sizes (*N*), age and length ranges of *Merluccius paradoxus* used for the final dataset of the otolith biochronology, sampled during Namibian hake biomass surveys 1991 to 2014.

Year	Months	*N*	Latitude range (°S)	Fish length range (cm)	Fish age range (years)
1991	10–11	15	20–28	35–55	3–6
1992	10–11	8	21–27	38–59	3–12
1994	10–11	2	23, 25	43, 78	5, 9
1997	1–2	31	18–29	35–84	4–15
2002	1–2	27	18–27	35–70	4–12
2008	1–2	23	23–29	35–65	3–10
2013	1–2	12	26–29	50–82	6–16
2014	1–2	22	25–29	36–70	4–11

users and computers. Each growth increment was measured from the end of the translucent zone to the end of the next translucent zone. Increments were measured from the dorsal edge to the nucleus of the sectioned otolith perpendicular to the annual growth zone. Some otoliths were measured along the axis of maximum growth (**Figure 2A**). However, for most otoliths, increments were only discernible on the nucleus-to-medial-edge axis of the otolith. In that case, they were measured along this axis from the medial edge to the nucleus of the sectioned otolith (**Figure 2B**). The axis of measurement was noted, and accounted for in the mixed effects model. The nuclear opaque area plus first translucent zone (age 0-year to 1-year growth) was not used as measurement. Only clearly discernible increments were measured, and thus of the initial 258 selected otoliths, only 140 were used in the final data set (**Table 1**).

Where possible (in cases when the time series and overlap of increments was long enough), increment measurements were visually cross-dated (Black et al., 2005).

Mixed Effects Modeling

Once increments were marked and cross-dated, each fish was assigned a final age-at-capture (AAC) and Cohort. Cohort was defined as the year of birth of the fish (calculated for February-caught fish as: year of capture – AAC – 1). Each raw otolith increment width measurement in mm (Inc) was assigned an age at the time of increment formation (Age) and calendar year of increment formation (Year). Before analysis, otolith increment-widths, Age, and AAC were log-transformed and mean-centered. These data were then used in a mixed effects model, to relate increment width (Inc), the response variable, to a series of intrinsic (fish-specific) and extrinsic (environmental, represented by inter-annual variation) factors (Morrongiello and Thresher, 2015). Intrinsic factors included Age, AAC, Sex (of the individual fish, male or female), allowing for the interaction between Age and Sex, measurement Axis ("Long" or "Short," see **Figure 2**) on the otolith, allowing for the interaction between Axis and Age, Cohort and FishID (each individual sample's unique identification). Age, AAC, Sex and Axis were treated as fixed effects. The effects of Cohort and FishID intercepts were treated as random effects. FishID accounts for pseudo-replication, i.e., correlation of the same individual due to genetic ID and sample preparation. Cohort accounts for density dependence and/or juvenile experience. The AAC term was included to correct for biases associated with sampling (skewed age distributions) and tests for bias associated with growth-rate based selectivity (Morrongiello and Thresher, 2015). Year intercept was treated as a random effect. Further random effects included were by-FishID, by-Cohort, and by-Year random slopes for the effects of age. Equation 1 shows the full model fitted to the entire otolith chronology data series 1982–2012 (**Table 1**).

$$\begin{aligned}\log(\text{Inc}) \sim\ & \text{c.}(\log(\text{Age})) + \text{Age} * \text{Sex} + \text{c.}(\log(\text{AAC})) \\ & + \text{Age} * \text{Axis} + \text{c.}(\log(\text{Age}))|\text{FishID} \\ & + \text{c.}(\log(\text{Age}))|\text{Cohort} + \text{c.}(\log(\text{Age}))|\text{Year} \quad (1)\end{aligned}$$

A series of mixed effects models (Weisberg et al., 2010; Morrongiello and Thresher, 2015) was used to test for the best possible combination of the explanatory variables, testing all possible combinations of fixed effects and random effects, intercept and slope for random effects [denoted by e.g., log(Age)|FishID, Equation 1]. The most parsimonious model was selected using maximum likelihood estimates of error and the lowest Akaike's Information Criterion (AIC) corrected for small sample sizes (AICc) (Burnham and Anderson, 2002; Zuur et al., 2009). The optimal selected model was refitted with restricted maximum likelihood (REML) to produce unbiased parameter estimates (Zuur et al., 2009), using the random effects of year (intercept) to produce a best linear unbiased predictor of growth (BLUP) for each year 1982–2012. The BLUP time series was used to visualize the temporal pattern of *M. paradoxus* growth variability and was correlated with an independently calculated growth rate, a fish condition index as well as environmental data/indices that represent local and remote forcing. All analyses were performed in R Version 3.5.0 (R Core Team, 2018), with libraries lme4 (Bates et al., 2015), AICcmodavg (Mazerolle, 2019), effects (Fox, 2003; Fox and Weisberg, 2019), and lattice (Sarkar, 2008) for plotting.

Annual Population-Level Age 3 Growth

Annual age-length-keys (ALKs), used in the Namibian hake stock assessments and read from whole otoliths collected in January-February of each year, were available from 2000 to 2016 (SP, MFMR, unpublished data). These were used to calculate mean lengths at each age 1 to 7 years for each calendar year (**Supplementary Table S1**). These data were used to calculate change in length from age 3 to 4 years (G3) from calendar year y to the next, at the population level, by the following equation:

$$\text{G3} = \text{L4}_{y+1} - \text{L3}_{y} \quad (2)$$

where y = the year of growth, $L3_y$ = length at age 3 in calendar year y, and $L4_{y+1}$ = length at age 4 in calendar year y + 1 (**Supplementary Table S1**). Growth from age 3 to 4 years was used because these fish are in the juvenile-to-sexually mature-adult transition (Wilhelm et al., 2015a) and are no longer influenced by cohort effects or hatch timing (this study, data not shown).

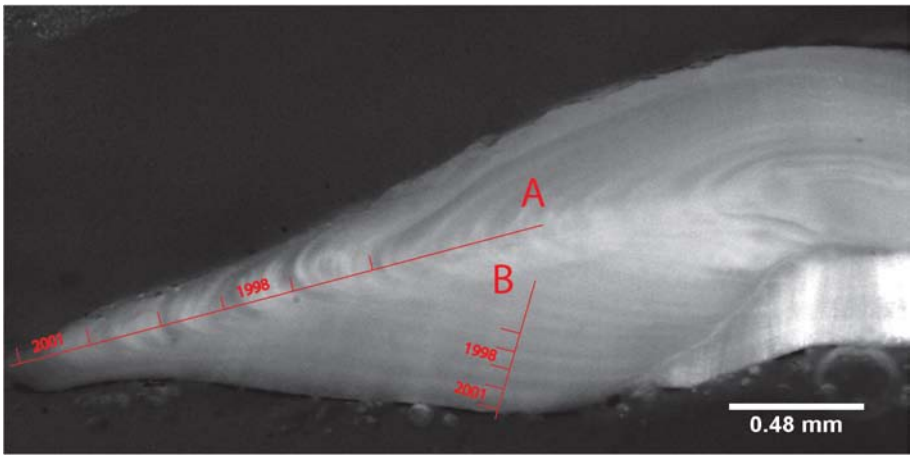

FIGURE 2 | Anterior view of a right-side sliced otolith of a 6-year old female *M. paradoxus* caught off Namibia in February 2002. The otolith is viewed with reflected light at 3.2× magnification. Lines show the end of a growth zone marked with the years (spring to spring) that they represent on (A) the "long" axis and (B) the "short" nucleus-to-medial-edge axis.

Fish Condition Index

Biological data collected from Namibian hake biomass surveys from 1994 to 2013 (**Table 2**) were used to calculate mean relative weight as a measure of fish condition for that year for *M. paradoxus*. Relative weight was calculated by dividing by survey-measured wet weight of each individual fish by the expected weight. Expected weight was calculated using a length-weight relationship:

$$\mathrm{Log}(\mathrm{W_e}) = \mathrm{b} * \mathrm{Log}(\mathrm{Lt}) + \mathrm{a} \quad (3)$$

where W_e = expected weight in g, Lt = total fish length in cm, and a and b are constants calculated for all fish measured for all surveys 1999–2013, $a = 3.10$ and $b = -2.31$ (**Supplementary Figure S1**).

After the data were cleaned for obvious errors using weight-length plots, the mean relative weight was calculated for each survey 1994 to 2013 for all fish between 25 and 59 cm. Most surveys were conducted in Quarter 1, January and February, while before 1997 surveys were also conducted in Quarter 2, April and May and Quarter 4, September to November (**Table 2**). Prior to 1997 not all years had surveys in the first quarter of the year, and there may also have been area and length sampling differences between these surveys. Thus, a General Linear Mixed Effects Model (GLMM) was performed in order to calculate a mean relative weight (condition index) for each year (keeping year as a random effect), taking into account all other variables (the unbalanced sampling design).

The full model, which was also the best-fit model (AICc = −78582.9, **Supplementary Table S2**) was as follows:

$$\mathrm{Log}(\mathrm{W}) \sim \mathrm{c.}(\log(\mathrm{Lt})) * \mathrm{Sex} + 1|\mathrm{Year} + \mathrm{Quarter} + \mathrm{Lat} \quad (4)$$

where W = wet weight of fish i in g, Lt = total length of fish i in cm (continuous variable). All other factors were added as categorical variables: Sex = male or female or unsexed, Lat = latitude to the nearest degree in which fish i was caught (17–29°S), Year = year of sampling (1994–2013), Quarter = sampling quarter of the year, either 1 (summer), 2 (autumn), or 4 (spring) using the same centring function, model selection procedures and R-packages as explained for Equation 1. Within the selection procedure, Quarter and Lat were also added as random effects to test for

TABLE 2 | Sample sizes of biological samples of *Merluccius paradoxus* females (F), males (M), and total used for each biomass survey, in austral summer (quarter 1), autumn (quarter 2) or spring (quarter 4) 1994 to 2013.

Year	Quarter	*F*	*M*	Total
1994	1	200	69	269
1994	2	466	205	671
1994	4	892	225	1117
1995	2	1465	414	1879
1996	1	428	153	581
1996	4	1022	561	1583
1997	1	249	65	314
1998	1	1463	520	1983
1999	1	1461	240	1701
2000	1	786	371	1157
2001	1	608	325	933
2002	1	550	341	891
2003	1	463	285	748
2004	1	1017	468	1485
2005	1	892	492	1384
2006	1	1382	607	1989
2007	1	2278	769	3047
2008	1	3151	583	3734
2009	1	2611	610	3221
2010	1	2080	641	2721
2011	1	832	511	1343
2012	1	1440	831	2271
2013	1	1528	717	2245
Total				37267

the best fit model. The model-estimated random intercept for each year was antilogged to obtain a relative weight for that year to be used for comparison with the otolith chronology annual growth estimate.

Environmental Data

The BLUP time series from the mixed effect model was correlated (Pearson's Correlation Coefficient) with an upwelling index, chlorophyll-a concentration, and sea surface temperature (SST) as indicators of local environmental drivers. The environmental variables were used as monthly, three-monthly and annual means and were correlated with the annual BLUP they overlapped with (lag 0 and lag 1 for spring), as well as lagged by 1 year for all (lag 1 and lag 2 for spring).

Similar to Lamont et al. (2018a), daily NCEP-DOE Reanalysis 2 wind vectors (Kanamitsu et al., 2002) along the coast were used to calculate daily values of Ekman transport (m^3 s^{-1}) per 100 m of coastline at the Lüderitz upwelling cell (27°30′′S) in the northern Benguela (15–29°S), and at the Namaqua upwelling cell in the southern Benguela (30°S). Daily values of cumulative offshore transport were summed per month to obtain total monthly values, which were then used as an indicator of upwelling variability.

Chlorophyll-a (chl-a) concentrations were calculated in mg m^{-3} using MODIS satellite data from the Giovanni website[3] for the period 2002–2013 at 4 km resolution (Acker and Leptoukh, 2007). The chl-a data were summarized to calculate monthly means for each of six zones within the northern part of the Benguela ecosystem. These were defined by homogeneity in severity and seasonality of the Chl-a concentration as: Zone 1: the Angola-Benguela Front (14–19°S, 7–12°E); Zone 2: nBUS N upwelling cell (19–21°S, 8–14°E); Zone 3: nBUS Center upwelling cell (21–23°S, 9–14°E); Zone 4: nBUS S upwelling cell (23–26°S, 10–15°E); Zone 5: Lüderitz upwelling cell (26–28°S, 10–15°E) and Zone 6: the Orange River-Namaqua upwelling cell (28–30°S, 11–17°E). For the purposes of overlap with the main *M. paradoxus* distribution, only Zones 4–6 were used.

Average monthly sea surface temperature (SST) values were extracted from the NOAA National Centre for Environmental System (NCEP) database[4] (Reynolds et al., 2002) for the area 24–28°S, 13–15°E from January 1982 to October 2016.

Indicators of remote drivers of *M. paradoxus* growth included the mean monthly multivariate ENSO index (MEI) (Wolter and Timlin, 1993) as an indicator of El Niño–Southern Oscillation (ENSO) as well as the Antarctic Annular Oscillation Index (AAO), which is the dominant 700 mb height anomalies poleward of 20°S that captures decadal-scale climate variability in the Southern Hemisphere (Thompson and Wallace, 2000). These climate indicators were correlated with the BLUP of annual *M. paradoxus* growth. MEI and AAO were obtained from KNMI Climate Explorer.[5]

[3]http://disc.sci.gsfc.nasa.gov/Giovanni

[4]https://iridl.ldeo.columbia.edu/SOURCES/.NOAA/.NCEP/.EMC/.CMB/.GLOBAL/.Reyn_SmithOIv2/

[5]climexp.knmi.nl/

Historical Length-at-Age

Finally, in order to view possible changes in fish growth over time over a period longer than the chronology time series, ALKs were retrieved from literature (ICSEAF, 1977, 1978, 1979, 1980, 1981, 1982, 1983b, 1984, 1985, 1987) for *M. paradoxus* caught in ICSEAF Divisions 1.3, 1.4 and 1.5 (off Namibia). ALKs from the three divisions and different countries and fleets were pooled by 3-month periods for each year (January–March, April–June, July–September, and October–December). Mean length at each age group *a* (1–8) was then calculated from each pooled ALK by:

$$\frac{\sum f_i x_i}{\sum fa} \tag{5}$$

where f_i = frequency of the age group in length class *i*, x_i = class mark of length class *i* and Σfa = total frequency in age group a. (Sum of lengths of each individual fish in that age group divided by the total number of fish in the age group). Historical (ICSEAF data) mean lengths-at-age were used together with the current (**Supplementary Table S1**), and time-related directional changes in fish growth were investigated by linear regressions of mean lengths against year of capture (for each age group).

RESULTS

The best supported model of the growth increment data (**Supplementary Figure S2**) was that which included fixed effects for Age and Axis, and random effects intercept and slope for Year and FishID (AICc = 603.14, Conditional R^2 = 0.820, **Supplementary Tables S3, S4** and **Table 3**). The selected model

TABLE 3 | Optimal model parameter estimates and test statistics describing Fixed and Random sources of growth variation in *Merluccius paradoxus* caught along the Namibian coast 1991 to 2013 (**Table 1**).

Fixed effects			
Covariate	**Estimate**	***SE***	***t*-value**
Intercept	−2.92	0.023	−127.01
Age	−0.48	0.022	−21.96
AxisLong	1.24	0.041	30.33
Random effects			
Covariate	**Variance component**	***SD***	**Correlation**
FishID	0.0319	0.1786	
Age| FishID	0.0170	0.1304	0.28
Year	0.0023	0.0479	
Residual	0.0925	0.3042	
Conditional R^2	**0.82**		

Growth modeling was limited to years with ≥3 increment measurements 1982–2013. Random effects age slopes for each individual are denoted by Age| FishID. Axis is the measurement axis on the otolith and is compared with respect to Short. SE is the standard error of the fixed effects covariate estimated as $s^2/(N-3)$, where s^2 = the sum square error of each component, and N = 834. For the random-effects section, the variance component is calculated as SD^2 (SD, standard deviation, which is estimated), with a correlation of 0.28 between by-FishID slope and intercept.

explained 82% of the variation in *M. paradoxus* growth. Age-at-capture did not add significantly to the explanation of otolith growth variation, meaning there was no evidence for biases associated with the sampling scheme. Sex of the fish, cohort, and latitude at which the individual fish was caught did not add significantly to changes in growth variation. Growth declined significantly with age (**Figure 3A**). The differences in mean increment width against age between short and long axes are shown in **Figures 3B,C**. From the random effects of Year, annual growth was lowest for 2003, after which mean growth rates appeared to increase toward 2013. However, no significant negative or positive trend in predicted growth was apparent over the time series from 1982 to 2013, which was dominated by decadal variability rather than a long-term trend (**Figure 4** and **Table 4**).

Mean annual population-level growth at age 3 years varied between 6 and 9 cm per year, 2000–2013 (**Figure 5**). Age-3 mean population-level growth per year was strongly positively correlated with the mean (individual-level) BLUP of growth from otolith increments ($\rho = 0.730$, $n = 14$, $p < 0.01$), overlapping from 2000 through 2013.

The GLMM-estimated relative weight (**Supplementary Table S5**) was used as an estimate of summer fish condition factor of *M. paradoxus* (see **Supplementary Figure S3**).

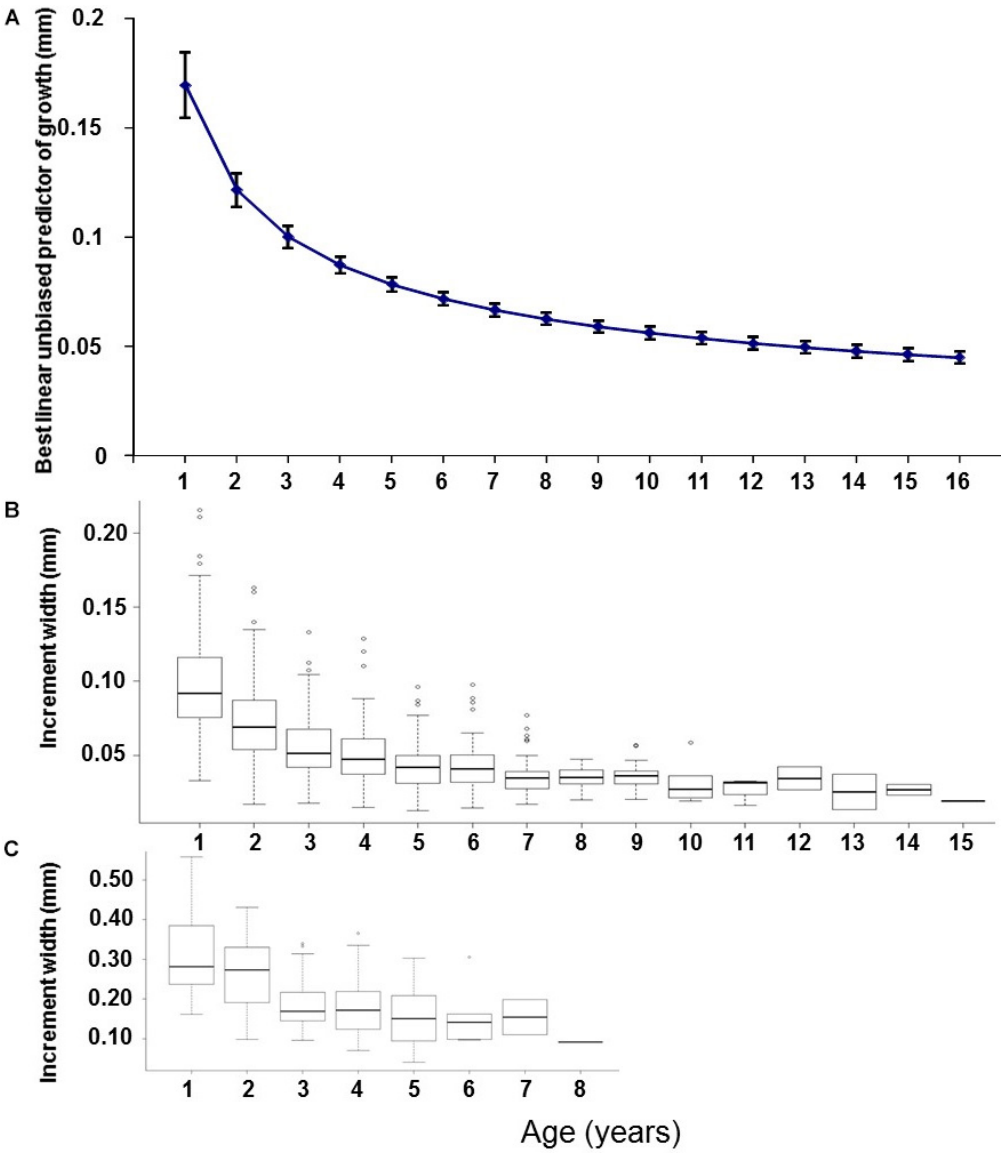

FIGURE 3 | (A) Predicted growth (mm) against age estimated in the full mixed effects model (mean age-related growth decline), back-transformed to the original scale. **(B)** Boxplots of absolute otolith increment width (mm) against age for the short measurement axis and **(C)** the long measurement axis, all for 140 otoliths of *M. paradoxus* caught off Namibia.

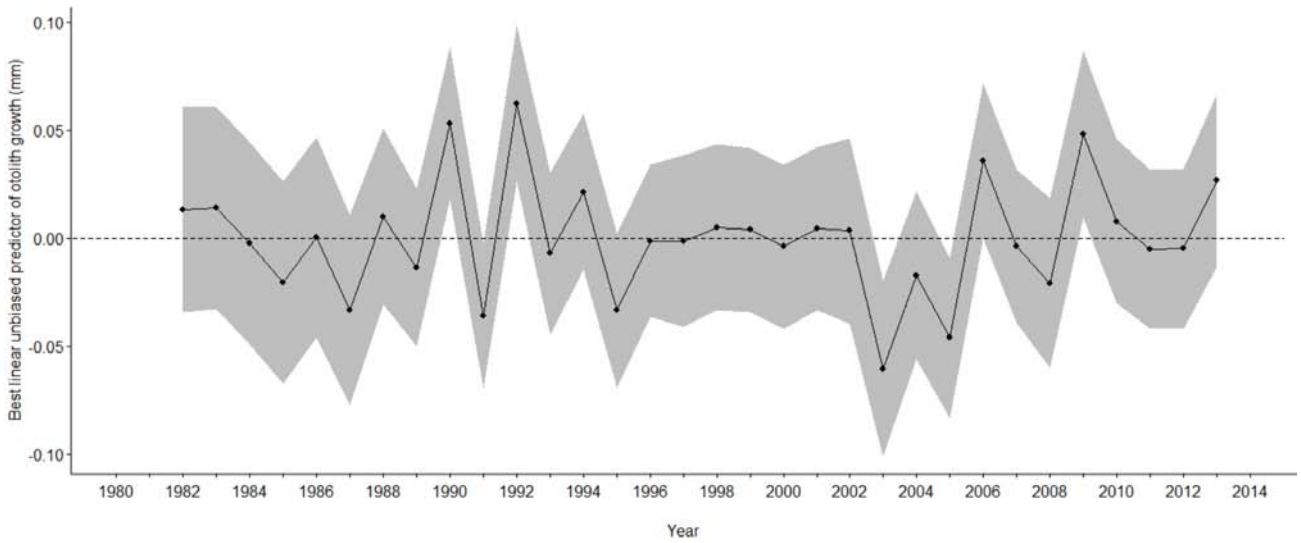

FIGURE 4 | Best linear unbiased predictor of growth, (dots and solid lines) against year of *M. paradoxus* caught off Namibia estimated from the most parsimonious mixed effects model on otolith increments (**Table 3**). Grayed areas indicate 95% confidence limits and the dashed line indicates mean growth.

Condition factor was weakly positively correlated with BLUP of growth from otolith increments ($\rho = 0.358$, $n = 20$, $p < 0.2$, **Figure 6**), overlapping in the period 1994–2013.

The best environmental indicators for *M. paradoxus* BLUP of growth from otolith increments were the August and July–September mean upwelling index in the 30°S area, southern Benguela (**Supplementary Figure S4B**), the August, October, and August–October (austral winter to spring) mean chl-a concentrations at the Namaqua upwelling cell in the southern Benguela (**Supplementary Figure S5B**) and the October and previous December–February SSTs in the 24–28°S area (**Supplementary Figure S6**). BLUP of otolith growth significantly positively correlated with the August upwelling index ($\rho = 0.411$, $n = 32$, $p < 0.05$) and the July–September upwelling index ($\rho = 0.414$, $n = 32$, $p < 0.05$) 1982–2013 at 30°S in the southern Benguela (**Figure 7**). BLUP of otolith growth also significantly positively correlated with the August ($\rho = 0.734$, $n = 12$, $p < 0.01$), October ($\rho = 0.587$, $n = 12$, $p < 0.05$) and August–October ($\rho = 0.600$, $n = 12$, $p < 0.05$) mean chlorophyll-a concentrations 2002–2013 in the 28–30°S area (**Figure 8**). Predicted growth significantly negatively correlated with October (austral spring) ($\rho = -0.381$, $n = 32$, $p < 0.05$) and previous December to February (austral summer) ($\rho = -0.355$, $n = 32$, $p < 0.05$) mean SSTs 24–28°S (**Figure 9**). Mean annual growth did not correlate with the upwelling index at the Lüderitz upwelling cell (**Supplementary Figure S4A**), the chlorophyll-a concentrations in all other areas (**Supplementary Figure S5**), the climate data lagged by 1 year (**Supplementary Figures S7–S9**) or the MEI or the AAO (**Supplementary Figure S10**).

Trends in mean population-level lengths-at-ages 1–8 from 1977 to 2016 showed that lengths-at-ages 1–4 increased by between 0.02 and 0.08 cm · year^{-1} and mean length-at-ages 5–8 decreased by between 0.004 and 0.25 cm · year^{-1} (**Figure 10** and **Table 4**). Significant time-related changes in mean lengths were seen for age 2 by 0.054 cm · year^{-1} ($t = 2.48$, df = 42, $p = 0.0017$), age 3 by 0.075 cm · year^{-1} ($t = 3.04$, df = 43, $p = 0.0040$), age 7 by −0.14 cm · year^{-1} ($t = -2.13$, df = 34, $p = 0.040$), and age 8 by −0.25 cm · year^{-1} ($t = -3.58$, df = 30, $p = 0.0012$) (**Table 4**).

DISCUSSION

In this study we developed a 32-year otolith chronology for *M. paradoxus*. This is the first study of its kind in the Benguela upwelling system. We showed that otolith chronologies (individual-level growth) as well as ALKs (population-level mean length at age) can be used as indicators of annual fish growth, fish condition and local climatic forcing, despite otoliths of the hakes and other species in the Benguela being notoriously difficult to read. By correlating annual otolith growth with annual fish growth age 3–4 using two independent methods of growth estimation, we indirectly validate age determination of *M. paradoxus* using the whole otolith method and its current age determination criteria. This confirms that *M. paradoxus* grow 6 to 9 cm year^{-1} at 3-years-old (**Figure 4**), with higher inter-annual variations (3–12 cm year^{-1}) apparent for other ages and in other years (**Figure 9**). Similarly, Wilhelm et al. (2015a, 2019) calculated growth of northern Benguela *M. paradoxus* using the von Bertalanffy growth curve fitted to 1999 to 2007 pooled lengths at ages as 7.3 cm year^{-1} at age group 1 to 4.4 cm year^{-1} at age group 8. The mean growth of 8.32 cm year^{-1} (all ages) that was estimated by a geostatistical model using survey length-frequency distributions of *M. paradoxus* caught off South Africa and Namibia (Jansen et al., 2017) is faster than this, probably driven by South African-caught *M. paradoxus* that grow 10–12 cm year^{-1} until about 50–60 cm length and age 5 years (Durholtz et al., 2015). This means that, compared to *M. capensis* in the northern Benguela

TABLE 4 | Regression results of **(A)** Mean length-at-age 1–8 years against year of sampling (Year), calculated from otolith-based age-length keys of *Merluccius paradoxus* caught off Namibia 1977 to 1987 from literature (ICSEAF, 1977, 1978, 1979, 1980, 1981, 1982, 1983b, 1984, 1985, 1987) and 1999 to 2016 from current data (SP, MFMR, and **Supplementary Table S1**) and **(B)** BLUP of growth from the otolith increments against year.

(A) Mean length-at-age *x*				
Coefficient	**Estimate**	***SE***	***t*-value**	***p*-value**
1-year, DF = 35				
Intercept	−14.40	60.93	−0.24	0.81
Year	0.019	0.031	0.61	0.55
2-years, DF = 42				
Intercept	−80.37	43.55	−1.85	0.072
Year	0.054	0.022	2.48	0.017*
3-years, DF = 43				
Intercept	−114.43	48.89	−2.34	0.024
Year	0.075	0.025	3.04	0.0040**
4-years, DF = 41				
Intercept	−22.52	60.26	−0.37	0.71
Year	0.032	0.030	1.06	0.29
5-years, DF = 39				
Intercept	133.63	79.01	1.69	0.10
Year	−0.042	0.040	−1.06	0.30
6-years, DF = 36				
Intercept	184.048	97.11	1.90	0.066
Year	−0.064	0.049	−1.32	0.19
7-years, DF = 34				
Intercept	349.56	135.20	2.59	0.014
Year	−0.14	0.068	−2.13	0.040*
8-years, DF = 30				
Intercept	555.06	136.29	4.07	0.00031
Year	−0.25	0.068	−3.59	0.0012**
(B) Otolith increments				
DF = 30				
Intercept	0.0056	1.06	0.0053	0.996
Year	−0.0000027	0.00052	−0.0053	0.996

*Year slopes that are significant at the 95% level are marked with *, and those significant at the 99% level are marked with **. SE is the standard error of each coefficient estimated as s^2/(DF), where s^2, the sum square error of the estimate, and DF, degrees of freedom (N − 2), which is also indicated for each model.*

(Wilhelm et al., 2015b, 2017, 2018, 2019), *M. paradoxus* exhibits slower growth, with stable and more consistent annual zone formation on their otoliths.

Otolith growth rates were dominated by high individual and inter-annual growth rate variation, rather than sex-specific or cohort-specific variation in the present study. The inter-annual variability of *M. paradoxus* growth appears to be influenced by local environmental conditions with long-term trends driven by other, possibly fisheries-induced, adaptive changes.

The best predictors for *M. paradoxus* growth were the July–September (austral winter-spring) upwelling index at 30°S and the August–October chl-a concentration in the 28–30°S area, the Namaqua upwelling cell, as well as spring and summer SSTs further northwards of this upwelling cell. Upwelling promotes primary productivity, reflected in the chlorophyll-a concentration, and gives rise to secondary productivity and increased abundances of forage fishes, and in that way promotes growth of predators. *M. paradoxus* at 35–50 cm (ages 3–5 years) mainly feed on krill (euphausiids and macrozooplankton) and myctophids (such as *Lampanyctodes hectoris*) (Wilhelm et al., 2015a) or other mesopelagic fishes such as *Maurolicus mueueri* (Armstrong and Prosch, 1991). Abundances and reproductive activity of these prey populations have been linked with the strength of upwelling (e.g., Hulley and Prosch, 1987; Hutchings et al., 1995; Landaeta and Castro, 2002). This provides evidence that *M. paradoxus* growth is limited by upwelling, i.e., productivity and consequently food availability, reflected by high chl-a concentrations, and cold sea surface temperatures in winter-spring at the Namaqua upwelling cell and slightly northwards. *M. paradoxus* growth also responds positively to cold summers (cold SST in November to February). Summer SST averaged over a large area is mostly a function of the seasonal surface irradiation signal rather than upwelling (Demarcq et al., 2007). Bottom temperatures usually lag SSTs by about 6 weeks (Wilhelm, 2012) and *M. paradoxus* have been associated with bottom temperatures between 6 and 8°C and were most negatively associated with warm (>10°C) bottom temperatures (Mbatha et al., 2019). We thus argue that warm water temperatures in summer would directly negatively affect growth rates of *M. paradoxus* (as opposed to reflecting upwelling productivity) when the increased energy demand generated by warm temperature is not matched with the necessary food supply (e.g., van der Sleen et al., 2018).

Demarcq et al. (2003, 2007) demonstrated, based on SeaWiFS satellite data 1997–2003, that phytoplankton blooms peaked in December to March off Lüderitz (26°S) and October to March off St. Helena Bay (33°S). On a broader spatial scale, a distinct chlorophyll-a minimum could be seen around Lüderitz (26–27°S), the main upwelling cell of the entire Benguela. They also demonstrated that chlorophyll-a was less variable in the southern than in the northern Benguela, but upwelling intensity at the Namaqua upwelling cell (29–31°S) peaked in October–December (Demarcq et al., 2003, 2007). In the present study, *M. paradoxus* growth, however, appeared to be driven by the austral winter–spring production of the Namaqua upwelling cell (28–30°S), where the peak in chl-a concentration was usually around that time (July–October) in recent years (**Supplementary Figure S11**). The reason for this discrepancy in seasonality of phytoplankton blooms in the Namaqua area between Demarcq et al. (2003, 2007) and values from the present study, is that Demarcq et al. (2003, 2007) used average coastal chl-a concentrations (20 km × 20 km), while the values in the present study were averaged from 11 to 17°E, 28 to 30°S, which stretches beyond the shelf edge to >1,000 m bottom depth (see **Figure 1**). Integrating chl-a concentrations between coastal and oceanic regions would have resulted in a different seasonality (Lamont et al., 2018b). Mesopelagic fishes are distributed from the coastal area to beyond the shelf edge (Hulley and Prosch, 1987). Their distribution, reproduction and vertical migration (and therefore availability to their predators) is dependent on upwelling productivity (Hulley and Prosch, 1987;

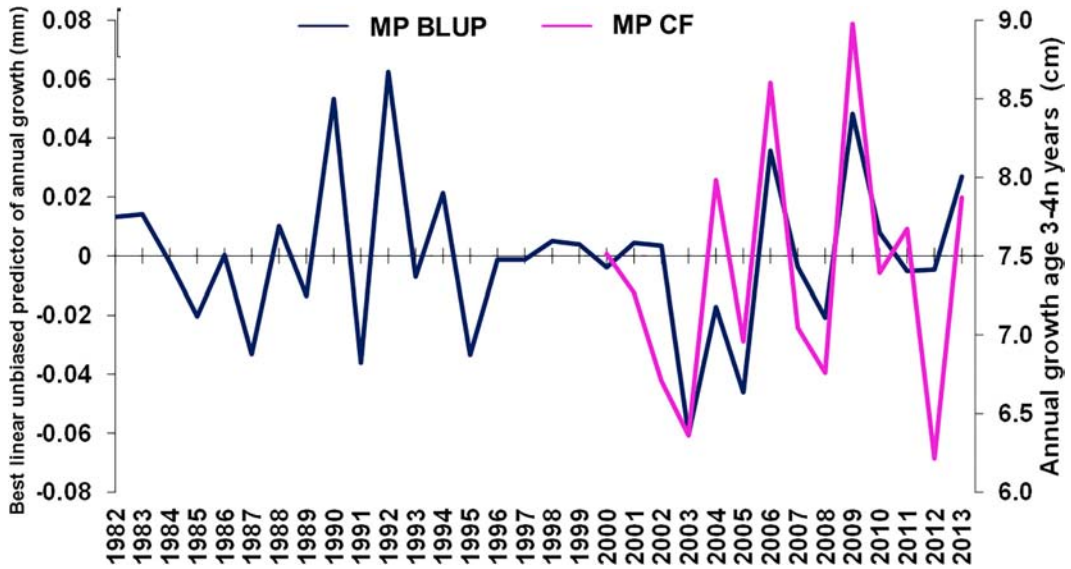

FIGURE 5 | *Merluccius paradoxus* (MP) caught in Namibia best linear unbiased predictor (BLUP) of annual growth from otolith increments (blue) and age 3 annual growth calculated from annual age-length keys (pink) against year.

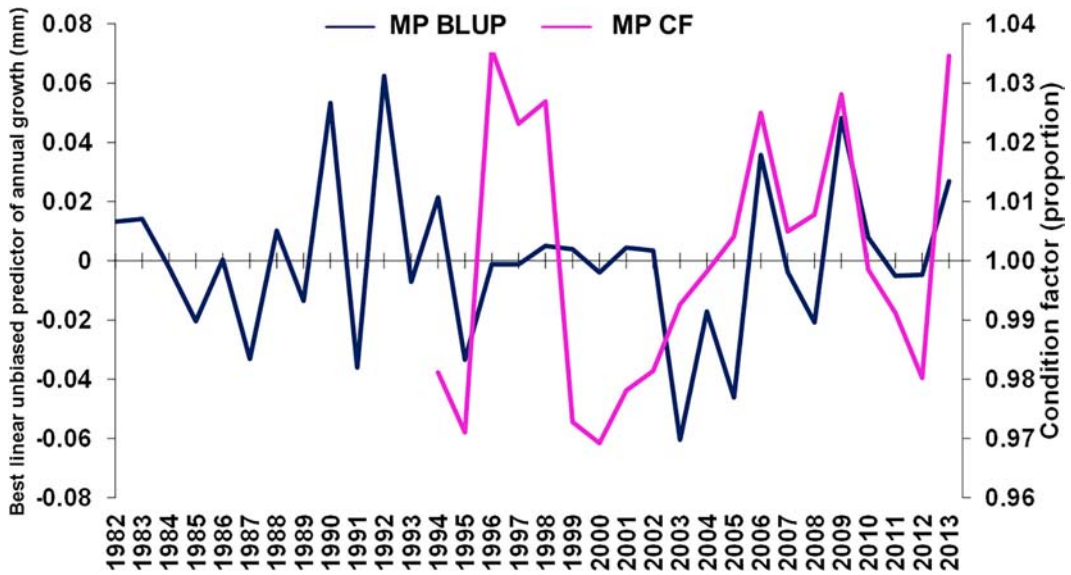

FIGURE 6 | *Merluccius paradoxus* (MP) caught in Namibia predicted annual growth from otolith increments (blue) and GLMM condition factor (CF, pink) against year.

Armstrong and Prosch, 1991), similar to mesopelagic fishes in other upwelling areas (e.g., Landaeta and Castro, 2002). This is a plausible explanation why *M. paradoxus* growth was sensitive to winter upwelling at the Namaqua upwelling cell in the present study. We thus establish that *M. paradoxus* growth variability is a suitable indicator for environmental variability and change, particularly upwelling and primary productivity along the *trans*-boundary area between the northern and southern Benguela, and between Namibia and South Africa (28–30°S).

Local/small-scale variability in the southern Benguela (as used in the present study) is not necessarily driven by large-scale climatic indices such as the ENSO or AAO. No significant correlations were found between SSTs and AAO by Rouault et al. (2010). According to Tim et al. (2015), El Niño events (ENSO) weakly increase upwelling, and La Niña events (AAO) strengthen upwelling in the southern Benguela. However, correlations between ENSO and upwelling indices were evident only in the summer months, where the strongest upwelling peaks were seen in the southern Benguela (Tim et al., 2015). Since *M. paradoxus* growth is most strongly related to winter upwelling/productivity, this explains why *M. paradoxus* growth was not sensitive to the MEI or AAO (remote forcing) in the present study. Similarly,

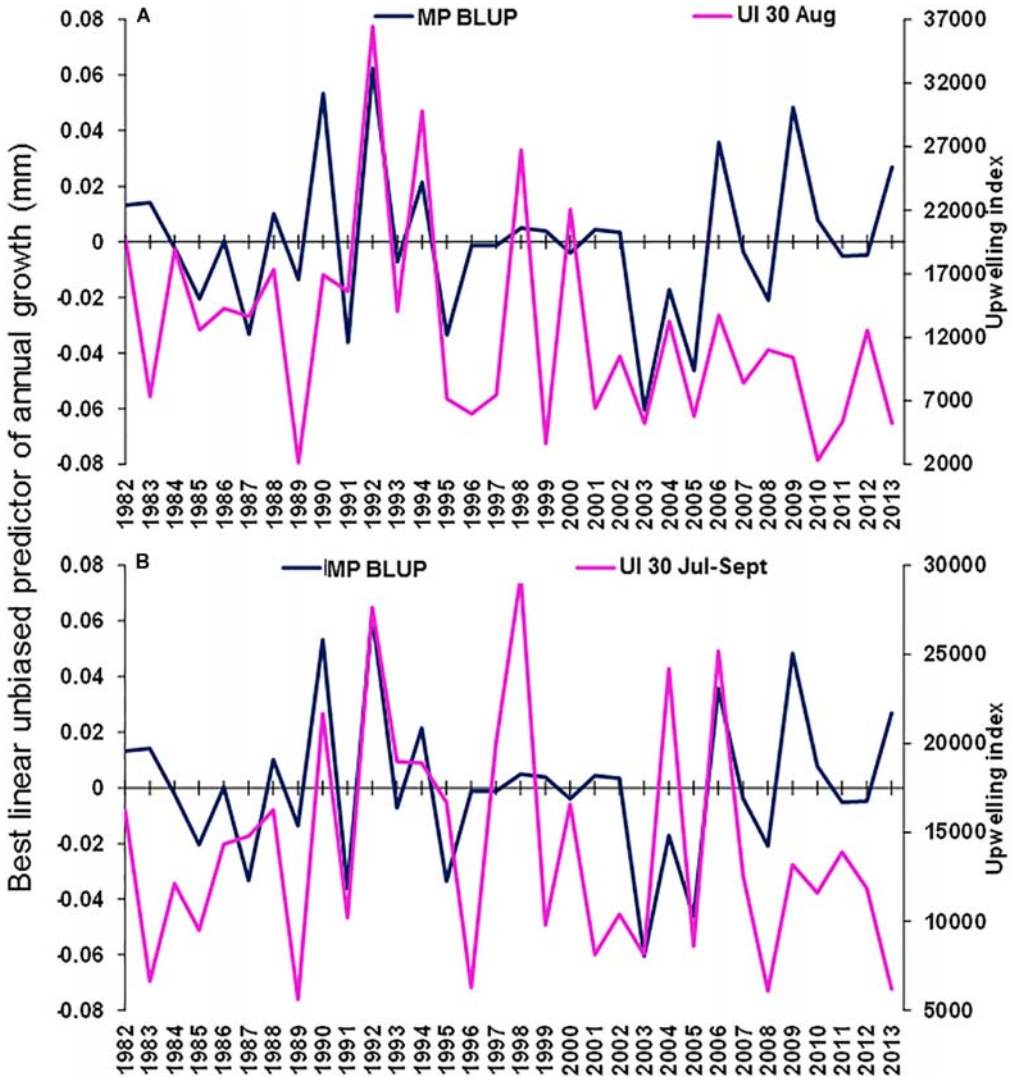

FIGURE 7 | *Merluccius paradoxus* (MP) caught in Namibia best linear unbiased predictor (BLUP) of annual growth from otolith increments (blue) and the **(A)** August and **(B)** August–October mean upwelling index (UI) along the coast for the southern Benguela at –30.0 latitude (30) (pink).

the summer upwelling mode in the California current (39°N) (June–August, corresponding to winter time in the Benguela), was not driven by the same forcing mechanism as the winter upwelling mode (sea level pressure and ENSO), but was instead linked with more local and fine-scale gradients and low-frequency processes (Black et al., 2011). Black et al. (2011, 2014) used fish growth from chronologies and fledging success across different taxa to show that some taxa were driven by the summer upwelling mode and some taxa by the winter upwelling mode. This could be the case in the Benguela upwelling system and linkages of growth of different species with winter and summer climate and with different local or remote drivers should be further explored.

Merluccius paradoxus growth sensitivity to upwelling variability may have changed over time, having a stronger correlation with upwelling indices in the present than the past. A different growth response to environmental variability is likely to be fishery-induced, similar to what was shown for purple wrasse in Tasmania (Morrongiello et al., 2019). Also, the directional change of fish growth seen in the population-scale data in the present study, is likely to be a fishery-induced adaptive change. Mean lengths at ages 2 and 3 have increased, so cumulative growth up to age 3 years has significantly increased since 1977. Since *M. paradoxus* A50 occurs at 4–6 years of age (Durholtz et al., 2015; Wilhelm et al., 2019), age 3 fish are pre-mature fish. Conversely, length-at-age of the 7–8-year-old post-mature fish have significantly decreased since 1977. All this occurred over a period of 40 years. This speaks to the evolutionary response to fishing, when fishing selection favors increased resource acquisition, faster growth, early maturation, and increased reproductive investment because of reduced longevity (Enberg et al., 2012). This is

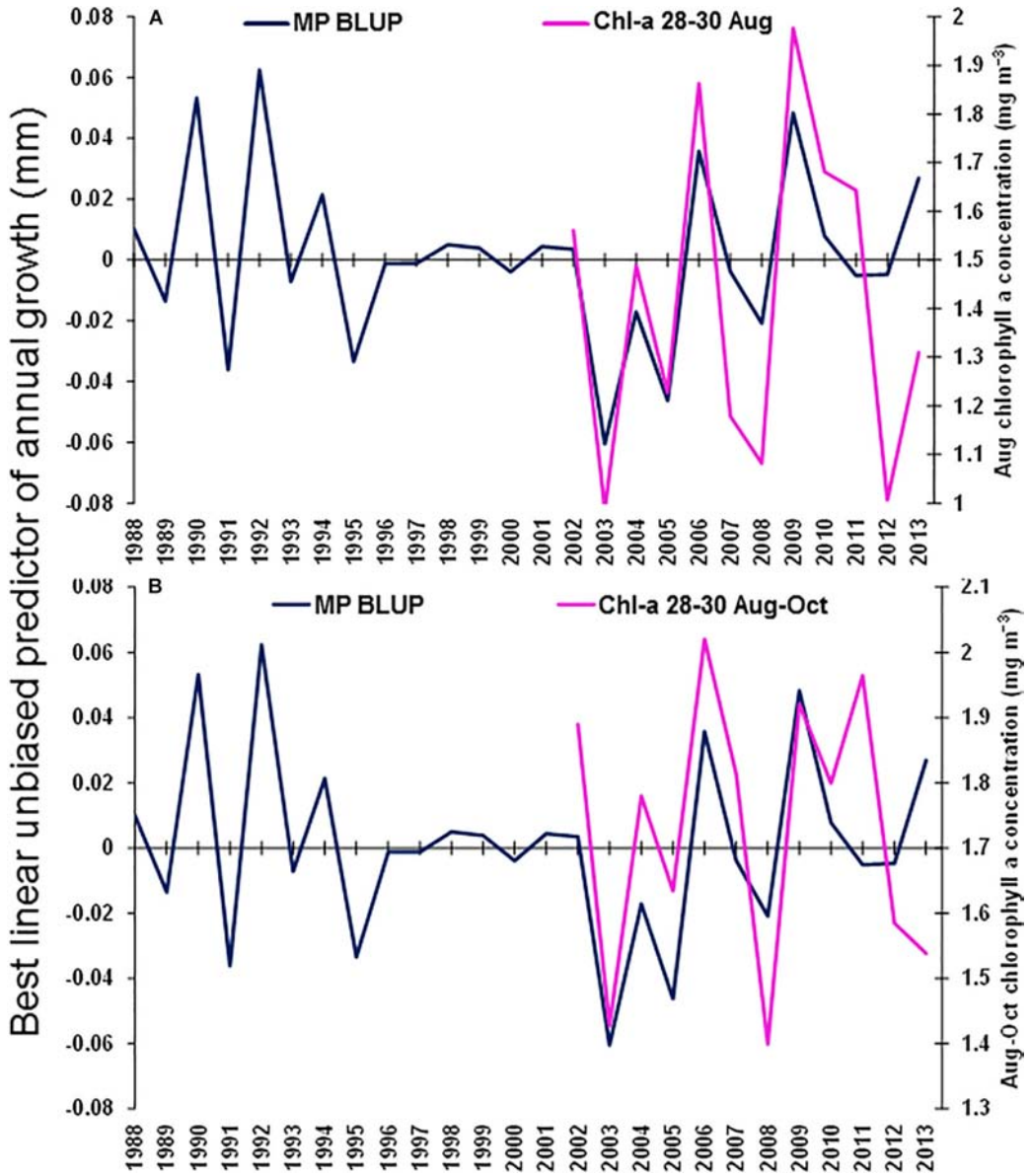

FIGURE 8 | *Merluccius paradoxus* (MP) caught in Namibia best linear unbiased predictor (BLUP) of annual growth from otolith increments (blue) and **(A)** August mean chlorophyll-a concentration (Chl-a 28–30 August); and **(B)** August to October mean chlorophyll-a concentration (Chl-a 28–30 August–October); both in the area −28.0 to −30.0 latitude and 11.0 to 17.0 longitude (pink).

visible in the population by increased growth rates up to sexual maturity, smaller post-mature fish (reduced size-at-age) and at the same time decreased length-at-maturity (Enberg et al., 2012). Overall growth rates of adults may also increase due to easing of density-dependent processes related to fishing (Lorenzen and Enberg, 2002; Morrongiello et al., 2019). In terms of fishing on *M. paradoxus* in Namibia, the maximum hake catches (for both species combined) in Namibia occurred in 1971 and after an initial stock decline again in 1985–1986 (Wilhelm et al., 2015a). Hake catch data in Namibia are only separated by hake species from 1997 onwards. However, given that the vessel strength and capacity and therefore fishing depth of the hake-directed fleet has increased since the start of the fishery (early 1960s), and while the *M. capensis* resource became heavily depleted toward 1990 (Kirchner et al., 2012), the proportion of *M. paradoxus* in the hake catches would have substantially increased in that period (1970–1990). From 1997 to current, between 50 and 80% of the total hake catch in Namibia consisted of *M. paradoxus* (Johnsen and Kathena, 2012), while in the 1980s the majority of the hake catch in Namibia was *M. capensis* (van der Westhuizen, 2001), leading to the evolutionary response of fast growth to this increased fishing mortality on *M. paradoxus* seen in the present study.

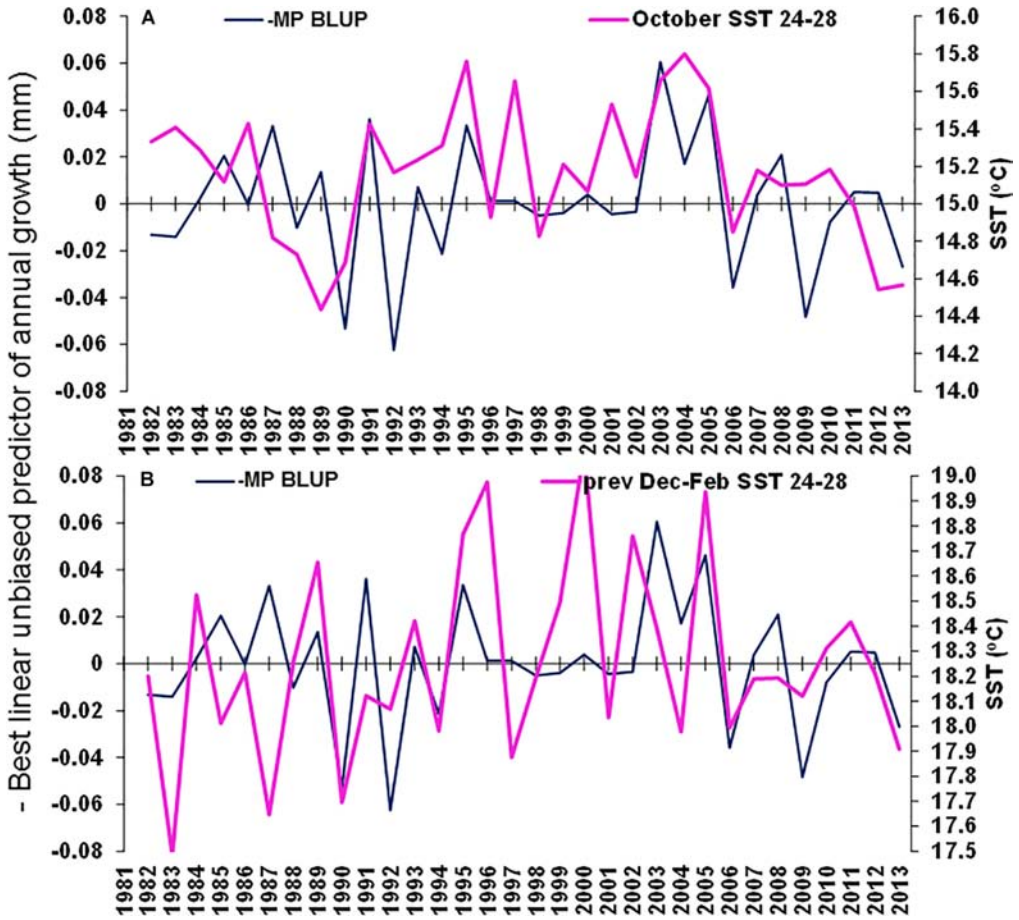

FIGURE 9 | *Merluccius paradoxus* (MP) caught in Namibia best linear unbiased predictor (BLUP) of annual growth from otolith increments (negative to demonstrate negative correlations) (blue) and **(A)** October Sea Surface temperature (SST) in the area –24.0 to –28.0 latitude, 13.0 to 15.0 longitude and **(B)** previous December to February SST in the area –24.0 to –28.0 latitude, 13.0 to 15.0 longitude.

The results of the present study are in line with results of previous studies on other species and/or in other areas. For example, Duncan (2019) developed a chronology of the resident temperate reef fish *Chrysoblephus laticeps* found along the South African South coast. He negatively correlated annual growth of this species with cumulative intensity of extreme cold-water events and positively correlated annual growth with austral autumn (growing season) water temperature. Duncan (2019) also showed that growth rates of young fish (<12 year-olds) were higher in the exploited population than those in the protected population, and for old (>18-year-old) fish this scenario switched, highlighting a fisheries-induced evolutionary effect similar to the effect described in the present study. In European hake (*M. merluccius*), Vieira et al. (2020) established a relationship between predicted otolith growth and both winter SSTs and spring bottom temperatures. They in fact showed that winter SSTs and spring bottom temperatures affected growth differently in different age groups. They also showed that *M. merluccius* predicted otolith growth was related to recruitment, ascribing this to density dependence. Using another species in the same genus as a species occurring in the Benguela, Atlantic horse mackerel *Trachurus trachurus*, Tanner et al. (2019) identified relationships between otolith growth and SSTs, primary productivity and fish biomass (density dependence). van der Sleen et al. (2018) also revealed density-dependent (SSB and CPUE) as well as temperature-dependent (autumn bottom temperature) changes in otolith growth of European plaice (*Pleuronectes platessa*) in the North Sea. Gillanders et al. (2012) determined strong correlations of otolith growth of a temperate reef fish in the southern hemisphere with summer SSTs.

The predicted climate-induced changes in in the Benguela are that upwelling-favorable winds will decrease in the northern Benguela as the pole-ward region of the Benguela, but increase toward the southern Benguela and the Namaqua area (Rykaczewski et al., 2015; Wang et al., 2015). This would negatively affect *M. paradoxus* growth in the northern Benguela as *M. paradoxus* growth was negatively correlated with SST in the northern Benguela (decreased upwelling would mean warmer SST), but conversely would affect *M. paradoxus* growth positively in the southern Benguela. Lamont et al. (2019) determined a general increase in chl-a concentration in the northern Benguela 1997 to 2017, with an increasing upwelling trend in summer

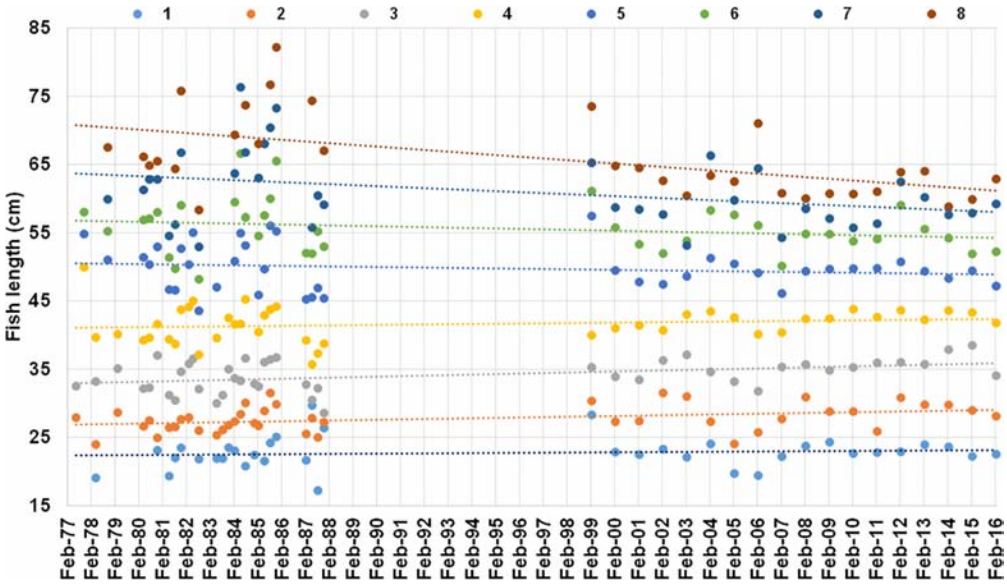

FIGURE 10 | Mean length at age 1–8 years (different color dots) from otolith-based age-length keys of *M. paradoxus* caught off Namibia 1977–1987 from literature (ICSEAF, 1977, 1978, 1979, 1980, 1981, 1982, 1983b, 1984, 1985, 1987) and 1999 to 2016 from current data (SP, MFMR unpublished data, **Supplementary Table S1**). Linear regression lines of mean length-at-age against date of capture are shown in the same color as the dots for each age (all regression outputs are shown in **Table 4**).

and winter; and a slight increasing trend in chl-a in the open ocean domain in the southern Benguela. This would have a positive effect on *M. paradoxus* growth rates. In addition to the climate-induced growth rate changes, there are other, age-specific and long-term (most likely fisheries-induced) effects on growth highlighted in the present study, which need to be considered in future population models. Individual-level growth rate affects fish population productivity (e.g., Morrongiello et al., 2014). This is important to take into account for an EAF management of fisheries on the heavily exploited resource, *M. paradoxus*, shared between the northern and southern Benguela. Time-varying growth should be incorporated in stock assessment and prediction models in the future (e.g., JABBA-Select, Winker et al., 2020), and ultimately, together with error estimates, feed into a comprehensive expert system approach as proposed by Jarre et al. (2006). Future models of *M. paradoxus* growth need to incorporate other environmental factors that have not been tested here, such as bottom temperatures and oxygen concentrations. Low oxygen events, which have been shown to affect hake distribution and mortality occur regularly in the northern Benguela (Hamukuaya et al., 1998; van der Lingen et al., 2006a). However, bottom temperatures and oxygen concentrations are not available on such a fine time-scale in the Benguela. It is therefore necessary and important to record temperature, oxygen and salinity regularly, including every bottom trawl station on fisheries-independent surveys, in the future.

The fact that pre-mature *M. paradoxus* growth has increased and post-mature fish growth has decreased shown by the ALK data in the present study, may explain why the overall individual growth rates from the chronology data (averaged over all age groups) show no significant long-term trend. Not enough samples were available for the otolith increment width data in the present study for these growth rates to be separated by age group. As Enberg et al. (2012) discuss, length-at-age data need to also usually be complemented with maturation information. However, L50 data for *M. paradoxus* in Namibia are only available from 1994 onwards, and from 1994 to present L50 remained constant. Age-at-50%-maturity (A50) data are available from 1999 onwards, and has remained constant between 5.5 and 8 years since then (MFMR, unpublished data). It is therefore imperative that age data (and consequently A50 data) are updated from otolith archives at MFMR back to 1990, and analyzed for the southern Benguela. For Cape horse mackerel *Trachurus capensis*, another heavily exploited fish resource in the northern Benguela, L50 decreased by about 2 cm from the 1950s to the early 2000s (van der Lingen et al., 2006b). For sardine *Sardinops sagax* in the Benguela, changes in condition factor (CF), gonad mass and L50 have been linked with density dependence, with CF and gonad mass increasing and L50 decreasing in years of low population density (van der Lingen et al., 2006c).

Apart from adding biological information from existing data on the hakes in the Benguela, there is a further need to investigate species-specific growth responses to environmental forces, especially in the Benguela upwelling system, and with longer time series of otoliths available. These types of analyses on individual species have been used, for example, to detect regime shifts, in the Bering Sea (van der Sleen et al., 2016) and the Baltic Sea (Smoliński and Mirny, 2017) and the Canary Current upwelling system (Tanner et al., 2019). In order to detect a regime shift in otolith growth for the Benguela, there is a need for using a longer otolith increment width time series spanning the time before and across the northern Benguela regime shift

that occurred during the 1980s (Cury and Shannon, 2004; van der Lingen et al., 2006b). Different taxa have different growth responses to extreme environmental forces and the same species respond differently in different regions (e.g., Izzo et al., 2016; van der Sleen et al., 2016), and even different age groups respond differently for the same species in the same region (e.g., van der Sleen et al., 2018; Vieira et al., 2020). In another example, species across different taxa and trophic levels in the same region, the California Current Upwelling System, were influenced by either winter or summer upwelling modes (Black et al., 2011). Tanner et al. (2019) illustrated that in the Canary Current many different factors, biotic and abiotic factors interacted to influence ecosystem productivity. All of these examples highlight a further need for investigating such responses for different taxa in the Benguela upwelling system (Morrongiello et al., 2012). Otolith chronologies, as well as long term time series of length-at-age of the aquatic resources in the Benguela, such as provided in the present study, prove useful for such long-term (ecosystem-level) indicators and for the possibility to forecast climate- and fisheries-induced changes in growth and ultimately population abundances.

DATA AVAILABILITY STATEMENT

The datasets generated for this study are available on request to the corresponding author.

ETHICS STATEMENT

Ethical review and approval was not required for the animal study because we were not working with any living animals, only otoliths and other secondary data that had been collected for other purposes on research surveys.

AUTHOR CONTRIBUTIONS

BB conceptualized the study. SP acquired and organized the condition index and age-length databases. TL, CB, and DL acquired and calculated the upwelling index, SST and chlorophyll datasets, respectively. MW developed the methods for and acquired the otolith chronology data, performed all the statistical analyses, and led the writing of the manuscript. All authors contributed to the manuscript revision, read and approved the submitted version.

FUNDING

This publication stemmed from research supported by the Marine Science Institute, University of Texas, Port Aransas, Texas, United States (MSI), the Ministry of Fisheries and Marine Resources, Namibia (MFMR), and the Department of Fisheries and Aquatic Sciences, University of Namibia (DFAS); and funded by the United States National Science Foundation Division of Ocean Sciences (Grant 1434732) and the ECOFISH project (Grant 2010/222387) in agreement with the Benguela Current Commission (BCC) and the National Institute for Aquatic Resources (DTU Aqua), Denmark.

ACKNOWLEDGMENTS

We thank the MFMR staff and crew on board all research surveys since 1991 for otolith, age and biological data collections. Wayne Hall (MSI) assisted with preparing and imaging otoliths. Rauha Shipindo, Veronica Kavela, Loide Ndatipo, and Titus Johannes (DFAS) typed up ALK data from hard copies of ICSEAF Sampling Bulletins. Analyses of chl-a data were produced with the Giovanni online data system, developed and maintained by the NASA GES DISC.

SUPPLEMENTARY MATERIAL

The Supplementary Material for this article can be found online at: https://www.frontiersin.org/articles/10.3389/fmars.2020.00315/full#supplementary-material

REFERENCES

Abramoff, M. D., Magelhaes, P. J., and Ram, S. J. (2004). Image processing with Image. *J. Biophotonics Int.* 11, 36–42.

Acker, J. G., and Leptoukh, G. (2007). Online analysis enhances use of NASA earth science data. *EOS Trans. Am. Geophys. Union* 88, 14–17.

Armstrong, M. J., and Prosch, R. M. (1991). Abundance and distribution of the mesopelagic fish *Maurolicus muelleri* in the southern Benguela system. *S. Afr. J. Mar. Sci.* 10, 13–28.

Bates, D., Maechler, M., Bolker, B., and Walker, S. (2015). Fitting linear mixed-effects models using lme4. *J. Stat. Softw.* 67, 1–48. doi: 10.18637/jss.v067.i01

Baudron, A. R., Needle, C. L., Rijnsdorp, A. D., and Marshall, C. T. (2014). Warming temperatures and smaller body sizes: synchronous changes in growth of North Sea fishes. *Glob. Change Biol.* 20, 1023–1031. doi: 10.1111/gcb.12514

BCC, (2015). *ECOFISH Workshop on Hake and Horse Mackerel Marginal Increment Analysis and Age Determination, 30 November – 11 December 2015*. Swakopmund: The Dome Conference Centre.

Black, B. A., Boehlert, G. W., and Yoklavich, M. M. (2005). Using tree-ring crossdating techniques to validate annual growth increments in long-lived fishes. *Can. J. Fish. Aquat. Sci.* 62, 2277–2284.

Black, B. A., Schroeder, I. D., Sydeman, W. J., Bograd, S. J., Wells, B. K., and Schwing, F. B. (2011). Winter and summer upwelling modes and their biological importance in the California current ecosystem. *Glob. Change Biol.* 17, 2536–2545.

Black, B. A., Sydeman, W. J., Frank, D. C., Griffin, D., Stahle, D. W., García-Reyes, M., et al. (2014). Six centuries of variability and extremes in a coupled marine-terrestrial ecosystem. *Science* 345, 1498–1502. doi: 10.1126/science.1253209

Boehlert, G. W., Yoklavich, M. M., and Chelton, D. B. (1989). Time series of growth in the genus *Sebastes* from the northeast Pacific Ocean. *Fish. Bull.* 87, 791–806. doi: 10.1890/04-1832

Burnham, K. P., and Anderson, D. R. (2002). *Model Selection and Inference: A Practical Information-Theoretic Approach*. New York: Springer.

Carey, M. P., and Zimmerman, C. E. (2014). Physiological and ecological effects of increasing temperature on fish production in lakes of Arctic Alaska. *Ecol. Evol.* 4, 1981–1993. doi: 10.1002/ece3.1080

Casselman, J. M., Brown, D. M., Hoyle, J. A., and Eckert, T. H. (2002). "Effects of climate and global warming on year-class strength and relative abundance of smallmouth bass in eastern Lake Ontario," in *Black Bass: Ecology, Conservation, and Management*, eds D. P. Philipp, and M. S. Ridgway (Bethesda, MA: American Fisheries Society), 73–90.

Cury, P., and Shannon, L. J. (2004). Regime shifts in upwelling ecosystems: observed changes and possible mechanisms in the northern and southern Benguela. *Prog. Oceanog.* 60, 223–243.

Demarcq, H., Barlow, R. G., and Shillington, F. A. (2003). Climatology and variability of sea surface temperature and surface chlorophyll in the Benguela and Agulhas ecosystems as observed by satellite imagery. *Afr. J. Mar. Sci.* 25, 363–372.

Demarcq, H., Barlow, R., and Hutchings, L. (2007). Application of a chlorophyll index derived from satellite data to investigate the variability of phytoplankton in the Benguela ecosystem. *Afr. J. Mar. Sci.* 29, 271–282.

Dorn, M. W. (1992). Detecting environmental covariates of Pacific whiting *Merluccius productus* growth using a growth-increment regression model. *Fish. Bull.* 90, 260–275.

Duncan, M. I. (2019). *A Physiological Study on a Commercial Reef Fish to Quantify the Relationship Between Exploitation and Climate Change Resilience*. Ph. D. thesis, Rhodes University, Grahamstown.

Duncombe Rae, C. M. (2005). A demonstration of the hydrographic partition of the Benguela upwelling ecosystem at 26°40'S. *Afr. J. Mar. Sci.* 27, 617–628.

Durholtz, M. D., Singh, L., Fairweather, T. P., Leslie, R. W., van der Lingen, C. D., Bross, C. A. R., et al. (2015). "Fisheries, ecology and markets of South African hake," in *Hakes: Biology and exploitation (1st edition)*, ed. H. Arancibia (Chichester: John Wiley & Sons, Ltd), 38–69.

Enberg, K., Jørgensen, C., Dunlop, E. S., Varpe, Ø, Boukal, D. S., Baulier, L., et al. (2012). Fishing—induced evolution of growth: concepts, mechanisms and the empirical evidence. *Mar. Ecol.* 33, 1–25. doi: 10.1111/j.1439-0485.2011.00460.x

Fox, J. (2003). Effect displays in R for generalised linear models. *J. Stat. Softw.* 8, 1–27.

Fox, J., and Weisberg, S. (2019). *An R Companion to Applied Regression*, 3rd Edn. Thousand Oaks, CA: Sage.

Gillanders, B. M., Black, B. A., Meekan, M. G., and Morrison, M. A. (2012). Climatic effects on the growth of a temperate reef fish from the Southern Hemisphere: a biochronological approach. *Mar. Biol.* 159, 1327–1333. doi: 10.1007/s00227-012-1913-x

Hamukuaya, H., O'Toole, M. J., and Woodhead, P. M. J. (1998). Observations of severe hypoxia and offshore displacement of Cape hake over the Namibian shelf in 1994. *S. Afr. J. Mar. Sci.* 19, 57–59.

Hardman-Mountford, N. J., Richardson, A. J., Agenbag, J. J., Hagen, E., Nykjaer, L., Shillington, F. A., et al. (2003). Ocean climate of the South East Atlantic observed from satellite and wind models. *Prog. Oceanogr.* 59, 181–221.

Hulley, P. A., and Prosch, R. M. (1987). Mesopelagic fish derivatives in the southern Benguela upwelling region. *S. Afr. J. Mar. Sci.* 5, 597–611.

Hutchings, L., Pitcher, G. C., Probyn, T. A., and Bailey, G. W. (1995). "The chemical and biological consequences of coastal upwelling," in *Upwelling in the Ocean: Modern Processes and Ancient Records*, eds C. P. Summerhayes, K. C. Emeis, M. V. Angel, R. L. Smith, and B. Zeitzschel (New York: John Wiley & Sons, Ltd), 65–81.

Hutchings, L., van der Lingen, C. D., Shannon, L. J., Crawford, R. J. M., Verheye, H. M. S., Bartholomae, C. H., et al. (2009). The Benguela current: an ecosystem in four components. *Prog. Oceanogr.* 83, 15–32.

ICSEAF (1977). Sampling bulletin. 1977. *Sampl. Bull. Int. Commn. SE Atl. Fish.* 6:177.

ICSEAF (1978). Sampling bulletin. 1978. *Sampl. Bull. Int. Commn. SE Atl. Fish.* 7:165. doi: 10.1177/1745691610369339

ICSEAF (1979). Sampling bulletin. 1979. *Sampl. Bull. Int. Commn. SE Atl. Fish.* 8:164.

ICSEAF (1980). Sampling bulletin. 1980. *Sampl. Bull. Int. Commn. SE Atl. Fish.* 9:277.

ICSEAF (1981). Sampling bulletin. 1981. *Sampl. Bull. Int. Commn. SE Atl. Fish.* 10:323.

ICSEAF (1982). Sampling bulletin. 1982. *Sampl. Bull. Int. Commn. SE Atl. Fish.* 11:217.

ICSEAF (1983a). ICSEAF Otolith interpretation guide. 1. *Hake Otol. Interp. Gde Int. Commn. SE Atl. Fish.* 1, 18.

ICSEAF (1983b). Sampling bulletin. 1983. *Sampl. Bull. Int. Commn. SE Atl. Fish.* 12:287.

ICSEAF (1984). Sampling bulletin. 1984. *Sampl. Bull. Int. Commn. SE Atl. Fish.* 13:263.

ICSEAF (1985). Sampling bulletin. 1985. *Sampl. Bull. Int. Commn. SE Atl. Fish.* 14:319.

ICSEAF (1987). Sampling bulletin. 1987. *Sampl. Bull. Int. Commn. SE Atl. Fish.* 16:282.

Izzo, C., Doubleday, Z. A., Grammer, G. L., Barnes, T. C., Delean, S., Ferguson, G. J., et al. (2016). Multi-species response to rapid environmental change in a large estuary system: a biochronological approach. *Ecol. Indic.* 69, 739–748. doi: 10.1016/j.ecolind.2016.05.019

Jansen, T., Kainge, P., Singh, L., Wilhelm, M. R., Durholtz, D., Strømme, T., et al. (2015). Spawning patterns of shallow-water hake (*Merluccius capensis*) and deep-water hake (*M. paradoxus*) in the Benguela current large marine ecosystem shown by gonadosomatic index. *Fish. Res.* 172, 168–180. doi: 10.1016/j.fishres.2015.07.009

Jansen, T., Kristensen, K., Fairweather, T. P., Kainge, P., Kathena, J. N., Durholtz, M. D., et al. (2017). Geostatistical modelling of the spatial life history of post-larval deepwater hake *Merluccius paradoxus* in the Benguela current large marine ecosystem. *Afr. J. Mar. Sci.* 39, 349–361. doi: 10.2989/1814232X.2017.1379437

Jarre, A., Moloney, C. L., Shannon, L. J., Fréon, P., van der Lingen, C. D., Verheye, H. M., et al. (2006). "Developing a basis for detecting and predicting long-term ecosystem changes," in *Large Marine Ecosystems*, Vol. 14, eds V. Shannon, G. Hempel, P. Malanotte-Rizzoli, C. Moloney, and J. Woods (Amsterdam: Elsevier), 239–272. doi: 10.1016/S1570-0461(06)80016-9

Jarre, A., Hutchings, L., Kirkman, S. P., Kreiner, A., Tchipalanga, P. C. M., Kainge, P., et al. (2015). Synthesis: climate effects on biodiversity, abundance and distribution of marine organisms in the Benguela. *Fish. Oceanogr.* 24, 122–149.

Johnsen, E., and Kathena, J. (2012). A robust method for generating separate catch time-series for each of the hake species caught in the Namibian trawl fishery. *Afr. J. Mar. Sci.* 34, 43–53.

Kanamitsu, M., Ebisuzaki, W., Woollen, J., Yang, S.-K., Hnilo, J. J., Fiorino, M., et al. (2002). NCEP-DOE AMIP-II Reanalysis (R-2). *Bull. Am. Meteorol. Soc.* 83, 1631–1643.

Kathena, J. N., Nielsen, A., Thygesen, U. H., and Berg, C. W. (2016). Hake species (*Merluccius capensis* and *M. paradoxus*) assessment in the Benguela current large marine ecosystem. *Environm. Dev.* 17, 193–201.

Kirchner, C., Kainge, P., and Kathena, J. (2012). Evaluation of the status of the Namibian hake resource (*Merluccius* spp.) using statistical catch-at-age analysis. *Environm. Dev.* 12, 1–52.

Lamont, T., García—Reyes, M., Bograd, S. J., van der Lingen, C. D., and Sydeman, W. J. (2018a). Upwelling indices for comparative ecosystem studies: variability in the benguela upwelling system. *J. Mar. Syst.* 188, 3–16. doi: 10.1016/j.jmarsys.2017.05.007

Lamont, T., Brewin, R. J. W., and Barlow, R. G. (2018b). Seasonal variation in remotely-sensed phytoplankton size structure around southern Africa. *Remote Sens. Env.* 204, 617–631.

Lamont, T., Barlow, R. G., and Brewin, R. J. W. (2019). Long—term trends in phytoplankton chlorophyll a and size structure in the Benguela Upwelling System. *J. Geophys. Res. Letters* 124, 1170–1195. doi: 10.1029/2018JC014334

Landaeta, M. F., and Castro, L. R. (2002). Spring spawning and early nursery zone of the mesopelagic fish *Maurolicus parvipinnis* at the coastal upwelling zone off Talcahuano, central Chile. *Mar. Ecol. Progr. Ser.* 226, 179–191.

Lorenzen, K., and Enberg, K. (2002). Density-dependent growth as a key mechanism in the regulation of fish populations: evidence from among-population comparisons. *Proc. R. Soc. Lond. B.* 269, 49–54. doi: 10.1098/rspb.2001.1853

Magnuson, J. J., Webster, K. E., Assel, R. A., Bowser, C. J., Dillon, P. J., Eaton, J. G., et al. (1997). Potential effects of climate changes on aquatic systems: laurentian great lakes and precambrian shield region. *Hydrol. Processes* 11, 825–871.

Mazerolle, M. J. (2019). *AICcmodavg: Model Selection and Multimodel Inference Based on (Q) AIC(c). R Package Version 2.2-2.* Available at: cran.r-project.org/package=AICcmodavg (accessed December 3, 2019).

Mbatha, F. L., Yemane, D., Ostrowski, M., Moloney, C. L., and Lipiński, M. R. (2019). Oxygen and temperature influence the distribution of deepwater Cape

hake *Merluccius paradoxus* in the southern Benguela: a GAM analysis of a 10-year time-series. *Afr. J. Mar. Sci.* 41, 413–427.

Morrongiello, J. R., Beatty, S. J., Bennett, J. C., Crook, D. A., Ikedife, D. N., Kennard, M. J., et al. (2011). Climate change and its implications for Australia's freshwater fish. *Mar. Freshw. Res.* 62, 1082–1098.

Morrongiello, J. R., Thresher, R. E., and Smith, D. C. (2012). Aquatic biochronologies and climate change. *Nat. Clim. Change* 2, 849–857. doi: 10.1038/nclimate1616

Morrongiello, J. R., Walsh, C. T., Gray, C. A., Stocks, J. R., and Crook, D. A. (2014). Environmental change drives long-term recruitment and growth variation in an estuarine fish. *Glob. Change Biol.* 20, 1844–1860. doi: 10.1111/gcb.12545

Morrongiello, J. R., and Thresher, R. E. (2015). A statistical framework to explore ontogenetic growth variation among individuals and populations: a marine fish example. *Ecol. Monogr.* 85, 93–115.

Morrongiello, J. R., Sweetman, P. C., and Thresher, R. E. (2019). Fishing constrains phenotypic responses of marine fish to climate variability. *J. Anim. Ecol.* 88, 1645–1656. doi: 10.1111/1365-2656.12999

Pilling, G. M., Kirkwood, G. P., and Walker, S. G. (2002). An improved method for estimating individual growth variability in fish, and the correlation between von Bertalanffy growth parameters. *Can. J. Fish. Aquat. Sci.* 59, 424–432.

Potts, W. M., Henriques, R., Santos, C. V., Munnik, K., Ansorge, I., Dufois, F., et al. (2014). Ocean warming, a rapid distributional shift, and the hybridization of a coastal fish species. *Glob. Change Biol.* 20, 2765–2777. doi: 10.1111/gcb.12612

R Core Team. (2018). *R: A Language and Environment for Statistical Computing. Version 3.5.0*. Vienna: R Foundation for Statistical Computing.

Reynolds, R. W., Rayner, N. A., Smith, T. M., Stokes, D. C., and Wang, W. (2002). An improved in situ and satellite SST Analysis for climate. *J. Clim.* 15, 1609–1625.

Rouault, M., Pohl, B., and Penven, P. (2010). Coastal oceanic climate change and variability from 1982 to 2009 around South Africa. *Afr. J. Mar. Sci.* 32, 237–246.

Rykaczewski, R. R., Dunne, J. P., Sydeman, W. J., García—Reyes, M., Black, B. A., and Bograd, S. J. (2015). Poleward displacement of coastal upwelling—favourable winds in the ocean's eastern boundary currents through the 21st century. *J. Geophys. Res. Lett.* 42, 6424–6431.

Sarkar, D. (2008). *Lattice: Multivariate Data Visualization with R*. New York: Springer.

Smoliński, S., and Mirny, Z. (2017). Otolith biochronology as an indicator of marine fish responses to hydroclimatic conditions and ecosystem regime shifts. *Ecol. Indic.* 79, 286–294.

Strømme, T., Lipinski, M. R., and Kainge, P. (2016). Life cycle of hake and likely management implications. *Rev. Fish Biol. Fish.* 26, 235–248.

Tanner, S. E., Vieira, A. R., Vasconcelos, R. P., Dores, S., Azevedo, M., Cabral, H. N., et al. (2019). Regional climate, primary productivity and fish biomass drive growth variation and population resilience in a small pelagic fish. *Ecol. Indic.* 103, 530–541.

Thompson, D., and Wallace, J. (2000). Annular modes in the extra-tropical circulation. 1. Month-to-month variability. *J. Climate* 13, 1000–1016. doi: 10.1038/s41598-019-39392-y

Tim, N., Zorita, E., and Hünicke, B. (2015). Decadal variability and trends of the Benguela upwelling system as simulated in a high-resolution ocean simulation. *Ocean Sci.* 11, 483–502.

van der Lingen, C. D., Fréon, P., Hutchings, L., Roy, C., Bailey, G. W., Bartholomae, C., et al. (2006a). "Forecasting shelf processes of relevance to living marine resources in the BCLME," in *Large Marine Ecosystems*, Vol. 14, eds V. Shannon, G. Hempel, P. Malanotte-Rizzoli, C. Moloney, and J. Woods (Amsterdam: Elsevier), 309–347.

van der Lingen, C. D., Shannon, L. J., Cury, P., Kreiner, A., Moloney, C. L., Roux, J.-P., et al. (2006b). "Resource and ecosystem variability, including regime shifts, in the Benguela Current System," in *Large Marine Ecosystems*, Vol. 14, eds V. Shannon, G. Hempel, P. Malanotte-Rizzoli, C. Moloney, and J. Woods (Amsterdam: Elsevier), 147–184.

van der Lingen, C. D., Fairweather, T. P., Fréon, P., and van der Westhuizen, J. J. (2006c). Density dependent changes in reproductive parameters and condition of southern Benguela sardine *Sardinops sagax*. *Afr. J. Mar. Sci.* 28, 625–636. doi: 10.2989/18142320609504212

van der Sleen, P., Dzaugis, M. P., Gentry, C., Hall, W. P., and Hamilton, V. (2016). Long-term Bering Sea environmental variability revealed by a centennial-length biochronology of Pacific ocean perch (*Sebastes alutus*). *Clim. Res.* 71, 33–45.

van der Sleen, P., Stransky, C., Morrongiello, J. R., Haslob, H., Peharda, M., and Black, B. A. (2018). Otolith increments in European plaice (*Pleuronectes platessa*) reveal temperature and density-dependent effects on growth. *ICES J. Mar. Sci.* 75, 1655–1663.

van der Westhuizen, A. (2001). A decade of exploitation and management of the Namibian hake stocks. *S. Afr. J. Mar. Sci.* 23, 307–315.

van Zuiden, T. M., Chen, M. M., Stefanoff, S., Lopez, L., and Sharma, S. (2016). Projected impacts of climate change on three freshwater fishes and potential novel competitive interactions. *Div. Distr.* 22, 603–614.

Verheye, H. M., Lamont, T., Huggett, J. A., Kreiner, A., and Hampton, I. (2016). Plankton productivity of the Benguela Current Large Marine Ecosystem (BCLME). *Environ. Dev.* 17, 75–92.

Vieira, A. R., Dores, S., Azevedo, M., and Tanner, S. E. (2020). Otolith increment width-based chronologies disclose temperature and density-dependent effects on demersal fish growth. *ICES J. Mar. Sci.* 77, 633–644. doi: 10.1093/icesjms/fsz243

Wang, D., Gouhier, T. C., Menge, B. A., and Ganguly, A. R. (2015). Intensification and spatial homogenization of coastal upwelling under climate change. *Nature* 518, 390–394. doi: 10.1038/nature14235

Weisberg, S., Spangler, G. R., and Richmond, L. S. (2010). Mixed effects models for fish growth. *Can. J. Fish. Aquat. Sci.* 67, 269–277.

Wilhelm, M. R. (2012). *Growth and Otolith Zone Formation of Namibian Hake Merluccius Capensis*. Ph. D. Thesis, University of Cape Town, Cape Town.

Wilhelm, M. R., Roux, J.-P., Moloney, C. L., and Jarre, A. (2013). Data from fur seal scats reveal when Namibian *Merluccius capensis* are hatched and how fast they grow. *ICES J. Mar. Sci.* 70, 1429–1438. doi: 10.1093/icesjms/fst101

Wilhelm, M. R., Kirchner, C. H., Roux, J.-P., Jarre, A., Iitembu, J. A., Kathena, J. N., et al. (2015a). "Biology and fisheries of the shallow-water hake (*Merluccius capensis*) and the deep-water hake (*M. paradoxus*) in Namibia," in *Hakes: Biology and exploitation*, 1st Edn, ed. H. Arancibia (Chichester: John Wiley & Sons, Ltd), 70–100. doi: 10.1002/9781118568262.ch3

Wilhelm, M. R., Roux, J.-P., Moloney, C. L., and Jarre, A. (2015b). Biannual otolith zone formation of young shallow-water hake *Merluccius capensis* in the northern Benguela: age validation using otoliths sampled by a top predator. *J. Fish Biol.* 87, 1–16. doi: 10.1111/jfb.12684

Wilhelm, M. R., Moloney, C. L., Paulus, S. C., and Roux, J.-P. (2017). Fast growth inferred for northern Benguela shallow-water hake *Merluccius capensis* using annual survey- and monthly commercial length-frequency distributions. *Fish. Res.* 193, 7–14. doi: 10.1016/j.fishres.2017.03.001

Wilhelm, M. R., Moloney, C. L., Paulus, S. C., Kashava, S., Brinkman, F. R. V., van der Plas, A. K., et al. (2018). Biannual otolith zonation of Cape hake (*Merluccius capensis*) in response to environment and fish physiology in the northern Benguela. *J. Mar. Syst.* 188, 98–108. doi: 10.1016/j.jmarsys.2017.08.001

Wilhelm, M. R., Paulus, S. C., and Kashava, S. (2019). New age determination method based on fast growth rate of Namibian *Merluccius capensis*. *Afr. J. Mar. Sci.* 41, 119–124. doi: 10.2989/1814232X.2019.1581659

Winker, H., Carvalho, F., Thorson, J. T., Kell, L. T., Parker, D., Kapur, M., et al. (2020). JABBA-Select: Incorporating life history and fisheries' selectivity into surplus production models. *Fish. Res.* 222:105355. doi: 10.1016/j.fishres.2019.105355

Wolter, K., and Timlin, M. S. (1993). "Monitoring ENSO in COADS with a seasonally adjusted principal component index," in *Proceedings of the 17th Climate Diagnostics Workshop* (Norman: NOAA), 52–57.

Zuur, A. F., Ieno, E. N., Walker, N. J., Saveliev, A. A., and Smith, G. M. (2009). *Mixed Effects Models and Extensions in Ecology with R*. New York, NY: Springer.

Conflict of Interest: The authors declare that the research was conducted in the absence of any commercial or financial relationships that could be construed as a potential conflict of interest.

Copyright © 2020 Wilhelm, Black, Lamont, Paulus, Bartholomae and Louw. This is an open-access article distributed under the terms of the Creative Commons Attribution License (CC BY). The use, distribution or reproduction in other forums is permitted, provided the original author(s) and the copyright owner(s) are credited and that the original publication in this journal is cited, in accordance with accepted academic practice. No use, distribution or reproduction is permitted which does not comply with these terms.

frontiers in Marine Science

ORIGINAL RESEARCH
published: 19 May 2020
doi: 10.3389/fmars.2020.00322

Growing Up Down South: Spatial and Temporal Variability in Early Growth of Fuegian Sprat *Sprattus fuegensis* From the Southwest Atlantic Ocean

Virginia A. García Alonso[1,2], Daniel R. Brown[3], Marcelo Pájaro[3] and Fabiana L. Capitanio[1,2]*

[1] Laboratorio de Zooplancton Marino, Departamento de Biodiversidad y Biología Experimental (DBBE), Facultad de Ciencias Exactas y Naturales, Universidad de Buenos Aires, Buenos Aires, Argentina, [2] Instituto de Biodiversidad y Biología Experimental Aplicada (IBBEA), CONICET-UBA, Facultad de Ciencias Exactas y Naturales, Universidad de Buenos Aires, Buenos Aires, Argentina, [3] Instituto Nacional de Investigación y Desarrollo Pesquero (INIDEP), Mar del Plata, Argentina

OPEN ACCESS

Edited by:
Alejandra Vanina Volpedo, University of Buenos Aires, Argentina

Reviewed by:
Mauricio F. Landaeta, University of Valparaíso, Chile
Guido Plaza, Pontificia Universidad Católica de Valparaíso, Chile

***Correspondence:**
Virginia A. García Alonso
garciaalonso.v.a@gmail.com

Specialty section:
This article was submitted to Marine Ecosystem Ecology, a section of the journal Frontiers in Marine Science

Received: *14 December 2019*
Accepted: *21 April 2020*
Published: *19 May 2020*

Citation:
García Alonso VA, Brown DR, Pájaro M and Capitanio FL (2020) Growing Up Down South: Spatial and Temporal Variability in Early Growth of Fuegian Sprat Sprattus fuegensis From the Southwest Atlantic Ocean. Front. Mar. Sci. 7:322. doi: 10.3389/fmars.2020.00322

The Fuegian sprat *Sprattus fuegensis* represents one of the most important pelagic resources in the Southwest Atlantic Ocean (SWAO), exerting a crucial ecological role as an intermediary link in Patagonian food webs. Otolith microstructure of 217 age-0 sprats were analyzed aiming to characterize growth patterns and possible environmental effects over them. Samples were gathered during three oceanographic surveys (spring 2014; autumns 2016, 2017) in Tierra del Fuego (TDF) and the Marine Protected Area Namuncurá-Burdwood Bank (MPAN-BB), the first Argentinian open-sea marine protected area. Daily growths (DG) of larvae and post-larvae were estimated by individually modeling size and otolith radius relationships through back-calculation procedures using potential and linear functions, respectively. Increment widths (IW) and DG values and trajectories were assessed for older sprats (i.e., survivors) sampled in the autumn surveys considering the habitat, year sampled and sprats' hatching seasons, and were additionally evaluated in relation to sea-surface temperature (SST). IW and DG trajectories differed primarily according to the habitat sampled and sprats' hatching seasons. Overall, strong coupling was detected between IW and DG trajectories with SST in both habitats. However, statistical assessment on particular comparisons showed that this general trend is not strictly invariant. Even though several results pinpointed a positive correlation between IW and DG with SST, the highest DG were estimated for summer- and autumn-born sprats sampled in 2016 in the MPAN-BB, period and habitat with the lowest SST values. These results unveil a complex relationship between spatial and temporal variability during early growth of Fuegian sprats, supplying relevant information that could be used in the creation of adequate ecosystem based management strategies in the SWAO.

Keywords: ***Sprattus fuegensis*, otolith microstructure, growth variability, environmental effect, Southwest Atlantic Ocean, Marine Protected Area Namuncurá-Burdwood Bank**

INTRODUCTION

The Fuegian sprat *Sprattus fuegensis* (i.e., Austral sprat, Patagonian sprat, Malvinas (Falkland) sprat) is a small clupeid that inhabits the coasts and shelves of southern South America (Cousseau, 1982; Aranis et al., 2007) and is usually referred to as the most important pelagic resource in the Southwest Atlantic Ocean (SWAO) south of 47°S (Bellisio et al., 1979). Despite representing a suitable target species, catches upon this clupeid are still incidental in the Patagonian Sea, with commercial extraction currently occurring only in Chile (Cerna et al., 2014). As many other small pelagic fishes, this zooplanktivorous sprat exerts an essential trophic role as an intermediary link between lower trophic levels and top predators of ecological and economical relevance (e.g., Ramírez, 1976; Bezzi, 1984; Schiavini et al., 1997; Ciancio et al., 2008; Belleggia et al., 2014; Scioscia et al., 2014). Furthermore, due to their high biomass schools and trophic position, *S. fuegensis* possibly controls the energy flux at the wasp-waist level (Cury et al., 2000; Bakun, 2006; Fauchald et al., 2011; Ricciardelli and Boy, unpublished data). Therefore, fluctuations in Fuegian sprat abundances could have major environmental and economic consequences.

Recruitment success in marine fishes is closely coupled to early stages' growth and survival (e.g., Hjort, 1926; Houde, 1987; Anderson, 1988; Cushing, 1990; Leggett and Deblois, 1994; Sogard, 1997; Köster et al., 2003). In turn, several biotic and abiotic factors have been linked to early growth variability and survival for other sprats such as *Sprattus sprattus*, with food availability, density-dependent processes and temperature being among the most significant ones (Nissling, 2004; Voss et al., 2006; Baumann et al., 2006a,b,c, 2007, 2008; Hinrichsen et al., 2010; Peck et al., 2012). Combined with the high susceptibility of small pelagic fishes to ocean-atmosphere variations (Alheit and Hagen, 2001; Peck et al., 2013), this background pinpoint the importance of understanding Fuegian sprat early stages' growth and the potential influence of environmental change over them, features poorly understood to the date.

Three different spawning/nursery grounds of *S. fuegensis* have been detected in the SWAO, the Malvinas Islands, the coasts of Tierra del Fuego (TDF) and the Marine Protected Area Namuncurá-Burdwood Bank (MPAN-BB), the first Argentinian open-sea marine protected area (Law no. 26,875) (Ciechomski and Weiss, 1974; Ciechomski et al., 1975; Sánchez and Ciechomski, 1995; Sánchez et al., 1995, 1997; Bruno et al., 2018; García Alonso et al., 2018). Located between 53°S and 55°S, the MPAN-BB and TDF encompass the southernmost extent inhabited by clupeids worldwide (**Figure 1**). Due to their similar latitudinal range and geographic proximity, these habitats exhibit shared environmental attributes: both of them are under the prevailing influence of intense westerly winds and high tidal variability, and their waters have a sub-Antarctic origin comprised mainly by the northernmost jets of the Antarctic Circumpolar Current and being partially fed by the Cape Horn Current (Piola et al., 2018). However, each habitat also possesses intrinsic physical characteristics, possibly imprinting environmentally induced variability over Fuegian sprats' early development.

Otolith microstructure analysis has proven to be a powerful tool for fishes' growth assessment, providing valuable growth information at an individual level (Stevenson and Campana, 1992). Daily increment counts and otolith growth trajectories enable not only age estimations, but also the detection of relevant life-history events and/or environmental influence over growth (Houde, 1989; Stevenson and Campana, 1992). Several studies have addressed the otolith microstructure analysis of young-of-the-year *S. sprattus* in the Baltic Sea, providing important information regarding growth and recruitment (e.g., Baumann et al., 2006a,b,c, 2007, 2008; Hinrichsen et al., 2010; Voss et al., 2012) and identifying ontogenetic variation in the relationship between fish length and otolith length (Günther et al., 2012). In contrast, few studies have addressed otolith analysis of early *S. fuegensis* in the Chilean Patagonia (Landaeta et al., 2012) or the SWAO (Sánchez et al., 1995, 1997; Brown and Sánchez, 2010; García Alonso et al., 2018), with growth being mainly assessed by modeling age-size relationships. However, habitat-induced variability over early stages' growth was reported for the latter, with reduced larval growth in the MPAN-BB compared to TDF (García Alonso et al., 2018).

In the light of these recent findings and given the intrinsic environmental characteristics encountered in TDF and the MPAN-BB, these habitats emerge as suitable settings for evaluating how variation in physical factors can impact early growth of *S. fuegensis*. Therefore, the aims of the present study were to (1) characterize and compare otolith microstructure of age-0 Fuegian sprats from the MPAN-BB and TDF through the analysis of daily otolith and somatic growth trajectories and to (2) explore possible environmental influence over the early growth of this species by comparing mean growth trajectories with surface seawater temperature variability. Understanding such patterns, would not only provide vital information to further comprehend Fuegian sprat recruitment, but could also constitute pivotal evidence for the generation of new ecosystem-based management strategies policies at the MPAN-BB as well as be used as a baseline to sustainably manage potential extractive activities in the Patagonian Sea.

MATERIALS AND METHODS

Study Area

The MPAN-BB is a shallow submarine plateau located 150 km east of Isla de los Estados where both spawning and nursery of early Fuegian sprats occur (**Figure 1**). Delimited by the 200 m isobath, the bank is surrounded by steep flanks of more than 3000 m depth through which strong currents circulate (Piola and Gordon, 1989; Reta et al., 2014; Matano et al., 2019). Intense upwelling and mixing occur over it, entraining deep nutrient-rich waters into the photic layer (Piola and Falabella, 2009; Matano et al., 2019) and resulting in a fairly homogeneous water column both spatially and temporally (Glorioso and Flather, 1995; Guerrero et al., 1999; Matano et al., 2019). Such features enhance the retention of eggs and early stages of Fuegian sprats along with abundant food (García Alonso et al., 2018). Moreover,

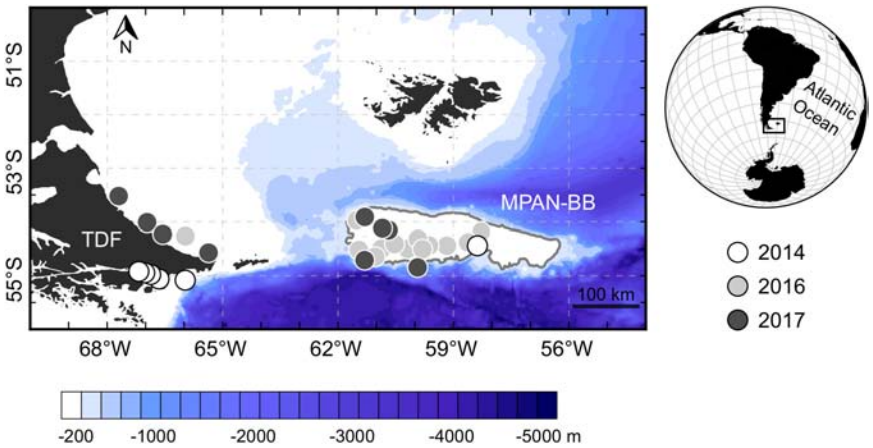

FIGURE 1 | Location of the studied habitats in the Southwest Atlantic Ocean: Tierra del Fuego (TDF) and the Marine Protected Area Namuncurá-Burdwood Bank (MPAN-BB). Stations from which Fuegian sprat *Sprattus fuegensis* where collected for analyzes are indicated according to the year sampled. The MPAN-BB is delimited by a gray solid line. Bathymetry from ETOPO1 Global Relief Model (Amante and Eakins, 2009).

physical features in the MPAN-BB are fairly stable, with salinity averaging 34 all year round and temperature ranging between 4 and 8°C overall (Guerrero et al., 1999; Acha et al., 2004; Piola and Falabella, 2009).

In contrast, TDF shows far more heterogeneous environmental characteristics. First, due to its shallowness and the proximity to the continent, the mass-heat exchange with the atmosphere is more pronounced than in the MPAN-BB, resulting not only in warmer temperatures, but also in significant seasonal stratification of the water column (Guerrero and Piola, 1997). Second, this habitat encompasses two different geographic regions, the Beagle Channel (BC) and the continental shelf. The BC is a 180 km strait where water is strongly diluted by intense precipitations occurring on the Southeast Pacific Ocean, continental run-offs and glacial melting (Guerrero and Piola, 1997; Piola and Rivas, 1997; Balestrini et al., 1998; Antezana, 1999; Isla et al., 1999). Eggs and early larvae found in the BC are energetically transported to warmer and more saline waters in the continental shelf where the transition to further developmental stages (i.e., transitional larvae/metamorphosing and juveniles) takes place (Sánchez et al., 1995, 1997; Acha et al., 1999).

Sample Collection

Fuegian sprats were collected during three oceanographic surveys carried out by the ARA "Puerto Deseado" oceanographic vessel in November 2014 (spring), March/April 2016 (autumn) and April/May 2017 (autumn) (**Figure 1**). Hauls were conducted through oblique tows for 5 min at 2–3 knots from 180 m to the surface or less, reaching bottom proximities when possible. Larvae were sampled using a 60 cm diameter Bongo net (300 μm), whereas post-larvae were collected using an Isaacs-Kidd Midwater Trawl (IKMT) employed only in 2017 in the same sampling positions surveyed with the Bongo net. Upon net recovery, several sprats per haul were sorted on board when available and stored frozen for biochemical analyses (article in preparation), while the remaining material was fixed in alcohol 80%. Since in 2014 unsorted sprats were fixed in 4% formaldehyde, they were excluded from this study.

Once in the laboratory, age-0 *S. fuegensis* from alcohol fixed samples were separated. Their developmental stages were determined distinguishing larval (yolk-sac, preflexion, flexion, and postflexion larvae) and post-larval sprats (transitional-larvae/metamorphosing) (Lebour, 1921; Kendall et al., 1984). Yolk-sac larvae were excluded from this study as they do not deposit daily increments (Alshuth, 1988). Standard lengths (SL) were measured from the tip of the snout to the end of the notochord and corrected for shrinkage (Fey, 1999). Larvae were measured to the nearest micrometer using a Carl Zeiss stereoscope equipped with Axio Vision software, while post-larvae were measured to the nearest millimeter with a scale. The same protocol was applied upon frozen sprats (previously thawed) without correcting SL (Petereit et al., 2008). Their heads were separated and preserved in 80% alcohol for posterior otolith microstructure analyzes.

Otolith Extraction and Microstructure Assessment

Sagittal otoliths were extracted from heads or complete specimens using fine dissection needles. They were cleaned, dried, placed on glass slides and covered with Pro-texx (transparent mounting medium).

Otolith's daily deposition patterns were established following the recommendations of Campana (1992) and assumed based on observations for *S. sprattus* (Alshuth, 1988). Otoliths radius (OR) were measured from the core to the edge of the otolith along the longest axis. Daily increments were counted and their widths were measured to the nearest 0.01 μm under a binocular optical microscope (400× or 1,000×) with transmitted light connected to a computer equipped with the Kontron software for image analysis. Because of their thickness, otoliths from sprats larger than 30 mm had to be manually grounded with

12, 9, and 3 μm lapping film papers. A 90% coincidence in the number of increments was assured between the two otoliths from the same individual, and one of them was then randomly selected for posterior analyzes. When only one otolith was available/undamaged, its number of increments was considered.

Data Analyzes

Ages of *S. fuegensis* were estimated by adding 6 days to the number of increments to compensate for the yolk-sac stage (Alshuth, 1988). Their hatching dates were inferred by subtracting their ages to the corresponding sampling date. Mean SL and their standard errors were calculated according to the habitat, year sampled, developmental stage and hatching season. Differences in larval SL (dependent continuous variable) across habitats and years (independent categorical variables) were statistically compared. Since data did not meet the assumptions of normal distribution (Shapiro–Wilk-test, $p < 0.05$) and equal variances (Levene's Test, $p < 0.05$), a linear model was fitted using generalized least squares (GLS) and variance was modeled with a constant variance function. This approach allowed for both assumptions to be met. The interaction between the independent variables was not significant ($p = 0.485$) and only the effect of the year was significant ($p < 0.001$). Therefore, a new model was fitted only considering the latter variable and Tukey HSD *post hoc* pairwise multiple comparisons were then performed.

Given the short life span of specimens sampled in the 2014 survey, sprats sampled in the autumn surveys (2016 and 2017, i.e., the survivors of the early larval stage which are closer to becoming recruits) were further assessed. The relationship between log-transformed larval SL and OR across different habitats (for each year) or years (within each habitat) was statistically tested through one-way ANCOVAs. A series of linear models were fitted considering SL as the dependent variable, OR and habitat/year as the independent variables. In order to standardize comparisons, only larvae with OR between 100 and 200 μm were included.

Daily growths (DG) were estimated for each individual sprat through proportional back-calculation procedures based on SL-OR relations (Francis, 1990). This approach was chosen due to the restricted ranges of SL shown by each cohort, allowing to estimate previous SL within a same cohort based on the corresponding otolith size. Preliminary assessment of the SL-OR relations evidenced distinct trajectories for different Fuegian sprats' developmental stages, being curvilinear along the larval phase and linear across the post-larval stage. Thus, a segmented approach was adopted and different growth models were employed to model the larval and post-larval phases, respectively (Laidig et al., 1991; Günther et al., 2012). Given the allometric relationship observed along the larval phase, a power function was selected to fit OR-SL data of sprat larvae (Eq. 1):

$$SL_t = a \times OR_t^b \quad (1)$$

where SL_t is the standard length at a given time t, OR_t the otolith radius at time t, and a and b the parameters of the power function. Parameters a and b of Eq. 1 were estimated for each larva by solving a system of two equations considering measures at capture (SL_c and OR_c) and at the first feeding day (SL_0 and OR_0), thus employing a biological intercept (Campana, 1990; Watanabe and Kuroki, 1997). OR_0 corresponded to OR at first increment deposition and SL_0 was established at 5.72 mm resembling the SL of the smaller larva sampled in its first feeding day (Age_0). SL at each day (i.e., SL at each OR_t) were back-calculated employing the individual estimated parameters with Eq. 1 and daily growth rates were then estimated as the difference in SL between two consecutive days (mm d^{-1}).

On the other hand, a linear regression was chosen to fit OR-SL data during the post-larval phase (Eq. 2):

$$SL_t = c + d \times OR_t \quad (2)$$

where c and d are the parameters of the linear equation. Given the different SL-OR relations evidenced by larval and post-larval stages, the growth trajectory of each post-larva was reconstructed by segmenting data and modeling each phase independently (**Figure 2**). To do so, we first estimated the point in which the growth trajectories shifted from curvilinear to linear by fitting general power and linear models to SL-OR data of larvae and post-larvae, respectively, by means of non-linear least squares. The interception between both models was estimated at OR_i and SL_i (**Figure 2A**) and the mean age at which OR_i is attained (Age_i) was interpolated (**Figure 2B**). Parameters c and d were then estimated by solving a system of two equations considering measures at capture (SL_c and OR_c) and at the interception (OR_i and SL_i) and SL during the post-larval phase were back-calculated with Eq. 2 from capture until Age_i (**Figure 2C**). SL during the larval phase of these specimens were estimated with Eq. 1 from Age_i to Age_0 as described above for sprat larvae considering measures at the first feeding day (SL_0 and OR_0) and at the interception (OR_i and SL_i). Results for larval and post-larval phases per specimen were concatenated, and daily growth rates were calculated as the difference in SL between consecutive days.

Increment widths and DG data were pooled in different groups accounting for each combination of habitat, year sampled and hatching season, and mean values and their standard deviations were estimated. Otolith and somatic growth trajectories in relation to age were graphically assessed by averaging IW and DG of each group every 10 days. IW and DG values were statistically compared at 5 different ages (20, 40, 60, 80, and 100 days) across habitats, years or hatching seasons by means of repeated measure analyses. In order to comply with the requirement of identical record lengths, individuals with one or more missing values at these ages were excluded. Given the nature of the response variables, different approaches were applied for IW and DG data, respectively. In the case of IW, data was modeled using a Gaussian distributed GLS whereas for DG, generalized estimation equations (GEE) with a Gamma distribution were applied. Several models of covariance structure were tested for both IW and DG. The best model was identified using the Akaike's information criterion (AIC; Akaike, 1974) for GLS models and the quasi-likelihood information criterion (QIC; Pan, 2001) for GEE models. Interaction between factors (habitat, year or season of hatching) and age was assessed in all the selected

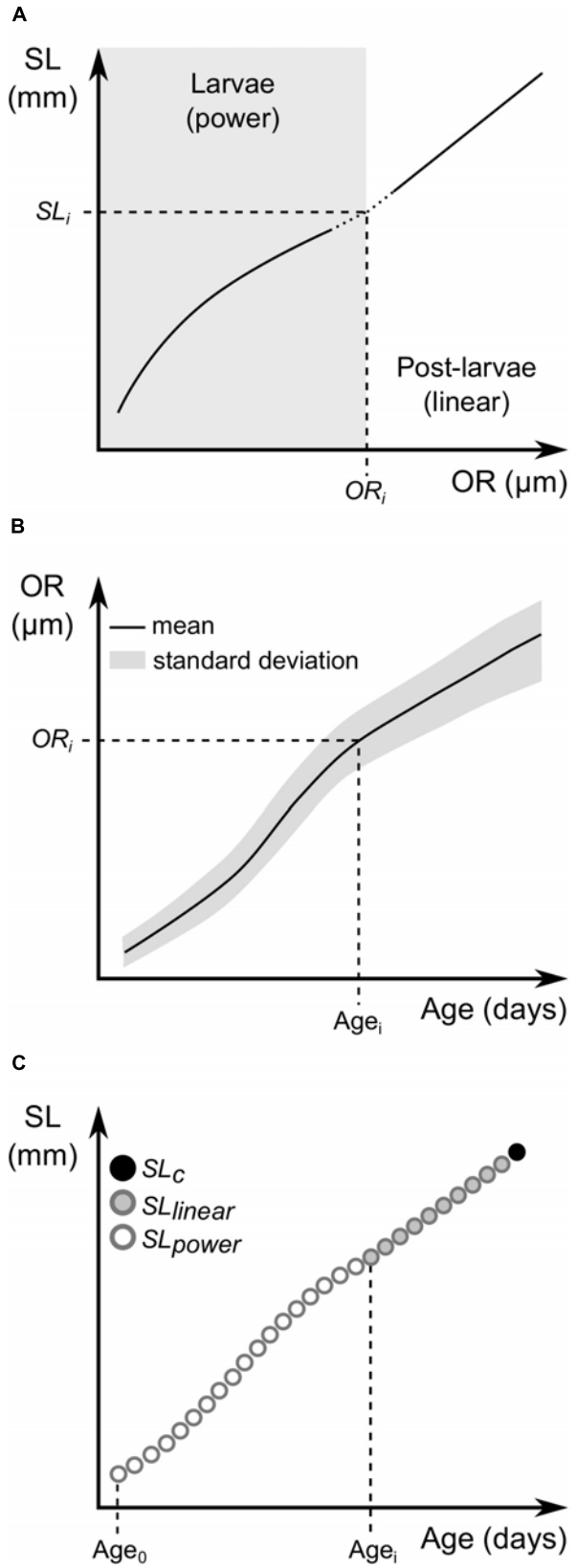

FIGURE 2 | Continued

FIGURE 2 | Schematic illustration of post-larval daily growth back-calculations. **(A)** General models were fitted to otolith radius (OR) and standard length (SL) relations according to developmental stage: a power relation for larvae (gray panel) and a linear function for post-larvae. The interception between both models was estimated at OR_i and SL_i. **(B)** The mean age at which OR_i is attained (Age_i) was interpolated. **(C)** SL back-calculations were performed from capture (SL_C) to Age_i applying a linear model (SL_{linear}) and from Age_i to the first feeding day (Age_0) with a power model (SL_{power}). SL of both stages from each specimen were concatenated and daily growth rates were estimated as the difference in SL between consecutive days.

models. When such interaction was significant, *post hoc* pair-wise comparisons for every combination of levels were carried out using least-squares and adjusting *p*-values with a Bonferroni correction. Otherwise, the main effect of each factor was assessed and a *post hoc* pair-wise comparison was performed across levels of the factors. Seasonal variability in the NMPA-BB was not assessed due to an insufficient number of observations.

Temperature variability was evaluated both spatially and temporally. Knowing that major abundances of Fuegian sprats usually occur in the sub-surface (Landaeta et al., 2013; Contreras et al., 2014), sea-surface temperature (SST) was assessed, thus allowing the acquisition of temperatures registered in periods not sampled. Time series were obtained through the Ocean Time Series Investigator App developed by Google Earth Engine (Gorelick et al., 2017). This platform computes level 3 sea surface temperature data from the MODIS-Aqua dataset (NASA, 2019). Five sites per habitat were chosen in order to cover the overall extension of the sampled areas. Data was downloaded, outliers were removed and smooth conditional means were displayed for each habitat using a "gam" smoothing function. Regression analyzes using generalized least squares were conducted to assess temperature variability (response continuous variable) across habitats and across years within each habitat separately (explanatory categorical variables), comparing equivalent date intervals in the latter. When detected, variance heterogeneity was modeled. The effect of temperature over patterns of growth trajectories was graphically assessed by aligning mean IW and DG trajectories of the groups considered to the corresponding SSTs registered. Pearson correlation coefficients between SST and IW and DG were estimated. To account for ontogenetic related variability, age-detrended IW and DG (i.e., residuals of the models of each variable in relation to age) models were used in the correlations.

Data analyzes were carried out within the R environment (R Core Team, 2019) with the stats (R Core Team, 2019), plyr (Wickham, 2011), tidyr (Wickham and Henry, 2018), dplyr (Wickham et al., 2019b), scales (Wickham, 2018), nlme (Pinheiro et al., 2018), geepack (Halekoh et al., 2006), lsmeans (Lenth, 2016), multcomp (Hothorn et al., 2008), modelr (Wickham, 2020), tidyverse (Wickham et al., 2019a), broom (Robinson and Hayes, 2020) and car (Fox and Weisberg, 2011) packages. Figures were visualized with ggplot2 (Wickham, 2016) and edited with the open-source software Inkscape[1].

[1]http://inkscape.org/

TABLE 1 | General information of Fuegian sprats *Sprattus fuegensis* analyzed in the Southwest Atlantic Ocean.

Survey	Habitat	Stage	Hatching season	*N*	Age	SL	Mean SL
2014	MPAN-BB	Larvae	Spring	6	6 – 9	6.39 – 9.69	8.21 ± 0.44
	TDF	Larvae	Spring	31	6 – 21	5.72 – 13.90	9.12 ± 0.36
2016	MPAN-BB	Larvae	Summer	92	30 – 123	16.96 – 32.07	25.11 ± 0.43
		Larvae	Autumn	9	17 – 42	11.93 – 17.76	15.61 ± 0.68
	TDF	Larvae	Summer	7	70 – 103	18.02 – 31.27	24.16 ± 1.59
2017	MPAN-BB	Larvae	Spring	1	165	28.82	–
		Larvae	Summer	26	76 – 152	20.07 – 30.30	24.84 ± 0.36
	TDF	Larvae	Summer	23	86 – 114	23.47 – 29.19	26.73 ± 0.30
		Post-larvae	Spring	22	155 – 202	33.00 – 51.00	40.32 ± 0.95

Number of specimens (N) are identified according to the survey, habitat (MPAN-BB, Marine Protected Area Namuncurá-Burdwood Bank; TDF, Tierra del Fuego), developmental stage and hatching season. Age (days) and standard length (SL; mm) ranges (minimum-maximum) and mean SL are informed, with variability around the mean displayed as standard error.

RESULTS

A total of 217 individuals were analyzed in this study, with 134 specimens sampled in the MPAN-BB and 83 in TDF. Larval sprats were found in all surveys in both habitats, while post-larval specimens were only captured during the autumn survey of 2017 in TDF (**Table 1**). Larvae sampled in the spring survey (2014) were the smallest sprats analyzed overall ($p < 0.001$), displaying mean SL of 9.12 and 8.21 mm for the MPAN-BB and TDF, respectively. Their ages varied between 6 and 21 days. Due to their short life span, the hatching season estimated resembled that of the survey. On the other hand, larvae from the autumn surveys (2016 and 2017) evidenced higher mean SL values ranging from 15.61 to 26.73 mm. Values measured in 2017 where significantly higher than those measured in 2016 in both habitats ($p < 0.001$). In terms of age, a wider range was observed both between and within habitats in 2016 and 2017 compared to 2014, with a range of more than 90 days of age among larvae from the MPAN-BB in 2016. This variability was replicated by the estimated hatching seasons, registering larval hatching during summer-autumn (2016) and spring-summer (2017) in the MPAN-BB but exclusively in summer in TDF. Furthermore, larvae in the MPAN-BB attained older ages than in TDF in both autumns sampled. Finally, post-larvae found in TDF had hatched entirely in spring. SL varied between 33.00 and 51.00 mm while ages ranged from 155 to 202 days. The oldest larvae found in 2017 in TDF were at least 40 days younger than post-larvae. On the contrary, older summer-born larvae from the MPAN-BB were 3 days younger, with the only spring-born larva being even older (165 days) than the youngest post-larvae (155 days).

The relationship between SL and OR revealed a marked ontogenetic variability (**Figure 3**). Regardless of the habitat and year sampled, larval SL-OR data displayed a distinct curvilinear relation. When statistically assessed, the interaction between OR and habitats/years (i.e., independent variables) were not significant in neither of the linear models assessed. Comparisons of the SL-OR relationships across habitats for each year sampled revealed inter-habitat differences. The MPAN-BB evidenced higher SL at equal OR compared to TDF in 2016 (ANCOVA, $F_{1,51} = 26.645$; $p < 0.001$), whereas it was the other way around in 2017 (ANCOVA, $F_{1,45} = 5.446$; $p = 0.024$). Also, a significant inter-annual difference was detected across older larvae sampled in the autumn surveys only in the MPAN-BB, attaining equal SL with smaller OR in 2016 than 2017 (ANCOVA, $F_{1,70} = 145.012$; $p < 0.001$). Post-larvae, on the other hand, exhibited a linear relation between SL and OR. The estimated age at which the transition between growth models occurred was approximately 110 days.

Increment Width Variability

Otolith IW of sprats sampled in the autumn surveys (see **Table 1**) varied between 0.17 and 6.23 μm overall, with the highest values measured in sprats captured in TDF in 2017 (**Table 2**). Both differences and similarities were recognized in otolith growth trajectories across habitats, hatching seasons and/or years sampled (**Figure 4**). Small IW were observed during the early larval phase (first 20 days) and did not vary significantly across the groups assessed in general, although they did differ across habitats when comparing summer-born larvae in 2016 and 2017, with values in both years being higher in TDF (**Table 3**). Further differences were observed across habitats and/or hatching seasons. Spring-born sprats sampled in TDF in 2017 displayed a clear dome-shaped deposition pattern, with major IW deposited around 90 days of age (**Figure 4D**) and with values close to the peak of the dome (60, 80, and 100 days) being significantly higher than those of summer-born sprats of that same year and habitat (**Table 3**). A similar vaulted pattern was exhibited by the only spring-born sprat analyzed in the MPAN-BB (**Figure 4A**), though the post-peak decline was more gentle. In contrast, summer-born sprats (**Figures 4B,E**) achieved a *plateau* of relatively slow variation in their IW after the first 40–50 days of age. Sprats from TDF (**Figure 4E**) remained in that *plateau* when captured, while a slow decrease was evidenced posterior to the *plateau* in the MPAN-BB (**Figure 4B**). Also, inter-habitat variability was statistically corroborated for summer-born sprats, with higher IW deposited in TDF in 2017 for all ages compared, and for the increments at 20 and 40 days of age in 2016 (**Table 3**). Inter-annual variability among summer-born sprats was graphically observed for both habitats, with curves in 2017 exhibiting higher values than 2016. When statistically assessed,

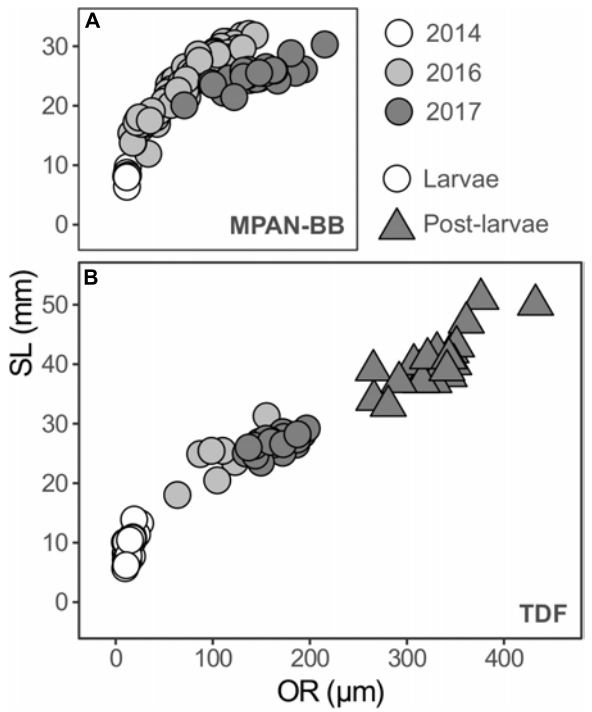

FIGURE 3 | Otolith radius (OR; μm) and standard length (SL; mm) relationships of Fuegian sprat *Sprattus fuegensis* in the Southwest Atlantic Ocean. Data is differentiated according to developmental stage, the survey in which sprats were captured and the habitat sampled: the Marine Protected Area Namuncurá-Burdwood Bank (MPAN-BB) **(A)** and Tierra del Fuego (TDF) **(B)**.

such variability was corroborated at 60 and 80 days of age in TDF and only at 40 days of age in the MPAN-BB (**Table 3**). Finally, sprats born in autumn in the MPAN-BB evidenced constant IW of approximately 0.75 μm in spite of increasing age (**Figure 4C**).

Comparisons of Daily Growth

Estimated DG varied between 0.02 and 1.52 mm d^{-1} overall, exhibiting different ranges across the groups assessed (**Table 4**). Growth trajectories also varied spatially and seasonally (**Figure 5**). Spring-born sprats displayed a dome-shaped pattern in their DG trajectories, similar to the one described for their IW, though in this case both habitats attained the highest DG at 60 days of age and their maximum values were not as uneven (**Figures 5A,D**). When compared with summer-born sprats captured in 2017 in TDF, DG at 60 and 80 days of age of spring-born sprats in TDF were significantly higher in the latter case (**Table 5**). DG of summer-born sprats did not resemble their IW growth patterns. In TDF (**Figure 5E**), DG increased from hatching until 20–30 days of age and decreased afterward, while in the MPAN-BB growth was maximum at the early larval phase and declined after the first 50 days of age (**Figure 5B**). Inter-annual variability also differed according to the habitat analyzed. The dissimilarity recognized in TDF laid in the position of the peak of maximum DG, occurring later for sprats sampled in 2017 than in those captured in 2016. However, DG did not statistically differ in neither of the ages assessed (20, 40, 60, 80, and 100 days of age) (**Table 5**). On the contrary, differences in the MPAN-BB did not involve variability in the shape of the trajectory but rather in the magnitude of the estimated values, with DG being significantly higher in sprats sampled in 2016 at all ages compared (**Table 5**). Finally, DG of sprats born in the MPAN-BB in autumn of 2016 decreased from hatching to capture (**Figure 5C**). Although they exhibited the maximum DG rates estimated, this group also displayed the major variability observed (in standard deviations) among all the groups considered.

Growth Trajectories and Temperature Time Series

Sea-surface temperature was assessed from December of 2015 (month of the first estimated hatching date) to June of 2017 (subsequent month to the last sampled date in the 2017 survey) in both habitats (**Figures 6A,B**). Temperatures differed significantly across habitats (chi-square = 123.66, df = 1, $p < 0.0001$), being higher in TDF (8.10 ± 1.94°C) than in the MPAN-BB (6.35 ± 1.19°C). Minimum temperatures registered (winter) were similar across habitats (approximately 3°C). In contrast, maximum temperatures (summer) were higher in TDF (11.69°C) (**Figure 6B**) than in the MPAN-BB, where they did not surpass the 9°C (**Figure 6A**). This difference was responsible for the wider temperature range of the former (8.33°C) compared to the latter (5.87°C). Moreover, inter-annual variability was also observed within habitats, with higher temperatures being registered in the summer of 2017 (compared to 2016) (chi-square = 38.49, df = 1, $p = 0.0024$ for TDF and chi-square = 60.61, df = 1, $p < 0.0001$ for the MPAN-BB).

Major coupling between mean growth trajectories of Fuegian sprats and SST was found for most of the groups considered (i.e., sprats according to the habitat, year sampled and season of hatching) (**Figures 6C,D**). The moment at which maximum IW and DG were first attained occurred roughly at the same time at which SST did in both habitats. The only exception was observed in spring-born sprats of TDF (larger trajectories in **Figure 6D**) sampled in 2017, which attained IW and DG peaks more than a month before temperature did. Although IW trajectories varied considerably after these peaks, DG consistently declined after these maximum values in all cases considered, therefore following the decrease in SST after its peak in summer.

Pearson correlation coefficients evidenced a significant positive correlation between SST and age-detrended IW and DG in 2017 for all the groups considered (**Table 6**), year in which maximum SST temperatures were registered. On the contrary, coefficients estimated for 2016 differed across groups, being positive for sprats from TDF, but mainly negative for sprats from the NMPA-BB. However, only the correlation between summer-born sprats' IW from the NMPA- BB was significant for the groups assessed in 2016.

TABLE 2 | Minimum (min), maximum (max) and mean otolith increment widths (IW; μm) of Fuegian sprats *Sprattus fuegensis* analyzed in the Marine Protected Area Namuncurá-Burdwood Bank (MPAN-BB) and Tierra del Fuego (TDF).

Survey	Hatching season	MPAN-BB			TDF		
		N	Min – max	Mean IW	N	Min – max	Mean IW
Total	–	10330	0.17 – 3.50	0.99 ± 0.33	6289	0.17 – 6.23	1.78 ± 0.87
2016	Total	7073	0.17 – 3.50	0.94 ± 0.30	590	0.17 – 2.52	1.12 ± 0.38
	Summer	6897	0.17 – 3.50	0.95 ± 0.30	590	0.17 – 2.52	1.12 ± 0.38
	Autumn	176	0.24 – 1.79	0.72 ± 0.29	–	–	–
2017	Total	3257	0.17 – 2.86	1.09 ± 0.37	5699	0.34 – 6.23	1.85 ± 0.88
	Spring	159	0.34 – 2.02	1.05 ± 0.38	3634	0.34 – 6.23	1.92 ± 0.99
	Summer	3098	0.17 – 2.86	1.10 ± 0.37	2065	0.34 – 4.25	1.72 ± 0.61

Number of increments measured (N) are informed according to the survey and season of hatching. Variability around the mean displayed as standard deviation.

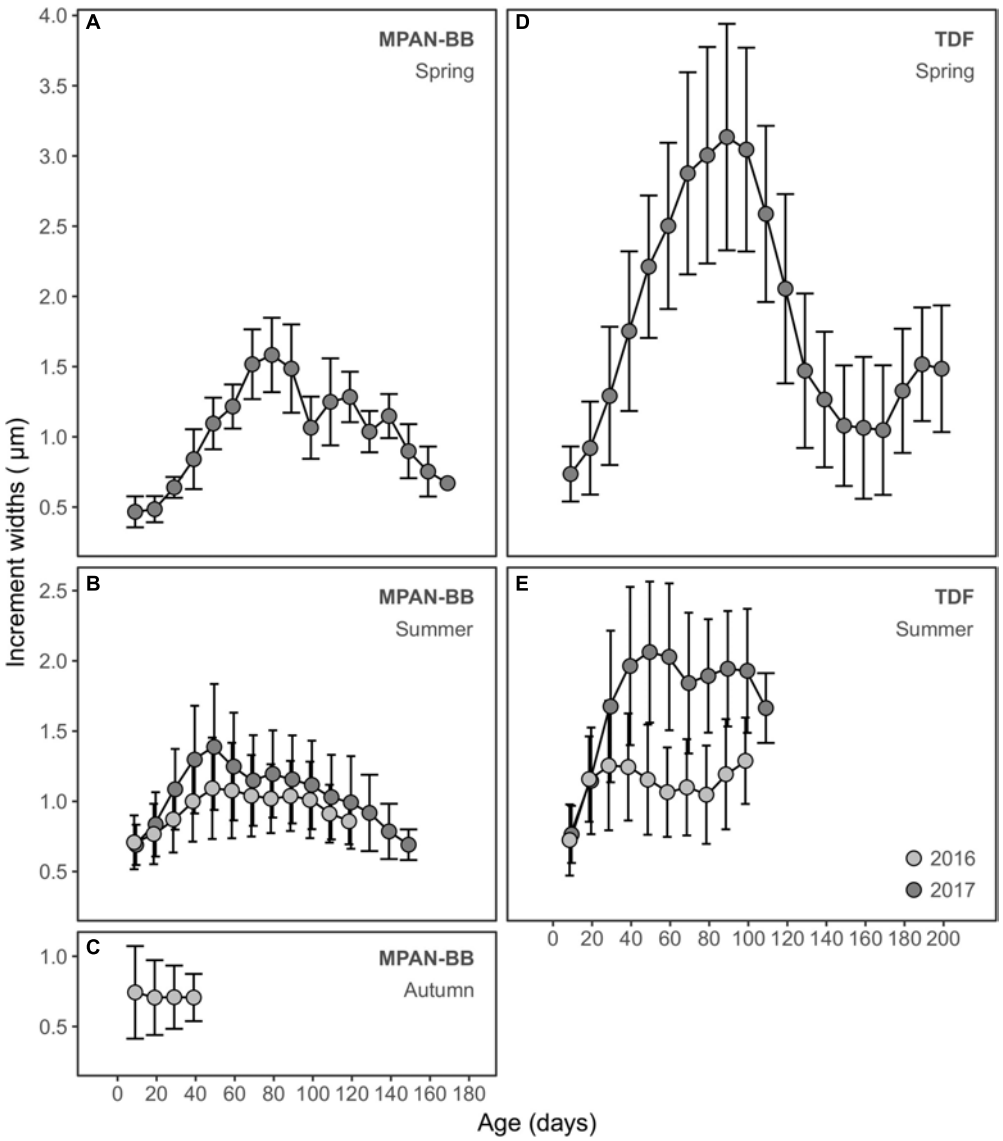

FIGURE 4 | Otolith increment widths (μm) in relation to age (days) of Fuegian sprat *Sprattus fuegensis* in the Marine Protected Area Namuncurá-Burdwood Bank (MPAN-BB) **(A–C)** and Tierra del Fuego (TDF) **(D–E)**. Records are grouped according to the year sampled (colors) and season of hatching: spring **(A,D)**, summer **(B,E)** and autumn **(C)**. Increment widths are averaged every 10 days, with variation around the mean displayed as standard deviations.

TABLE 3 | Results of repeated measure analyses of otolith increment widths at 20, 40, 60, 80, and 100 days of age of Fuegian sprats *Sprattus fuegensis* in the Marine Protected Area Namuncurá-Burdwood Bank (MPAN-BB) and Tierra del Fuego (TDF).

Factor	Data	Model statistics				Pair-wise comparisons				
		Effect	df	χ^2	*p*-value	20	40	60	80	100
Habitat	Summer-born/2016	Habitat	1	29.851	<0.001	*	*	–	–	–
		Age	4	95.323	<0.001					
		Habitat*Age	4	25.096	<0.001					
	Summer-born/2017	Habitat	1	8.419	0.004	*	*	*	*	*
		Age	4	40.093	<0.001					
		Habitat*Age	4	9.458	0.051					
Year	Summer-born/MPAN-BB	Year	1	1.157	0.218	–	*	–	–	–
		Age	4	91.853	<0.001					
		Year*Age	4	13.676	0.008					
	Summer-born/TDF	Year	1	0	0.767	–	–	*	*	–
		Age	4	10.997	0.027					
		Year*Age	4	23.797	<0.001					
Hatching season	Spring- and summer-born/TDF/2017	Hatching season	1	3.699	0.054	–	–	*	*	*
		Age	4	313.678	<0.001					
		Hatching season*Age	4	53.581	<0.001					

Data used in each analysis is specified according to the factor assessed (habitat, years or hatching seasons). Test statistics for main effects and interactions of the models selected are informed. Asterisks (*) represent significant differences (p-value < 0.05) obtained in the post hoc pair-wise comparison across levels of each factor for equivalent ages.

TABLE 4 | Minimum (min), maximum (max) and mean daily growth rates (mm d^{-1}) of Fuegian sprats *Sprattus fuegensis* sampled in the autumn surveys in the Marine Protected Area Namuncurá-Burdwood Bank (MPAN-BB) and Tierra del Fuego (TDF).

Survey	Hatching season	MPAN-BB		TDF	
		Min – max	Mean daily growth	Min – max	Mean daily growth
All	–	0.03 – 1.52	0.23 ± 0.10	0.02 – 0.70	0.22 ± 0.09
2016	total	0.05 – 1.52	0.26 ± 0.09	0.05 – 0.51	0.22 ± 0.08
	summer	0.05 – 0.73	0.26 ± 0.08	0.05 – 0.51	0.22 ± 0.08
	autumn	0.17 – 1.52	0.51 ± 0.21	–	–
2017	total	0.03 – 0.44	0.16 ± 0.06	0.02 – 0.67	0.22 ± 0.09
	spring	0.05 – 0.28	0.15 ± 0.05	0.02 – 0.67	0.21 ± 0.09
	summer	0.03 – 0.44	0.16 ± 0.06	0.07 – 0.56	0.23 ± 0.08

*Growth values considered are equivalent to the ones informed in **Table 2**. Variability around the mean displayed as standard deviation.*

DISCUSSION

Otolith microstructure analyzes provide important life-history knowledge (Campana and Neilson, 1985; Stevenson and Campana, 1992; Morales-Nin, 2000; Sponaugle, 2010), with information from field-caught fishes being particularly valuable for species which are difficult to rear in the laboratory, such as sprats (Peck et al., 2004; Baumann et al., 2005; Petereit et al., 2008; Leal et al., 2017). In this context, collecting samples in two environmentally distinct habitats represented a unique opportunity to evaluate early growth variability of Fuegian sprats in relation to physical characteristics such as temperature. However, sampling in an open-sea area as the MPAN-BB is both logistically and meteorologically challenging. Recurrent oceanographic surveys were recently carried out in this submarine *plateau* of high biodiversity and conservational importance (e.g., Schejter et al., 2016; Fraysse et al., 2018; Di Luca and Zelaya, 2019; Schejter and Bremec, 2019) and its adjacent areas as a result of the implementation of the Argentinian national initiative "Pampa Azul". Results shown here not only represent the first comparison of age-0 *S. fuegensis* growth trajectories from these spawning/nursery grounds of the SWAO, but also represent an update on early sprats' knowledge sampled for the last time over 20 years ago.

Determining when successful recruits are predominantly produced represents crucial information in the attempt to understand the recruitment dynamic of batch spawner fishes (Baumann et al., 2008) such as the Fuegian sprat (Shirokova, 1978; Hansen, 1999). Survivors sampled in the autumn surveys (2016 and 2017) were born during spring/summer in TDF or spring/autumn in the MPAN-BB. In the latter, only one spring-born specimen was captured during these surveys, with no post-larvae being captured at all, thus suggesting a selective

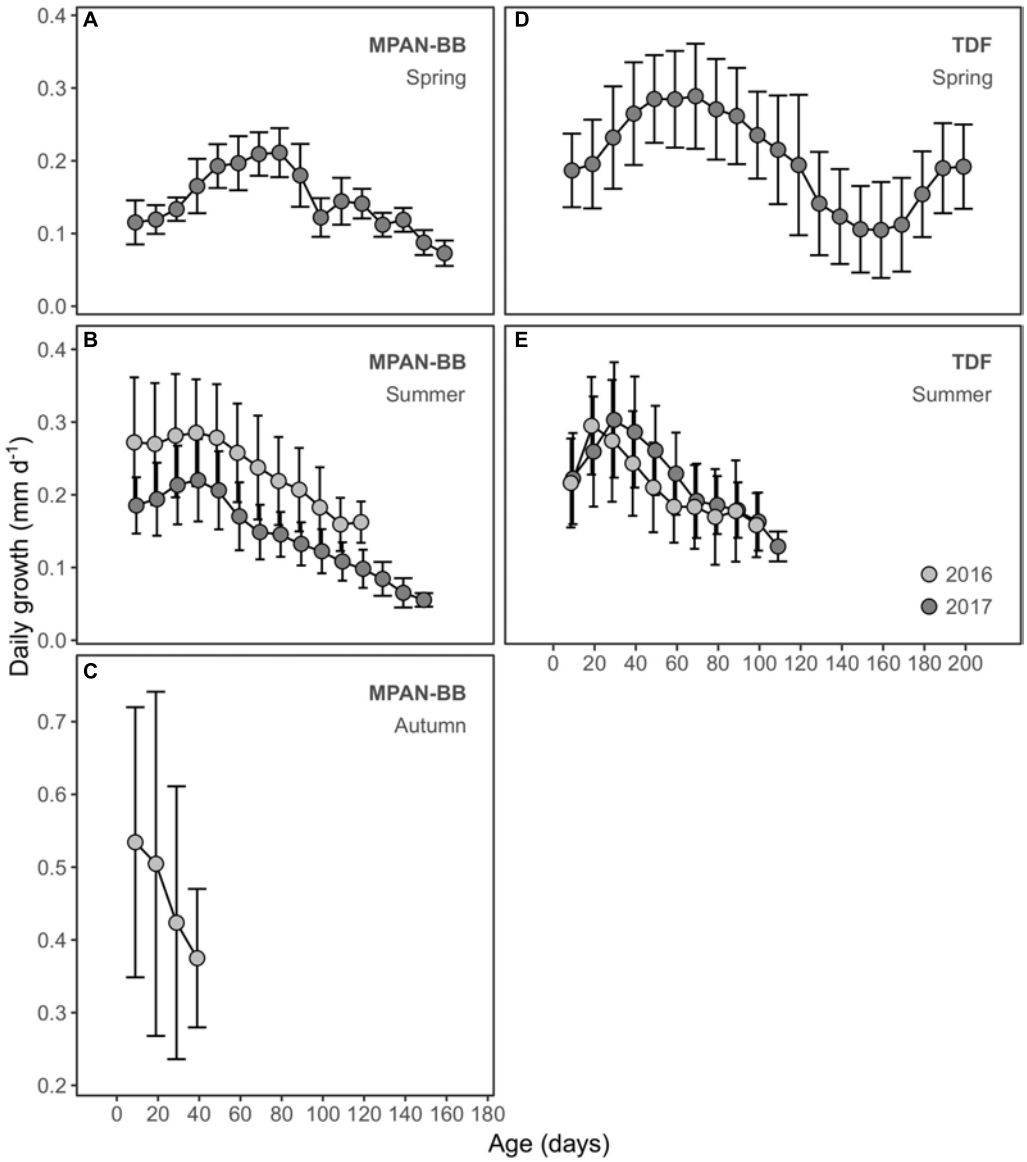

FIGURE 5 | Daily growth (mm d^{-1}) in relation to age (days) of Fuegian sprat *Sprattus fuegensis* in the Marine Protected Area Namuncurá-Burdwood Bank (MPAN-BB) **(A–C)** and Tierra del Fuego (TDF) **(D–E)**. Records are grouped according to the year sampled (colors) and season of hatching: spring **(A,D)**, summer **(B,E)** and autumn **(C)**. Daily growths are averaged every 10 days, with variation around the mean displayed as standard deviations.

survival of later born sprats. Colder conditions experienced in spring may be disadvantageous for larval development (Baumann et al., 2008), although this warrants a more detailed assessment since the response to cold water temperatures of clupeid larvae can vary rapidly and is species-specific (Molina-Valdivia et al., 2020). Also, density-dependent control (Baumann et al., 2007) could be taking place during this period of major spawning in the MPAN-BB (García Alonso et al., 2018). However, in the light of recent results from numerical models addressing water circulation in the bank (Matano et al., 2019), combined with the fact that sprats generally reside close to coastlines (Whitehead, 1985), an alternative explanation for this outcome implies that nursery of these older/bigger specimens may not occur within the bank. In this regard, the Malvinas (Falkland) Islands area arises as the most probable destination given their geographic proximity and estimated water circulation pattern. In TDF, similar cautions should be taken before jumping into conclusions over selective survival. Spring-born were only captured with the IKMT net in 2017, an appropriate sampling gear for bigger/faster specimens (Fey, 2015). Although the absence of spring-born sprats in 2016 could be the result of selective survival of summer-born specimens, this outcome is most likely to be reflecting the selectivity of the net employed. Employing the IKMT net and broadening the sampled areas are therefore necessary to untangle these uncertainties.

TABLE 5 | Results of repeated measure analyses of daily growth rates at 20, 40, 60, 80, and 100 days of age of Fuegian sprats *Sprattus fuegensis* in the Marine Protected Area Namuncurá-Burdwood Bank (MPAN-BB) and Tierra del Fuego (TDF).

Factor	Data	Model statistics				Pair-wise comparisons				
		Effect	df	χ^2	*p*-value	20	40	60	80	100
Habitat	Summer-born/2016	Habitat	1	9.792	0.002	–	–	*	–	–
		Age	4	63.600	<0.001					
		Habitat*Age	4	29.795	<0.001					
	Summer-born/2017	Habitat	1	67.608	<0.001	*	*	*	*	*
		Age	4	109.143	<0.001					
		Habitat*Age	4	0.858	0.931					
Year	Summer-born/MPAN-BB	Year	1	185.530	<0.001	*	*	*	*	*
		Age	4	120.133	<0.001					
		Year*Age	4	2.569	0.632					
	Summer-born/TDF	Year	1	0.886	0.347	–	–	–	–	–
		Age	4	58.057	<0.001					
		Year*Age	4	10.563	0.031					
Hatching season	Spring- and summer-born/TDF/2017	Hatching season	1	6.068	0.014	*	–	*	*	–
		Age	4	22.653	<0.001					
		Hatching season*Age	4	50.952	<0.001					

Data used in each analysis is specified according to the factor assessed (habitat, years or hatching seasons). Test statistics for main effects and interactions of factors with age are informed. Asterisks (*) represent significant differences (p-value < 0.05) obtained in the post hoc pair-wise comparison across levels of each factor for equivalent ages.

As previously mentioned, otolith microstructure analysis is a powerful tool which can provide growth information of life-history events and environmental effects over growth. Before analyzing otolith growth trajectories, sprats' ages and developmental stages already provided strong evidence of differential growth across habitats. Spring-born sprats of 155 days or older were post-larval specimens in TDF, with transition estimated to occur around 110 days of age. However, several sprats captured in the MPAN-BB were more than 110 days old, reaching similar ages (152 days) or even older (165 days) than post-larvae from TDF, yet still evidencing larval morphology, thus further supporting a protracted larval stage in the former habitat (García Alonso et al., 2018). Stage durations tend to be both longer and potentially more variable in higher latitudes subject to colder temperatures (Houde, 1989). Although the MPAN-BB occupies a similar latitudinal range than TDF, this habitat is subject to colder temperatures which would account for this difference in larval stage duration.

Modeling age-size relations constitutes one of the most common methodologies used to assess early growth of *S. fuegensis* in both the Southeast Pacific Ocean (Cerna et al., 2014; Leal et al., 2017) and the SWAO (Sánchez et al., 1995, 1997; Brown and Sánchez, 2010; García Alonso et al., 2018). Given that collected sprats corresponded to different cohorts and the restricted SL ranges covered, back-calculating previous SL based on SL-OR relations (Stevenson and Campana, 1992) was the chosen methodology to estimate daily growth rates in this study. Many authors employed otolith growth (i.e., IW or mean standardized IW) as a direct proxy for somatic growth (e.g., Baumann et al., 2006a, 2008; Hinrichsen et al., 2010). However, in the light of differential SL-OR relationships observed among larval and post-larval stages (Günther et al., 2012; this study) and with IW being highly autocorrelated and age dependent (Hinrichsen et al., 2010), modeling SL-OR relations and generating SL daily back-calculations arises as a more adequate approach in the estimation of DG rates of Fuegian sprats. Furthermore, inter-annual variability should also be considered when pooling data from a particular population. Increment deposition during the firsts 20 days of age of Fuegian sprats did not vary considerably across habitats nor hatching seasons. Even more, they closely resembled the pattern described for the Chilean Patagonian population of *S. fuegensis* (Landaeta et al., 2012). However, when comparing data from the autumn surveys, OR in the year 2017 were wider that in sprats of equivalent SL in 2016 in both habitats. This was a direct consequence of wider IW being deposited in 2017 (**Table 2**) in accordance to higher temperatures registered in both habitats during that year (**Figure 6**).

Besides selecting adequate SL-OR models (Günther et al., 2012), other considerations should also be taken when assessing sprats' growth on the basis of otolith IW such as otolith growth-somatic growth decoupling. Decoupling in length and otolith growth of age-0 Fuegian sprats has been previously reported (García Alonso et al., 2018), with variable environmental conditions including feeding condition, salinity and vertical stratification (Baumann et al., 2005; Landaeta et al., 2012; Zenteno et al., 2014) and/or ontogenetic shifts (Günther et al., 2012) being among the possible causes for such decoupling. Our results not only yield evidence supporting the existence of otolith length-fish length decoupling in Fuegian sprats in all the groups considered (Contreras et al., 2017), but also suggest that this decoupling becomes more pronounced toward the end of the hatching period. Spring-born sprats from TDF only evidenced a dissociation between IW and DG peaks but did not display major variations in the overall trajectories, with moderate decoupling exhibited in the MPAN-BB overall. On the contrary, summer-born sprats in both

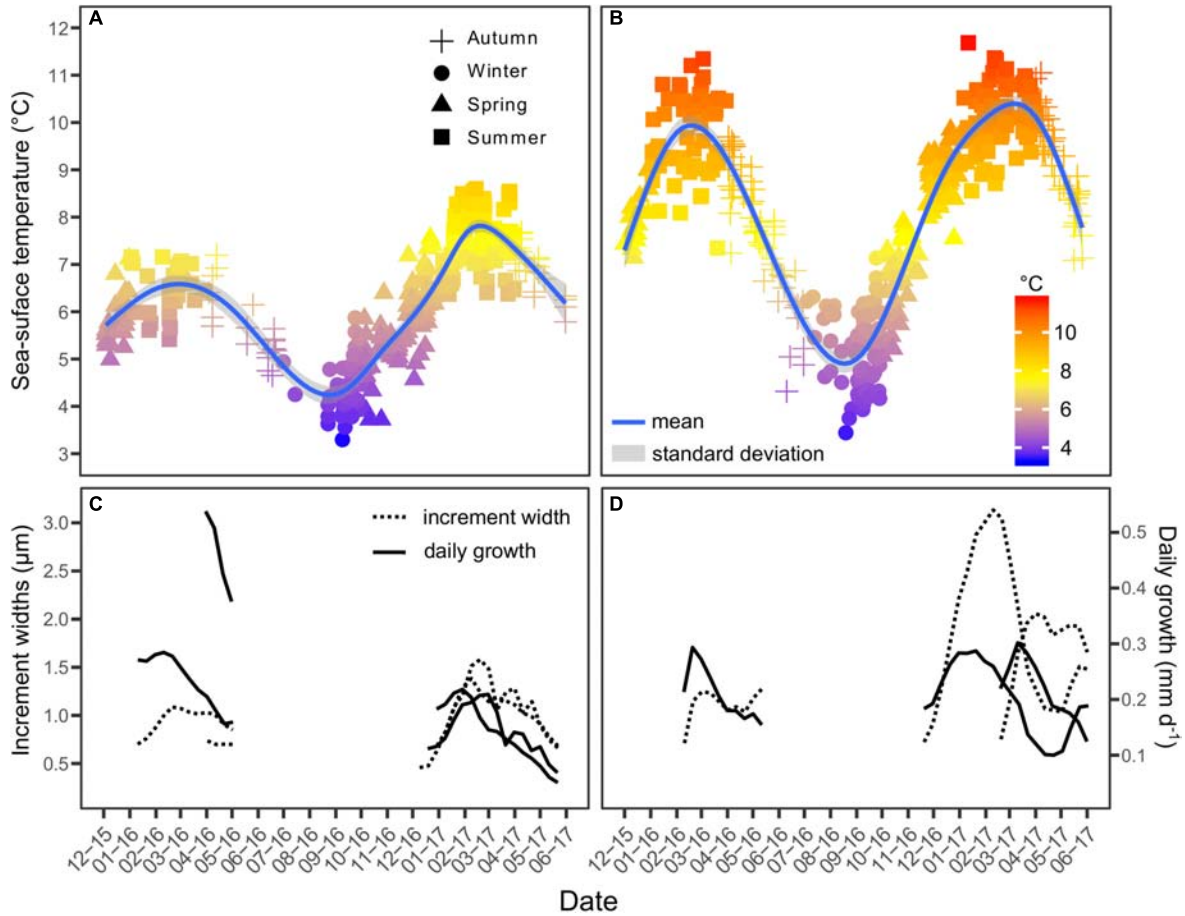

FIGURE 6 | Sea-surface temperature (°C) time series in the Marine Protected Area Namuncurá-Burdwood Bank (MPAN-BB) **(A)** and in Tierra del Fuego (TDF) **(B)**. Sites from which data was obtained are shown in the reference maps. Shapes indicate the season of the record. Mean trajectories of increment widths (µm; dotted lines) and daily growths (mm d^{-1}; solid lines) for each habitat, survey and season of hatching are displayed **(C–D)**.

habitats did show distinct IW and DG patterns. For sprats sampled in TDF, decoupling was observed after the first 30 days of age during which IW remained in a *plateau* of high values, but DG constantly decreased. A similar decoupling was detected for sprats sampled in the MPAN-BB, but this discrepancy took place between 50 and 100 days, after which IW trajectories started decreasing. Moreover, autumn-born sprats not only evidenced discordant growth trajectories patterns, but displayed the lowest IW and highest DG (**Figure 6**), further supporting the idea that estimating somatic growth by direct comparison with IW values could lead to major inconsistencies.

Notwithstanding the particular differences mentioned above, an important general coupling was observed between these growth trajectories' patterns and SST time series, thus corroborating an important effect of temperature variability over them. With the exception of spring-born sprats sampled in 2017 in TDF, the dates at which maximum temperatures were registered correlated with the moment at which maximum IW and DG values were first attained, with DG trajectories closely resembling temperature patterns overall (**Figure 6**). Furthermore, significant positive correlations were estimated for both IW and DG with SST in most of the cases considered (**Table 6**) further supporting such association.

TABLE 6 | Pearson correlation coefficients for age-detrended increment widths (IW) and daily growth rates (DG) of Fuegian sprats *Sprattus fuegensis* in relation to sea surface temperature in the Marine Protected Area Namuncurá-Burdwood Bank (MPAN-BB) and Tierra del Fuego (TDF).

Survey	Habitat	Hatching season	IW	DG
2016	MPAN-BB	Summer	**−0.074**	−0.021
		Autumn	0.154	−0.091
	TDF	Summer	0.012	0.024
2017	MPAN-BB	Spring	**0.536**	**0.686**
		Summer	**0.245**	**0.228**
	TDF	Summer	**0.071**	**0.149**
		Spring	**0.197**	**0.308**

Correlations were performed according to the survey, habitat and sprats' hatching seasons. Statistically significant estimates are visualized in bold.

However, although higher DG are expected to occur in warmer environmental conditions, highest mean DG values of 0.26 and 0.51 mm d^{-1} were estimated for summer- and autumn-born sprats in the MPAN-BB in 2016, habitat and year with the coldest maximum temperatures registered. In fact, the mean growth of autumn-born sprats from the MPAN-BB was higher than the one estimated for *S. fuegensis* from Chilean Patagonia (0.45 mm d^{-1}) where temperatures measured were about 2°C above the ones measured in the NMPA-BB (Landaeta et al., 2012). Lower temperatures could be advantageous for faster growth in the NMAP-BB by setting lower food ingestion requirements to support growth in such a cold habitat (Houde, 1989). Salinity could also be considered a possible factor affecting growth, however, Landaeta et al. (2012) found that this environmental forcing did not significantly correlate with larval otolith growth of *S. fuegensis*. Another possible explanation for this outcome lies in the high phytoplankton biomass detected during the 2016 survey over the MPAN-BB, composed mainly of *Rhizosolenia crassa* diatom (Bértola pers. comm.). Although these organisms are not the most adequate food source for Fuegian sprats, their high abundances indicates the existence of favorable environmental conditions for phytoplankton proliferation and, thus, zooplankters which are the main prey items in *S. fuegensis* diet.

Further analyzes are still necessary to unravel underlying mechanisms during early development of Fuegian sprats not evaluated yet. However, the results from the present study comprise a fundamental baseline in the understanding of environmental variation over growth of age-0 *S. fuegensis* in the SWAO. Strong correlation with temperature appears to be a key factor implied in growth modulation, but the habitat, seasonal and inter-annual variability observed revealed a high complexity in the early development of this species, which in turn can influence recruitment success. Biological mechanisms involved in the multiple processes simultaneously affecting recruitment need to be thoroughly understood before predictions and/or suggestions can be proposed (Baumann et al., 2006b; Voss et al., 2012). Nonetheless, otolith microstructure analyzes emerges as powerful tool in the assessment of life-history of Fuegian sprats, and information gathered in this study provides keystone information upon which adequate ecosystem based management strategies for the different habitats existing in the SWAO can be based on.

DATA AVAILABILITY STATEMENT

The datasets generated for this study are available on request to the corresponding author.

ETHICS STATEMENT

The research reported here has been conducted in an Ethical and responsible manner, complying with all applicable international, national, and/or institutional guidelines for the care and use of fish larvae and post-larvae.

AUTHOR CONTRIBUTIONS

VG and FC conceived and designed the study. VG and DB conducted the field work and performed the otolith microstructure analyzes. MP and FC provided the necessary sampling gear and materials. VG organized the database, performed the data analyzes, and wrote the manuscript. All authors participated in the edition and discussion of the manuscript making valuable contributions.

FUNDING

Operating costs were afforded with funds from the MPA Namuncurá-Banco Burdwood creation law (Law 26.875). This research is part of the Pampa Azul interministerial initiative promoted by Argentine Ministry for Science, Technology and Productive Innovation. This study is part of the Ph.D. by VGA who was supported by a Doctoral Fellowship awarded by the National Scientific and Technical Research Council-Argentina (CONICET-Argentina). FC was funded by CONICET-Argentina (PIP 11220150100109CO 2015-2017) and the University of Buenos Aires, Argentina (UBACYT 20020160100045BA 2017-2020).

ACKNOWLEDGMENTS

The authors would like to thank Luciano Padovani and Alejandro Martinez for their collaboration during sample collection and preparation and to Pablo S. Milla Carmona for his statistical advices. We extend our thanks to both reviewers for their suggestions and corrections, which greatly improved the manuscript. This is INIDEP contribution N° 2207 and Marine Protected Area Namuncurá-Burdwood Bank (Law 26,875) contribution N° 35 MODIS data was distributed by the NASA Ocean Biology Processing Group. Parts of these results were presented in the "II Workshop Latinoamericano de Otolitos."

REFERENCES

Acha, E. M., Mianzan, H. W., Guerrero, R. A., Favero, M., and Bava, J. (2004). Marine fronts at the continental shelves of austral South America: physical and ecological processes. *J. Mar. Syst.* 44, 83–105. doi: 10.1016/j.jmarsys.2003.09.005

Acha, E. M., Pájaro, M., and Sánchez, R. P. (1999). "The reproductive response of clupeoid fishes to different physical scenarios. three study cases in the Southwest Atlantic," in *Proceedings of the ICES Annual Science Conference, ICES CM 1997_K:12*, Copenhagen.

Akaike, H. (1974). A new look at the statistical model identification. *IEEE Trans. Autom. Control* 19, 716–723. doi: 10.1109/TAC.1974.1100705

Alheit, J., and Hagen, E. (2001). "The effect of climatic variation on pelagic fish and fisheries," in *History and Climate*, eds P. D. Jones, A. E. J. Ogilvie, T. D. Davies, and K. R. Briffa (Boston, MA: Springer), 247–265.

Alshuth, S. (1988). Daily growth increments on otoliths of laboratory reared sprat, *Sprattus sprattus* L., larvae. *Meeresforsch* 32, 23–29.

Amante, C., and Eakins, B. W. (2009). *ETOPO1 1 Arc-Minute Global Relief Model: Procedures, Data Sources and Analysis*. NOAA Technical Memorandum NESDIS NGDC-24. Silver Spring: NOAA.

Anderson, J. T. (1988). A review of size dependent survival during pre-recruit stages of fishes in relation to recruitment. *J. Northwest Atlant. Fish. Sci.* 8, 55–66.

Antezana, T. (1999). Hydrographic features of Magellan and Fuegian inland passages and adjacent Subantarctic waters. *Sci. Mar.* 63, 23–34.

Aranis, A., Meléndez, R., Pequeño, G., and Cerna, F. (2007). *Sprattus fuegensis* en aguas interiores de Chiloé, Chile (Osteichthyes: Clupeiformes: Clupeidae). *Gayana* 71, 102–113.

Bakun, A. (2006). Wasp-waist populations and marine ecosystem dynamics: navigating the "predator pit" topographies. *Prog. Oceanogr.* 68, 271–288. doi: 10.1016/j.pocean.2006.02.004

Balestrini, C., Manzella, G., and Lovrich, G. A. (1998). Simulación de corrientes en el Canal Beagle y Bahía Ushuaia, mediante un modelo bidimensional. *Serv. Hidrografía Naval* 98, 1–58. doi: 10.13140/RG.2.1.1196.272

Baumann, H., Gröhsler, T., Kornilovs, G., Makarchouk, A., Feldmann, V., and Temming, A. (2006a). Temperature-induced regional and temporal growth differences in Baltic young-of-the-year sprat *Sprattus sprattus*. *Mar. Ecol. Prog. Ser.* 317, 225–236. doi: 10.3354/meps317225

Baumann, H., Hinrichsen, H. H., Möllmann, C., Köster, F. W., Malzahn, A. M., and Temming, A. (2006b). Recruitment variability in Baltic Sea sprat (*Sprattus sprattus*) is tightly coupled to temperature and transport patterns affecting the larval and early juvenile stages. *Can. J. Fish. Aquat. Sci.* 63, 2191–2201. doi: 10.1139/f06-112

Baumann, H., Hinrichsen, H. H., Voss, R., Stepputtis, D., Grygiel, W., Clausen, L. W., et al. (2006c). Linking growth to environmental histories in central Baltic young-of-the-year sprat, *Sprattus sprattus*: an approach based on otolith microstructure analysis and hydrodynamic modelling. *Fish. Oceanogr.* 15, 465–476. doi: 10.1111/j.1365-2419.2005.00395.x

Baumann, H., Peck, M. A., Götze, H. E., and Temming, A. (2007). Starving early juvenile sprat *Sprattus sprattus* (L.) in western Baltic coastal waters: evidence from combined field and laboratory observations in August and September 2003. *J. Fish Biol.* 70, 853–866. doi: 10.1111/j.1095-8649.2007.01346.x

Baumann, H., Peck, M. A., and Herrmann, J. P. (2005). Short-term decoupling of otolith and somatic growth induced by food level changes in postlarval Baltic sprat, *Sprattus sprattus*. *Mar. Freshw. Res.* 56, 539–547. doi: 10.1071/MF04140

Baumann, H., Voss, R., Hinrichsen, H. H., Mohrholz, V., Schmidt, J. O., and Temming, A. (2008). Investigating the selective survival of summer-over spring-born sprat, *Sprattus sprattus*, in the Baltic Sea. *Fish. Res.* 91, 1–14. doi: 10.1016/j.fishres.2007.11.004

Belleggia, M., Figueroa, D. E., Irusta, G., and Bremec, C. (2014). Spatio-temporal and ontogenetic changes in the diet of the Argentine hake *Merluccius hubbsi*. *J. Mar. Biol. Assoc. U. K.* 94, 1701–1710. doi: 10.1017/S0025315414000629

Bellisio, N. B., López, R. B., and Torno, A. (1979). *Peces Marinos Patagónicos. Secretaria de Estado de Intereses Maítimos, Subsecretaría de Pesca*. Argentina: Buenos Aires.

Bezzi, S. I. (1984). Aspectos biológicos pesqueros de la merluza de cola del Atlántico Sudoccidental. *Rev. Investig. Desarrollo Pesquero INIDEP* 4, 63–80.

Brown, D. R., and Sánchez, R. P. (2010). Larval and juvenile growth of two Patagonian small pelagic fshes: *Engraulis anchoita* and *Sprattus fuegensis*. *Rev. Investig. Desarrollo Pesquero INIDEP* 20, 35–50.

Bruno, D. O., Victorio, M. F., Acha, E. M., and Fernández, D. A. (2018). Fish early life stages associated with giant kelp forests in sub-Antarctic coastal waters (Beagle Channel, Argentina). *Polar Biol.* 41, 365–375. doi: 10.1007/s00300-017-2196-y

Campana, S. E. (1990). How reliable are growth back-calculations based on otoliths? *Can. J. Fish. Aquat. Sci.* 47, 2219–2227. doi: 10.1139/f90-246

Campana, S. E. (1992). "Measurement and interpretation of the microstructure of fish otoliths," in *Otolith Microstructure Examination and Analysis*, eds D. K. Stevenson and S. E. Campana (Ottawa: Canada Communication Group - Publishing), 59–71.

Campana, S. E., and Neilson, J. D. (1985). Microstructure of fish otoliths. *Can. J. Fish. Aquat. Sci.* 42, 1014–1032. doi: 10.1139/f85-127

Cerna, F., Leal, E., López, A., and Plaza, G. (2014). Age, growth and natural mortality of the Patagonian sprat *Sprattus fuegensis* (Jenyns, 1842) in Chiloé inland sea, southern Chile. *Latin Am. J. Aquat. Res.* 42, 580–587. doi: 10.3856/vol42-issue3-fulltext-15

Ciancio, J. E., Pascual, M. A., Botto, F., Frere, E., and Iribarne, O. (2008). Trophic relationships of exotic anadromous salmonids in the southern Patagonian Shelf as inferred from stable isotopes. *Limnol. Oceanogr.* 53, 788–798. doi: 10.4319/lo.2008.53.2.0788

Ciechomski, J. D., Cassia, M. C., and Weiss, G. (1975). Distribución de huevos, larvas y juveniles de peces en los sectores surbonaerenses, patagónico y fueguino del mar epicontinental argentino, en relación con las condiciones ambientales, en noviembre 1973-enero 1974. *Ecosur* 2, 219–248.

Ciechomski, J. D., and Weiss, G. (1974). Consideraciones sobre la reproducción y distribución cuantitativa de huevos y larvas de la sardina fueguina *Sprattus fuegensis*, en sector patagónico del Atlántico. FAO/CARPAS/6. *Docu. Técn.* 12, 1–11.

Contreras, J. E., Rodriguez-Valentino, C., Landaeta, M. F., Plaza, G., Castillo, M. I, and Alvarado-Niño, M. (2017). Growth and mortality of larval anchoveta *Engraulis ringens*, in northern Chile during winter and their relationship with coastal hydrographic conditions. *Fish. Oceanogr.* 26, 603–614. doi: 10.1111/fog.12219

Contreras, T., Castro, L. R., Montecinos, S., Gonzalez, H. E., Soto, S., Muñoz, M. I., et al. (2014). Environmental conditions, early life stages distributions and larval feeding of patagonian sprat *Sprattus fuegensis* and common sardine *Strangomera bentincki* in fjords and channels of the northern Chilean patagonia. *Prog. Oceanogr.* 129, 136–148. doi: 10.1016/j.pocean.2014.10.005

Cousseau, M. B. (1982). Revisión taxonómica y análisis de los caracteres morfométricos y merísticos de la sardina fueguina, *Sprattus fuegensis* (Jenyns, 1842) (Pisces, Clupeidae). *Rev. Investig. Desarrollo Pesquero INIDEP* 3, 77–94.

Cury, P., Bakun, A., Crawford, R. J., Jarre, A., Quinones, R. A., Shannon, L. J., et al. (2000). Small pelagics in upwelling systems: patterns of interaction and structural changes in "wasp-waist" ecosystems. *ICES J. Mar. Sci.* 57, 603–618. doi: 10.1006/jmsc.2000.0712

Cushing, D. H. (1990). Plankton production and year-class strength in fish populations: an update of the match/mismatch hypothesis. *Adv. Mar. Biol.* 26, 249–293. doi: 10.1016/S0065-2881(08)60202-3

Di Luca, J., and Zelaya, D. G. (2019). Gastropods from the Burdwood Bank (southwestern Atlantic): an overview of species diversity. *Zootaxa* 4544, 41–78. doi: 10.11646/zootaxa.4544.1.2

Fauchald, P., Skov, H., Skern-Mauritzen, M., Johns, D., and Tveraa, T. (2011). Wasp-waist interactions in the North Sea ecosystem. *PLoS One* 6:e22729. doi: 10.1371/journal.pone.0022729

Fey, D. P. (1999). Effects of preservation technique on the length of larval fish: methods of correcting estimates and their implication for studying growth rates. *Arch. Fish. Mar. Res.* 47, 17–29.

Fey, D. P. (2015). Size and growth rate differences of larval Baltic sprat *Sprattus sprattus* collected with bongo and MIK nets. *J. Fish Biol.* 86, 355–359. doi: 10.1111/jfb.12528

Fox, J., and Weisberg, S. (2011). *An {R} Companion to Applied Regression, Second Edition*. Thousand Oaks, CA: Sage.

Francis, R. I. C. C. (1990). Back-calculation of fish length: a critical review. *J. Fish Biol.* 36, 883–902. doi: 10.1111/j.1095-8649.1990.tb05636.x

Fraysse, C., Calcagno, J., and Pérez, A. F. (2018). Asteroidea of the southern tip of South America, including Namuncurá Marine Protected Area at Burdwood Bank and Tierra del Fuego Province, Argentina. *Polar Biol.* 41, 2423–2433. doi: 10.1007/s00300-018-2377-3

García Alonso, V. A., Brown, D., Martín, J., Pájaro, M., and Capitanio, F. L. (2018). Seasonal patterns of Patagonian sprat *Sprattus fuegensis* early life stages in an open sea Sub-Antarctic Marine Protected Area. *Polar Biol.* 41, 2167–2179. doi: 10.1007/s00300-018-2352-z

Glorioso, P. D., and Flather, R. A. (1995). A barotropic model of the currents off SE South America. *J. Geophys. Res. Oceans* 100, 13427–13440. doi: 10.1029/95JC00942

Gorelick, N., Hancher, M., Dixon, M., Ilyushchenko, S., Thau, D., and Moore, R. (2017). Google Earth Engine: planetary-scale geospatial analysis for everyone. *Remote Sens. Environ.* 202, 18–27. doi: 10.1016/j.rse.2017.06.031

Guerrero, R. A., Baldoni, A. G., and Benavides, H. R. (1999). Oceanographic conditions at the southern end of the Argentine continental slope. *Docu. Científico INIDEP* 5, 7–22.

Guerrero, R. A., and Piola, A. R. (1997). "Masas de agua en la plataforma continental," in *El Mar Argentino y Sus Recursos Pesqueros. Tomo 1. Antecedentes Históricos de las Exploraciones en el Mar Argentino y las Características Ambientales*, ed. E. E. Boschi (Mar del Plata, BA: Instituto Nacional de Investigación y Desarrollo Pesquero), 107–118.

Günther, C. C., Temming, A., Baumann, H., Huwer, B., Möllmann, C., Clemmesen, C., et al. (2012). A novel length back-calculation approach accounting for ontogenetic changes in the fish length–otolith size relationship during the early life of sprat (*Sprattus sprattus*). *Can. J. Fish. Aquat. Sci.* 69, 1214–1229. doi: 10.1139/f2012-054

Halekoh, U., Højsgaard, S., and Yan, J. (2006). The R package geepack for generalized estimating equations. *J. Stat. Softw.* 15, 1–11. doi: 10.18637/jss.v015.i02

Hansen, J. E. (1999). Estimación de parámetros poblacionales del efectivo de sardina fueguina (*Sprattus fuegensis*) de la costa continental Argentina. *Informe Técn. INIDEP* 27, 1–18.

Hinrichsen, H. H., Voss, R., Huwer, B., and Clemmesen, C. (2010). Variability of larval Baltic sprat (*Sprattus sprattus* L.) otolith growth: a modeling approach combining spatially and temporally resolved biotic and abiotic environmental key variables. *Fish. Oceanogr.* 19, 463–479. doi: 10.1111/j.1365-2419.2010.00557.x

Hjort, J. (1926). Fluctuations in the year classes of important food fishes. *ICES J. Mar. Sci.* 1, 5–38. doi: 10.1093/icesjms/1.1.5

Hothorn, T., Bretz, F., and Westfall, P. (2008). Simultaneous inference in general parametric models. *Biometr. J.* 50, 346–363. doi: 10.1002/bimj.200810425

Houde, E. D. (1987). Fish early dynamics and recruitment variability. *Am. Fish. Soc. Symp.* 2, 17–29.

Houde, E. D. (1989). Comparative growth, mortality and energetics of marine fish larvae: temperature and implied latitudinal effects. *Fish. Bull.* 87, 471–495.

Isla, F., Bujalesky, G., and Coronato, A. T. (1999). Procesos estuarinos en el canal Beagle, Tierra del Fuego. *Rev. Asoc. Geol. Argent.* 54, 307–318.

Kendall, A. W., Ahlstrom, E. H., and Moser, H. G. (1984). ""Early life history stages of fishes and their characters,"," in *Ontogeny and Systematics of Fishes*, eds H. G. Moser, W. J. Richards, D. M. Cohen, M. P. Fahay, A. W. Kendall, and S. L. Richardson (Lawrence, KS: Allen Press Inc), 11–22.

Köster, F. W., Hinrichsen, H. H., Schnack, D., John, M. A. S., Mackenzie, B. R., Tomkiewicz, J., et al. (2003). Recruitment of Baltic cod and sprat stocks: identification of critical life stages and incorporation of environmental variability into stock-recruitment relationships. *Sci. Mar.* 67, 129–154. doi: 10.3989/scimar.2003.67s1129

Laidig, T. E., Ralston, S., and Bence, J. R. (1991). Dynamics of growth in the early life history of shortbelly rockfish *Sebastes jordani*. *Fish. Bull.* 89, 611–621.

Landaeta, M. F., López, G., Suárez-Donoso, N., Bustos, C. A., and Balbontín, F. (2012). Larval fish distribution, growth and feeding in Patagonian fjords: potential effects of freshwater discharge. *Environ. Biol. Fishes* 93, 73–87. doi: 10.1007/s10641-011-9891-2

Landaeta, M. F., Martínez, R. A., Bustos, C. A., and Castro, L. R. (2013). Distribution of microplankton and fish larvae related to sharp clines in a Patagonian fjord. *Rev. Biol. Mar. Oceanogr.* 48, 401–407. doi: 10.4067/S0718-19572013000200020

Leal, E., Muñoz, C., Moyano, G., Bernal, C., and Aranis, A. (2017). A first experience of Patagonian sprat *Sprattus fuegensis* spawning in captivity: adult acclimation, egg and larval measurements. *Rev. Biol. Mar. Oceanogr.* 52, 641–645. doi: 10.4067/S0718-19572017000300021

Lebour, M. V. (1921). The larval and post-larval stages of the pilchard, sprat and herring from Plymouth district. *J. Mar. Biol. Assoc. U. K.* 12, 427–457. doi: 10.1017/S0025315400006299

Leggett, W. C., and Deblois, E. (1994). Recruitment in marine fishes: is it regulated by starvation and predation in the egg and larval stages? *Netherlands J. Sea Res.* 32, 119–134. doi: 10.1016/0077-7579(94)90036-1

Lenth, R. V. (2016). Least-squares means: the R Package lsmeans. *J. Stat. Softw.* 69, 1–33. doi: 10.18637/jss.v069.i01

Matano, R. P., Palma, E. D., and Combes, V. (2019). The Burdwood bank circulation. *J. Geophys. Res. Oceans* 124, 6904–6926. doi: 10.1029/2019JC015001

Molina-Valdivia, V., Landaeta, M. F., Castillo, M. I., Alarcón, D., and Plaza, G. (2020). Short-term variations in the early life history traits of common sardine *Strangomera bentincki* and anchoveta *Engraulis ringens* off central Chile. *Fish. Res.* 224:105460. doi: 10.1016/j.fishres.2019.105460

Morales-Nin, B. (2000). Review of the growth regulation processes of otolith daily increment formation. *Fish. Res.* 46, 53–67. doi: 10.1016/S0165-7836(00)00133-8

NASA (2019). *Data from: Goddard Space Flight Center, Ocean Ecology Laboratory, Ocean Biology Processing Group*. Greenbelt, MD: NASA.

Nissling, A. (2004). Effects of temperature on egg and larval survival of cod (*Gadus morhua*) and sprat (*Sprattus sprattus*) in the Baltic Sea - implications for stock development. *Hydrobiologia* 514, 115–123. doi: 10.1023/B:hydr.0000018212.88053.aa

Pan, W. (2001). Akaike's information criterion in generalized estimating equations. *Biometrics* 57, 120–125. doi: 10.1111/j.0006-341X.2001.00120.x

Peck, M. A., Baumann, H., Bernreuther, M., Clemmesen, C., Herrmann, J. P., Haslob, H., et al. (2012). The ecophysiology of *Sprattus sprattus* in the Baltic and North Seas. *Prog. Oceanogr.* 103, 42–57. doi: 10.1016/j.pocean.2012.04.013

Peck, M. A., Clemmesen, C., Baumann, H., Herrmann, J. P., Stäcker, S., and Temming, A. (2004). *The Growth-Feeding Relationship in Post-Larval Baltic sprat (Sprattus sprattus L.): Comparison of Somatic, Nucleic Acid- and Otolith-Based Growth Rates. ICES CM 2004/L:25*. Available at http://www.ices.dk/products/cmdocs/2004/CM[[AQ16]]

Peck, M. A., Reglero, P., Takahashi, M., and Catalán, I. A. (2013). Life cycle ecophysiology of small pelagic fish and climate-driven changes in populations. *Prog. Oceanogr.* 116, 220–245. doi: 10.1016/j.pocean.2013.05.012

Petereit, C., Haslob, H., Kraus, G., and Clemmesen, C. (2008). The influence of temperature on the development of Baltic Sea sprat (*Sprattus sprattus*) eggs and yolk sac larvae. *Mar. Biol.* 154, 295–306. doi: 10.1007/s00227-008-0923-1

Pinheiro, J., Bates, D., DebRoy, S., Sarkar, D., and R Core Team (2018). *nlme: Linear and Nonlinear Mixed Effects Models_. R package version 3.1-137*.

Piola, A. R., and Falabella, V. (2009). "The Patagonian Sea," in *Atlas of the Patagonian Sea, Species and Spaces*, eds V. Falabella, C. Campagna, and J. Croxall (Buenos Aires: Wildlife Conservation Society and Bird Life International), 55–75.

Piola, A. R., and Gordon, A. L. (1989). Intermediate waters in the southwest South Atlantic. *Deep Sea Res. A Oceanogr. Res. Pap.* 36, 1–16. doi: 10.1016/0198-0149(89)90015-0

Piola, A. R., Palma, E. D., Bianchi, A. A., Castro, B. M., Dottori, M., Guerrero, R. A., et al. (2018). ""Physical oceanography of the SW Atlantic shelf: a review,"," in *Plankton Ecology of the Southwestern Atlantic*, eds M. Hoffmeyer, M. Sabatini, F. Brandini, D. Calliari, and N. Santinelli (Cham, ZG: Springer), 37–56.

Piola, A. R., and Rivas, A. L. (1997). "Corrientes en la plataforma continental," in *El Mar Argentino y Sus Recursos Pesqueros. Tomo 1. Antecedentes Históricos de las Exploraciones en el Mar Argentino y las Características Ambientales*, ed. E. E. Boschi (Mar del Plata, BA: Instituto Nacional de Investigación y Desarrollo Pesquero), 119–132.

R Core Team (2019). *R: A Language and Environment for Statistical Computing*. Vienna: R Foundation for Statistical Computing.

Ramírez, F. C. (1976). Contribución al conocimiento del espectro alimenticio de la sardina fueguina (Clupeidae, *Sprattus fuegensis* Jenyns). *Neotrópica* 22, 137–141.

Reta, R., Guerrero, R., Molinari, G., Fenco, H., Allega, L., Cozzolino, E., et al. (2014). *Oceanografía del Banco Burdwood: Estado Actual del Conocimiento y Perspectivas*. Buenos Aires: Informe Técnico INIDEP, 15.

Robinson, D., and Hayes, A. (2020). *broom: Convert Statistical Analysis Objects into Tidy Tibbles. R package version 0.5.5*.

Sánchez, R. P., and Ciechomski, J. D. (1995). Spawning and nursery grounds of pelagic fish species in the sea-shelf off Argentina and adjacent areas. *Sci. Mar.* 59, 455–478.

Sánchez, R. P., Madirolas, A., Reta, R., Ehrlich, M. D., Álvarez Colombo, G., and Macchi, G. (1997). "The reproductive biology of the Patagonian sprat (*Sprattus fuegensis*): several facts and still some speculations," in *Proceedings of the ICES Annual Science Conference, ICES CM 1997_HH:22*, Copenhagen.

Sánchez, R. P., Remeslo, A., Madirolas, A., and de Ciechomski, J. D. (1995). Distribution and abundance of post-larvae and juveniles of the Patagonian sprat, *Sprattus fuegensis* and related hydrographic conditions. *Fish. Res.* 23, 47–81. doi: 10.1016/0165-7836(94)00339-X

Schejter, L., and Bremec, C. S. (2019). Stony corals (Anthozoa: Scleractinia) of Burdwood Bank and neighbouring areas, SW Atlantic Ocean. *Sci. Mar.* 83, 247–260. doi: 10.3989/scimar.04863.10A

Schejter, L., Rimondino, C., Chiesa, I., Díaz de Astarloa, J. M., Doti, B., Elías, R., et al. (2016). Namuncurá Marine Protected Area: an oceanic hot spot of benthic biodiversity at Burdwood Bank, Argentina. *Polar Biol.* 39, 2373–2386. doi: 10.1007/s00300-016-1913-2

Schiavini, A. C., Goodall, R. N. P., Lescrauwaet, A. K., and Alonso, M. K. (1997). Food habits of the Peales dolphin *Lagenorhynchus australis*; review and new information. *Rep. Int. Whal. Comm.* 47, 827–834.

Scioscia, G., Raya Rey, A., Saenz Samaniego, R. A., Florentín, O., and Schiavini, A. (2014). Intra-and interannual variation in the diet of the Magellanic penguin (*Spheniscus magellanicus*) at Martillo Island, Beagle Channel. *Polar Biol.* 37, 1421–1433. doi: 10.1007/s00300-014-1532-8

Shirokova, E. N. (1978). Some biological features of Tierra del Fuego sprat. *Soviet J. Mar. Biol.* 4, 697–702.

Sogard, S. M. (1997). Size-selective mortality in the juvenile stage of teleost fishes: a review. *Bull. Mar. Sci.* 60, 1129–1157.

Sponaugle, S. (2010). Otolith microstructure reveals ecological and oceanographic processes important to ecosystem-based management. *Environ. Biol. Fish.* 89, 221–238. doi: 10.1007/s10641-010-9676-z

Stevenson, D. K., and Campana, S. E. (1992). *Otolith Microstructure Examination and Analysis*. Ottawa: Canada Communication Group - Publishing.

Voss, R., Clemmesen, C., Baumann, H., and Hinrichsen, H. H. (2006). Baltic sprat larvae: coupling food availability, larval condition and survival. *Mar. Ecol. Prog. Ser.* 308, 243–254. doi: 10.3354/meps308243

Voss, R., Peck, M. A., Hinrichsen, H. H., Clemmesen, C., Baumann, H., Stepputtis, D., et al. (2012). Recruitment processes in Baltic sprat–A re-evaluation of GLOBEC Germany hypotheses. *Prog. Oceanogr.* 107, 61–79. doi: 10.1016/j.pocean.2012.05.003

Watanabe, Y., and Kuroki, T. (1997). Asymptotic growth trajectories of larval sardine (*Sardinops melanostictus*) in the coastal waters off western Japan. *Mar. Biol.* 127, 369–378. doi: 10.1007/s002270050023

Whitehead, P. J. P. (1985). King herring: his place amongst the clupeoids. *Can. J. Fish. Aquat. Sci.* 42, s3–s20. doi: 10.1139/f85-258

Wickham, H. (2011). The split-apply-combine strategy for data analysis. *J. Stat. Softw.* 40, 1–29.

Wickham, H. (2016). *ggplot2: Elegant Graphics for Data Analysis*. New York: Springer-Verlag.

Wickham, H. (2018). *scales: Scale Functions for Visualization. R package version 1.0.0*.

Wickham, H. (2020). *modelr: Modelling Functions that Work with the Pipe. R package version 0.1.6*.

Wickham, H., Averick, M., Bryan, J., Chang, W., McGowan, L., François, R., et al. (2019a). Welcome to the Tidyverse. *J. Open Source Softw.* 4:1686. doi: 10.21105/joss.01686

Wickham, H., François, R., Henry, L., and Müller, K. (2019b). *dplyr: A Grammar of Data Manipulation. R package version 0.8.0.1*.

Wickham, H., and Henry, L. (2018). *tidyr: Easily Tidy Data with 'spread()' and 'gather()' Functions. R package version 0.8.2*.

Zenteno, J. I., Bustos, C. A., and Landaeta, M. F. (2014). Larval growth, condition and fluctuating asymmetry in the otoliths of a mesopelagic fish in an area influenced by a large *Patagonian glacier*. *Mar. Biol. Res.* 10, 504–514. doi: 10.1080/17451000.2013.831176

Conflict of Interest: The authors declare that the research was conducted in the absence of any commercial or financial relationships that could be construed as a potential conflict of interest.

The handling Editor declared a shared affiliation, though no other collaboration, with the authors VG and FC, at time of review.

Copyright © 2020 García Alonso, Brown, Pájaro and Capitanio. This is an open-access article distributed under the terms of the Creative Commons Attribution License (CC BY). The use, distribution or reproduction in other forums is permitted, provided the original author(s) and the copyright owner(s) are credited and that the original publication in this journal is cited, in accordance with accepted academic practice. No use, distribution or reproduction is permitted which does not comply with these terms.

frontiers in Marine Science

BRIEF RESEARCH REPORT
published: 20 May 2020
doi: 10.3389/fmars.2020.00291

Polymorphism in Conservative Structures? The Scapulocoracoids in Skates Genus *Psammobatis* (Chondrichthyes, Arhynchobatidae) and the Validity of *P. parvacauda*

E. Mabragaña*, M. González-Castro, V. Gabbanelli, D. M. Vazquez and J. M. Díaz de Astarloa

Laboratorio de Biotaxonomía Morfológica y Molecular de Peces, Instituto de Investigaciones Marinas y Costeras (IIMyC), CONICET, Universidad Nacional de Mar del Plata, Mar del Plata, Argentina

OPEN ACCESS

Edited by:
Alejandra Vanina Volpedo, University of Buenos Aires, Argentina

Reviewed by:
William Driggers, National Marine Fisheries Service (NOAA), United States
Paul Brickle, South Atlantic Environmental Research Institute, Falkland Islands

***Correspondence:**
E. Mabragaña
emabraga@mdp.edu.ar

Specialty section:
This article was submitted to Marine Ecosystem Ecology, a section of the journal Frontiers in Marine Science

Received: *13 December 2019*
Accepted: *14 April 2020*
Published: *20 May 2020*

Citation:
Mabragaña E, González-Castro M, Gabbanelli V, Vazquez DM and Díaz de Astarloa JM (2020) Polymorphism in Conservative Structures? The Scapulocoracoids in Skates Genus Psammobatis (Chondrichthyes, Arhynchobatidae) and the Validity of P. parvacauda. Front. Mar. Sci. 7:291. doi: 10.3389/fmars.2020.00291

Skeletal structures, especially the claspers, neurocrania, and scapulocoracoids have been widely used to characterize and describe new species of elasmobranchs. Intra and interspecific variation of scapulocoracoids in 3 species of *Psammobatis* ($n = 94$) from the Southwest Atlantic Ocean were analyzed to assess its utility as a diagnostic character in skates. Moreover, based on scapulocoracoids and body morphometric analyses, the validity of *Psammobatis parvacauda* McEachran, 1983 was evaluated. A remarkable sexual dimorphism in scapulocoracoids was observed in all species in accordance with original descriptions, which was also evident in the principal component (PCA) and Discriminant Analyses. The number and arrangement of post-dorsal and post-ventral fenestra were highly variable at intra-specific level, in contrast with original descriptions. Particularly, one of the morphotypes observed in females of *P. normani* was identical to the one reported in *P. parvacauda*. Results showed intraspecific variation in this structure, as was previously observed in *Sympterygia* species. Therefore, this structure should not be used as a diagnostic character in skates, at least for these genera. Regarding body morphometry the PCA showed that *P. parvacauda* grouped with *P. normani* females and the cross-validated analysis showed that *P. parvacauda* was classified in the group of *P. normani* females. *P. parvacauda* is only known from its original description (one female) and a likely second specimen, but our analyses revealed a lack of diagnostic characteristics. Based on observations and measurements of the holotype of *P. parvacauda*, and comparisons with congenerics, *P. normani* is regarded a senior synonym of *P. parvacauda.*

Keywords: Rajiformes, *Psammobatis*, scapulocoracoids, intraspecific polymorphism, *P. parvacauda*, synonymization

INTRODUCTION

Skates (Chondrichthyes, Rajiformes), constitute a monophyletic and cosmopolitan group of cartilaginous fishes, with representatives in all oceans. The Order includes approximately 290 species and is composed by two highly diverse families (Rajidae and Arhynchobatidae) and two smaller families (Anacanthobatidae and Gurgesiellidae) (Last et al., 2016a,b; Séret et al., 2016;

Weigmann et al., 2016). The endoskeleton of skates -like all chondrichthyan fishes- is comprised predominantly of a hyaline-like cartilage that persists throughout the entire life and is not replaced by bone (Compagno, 1999; Seidel et al., 2017). During ontogeny the matrix undergoes a distinctive calcification, developing an outer calcified rind of hydroxyapatite or tesserae, located between the cartilaginous core and the outer, perichondrium (Seidel et al., 2017).

Skeletal structures, especially the claspers, neurocrania and scapulocoracoids have been widely used not only to characterize and describe new species of skates (McEachran and Compagno, 1982; Stehmann and Seret, 1983; McEachran and Last, 1994; de Carvalho et al., 2005; Last and McEachran, 2006; Last and Gledhill, 2007; Jeong and Nakabo, 2009), but also for conducting comprehensive systematic studies (Stehmann, 1970; Hulley, 1972; McEachran and Miyake, 1990; McEachran and Dunn, 1998). The scapulocoracoid or pectoral girdle is located just posterior to the branchial arches and is attached to the vertebral column dorsally (Compagno, 1999). The scapulocoracoid consists basically of a ventral and transverse coracoid bar, a dorsolateral scapular process on each side and, in some species an articulated suprascapula above the scapular process. The lateral face of the scapulocoracoid has an articular surface for the pectoral basal cartilages and foramina for blood vessels and nerves (Compagno, 1999). Fenestrae on the lateral face of the scapulocoracoid of primitive batoids include anterodorsal and anteroventral fenestrae between the pro and mesocondyles, and postdorsal and posventral fenestrae between the meso and metacondyles (Compagno, 1999).

McEachran (1982, 1983) conducted a comprehensive review of skate species from the *Sympterygia* and *Psammobatis* genera, and described their skeletal structures including scapulocoracoids. He found a strong sexual dimorphism in this part of the skeleton in *Psammobatis* species, and defined the overall morphological pattern of this structure for each species, endorsing it as a diagnostic character. Recent studies have called into question the usefulness of scapulocoracoids as a diagnostic character at the specific level. Jurado et al. (2017), reported a high variability in this structure at the intraspecific level in *Sympterygia* species, especially in the number of postdorsal and postventral fenestrae. On this basis, it would be relevant to investigate potential morphological variability in scapulocoracoids within *Psammobatis*, a closely related genus (McEachran and Dunn, 1998), to determine whether a similarly non-conservative pattern is observed.

The genus *Psammobatis* (Rajiformes, Arhynchobatidae) is endemic of South America and is comprised of eight small to medium sized skates. Thorough taxonomic revision of the genus was conducted by McEachran (1983) and completed by de Carvalho and Figueiredo (1994). The genus currently includes two amphioceanic species, *P. rudis* Gunther, 1870 and *P. normani* McEachran, 1983, both occurring in the Southwest Atlantic Ocean (SWA) and the South-east Pacific Ocean (SEP), one species exclusively found in the SEP, *P. scobina* (Philippi, 1857), and 5 species exclusively distributed in the SWA, *P. bergi* Marini, 1932, *P. rutrum* Jordan, 1890, *P. extenta* (Garman, 1913), *P. lentiginosa* McEachran, 1983, and *Psammobatis parvacauda* McEachran, 1983. The latter was described based on a single female collected around Malvinas/Falkland Islands, whose external morphological characteristics and skeletal structures, particularly the scapulocoracoid, were unique (McEachran, 1983). After the revision of McEachran (1983), several studies were conducted on almost all *Psammobatis* species including reproductive biology (Braccini and Chiaramonte, 2002b; Mabragaña and Cousseau, 2004; San Martín et al., 2005, Mabragaña, 2007; Perier et al., 2011; Mabragaña et al., 2012; Martins and Oddone, 2017), feeding ecology (Braccini and Perez, 2005; Mabragaña, 2007; Mabragaña and Giberto, 2007; San Martín et al., 2007; Barbini and Lucifora, 2012), morphology (Braccini and Chiaramonte, 2002a; Mabragaña, 2007), egg cases (Concha et al., 2009; Mabragaña et al., 2011; Vazquez et al., 2016), and their parasites community (Irigoitia et al., 2019). Strikingly, no further studies were conducted in *P. parvacauda*. In fact, no new records of this species were published since McEachran's (1983) original description.

The objectives of this study are (1) to analyze the morphological variability of scapulocoracoids in three *Psammobatis* species from the SWA, (2) to assess the usefulness of scapulocoracoid as a diagnostic character in this genus, and (3) in the light of objectives 1 and 2, to assess the validity of *P. parvacauda* McEachran, 1983 based on morphological and skeletal analyses.

MATERIALS AND METHODS

Sample Collection

Skeletal material was obtained from specimens of *P. rudis* (males n = 13, females n = 18) and *P. normani* (males n = 18, females n = 19), collected by trawl fishing during research cruises conducted by the National Institute for Fisheries Research and Development (INIDEP) in southern Patagonian waters (49°28′S, 67°03′W to 52°00′S, 53°49′W, and from 84 to 182 m) in April 2000, and from specimens of *P. lentiginosa* (males n = 13, females n = 13) collected off Buenos Aires Province (36°23′S, 63°59′W to 39°05′S, 58°04′W, from 66 to 99 m depth) in October 2006.

Total length (TL) and disc width (DW) in millimeters, sex and maturity (following Mabragaña and Cousseau, 2004) were recorded for each specimen in the laboratory. Scapular girdles were dissected and kept frozen for subsequent study. In order to reveal scapulocoracoid structure (shape, number, and fenestrae pattern), dissected material was submerged in water at 90–95°C for easy flesh removal. Once cartilaginous structures were cleaned, they were stored in ethanol 70%.

Scapulocoracoid Morphometric Analysis

Morphometric (linear morphometric measurements; LMM) were taken following McEachran and Compagno (1979). Morphometric variables included greatest length and height, anterior and posterior length to mesocondyle (pre- and postmesocondyle, respectively), and height of rear corner. These variables were taken on the left scapulocoracoid side. Given that in *P. lentiginosa* only 10 scapulocoracoids could be measured, the total of observations was 78. A digital caliper with a

0.01 mm error was used for taking each measurement. Digital photographs were taken from the lateral face of scapulocoracoids for illustrative purposes.

Statistical and mathematical procedures for the LMM analysis followed González-Castro et al. (2012, 2016). The morphometric characters were organized by sexes and species. A normalization technique to scale the data that exhibit allometric growth was employed following Lleonart et al. (2000). Scapulacoracoid length (ScL) was used as the independent variable. ScL0 represents a references value of ScL (23 mm) to which all scapulocoracoids were either reduced or amplified (Lombarte and Lleonart, 1993). After transformation, a principal component analysis (PCA) was performed using MULTIVARIADO®software (Salomón et al., 2004). Finally, principal component scores (PCs) were submitted to cross-validated discriminant analysis (DA) using SPSS®vers. 13.0 (Nie et al., 2004), in order to build a predictive model of group membership based on the observed characteristics of each case. This procedure generates a set of discriminant functions based on linear combinations of the predictor variables that provide the best discrimination between groups.

Scapulocoracoid Morphological Analysis

Morphological variables were taken following McEachran and Compagno (1979). The variables included number of postdorsal and postventral fenestrae, and were taken in both left and right sides of scapulocoradoids. Therefore the total of observations arise to 188. Morphological variation was quantitatively and qualitatively evaluated by comparing number, shape and arrangement of posterior fenestrae, both dorsal and ventral. The number of fenestrae was analyzed through a Mann–Whitney test. Statistical analyses were performed using Statistica 7.0 (Stat. Soft. Inc). For illustrative purposes, digital photographs were taken from the lateral face of scapulocoracoids.

Morphological and Morphometric Analyses of *P. parvacauda*

To assess the validity of *P. parvacauda*, the holotype was examined. The specimen is stored at Zoologisches Museum Hamburg [ZMH 25234 (ex ISH 1671-1966 ISH Aussenstelle Ichthyologie des Instituts für Seefischerei)] Germany. Morphological features as well as body morphometric LMM of the specimen were taken.

For comparison purposes, 12 morphometric variables LMM were selected and measured on dorsal and ventral sides of specimens of *P. normani* (n = 81), *P. rudis* (n = 34) and *P. lentiginosa* (n = 35) following Last et al. (2008), and compared to those of *P. parvacauda*. The variables were: DW, disc length, snout length, preoral length, prenasal length, orbit diameter, interorbital distance, mouth width, distance between first gill openings, distance between fifth openings, distance snout to cloaca, and distance cloaca to caudal tip. As in scapulocoracoid analysis, a normalization technique to scale the data that exhibit allometric growth was employed following Lleonart et al. (2000). In this case, DW was used as the independent variable and DW0 represents a reference value of DW (230 mm) to which all specimens were either reduced or amplified. Even though TL was also measured in all individuals, this variable was removed from the analysis because of the damage tail of the holotype of *P. parvacauda*.

RESULTS AND DISCUSSION

Scapulocoracoid Morphometric Analysis

A sexual dimorphism has been observed in the three *Psammobatis* species analyzed, according to the original descriptions (McEachran, 1983), being the scapulocoracoids of females more rectangular than those of males, which were more triangular shaped. The PCA of the correlation matrix of LMM of scapulocoracoid, generated by the normalization procedure, produced 2 eigenvalues of >1 (data not shown) and 8 PCs. Correlations between variables and components >0.59 were considered significant (data not shown). The PCA based on LMM allowed a clear differentiation along the PC1 of the females from the males of the three species analyzed (**Figure 1**). Males showed higher loadings for pre-mesocondyle, greatest height, height of rear corner, and pre-dorsal fenestrae height, whereas higher loadings of variables, post-mesocondyle, and post-dorsal fenestrae length characterized females of the three species analyzed (data not shown). Moreover, the characterization of the species by sexes was only partial, because some overlap between them was detected (**Figure 1**). The DA on the variations in the 78 individuals of *Psammobatis* classified by sexes and species were explained by 5 canonical discrimination functions, of which the first 2 explained 93.4% (63.3 and 30.1%, respectively) of the total variance in the data, (Wilks' lambda = 0.076, $p < 0.000$). The DA correctly classified 74.4% of the original grouped cases, whereas the cross-validated analysis correctly classified only the 59.4% of the fishes according to their LMM of scapulocoracoid. Moreover, the cross-validated analysis showed that misclassifications varied from 5.3 to 33.3%, depending on the group analyzed (**Table 1A**). Again, the sexual dimorphism was evidenced as a variable equal, or even stronger than species influence in the group discrimination.

Scapulocoracoids Morphological Analysis

The number of pre-dorsal and pre-ventral fenestra observed were identical to those described by McEachran (1983). However, a high variability in the number and arrangement of post-dorsal and post-ventral fenestra (pdf and pvf, respectively) was observed, in contrast with original descriptions. This variation was also shown when comparing left and right sides. Both, in *P. rudis* and *P. normani*, about 16% of specimens showed differences in the number of postdorsal or postventral fenestrae on each side, and 31% in *P. lentiginosa*.

Psammobatis rudis showed no differences between males and females in number of pdf and pvf. On the contrary, *P. normani* showed sexual differences in number of left pvf (p = 0.013). On the other hand, *P. lentiginosa* showed differences between males and females in both, number of pdf (p = 0.015 left side, p = 0.006 right side), and pvf (p = 0.003 left side, $p < 0.001$).

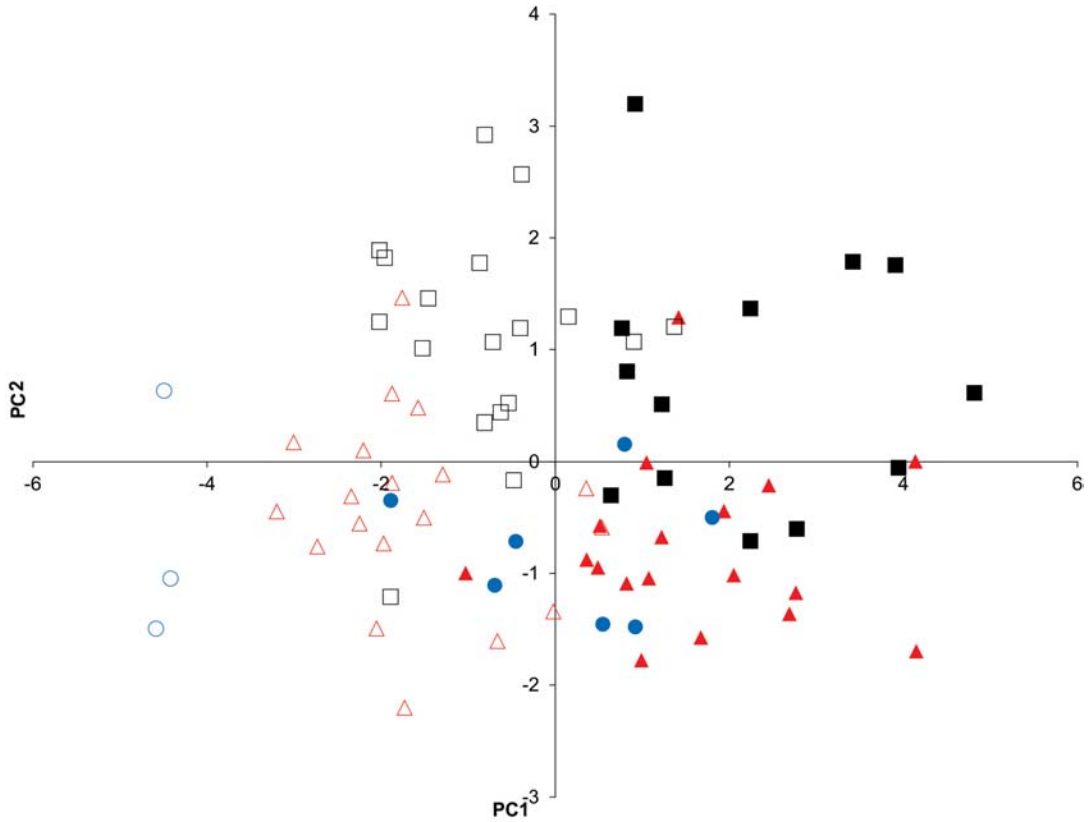

FIGURE 1 | Principal component (PC) analysis (PC1 vs. PC2) based on linear morphometric measurements of scapulocoracoids. The 1st 2 PCs explained 71.3% of the variance in the data. *Psammobatis rudis* males (black squares); *P. rudis* females (white squares); *P. normani* males (red triangles); *P. normani* females (white triangles); *P. lentiginosa* males (black circles); and *P. lentiginosa* females (white circles).

Overall, no differences in the number of pdf between males of the three species were observed. Similarly, no differences in the number of pvf between males of *P. rudis* and *P. normani* were observed. On the contrary, females of *P. rudis* presented more pvf than those of *P. normani* ($p = 0.015$ left side, $p = 0.035$ right side). On the other hand, males of *P. lentiginosa* presented more pvf than those of *P. rudis* ($p < 0.001$ left side, $p = 0.013$ right side). Similarly, females of *P. lentiginosa* had more pdf ($p = 0.004$ left side, $p < 0.001$ right side) and pvf ($p < 0.001$ left side, $p = 0.013$ right side) than those of *P. rudis*. Finally, males of *P. lentiginosa* had more pvf ($p = 0.001$ left side, $p = 0.007$ right side) than those of *P. normani*, and females of *P. lentiginosa* presented more pdf ($p = 0.003$ left side), and pvf ($p < 0.001$ left side, $p < 0.001$ right side) than those of *P. normani*.

Regarding arrangement of fenestrae, in males of *P. rudis*, three different morphotypes were observed. Twenty-three percent of the samples were identical to those reported by McEachran (1983), (i.e., with one pdf and two pvf), 73% of the samples possessed 1 pdf and 1 pvf, whereas 4% had 1 pdf and 3 pvf (**Figure 2A**). In females of *P. rudis* two morphotypes were observed, 67% were coincident with original description, (i.e., with one pdf and one pvf), and 33% presented 2 pvf (**Figure 2A**).

In males of *P. normani*, three morphotypes were observed, 72% of the samples were identical to those described by McEachran (1983), having one pdf and one pvf, but 22% possessed 2 pvf and the remaining 6% possessed 3 pvf (two bigger and between them a third little foramina; **Figure 2B**). In females of *P. normani* three morphotypes were also observed. 71% of the samples were identical to those described by McEachran (1983), 21% possessed 1 pvf, and 8% (3 specimens) possessed two pdf and one pvf (**Figure 2B**).

In males of *P. lentiginosa* three morphotypes were observed, 27% of the specimens are coincident with original descriptions made by McEachran (1983), with one pdf and three pvf, whereas 58% possessed 2 pvf, and 15% had only one pvf (**Figure 2C**). Finally, in females of *P. lentiginosa* at least 5 fenestrae arrangement patterns were observed, and only 20% of the samples were coincident with original descriptions, with one large pdf and 4 pvf. The remaining morphotypes were distributed as follows: 38% has one large pdf and 3 pvf, 27% had 2 pdf and 3 pvf, 12% possessed 2 pdf and 4 pvf, and 4% possessed 3 pdf and 3 pvf (**Figure 2C**).

The aforementioned results showed a high variability in fenestrae arrangement at intraspecific level at least within the genus *Psammobatis*, similar to what have been observed in *Sympterygia* spp. (Jurado et al., 2017). Both results call into question the conservative character of this structure and also indicate the lack of taxonomic value, at least in this skates'

TABLE 1 | Percent values of the cross-validated discriminant analysis, based on the principal component (PC) scores of: (A) Scapulocoracoid linear morphometric measurements, (B) Body linear morphometric. Group codes are: Pru = *Psammobatis rudis*, Pno = *P. normani*, Ple = *P. lentiginosa*, Ppa = *P. parvacauda*, M = males, F = females.

Species	Predicted group membership (%)					
	Pru_M	Pno_M	Ple_M	Pru_F	Pno_F	Ple_F
(A)						
Pru_M	53.85	30.77	7.69	7.69	0	0
Pno_M	11.11	55.56	27.78	5.56	0	0
Ple_M	0	28.57	57.14	0	14.29	0
Pru_F	16.67	0	0	61.11	22.22	0
Pno_F	0	0	10.53	21.05	63.16	5.26
Ple_F	0	0	0	0	33.33	66.67
Note: 59.0% of the cross-validated grouped cases were correctly classified.						

Species	Pru_M	Pru_F	Pno_M	Pno_F	Ple_M	Ple_F	Ppa_F
(B)							
Pru_M	0	92.3	0	7.7	0	0	0
Pru_F	76.2	9.5	14.3	0	0	0	0
Pno_M	17.1	0	80.5	2.4	0	0	0
Pno_F	0	7.5	2.5	90	0	0	0
Ple_M	0	0	0	0	100	0	0
Ple_F	0	0	0	0	4.8	95.2	0
Ppa_F	0	0	0	100	0	0	0
Note: 86.8% of the cross-validated grouped cases were correctly classified.							

genera. In this respect, one of the morphotypes observed in females of *P. normani* (with two pdf and one pvf, **Figure 2B**) was identical to the one reported in *P. parvacauda* by McEachran (1983) who stated "scapulocoracoids of *P. parvacauda* are derived in possessing: two postdorsal foramina and an expanded postventral fenestra."

Morphological and Morphometric Analysis of *Psammobatis* spp.

The morphometric analysis of the holotype of *P. parvacauda* and specimens of *P. normani*, *P. rudis,* and *P. lentiginosa* (present study) yielded the following results: the PCA of the correlation matrix of LMM of body, generated by the normalization procedure, produced 3 eigenvalues of >1 (data not shown) and 11 PCs. Correlations between variables and components of >0.59 were considered significant (data not shown). As in the scapulocoracoid morphometric analysis, differences between sexes but also species were recorded. Notably, the PCA showed that *P. parvacauda* (a female) grouped with *P. normani* females in the PC1-PC2 plot, denoting higher loadings of distance between first gill openings and distance between fifth openings, variables. The characterization of the species by sexes was only partial, because some overlap between them was detected (**Figure 3**). The DA on the variations in the 151 individuals of *Psammobatis* classified by sexes and species were explained by 6 canonical discrimination functions, of which the first two explained 84.4% (58.6 and 25.8%, respectively) of the total variance in the data, (Wilks' lambda = 0.007, $p < 0.000$). The DA correctly classified 94.7% of the original grouped cases, whereas the cross-validated analysis correctly classified 86.8% of the fishes according to their LMM of body. Moreover, the cross-validated analysis showed that the specimen of *P. parvacauda* was classified by cross validation analysis in the group of *P. normani* females (**Table 1B**).

Is *Psammobatis parvacauda* a Valid Species?

Psammobatis parvacauda was described based on a single female collected around Malvinas/Falkland Islands (McEachran, 1983). According to the author, "*P. parvacauda* most closely resembles *P. rudis* and *P. scobina*, but can be distinguished from the latter by morphometrics, in addition to skeletal structures. In *P. parvacauda* the preorbital length is less than the preoral length (preorbital snout length is equal to or greater than preoral snout length in *P. rudis*), the tail length is less than the distance from tip of the snout to the center of the cloaca (the tail length is greater than the distance from the tip of the snout to the center of the cloaca in *P. rudis* and *P. normani*, and in all other known species of *Psammobatis*)." McEachran (1983) also reported 37 tooth rows in the upper jaw and described its spinulation pattern: two suprascapular and two scapular thorns, not forming distinct triangular patch; tail with three irregular rows of thorns on dorsal and dorsolateral surfaces. Finally, coloration was described as dorsal surface tan and scattered with small, faint, white blotches. However, none of these features are diagnostic for *P. parvacauda*, indeed, the only character used in the key of species provided by McEachran (1983, p. 50) was the length of the tail.

Regarding skeletal structures, as no males are known from this species, the claspers features and their components are obviously

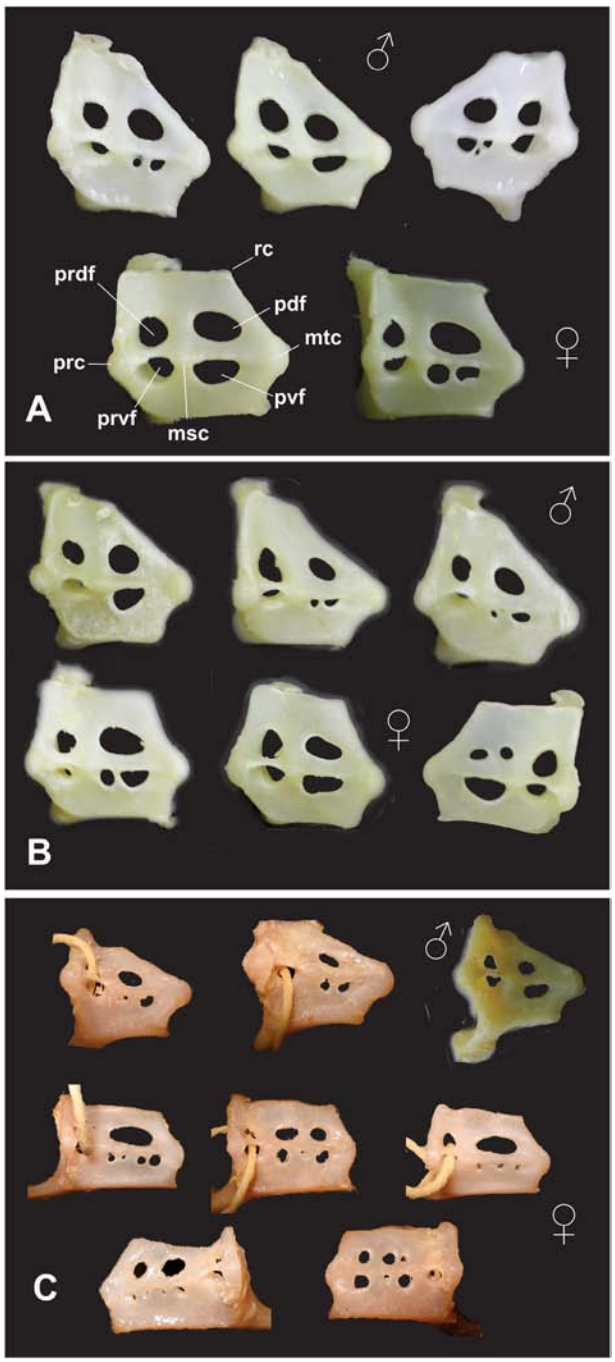

FIGURE 2 | Scapulocoracoid morphotypes observed in 3 species of *Psammobatis*: **(A)** *P. rudis* (above males, below females); **(B)** *P. normani* (above males, below females); and **(C)** *P. lentiginosa* (above males, below females. Msc = mesocondyle, mtc = metacondyle, pdf = postdorsal foramina or fenestra, prc = procondyle, prdf = predorsal fenestra, prvf = preventral fenestra, pvf = postventral foramina or fenestra, and rc = rear corner.

unknown. The neurocranium and the scapulocoracoid are the only skeletal structure available for this species. As noticed by McEachran (1983, p. 42) neurocrania of *P. parvacauda* and *P. normani* are similar, but, the scapulocoracoid of *P. parvacauda* is distinct from the other *Psammobatis* species in possessing two pdf and an expanded pvf (McEachran, 1983). However, as previously demonstrated, the scapulocoracoid in *Psammobatis* species is highly variable not only among species but also within species. Moreover, as previously indicated the scapulocoracoid pattern of *P. parvacauda* was observed in three specimens of *P. normani* (present study). Interestingly, the spinulation pattern and morphometrics of these specimens were in accordance with original descriptions and the remaining *P. normani* analyzed in the present study. Particularly, they did not have a short tail (length from tip of snout to center of cloaca was similar to length from center of cloaca to tail tip), and eye diameter was not large (4.4% of TL). Therefore, there is no skeletal structures with exclusive characteristic of *P. parvacauda*.

With respect to *P. parvacauda*, Weigmann (2016) stated "Possibly an aberrant specimen of another *Psammobatis* species as the postdorsal tail section of the holotype is apparently incomplete and, despite precise registrations of catches in this area, only one further specimen has been found (Stehmann, 2014, pers. comm.) Nevertheless, the apparently undamaged tail of the second specimen and the very large eyes of the species indicate that the species indeed might be valid despite its close similarity to *P. rudis* and *P. scobina* (Weigmann, unpubl. data)." In the present work, the holotype was examined by one of the co-authors and in fact, the tail section is incomplete (the caudal fin base measured 1.8 mm). Indeed, McEachran (1983) mentioned that epicordal lobe of caudal fin was barely developed in *P. parvacauda*. There is no reliable record of the second specimen reported, because it was not published. Therefore, no information regarding this specimen is available (photos, measurements, meristic, and genetics), only a personal communication by Stehmann to Weigmann is offered. Weigmann highlighted "the very large eyes of the species." However, McEachran (1983) did not regard this feature as a diagnostic characteristic for the species. He only reported its value as 5.6% of TL (TL 347 mm, OD 19.4 mm).

In addition, Last et al. (2016b) pointed out that "*P. parvacauda* is very poorly known and its distinction from some sandskates has been questioned. However, based on its relatively large eyes (5.6–6.7% of TL), compared to other members of the genus, we provisionally consider it to be valid." The authors also indicated that the species is distributed in northeast Malvinas/Falkland Islands (type locality) and in northern Patagonian waters (130 m). However, no record of the latter specimen has been published. On the other hand, the features observed in the "new" sample are not totally in accordance with the holotype. Indeed, Last et al. (2016b) mentioned "Tail rather slender and short, tapering strongly, its length ∼0.9–1 times precloacal length." Therefore, in the "new specimen" tail length is equal to precloacal length and no shorter as was diagnosed in the first description made by McEachran (1983). Regarding the eye diameter, the values reported by McEachran (1983) for the holotype was 5.6% of TL, slightly higher than those reported for the holotype of *P. normani* (5.4% TL; McEachran, 1983, table 3, p. 53), whereas for *P. rudis* and *P. scobina* the author provided only the mean values and those were lower than 4.5%. From 152 specimens of *P. normani* analyzed, Mabragaña (2007) showed that this

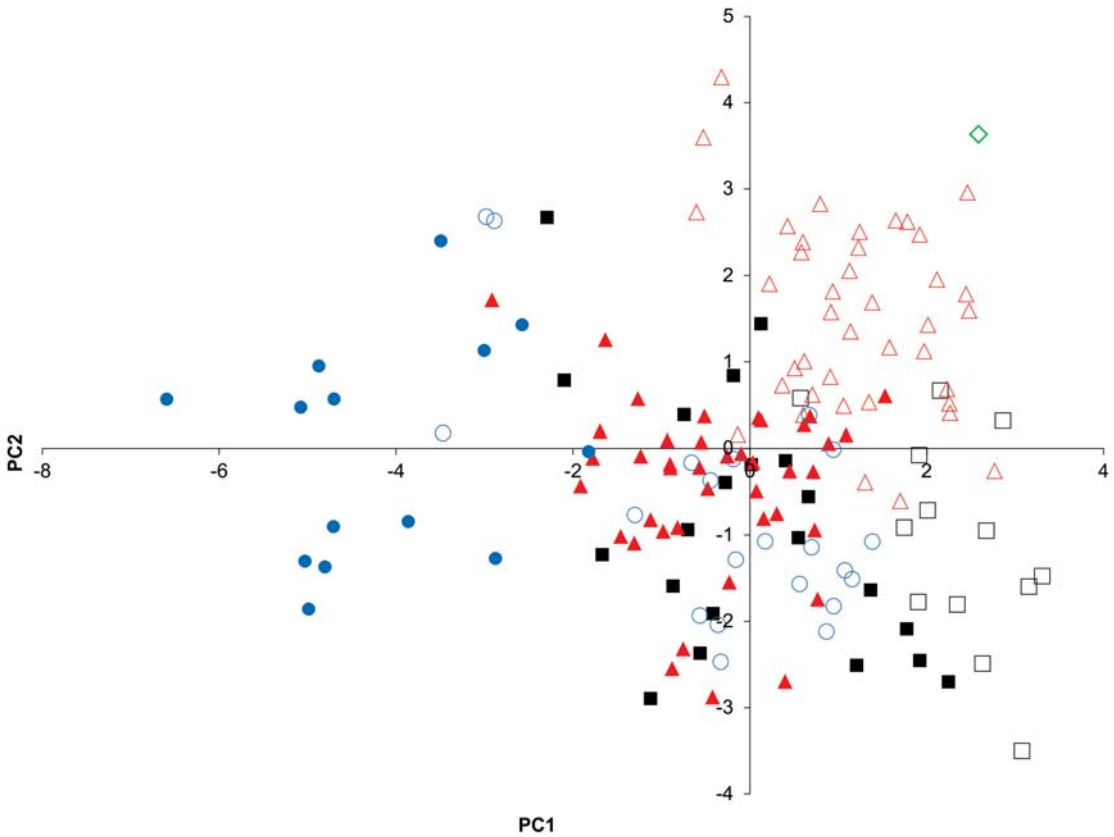

FIGURE 3 | Principal component (PC) analysis (PC1 vs. PC2) based on linear morphometric measurements of body. The 1st 2 PCs explained 55.6% of the variance in the data. *Psammobatis rudis* males (black squares); *P. rudis* females (white squares); *P. normani* males (red triangles); *P. normani* females (white triangles); *P. lentiginosa* males (blue circles); and *P. lentiginosa* females (white circles). Holotype of *P. parvacauda* (white diamond).

characteristic could reach 5.6% of TL, a value observed in the holotype of *P. parvacauda*. Therefore, there would be no diagnostic characters for the species.

It is suspicious that after almost 40 years from its original description, no novel specimens from this species were reported so far, and a likely second specimen quoted by Last et al. (2016b) and Weigmann (2016) would be another report of the species, even more if we consider that species from this genus are conspicuous and abundant in the Patagonian shelf (Cousseau et al., 2007). Furthermore, Mabragaña (2007) in spite of revising more than 600 specimens of its congeners *P. rudis* and *P. normani* along their entire distribution in the SWA, only found males with clasper morphology typical of *P. rudis* or *P. normani*.

The morphological features of the holotype of *P. parvacauda*, specially the spinulation pattern of tail with 3 irregular rows of tail thorns and no dermal denticles or minute spines on dorsolateral aspects of tail, resemble that of *P. normani* more than *P. rudis* (McEachran, 1983; Mabragaña, 2007). In the same way, the number of tooth rows on upper jaw (37) is within the range of both *P. rudis* (31–37, mean = 34, and n = 34) and *P. normani* (33–44, mean = 39, and n = 46; Mabragaña, 2007). Orbital nuchal and scapular thorns are also large and visible as in *P. normani*, and similarly the dorsal surface of disk is not covered with coarse dermal denticles as it happens in *P. rudis* (McEachran, 1983; Mabragaña, 2007). Also, as was already demonstrated, the specimen of *P. parvacauda* was statistically classified (cross-validated analysis of DA) in the *P. normani* female group. The external similarities between *P. parvacauda* and *P. normani*, as well as the presence of that particular fenestrae arrangement in the scapulocoracoid of some *P. normani* similar to that reported for *P. parvacauda*, the lack of a particular diagnostic character in the holotype, and the absence of a reported male for this species, strongly suggest that *P. parvacauda* is a junior synonym of *P. normani*. As Weigmann (2016) stated, this specimen surely constitutes "an aberrant female of other *Psammobatis* species." Both, *P. rudis* and *P. normani* are simpatrically distributed in the SWA, and although *P. rudis* is more abundant in the southern south-west Atlantic Ocean, *P. normani* inhabits also in Patagonian waters (Mabragaña and Cousseau, 2004; Mabragaña and Giberto, 2007).

In conclusion our data strongly indicate that *P. parvacauda* and *P. normani* correspond to the same species. Given that both species were described in the same moment, but considering that description of *P parvacauda* is possible based in an aberrant specimen, *P. normani* McEachran should be the senior synonym.

DATA AVAILABILITY STATEMENT

The raw data supporting the conclusions of this article are available on Figshare at doi: 10.6084/m9.figshare.12142302.v1.

ETHICS STATEMENT

Ethical review and approval was not required for the animal study because It was based on specimen collected with bottom trawls, in research cruises conducted more than 10 years ago, and specimens were landed already dead.

AUTHOR CONTRIBUTIONS

EM conceived the study. EM, VG, DV, and JD process the sample material. MG-C performed the statistical analyses. EM and MG-C interpreted the results and wrote the first draft of the manuscript. All authors wrote and revised the final draft of the manuscript.

FUNDING

The work was partially supported by Consejo Nacional de Investigaciones Científicas y Técnicas (CONICET, PIP 0339), MINCYT (PICT-2018-0790), and Facultad de Ciencias Exactas y Naturales, Universidad Nacional de Mar del Plata (EXA767/16 and EXA 867/18).

ACKNOWLEDGMENTS

We thank the skippers, crews and scientists of the R.V. O. Balda and R.V. E. L. Holmberg from the Instituto Nacional de Investigación y Desarrollo Pesquero for their assistance in the collection of samples. We also thank Patrice Pruvost and Romain Causse from Muséum national d'Histoire naturelle (Paris) for their effort and assistance in the acquisition of the holotype of *P. parvacauda*.

REFERENCES

Barbini, S. A., and Lucifora, L. O. (2012). Ontogenetic diet shifts and food partitioning between two small sympatric skates (Chondrichthyes, Rajidae) in the Southwestern Atlantic. *Mar. Freshw. Res.* 63, 905–913.

Braccini, J. M., and Chiaramonte, G. E. (2002a). Reproductive biology of *Psammobatis extenta*. *J. Fish. Biol.* 61, 272–288.

Braccini, J. M., and Chiaramonte, G. E. (2002b). Intraspecific variation in the external morphology of the sand skate. *J. Fish. Biol.* 61, 959–972.

Braccini, J. M., and Perez, J. E. (2005). Feeding habits of the sandskate *Psammobatis extenta* (Garman, 1913): sources of variation in dietary composition. *Mar. Freshw. Res.* 56, 395–403.

Compagno, L. J. V. (1999). "Endoskeleton," in *Sharks, Skates and Rays. The Biology of Elasmobranch Fishes*, Chap. 3, ed. W. C. Hamlett, (Maryland: Johns Hopkins Press), 69–92.

Concha, F., Hernández, S., and Oddone, M. C. (2009). Egg capsules of the raspthorn sandskate, *Psammobatis scobina* (Philippi, 1857)(Rajiformes, Rajidae). *Rev. Biol. Mar. Oceanogr.* 44, 253–256.

Cousseau, M. B., Figueroa, D. E., Díaz de Astarloa, J. M., Mabragaña, E., and Lucifora, L. O. (2007). *Rayas, Chuchos y Otros Batoideos del Atlántico Sudoccidental*. Buenos Aires: INIDEP.

de Carvalho, M. R., and Figueiredo, J. L. (1994). *Psammobatis extenta* (Garman, 1913): a senior synonym of *Psammobatis glansdissimilis* McEachran, 1983 (Chondrichthyes, Rajidae). *Copeia* 1994, 1029–1033.

de Carvalho, M. R., Gomes, U. L., and Gadig, O. B. F. (2005). Description of a new species of skate of the genus *Malacoraja* Stehmann, 1970: the first species from the southwestern Atlantic Ocean, with notes on generic monophyly and composition (Chondrichthyes: Rajidae). *Neotrop. Ichthyol.* 3, 239–258. doi: 10.1590/S1679-62252005000200002

González-Castro, M., Ibáñez, A. L., Heras, S., Roldán, M. I., and Cousseau, M. B. (2012). Assesment of lineal versus landmarks-based morphometry for discriminating species of Mugilidae (*Actinopterygii*). *Zool. Stud.* 51, 1515–1528.

González-Castro, M., Rosso, J. J., Mabragaña, E., and Díaz de Astarloa, J. M. (2016). Surfing among species, populations and morphotypes: inferring boundaries between two species of new world silversides (Atherinopsidae). *CR Biol.* 339, 10–23. doi: 10.1016/j.crvi.2015.11.004

Hulley, P. A. (1972). The origin, interrelationships and distribution of southern African Rajidae (Chondrichthyes, Batoidei). *Ann. S. Afr. Mus.* 60, 1–103.

Irigoitia, M. M., Braicovich, P. E., Rossin, M. A., Canel, D., Levy, E., Farber, M. D., et al. (2019). Diversity of *Empruthotrema* Johnston and Tiegs, 1992 parasitizing batoids (Chondrichthyes: Rajiformes and Myliobatiformes) from the Southwest Atlantic Ocean, with description of three new species. *Parasitol. Res.* 118, 3113–3127. doi: 10.1007/s00436-019-06456-x

Jeong, C. H., and Nakabo, T. (2009). *Hongeo*, a new skate genus (Chondrichthyes: Rajidae), with redescription of the type species. *Ichthyol. Res.* 56, 140–155. doi: 10.1007/s10228-008-0083-9

Jurado, C. D., Mabragaña, E., and Díaz de Astarloa, J. M. D. (2017). Morphological variation in a conservative structure: the scapulocoracoids in *Sympterygia acuta* Garman, 1837 and *Sympterygia bonapartii* Müller & Henle, 1841 (Chondrichthyes: Rajidae). *Zootaxa* 4318, 157–166.

Last, P. R., and Gledhill, D. C. (2007). The Maugean Skate, *Zearaja maugeana* sp. nov. (Rajiformes: Rajidae) –A micro-endemic, gondwanan relict from *Tasmanian estuaries*. *Zootaxa* 1494, 45–65.

Last, P. R., and McEachran, J. D. (2006). *Notoraja hirticauda*, a new species of skate (Chondrichthyes: Rajoidei) from the south-eastern Indian Ocean. *Mem. Mus. Vic.* 63, 65–75. doi: 10.24199/j.mmv.2006.63.9

Last, P. R., Stehmann, M. F. W., Séret, B., and Weigmann, S. (2016a). "Skates, family rajidae," in *Rays of the World*, eds P. R. Last, W. T. White, M. R. Carvalho, B. de Séret, M. F. W. Stehmann, and G. J. P. Naylor, (Melbourne: CSIRO Publishing), 204–363.

Last, P. R., Stehmann, M. F. W., Séret, B., and Weigmann, S. (2016b). "Softnose skates, family arhynchobatidae," in *Rays of the World*, eds P. R. Last, W. T. White, M. R. Carvalho, B. de Séret, M. F. W. Stehmann, and G. J. P. Naylor, (Melbourne: CSIRO Publishing), 364–472.

Last, P. R., White, W. T., Pogonoski, J. J., and Gledhill, D. C. (2008). "New Australian skates (Batoidea: Rajoidei) – background and methodology," in *Description of New Australian Skates (Batoidea: Rajoidei)*, eds P. R. Last, W. T. White, J. J. Pogonoski, and D. C. Gledhill (Canberra: CSIRO Marine and Atmospheric Research), 1–8.

Lleonart, J., Salat, G., and Torres, J. (2000). Removing allometrics effects of body size in morphological analysis. *J. Theor. Biol.* 205, 85–93. doi: 10.1006/jtbi.2000.2043

Lombarte, A., and Lleonart, J. (1993). Otolith size changes related with body growth, habitat depth and temperature. *Environ. Biol. Fish.* 37, 297–306.

Mabragaña, E. (2007). *Las Rayas del Género Psammobatis de la Plataforma Argentina: Biología y Ecología*. Ph.D. Thesis, Universidad Nacional de Mar del Plata, Mar del Plata.

Mabragaña, E., and Cousseau, M. B. (2004). Reproductive biology of two sympatric skates in the south-west Atlantic: *Psammobatis rudis* and *Psammobatis normani*. *J. Fish. Biol.* 65, 559–573.

Mabragaña, E., Figueroa, D. E., Scenna, L. B., Díaz de Astarloa, J. M., Colonello, J. H., and Delpiani, G. (2011). Chondrichthyan egg cases from the south-west Atlantic Ocean. *J. Fish. Biol.* 79, 1261–1290. doi: 10.1111/j.1095-8649.2011.03111.x

Mabragaña, E., and Giberto, D. A. (2007). Feeding ecology and abundance of two sympatric skates, the shortfin sand skate *Psammobatis normani* McEachran, and the smallthorn sand skate *P. rudis* Günther (Chondrichthyes, Rajidae), in the southwest Atlantic. *ICES J. Mar. Sci.* 64, 1017–1027.

Mabragaña, E., Ibáñez, P., and Cousseau, M. B. (2012). Reproductive biology and abundance of the freckled sandskate *Psammobatis lentiginosa* McEachran, 1983 in the southwest Atlantic. *Mar. Biol. Res.* 8, 292–299.

Martins, M. F., and Oddone, M. C. (2017). Reproductive biology of *Psammobatis rutrum* (Chondrichthyes: Arhynchobatidae) in south Brazil, south-west Atlantic. *J. Fish. Biol.* 91, 443–459. doi: 10.1111/jfb.13350

McEachran, J. D. (1982). Revision of the South American skate genus *Sympterygia* (Elasmobranchii, Rajiformes). *Copeia* 4, 867–890. doi: 10.2307/1444098

McEachran, J. D. (1983). Results of the research cruises of FRV "Walter Herwig" to South America LXI. Revision of the South American skate genus *Psammobatis* Günther, 1873 (Elasmobranchii, Rajiformes, Rajidae). *Arch. Fischereiwiss* 34, 23–80.

McEachran, J. D., and Compagno, L. J. V. (1979). A further description of *Gurgesiella furvesens* with comments on the interrelationships of Gurgesiellidae and Pseudorajidae (Pisces, Rajoidei). *Bull. Mar. Sci.* 29, 530–553.

McEachran, J. D., and Compagno, L. J. V. (1982). Interrelationships of and within *Breviraja* based on anatomical structures (Pisces: Rajoidei). *Biol. Mar. Sci.* 32, 399–425.

McEachran, J. D., and Dunn, K. A. (1998). Phylogenetic analysis of skates, a morphologically conservative clade of elasmobranchs (Chondrichthyes: Rajidae). *Copeia* 1998, 271–290. doi: 10.2307/1447424

McEachran, J. D., and Last, P. R. (1994). New species of Skate, *Notoraja ochroderma*, from off Queensland, Australia, with comments on the taxonomic limits of *Notoraja* (Chondrichthyes, Rajoidei). *Copeia* 1994, 413–421. doi: 10.2307/1446989

McEachran, J. D., and Miyake, T. (1990). "Phylogenetic interrelationships of skates: a working hypothesis (Condrichthyes: Rajoidei)," in *Elasmobranchs as Living Resources: Advances in the Biology, Ecology, Systematics and the Status of Fisheries*, eds H. L. Pratt, S. H. Gruber, and T. Taniuchi, (Silver Spring, MA: NOAA), 285–304.

Nie, N. H., Hadlai Hull, C., and Bent, D. H. (2004). *SPSS for Windows. Version 13.0*.

Perier, R., Estalles, M., Coller, M., and Di Giacomo, E. E. (2011). Reproductive biology of the endemic skate *Psammobatis lentiginosa* in the San Matías Gulf (south-western Atlantic). *J. Mar. Biol. Assoc. U.K.* 91, 1165–1173.

Salomón, R., Melo, S., and Winzer, N. (2004). *MULTIVARIADO Software*. Bahía Blanca: Departamento de Matemática, Univ. Nacional del Sur.

San Martín, M. J., Braccini, J. M., Tamini, L. L., Chiaramonte, G. E., and Perez, J. E. (2007). Temporal and sexual effects in the feeding ecology of the marbled sand skate *Psammobatis bergi* Marini, 1932. *Mar. Biol.* 151, 505–513.

San Martín, M. J., Perez, J. E., and Chiaramonte, G. E. (2005). Reproductive biology of the south west Atlantic marbled sand skate *Psammobatis bergi* Marini, 1932 (Elasmobranchii, Rajidae). *J. Appl. Ichthyol.* 21, 504–510.

Seidel, R., Blumer, M., Pechriggl, E. J., Lyons, K., Hall, B. K., Fratzl, P., et al. (2017). Calcified cartilage or bone? Collagens in the tessellated endoskeletons of cartilaginous fish (sharks and rays). *J. Struct. Biol.* 200, 54–71. doi: 10.1016/j.jsb.2017.09.005

Séret, B., Last, P. R., Weigmann, S., and Stehmann, M. F. W. (2016). "Legskates, family Anacanthobatidae," in *Rays of the World*, eds P. R. Last, W. T. White, M. R. Carvalho, B. de Séret, M. F. W. Stehmann, and G. J. P. Naylor, (Melbourne: CSIRO Publishing), 494–508.

Stehmann, M. (1970). Vergleichend morphologische und anatomische Untersuchungen zur Neuordnung der Systematik der nordostatlantischen Rajidae (Chondrichthyes, Batoidei). *Arch. Fischereiwiss* 21, 73–164.

Stehmann, M., and Seret, B. (1983). A new species of deep-water skate, *Breviraja africana* sp. n. (Pisces, Batoidea, Wajidae), from the Eastern Central Atlantic slope, and remarks on the taxonomic status of *Breviraja* Bigelow & Schroeder, 1948. *B Mus. Natl. Hist. Nat.* 5, 903–925.

Vazquez, D. M., Mabragaña, E., Gabbanelli, V., and Díaz de Astarloa, J. M. (2016). Exploring nursery sites for oviparous chondrichthyans in the Southwest Atlantic (36° S–41° S). *Mar. Biol. Res.* 12, 715–725.

Weigmann, S. (2016). Annotated checklist of the living sharks, batoids and chimaeras (Chondrichthyes) of the world, with a focus on biogeographical diversity. *J. Fish. Biol.* 88, 837–1037. doi: 10.1111/jfb.13234

Weigmann, S., Séret, B., Last, P. R., and McEachran, J. D. (2016). "Pygmy skates, Family Gurgesiellidae," in *Rays of the World*, eds P. R. Last, W. T. White, M. R. Carvalho, B. Séret, M. F. W. Stehmann, and G. J. P. Naylor, (Melbourne: CSIRO Publishing), 473–493.

Conflict of Interest: The authors declare that the research was conducted in the absence of any commercial or financial relationships that could be construed as a potential conflict of interest.

Copyright © 2020 Mabragaña, González-Castro, Gabbanelli, Vazquez and Díaz de Astarloa. This is an open-access article distributed under the terms of the Creative Commons Attribution License (CC BY). The use, distribution or reproduction in other forums is permitted, provided the original author(s) and the copyright owner(s) are credited and that the original publication in this journal is cited, in accordance with accepted academic practice. No use, distribution or reproduction is permitted which does not comply with these terms.

frontiers in Marine Science

ORIGINAL RESEARCH
published: 25 May 2020
doi: 10.3389/fmars.2020.00258

Otolith Chemistry Reveals Natal Region of Larval Capelin in Coastal Newfoundland, Canada

*Ashley Tripp[1], Hannah M. Murphy[2] and Gail K. Davoren[1]**

[1] Department of Biological Sciences, University of Manitoba, Winnipeg, MB, Canada, [2] Northwest Atlantic Fisheries Centre, Fisheries and Oceans Canada, St. John's, NL, Canada

Identifying natal origins of animals is key to determining the relative productivity of natal habitats, dispersal of individuals among local populations (i.e., connectivity), and, ultimately, metapopulation dynamics. As marine fish larvae have a high potential for dispersal, natural tags such as otolith chemistry are often used to determine natal origins. Trace elements may be incorporated into embryonic otoliths while larvae are developing in the egg, resulting in chemical signatures in the pre-hatch region of the otolith that reflect the natal habitat. Our goal was to determine whether the natal origins of 1- to 3-day-old larval capelin (*Mallotus villosus*), a key forage fish in many northern marine ecosystems, could be determined using otolith chemistry. We sampled larvae from five Newfoundland regions (i.e., embayments: Placentia Bay, St. Mary's Bay, Witless Bay, Trinity Bay, and Notre Dame Bay) during July–August 2019 to quantify regional differences in otolith chemistry. Additionally, eggs/larvae were field-reared within two regions over multiple years (Notre Dame Bay: 2014, 2015, 2018, and 2019; Trinity Bay: 2018 and 2019) to quantify interannual variation in region-specific otolith chemistry. Multielemental otolith signatures (i.e., Mg, Mn, Zn, Sr, and Ba), as determined by laser ablation inductively coupled plasma–mass spectrometry (LA ICP–MS), differed significantly among regions, with individuals classified into their natal region with 78% success (region-specific success: 68–100%). Classification success into natal region remained high (67–76%) despite interannual variation in otolith trace element concentrations within regions. Characterizing region-specific otolith chemical signatures that reflect natal origins of capelin larvae is the first step in determining the productivity and relative contributions of different regions of coastal Newfoundland to capelin recruitment.

Keywords: ***Mallotus villosus*, larvae, laser ablation ICP–MS, natal origin, Newfoundland**

OPEN ACCESS

Edited by:
Benjamin D. Walther, Texas A&M University Corpus Christi, United States

Reviewed by:
Troy A. Rogers, University of Adelaide, Australia
Jed Ian Macdonald, Pacific Community (SPC), New Caledonia

***Correspondence:**
Gail K. Davoren
Gail.Davoren@umanitoba.ca

Specialty section:
This article was submitted to Marine Ecosystem Ecology, a section of the journal Frontiers in Marine Science

Received: *16 December 2019*
Accepted: *31 March 2020*
Published: *25 May 2020*

Citation:
Tripp A, Murphy HM and Davoren GK (2020) Otolith Chemistry Reveals Natal Region of Larval Capelin in Coastal Newfoundland, Canada. Front. Mar. Sci. 7:258. doi: 10.3389/fmars.2020.00258

INTRODUCTION

Natal origins of animals are used to evaluate relative productivity of natal habitats and determine dispersal and connectivity of individuals among local populations and metapopulations (Cowen et al., 2007). Natal origin can be difficult to determine for marine species due to their high potential dispersal rates, which are typically associated with the planktonic duration of the larval stage (Bohonak, 1999). However, there is growing evidence that some larvae are retained and recruited

locally (e.g., Bradbury et al., 2008; Stanley et al., 2013). To determine the natal origins of fish larvae, tagging or marking is required. Natural tags have determined natal origins of fish larvae, providing important information on local retention (e.g., Jones et al., 1999; Swearer et al., 1999) and connectivity (e.g., Davoren and Halden, 2014). Trace elements in the surrounding aquatic environment are incorporated into the calcium carbonate structure of fish otoliths as individuals grow, allowing chronological reconstruction of environmental histories including natal origin (Campana, 1999; Elsdon and Gillanders, 2003). Some essential elements that are required for growth [e.g., magnesium (Mg) and manganese (Mn)] are actively incorporated into the otolith, while nonessential elements [e.g., strontium (Sr) and barium (Ba)] are inadvertently incorporated during calcium uptake due to their chemical similarity to calcium (Ca) (Crichton, 2008; Loewen et al., 2016). Although ambient water chemistry primarily influences trace element incorporation into the otoliths, other extrinsic factors including salinity and temperature also influence trace element incorporation rates (reviewed in Loewen et al., 2016).

Capelin (*Mallotus villosus*) is a small, short-lived (3–6 years) circumpolar marine forage fish species in the sub-Arctic (Carscadden and Vilhjálmsson, 2002). Capelin is also a commercially fished species, with Newfoundland and Labrador representing one of three economically important capelin fisheries along with Iceland and the Barents Sea (Carscadden et al., 2013). Capelin occupies a vital position in marine food webs as it is one of a few species that transfer energy from lower trophic levels (i.e. zooplankton) to upper-trophic-level predators, including whales, seabirds, and large piscivorous fish species, such as Atlantic cod (*Gadus morhua*; Carscadden and Vilhjálmsson, 2002). Capelin is primarily distributed offshore on the Newfoundland shelf and undergoes annual migrations into coastal embayments during June and July (Carscadden et al., 2013) to spawn at both beach (intertidal) and deepwater (subtidal, 15–40 m) sites (Crook et al., 2017). Post-spawning mortality in capelin is high, with higher proportions of dead males than females observed at spawning beaches (Templeman, 1948). Fertilized capelin eggs adhere to sediment at spawning sites, where they incubate until hatch and larvae are dispersed to offshore nursery habitats. Tagging (Nakashima, 1992) and genetic studies (Kenchington et al., 2015) suggest that capelin from the southeast and eastern coast of Newfoundland [Northwest Atlantic Fisheries Organization (NAFO) Divisions 2J3KL] represent one stock/management unit (Carscadden et al., 2013). The importance of specific embayments to stock productivity is unknown.

Trace elements are incorporated into embryonic otoliths (i.e. pre-hatch region) of capelin while larvae are developing in the egg (Loeppky et al., 2018), resulting in chemical signatures in the embryonic otolith that reflect the natal habitat (Davoren et al., 2015; Loeppky et al., 2018; Loeppky and Davoren, 2018). Furthermore, previous work revealed divergent otolith chemical signatures from 1- to 3-day-old larvae incubated within nearby (<20 km) beach and deepwater sites in coastal Newfoundland (Davoren et al., 2015; Loeppky and Davoren, 2018). As ambient water chemistry and salinity did not differ between these sites throughout the incubation period (2–4 weeks), habitat-specific otolith elemental concentrations appeared to result from divergent temperatures in the two habitats. This hypothesis was supported by laboratory and field experiments where treatments that varied by 4°C resulted in high classification success (73–88%) of larvae into their natal habitat (beach or deepwater; Loeppky and Davoren, 2018). Lazartigues et al. (2016) also successfully classified capelin larvae from different hatching sites within the St. Lawrence Estuary primarily based on otolith concentrations of Ba and Mg, with the highest misclassification rate (17%) occurring between nearby relative and more distant sites. Although these regional comparisons have not been conducted on capelin in coastal Newfoundland, a recent study found that juvenile cod could be successfully classified into coastal regions of Newfoundland, with success rates increasing with geographic scale (i.e., sites, bays, and coastal regions; Stanley et al., 2016). Together, these studies suggest that the natal origin of capelin larvae can be identified from geographically distant (>100 km) coastal regions of Newfoundland using otolith chemistry.

The objectives of this study were to investigate whether otolith chemical signatures of larval capelin differ among regions (i.e., embayments) of Newfoundland, Canada, and among years within regions. Region-specific otolith chemical signatures in the embryonic otolith prior to larvae dispersing offshore could be used to identify natal origins of capelin larvae. Therefore, this study will evaluate the potential use of chemical signatures in adult capelin otoliths to address knowledge gaps related to connectivity and productivity, such as the relative contribution of different regions of coastal Newfoundland to capelin recruitment.

MATERIALS AND METHODS

Field Sampling

For regional comparisons of otolith chemistry, preemergent larvae (3–6 mm, yolk sac present) within sediments at spawning beaches were opportunistically collected during July and August 2019 in Placentia Bay (St. Brides Beach), St. Mary's Bay (Branch Beach), Witless Bay (Burnt Cove Beach), and Notre Dame Bay (Mussel Shells Beach; **Figure 1** and **Table 1**). Preemergent larvae were collected by scooping beach sediment with adherent eggs in late developmental stages (stages V–VII; Fridgeirsson, 1976) into plastic bags, and then the bags were filled with seawater to separate eggs and sediment from preemergent larvae. The seawater was then poured over a 0.270-mm sieve, and preemergent capelin larvae were retained and preserved in 95% ethanol. Although we did not aim to examine mechanisms underlying otolith chemical variation, one water sample was collected at each site either on the same day or up to 17 days prior to the collection of preemergent larvae to characterize the ambient water chemistry during egg/larval development (**Table 1**). Multiple water samples were not collected because previous studies in coastal Newfoundland found negligible variation in ambient water chemistry from samples collected during capelin egg incubation (∼10 days apart) and across years (Davoren et al., 2015; Loeppky and Davoren, 2018). Water samples were collected in a 60-ml disposable syringe, filtered

using a 0.45-μm filter into a plastic sample bottle and preserved with 3 ml of 1:3 ultrapure nitric acid (HNO_3)/deionized water. Field-reared larvae (see below) from Trinity Bay (Bellevue Beach) were also included in regional comparisons.

To determine whether interannual variation in otolith chemistry could influence classification success of larvae into their natal regions, capelin larvae (1–3 days old) were field-reared within two bays across multiple years (Notre Dame Bay: 2014, 2015, 2018, and 2019; Trinity Bay: 2018 and 2019; **Figure 1** and **Table 1**) by placing naturally fertilized eggs in early developmental stages (stages I and II; Fridgeirsson, 1976) from spawning beaches in incubation canisters, which were moored near the beach in ∼1 m of water (see details in Davoren et al., 2015; Loeppky and Davoren, 2018). In brief, the incubation canisters consisted of 20-ml plastic vials (n = 10 per site) perforated with holes and covered in 0.28-mm mesh. The canisters were retrieved close to the hatching date, which was estimated using water temperature measurements taken at waist height from the beach using a YSI Pro30 every 48 h (Nakashima and Wheeler, 2002; Penton et al., 2012). Upon retrieval, canister contents were poured over a 0.270-mm sieve, and capelin larvae (3–6 mm, yolk sac present) were retained and preserved with 95% ethanol. One water sample was collected per site during field rearing using the same method as above (**Table 1**).

Lab Processing

Each larva was placed in a drop of deionized water on a clean glass slide (similar to Loeppky and Davoren, 2018), and one sagittal otolith was removed using tungsten needles (Roboz) under a dissecting microscope (Olympus SZX7) with a polarizing lens (Olympus SZX-PO). Otoliths were left to dry for 30 s before being mounted on a 1-cm^2 square grid (5 × 5) microscope slide using double-sided tape (Scotch^{TM}), following Loeppky and Davoren (2018). Individual otoliths were centered in each square and photographed for easier detection during processing. Concentrations of six trace elements (i.e., ^{25}Mg, ^{43}Ca, ^{55}Mn, ^{66}Zn, ^{88}Sr, and ^{137}Ba) were quantified using laser ablation inductively coupled plasma–mass spectrometry (LA ICP–MS; Perkin-Elmer DRC II, Loeppky and Davoren, 2018). Laser ablation inductively coupled plasma–mass spectrometry analyses were conducted at the Department of Geological Sciences, University of Manitoba, using a Thermo Finnigan Element 2 ICP–MS coupled to a Merchantek LUV 213 neodymium : yttrium aluminum garnet (Nd-YAG) laser. A Ca standard (MACS-3) was used as an external standard to calibrate the LA ICP–MS and was ablated in triplicate before and after ablation of all otoliths on each microscope slide (25 otoliths per slide). Otoliths were ablated using a spot technique (beam size = 40 μm) to ensure ablation of the entire otolith (diameter ∼30 μm). As the beam size was slightly larger than the circular otoliths, the tape was tested for any background chemical signatures, and none were found. Laser parameters were 56% output (3.3 J/cm^2), 2-Hz repetition rate, and a dwell time of 40 s. Background trace element concentrations were measured for 40 s prior to ablating each otolith for 40 s followed by a 60-s washout, whereby the laser stopped firing but detection continued to remove any remaining material before ablating the next otolith to avoid contamination.

Data reduction was performed in *Igor Pro* graphing software with *Iolite* version 3.71 by first removing spurious spikes (>3 SD), indicating surface-level contamination in trace element concentrations. Calcium (^{43}Ca) in counts per second (CPS) was then used to standardize trace element concentrations (40.04 wt.%) to account for changes in sample volume. Mean concentrations and standard error (ppm ± SE) of otolith trace elements were calculated by averaging each trace element concentration over the period the otolith was ablated, which was indicated by high and relatively stable ^{43}Ca CPS. As the otolith center, or primordial, region had Mn concentrations that were 6–10 times higher than those of the outer otolith region, similar to previous findings (Lazartigues et al., 2014), and more likely represent maternal investment instead of the natal environment (Loeppky et al., 2018), mean Mn concentrations were calculated excluding the higher concentrations in the center, similar to those of DiMaria et al. (2010). Mn concentrations were averaged starting from the edge of the otolith, which was visually indicated in *Igor Pro* by high and relatively stable Ca concentrations, and ending just before Mn concentrations spiked, indicating the center otolith region. External precision estimates (%RSD) and limits of detection (LODs) were as follows: ^{43}Ca = 2.1%, 0 μg/g; ^{25}Mg = 1.1%, 28.6 μg/g; ^{55}Mn = 0.88%, 3.7 μg/g; ^{66}Zn = 1.0%, 9.5 μg/g; ^{88}Sr = 1.2%, 84.2 μg/g; and ^{137}Ba = 0.82%, 9.0 μg/g. Laser ablation inductively coupled plasma–mass spectrometry recoveries were as follows: ^{25}Mg = 2.02%; ^{55}Mn = 8.71%; ^{66}Zn = 13.6%; ^{88}Sr = 2.16%; and ^{137}Ba = 8.66%.

Water samples were analyzed for trace element concentrations at ALS Environmental Laboratories (Burnaby, BC). Samples were diluted 10×, and major elements (e.g., Ca) were quantified by ICP–optical emission spectroscopy (OES) (Thermo iCAP 6500), while trace elements (e.g., Mg, Mn, Sr, and Ba) were quantified by solution-based ICP–MS following EPA Method 6010B (see Davoren et al., 2015). To correct for drift and matrix effects, ^{6}Li, ^{45}Sc, ^{74}Ge, ^{115}In, and ^{175}Lu were used as internal standards. Laboratory control spikes were used in all water sample analyses, and external standards for spike recovery were ^{43}Ca (101.6%), ^{25}Mg (99.6%), ^{55}Mn (99.4%), ^{88}Sr (101.8%), and ^{137}Ba (98.8%).

Statistical Analysis

Individuals with mean trace element concentrations of >2 SD from the mean of all larvae within a region were considered outliers and excluded from statistical analyses. These individuals were considered outliers based on previous studies on larval capelin otolith microchemistry (Loeppky et al., 2018; Loeppky and Davoren, 2018) that found abnormal trace element concentrations resulted from the laser not ablating the entire otolith or the otolith exploding prematurely. For regional comparisons, four to six otoliths per region were removed as outliers (24 total), resulting in a total of 72 otoliths used in analyses (8–19 per region; **Table 2**). For interannual comparisons, two to eight otoliths per year were removed as outliers (26 total), resulting in 113 otoliths (9–24 per region per year) used in analyses. All otolith trace element concentrations were log-transformed to meet the underlying assumptions of parametric statistics. For regional comparisons, a principal component analysis (PCA) was used to explore

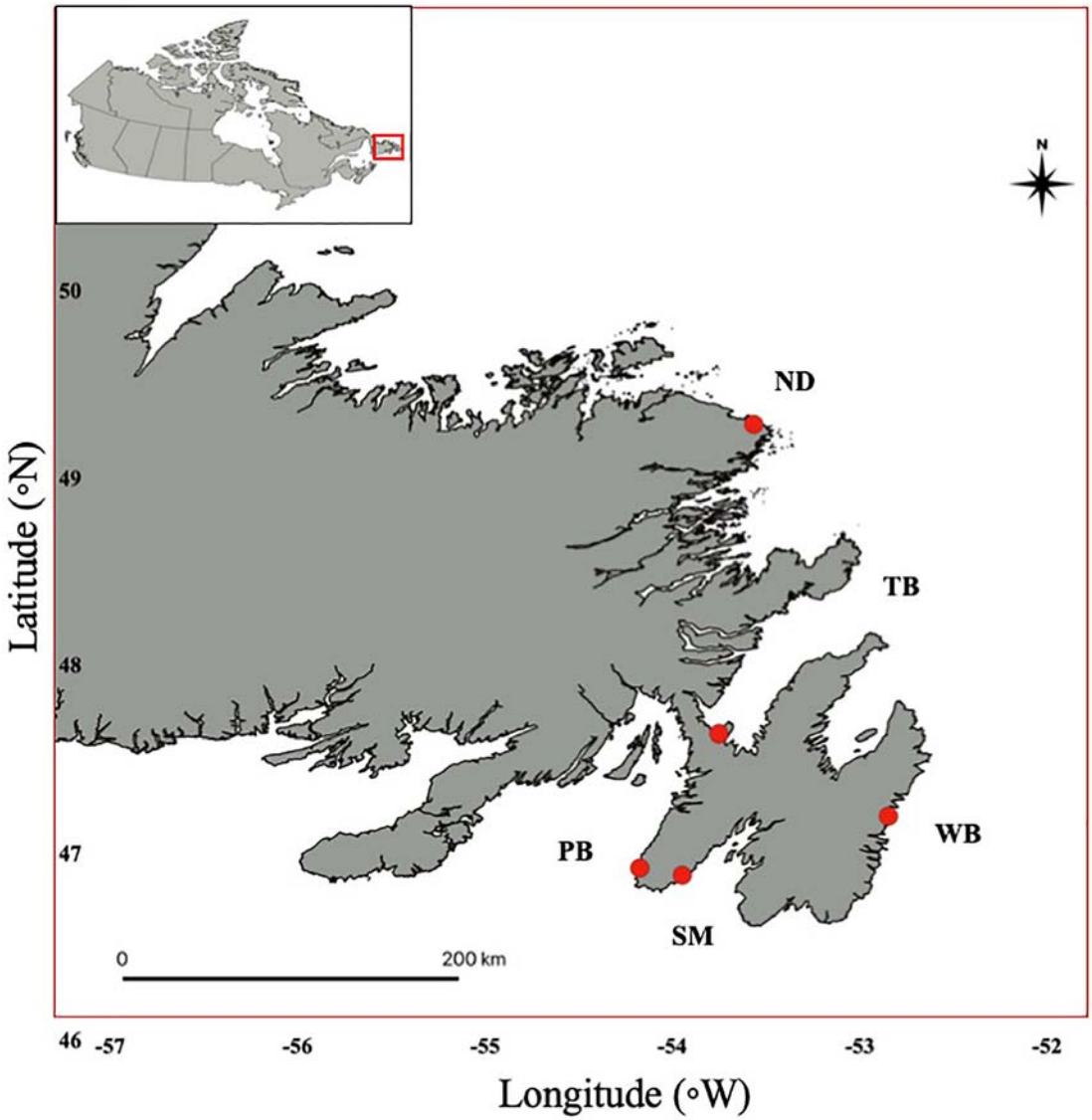

FIGURE 1 | Map of Newfoundland, Canada, indicating locations where capelin larvae were sampled in five coastal regions: Notre Dame Bay (ND; Mussel Shells Beach; 49.2856, -53.5673), Trinity Bay (TB; Bellevue Beach; 47.6338, -53.7519), Witless Bay (WB; Burnt Cove Beach; 47.1965, -52.8486), St. Mary's Bay (SM; Branch Beach; 46.8824, -53.9470), and Placentia Bay (PB; St. Brides Beach; 46.9204, -54.1748).

which otolith trace element concentrations (i.e., Mg, Mn, Zn, Sr, and Ba) were important in explaining the variation in the dataset without considering *a priori* groupings. To determine whether larvae could be correctly classified into their natal regions based on otolith chemical signatures, all five otolith trace element concentrations were used in a backward stepwise discriminant function analysis (DFA), and based on a p to enter of 0.05 and a p to exit of 0.25 (Davoren and Halden, 2014), all elements were retained by the model. Therefore, all five trace elements were included in a quadratic discriminant function analysis (QDFA). One-way ANOVAs were then used to determine whether each trace element concentration in otoliths differed among regions. When otolith concentrations of a trace element differed significantly among regions, *post hoc* Tukey's HSD tests were used to determine which regions differed from each other.

For interannual comparisons (Notre Dame Bay: 2014, 2015, 2018, and 2019; Trinity Bay: 2018 and 2019), MANOVAs and ANOVAs were used to test whether otolith chemistry differed among years within the two regions. If otolith chemistry differed among years within a region, the QDFA for regional comparisons was rerun, each time substituting the 2019 data with another year to determine if the regional classification rate varied as a result of this interannual variability. For the interannual comparison, Mn was excluded from the analysis as mean Mn concentrations were averaged across the entire embryonic otolith for 2014 and 2015 in Notre Dame Bay (see Loeppky and Davoren, 2018), but the center region was excluded from averages in 2018 and 2019.

TABLE 1 | Regions where capelin larvae and water chemistry were sampled from Notre Dame Bay (ND), Trinity Bay (TB), Witless Bay (WB), St. Mary's Bay (SM), and Placentia Bay (PB), with the dates of larvae/water sampling, along with water trace element concentrations from one water sample per region.

Region	Year	Date	Magnesium (mg/L)	Manganese (mg/L)	Zinc (mg/L)	Strontium (mg/L)	Barium (mg/L)
Regional comparison							
ND	2019	August 8/August 8	1,280	<LOD	<LOD	7.08	<LOD
TB	2019	August 7*/August 7	1,350	<LOD	<LOD	7.17	<LOD
WB	2019	July 29/July 29	1,120	0.120	<LOD	6.21	<LOD
SM	2019	July 18/July 18	1,260	0.042	<LOD	7.04	<LOD
PB	2019	July 19/July 19	1,250	<LOD	<LOD	6.79	<LOD
Interannual comparison							
ND	2014	July 10*/July 7	1,070	0.001	<LOD	6.14	0.007
	2015	August 17*/July 30	1,040	0.003	<LOD	6.16	0.007
	2018	August 1*/July 23	1,190	<LOD	0.24	6.52	<LOD
TB	2018	August 18*/August 1	1,250	<LOD	<LOD	6.98	<LOD

*Trace element concentrations below the limits of detection are indicated as <LOD. *Indicates field-reared larval samples.*

All statistical analyses were performed in JMP Pro (version 14.1), with $\alpha = 0.05$ and means reported as $\pm$ SE.

RESULTS

Otolith chemistry differed for some trace elements between field-reared larvae in incubation canisters and preemergent larvae collected from sediments in Notre Dame Bay during 2019, with significant differences in Zn ($t_{38} = 3.24$, $p = 0.0025$), Mn ($t_{42} = 2.504$, $p = 0.0163$), and Ba ($t_{41} = 2.023$, $p = 0.0496$). Consequently, otoliths from preemergent larvae were used in all analyses for regional comparisons, with the exception of Trinity Bay where only field-reared larvae were available for 2019. For interannual comparisons, only field-reared larvae from incubation canisters were used in the analyses.

Regional Comparisons

The PCA had two components with eigenvalues over 1, explaining cumulatively 60.1% of the variation (PC1: 35.7%; PC2: 24.4%). The otolith trace elements with the highest loadings on PC1 were Mn (0.8764) and Mg (0.8525), and those with the highest loadings on PC2 were Sr (0.7102), Zn (0.5855), and Ba (0.5613). Therefore, PC1 represented variability in most essential elements (i.e., Mn and Mg), while PC2 primarily represented variability in nonessential elements (i.e., Sr and Ba). Capelin larvae could be correctly classified into their natal region based on otolith chemistry (QDFA: Wilk's $\lambda = 0.172$; approximate $F_{20,210} = 7.332$, $p < 0.0001$; **Figure 2**) with an overall classification success of 78% (region-specific classification success: 68–100%; **Table 2**). Univariate analyses revealed that all otolith trace element concentrations differed significantly across regions (Mg: $F_{4,84} = 13.67$, $p < 0.0001$; Mn: $F_{4,89} = 22.11$, $p < 0.0001$; Zn: $F_{4,85} = 3.142$, $p = 0.0184$; Sr: $F_{4,86} = 4.817$, $p = 0.0015$; and Ba: $F_{4,85} = 10.19$, $p < 0.0001$), especially between Witless Bay and all other bays (**Figure 3**). Ambient water chemistry did not appear to vary considerably among regions during 2019, and only Sr and Mg concentrations were consistently above LODs (**Table 1**). While Sr concentrations in larval otoliths followed similar regional trends as ambient water concentrations, Mg concentrations in otoliths and ambient water did not show similar regional patterns (**Table 1** and **Figure 3**).

TABLE 2 | The number of larval otoliths included in analysis per region (number of outliers discarded from analysis in parentheses), as well as the number of otoliths classified into each region ("predicted region," columns).

		Predicted region				
Region	**No. of otoliths**	**ND**	**TB**	**WB**	**SM**	**PB**
ND	19 (5)	13	0	0	1	2
TB	8 (4)	0	7	0	1	0
WB	12 (6)	2	0	12	1	2
SM	15 (4)	2	1	0	11	2
PB	18 (5)	2	0	0	1	13
Classification Success (%)		68.4	84.5	100	73.3	72.2

Overall classification success of each region was based on a quadratic discriminant function analysis on otolith trace element concentrations of magnesium, manganese, zinc, strontium, and barium from larvae collected from Notre Dame Bay (ND), Trinity Bay (TB), Witless Bay (WB), St. Mary's Bay (SM), and Placentia Bay (PB).

Interannual Comparisons

Capelin larval otolith chemical signatures within Trinity Bay did not differ significantly between 2018 and 2019 (MANOVA: Wilk's $\lambda = 0.774$; approximate $F_{4,26} = 1.897$, $p = 0.141$; **Figure 4**). In contrast, otolith chemical signatures differed significantly among years (2014, 2015, 2018, and 2019) in Notre Dame Bay (MANOVA: Wilk's $\lambda = 0.120$; approximate $F_{12,199} = 20.46$, $p < 0.0001$). Univariate analyses revealed significant differences in all trace elements across years within Notre Dame Bay (Mg: $F_{3,88} = 38.42$, $p < 0.0001$; Zn: $F_{3,85} = 22.47$, $p < 0.0001$; Sr: $F_{3,87} = 9.68$, $p < 0.0001$; and Ba: $F_{3,86} = 23.76$, $p < 0.0001$; **Figure 5**). *Post hoc* tests revealed that while otolith Mg concentrations varied among all years, Zn and Sr were relatively stable across 2014, 2015, and 2018 but differed significantly in 2019, during which Zn was higher and Sr was lower (**Figure 5**). Otolith Ba concentrations were more similar within samples

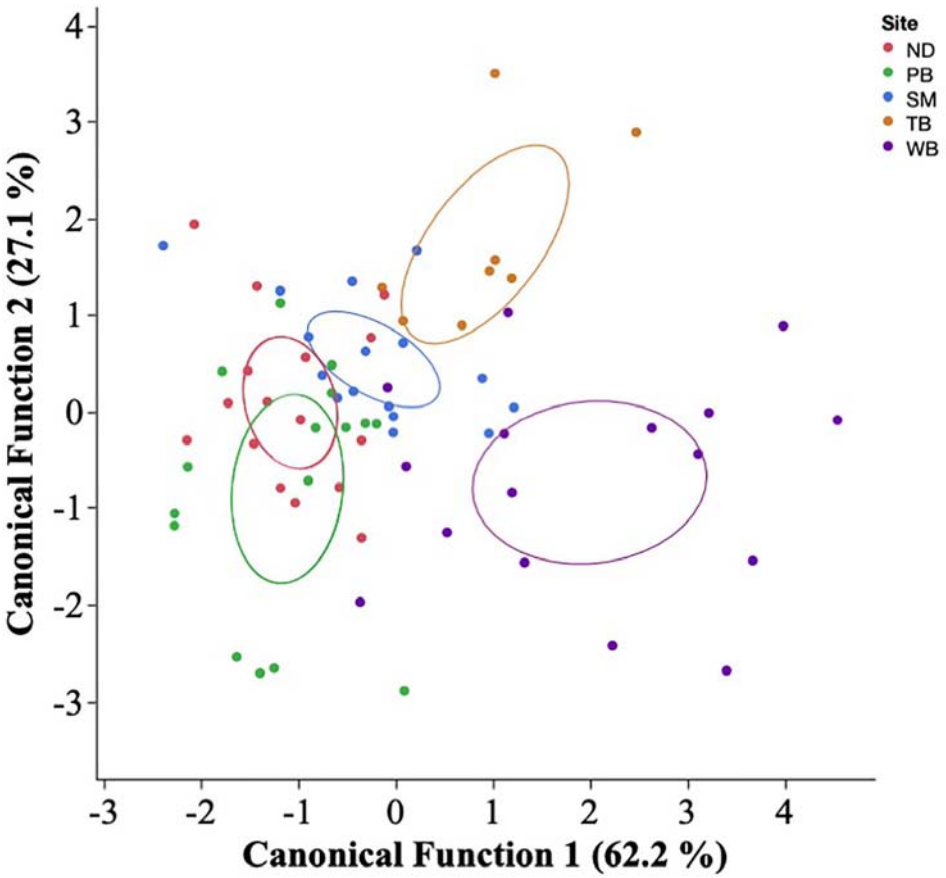

FIGURE 2 | Quadratic discriminant function analysis based on larval capelin otolith trace element concentrations of Mg, Mn, Zn, Sr, and Ba, where each dot represents each individual sampled during July–August 2019 from one of five regions: Notre Dame Bay (ND), Placentia Bay (PB), St. Mary's Bay (SM), Trinity Bay (TB), and Witless Bay (WB). Ellipses indicate the mean 95% confidence level contours for each bay.

from consecutive years relative to samples from nonconsecutive years (**Figure 5**).

Owing to interannual variation in otolith chemistry within Notre Dame Bay, we reran QDFAs for regional comparison three times, each time replacing the 2019 Notre Dame Bay data with one of the three earlier years. Otolith trace element concentrations remained significantly different among regions regardless of interannual variability in otolith chemical signatures ($p < 0.0001$), with similar regional classification success (67–76%) relative to the original model using 2019 data only and excluding otolith Mn concentrations (i.e., 66%). The removal of Mn did result in a slightly lower classification success compared to the original model using the 2019 data from all five embayments and all elements (i.e., Mg, Mn, Zn, Sr, and Ba). To further explore whether interannual variation in otolith chemical signatures could influence regional classification success, we used a MANOVA to test if otolith chemical signatures differed between Notre Dame Bay and Trinity Bay in 2018. The MANOVA revealed that otolith trace element concentrations differed significantly between field-reared larvae from Notre Dame Bay and Trinity Bay in 2018 (Wilk's $\lambda = 0.664$; approximate $F_{4,46} = 5.83$, $p = 0.0007$). Ambient water chemistry did not appear to vary considerably among years within regions, and, again, only Sr and Mg concentrations were consistently above LODs (**Table 1**).

DISCUSSION

Our classification success of capelin larvae into natal embayments (78%) was similar to the classification success (83%) of another study using otolith chemical signatures to examine regional differences of dispersing larval capelin in the Gulf of St. Lawrence (Lazartigues et al., 2016). Classification success of juvenile cod at the broad scale of southern and northern bays of Newfoundland was also similar to this study (75%), although classification success into specific bays was more variable (27–77%; Stanley et al., 2016), possibly due to variable environmental conditions. Classification success also remained consistent among regions in our study despite interannual differences in otolith trace element signatures within one region (Notre Dame Bay). Indeed, interannual variability in otolith chemical signatures had been shown previously for capelin (Davoren et al., 2015; Loeppky et al., 2018) along with a variety of other marine species

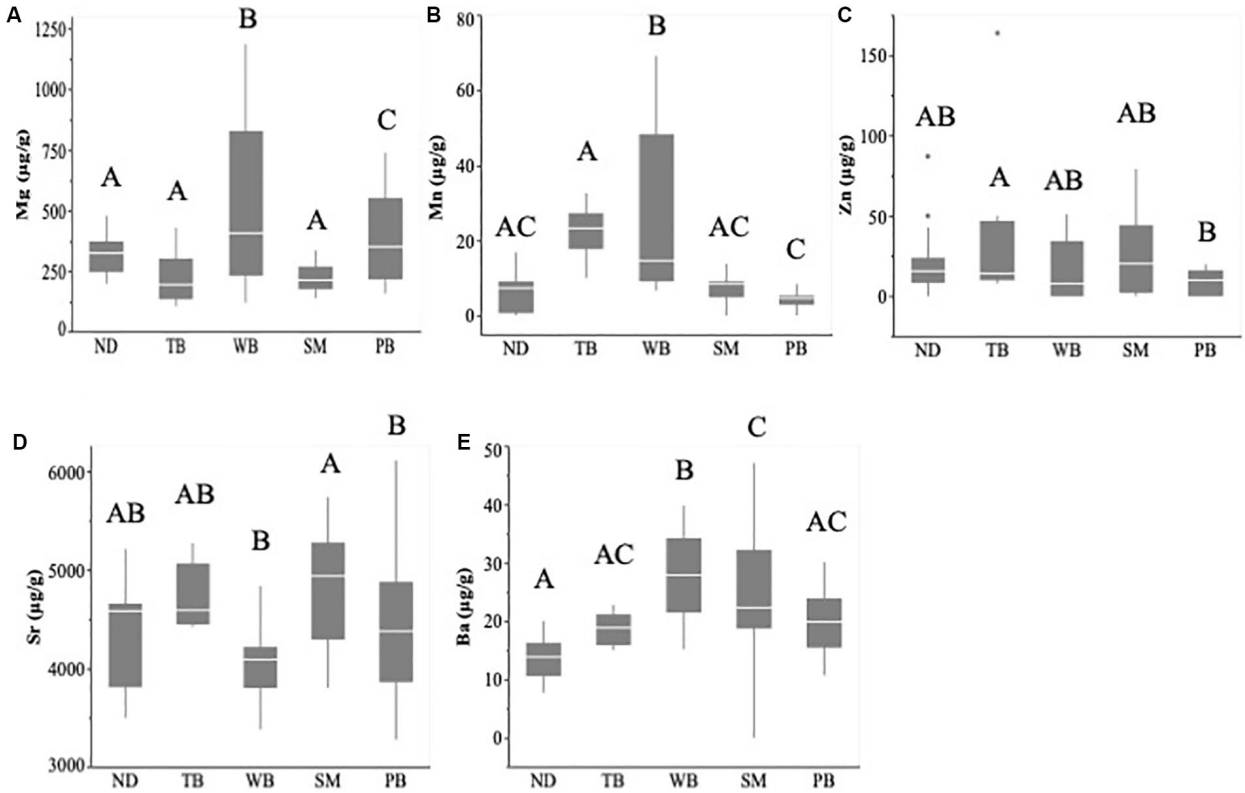

FIGURE 3 | Larval capelin otolith concentrations (µg/g ± SE) of magnesium **(A)**, manganese **(B)**, zinc **(C)**, strontium **(D)**, and barium **(E)** sampled during July–August 2019 from five coastal regions of Newfoundland: Notre Dame (ND), Trinity (TB), Witless (WB), St. Mary's (SM), and Placentia (PB). Boxplots show the mean (horizontal bar), 25th percentile (lower bar), 75th percentile (upper bar), and outliers. Significantly different mean otolith concentrations ($p < 0.05$) are indicated with different letters, while values that are not significantly different ($p > 0.05$) have the same letters.

[e.g., King George whiting, *Sillaginodes punctatus*, Rogers et al., 2019; juvenile snapper, *Pagrus auratus* (formerly known as *Chrysophyrs auratus*), Hamer et al., 2003; and common sole, *Solea solea*, and Senegalese sole, *Solea senegalensis*, Tanner et al., 2012]. Despite significant interannual variation in otolith chemistry, larvae in other studies can often still be classified into their natal regions, as was found for King George whiting in southern Australia (82% classification success; Rogers et al., 2019). Overall, these findings suggest that regional differences in otolith chemistry are robust to among-year variation. Otolith chemical differences between Trinity Bay and other regions, however, should be interpreted with caution due to divergent otolith chemistry between field-reared larvae in canisters (subtidal; ∼1 m water; Trinity Bay) relative to preemergent larvae collected within beach spawning sediment (intertidal; all other bays).

Our results support a growing body of evidence that otolith chemistry is a useful tool to identify the natal origin of early life history stages of marine fish (e.g., Vasconcelos et al., 2007; Clarke et al., 2009; Di Franco et al., 2012; Rogers et al., 2019). Indeed, this approach was used successfully for juvenile snapper in southern Australia where chemical signatures in juvenile otoliths demonstrated high connectivity among coastal regions and identified one high-productivity region to target for fisheries management (Hamer et al., 2011). Given that region-specific chemical signatures can be identified in larval capelin otoliths (Lazartigues et al., 2016; this study), the next step is to use these distinct signatures to determine the natal origin of spawning adults by quantifying otolith chemistry in the pre-hatch region. This research will address knowledge gaps regarding embayment-specific productivity of capelin along with connectivity among embayments.

Although the goal of this study was not to investigate the mechanisms underlying region-specific differences in otolith chemistry, we did expect otolith chemical signatures to generally reflect variation in ambient water chemistry, especially for nonessential trace elements (i.e., Sr and Ba; reviewed in Campana, 1999; Loewen et al., 2016). However, this was not the case for most trace elements in this study. For Mg, an essential element, ambient concentrations varied among regions, but this variation was not reflected in otolith concentrations. There was also no trend between ambient and otolith Mn concentrations, another essential element, which may be due to the enrichment of this element in the pre-hatch region of larval otoliths, possibly due to maternal investment (Brophy et al., 2004; Ruttenberg et al., 2005; DiMaria et al., 2010; Lazartigues et al., 2014). For the nonessential element Ba, otolith concentrations also likely reflect maternal investment rather than differences in ambient

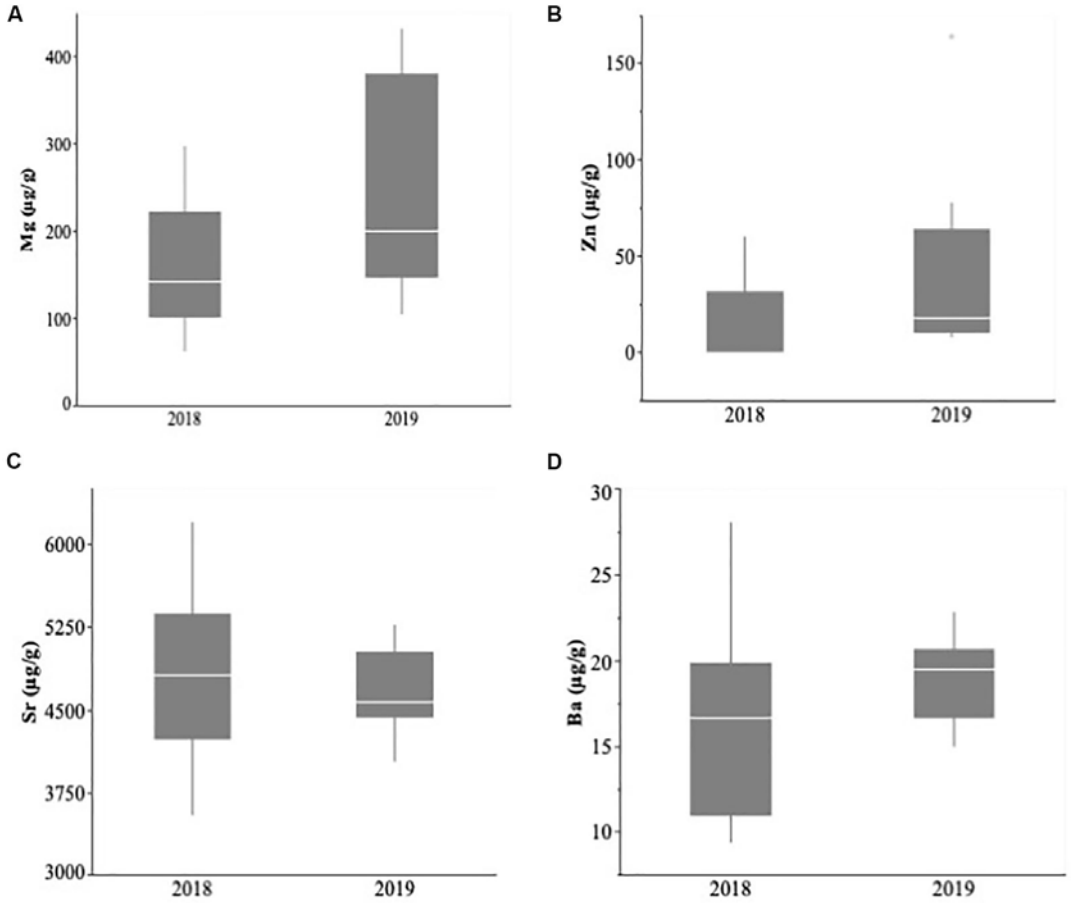

FIGURE 4 | Larval capelin otolith concentrations (µg/g ± SE) of magnesium **(A)**, zinc **(B)**, strontium **(C)**, and barium **(D)** sampled during July–August 2018 and 2019 in Trinity Bay. Boxplots show the mean (horizontal bar), 25th percentile (lower bar), 75th percentile (upper bar), and outliers.

water chemistry in capelin (Loeppky et al., 2018). Differing maternal investment of otolith Ba concentrations from repeat spawners may explain our finding of more similar concentrations of this element between consecutive years compared to those between nonconsecutive years. Although Sr, another nonessential element, may be maternally invested in other marine species (e.g., salmonids, Volk et al., 2000; Limburg et al., 2001; Zimmerman and Reeves, 2002), this element is known to be incorporated into the pre-hatch region of capelin otoliths during egg incubation and appears to be less maternally derived than Ba (Loeppky et al., 2018). In support, pre-hatch otolith Sr concentrations were higher in regions with higher ambient Sr concentrations in this study. Overall, the inconsistencies between otolith chemistry and most trace element concentrations in ambient water in this study have been found in other studies (Brown and Severin, 2009; Sturrock et al., 2014, 2015; Loewen et al., 2015). While our sampling regime was unable to determine if water chemistry varied throughout incubation, trace element concentrations in ambient water both within and among years were consistent in previous coastal Newfoundland studies (Davoren et al., 2015; Loeppky and Davoren, 2018), suggesting there are other drivers of variability in larval otolith chemical signatures.

Temperature and salinity are known to influence chemical signatures in the embryonic otolith of capelin larvae (Davoren et al., 2015; Loeppky and Davoren, 2018; Loeppky et al., 2018), as also found for other marine species (black bream, *Acanthopagrus butcheri*, Elsdon and Gillanders, 2005; Izzo et al., 2018; and European plaice, *Pleuronectes platessa*, Sturrock et al., 2014, 2015) and, thus, may have influenced otolith chemistry differences among regions. Preemergent capelin larvae were likely exposed to region-specific microclimates during incubation as capelin eggs are sticky and adhere to beach sediments for 10+ days before hatching (Frank and Leggett, 1981; Penton et al., 2012). Temperature is known to vary among capelin spawning beaches within a region (Crook et al., 2017), and temperature can indirectly influence otolith chemistry through its impact on somatic growth and transport kinetics, whereby higher temperatures increase larval growth which affects incorporation rates of essential trace elements (e.g., Mg and Mn; Loewen et al., 2016). Indeed, altered otolith biomineralization (e.g., stable isotopes, trace elements, and microstructure) can result from differing growth rates (Limburg et al., 2018; Freshwater et al., 2019), metabolic or energy demands (Chung et al., 2019), and ontogeny (Clarke et al., 2011). In contrast, several

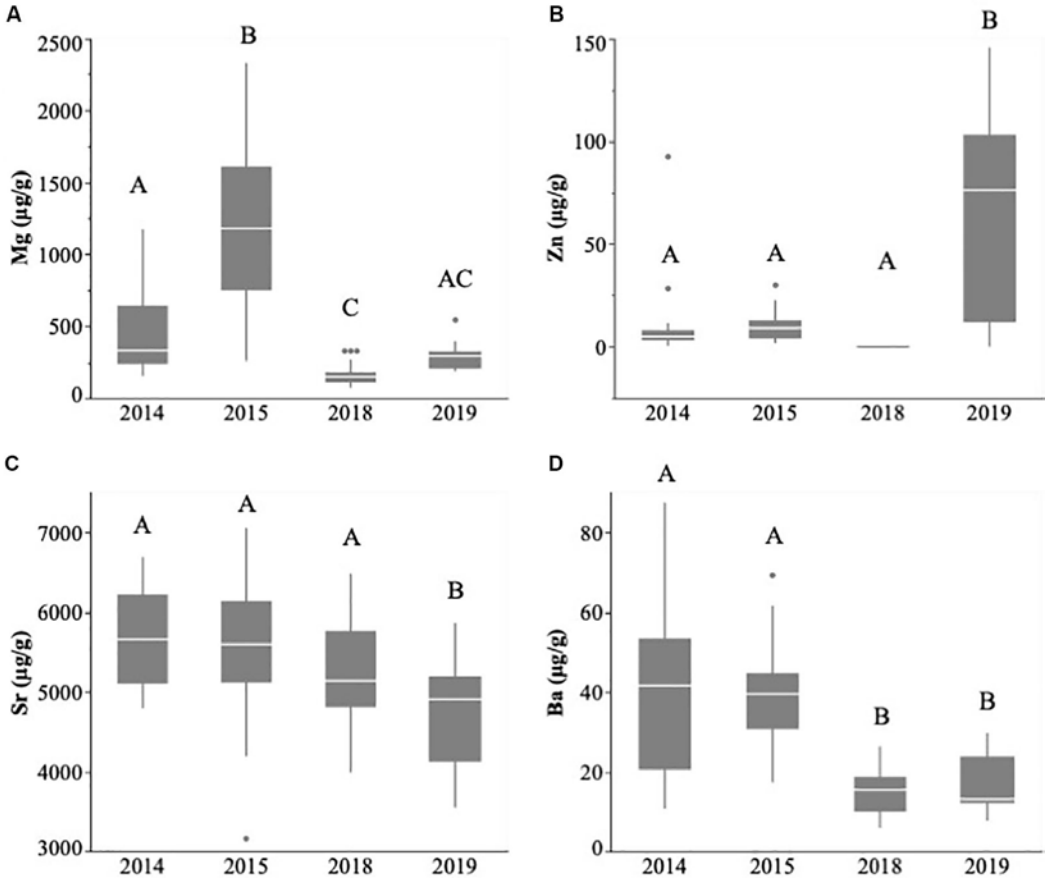

FIGURE 5 | Larval capelin otolith concentrations (µg/g ± SE) of magnesium **(A)**, zinc **(B)**, strontium **(C)**, and barium **(D)** sampled during July–August 2014, 2015, 2018, and 2019 in Notre Dame Bay. Boxplots show the mean (horizontal bar), 25th percentile (lower bar), 75th percentile (upper bar), and outliers. Significantly different mean otolith concentrations ($p < 0.05$) are indicated with different letters, while values that are not significantly different ($p > 0.05$) have the same letters.

lab-based studies found either no effect or a weak effect of growth on both nonessential (i.e., Sr and Ba; Bath et al., 2000; Martin et al., 2004) and essential elements (i.e., Mg and Mn; Martin and Thorrold, 2005). Capelin spawning beaches are frequently associated with varying freshwater inputs (Beirão et al., 2018; Purchase, 2018), influencing the salinity of incubating water, which is likely further influenced by regional variability in summer rainfall. As Sr concentrations are positively related to environmental salinity (Panfili et al., 2015), the otolith concentrations of this trace element have been used as a marker of anadromy in many species (e.g., Arctic char, *Salvelinus alpinus*, Halden et al., 1995; black bream, Elsdon and Gillanders, 2005; and European bass, *Dicentrarchus labrax*, Reis-Santos et al., 2013). Salinity is also known to influence the incorporation rates of Sr into the embryonic otoliths of capelin (Loeppky and Davoren, 2018; Loeppky et al., 2018). Overall, microclimate variation during capelin egg incubation likely contributed to divergent otolith chemistry of larvae among regions, among years within a region, and between preemergent larvae within beach spawning sediment (intertidal) relative to field-reared larvae in incubation canisters (subtidal; ∼1 m water).

CONCLUSION

In conclusion, although the mechanisms underlying the observed regional differences in larval otolith chemistry are unclear due to limited sampling of ambient water conditions, our findings support the use of capelin otolith chemical signatures to evaluate the regional productivity and connectivity of this stock. Preemergent (1- to 3-day-old) larval capelin show region-specific otolith chemistry signatures which allowed larvae to be classified into their natal region and provide the basis for future studies to assess the natal origins of juvenile and adult capelin sampled offshore. As a result of the interannual variation in otolith chemistry, capelin recruits will need to be of the same cohort as the larvae sampled for baseline measurements (e.g., Hamer et al., 2011). This will allow for the identification of key coastal regions for larval production that contribute to recruitment (i.e., source and sink regions) and provide information on the scale of dispersal and connectivity among regions. Overall, identifying the natal origins of larval and adult capelin is critical for marine spatial planning and informing stock structure for management of this key forage fish species in the Newfoundland ecosystem.

DATA AVAILABILITY STATEMENT

The datasets generated for this study are available on reasonable request to the corresponding author.

ETHICS STATEMENT

We confirm that the research conducted was in adherence with guidelines of the Canadian Council of Animal Care (Protocol: F16-017/1/2/3).

AUTHOR CONTRIBUTIONS

AT wrote the manuscript and conducted all lab processing. GD and HM acquired funding for the project, conceived of the manuscript, and led the development of the manuscript. All authors were involved in determining appropriate data analyses and manuscript structure and in editing/revising the manuscript.

FUNDING

Principal funding was provided by the Natural Sciences and Engineering Research Council of Canada Discovery (2019-06290) and Ship Time Grant (486208-2019) to GD, along with a University of Manitoba Faculty of Science Fieldwork Support Program Grant (2019) and a Coastal Restoration Fund grant (funded by WorldWildlife Fund Canada) to GD.

ACKNOWLEDGMENTS

We are indebted to the captain and crew of the *Lady Easton* for their assistance with fieldwork. Thanks also to B. Squires and the DFO team for sample collection in Trinity Bay and to S. Morrison and L. Bliss for larval collection in Placentia and surrounding bays. Thanks also to A. Loeppky for assistance with lab processing techniques and to P. Yang for laser expertise. Thank you to our two reviewers for their helpful feedback and comments.

REFERENCES

Bath, G. E., Thorrold, S. R., Jones, C. M., Campana, S. E., McLaren, J. W., and Lam, J. W. H. (2000). Strontium and barium uptake in aragonitic otoliths of marine fish. *Geochim. Cosmochim. Acta* 64, 1705–1714. doi: 10.1016/S0016-7037(99)00419-6

Beirão, J., Lewis, J. A., Wringe, B. F., and Purchase, C. F. (2018). A novel sperm adaptation to evolutionary constraints on reproduction: pre-ejaculatory sperm activation in the beach spawning capelin (*Osmeridae*). *Ecol. Evol.* 8, 2343–2349. doi: 10.1002/ece3.3783

Bohonak, A. J. (1999). Dispersal, gene flow, and population structure. *Q. Rev. Biol.* 74, 21–45.

Bradbury, I. R., Laurel, B. J., Robichaud, D., Rose, G. A., Snelgrove, P. V. R., Gregory, R. S., et al. (2008). Discrete spatial dynamics in a marine broadcast spawner: Re-evaluating scales of connectivity and habitat associations in Atlantic cod (*Gadus morhua* L.) in coastal Newfoundland. *Fish. Res.* 91, 299–309. doi: 10.1016/j.fishres.2007.12.006

Brophy, D., Jeffries, T. E., and Danilowicz, B. S. (2004). Elevated manganese concentrations at the cores of clupeid otoliths: possible environmental, physiological, or structural origins. *Mar. Biol.* 144, 779–786. doi: 10.1007/s00227-003-1240-3

Brown, R. J., and Severin, K. P. (2009). Otolith chemistry analyses indicate that water Sr:Ca is the primary factor influencing otolith Sr:Ca for freshwater and diadromous fish but not for marine fish. *Can. J. Fish. Aquat. Sci.* 66, 1790–1808. doi: 10.1139/F09-112

Campana, S. E. (1999). Chemistry and composition of fish otoliths: pathways, mechanisms and applications. *Mar. Ecol. Prog. Ser.* 188, 263–297. doi: 10.3354/meps188263

Carscadden, J. E., Gjøsæter, H., and Vilhjálmsson, H. (2013). Recruitment in the Barents Sea, Icelandic, and eastern Newfoundland/Labrador capelin (*Mallotus villosus*) stocks. *Prog. Oceanogr.* 114, 84–96. doi: 10.1016/j.pocean.2013.05.006

Carscadden, J. E., and Vilhjálmsson, H. (2002). Capelin - What are they good for? Introduction. *ICES J. Mar. Sci.* 59, 863–869. doi: 10.1006/jmsc.2002.1283

Chung, M. T., Trueman, C. N., Godiksen, J. A., Holmstrup, M. E., and Grønkjær, P. (2019). Field metabolic rates of teleost fishes are recorded in otolith carbonate. *Commun. Biol.* 2, 1–10. doi: 10.1038/s42003-018-0266-5

Clarke, L. M., Conover, D. O., and Thorrold, S. R. (2011). Population differences in otolith chemistry have a genetic basis in *Menidia menidia*. *Can. J. Fish. Aquat. Sci.* 68, 105–114. doi: 10.1139/F10-147

Clarke, L. M., Walther, B. D., Munch, S. B., Thorrold, S. R., and Conover, D. O. (2009). Chemical signatures in the otoliths of a coastal marine fish, *Menidia menidia*, from the northeastern united states: spatial and temporal differences. *Mar. Ecol. Prog. Ser.* 384, 261–271. doi: 10.3354/meps07927

Cowen, R. K., Gawarkiewicz, G., Pineda, J., Thorrold, S. R., and Werner, F. E. (2007). Population connectivity in marine systems an overview. *Oceanography* 20, 14–21.

Crichton, R. R. (2008). *Biological Inorganic Chemistry*. Amsterdam: Elsevier.

Crook, K. A., Maxner, E., and Davoren, G. K. (2017). Temperature-based spawning habitat selection by Capelin (*Mallotus villosus*) in Newfoundland. *ICES J. Mar. Sci.* 74, 1622–1629. doi: 10.1093/icesjms/fsx023

Davoren, G. K., and Halden, N. M. (2014). Connectivity of capelin (*Mallotus villosus*) between regions and spawning habitats in Newfoundland inferred from otolith chemistry. *Fish. Res.* 159, 95–104. doi: 10.1016/j.fishres.2014.05.010

Davoren, G. K., Woloschiniwsky, C. S. A., Halden, N. M., and Wang, F. (2015). Does otolith chemistry indicate the natal habitat of Newfoundland capelin *Mallotus villosus*? *J. Exp. Mar. Bio. Ecol.* 464, 88–95. doi: 10.1016/j.jembe.2014.10.025

Di Franco, A., Gillanders, B. M., De Benedetto, G., Pennetta, A., De Leo, G., and Guidetti, P. (2012). Dispersal patterns of coastal fish: implications for designing networks of marine protected areas. *PLoS One* 7:e13681. doi: 10.1371/journal.pone.0031681

DiMaria, R. A., Miller, J. A., and Hurst, T. P. (2010). Temperature and growth effects on otolith elemental chemistry of larval Pacific cod, *Gadus macrocephalus*. *Environ. Biol. Fish.* 89, 453–462. doi: 10.1007/s10641-010-9665-2

Elsdon, T. S., and Gillanders, B. M. (2003). Relationship between water and otolith elemental concentrations in juvenile black bream *Acanthopagrus butcheri*. *Mar. Ecol. Prog. Ser.* 260, 263–272. doi: 10.3354/meps260263

Elsdon, T. S., and Gillanders, B. M. (2005). Consistency of patterns between laboratory experiments and field collected fish in otolith chemistry: an example and applications for salinity reconstructions. *Mar. Freshw. Res.* 56, 609–617. doi: 10.1071/MF04146

Frank, K. T., and Leggett, W. C. (1981). Prediction of egg development and mortality rates in Capelin (*Mallotus villosus*) from meteorological, hydrographic, and biological factors. *Can. J. Fish. Aquat. Sci.* 38, 1327–1338. doi: 10.1139/f81-179

Freshwater, C., Trudel, M., Beacham, T. D., Gauthier, S., Johnson, S. C., Neville, C. E., et al. (2019). Individual variation, population-specific behaviours and stochastic processes shape marine migration phenologies. *J. Anim. Ecol.* 88, 67–78. doi: 10.1111/1365-2656.12852

Fridgeirsson, E. (1976). Observation on spawning behaviour and embryonic development of the Icelandic capelin. *Rit Fiskideildar.* 5, 1–35.

Halden, N. M., Babaluk, J. A., Campbell, J. L., and Teesdale, W. J. (1995). Scanning proton microprobe analysis of strontium in an Arctic charr, *Salvelinus alpinus*, otolith: implications for the interpretation of anadromy. *Environ. Biol. Fishes* 43, 333–339. doi: 10.1007/BF00001166

Hamer, P. A., Acevedo, S., Jenkins, G. P., and Newman, A. (2011). Connectivity of a large embayment and coastal fishery: spawning aggregations in one bay source local and broad-scale fishery replenishment. *J. Fish Biol.* 78, 1090–1109. doi: 10.1111/j.1095-8649.2011.02921.x

Hamer, P. A., Jenkins, G. P., and Gillanders, B. M. (2003). Otolith chemistry of juvenile snapper *Pagrus auratus* in victorian waters: natural chemical tags and their temporal variation. *Mar. Ecol. Prog. Ser.* 263, 261–273. doi: 10.3354/meps263261

Izzo, C., Reis-Santos, P., and Gillanders, B. M. (2018). Otolith chemistry does not just reflect environmental conditions: a meta-analytic evaluation. *Fish Fish.* 19, 441–454. doi: 10.1111/faf.12264

Jones, G., Milicich, M., Emslie, M., and Lunow, C. (1999). Self-recruitment in a coral reef fish population. *Nature* 402, 802–804. doi: 10.1038/45538

Kenchington, E. L., Nakashima, B. S., Taggart, C. T., and Hamilton, L. C. (2015). Genetic structure of capelin (Mallotus villosus) in the northwest Atlantic Ocean. *PLoS One* 10:e0122315. doi: 10.1371/journal.pone.0122315

Lazartigues, A. V., Plourde, S., Dodson, J. J., Morissette, O., Ouellet, P., and Sirois, P. (2016). Determining natal sources of capelin in a boreal marine park using otolith microchemistry. *ICES J. Mar. Sci. J. Cons.* 73, 2644–2652. doi: 10.1093/icesjms/fsw104

Lazartigues, A. V., Sirois, P., and Savard, D. (2014). LA-ICP-MS analysis of small samples: carbonate reference materials and larval fish otoliths. *Geostand. Geoanalytical. Res.* 38, 225–240. doi: 10.1111/j.1751-908X.2013.00248.x

Limburg, K. E., Landergren, P., Westin, L., Elfman, M., and Kristiansson, P. (2001). Flexible modes of anadromy in Baltic sea trout: making the most of marginal spawning streams. *J. Fish. Biol.* 59, 682–695.

Limburg, K. E., Wuenschel, M. J., Hüssy, K., Heimbrand, Y., and Samson, M. (2018). Making the otolith magnesium chemical calendar-clock tick: plausible mechanism and empirical evidence. *Rev. Fish. Sci. Aquac.* 26, 479–493. doi: 10.1080/23308249.2018.1458817

Loeppky, A. R., and Davoren, G. K. (2018). Temperature and salinity influence the chemistry in the pre-hatch otolith region of capelin, *Mallotus villosus*, during lab and field egg incubation experiments. *J. Exp. Mar. Bio. Ecol.* 501, 65–73. doi: 10.1016/j.jembe.2018.01.003

Loeppky, A. R., Purchase, C. F., and Davoren, G. K. (2018). Chemical signatures in embryonic otoliths of capelin (*Mallotus villosus*) influence of family and environmental conditions. *J. Exp. Mar. Bio. Ecol.* 498, 25–31.

Loewen, T. N., Carriere, B., Reist, J. D., Halden, N. M., and Anderson, W. G. (2016). Linking physiology and biomineralization processes to ecological inferences on the life history of fishes. *Comp. Biochem. Physiol. A Mol. Integr. Physiol.* 202, 123–140. doi: 10.1016/j.cbpa.2016.06.017

Loewen, T. N., Reist, J. D., Yang, P., Koleszar, A., Babaluk, J. A., Mochnacz, N., et al. (2015). Discrimination of northern form Dolly Varden Char (*Salvelinus malma* malma) stocks of the North Slope, Yukon and Northwest Territories, Canada via otolith trace elements and 87Sr/86Sr isotopes. *Fish. Res.* 170, 116–124. doi: 10.1016/j.fishres.2015.05.025

Martin, G. B., and Thorrold, S. R. (2005). Temperature and salinity effects on magnesium, manganese, and barium incorporation in otoliths of larval and early juvenile spot *Leiostomus xanthurus*. *Mar. Ecol. Prog. Ser.* 293, 223–232. doi: 10.3354/meps293223

Martin, G. B., Thorrold, S. R., and Jones, C. M. (2004). Temperature and salinity effects on strontium incorporation in otoliths of larval spot (*Leiostomus xanthurus*). *Can. J. Fish. Aquat. Sci.* 61, 34–42. doi: 10.1139/f03-143

Nakashima, B. S. (1992). Patterns in coastal migration and stock structure of capelin (*Mallotus villosus*). *Can. J. Fish. Aquat. Sci.* 49, 2423–2429. doi: 10.1139/f92-268

Nakashima, B. S., and Wheeler, J. P. (2002). Capelin (*Mallotus villosus*) spawning behaviour in Newfoundland waters - the interaction between beach and demersal spawning. *ICES J. Mar. Sci.* 59, 909–916. doi: 10.1006/jmsc.2002.1261

Panfili, J., Darnaude, A. M., Vigliola, L., Jacquart, A., Labonne, M., and Gilles, S. (2015). Experimental evidence of complex relationships between the ambient salinity and the strontium signature of fish otoliths. *J. Exp. Mar. Bio. Ecol.* 467, 65–70. doi: 10.1016/j.jembe.2015.03.007

Penton, P. M., Davoren, G. K., Montevecchi, W. A., and Andrews, D. W. (2012). Beach and demersal spawning in capelin *(Mallotus villosus*) on the northeast Newfoundland coast: egg developmental rates and mortality. *Can. J. Zool.* 90, 248–256. doi: 10.1139/Z11-132

Purchase, C. F. (2018). Low tolerance of salt water in a marine fish: new and historical evidence for surprising local adaption in the well-studied commercially exploited capelin. *Can. J. Fish. Aquat. Sci.* 75, 673–681. doi: 10.1139/cjfas-2017-0058

Reis-Santos, P., Tanner, S. E., Elsdon, T. S., Cabral, H. N., and Gillanders, B. M. (2013). Effects of temperature, salinity and water composition on otolith elemental incorporation of Dicentrarchus labrax. *J. Exp. Mar. Bio. Ecol.* 446, 245–252. doi: 10.1016/j.jembe.2013.05.027

Rogers, T. A., Fowler, A. J., Steer, M. A., and Gillanders, B. M. (2019). Discriminating natal source populations of a temperate marine fish using larval otolith chemistry. *Front. Mar. Sci.* 6:711. doi: 10.3389/fmars.2019.00711

Ruttenberg, B. I., Hamilton, S. L., Hickford, M. J. H., Paradis, G. L., Sheehy, M. S., Standish, J. D., et al. (2005). Elevated levels of trace elements in cores of otoliths and their potential for use as natural tags. *Mar. Ecol. Prog. Ser.* 297, 273–281. doi: 10.3354/meps297273

Stanley, R. R. E., deYoung, B., Snelgrove, P. V. R., and Gregory, R. S. (2013). Factors regulating early life history dispersal of Atlantic cod (*Gadus morhua*) from coastal Newfoundland. *PLoS One* 8:75889. doi: 10.1371/journal.pone.0075889

Stanley, R. R. E., Dibacco, C., Thorrold, S. R., Snelgrove, P. V. R., Morris, C. J., Gregory, R. S., et al. (2016). Regional variation in otolith geochemistry of juvenile Atlantic cod *(Gadus morhua*) in coastal Newfoundland. *Can. J. Fish. Aquat. Sci.* 73, 1507–1519. doi: 10.1139/cjfas-2015-0353

Sturrock, A. M., Hunter, E., Milton, J. A., Johnson, R. C., Waring, C. P., Trueman, C. N., et al. (2015). Quantifying physiological influences on otolith microchemistry. *Methods Ecol. Evol.* 6, 806–816. doi: 10.1111/2041-210X.12381

Sturrock, A. M., Trueman, C. N., Milton, J. A., Waring, C. P., Cooper, M. J., and Hunter, E. (2014). Physiological influences can outweigh environmental signals in otolith microchemistry research. *Mar. Ecol. Prog. Ser.* 500, 245–264. doi: 10.3354/meps10699

Swearer, S. E., Caselle, J. E., Lea, D. W., and Warner, R. R. (1999). Larval retention and recruitment in an island population of a coral-reef fish. *Nature* 402:799.

Tanner, S. E., Reis-Santos, P., Vasconcelos, R. P., França, S., Thorrold, S. R., and Cabral, H. N. (2012). Otolith geochemistry discriminates among estuarine nursery areas of Solea solea and S. senegalensis over time. *Mar. Ecol. Prog. Ser.* 452, 193–203. doi: 10.3354/meps09621

Templeman, W. (1948). The life history of the capelin (*Mallotus villosus* O.F. Müller) in Newfoundland waters. *Res. Bull. Newfoundland. Dept. Nat. Res.* 17, 1–15.

Vasconcelos, R. P., Reis-Santos, P., Tanner, S., Fonseca, V., Latkoczy, C., Günther, D., et al. (2007). Discriminating estuarine nurseries for five fish species through otolith elemental fingerprints. *Mar. Ecol. Prog. Ser.* 350, 117–126. doi: 10.3354/meps07109

Volk, E. C., Blakley, A., Schroder, S. L., and Kiehner, S. M. (2000). Otolith chemistry reflects migratory characteristics of Pacific salmonids: using otolith core chemistry to distinguish maternal associations with sea and freshwaters. *Fish. Res.* 46, 251–266.

Zimmerman, C. E., and Reeves, G. H. (2002). Identification of steelhead and resident rainbow trout progeny in the deschutes River, Oregon, revealed with otolith microchemistry. *Trans. Am. Fish. Soc.* 131, 986–993.

Conflict of Interest: The authors declare that the research was conducted in the absence of any commercial or financial relationships that could be construed as a potential conflict of interest.

Copyright © 2020 Tripp, Murphy and Davoren. This is an open-access article distributed under the terms of the Creative Commons Attribution License (CC BY). The use, distribution or reproduction in other forums is permitted, provided the original author(s) and the copyright owner(s) are credited and that the original publication in this journal is cited, in accordance with accepted academic practice. No use, distribution or reproduction is permitted which does not comply with these terms.

frontiers in Marine Science

ORIGINAL RESEARCH
published: 26 May 2020
doi: 10.3389/fmars.2020.00347

Water and Otolith Chemistry: Implications for Discerning Estuarine Nursery Habitat Use of a Juvenile Flatfish

Filipe Martinho[1†], Beatriz Pina[1†], Margarida Nunes[1], Rita P. Vasconcelos[2], Vanessa F. Fonseca[3,4], Daniel Crespo[1,5], Ana Lígia Primo[1], Ana Vaz[1], Miguel A. Pardal[1], Bronwyn M. Gillanders[6], Susanne E. Tanner[3,4‡] and Patrick Reis-Santos[3,6‡]*

[1] Centre for Functional Ecology – CFE, Department of Life Sciences, Calçada Martim de Freitas, University of Coimbra, Coimbra, Portugal, [2] IPMA – Portuguese Sea and Atmosphere Institute, Av. Dr. Alfredo Magalhães Ramalho, Lisbon, Portugal, [3] MARE – Marine and Environmental Sciences Centre, Faculdade de Ciências, Universidade de Lisboa, Campo Grande, Lisbon, Portugal, [4] Departamento de Biologia Animal, Faculdade de Ciências, Universidade de Lisboa, Campo Grande, Lisbon, Portugal, [5] MARE – Marine and Environmental Sciences Centre, Polytechnic of Leiria, Edifício CETEMARES, Av. Porto de Pesca, Peniche, Portugal, [6] Southern Seas Ecology Laboratories, School of Biological Sciences, The University of Adelaide, Adelaide, SA, Australia

OPEN ACCESS

Edited by:
Esteban Avigliano,
Consejo Nacional de Investigaciones Científicas y Técnicas (CONICET), Argentina

Reviewed by:
Pia Schuchert,
Agri-Food and Biosciences Institute (AFBI), United Kingdom
Felippe Alexandre Daros,
São Paulo State University, Brazil

***Correspondence:**
Filipe Martinho
fmdm@ci.uc.pt;
fmartinho@gmail.com

† These authors have contributed equally to this work

‡ These authors share senior authorship

Specialty section:
This article was submitted to Marine Ecosystem Ecology, a section of the journal Frontiers in Marine Science

Received: 31 January 2020
Accepted: 24 April 2020
Published: 26 May 2020

Citation:
Martinho F, Pina B, Nunes M, Vasconcelos RP, Fonseca VF, Crespo D, Primo AL, Vaz A, Pardal MA, Gillanders BM, Tanner SE and Reis-Santos P (2020) Water and Otolith Chemistry: Implications for Discerning Estuarine Nursery Habitat Use of a Juvenile Flatfish. Front. Mar. Sci. 7:347. doi: 10.3389/fmars.2020.00347

Variations in otolith elemental composition are widely used to reconstruct fish movements. However, reconstructing habitat use and environmental histories of fishes within estuaries is still a major challenge due to the dynamic nature of these coastal environments. In this study, we performed a laboratory experiment to investigate the effects of variations in salinity (three levels; 5, 18, 30) and temperature (two levels; 16, 21°C) on the otolith elemental composition (Mg:Ca, Mn:Ca, Sr:Ca, Ba:Ca) of juvenile Senegalese sole *Solea senegalensis.* Temperature and salinity treatments mirrored the natural conditions of the estuarine habitats occupied by juvenile Senegalese sole, thereby providing information on the applicability of otolith microchemistry to reconstruct habitat use patterns within estuarine nurseries, where individual fish move across complex salinity and temperature gradients. While Sr:Ca and Ba:Ca in otoliths were both positively related to salinity, no temperature effect was observed. Partition coefficients, proxies for element incorporation rates increased with increasing salinity for Sr (D_{Sr}) and Ba (D_{Ba}). In contrast, salinity and temperature had little influence on otolith Mn:Ca and Mg:Ca, supporting physiological control on the incorporation of these elements. Our results are a stepping stone for the interpretation of otolith chemical profiles for fish collected in their natural habitats and contribute to better understanding the processes involved in otolith element incorporation.

Keywords: connectivity, flatfish, nursery areas, estuaries, migrations, otoliths

INTRODUCTION

Estuaries are key nursery areas for many marine fish (Beck et al., 2001; Sheaves et al., 2006; Nagelkerken et al., 2013), including flatfishes (Le Pape et al., 2003; Martinho et al., 2010; Vasconcelos et al., 2011; Freitas et al., 2012). These species often have complex life cycles, which include migrations between coastal areas and inshore nurseries of up to 100s of kilometers. In this

sense, development of management and protection plans should take into account connectivity between the distinct ontogenetic habitats, as connectivity is directly linked to population dynamics, productivity and resilience to harvest (Cowen et al., 2000; Thorrold et al., 2001; Pihl et al., 2002).

Otolith chemistry has become a benchmark for reconstructing fish movements and migrations (Elsdon et al., 2008; Izzo et al., 2018; Walther, 2019). The use of otoliths as natural tags is feasible because these paired calcium carbonate structures are metabolically inert, grow continuously forming daily and annual patterns, and incorporate trace elements as they grow without evidence of resorption or reworking of the chemical composition (Campana, 1999; Elsdon et al., 2008). The elemental composition of otoliths is generally influenced by the concentration of the elements in the surrounding water, providing a natural tag in which all individuals are marked similarly, even though individual-based physiological and genetic processes take part (Sturrock et al., 2015; Izzo et al., 2018). For reconstructing migration patterns between the sea and the river, Strontium (Sr) and Barium (Ba) are commonly used as their concentrations tend to inversely related in fresh and saltwater (e.g., Walther and Limburg, 2012; Smith and Kwak, 2014). Yet, a suite of other elements, such as magnesium (Mg) or manganese (Mn), also reflect multiple environmental and physiological responses of individual fish to the surrounding ambient water conditions and can aid in environmental reconstructions (Martin and Thorrold, 2005; Tanner et al., 2013a).

Presently, there is still some debate regarding the use of otolith chemistry to discern movements and habitat use within complex and dynamic environments such as estuaries (Elsdon and Gillanders, 2004; Reis-Santos et al., 2018; Williams et al., 2018; Walther, 2019). Several factors may contribute to variations in otolith elemental composition, particularly environmental factors such as water temperature, salinity and ambient element concentrations, which can play an important role in the control of element uptake, as well as several intrinsic factors such as the genetic background, fish diet and physiological processes (Clarke et al., 2011; Woodcock et al., 2012; Sturrock et al., 2014; Grammer et al., 2017; Izzo et al., 2018). In addition, variations in otolith elemental composition also seem to be species-specific (Reis-Santos et al., 2008; Chang and Geffen, 2012).

Water temperature and salinity are known to influence the concentration of elements in the water, whose variation is often inter-dependent. Moreover, the effects of salinity on the elemental ratios in otoliths generally rises with increasing temperature (Elsdon and Gillanders, 2002), although differential results of temperature response among species and elements have been observed (see Miller, 2009; Izzo et al., 2018). Hence, before using otolith chemistry to reconstruct fish life history or habitat use patterns, we need to evaluate the degree to which movements along salinity gradients within estuaries can be determined with accuracy, and unravel the role of temperature on otolith elemental composition (Miller, 2011; Reis-Santos et al., 2013; Tanner et al., 2013a).

Considering that juveniles of many commercially important fishes use estuaries as nursery areas over prolonged periods of their lives (months to years; Gillanders et al., 2003), a better understanding of the ability of otolith chemistry to discern intra-estuarine habitat use patterns can provide key information for species management and habitat conservation. Thus, the objective of this work was to evaluate the effects of salinity and water temperature on otolith chemical composition (Mg:Ca, Mn:Ca, Sr:Ca, Ba:Ca).

In a controlled laboratory experiment, juveniles of the flatfish Senegalese sole *Solea senegalensis* Kaup, 1858 were exposed to combinations of three salinity and two temperature treatments, representative of estuarine environments, to evaluate if otolith chemistry can accurately reflect movement and habitat use within estuarine nursery areas.

MATERIALS AND METHODS

Study Species

The Senegalese sole is a flatfish of high commercial value and widely distributed along the eastern Atlantic from the Bay of Biscay to Senegal, and in the western Mediterranean. Spawning and larval development takes place in shelf waters, with metamorphosis and shift to a benthic life form occurring before recruitment to estuarine nursery grounds, where juveniles remain for up to 2 years (Cabral and Costa, 1999; Primo et al., 2013). Despite key estuarine areas for this species having been identified and population connectivity between estuaries and coastal areas quantified (Vasconcelos et al., 2010; Tanner et al., 2013b), there still is a clear lack of detailed knowledge on juvenile habitat use patterns within estuaries.

Experimental Design

Solea senegalensis juveniles with an average total length (TL) of 9.8 cm (± 1.1 cm standard deviation), approximately 7 months old, were obtained from a hatchery (where they were born) and acclimatized to laboratory conditions over 30 days in 200 L tanks equipped with aeration and filtration, at constant temperature (19°C) and salinity (20; reconstructed with artificial sea salt TMC REEF – Premium REEF Salt) levels. Afterward, all fish (n = 93) were randomly distributed to 18 tanks (20 L) at a density of 6 to 7 individuals per tank to initiate the acclimatization to the test conditions. These tanks were also equipped with aeration and filtration systems and had the same temperature and salinity (19 and 20°C, respectively) to minimize the stress-induced from fish handling and rearing conditions. Over 21 days, water temperature and salinity in the tanks were gradually altered to acclimatize fish to the experimental temperature (16, 21°C) and salinity (5, 18, and 30) combined treatments. Photoperiod was set at 12 h day (dim) and 12 h night (dark) daily cycles. The final experimental design was composed of six test conditions (2 temperatures × 3 salinities) with three replicates each. Salinity and temperature ranges of the experiment represent typical environmental conditions that *S. senegalensis* juveniles experience over spring and summer during their estuarine residency and among intra-estuarine nursery areas (Vinagre et al., 2009; Vasconcelos et al., 2010).

During the experiment, salinity was controlled by adding fresh dechlorinated water with artificial marine salt (TMC

REEF- Premium REEF Salt) to match each test condition (5, 18, and 30). Experiments were run in a room with controlled temperature, which was maintained constant at 21°C, with the low-temperature treatments achieved via an open water bath system connected to a chiller kept stable at 16°C. Approximately 40% of the water in each tank was changed every 3 days. Salinity, water temperature (°C), oxygen (mg/L) and pH were measured daily, whilst ammonia, nitrite and nitrate levels were analyzed weekly throughout the experiment to ensure the best possible water quality.

Fish were maintained under experimental conditions for 98 days and fed daily with specialized food pellets (provided by the hatchery) until apparent satiation, corresponding to 1–2% of their body weight. Fish feed was the same given at the hatchery. Excess food and debris were siphoned within 1 h. All fish were measured for total length (TL, cm) in the beginning and at the end of the experiment, to determine the respective mean growth rate (cm day^{-1}) per treatment.

This study was carried out following the principles of the Basel Declaration and recommendations of Directive 2010/63/EU and Art° 44 of the Decree-Law no. 113/2013 of 7th August. The protocol was approved by the Portuguese National Authority for Animal Health (DGAV; Ref. 0421/000/000/2017).

Water Analyses

On day seven and approximately every 2 weeks from then on, duplicate water samples from each treatment were collected with polypropylene syringes to characterize water elemental concentrations. Over the course of the experiment there were a total of eight water collection times per treatment. Water samples were filtered (GF/F, 0.2 μm) into 60 mL flasks and acidified with concentrated ultrapure nitric acid (HNO_3) in a 1:50 ratio and stored at 4°C until analysis. Prior to elemental quantification by inductively coupled plasma mass spectrometry (ICP-MS), 3 mL of each water sample were further acidified (1:10) by adding 3 mL of a previously distilled 10% nitric acid solution. Water samples were analyzed for ^{24}Mg, ^{43}Ca, ^{55}Mn, ^{88}Sr, and ^{138}Ba using a Thermo Fisher Scientific Model iCAP Q spectrophotometer (Bremen, Germany). The calibration of the ICP-MS measurements was done using a five-point calibration curve per element. Standard solutions were prepared with dilutions of a multi-element standard (92091, Periodic table mix 1 for ICP, Sigma-Aldrich), and a standard curve was generated per element at 0, 1, 10, 100, 1000, and 2000 ppm concentrations. Blank controls consisted of ultrapure water acidified with HNO_3 at 10%. Standards and blanks were analyzed at the beginning and throughout the session. The detection limits were 1.1213, 2.0350, 0.0122, 0.0188 and 0.0380 ppb for ^{24}Mg, ^{43}Ca, ^{55}Mn, ^{88}Sr, and ^{138}Ba, respectively.

Otolith Analyses

After the 98-day experimental procedure, all fish were measured and weighed, and their sagittal otoliths removed, cleaned with distilled water and the left otolith mounted on microscope slides with cyanoacrylate glue. Subsequently, otoliths were polished with 3 μm lapping film under a binocular lens to expose an even surface between the core and the edge of the otolith. Otoliths were then sonicated in ultrapure water until they detached from the microscope slide, and were subsequently dried in a laminar flow cabinet and attached to a new microscope slide using double-sided tape (see Tanner et al., 2013a).

Otolith chemical analysis followed the procedure in Reis-Santos et al. (2018). Briefly, a 213 nm high-performance UV (Nd: YAG) laser microprobe coupled to an Agilent 7900 inductively coupled plasma mass spectrometer (ICP-MS) was used to quantify ^{24}Mg, ^{55}Mn,^{44}Ca, ^{88}Sr, and ^{138}Ba concentrations in otoliths. Ca was used as an internal standard to normalize variations in ablation yield (Yoshinaga et al., 2000). Three spots with a diameter of 25 μm were ablated (power ∼10 J cm^{-2}, and fluence 5 Hz) on the marginal edge of all otoliths. These spot analyses targeted otolith material deposited during the experimental period and represent recent elemental incorporation. All spots were pre-ablated to remove any potential surface contamination. Laser ablations occurred in a sealed chamber with resulting analyte transported to the ICP-MS via a smoothing manifold in an argon (Ar) and helium (He) stream. A glass certified reference material (NIST 612 – National Institute of Standards and Technology) was analyzed at the start and end of each session and after every 10 otoliths to correct for mass bias and machine drift. External precision (% relative standard deviation) was determined based on a calcium carbonate certified reference material, MACS-3 (United States Geological Survey) (RSD $\leq$ 5%). All data reduction, including background corrections, limits of detections and mass count to ppm conversions were done using Iolite software (v 3.1) (Paton et al., 2011).

Data Analyses

Variation in growth rates (cm day^{-1}) per treatment was analyzed with permutational analysis of variance (PERMANOVA), using PRIMER v6 & PERMANOVA + v1 software (PRIMER-E, Ltd.), based on Euclidean distance matrices with unrestricted permutations. Temperature and salinity were treated as fixed categorical factors, and replicate tanks were included as a random factor nested within both fixed factors. Pairwise *post hoc* tests were performed whenever significant differences were found.

Otolith elemental concentration (Me, ppm) values were converted to molar concentrations and standardized to calcium ($Me{:}Ca_{Otolith}$), and all further data analyses were carried out on the $Me{:}Ca_{Otolith}$ data. The same procedure was adopted for the water samples ($Me{:}Ca_{Water}$). The $Me{:}Ca_{Otolith}$ values were calculated per individual, and the three tank averages were used as replicates for each experimental condition. Partition coefficients of an element (D_{Me}) depict otolith chemical concentrations relative to water chemical concentrations, and reflect the fractionation and physiological regulation of element incorporation into biogenic carbonates (Morse and Bender, 1990; Reis-Santos et al., 2013). D_{Me} were calculated for each element dividing the $Me{:}Ca_{Otolith}$ by the $Me{:}Ca_{Water}$. The partition coefficient (D_{Me}) provides an easy and useful metric to compare incorporation of elements in various treatments, since it describes the chemical concentrations of otoliths in relation to the chemical concentration in the water, and is a valuable tool to evaluate

TABLE 1 | Summary of the experimental conditions of salinity and temperature along with water Me:Ca ratios in each treatment, showing mean and standard deviation of water salinity, temperature (°C), and Mg:Ca_{Water} (mol mol^{-1}), Mn:Ca_{Water} (μmol mol^{-1}), Sr:Ca_{Water} (mmol mol^{-1}) and Ba:Ca_{Water} (μmol mol^{-1}) ratios.

Treatment							
Temperature	**Salinity**	**Salinity**	**Temperature**	**Mg:Ca**	**Mn:Ca**	**Sr:Ca**	**Ba:Ca**
16	5	5.047 ± 0.142	15.933 ± 0.096	10.828 ± 1.564	183.276 ± 105.022	15.374 ± 4.366	80.9 11 ± 34.692
	18	18.173 ± 0.322	15.913 ± 0.136	12.315 ± 1.234	41.546 ± 48.758	14.631 ± 4.262	36.062 ± 25.649
	30	30.041 ± 0.204	16.052 ± 0.133	12.594 ± 1.085	49.284 ± 51.206	13.377 ± 3.514	22.877 ± 13.914
21	5	5.017 ± 0.157	21.359 ± 0.804	10.284 ± 0.450	166.882 ± 189.070	14.218 ± 3.514	113.939 ± 41.147
	18	18.247 ± 0.312	20.990 ± 0.900	12.045 ± 0.409	51.228 ± 68.776	13.551 ± 3.050	33.783 ± 11.382
	30	30.056 ± 0.292	21.449 ± 0.950	12.407 ± 0.666	25.148 ± 23.793	12.536 ± 2.324	21.463 ± 6.723

Total number of water collections throughout the experimental 98 day period = 8.

TABLE 2 | Results of the permutational analysis of variance (PERMANOVA) investigating the effects of salinity and temperature on the Mg:Ca_{Water}, Mn:Ca_{Water}, Sr:Ca_{Water}, and Ba:Ca_{Water} of the rearing conditions.

		Mg:Ca		Mn:Ca		Sr:Ca		Ba:Ca	
Source of variation	**df**	**MS**	**Pseudo-F**	**MS**	**Pseudo-F**	**MS**	**Pseudo-F**	**MS**	**Pseudo-F**
Water									
Temperature	1	0.013	2.105	2.064	1.791	0.081	1.604	0.767	3.275
Salinity	2	0.240	37.922**	25.300	21.950**	0.112	2.212	12.801	54.638**
Temperature x Salinity	2	0.002	0.300	0.524	0.454	0.001	0.012	0.100	0.426
Residual	78	0.006		1.153		0.051		0.234	

$^{**}p < 0.01$.

abiotic and biotic effects on otolith elemental incorporation and to perform comparisons between species and studies.

Differences among treatments in Me:Ca_{Water}, Me:$Ca_{Otolith}$ and D_{Me} were analyzed separately with permutational analysis of variance (PERMANOVA), using PRIMER v6 & PERMANOVA + v1 software (PRIMER-E, Ltd.), based on Euclidean distance matrices with unrestricted permutations of log(x + 1) transformed data. Salinity and temperature were treated as fixed factors, and replicate tanks as random factors nested within both fixed factors (only for Me:$Ca_{Otolith}$ and D_{Me}). Pearson correlation analyses were used to determine the relationship between the elemental ratio in the rearing water and the elemental ratio in the juvenile *S. senegalensis* otoliths. A significance level of 0.05 was considered for all test procedures.

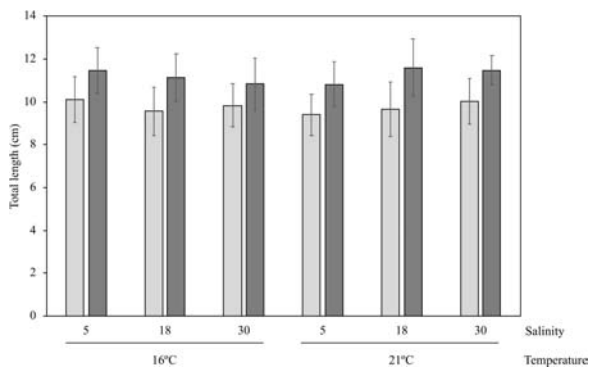

FIGURE 1 | Average total length of juvenile *Solea senegalensis* at the beginning (light gray) and at the end (dark gray) of the experimental procedure for all treatments.

RESULTS

Experimental Conditions

Temperature and salinity reflected the required experimental levels and were kept stable throughout the experiment (**Table 1**). Elemental ratios in the water were within the range found in a temperate estuary in Portugal (Tejo; see Tanner et al., 2013a) and were influenced by the different salinity treatments, but not by temperature. Specifically, Mg:Ca_{Water} decreased with increasing salinity, being significantly higher at salinity five treatments than at 18 and 30, but with no distinction between the two latter ($P_{(perm)}$ = 0.001 and $P_{(perm)}$ = 0.001, respectively). Mn:Ca_{Water} increased with salinity, being significantly lower at salinity five than at the 18 and 30 treatments, also which did not vary from one another ($P_{(perm)}$ = 0.001 and $P_{(perm)}$ = 0.001, respectively). Sr:Ca_{Water} was constant among all salinity and temperature treatments, while Ba:Ca_{Water} decreased with increasing salinity, with significant differences among all treatments ($P_{(perm)}$ = 0.001, $P_{(perm)}$ = 0.001, and $P_{(perm)}$ = 0.007, respectively) (**Tables 1**, **2**).

Juvenile *S. senegalensis* increased in total length in all treatments during the 98-day experimental procedure: initial average TL 9.8 ± 1.1 cm; final average TL 11.2 ± 1.1 cm (**Figure 1**). There were no differences in growth rates among treatments, with only a significant tank effect (**Table 3**), which was most probably due to a single tank with lower growth rates (one of the three replicates of the 21°C, 30 salinity treatment).

TABLE 3 | Results of the permutational analysis of variance (PERMANOVA) investigating the effects of salinity and temperature on the growth rates of juvenile *Solea senegalensis*.

Source of variation	df	MS	Pseudo-F
Growth rates			
Temperature	1	2.4×10^{-4}	1.205
Salinity	2	1.9×10^{-4}	0.972
Temperature x Salinity	2	3.5×10^{-8}	1.8×10^{-4}
Tank (Temperature x Salinity)	12	2.1×10^{-4}	6.989**
Residual	75	3.0×10^{-5}	

**$p < 0.01$.

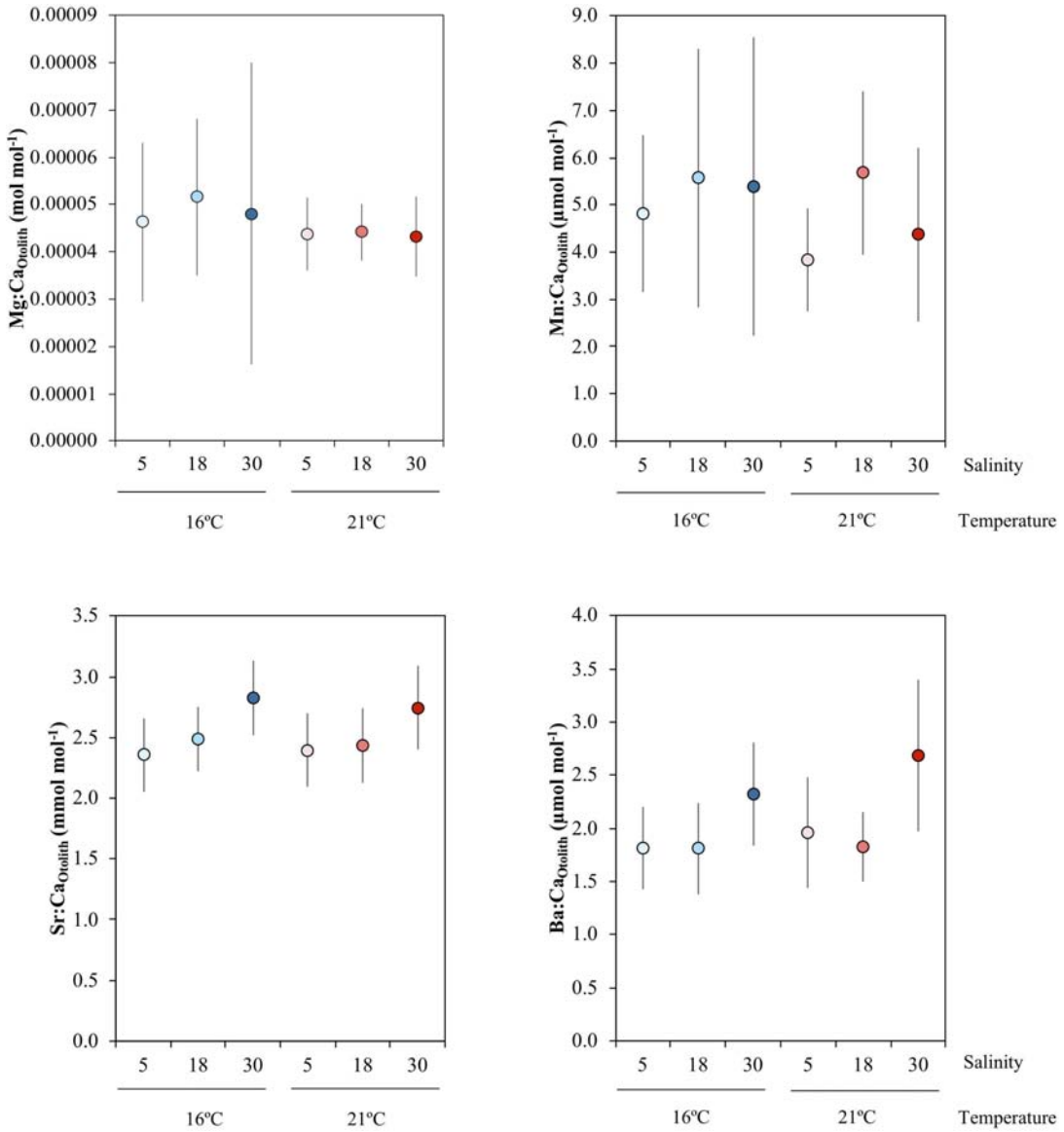

FIGURE 2 | Mean and standard error of Mg:Ca$_{Otolith}$, Mn:Ca$_{Otolith}$, Sr:Ca$_{Otolith}$, and Ba:Ca$_{Otolith}$ across the salinity (5, 18, 30) and temperature (16 and 21°C) experimental treatments, which are indicated by the different colors: blue colors – 16°C, red colors – 21°C; light tone – 5 salinity, medium tone – 18 salinity, dark tone – 30 salinity.

TABLE 4 | Results of the permutational analysis of variance (PERMANOVA) investigating the effects of salinity and temperature on log transformed $Mg:Ca_{Otolith}$, $Mn:Ca_{Otolith}$, $Sr:Ca_{Otolith}$ and $Ba:Ca_{Otolith}$ of juvenile *Solea senegalensis* otoliths.

		Mg:Ca		Mn:Ca		Sr:Ca		Ba:Ca	
Source of variation	**df**	**MS**	**Pseudo-F**	**MS**	**Pseudo-F**	**MS**	**Pseudo-F**	**MS**	**Pseudo-F**
Otolith									
Temperature	1	0.013	0.493	0.024	0.348	0.002	0.127	0.064	2.297
Salinity	2	0.085	3.132	0.261	3.711	0.176	10.193**	0.415	14.891**
Temperature x Salinity	2	0.058	2.137	0.088	1.244	0.001	0.086	0.018	0.630
Tank (Temperature x Salinity)	12	0.027	1.092	0.071	1.209	0.017	1.230	0.028	0.925
Residual	75	0.025		0.059		0.014		0.030	

**$p < 0.01$.

Effect of Salinity and Temperature on Otolith Chemistry

Otolith elemental concentrations varied according to the different salinity treatments, but not with temperature (**Figure 2** and **Table 4**). No effects of temperature, salinity or their interaction were observed for $Mn:Ca_{Otolith}$ and $Mg:Ca_{Otolith}$. In contrast, a significant effect of salinity was observed for $Sr:Ca_{Otolith}$, where pairwise comparisons found that $Sr:Ca_{Otolith}$ in the highest (30) salinities were higher than in the medium (18) and lowest salinities (5) ($P_{(perm)} = 0.004$ and $P_{(perm)} = 0.016$, respectively). No significant differences were observed between the low (5) and medium (18) salinity treatments. A similar result was obtained for $Ba:Ca_{Otolith}$, which increased with salinity (**Figure 2** and **Table 4**). *Post hoc* pairwise tests found significant differences between salinities 5 and 30, as well as between 18 and 30 ($P_{(perm)} = 0.006$ and $P_{(perm)} = 0.005$, respectively) (**Figure 2** and **Table 4**).

The partition coefficients for magnesium (D_{Mg}) were extremely low, ranging between $3.48 \times 10^{-6} \pm 6.89 \times 10^{-7}$ and $4.28 \times 10^{-6} \pm 1.56 \times 10^{-6}$, with no differences among treatments. For manganese, D_{Mn} values ranged between 0.02 ± 0.01 and 0.17 ± 0.07. An effect of salinity was observed for D_{Mn}, with *post hoc* pairwise tests identifying a significant increase between salinities 5 and 18, as well as between 5 and 30 ($P_{(perm)} = 0.001$ and $P_{(perm)} = 0.002$, respectively). For strontium, D_{Sr} ranged between 0.15 ± 0.02 and 0.22 ± 0.03 and with a significant positive effect of salinity between 5 and 30, and between 18 and 30 ($P_{(perm)} = 0.001$ and $P_{(perm)} = 0.002$, respectively). For barium, D_{Ba} ranged between 0.02 ± 0.01 and 0.13 ± 0.03, and showed a significant increase between salinities 5 and 18, as well as between 5 and 30 ($P_{(perm)} = 0.007$ and $P_{(perm)} = 0.001$, respectively) (**Figure 3** and **Table 5**).

There were no significant relationships between water and otolith elemental concentrations for all elements ($p > 0.1$) (**Figure 4**).

DISCUSSION

Resolving estuarine habitat use with otolith chemistry can provide key knowledge on species habitat use, movements and connectivity particularly for species that use estuaries as nursery grounds. Such knowledge can represent important information for protection and management programs. The main finding of our work was related to the ability to use otolith Sr:Ca and Ba:Ca of juvenile Senegalese sole *S. senegalensis* to distinguish between the tested low and high salinity environments, irrespective of the tested temperature regimes. Yet, we were not able to successfully discern the intermediate salinity tested. Therefore, whilst our results support the use of otolith chemistry to disentangle brackish waters, namely oligohaline (salinity $\pm$ 5) from polyhaline waters (salinity $\pm$ 30), there were limitations differentiating mesohaline waters (salinity $\pm$ 18).

We observed no clear temperature effect on Mg, Mn, Sr, and Ba elemental concentration in juvenile *S. senegalensis* otoliths, which follows findings from other fish species (e.g., Gallahar and Kingsford, 1996; Elsdon and Gillanders, 2004; Martin et al., 2004; Martin and Thorrold, 2005; Mazloumi et al., 2017). Despite the 5°C difference in treatments, the experimental temperatures chosen (16 and 21°C) are within the range this species typically experience in temperate estuaries and coastal zones, which may explain the little effect on the elemental assimilation rates in the otolith matrix. Nonetheless, it is important to bear in mind that the relationship between otolith chemistry and temperature varies among species, families and life history traits (Collingsworth et al., 2010; Mazloumi et al., 2017). Overall, the high degree of inter-specific variability in the isolated and interactive effects of temperature and salinity on element uptake into otoliths hinders the development of universal models based on otolith chemistry to understand life history patterns (Stanley et al., 2015).

We also found no significant differences between salinity and temperature treatments for both $Mg:Ca_{Otolith}$ and $Mn:Ca_{Otolith}$ in juvenile Senegalese sole, in agreement with other laboratory experiments (Elsdon and Gillanders, 2002; Martin and Wuenschel, 2006; DiMaria et al., 2010). For magnesium, the lack of correlation between the chemical composition of otoliths and water likely indicates that this element is under significant physiological control (Woodcock et al., 2012; Grammer et al., 2017), and supported by the fact Mg is very abundant in the marine environment and required in many metabolic pathways, regulating cell function, bone development and growth. According to Elsdon and Gillanders (2003b), manganese is key to multiple metabolic processes, yet it can become toxic at high levels, and thus it is highly regulated within the organism. In addition, the presence of Mn is also

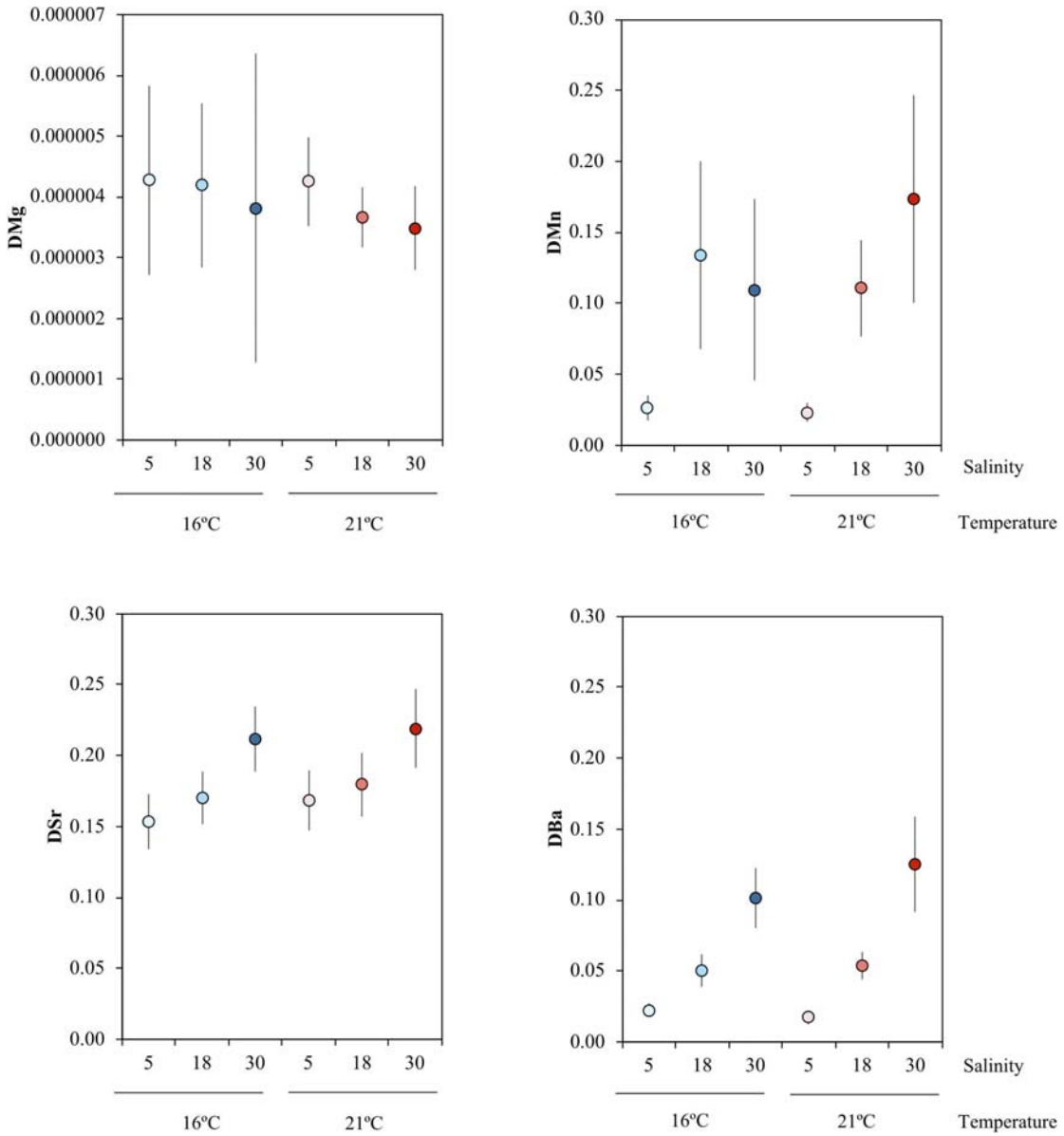

FIGURE 3 | Mean and standard error of partition coefficients of magnesium (D_{Mg}), manganese (D_{Mn}), strontium (D_{Sr}) and barium (D_{Ba}), across the salinity (5, 18, 30) and temperature (16 and 21°C) experimental treatments, which are indicated by the different colors: blue colors – 16°C, red colors – 21°C; light tone – 5 salinity, medium tone – 18 salinity, dark tone – 30 salinity.

essential for the biomineralization process in otoliths (Thomas et al., 2018). The use of Mn:$Ca_{Ototlith}$ as a marker to understand life history patterns has not yet been thoroughly validated, given the likely confounding effects of diet composition, temperature variations, physiology and growth (Pentreath, 1976; Miller, 2009; Sturrock et al., 2015). Our results were not able to disentangle the effects of salinity and temperature on Mn:$Ca_{Ototlith}$, which is indicative of physiological regulation. Overall, although still poorly understood, the incorporation of Mn into otoliths is presumed to be essentially under metabolic control, rather than determined by environmental factors (Tanner et al., 2012; Limburg et al., 2015; Sturrock et al., 2015). While there were no differences in the elemental composition of Mg:$Ca_{O\,tolith}$ and Mn:$Ca_{O\,tolith}$, there was a significant effect of salinity on the incorporation of manganese (D_{Mn}), which mainly reflected the different environmental levels in the rearing water and further highlights the role of physiology in regulating otolith Mn. Earlier works have suggested that Mn:$Ca_{Ototlith}$ has potential as an environmental marker of exposure to hypoxia (Mohan et al., 2014; Limburg et al., 2015). Further explored, this facet of Mn and otolith chemistry may provide useful information on fish populations in estuaries, since hypoxic events are increasing in

TABLE 5 | Results of the permutational analysis of variance (PERMANOVA) investigating the effects of salinity and temperature on the partition coefficients of magnesium (D_{Mg}), manganese (D_{Mn}), strontium (D_{Sr}) and barium (D_{Ba}).

		D_{Mg}		D_{Mn}		D_{Sr}		D_{Ba}	
Source of variation	**df**	**MS**	**Pseudo-F**	**MS**	**Pseudo-F**	**MS**	**Pseudo-F**	**MS**	**Pseudo-F**
DMe									
Temperature	1	0.012	0.002	0.978	1.308	0.038	0.055	0.005	0.004
Salinity	2	9.056	1.201	28.137	37.520**	2.879	4.179**	17.346	13.864**
Temperature x Salinity	2	2.672	0.354	1.066	1.421	3.367	4.887**	0.961	0.768
Tank (Temperature x Salinity)	12	7.657	1.486	0.766	1.831	0.686	0.906	1.264	1.274
Residual	75	5.152		0.419		0.756		0.992	

**$p < 0.01$.

time and space throughout the world, particularly during the warm season (Breitburg et al., 2018; Schmidt et al., 2019).

The use of Sr as a recorder of past salinity history is based on the premise that it replaces Ca in otolith aragonite as fish grow, and especially that there is generally more Sr in seawater than in freshwater (Campana, 1999; Elsdon et al., 2008; Doubleday et al., 2014). In this work, we found a positive influence of salinity on $Sr:Ca_{Otolith}$, as it was higher in the treatment close to marine water (30) when compared with the brackish treatment (18) and the one close to freshwater (5). Our results generally agree with experimental studies on other fish species based on salinity and temperature manipulations (Martin and Wuenschel, 2006; Stanley et al., 2015), but also contrast with others, in which a negative relationship with salinity was reported (Elsdon and Gillanders, 2002; Mazloumi et al., 2017). Considering that most elemental uptake into otoliths is usually acknowledged as species-specific (Swearer et al., 2003; Reis-Santos et al., 2008; Chang and Geffen, 2012), our results also support the use of Sr as a marker for reconstructing past habitat use, preferably between high and low salinities. However, $Sr:Ca_{Otolith}$ could not resolve the lower and brackish salinities. This limits its application to discern intra-estuarine habitat use in marine juvenile fishes, particularly if they spend a significant amount of time at mid and upper areas of estuaries, which is the case for the Senegalese sole (Vinagre et al., 2009; Primo et al., 2013). One possible reason is that Sr can be highly variable in estuaries due to tidal mixing with freshwater discharge, suggesting that the increase in Sr:Ca with salinity in these waters might not follow a linear trend (Phillis et al., 2011; Walther and Nims, 2014). Indeed, key to discerning habitat use by marine fish in transitional ecosystems is the elemental mixing kinetics (Walther, 2019), which depend greatly on the hydrodynamics and endmember contributions of each system. The temporal lag between exposure to a water mass (either freshwater, brackish or marine) and the incorporation in otoliths is also an important feature for the correct use of otolith chemistry for tracking fish movements (Elsdon and Gillanders, 2005c; Izzo et al., 2018).

Similarly to $Sr:Ca_{Otolith}$, $Ba:Ca_{Otolith}$ also increased with salinity, with higher values in the marine-like treatment (30) than in the near freshwater (5) and brackish (18) experimental conditions. Barium has been used typically in combination with Sr to unravel environmental and migratory histories (Bath et al., 2000; Elsdon and Gillanders, 2002; de Vries et al., 2005; Reis-Santos et al., 2013), given the natural inverse concentration of Sr and Ba in riverine and marine waters (Turner et al., 1981; Coffey et al., 1997; Elsdon and Gillanders, 2005a). Nevertheless, akin to Sr levels, our results for Ba revealed a potential shortcoming due to the inability to resolve near freshwater and brackish environments. Accordingly, $Sr:Ca_{Otolith}$ and $Ba:Ca_{Otolith}$ in juvenile *S. senegalensis* can only be used to accurately resolve between low and high salinity environments, without the possibility to resolve habitat use patterns at finer spatial scales.

The incorporation of Sr and Ba, given by their partition coefficients (D_{Me}), was positively influenced by salinity, and was a good metric for comparing the relation between elemental concentrations in the otoliths and in the water (as in Miller, 2009), even if there were no significant differences in $Sr:Ca_{Water}$ between treatments. Although the element concentrations in the otoliths were one (Sr) and two (Ba) orders of magnitude lower than the experimental medium, they still reflected the existing variations in salinity, and were within the range reported for other fish species (Elsdon and Gillanders, 2003a; Reis-Santos et al., 2012, 2013). An increase in $Sr:Ca_{Otolith}$ and D_{Sr} with salinity suggests that the incorporation of Sr may be facilitated by higher salinity, as there were no differences in $Sr:Ca_{Water}$ of the rearing treatments. On the other hand, a decrease in $Ba:Ca_{Water}$ with increasing salinity resulted in higher elemental incorporation in otoliths and an increase in the D_{Ba}, which has been suggested to occur at higher Sr:Ca levels in brackish waters, suggesting facilitation of Ba uptake (de Vries et al., 2005). In elements with high physiological regulation such as Mg and Mn, the use of partition coefficients may be misleading as a series of complex but still poorly understood mechanisms influence the chemical incorporation through multiple osmoregulatory barriers between the environment and the endolymph. The use of partition coefficients (D_{Me}) whilst of great applicability in experimental studies, may have some limitations for *in situ* evaluations, particular in such dynamic and complex environments as estuaries, since sudden changes in salinity and/or temperature may not be reflected in the incorporation of elements, thus being more useful for prolonged exposures.

In this work, we did not find a significant correlation between element concentration in the otolith ($Me:Ca_{Otolith}$) and the

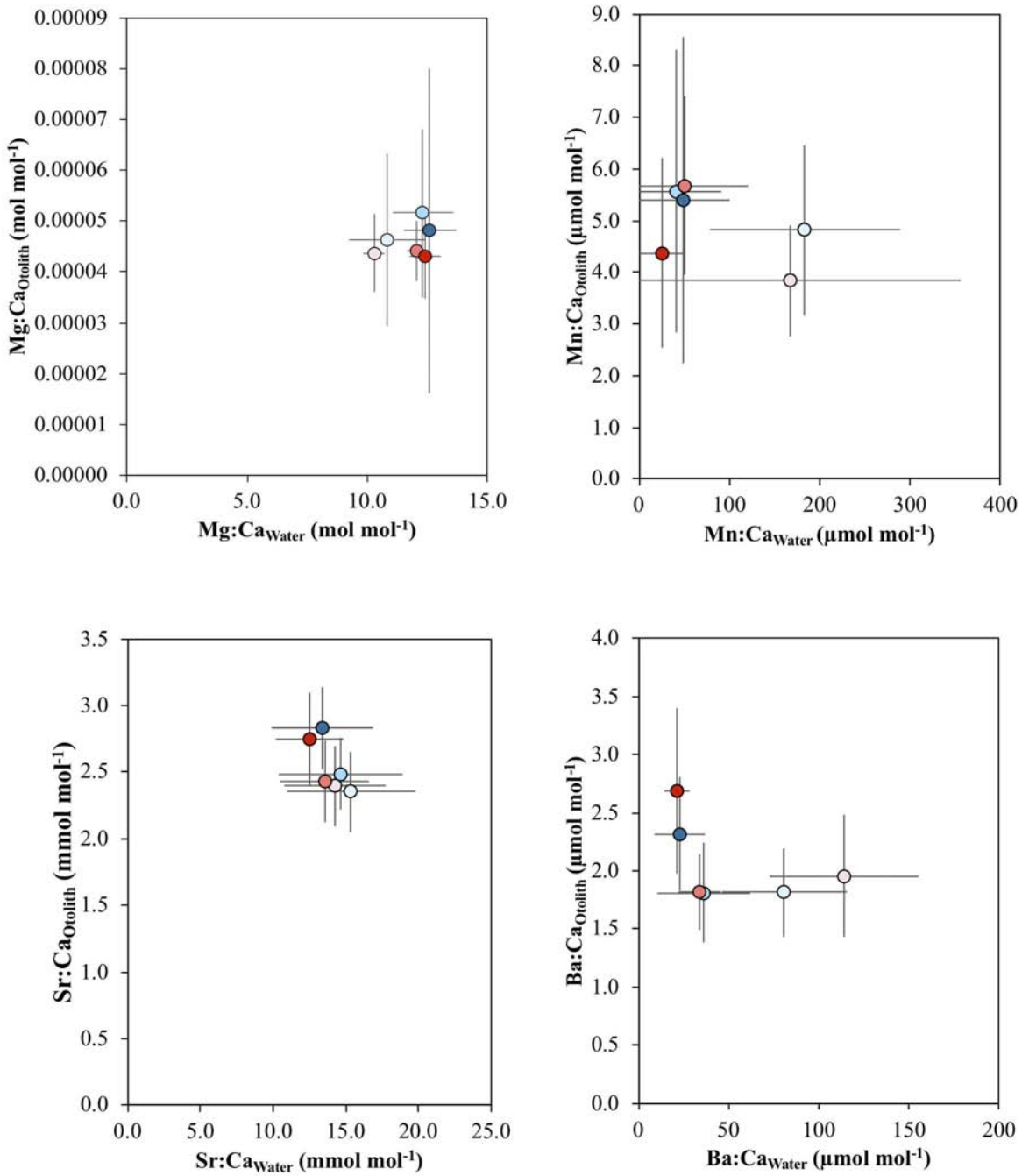

FIGURE 4 | Mean and standard error of the relationship between Mg:Ca$_{Otolith}$ and Mg:Ca$_{Water}$, Mn:Ca$_{Otolith}$ and Mn:Ca$_{Water}$, Sr:Ca$_{Otolith}$ and Sr:Ca$_{Water}$, and Ba:Ca$_{Otolith}$ and Ba:Ca$_{Water}$ across the salinity (5, 18, 30) and temperature (16 and 21°C) experimental treatments, which are indicated by the different colors: blue colors – 16°C, red colors – 21°C; light tone – 5 salinity, medium tone – 18 salinity, dark tone – 30 salinity.

water (Me:Ca$_{Water}$) for any of the considered elements. The complex nature of the relationship between Me:Ca$_{Otolith}$ and Me:Ca$_{Water}$ is emphasized by the disparity in results from previous studies mostly on Sr:Ca, Ba:Ca and water chemistry, which described linear (Martin and Wuenschel, 2006; Macdonald and Crook, 2010), exponential (Dorval et al., 2007) and even no relationships (Elsdon and Gillanders, 2005b; Mazloumi et al., 2017) as in the present study, and can be related with the different mode of element uptake by each species. Element uptake is a multi-stage process, characterized by a succession of barriers with varying degrees of inter-dependence from the ambient water to blood plasma through gills, endolymph and finally into the otolith (Campana, 1999). To our knowledge, few experimental procedures on otolith chemistry have been

performed with flatfishes (e.g., Sturrock et al., 2014), whose particular ecological characteristics (life history, metamorphosis, physiology) might drive some of the differences observed in terms of $Me:Ca_{Otolith}$ and $Me:Ca_{Water}$ relationships. In addition, the lack of discrimination between water and otolith composition may also be due to the use of a reduced range of temperatures (Elsdon and Gillanders, 2002) and/or elemental concentrations in water (Elsdon and Gillanders, 2003a).

Despite the limitations described above, this study is a stepping-stone for the interpretation of otolith chemical profiles and for the reconstruction of estuarine habitat use. Very few studies have focused on flatfishes, whose specific ecological features might be responsible for the distinct patterns observed, and several questions arose that foster further research to improve our ability to reconstruct past estuarine habitat use by fishes. Among others, these include experimental work based on a wider range of temperatures covering the range of wintering conditions, as well as establishing a parallel with field conditions, since the complex dynamics and interactions between the chemical elements in the environment might lead to discrepancies with laboratory results (Elsdon and Gillanders, 2005b; Dorval et al., 2007; Tanner et al., 2013a; Williams et al., 2018). Additional research should address element mixing dynamics between heterogenous water masses, as well as the kinetics of element incorporation, ion transport and internal regulation in fish, with the ultimate goal of elucidating the suitability of the selected elements as environmental tracers. Indeed, the suite of factors that govern otolith elemental composition from that found in the environment are complex and, in most cases, poorly understood (Izzo et al., 2018; Reis-Santos et al., 2018; Walther, 2019). Apart from salinity, temperature and ambient elemental concentration, other examples of biological factors play a role in determining the elemental concentrations in the otolith, such as genetic profiles, size, sex or age (Barnes and Gillanders, 2013; Izzo et al., 2018; Reis-Santos et al., 2018; Walther, 2019). These are factors that should be considered early in the experimental design to control for their confounding effects. Accordingly, all fish in our experiment were obtained from the same hatchery, brood stock, age and size range to minimize potential ontogenic and genetic effects, while a commercial feed designed for the selected size range was provided to avoid any potential bias related to dietary variations. The absence of significant differences in growth rates between treatments also contributed to mitigating any other effects related to individual responses to the test conditions. Further studies using prey from the field should be performed to disentangle the possible effects of diet composition on the otolith chemistry of fishes in estuaries.

CONCLUSION

The measured elemental composition of otoliths of *S. senegalensis* were linked to the tested environmental factors. In particular, Sr and Ba were suitable elements for the reconstruction of juvenile *S. senegalensis* movements along natural salinity gradients, but with limited resolving power for finer scale variations, namely between oligo- and mesohaline, and meso- and polyhaline waters. Ultimately, further work should focus on combining laboratory experiments with species-specific information on the elemental incorporation of otoliths and field trials, to better improve our knowledge of the processes involved under natural conditions, as well as the timeframe between element uptake and otolith assimilation.

DATA AVAILABILITY STATEMENT

The datasets generated for this study are available on request to the corresponding author.

ETHICS STATEMENT

The animal study was reviewed and approved by Portuguese National Authority for Animal Health (DGAV; Ref. 0421/000/000/2017).

AUTHOR CONTRIBUTIONS

ST, RV, VF, PR-S, and FM designed the experiment and approach. BP, MN, AV, DC, AP, MP, and FM executed the experiment and laboratory work. PR-S and BG executed the otolith chemical analyses. BP and FM analyzed the data and wrote the manuscript. All authors commented on and approved the final version of the manuscript.

FUNDING

This research was supported by the Portuguese Foundation for Science and Technology (FCT, I.P.) via a post-doctoral grant to PR-S (SFRH/BPD/95784/2013), a Ph.D. grant to AV (SFRH/BD/137862/2018), and researcher contracts to ST (DL57/2016/CP1479/CT0022), VF (DL57/2016/CP1479/CT0024), FM, and AP, in the scope of the framework contract foreseen in the numbers 4, 5, and 6 of the article 23, of the Decree-Law 57/2016, of August 29, changed by Law 57/2017, of July 19. FCT, I.P. also provided support through the research project "Mytag – Integrating natural and artificial tags to reconstruct fish migrations and ontogenetic niche shifts" (PTDC/MAR-EST/2098/2014), under the Project 9471 – Reforçar a Investigação, o Desenvolvimento Tecnológico e a Inovação (Projeto 9471-RIDTI) and subsidized by the European Regional Development Fund (FEDER, POCI-01-0145-FEDER-016787), the Centre for Functional Ecology Strategic Project (UID/BIA/04004/2019) within the PT2020 Partnership Agreement and COMPETE 2020, and the Marine and Environmental Sciences Centre Strategic Project (UID/MAR/04292/2019). Financial support was also provided by FEDER through the project ReNATURE – Valorization of the Natural Endogenous Resources of the Centro Region (Centro 2020, Centro-01-765-0145-FEDER-000007).

ACKNOWLEDGMENTS

We are grateful to Ana Varela and João Rito for their help during the experimental setup and laboratory work. We also thank Sarah Gilbert for her assistance and acknowledge Adelaide Microscopy, The University of Adelaide and the Australian Microscopy and Microanalysis Research Facility (AMMRF) for use of equipment.

REFERENCES

Barnes, T. C., and Gillanders, B. M. (2013). Combined effects of extrinsic and intrinsic factors on otolith chemistry: implications for environmental reconstructions Ed K. Rose. *Can. J. Fish. Aquat. Sci.* 70, 1159–1166. doi: 10.1139/cjfas-2012-0442

Bath, G. E., Thorrold, S. R., Jones, C. M., Campana, S. E., McLaren, J. W., and Lam, J. W. H. (2000). Strontium and barium uptake in aragonitic otoliths of marine fish. *Geochim. Cosmochim. Acta* 64, 1705–1714. doi: 10.1016/S0016-7037(99)00419-6

Beck, M., Heck, K., Able, K., Childers, D., Eggleston, D., Gillanders, B. M., et al. (2001). The identification, conservation, and management of estuarine and marine nurseries for fish and invertebrates. *Bioscience* 51, 633–641.

Breitburg, D., Levin, L. A., Oschlies, A., Grégoire, M., Chavez, F. P., Conley, D. J., et al. (2018). Declining oxygen in the global ocean and coastal waters. *Science* 359:eaam7240. doi: 10.1126/science.aam7240

Cabral, H. N., and Costa, M. J. (1999). Differential use of nursery areas within the Tagus estuary by sympatric soles, *Solea solea* and *Solea senegalensis*. *Environ. Biol. Fish.* 56, 389–397.

Campana, S. E. (1999). Chemistry and composition of fish otoliths: pathways, mechanisms and applications. *Mar. Ecol. Progr. Ser.* 188, 263–297.

Chang, M.-Y., and Geffen, A. J. (2012). Taxonomic and geographic influences on fish otolith microchemistry. *Fish Fish.* 14, 458–492. doi: 10.1111/j.1467-2979.2012.00482.x

Clarke, L. M., Thorrold, S. R., and Conover, D. O. (2011). Population differences in otolith chemistry have a genetic basis in *Menidia menidia*. *Can. J. Fish. Aquat. Sci.* 68, 105–114. doi: 10.1139/F10-147

Coffey, M., Dehairs, F., Collette, O., Luther, G., Church, T., and Jickells, T. (1997). The behaviour of dissolved barium in estuaries. *Estuar. Coast. Shelf Sci.* 45, 113–121. doi: 10.1006/ecss.1996.0157

Collingsworth, P. D., Van Tassell, J. J., Olesik, J. W., and Marschall, E. A. (2010). Effects of temperature and elemental concentration on the chemical composition of juvenile yellow perch (*Perca flavescens*) otoliths. *Can. J. Fish. Aquat. Sci.* 67, 1187–1196. doi: 10.1139/F10-050

Cowen, R. K., Lwiza, K. M. M., Sponaugle, S., Paris, C. B., and Olson, D. B. (2000). Connectivity of marine populations: open or closed? *Science* 287, 857–859. doi: 10.1126/science.287.5454.857

de Vries, M. C., Gillanders, B. M., and Elsdon, T. S. (2005). Facilitation of barium uptake into fish otoliths: influence of strontium concentration and salinity. *Geochim. Cosmochim. Acta* 69, 4061–4072. doi: 10.1016/j.gca.2005.03.052

DiMaria, R. A., Miller, J. A., and Hurst, T. P. (2010). Temperature and growth effects on otolith elemental chemistry of larval Pacific cod, *Gadus macrocephalus*. *Environ. Biol. Fish.* 89, 453–462. doi: 10.1007/s10641-010-9665-2

Dorval, E., Jones, C. M., Hannigan, R., and Montfrans, J. V. (2007). Relating otolith chemistry to surface water chemistry in a coastal plain estuary. *Can. J. Fish. Aquat. Sci.* 64, 411–424. doi: 10.1139/f07-015

Doubleday, Z. A., Harris, H. H., Izzo, C., and Gillanders, B. M. (2014). Strontium randomly substituting for calcium in fish otolith aragonite. *Analyt. Chem.* 86, 865–869. doi: 10.1021/ac4034278

Elsdon, T. S., and Gillanders, B. M. (2002). Interactive effects of temperature and salinity on otolith chemistry: challenges for determining environmental histories of fish. *Can. J. Fish. Aquat. Sci.* 59, 1796–1808. doi: 10.1139/f02-154

Elsdon, T. S., and Gillanders, B. M. (2003a). Reconstructing migratory patterns of fish based on environmental influences on otolith chemistry. *Rev. Fish Biol. Fish.* 13, 217–235.

Elsdon, T. S., and Gillanders, B. M. (2003b). Relationship between water and otolith elemental concentrations in juvenile black bream *Acanthopagrus butcheri*. *Mar. Ecol. Prog. Ser.* 260, 263–272. doi: 10.3354/meps260263

Elsdon, T. S., and Gillanders, B. M. (2004). Fish otolith chemistry influenced by exposure to multiple environmental variables. *J. Exp. Mar. Biol. Ecol.* 313, 269–284. doi: 10.1016/j.jembe.2004.08.010

Elsdon, T. S., and Gillanders, B. M. (2005a). Alternative life-history patterns of estuarine fish: barium in otoliths elucidates freshwater residency. *Can. J. Fish. Aquat. Sci.* 62, 1143–1152. doi: 10.1139/f05-029

Elsdon, T. S., and Gillanders, B. M. (2005b). Consistency of patterns between laboratory experiments and field collected fish in otolith chemistry: an example and applications for salinity reconstructions. *Mar. Freshw. Res.* 56:609. doi: 10.1071/MF04146

Elsdon, T. S., and Gillanders, B. M. (2005c). Strontium incorporation into calcified structures: separating the effects of ambient water concentration and exposure time. *Mar. Ecol. Prog. Ser.* 285, 233–243. doi: 10.3354/meps285233

Elsdon, T. S., Wells, B. K., Campana, S. E., Gillanders, B. M., Jones, C. M., Limburg, K. E., et al. (2008). Otolith chemistry to describe movements and life-history parameters of fishes: hypotheses, assumptions, limitations and inferences. *Oceanogr. Mar. Biol. Annu. Rev.* 46, 297–330.

Freitas, V., Kooijman, S., and van der Veer, H. W. (2012). Latitudinal trends in habitat quality of shallow-water flatfish nurseries. *Mar. Ecol. Prog. Ser.* 471, 203–214. doi: 10.3354/meps10025

Gallahar, N. K., and Kingsford, M. J. (1996). Factors influencing Sr/Ca ratios in otoliths of *Girella elevata*: an experimental investigation. *J. Fish Biol.* 48, 174–186. doi: 10.1111/j.1095-8649.1996.tb01111.x

Gillanders, B. M., Able, K., Brown, J. A., Eggleston, D., and Sheridan, P. (2003). Evidence of connectivity between juvenile and adult habitats for mobile marine fauna: an important component of nurseries. *Mar. Ecol. Prog. Ser.* 247, 281–295.

Grammer, G. L., Morrongiello, J. R., Izzo, C., Hawthorne, P. J., Middleton, J. F., and Gillanders, B. M. (2017). Coupling biogeochemical tracers with fish growth reveals physiological and environmental controls on otolith chemistry. *Ecolo. Monogr.* 87, 487–507. doi: 10.1002/ecm.1264

Izzo, C., Reis-Santos, P., and Gillanders, B. M. (2018). Otolith chemistry does not just reflect environmental conditions: a meta-analytic evaluation. *Fish Fish.* 1:291. doi: 10.1016/j.gca.2012.07.003

Le Pape, O., Holley, J., Guerault, D., and Desaunay, Y. (2003). Quality of coastal and estuarine essential fish habitats: estimations based on the size of juvenile common sole (*Solea solea* L.). *Estuar. Coast. Shelf Sci.* 58, 793–803. doi: 10.1016/S0272-7714(03)00185-9

Limburg, K. E., Walther, B. D., Lu, Z., Jackman, G., Mohan, J., Walther, Y., et al. (2015). In search of the dead zone: use of otoliths for tracking fish exposure to hypoxia. *J. Mar. Syst.* 141, 167–178. doi: 10.1016/j.jmarsys.2014.02.014

Macdonald, J. I., and Crook, D. A. (2010). Variability in Sr:Ca and Ba:Ca ratios in water and fish otoliths across an estuarine salinity gradient. *Mar. Ecol. Prog. Ser.* 413, 147–161. doi: 10.3354/meps08703

Martin, G. B., and Thorrold, S. R. (2005). Temperature and salinity effects on magnesium, manganese, and barium incorporation in otoliths of larval and early juvenile spot *Leiostomus xanthurus*. *Mar. Ecol. Prog. Ser.* 293, 223–232. doi: 10.3354/meps293223

Martin, G. B., Thorrold, S. R., and Jones, C. M. (2004). Temperature and salinity effects on strontium incorporation in otoliths of larval spot (*Leiostomus xanthurus*). *Can. J. Fish. Aquat. Sci.* 61, 34–42. doi: 10.1139/f03-143

Martin, G. B., and Wuenschel, M. J. (2006). Effect of temperature and salinity on otolith element incorporation in juvenile gray snapper *Lutjanus griseus*. *Mar. Ecol. Prog. Ser.* 324, 229–239. doi: 10.3354/meps324229

Martinho, F., Dolbeth, M., Viegas, I., Baptista, J., Cabral, H. N., and Pardal, M. A. (2010). Does the flatfish community of the Mondego estuary (Portugal) reflect environmental changes? *J. Appl. Ichthyol.* 26, 843–852. doi: 10.1111/j.1439-0426.2010.01486.x

Mazloumi, N., Doubleday, Z. A., and Gillanders, B. M. (2017). The effects of temperature and salinity on otolith chemistry of King George whiting. *Fish. Res.* 196, 66–74. doi: 10.1016/j.fishres.2017.08.010

Miller, J. A. (2009). The effects of temperature and water concentration on the otolith incorporation of barium and manganese in black rockfish *Sebastes melanops*. *J. Fish Biol.* 75, 39–60. doi: 10.1111/j.1095-8649.2009.02262.x

Miller, J. A. (2011). Effects of water temperature and barium concentration on otolith composition along a salinity gradient: implications for migratory reconstructions. *J. Exp. Mar. Biol. Ecol.* 405, 42–52. doi: 10.1016/j.jembe.2011.05.017

Mohan, J., Rahman, M., Thomas, P., and Walther, B. (2014). Influence of constant and periodic experimental hypoxic stress on Atlantic croaker otolith chemistry. *Aquat. Biol.* 20, 1–11. doi: 10.3354/ab00542

Morse, J. W., and Bender, M. L. (1990). Partition coefficients in calcite: examination of factors influencing the validity of experimental results and their application to natural systems. *Chem. Geol.* 82, 265–277. doi: 10.1016/0009-2541(90)90085-L

Nagelkerken, I., Sheaves, M., Baker, R., and Connolly, R. M. (2013). The seascape nursery: a novel spatial approach to identify and manage nurseries for coastal marine fauna. *Fish Fish.* 16, 362–371. doi: 10.1111/faf.12057

Paton, C., Hellstrom, J., Paul, B., Woodhead, J., and Hergt, J. (2011). Iolite: freeware for the visualisation and processing of mass spectrometric data. *J. Analyt. Atom. Spectrom.* 26, 2508–2511. doi: 10.1039/c1ja10172b

Pentreath, R. J. (1976). Some further studies on the accumulation and retention of 65Zn and 54Mn by the plaice, *Pleuronectes platessa* L. *J. Exp. Mar. Biol. Ecol.* 21, 179–189. doi: 10.1016/0022-0981(76)90038-1

Phillis, C. C., Ostrach, D. J., Ingram, B. L., and Weber, P. K. (2011). Evaluating otolith Sr/Ca as a tool for reconstructing estuarine habitat use. *Can. J. Fish. Aquat. Sci.* 68, 360–373. doi: 10.1139/F10-152

Pihl, L., Cattrijsse, A., Codling, I., Mathieson, S., McLusky, D. S., and Roberts, C. M. (2002). "Habitat use by fishes in estuaries and other brackish areas," in *Fishes in Estuaries*, eds M. Elliott and K. L. Hemingway (Hoboken, NJ: Blackwell Publishing Ltd), 10–53.

Primo, A. L., Azeiteiro, U. M., Marques, S. C., Martinho, F., Baptista, J., and Pardal, M. A. (2013). Colonization and nursery habitat use patterns of larval and juvenile flatfish species in a small temperate estuary. *Cell* 76, 126–134. doi: 10.1016/j.seares.2012.08.002

Reis-Santos, P., Gillanders, B. M., Tanner, S. E., Vasconcelos, R. P., Elsdon, T. S., and Cabral, H. N. (2012). Temporal variability in estuarine fish otolith elemental fingerprints: implications for connectivity assessments. *Estuar. Coast. Shelf Sci.* 112, 216–224. doi: 10.1016/j.ecss.2012.07.027

Reis-Santos, P., Tanner, S. E., Elsdon, T. S., Cabral, H. N., and Gillanders, B. M. (2013). Effects of temperature, salinity and water composition on otolith elemental incorporation of *Dicentrarchus labrax*. *J. Exp. Mar. Biol. Ecol.* 446, 245–252. doi: 10.1016/j.jembe.2013.05.027

Reis-Santos, P., Vasconcelos, R. P., Ruano, M., Latkoczy, C., Gnther, D., Costa, M. J., et al. (2008). Interspecific variations of otolith chemistry in estuarine fish nurseries. *J. Fish Biol.* 72, 2595–2614. doi: 10.1111/j.1095-8649.2008.01871.x

Reis-Santos, P., Vasconcelos, R. P., Tanner, S. E., Fonseca, V. F., Cabral, H. N., and Gillanders, B. M. (2018). Extrinsic and intrinsic factors shape the ability of using otolith chemistry to characterize estuarine environmental histories. *Mar. Environ. Res.* 140, 332–341. doi: 10.1016/j.marenvres.2018.06.002

Schmidt, S., Diallo, I. I., Derriennic, H., Fallou, H., and Lepage, M. (2019). Exploring the susceptibility of turbid estuaries to hypoxia as a prerequisite to designing a pertinent monitoring strategy of dissolved oxygen. *Front. Mar. Sci.* 6:613. doi: 10.3389/fmars.2019.00352

Sheaves, M., Baker, R., and Johnston, R. (2006). Marine nurseries and effective juvenile habitats: an alternative view. *Mar. Ecol. Prog. Ser.* 318, 303–306. doi: 10.3354/meps318303

Smith, W. E., and Kwak, T. J. (2014). Otolith microchemistry of tropical diadromous fishes: spatial and migratory dynamics. *J. Fish Biol.* 84, 913–928. doi: 10.1111/jfb.12317

Stanley, R. R. E., Bradbury, I. R., DiBacco, C., Snelgrove, P. V. R., Thorrold, S. R., and Killen, S. S. (2015). Environmentally mediated trends in otolith composition of juvenile Atlantic cod (*Gadus morhua*). *ICES J. Mar. Sci.* 72, 2350–2363. doi: 10.1093/icesjms/fsv070

Sturrock, A. M., Hunter, E., Milton, J. A., Johnson, R. C., Waring, C. P., and Trueman, C. N. (2015). Quantifying physiological influences on otolith microchemistry. *Methods Ecol. Evol.* 6, 806–816. doi: 10.1111/2041-210X.12381

Sturrock, A. M., Trueman, C. N., Milton, J. A., Waring, C. P., Cooper, M. J., and Hunter, E. (2014). Physiological influences can outweigh environmental signals in otolith microchemistry research. *Mar. Ecol. Prog. Ser.* 500, 245–264. doi: 10.3354/meps10699

Swearer, S., Forrester, G., Steele, M., Brooks, A., and Lea, D. (2003). Spatio-temporal and interspecific variation in otolith trace-elemental fingerprints in a temperate estuarine fish assemblage. *Estuar. Coast. Shelf Sci.* 56, 1111–1123. doi: 10.1016/S0272-7714(02)00317-7

Tanner, S. E., Reis-Santos, P., Vasconcelos, R. P., Fonseca, V. F., Franca, S., Cabral, H. N., et al. (2013a). Does otolith geochemistry record ambient environmental conditions in a temperate tidal estuary? *J. Exp. Mar. Biol. Ecol.* 441, 7–15. doi: 10.1016/j.jembe.2013.01.009

Tanner, S. E., Reis-Santos, P., Vasconcelos, R. P., Thorrold, S. R., and Cabral, H. N. (2013b). Population connectivity of *Solea solea* and *Solea senegalensis* over time. *J. Sea Res.* 76, 82–88. doi: 10.1016/j.seares.2012.11.005

Tanner, S. E., Vasconcelos, R. P., Cabral, H. N., and Thorrold, S. R. (2012). Testing an otolith geochemistry approach to determine population structure and movements of European hake in the northeast Atlantic Ocean and Mediterranean Sea. *Fish. Res.* 12, 198–205. doi: 10.1016/j.fishres.2012.02.013

Thomas, O. R. B., Swearer, S. E., Kapp, E. A., Peng, P., Tonkin Hill, G. Q., Papenfuss, A., et al. (2018). The inner ear proteome of fish. *FEBS J.* 286, 66–81. doi: 10.1111/febs.14715

Thorrold, S. R., Latkoczy, C., Swart, P. K., and Jones, C. M. (2001). Natal homing in a marine fish metapopulation. *Science* 291, 297–299. doi: 10.1126/science.291.5502.297

Turner, D. R., Whitfield, M., and Dickson, A. G. (1981). The equilibrium speciation of dissolved components in freshwater and sea water at 25°C and 1 atm pressure. *Geochim. Cosmochim. Acta* 45, 855–881. doi: 10.1016/0016-7037(81)90115-0

Vasconcelos, R. P., Reis-Santos, P., Costa, M. J., and Cabral, H. N. (2011). Connectivity between estuaries and marine environment: integrating metrics to assess estuarine nursery function. *Ecol. Indic.* 11, 1123–1133. doi: 10.1016/j.ecolind.2010.12.012

Vasconcelos, R. P., Reis-Santos, P., Maia, A., Fonseca, V. F., Franca, S., Wouters, N., et al. (2010). Nursery use patterns of commercially important marine fish species in estuarine systems along the Portuguese coast. *Estuar. Coast. Shelf Sci.* 86, 613–624. doi: 10.1016/j.ecss.2009.11.029

Vinagre, C., Maia, A., Reis-Santos, P., Costa, M. J., and Cabral, H. N. (2009). Small-scale distribution of *Solea solea* and *Solea senegalensis* juveniles in the Tagus estuary (Portugal). *Estuar. Coast. Shelf Sci.* 81, 296–300. doi: 10.1016/j.ecss.2008.11.008

Walther, B. D. (2019). The art of otolith chemistry: interpreting patterns by integrating perspectives. *Mar. Freshw. Res.* 70:1643. doi: 10.1071/MF18270

Walther, B. D., and Limburg, K. E. (2012). The use of otolith chemistry to characterize diadromous migrations. *J. Fish Biol.* 81, 796–825. doi: 10.1111/j.1095-8649.2012.03371.x

Walther, B. D., and Nims, M. K. (2014). Spatiotemporal variation of trace elements and sable isotopes in subtropical estuaries: I. Freshwater endmembers and mixing curves. *Estuar. Coast. Shelf Sci.* 38, 754–768. doi: 10.1007/s12237-014-9881-7

Williams, J., Jenkins, G. P., Hindell, J. S., and Swearer, S. E. (2018). Fine-scale variability in elemental composition of estuarine water and otoliths: developing environmental markers for determining larval fish dispersal histories within estuaries. *Limnol. Oceanogr.* 63, 262–277. doi: 10.1002/lno.10627

Woodcock, S. H., Munro, A. R., Crook, D. A., and Gillanders, B. M. (2012). Incorporation of magnesium into fish otoliths: determining contribution from water and diet. *Geochim. Cosmochim. Acta* 94, 12–21. doi: 10.1016/j.gca.2012.07.003

Yoshinaga, J., Nakama, A., Morita, M., and Chemistry, J. E. M. (2000). Fish otolith reference material for quality assurance of chemical analyses. *Elsevier* 69, 91–97. doi: 10.1016/S0304-4203(99)00098-5

Conflict of Interest: The authors declare that the research was conducted in the absence of any commercial or financial relationships that could be construed as a potential conflict of interest.

Copyright © 2020 Martinho, Pina, Nunes, Vasconcelos, Fonseca, Crespo, Primo, Vaz, Pardal, Gillanders, Tanner and Reis-Santos. This is an open-access article distributed under the terms of the Creative Commons Attribution License (CC BY). The use, distribution or reproduction in other forums is permitted, provided the original author(s) and the copyright owner(s) are credited and that the original publication in this journal is cited, in accordance with accepted academic practice. No use, distribution or reproduction is permitted which does not comply with these terms.

frontiers in Marine Science

ORIGINAL RESEARCH
published: 26 May 2020
doi: 10.3389/fmars.2020.00320

Growth Rate, Ration, and Temperature Effects on Otolith Elemental Incorporation

Jessica A. Miller[1]* *and Thomas P. Hurst*[2]

[1] Department of Fisheries and Wildlife, Coastal Oregon Marine Experiment Station, Oregon State University, Newport, OR, United States, [2] Fisheries Behavioral Ecology Program, Resource Assessment and Conservation Engineering Division, Alaska Fisheries Science Center, National Marine Fisheries Service, National Oceanic and Atmospheric Administration, Hatfield Marine Science Center, Newport, OR, United States

The application and utility of otolith chemistry continues to expand despite an incomplete understanding of the mechanisms that regulate elemental incorporation. An unresolved question is what role individual factors such as growth play in regulating elemental incorporation. Disentangling growth variation from thermal effects is particularly challenging in fishes yet integral to understanding the mechanisms of incorporation and interpreting patterns of variation in the field. Juvenile Pacific cod (*Gadus macrocephalus*) were maintained in a controlled laboratory setting to evaluate the relative importance of growth rate, ration, and temperature on otolith elemental incorporation. Fish were held at four temperatures (2, 5, 9, 13°C) and fed daily to apparent satiation. An additional treatment included fish that were held at 9°C and fed a reduced ration (1% body mass d^{-1}). Fish were maintained for variable duration (40–147 d), depending on ration and temperature, to ensure adequate otolith growth for analysis. Water samples for chemical analysis were collected to determine elemental partition coefficients (D_{Me}). Overall, mean growth rates ranged from −0.09 to 1.52% d^{-1}. For the 9°C fish, there was a clear ration effect on D_{Mn} (2.6X higher at high ration) and D_{Sr} (1.5X higher at low ration), a small effect for D_{Mg} (1.1X higher at high ration), and no effect for D_{Ba}. For high ration fish, there was a positive effect of temperature on D_{Mn} and D_{Mg}, due solely to differences associated with the 2°C treatment, and no effect on D_{Sr} and D_{Ba}. Correlations between growth and D_{Me} within temperature treatments were variable, but for D_{Mn} and D_{Sr} the directionality mirrored the ration effect with positive correlations for D_{Mn} and negative correlations for D_{Sr}. Overall, the observed ration effects were greater than any growth rate effect, indicating that the effect of ration is due to more than growth variation.

Keywords: partition co-efficients, manganese, strontium, barium, magnesium, Pacific cod

OPEN ACCESS

Edited by:
Benjamin D. Walther,
Texas A&M University Corpus Christi,
United States

Reviewed by:
Susanne Eva Tanner,
University of Lisbon, Portugal
Ewan Hunter,
Centre for Environment, Fisheries and Aquaculture Science (CEFAS),
United Kingdom
Patrick Reis-Santos,
University of Adelaide, Australia

****Correspondence:***
Jessica A. Miller
jessica.miller@oregonstate.edu

Specialty section:
This article was submitted to Marine Ecosystem Ecology, a section of the journal Frontiers in Marine Science

Received: *16 December 2019*
Accepted: *20 April 2020*
Published: *26 May 2020*

Citation:
Miller JA and Hurst TP (2020) Growth Rate, Ration, and Temperature Effects on Otolith Elemental Incorporation. Front. Mar. Sci. 7:320. doi: 10.3389/fmars.2020.00320

INTRODUCTION

Elemental analysis of accretionary hard tissues in aquatic animals is now widely used in a variety of disciplines, such as aquaculture (Yamada and Mulligan, 1982; Gibson-Reinemer et al., 2009) and climatology (Wurster and Patterson, 2001; Schloesser et al., 2009). While incomplete, our mechanistic understanding of the factors regulating elemental incorporation into hard structures, such as fish scales and otoliths, mollusk shells, and coral skeletons, has advanced through controlled

experiments on (1) abiotic crystals, such as calcite and aragonite (Gaetani and Cohen, 2006; Lopez et al., 2009); (2) animal tissues that grow in direct contact with the water, such as coral skeletons and bivalve shells (Mitsuguchi et al., 2003; Holcomb et al., 2009; Marchitto et al., 2018); and (3) animal tissues that grow internally with multiple interfaces for the discrimination, or partitioning, of elements, such as teleost otoliths (Elsdon and Gillanders, 2003; Miller, 2009, 2011). For otolith elemental incorporation, physical characteristics, such as water elemental concentrations, temperature, salinity, and pH (Bath et al., 2000; Elsdon and Gillanders, 2004; DiMaria et al., 2010), as well as biological characteristics, such as growth, diet, and reproductive state (Buckel et al., 2004; Walther et al., 2010; Sturrock et al., 2015), have all been identified as factors that can influence elemental incorporation.

For many ecological applications, it is assumed that the dominant mechanisms regulating elemental incorporation are related to physical water characteristics with minor or minimal effects of biological traits, such as diet or growth. While there are laboratory experiments and reviews that highlight some of these potentially confounding factors (Sturrock et al., 2014; Izzo et al., 2018), many field studies do not explicitly address them, and the occurrence of strong biotic effects has the potential to confound interpretation of field observations. Direct effects of growth and metabolic variation are of interest because, if dominant, such effects could result in substantial variation among individuals residing in the same locations or water masses, which would violate one of the most common assumptions. Thus, it is important to determine the relative importance of abiotic (or "kinetic") and biotic (or "vital") effects on elemental incorporation in general and of growth variation specifically.

There is some evidence for growth rate effects on otolith elemental incorporation (Sadovy and Severin, 1994; Walther et al., 2010; Stanley et al., 2015); however, most studies are confounded by temperature. Growth of ectotherms covaries with temperature and relatively few studies have reported growth effects on otolith elemental incorporation within comparable thermal environments (Martin et al., 2004; Martin and Thorrold, 2005; DiMaria et al., 2010; Walther et al., 2010; Stanley et al., 2015). Overall, variable effects of growth are reported, with positive, negative, and no effects on incorporation reported for the most commonly examined elements: magnesium (Mg), manganese (Mn), strontium (Sr), and barium (Ba) (**Tables 1**, **2**). These findings are further complicated because there are multiple opportunities for partitioning, i.e., at the gills, in the blood and endolymph, and during crystal formation. However,

TABLE 1 | Laboratory studies that examined temperature and/or growth effects on otolith elemental incorporation of immature marine or euryhaline fish species.

Study	Species	Temp. (°C)	Elements	Growth or ration evaluation
Walther et al. (2010)	*Acanthochromis polycanthus*	26, 28, 31	Sr, Ba	Two rations at all three temperatures.
[1]Elsdon and Gillanders (2002)	*Acanthopagrus butcheri*	16, 20, 24	Mg, Mn, Sr, Ba	
[2]Webb et al. (2012)	*Acanthopagrus butcheri*	12, 16, 20, 24, 28	Sr, Ba	% contribution water vs. food
Marohn et al. (2011)	*Anguilla Anguilla*	14, 19, 24	Mg, Mn, Sr, Ba	Regression analysis within temp.
Barnes and Gillanders (2013)	*Argyrosomaus japonicas*	16, 20, 24	Mg, Sr, Ba	
Chesney et al. (1998)	*Brevoortia patronus*	18, 22, 26	Sr	
Reis-Santos et al. (2013)	*Dicentrarchus labrax*	21, 25	Sr, Ba	
Radtke (1989)	*Fundulus heteroclitus*	18, 22, 26, 30	Sr	
[1]DiMaria et al. (2010)	*Gadus macrocephalus*	2, 5, 8	Mg, Sr, Ba	Correlation analysis within temp.
[2]Miller and Hurst, this study	*Gadus macrocephalus*	2, 5, 9, 13	Mg, Mn, Sr, Ba	Two rations at 9°C Correlation analysis within temp.
Stanley et al. (2015)	*Gadus morhua*	5, 8.5, 12	Mg, Mn, Sr, Ba	Correlation analysis within temp. mixed-effect model
Gallahar and Kingsford (1996)	*Girella elevate*	19, 28	Sr	
Izzo et al. (2015)	*Lates calcarifer*	26, 30	Sr, Ba	% contribution water vs. food mixed-effect model
[1]Bath et al. (2000)	*Leiostomus xanthurus*	20, 25	Sr, Ba	Correlation analysis within temp.
[2]Martin et al. (2004)	*Leiostomus xanthurus*	17, 20, 23, 26	Sr	
[3]Martin and Thorrold (2005)	*Leiostomus xanthurus*	17, 20, 23, 26	Mg, Mn, Ba	Correlation analysis within temp.
Martin and Wuenschel (2006)	*Lutjanus griseus*	18, 23, 28, 33	Mg, Mn, Sr, Ba	
[1]Gauldie (1996)	*Oncorhynchus tshawytscha*	8, 10, 12, 14, 16	Mn, Mg, Sr	
[2]Miller (2011)	*Oncorhynchus tshawytscha*	9, 12, 15	Mg, Sr, Ba	Correlation analysis within temp.
Walsh and Gillanders (2018)	*Percalates novemaculeata*	16, 20, 24	Sr, Ba	
Hoff and Fuiman (1995)	*Sciaenops ocellatus*	21, 23, 27, 30, 34	Mg, Sr	
Miller (2009)	*Sebastes melanops*	7.4, 13	Mn, Ba	Correlation analysis within temp.

Temperature treatments and elements examined, ration, if variable, and the statistical approach, if used, to separate growth and temperature effects are included. Two studies used tracers to estimate the percent contribution of water and food to otolith elemental composition. General findings of these studies are presented in ***Table 2****. Subscripts link study in* ***Table 1*** *with results in* ***Table 2*** *when there is more than one study per species.*

TABLE 2 | Review of studies that examined temperature and growth effects on otolith elemental incorporation of immature marine or euryhaline fish species.

Species	Mg			Mn			Sr			Ba		
	T	G	T:G	T	G	T:G	T	G	T:G	T	G	T:G
Acanthochromis polycanthus							⊘	Ration		⊘	Ration	
[1]*Acanthopagrus butcheri*			⊘			⊘	NL		TxS			TxS
[2]*Acanthopagrus butcheri*									TxS			TxS
Anguilla anguilla											⊘	
Argyrosomus japonicus									TxS			TxS
Brevoortia patronus								⊘	⊘			
Dicentrarchus labrax												
Fundulus heteroclitus												
[1]*Gadus macrocephalus*		⊘	⊘					⊘			⊘	
[2]*Gadus macrocephalus*		Ration			Ration			Ration			Ration	⊘
Gadus morhua		⊘		TxS	2 of 9			3 of 9		TxS	⊘	TxS
Girella elevata									⊘			
Lates calcarifer								Cond	TxS		Cond	
[1]*Leiostomus xanthurus*								⊘			⊘	⊘
[2]*Leiostomus xanthurus*								3 of 23				
[3]*Leiostomus xanthurus*	⊘				⊘	TxS				⊘	⊘	
Lutjanus griseus			⊘			⊘						⊘
[1]*Oncorhynchus tshawytscha*			⊘			⊘						
[2]*Oncorhynchus tshawytscha*	TxS	⊘	⊘				⊘	⊘	TxS	TxS	1 of 3	
Percalates novemaculeata			⊘						TxS			TxS
Sciaenops ocellatus			⊘									
Sebastes melanops					⊘						⊘	

Reported results for temperature (T) and growth (G) effects on the otolith incorporation of magnesium (Mg), manganese (Mn), Strontium (Sr), and barium (Ba) are included as well as observed effects that could be influenced by variation in growth (T:S). Green, positive effect, black, negative effect, gray with "⊘" symbol, examined but no effect, blank or white, not examined. "TxS" indicates a reported interaction between temperature and salinity. "NL" indicates non-linear relationship. Notations indicate the number of within-temperature growth correlations that were statistically significant. For example, a black box with "3 of 9" indicates that three temperature-specific correlations were significantly, negatively correlated with incorporation of that element. Studies represented are presented in ***Table 1****. Subscripts link study in* ***Table 1*** *with results in* ***Table 2*** *when there is more than one study per species.*

in studies that attempted to account for growth variation by limiting comparisons to individuals in similar temperature treatments, the results are more consistent with primarily positive or no growth effects on the incorporation of Mg and Mn and negative or no effects on the incorporation of Sr and Ba (**Table 2**). Therefore, growth and temperature could have independent, differential, additive, or multiplicative effects across these interfaces, which could vary across species and in relation to the species' thermal range.

To separate temperature and growth effects on otolith elemental incorporation, we manipulated both temperature and ration in a controlled laboratory experiment on juvenile Pacific cod (*Gadus macrocephalus*). By maintaining fish at realistic temperatures that can be experienced during their first year of life (2, 5, 9, 13°C) and manipulating ration within the 9°C treatments, which reflects the species' optimal temperature for growth (Hurst et al., 2010), we independently examined the effects of temperature and growth on elemental incorporation.

MATERIALS AND METHODS

Fish Collections and Laboratory Experiment

Age-0 Pacific cod were collected within a Kodiak Island juvenile nursery using a 36-m beach seine. Fish were maintained for at least 48 h at the Alaska Fisheries Science Center (AFSC) Kodiak Laboratory in ambient seawater prior to shipment to the AFSC Laboratory in Newport, Oregon. Fish were shipped overnight in insulated containers filled with seawater and oxygen. Prior to use in laboratory experiments, fish were maintained in 1-m diameter round tanks with flow-through seawater maintained at 8–10°C. During this acclimation period fish were fed thawed krill and a gelatinized combination of squid, krill, herring, commercial fish food, amino acid supplements, and vitamins three times per week.

After 2 months of laboratory acclimation, 225 fish were randomly assigned to 15 tanks at densities of 15 fish per tank. Experimental tanks were 1 m in diameter and filled to a depth of

TABLE 3 | Mean (standard deviation) water elemental concentrations during the experiment.

Treatment °C	Exp. days	Ca, ppm	Mg, ppm	Sr, ppm	Ba, ppb	Mn, ppb	Mg:Ca, mMM	Sr:Ca, mMM	Ba:Ca, μMM	Mn:Ca, μMM
2	147	383.6 (14.1)	1,208 (43.9)	7.10 (0.28)	5.1 (0.9)	2.3 (1.2)	5,198 (17.5)	8.47 (0.04)	3.9 (0.08)	4.3 (0.02)
5	84	381.4 (10.7)	1,202 (33.6)	7.07 (0.21)	5.3 (0.9)	2.7 (1.7)	5,200 (18.7)	8.49 (0.03)	4.0 (0.07)	5.3 (0.03)
9L	56	379.3 (11.0)	1,194 (32.9)	7.03 (0.22)	4.8 (0.7)	2.9 (1.5)	5,198 (18.2)	8.49 (0.03)	3.7 (0.06)	5.7 (0.03)
9H, 13	40	380.4 (12.2)	1,198 (36.4)	7.05 (0.24)	5.1 (0.8)	3.0 (1.7)	5,197 (19.1)	8.47 (0.03)	3.9 (0.07)	4.3 (0.03)

Values were averaged using samples collected over the duration of the experiment within each temperature treatment. The number of days for each treatment is included. Experimental dates were 10 Dec 09 to 09 Jan 10 for the 9 and 13°C high-ration treatments; 10 Dec 09 to 01 Feb 10 for the 9°C low-ration treatment; 10 Dec 09 to 24 Feb 10 for the 5°C high-ration treatment; and 10 Dec 09 to 25 Apr 10 for the 2°C high-ration treatment.

55 cm. After 5 d, tank temperatures were adjusted to treatment temperatures at a rate of 1°C per day. Three tanks were assigned to the 2, 5, and 13°C treatments and six tanks were assigned to the 9°C treatment. Lights were maintained on a 12:12 h light:dark photoperiod throughout the experiment. Tanks were checked twice daily for mortalities, which were removed, weighed, and measured. During the tank and temperature acclimation period, fish were fed three times per week.

Following 2 weeks of temperature acclimation, all fish in the experiment were measured and experimental feeding conditions initiated (experiment day 0). Initial mean sizes of the fish were 95.7 mm SL (± 10.1 SD) and 9.2 g wet weight (± 2.7 SD). Three of the 9°C tanks were assigned to a restricted ration treatment with all other tanks being fed thawed krill (*Euphausia pacifica*) to apparent satiation once per day. The restricted ration treatment was offered food at a rate of 1% wet mass per day, with the ration adjusted following fish measurements. This ration level was slightly above the estimated "maintenance ration" for juvenile Pacific cod and expected to support low levels of somatic growth. All fish in the 9 and 13°C treatments were measured every 2 weeks and fish in the 2 and 5°C treatments were measured every 3 weeks. Due to the expected differences in growth rates, lower temperature and low-ration treatments were extended to allow time for enough otolith deposition for chemical analyses. Therefore, the sampling interval and experimental duration varied among the treatments (**Table 3**). At the end of the experiment, all fish were euthanized with 250 mg/L of tricaine methanesulfonate (MS-222) buffered to a pH of 7.0 with sodium bicarbonate [American Veterinary Medical Association (AVMA), 2007] and frozen prior to dissection and extraction of otoliths.

Somatic growth rates were determined individually for each fish in the experiment. In lieu of individual marking of the fish, we used the size disparity among fish in each tank as an indicator of identity, assuming maintenance of relative size ranks throughout (Hurst et al., 2012). Weight-specific growth rate (SGR, % body mass d^{-1}) of each fish was calculated by regression of ln-transformed wet mass against sampling date. An indicator of body condition, the hepatosomatic index (HSI), was also calculated (wet liver mass/body mass · 100). Fish size at the end of the experiment, SGR, and the HSI were compared across all five treatments (2, 5, 9_low, 9_high, and 13°C) with one-way Analysis of Variance (ANOVA) and Tukey HSD *post-hoc* comparisons using R version 3.6.0. Data were log-transformed to satisfy parametric assumptions.

All tanks in the experiment shared the same water source. Coastal oceanic water was pumped from Yaquina Bay during flooding tides into a 3 million L reservoir. Water was pumped from the reservoir through a sand filter to the fish holding facilities where it was heated or chilled to achieve the target temperatures. Given that the water source was the same for all tanks, water samples were collected haphazardly from two of the 15 tanks every 10–14 d for elemental analysis. Water samples were filtered (0.25 μm) and acidified (< 2 pH) with ultrapure HNO_3 (ULTREX, J.T. Baker). Dissolved elemental concentrations were measured using a Leeman-Teledyne inductively coupled plasma optical emission spectrometer (ICP-OES) (Mg at 279.1 nm, Ca at 317.9 nm, Mn at 259.4 nm, Sr at 421.5 nm, and Ba at 455.4 nm). Filtered, acidified samples were diluted 150x for the determination of Mg, Ca, and Sr and 20x for Mn and Ba. Matrix-matched standards were created using SPEX Certiprep Group® certified reference materials, National Institute of Standards and Technology (NIST) liquid standard (1643e), and a sodium chloride (NaCl) solution. Matrix-matched NIST standards and HNO_3 blanks were used to evaluate accuracy. Measured Mg, Ca, Mn, Sr, and Ba concentrations were within 6, 2, 4, 1, and 6%, respectively, of certified values. Repeated measurements of the same standards indicated that precision was within 5% for all elements ($n = 5$). Elemental concentrations are presented in ppm (Mg, Ca, Sr) or ppb (Mn, Ba) or in mmol mol^{-1} (Mg:Ca, Sr:Ca) or μmol mol^{-1} (Mn:Ca, Ba:Ca). We used paired *t*-tests to compare the two separate tank water samples collected on the same days. If there were no differences in water elemental concentrations between tank samples, then the water Me:Ca ratios for the two samples were averaged and used for comparison with otolith chemistry. Elemental ratios were ln-transformed to normalize data distributions and homogenize the variance.

Otolith Preparation and Analysis

Juveniles were weighed (to 0.01 mg) and measured (standard length SL, to 1.0 mm), and both sagittae were removed using standard methods to minimize contamination. The left otolith was mounted on a glass slide using thermoplastic resin and polished to expose the core using 3M™ tri-mite Wetordry™ paper (240–1,200 grit) and diamond lapping film. Polished otoliths were imaged at 400× magnification using a Leica DM1000 compound microscope and Micropublisher camera. The mean otolith deposition in each temperature-ration treatment was determined by measuring the total

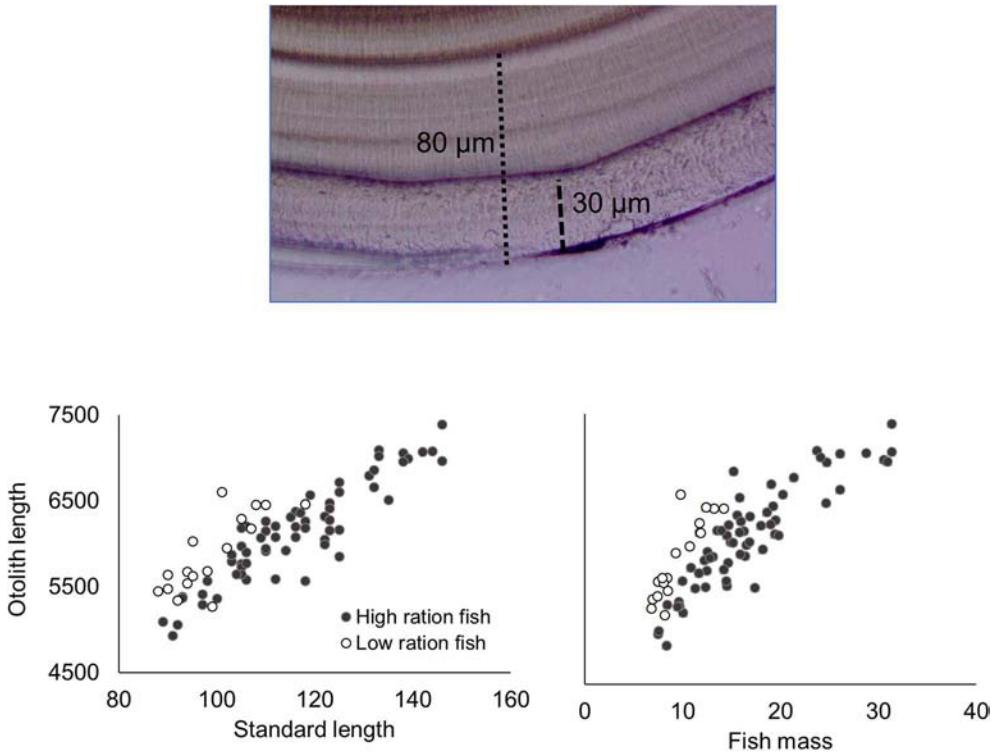

FIGURE 1 | Image of otolith from the low-ration treatment (top image) with apparent stress check (at 80 µm) and ablation scar (30 µm) indicated. Otolith length plotted against fish standard length (left graph) and fish mass (right graph) at the end of the experiment are also included, with the low- and high-ration fish indicated.

otolith deposition during the experiment based on increment counts. For most fish, particularly in the low-ration treatments, the otoliths displayed a prominent check that aligned with the initiation of the experiment (**Figure 1**). Daily increments (Narimatsu et al., 2007) within the final 30 µm, which represented the otolith material that was ablated to estimate elemental composition, were measured using ImagePro®. Otoliths were interpreted at least twice with at least 90% agreement for estimates included in subsequent analyses. The duration of the experiment varied across treatments with the 2°C fish maintained for 147 d; the 5°C fish for 84 d; the 9°C low-ration fish for 56 d; and the 9 °C high-ration and 13 °C fish for 40 d. For the 2°C treatment otolith deposition = 198 µm (27 SD); 5°C = 129 µm (16 SD); 9°C low-ration = 81 µm (6 SD); 9°C high-ration = 70 µm (10 SD); and 13°C = 91 µm (12 SD). Individual increment widths during the final 30 µm of otolith deposition experiment were averaged and log-transformed to meet parametric assumptions prior to analysis. Variation across treatments was examined with a one-way ANOVA and Tukey HSD *post-hoc* tests for pairwise comparisons using R version 3.6.0.

The left sagittae were also used for elemental analysis. Otolith thin sections were cleaned ultrasonically in NANOpure® water (18 MΩ·cm), dried in a Class 100 clean bench, and mounted randomly onto clean glass slides. To remove any surface contamination, each otolith was pre-ablated along a transect (500 µm in length) parallel to the outer otolith edge in the anterior-dorsal quadrant; the laser was set at a pulse rate of 2 Hz with a 100-µm spot moving at 100 µm s^{-1}. To collect otolith elemental data, the laser was set at a pulse rate of 7 Hz with a spot of 30 µm moving at 2 µm s^{-1}. Given that a minimum average otolith deposition during the experiment was 70 µm (±10 µm SD), the 30-µm spot size only sampled material deposited during the experiment.

Otolith analyte count data were normalized by ^{43}Ca to adjust for variability in instrument sensitivity and the amount of ablated material and converted to elemental ratios based on measurements of the NIST 612 standard. Elemental ratios are presented in mmol mol^{-1} (Mg, Sr) or µmol mol^{-1} (Mn, Ba). Precision (%RSD) was determined based on repeated measurements of NIST 612 glass slides (^{24}Mg:^{43}Ca = 6.0%, ^{55}Mn:^{43}Ca = 3.3%, ^{86}Sr:^{3}Ca = 2.6%, ^{138}Ba:^{43}Ca = 3.7%). Accuracy was measured using repeated analysis of USGS calcium carbonate standards MACS-1 and MACS-3 (mean ± SD for Mg:Ca = 114% ± 6.9, Mn:Ca = 99.4% ± 2.5, Sr:Ca = 102% ± 3.8, Ba:Ca = 113% ± 5.5). To describe elemental composition of otolith carbonate deposited during the experiment, Me:Ca values across 250–350 µm of each transect were averaged for each otolith.

There are various points at which discrimination, or partitioning, of elements can occur within teleosts, including at the water-gill interface, incorporation into blood plasma and endolymph, and during crystallization (Campana, 1999). Therefore, comparison of partition coefficients is common

TABLE 4 | Tank number, water temperature (T), ration, and mean (SD) fish size at end of the experiment (standard length, SL) and specific growth rate (SGR) and otolith growth rate during the experiment.

Tank	T	Ration	SL, mm	SGR (% g d^{-1})	n_{SGR}	Otolith growth μm d^{-1}	$n_{otolith}$
10	2°C	High	126.0 (20.7)	0.41 (0.09)	7	1.57 (0.34)	4
12	2°C	High	112.5 (7.8)	0.41 (0.05)	6	1.30 (0.24)	6
1	5°C	High	129.2 (6.1)	0.84 (0.05)	6	1.29 (0.14)	4
2	5°C	High	118.8 (12.7)	0.88 (0.06)	6	1.65 (0.24)	5
3	5°C	High	131.5 (10.4)	0.87 (0.06)	6	1.67 (0.21)	6
4	9°C	Low	103.0 (6.8)	0.06 (0.08)	6	1.27 (0.11)	6
6	9°C	Low	104.8 (7.5)	0.09 (0.19)	6	1.57 (0.09)	6
14	9°C	Low	91.3 (2.4)	−0.09 (0.12)	6	1.49 (0.13)	6
13	9°C	High	103.8 (12.8)	1.22 (0.10)	6	1.45 (0.32)	6
5	9°C	High	106.5 (11.1)	1.21 (0.14)	6	1.89 (0.31)	6
8	13°C	High	119.7 (4.7)	1.45 (0.12)	3	2.80 (NA)	1
9	13°C	High	112.3 (7.9)	1.52 (0.16)	6	2.15 (0.33)	6

Sample sizes for SGR and otolith growth analyses are also included.

(Morse and Bender, 1990) and allows for a more appropriate comparison of otolith elemental incorporation, particularly given the variable experimental duration across treatments in this study. Partition coefficients (D_{Me}) were calculated using the following equation:

$$\mathbf{D_{Me}} = \frac{[\mathbf{Me{:}Ca}]_{\mathbf{otolith}}}{[\mathbf{Me{:}Ca}]_{\mathbf{water}}}$$

To evaluate temperature effects on D_{Me}, we used a one-way ANOVA with temperature as a fixed factor and tank as the level of replication for all high-ration fish. To evaluate the effect of ration on $D_{Me,}$ we also used a one-way ANOVA with ration as the fixed factor for the 9°C fish only. Data were log-transformed (Sr:Ca, Ba:Ca) or square root transformed (Mg:Ca, Mn:Ca) to meet parametric assumptions. In order to further evaluate the potential effects of growth, we determined Pearson correlation coefficients between SGR and D_{Me} and between otolith increment width and D_{Me} for all fish within the same temperature and ration treatment. Analyses were completed using R version 3.6.0.

Finally, we compiled available literature information on growth and temperature effects on otolith elemental incorporation in order to separate results that are potentially confounded by a temperature x growth interaction from those results that examined, or accounted for in some manner, growth variation. We limited this review to controlled laboratory studies that examined the otolith incorporation of one or more of the most commonly used elements (Mg, Mn, Sr, or Ba). We further limited this analysis to studies on larval or juvenile marine and euryhaline fish in order to avoid potential confounding factors associated with large differences in salinity or maturity.

This experiment was conducted in NOAA's Alaska Fisheries Science Center Laboratory in Newport, Oregon. This research was carried out in accordance with all applicable institutional and national guidelines at the time that the study was conducted; all work followed American Fisheries Society policies on the Guidelines for Use of Fishes in Research (https://fisheries.org/docs/policy_useoffishes.pdf) and AVMA (American Veterinary Medical Association) Guidelines on Euthanasia (https://olaw.nih.gov/sites/default/files/Euthanasia2007.pdf). Fish were collected under permit CF-09-081 from the Alaska Department of Fish and Game. There was no formal ethics review of this study because NOAA National Marine Fisheries Service does not have an Institutional Animal Care and Use Committee (IACUC) or an ethics approval processes for research on fishes and, at the time of this study (2009–2010), OSU's IACUC did not provide review of research that was completed in US federal facilities.

RESULTS

There were very few mortalities during the experiment (one fish in the 5°C and two fish in 9°C low-ration treatment); these were removed from the tank and excluded from all analyses. Due to a handling error, fish from two tanks were irretrievably lost (Tanks five and seven). One additional tank (15) was removed due to consistently high values for otolith Mg:Ca (>6 SD greater than the overall tank mean) and Mn:Ca (4 SD greater than the tank mean). We identified no reason for these values and determined removal of the tank was the best option.

For the remaining 12 tanks, fish metrics (SL, SGR, HSI, and otolith increment width) were compared across all treatments (2, 5, 9 low-ration, 9 high-ration, and 13°C). Tank mean SL ranged from 91.3 to 131.5 mm, and there were differences among treatments ($F_{4,7} = 12.84$, $P = 0.002$) (**Table 4** and **Table S2**). Mean length of the 9°C, low-ration fish was less than the 2, 5, and 13°C fish (pairwise $P < 0.045$). Mean SGR ranged from −0.09 g d^{-1} to 1.52% g d^{-1} and also varied with treatment ($F_{4,7} = 263.1$, $P < 0.0001$) (**Figure 2**). Mean SGR consistently increased with temperature except for the 9°C, low-ration fish, which grew more slowly than the 2°C fish. The low-ration fish also displayed the most variable growth (−0.31 to 0.31). However, only two low-ration fish displayed a negative SGR or even a value < 0.1 g d^{-1}, which indicates that the ration, while low, was

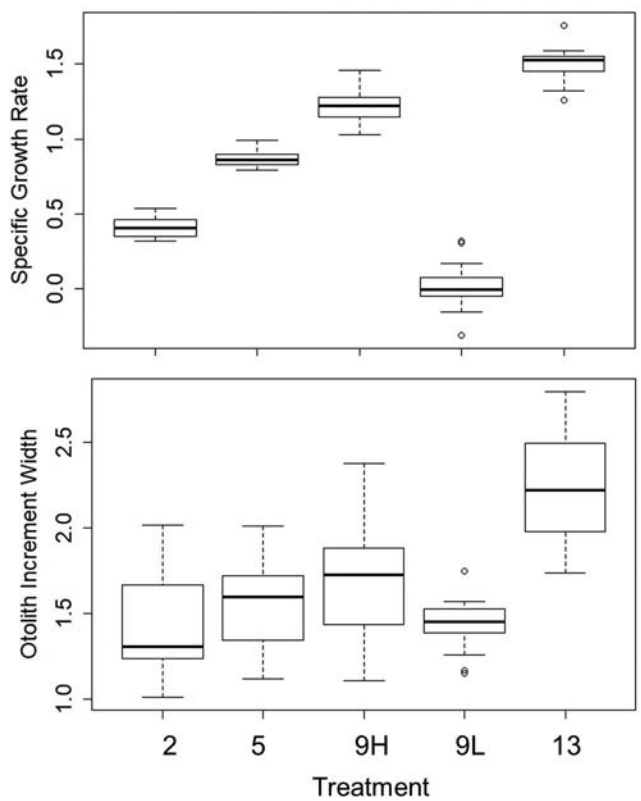

FIGURE 2 | Median, first, and third quartiles and outlying points for specific growth rate (% body mass d^{-1}) and otolith increment width (μm) during the experiment for the 2, 5, 9_low, 9_high, and 13°C treatments.

effectively a maintenance ration. Pairwise contrasts demonstrated that SGR differed among all treatments (pairwise $P < 0.002$ for all except the 9 and 13°C comparison, $P = 0.012$). Mean HSI ranged from 1.68 to 4.78 and varied with treatment ($F_{4,7} = 13.85$, $P = 0.002$). The differences were due to consistently low HSI values in the low-ration, 9°C treatment compared to the four other treatments ($P < 0.027$) (**Figure S1**). Mean otolith increment width also increased with temperature, although differences among treatments were relatively small (**Figure 2**). Overall, there was an effect of treatment on otolith increment width ($F_{4,7} = 4.86$, $P = 0.034$) with the smallest increments observed in the 9°C low-ration and the largest observed in the 13°C treatment (**Figure 2**). However, pairwise comparisons indicated that the differences were primarily due to smaller increment widths in the 2°C ($P = 0.044$), 5°C ($P = 0.056$), and 9°C low-ration ($P = 0.035$) compared with the 13°C treatments (**Table 4**). The otolith length was positively related to fish length and mass, and the low-ration fish had larger otoliths at size than the high-ration fish (**Figure 1**). Tank mean otolith increment width and SGR were positively correlated ($r = 0.69$; $P = 0.012$).

Elemental concentrations between the two tank water samples collected on the same day were similar (paired *t*-test, $n = 14$, $P > 0.30$). Therefore, the mean of the two samples taken on each of 14 sampling days was used to describe water elemental concentrations during the experiment (**Table S1**) and values were then averaged for each temperature treatment according to the duration of each treatment (**Table 3**). There was some seasonal variation observed. Therefore, otolith Me:Ca values are presented (**Table 5**) but all statistical analyses were based on D_{Me}, which accounts for variation in water chemistry (**Figure 3**).

The effect of temperature on partition coefficients, which was evaluated using only high- ration fish, varied across elements with positive effects on D_{Mn} and D_{Mg}, inconclusive effects on D_{Sr}, and no effect on D_{Ba} (**Figure 3**; **Table S2**). For D_{Mn}, there was a positive effect of temperature ($F_{3,5} = 32.73$, $P = 0.001$) where the 2°C treatment was lower than the 5°C ($P = 0.003$), 9°C ($P < 0.001$), and 13°C ($P = 0.005$) treatments. For D_{Mg}, there was also a positive effect of temperature ($F_{3,5} = 8.54$, $P = 0.021$) where the 2°C treatment was lower than the 5°C ($P = 0.028$) and 13°C ($P = 0.022$) treatments. For D_{Sr}, there was a minor association with temperature ($F_{3,5} = 4.09$, $P = 0.082$) due to slightly higher values in the 2°C treatment than in the 5°C treatment ($P = 0.080$). There was no effect of temperature on D_{Ba} ($F_{3,5} = 1.31$, $P = 0.368$). Overall, any observed temperature effects on otolith elemental incorporation were due to the 2°C treatment (**Figure S2**).

There was a strong, positive effect of ration on the partitioning of Mn ($F_{1,3} = 380.9$, $P = 0.0003$) and negative effect on the partitioning of Sr ($F_{1,3} = 111.9$, $P = 0.002$) (**Figure 3**; **Table S2**). There was a small, positive effect of ration on partitioning for Mg ($F_{1,3} = 10.21$, $P = 0.05$) and no effect for Ba ($F_{1,3} = 1.31$, $P = 0.368$). Overall, D_{Mn} was 2.6X greater and D_{Mg} was 1.1X in high-ration compared with low-ration fish. In contrast, D_{Sr} was 1.5X greater in low-ration compared with high-ration fish.

We also determined the Pearson correlation coefficients between SGR and D_{Me} and increment width and D_{Me} within the temperature treatments to further evaluate the potential effects of growth rate (**Table 6**). There were no wholly consistent patterns observed for any partition coefficients at all temperatures (**Figure 4**) and no *P*-values were smaller than 0.05 after conservative adjustments for multiple comparisons. However, the directionality of the correlations between SGR and D_{Me} were similar to that of the ration effect for D_{Mn}, positive for four of the five correlations and for D_{Sr}, negative for four of the five correlations. For D_{Mg}, three of the five correlations were negative, which is opposite the observed, relatively small ration effect. The pattern of correlations between mean otolith increment width and D_{Me} were similar to SGR. The coefficient of variation for otolith increment width was greater than for SGR, except for the low ration treatment in which variation in SGR was very high (**Table 6**). The patterns between D_{Me} and HSI were similar to SGR and otolith growth (**Figure S1**).

The observed ration effects were consistently greater than the observed temperature effects. The ration effects are also greater than any observed effects due to growth variation within temperature treatments. For example, the mean difference in SGR between the 2 and 13°C treatments (1.09% g d^{-1}) was similar to the difference between the low- and high-ration 9°C treatments (1.20% g d^{-1}). In contrast, the mean difference in D_{Mn} between the 2 and 13°C fish (1.3X) was half of the observed difference between the low- and high-ration fish (2.6X). Additionally, mean D_{Sr} was similar in the 2 and 13°C fish (0.244

TABLE 5 | Tank mean (standard deviation) for otolith elemental concentrations (Me:Ca) and partition coefficients (D_{Me}) during the experiment.

Tank	T	Ration	Mg:Sr (mMM^{-1})	Mn:Ca (μMM^{-1})	Sr:Ca (mMM^{-1})	Ba:Ca (μMM^{-1})	D_{Mg} (x1000)	D_{Mn}	D_{Sr}	D_{Ba}
10	2°C	High	0.280	18.6 (8.1)	2.00 (0.46)	1.40 (0.46)	0.054 (0.02)	4.29 (1.8)	0.236 (0.05)	0.355 (0.12)
12	2°C	High	0.284	17.7 (4.1)	2.13 (0.44)	1.29 (0.44)	0.055 (0.01)	4.08 (0.9)	0.252 (0.05)	0.328 (0.07)
1	5°C	High	0.316	24.3 (4.7)	1.51 (0.17)	1.26 (0.25)	0.061 (0.01)	5.62 (1.1)	0.178 (0.20)	0.320 (0.06)
2	5°C	High	0.344	23.2 (8.2)	1.91 (0.56)	1.74 (0.42)	0.066 (0.02)	5.35 (1.9)	0.226 (0.07)	0.440 (0.11)
3	5°C	High	0.336	23.5 (2.3)	1.61 (0.17)	1.50 (0.22)	0.064 (0.01)	5.42 (0.5)	0.190 (0.02)	0.380 (0.06)
4	9°C	Low	0.282	12.0 (3.3)	2.82 (0.33)	1.88 (0.68)	0.054 (0.01)	2.10 (0.6)	0.332 (0.03)	0.505 (0.18)
6	9°C	Low	0.287	13.3 (3.7)	2.64 (0.39)	1.48 (0.47)	0.055 (0.01)	2.34 (0.6)	0.311 (0.01)	0.397 (0.13)
14	9°C	Low	0.254	13.3 (1.9)	2.88 (0.26)	1.62 (0.26)	0.049 (0.01)	2.34 (0.3)	0.340 (0.03)	0.435 (0.09)
13	9°C	High	0.321	24.8 (3.2)	1.88 (0.24)	1.52 (0.24)	0.062 (0.01)	5.73 (0.7)	0.222 (0.03)	0.384 (0.09)
5	9°C	High	0.312	26.7 (3.0)	1.89 (0.18)	1.84 (0.41)	0.060 (0.01)	6.16 (0.7)	0.223 (0.05)	0.465 (0.10)
8	13°C	High	0.327	23.0 (9.0)	1.93 (0.11)	1.38 (0.34)	0.063 (0.01)	5.31 (2.0)	0.227 (0.03)	0.350 (0.09)
9	13°C	High	0.352	23.8 (3.2)	1.95 (0.22)	1.35 (0.17)	0.068 (0.01)	5.50 (0.7)	0.230 (0.05)	0.343 (0.04)

Tank temperature and ration level are also included.

and 0.229, respectively) whereas D_{Sr} values for the low-ration 9°C fish were, on average, 1.5X greater than the high-ration 9°C fish, despite the similar growth rate variation. Similarly, the HSI was, on average, 1.2X greater in the 13°C treatments compared with the 2°C treatments but was 2.8X greater in fish from the high-ration vs. low-ration 9°C treatments. Thus, the difference in condition, as measured by the HSI, reflects the variation in D_{Me} better than somatic or otolith growth.

We identified 21 studies in our literature review of growth and temperature effects on otolith elemental incorporation, which was limited to laboratory studies on larval and juvenile marine and euryhaline fish. Only 10 of these studies explicitly attempted to account for growth vs. temperature effects and only one other study directly manipulated growth through ration (Walther et al., 2010). An important consideration is that most other studies used a correlative approach to examine growth effects within or across temperature treatments (**Tables 1**,**2**).

For magnesium, the most commonly reported finding was no effect or a positive effect of temperature when comparisons did not explicitly account for growth (Gauldie, 1996; DiMaria et al., 2010; Miller, 2011; Stanley et al., 2015). When growth was examined at least somewhat independently, no effect of growth was most common (four studies) with one report of positive and one of negative growth effects on Mg incorporation. Marohn et al. (2011) observed a positive effect of growth for the European eel (*Anguilla anguilla*) but only at 19°C whereas Martin and Thorrold (2005) observed a negative growth effect for juvenile spot (*Leiostomus xanthurus*).

For manganese, there is evidence for positive temperature effects in two species (Marohn et al., 2011; Stanley et al., 2015), no effects in three species (Elsdon and Gillanders, 2002; Martin and Wuenschel, 2006; Miller, 2009) and negative effects for one species (Miller, 2009) although these observations are all potentially confounded by growth variation. However, when attempts to isolate growth effects were made, there are only reports of positive or no effect of growth on elemental incorporation.

For strontium, there are numerous studies with findings of positive, negative, or no effects of temperature; however, the majority of those are also confounded by potential growth effects (**Table 2**). For studies that controlled ration or examined body condition or growth within comparable temperatures, only negative (five of eight studies) or no effects (three of eight) of growth are reported. For example, DiMaria et al. (2010) examined temperature and growth effect on D_{Sr} of larval Pacific cod and observed a negative effect of temperature across temperature treatments, an observation that was confounded by temperature-induced growth variation. Within temperature treatments, there was evidence for a growth effect on D_{Sr} only within the 5°C treatment.

For barium, variable effects of temperature on incorporation, including positive, negative, and no effects, have been reported although most of these are also potentially confounded by growth (**Table 2**). However, similar to Sr, for studies that manipulated ration or examined growth or condition at comparable temperatures, there were no (six of nine studies) or negative (three of nine studies) effects of growth on otolith incorporation reported.

DISCUSSION

The use of otolith chemistry to address ecological questions, such as identification of natal origins or estimation of mixing among groups of individuals, and environmental challenges, such as reconstruction of water temperature or salinity, usually requires the implicit assumption that individual variation in growth has minimal effect on the elemental signatures. While there are some indications that this assumption is not wholly supported in immature (Walther et al., 2010; Marohn et al., 2011; Stanley et al., 2015) or mature (Kalish, 1991; Sadovy and Severin, 1994; Sturrock et al., 2014) fishes, independent evaluations are scarce due to the inherent covariation of temperature and growth in fishes. While we observed a relatively large effect of ration on the incorporation of Mn (+) and Sr (−), there was a relatively small

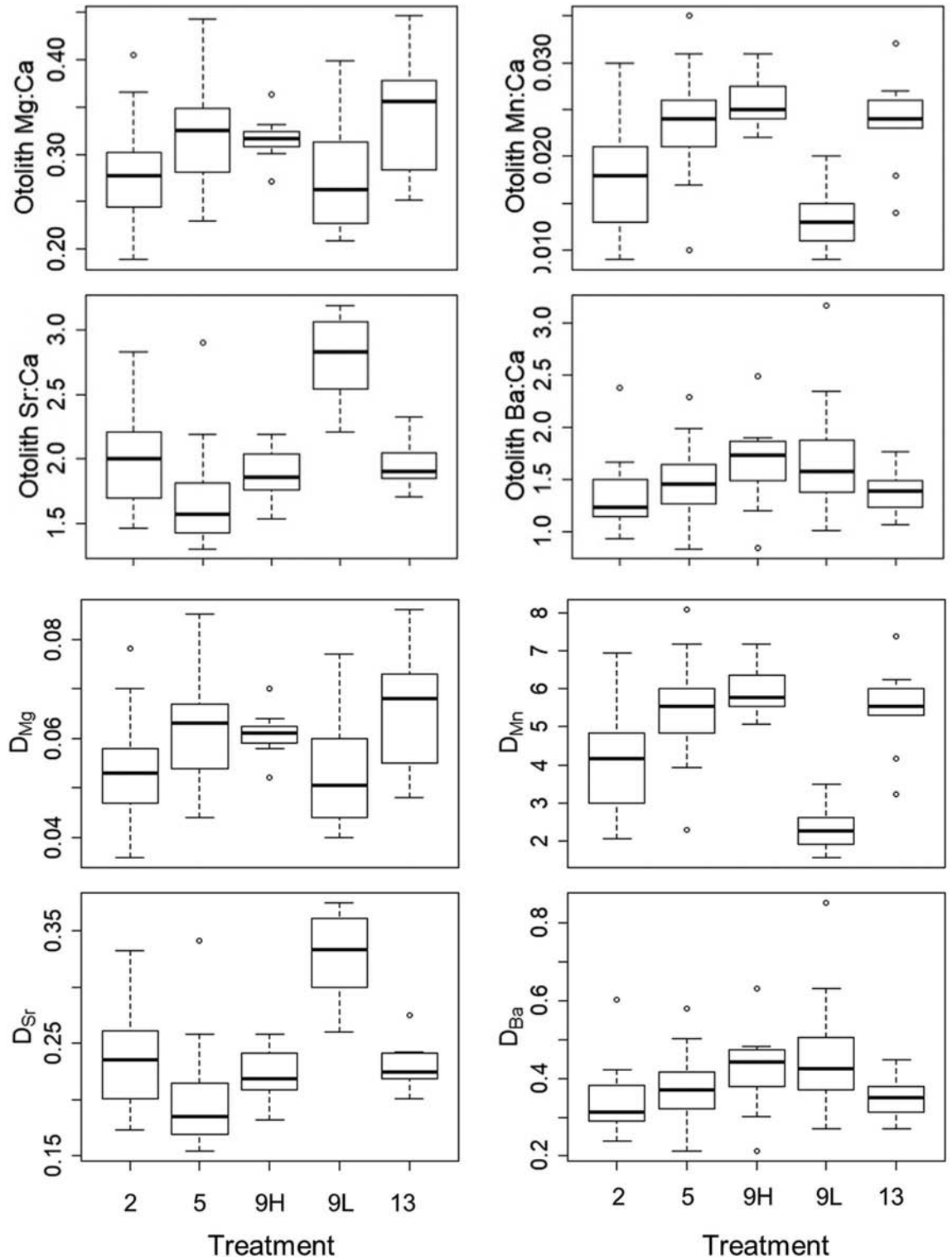

FIGURE 3 | Median, first, and third quartiles and outlying points for otolith Me:Ca (upper four graphs) and D_{Me} (lower four graphs) for the 2, 5, 9_low ration (9L), 9_high ration (9H), and 13°C treatments.

effect for Mg (+), and no effect for Ba. Temperature effects were only observed for D_{Mn} and D_{Mg} and only associated with the 2°C treatments. Furthermore, the data were inconclusive regarding the effect of growth rate within temperature treatments although the observed directionality of the potential growth effects were similar to the ration effect for Mn and for Sr but not for Mg.

TABLE 6 | Correlation coefficients between D_{Me} and specific growth rate (SGR, % body mass per day) and partition coefficients (D_{Me}) for fish within the same treatments.

Temp °C	D_{Mg}	D_{Mn}	D_{Sr}	D_{Ba}	*n*	CV
Specific growth rate (% body mass per day)						
2	0.522	0.583*	−0.640*	−0.230	13	16.2%
5	−0.021	0.242	0.068	0.404	18	6.6%
9H	−0.093	−0.133	−0.400	−0.588*	12	9.6%
9L	0.333	0.170	−0.346	−0.083	18	844.4%
13	−0.673*	0.131	−0.432	−0.244	9	9.8%
Mean otolith increment width (μm)						
2	0.120	0.016	−0.204	0.062	10	21.7%
5	0.358	0.390	−0.152	0.389	15	16.3%
9H	−0.574	0.372	−0.641	−0.251	6	21.8%
9L	0.017	0.282	−0.050	−0.292	18	11.5%
13	−0.737*	−0.365	−0.571	−0.460	7	17.2%

**indicates correlations with $P < 0.05$ and no correlations meet a more conservative P-value adjusted for multiple comparisons. The sample sizes (n) for each comparison and the coefficient of variation for SGR and otolith increment width are included. "9H" and "9L" refer to the high- and low-ration treatments at 9°C.*

The proposed mechanisms by which trace elements become associated with an otolith include: substitution for calcium; trapped in interstitial spaces within the crystal; passive or active association with the organic component; or incorporation as a biochemical co-factor (Campana, 1999; Doubleday et al., 2014; Thomas et al., 2017). Determining definitively which of these processes occurs is challenging. However, several studies have examined elemental concentrations throughout the pathway leading to crystallization, i.e., in the blood, endolymph, and otolith (Kalish, 1991; Payan et al., 1999; Melancon et al., 2009; Sturrock et al., 2014, 2015), while other studies focused on determining which elements were associated with the organic, proteinaceous component of the endolymph and otolith (Miller et al., 2006; Izzo et al., 2016).

Recently, Thomas et al. (2017) used size-exclusion chromatography with inductively coupled plasma mass spectrometry to determine if elements within the endolymph were associated with proteins, present only as free ions, or both. They propose that elements occurring only as free ions (or within the "salt" fraction) are the most likely to be substituted for calcium and therefore reflect environmental variation whereas elements found only associated with proteins (within the "proteinaceous" fraction) would be more likely to be associated with the organic component and to reflect physiological variation. Elements found in both fractions could reflect both environmental and physiological process, thereby complicating interpretation of otolith concentrations. Magnesium and manganese were found only in the salt fraction whereas calcium, strontium, and barium were all found in both the proteinaceous and salt fractions (Thomas et al., 2017). The substitution of other ions for calcium in aragonite appears to be dependent on size with some authors suggesting that those with larger ionic radii than calcium (Sr and Ba) are more likely to substitute (Thomas et al., 2017) whereas others indicate those with smaller ionic radii (Mg) are energetically favored as substitutes (Menadakis et al., 2008). Magnesium has a smaller ionic radius than calcium and could also be trapped within the growing otolith matrix. Thomas et al. (2017) propose that their observation of Mn only in the salt fraction of the endolymph, combined with its potential to form a dimer with an ionic radius similar to calcium, is an indication that Mn otolith incorporation could occur through substitution for calcium. However, several studies have reported Mn associated with otolith proteins (Miller et al., 2006; Izzo et al., 2016; Thomas and Swearer, 2019). Despite the progress made on understanding the mechanisms of otolith elemental incorporation, uncertainty regarding how various factors, such as temperature or growth, influence those mechanisms remains high.

Seasonal variation in plasma or endolymph chemistry has been reported in adult fish (Kalish, 1991; Sturrock et al., 2014, 2015). However, there is less information on seasonality for immature, marine or euryhaline fish. The experimental phase of our study ranged from 40 to 147 d, and the difference in duration between the low- and high-ration 9°C fish, which showed the largest treatment effect, was 16 d. Therefore, it is unlikely the changes due to seasonality could explain our observations although it is not out of the realm of possibility for the temperature effect observed for the 2°C treatment. For mature, female bearded rock cod (*Pseudophycis barbatus*), Kalish (1991) observed that protein, Sr, and Sr:Ca levels in the endolymph, the calcifying fluid in which the otolith grows, all reached their lowest levels in March, which was also when the otolith Sr:Ca reached its nadir. Kalish (1991) concluded that these seasonal patterns were most likely related to changes in protein concentrations and composition within the plasma and endolymph that were associated with reproduction. He noted that changes in endolymph composition associated with gonad development cannot explain otolith Sr:Ca changes in immature fish but postulated that stress could change the protein complement and ultimately affect the relative proportions of calcium and strontium in the endolymph.

Given that the largest incorporation effects in this study were associated with ration rather than growth or temperature, could the pattern be explained by a stress response? We did not assess stress directly, and therefore cannot objectively determine if the low-ration fish were stressed. As noted, stress could alter the protein quantity and composition and ultimately affect the relative proportions of calcium and strontium in the endolymph. Kalish (1989) and Townsend et al. (1992) reported higher otolith Sr:Ca in presumably stressed immature fish with relatively low condition indices compared with unstressed fish that had higher condition indices. Stress in fishes can lead to increased production of hormones, such as corstisol and other glucocorticoids, which can increase permeability of gill and intestinal membranes potentially altering ion transport (Wendelaar Bonga, 1997). If such alterations occurred, they could affect endolymph chemistry and otolith composition. However, studies that examined endolymph chemistry of fish that were stressed through starvation (Payan et al., 1998) or through Cl_2-stress (Payan et al., 2004b) report no change in Ca, sodium (Na), or potassium (K) concentrations within the

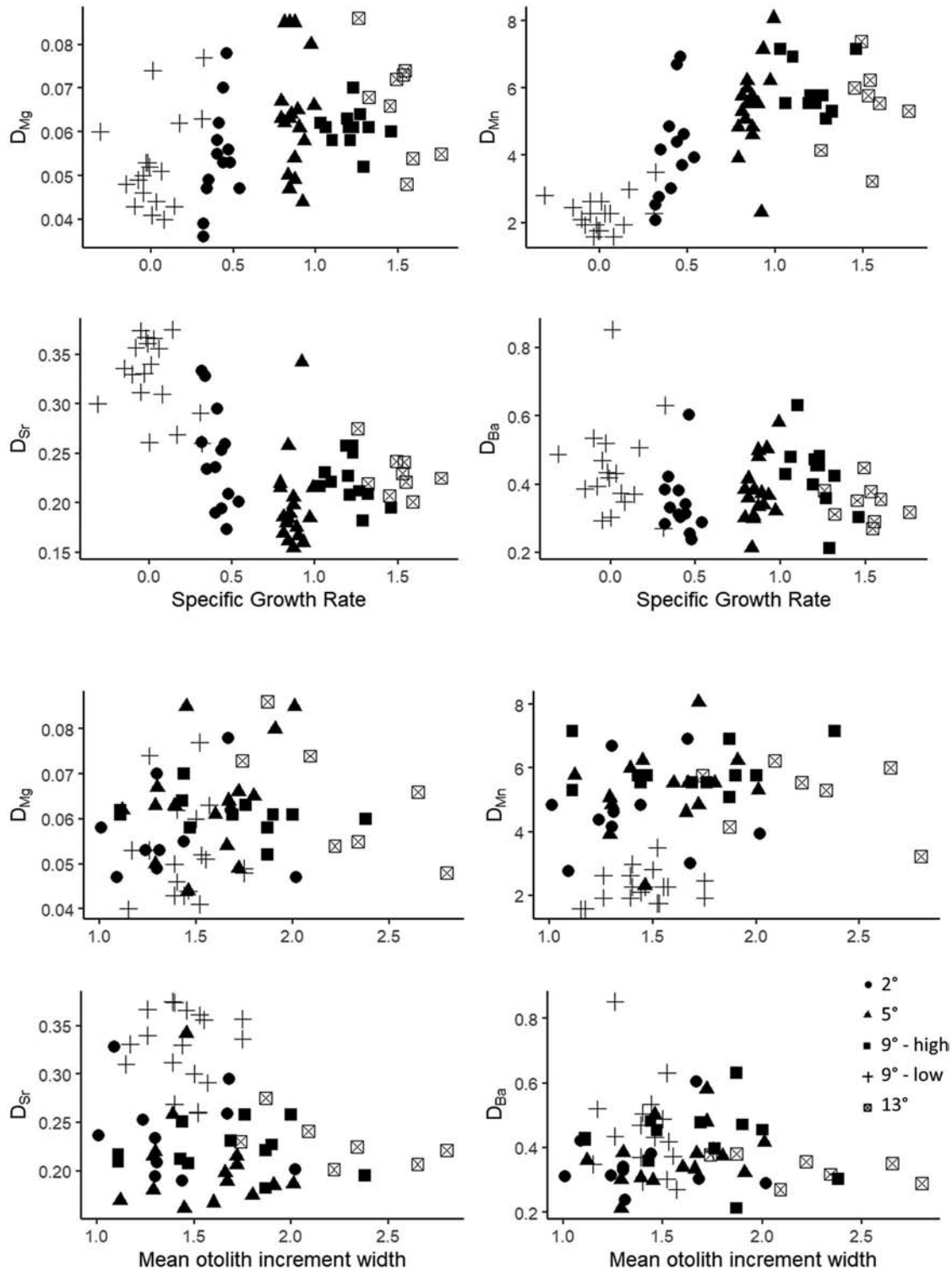

FIGURE 4 | Scatter plot of D_{Me} and specific growth rate (% body mass d^{-1}) for all fish in the 2, 5, 9_low ration (9L), 9_high ration (9H), and 13°C treatments (top four graphs) and for D_{Me} and mean otolith increment width (bottom four graphs).

endolymph. Furthermore, a notable change in endolymph Ca concentrations, which are regulated through active transport and ion exchange, could be expected to similarly affect other elements that can substitute for Ca. However, we observed a negative effect of ration only for $D_{Sr.}$ Alternatively, if the low-ration fish experienced this type of stress response that led to increases in Sr

concentrations while there was a greater level of ion regulation for Ca, it is plausible that the observed increase in D_{Sr} was due to increases in strontium concentrations within the endolymph rather than declines in calcium (Payan et al., 2002, 2004b). Additionally, as noted, the concentration of proteins within the endolymph can vary (Mugiya, 1987; Payan et al., 1999; Edeyer et al., 2000), which could also influence the incorporation of protein-associated elements. If there was a decline in protein concentration within the endolymph associated with the low-ration treatment, that could potentially result in a decline in the incorporation of manganese, which is reported to be associated with matrix proteins (Miller et al., 2006; Izzo et al., 2016; Thomas and Swearer, 2019), in the low-ration fish as we observed.

Overall, we identified modest effects of temperature only for D_{Mn} and D_{Mg}. These relatively small incorporation effects associated with temperature were due entirely to differences in the 2°C treatment and thus appear unlikely to be solely the result of growth variation. For D_{Mn}, we observed a moderate, positive effect of temperature (1.3X) and the relationships between D_{Mn} and somatic and otolith growth were inconclusive. As noted earlier, for the few other studies that attempted to separate growth and temperature effects, there are only reports of positive or no relationships between D_{Mn} and growth (Martin and Thorrold, 2005; Miller, 2009; Marohn et al., 2011; Stanley et al., 2015). For D_{Mg}, we observed a small, positive effect of temperature, a relatively small effect of ration, and no consistent effect of growth on D_{Mg}. In fact, two low-ration fish with relatively high D_{Mg} exhibited the fastest and one of the slowest growth rates in the entire study ($D_{Mg} = 0.77$ and 0.74 and SGR = 0.01 and 0.32% g d^{-1}, respectively). For D_{Sr} and D_{Ba} there was no effect of temperature even though growth rates varied across treatments. Overall, these differences in elemental incorporation associated with ration or temperature do not appear to simply reflect growth variation.

The observed growth variation across treatments was greatest in terms of change in mass, followed by length, with the smallest differences observed for otolith increment width. While this could initially appear incongruous, there are several plausible explanations for the smaller growth effects within the otoliths. Studies report continued otolith deposition during periods of starvation (Campana, 1983; Mosegaard and Titus, 1987) whereas others report continued otolith deposition with a decrease in the frequency of increment formation (Jones and Brothers, 1987; Zhang and Runham, 1992). However, Jones and Brothers (1987) determined that, for striped bass (*Morone saxatilis*), this apparent reduction was likely due to a limited ability to detect increments using light microscopy as daily increments were successfully identified using scanning electron microscopy. Additionally, studies demonstrate a positive relationship between metabolic rate and otolith deposition independent of somatic growth rate (Mosegaard and Titus, 1987; Wright, 1991). In this experiment, the low-ration fish were maintained at 9°C. Therefore, it is plausible that these low-ration fish maintained a relatively high metabolic rate in comparison with the 2 and 5°C fish, which could influence their otolith deposition. Additionally, the process of otolith growth and the deposition of incremental and discontinuous zones is thought to be under circadian control, thus maintained under periods of reduced food (Mugiya, 1984, 1987; Payan et al., 2004a; Thomas and Swearer, 2019). Another observation that indicates otolith deposition occurred in all of our treatments is that the otoliths for these low ration fish were larger than the otoliths of fish of comparable body size in the other treatments, which indicates continued otolith deposition with no or minimal growth.

Our D_{Mn} values were relatively high (2.1–6.2), and exceeded estimates reported from other laboratory studies. Martin and Wuenschel (2006) reported D_{Mn} values just over 1.0 for juvenile gray snapper *Lutjanus griseus* and Miller (2009) documented D_{Mn} values from 0.01 to 0.41 for juvenile black rockfish (*Sebastes melanops*) across a wide range of water concentrations (4.6–118.9 μM M^{-1}). However, Dorval et al. (2007) collected water and juvenile spotted sea trout (*Cynoscion nebulosus*) in Chesapeake Bay and also reported relatively high estimates of D_{Mn}, ranging from 7.7 to 32.8. Their otolith Mn:Ca values (21–40 μM M^{-1}) were similar to or greater than our observations for Pacific cod (12–26.7 μM M^{-1}) with lower or similar water Mn:Ca levels. This relatively large range of D_{Mn} values in wholly marine species indicates that multiple mechanisms could be influencing otolith incorporation of manganese.

An additional consideration with otolith incorporation of Mn is recent work that indicates Mn uptake is related to dissolved oxygen levels, with hypoxia-induced increases in Mn^{+2} due to favorable redox conditions (Limburg et al., 2011, 2015; Limburg and Casini, 2018). Although our dissolved oxygen levels were not constantly monitored in our experiment, values were typically >7 mg L^{-1} and the maximum fish density was <0.75 g L^{-1} with uneaten food biomass <2% of the total fish biomass in each tank. Additionally, there was no evidence in the water samples for elevated Mn in the high-ration treatment. There is also evidence for positive relationships between otolith Mn:Ca and growth: Turner and Limburg (2015) observed positive relationships between otolith growth and otolith Mn:Ca in blueblack (*Alosa aestivalis*) and river herring (*A. pseudoharengus*). Across an ~2.5 to 4x increase in otolith growth, they observed increases in otolith Mn:Ca comparable to or greater than our observed ration effect. Therefore, although multiple lines of evidence support a positive effect of growth on otolith incorporation of Mn, it is not yet entirely clear how growth and temperature, and potentially other factors, interact to regulate this element in otoliths.

Effects of ration, condition, or growth on otolith elemental incorporation have been reported previously. Izzo et al. (2015) isotopically spiked water and evaluated the effects of variable salinity and temperature on otolith elemental incorporation in barramundi (*Lates calcarifer*) and also determined if there were shifts in the percent contribution of food vs. water across treatments. Using a mixed-model approach, they found that temperature and indices of body condition (Fulton's *K* for Sr:Ca) or growth (RNA:DNA for Ba:Ca) combined were the best predictors of otolith chemistry. In their experiment, they observed higher D_{Me} at warmer temperatures (30°C) but fish at

the lower temperature (26°C) were in better condition, which indicates negative effects of condition and positive effects of temperature on otolith incorporation of Sr and Ba. They also observed a reduction in the percent contribution of water to otolith Sr:Ca and Ba:Ca (and an increase in the food contribution) at the lower temperature, which was the treatment with the higher condition fish. The observation of a negative effect of ration and condition on D_{Sr} is similar to our results as well as those of Walther et al. (2010), who reported a negative effect of ration on D_{Sr} and D_{Ba} in juvenile spotted chromis (*Acanthochromis polycanthus)* and observed negative relationships between fish growth and D_{Sr} and D_{Ba}. Therefore, for the few studies that manipulated or evaluated the effects of ration, there are consistently negative effects of increased ration, higher condition, or elevated growth on D_{Sr} and some consistency (two out of three studies) for D_{Ba}. Combined with our observations of positive effects of ration on D_{Mn}, these findings indicate that there may be stress-, condition-, or nutrition-mediated effects on otolith elemental incorporation, at least for some elements.

An important question is whether or not it is reasonable to expect a general pattern for growth effects on elemental incorporation to emerge if enough species are studied. Given the structural differences in calcium carbonate morphology (trigonal, orthorhombic, and hexagonal) across crystal types (calcite, aragonite, vaterite) and the observations of variable growth effects across crystal types (De Choudens-Sánchez and González, 2009), comparisons with abiotic aragonite, which is the common morphology of sagittae, are the most relevant. Experimental manipulations of abiotic aragonite have demonstrated that incorporation of alkaline earth cations (Mg^{+2}, Ca^{+2}, Sr^{+2}, and Ba^{+2}) have an inverse relationship with temperature (Gaetani and Cohen, 2006). Furthermore, aragonite precipitation rate also influenced elemental incorporation rates with positive effects for Mg:Ca and negative effects for Sr:Ca and Ba:Ca, and models that reconstruct temperature based on Me:Ca in coral aragonite were improved by inclusion of these precipitation rate effects (Gaetani et al., 2011). Therefore, it does not seem unreasonable to expect some consistent patterns to emerge in regard to growth rate effects on otolith elemental incorporation.

Given the collective evidence currently available, there is support for ration, growth, or condition effects on otolith elemental incorporation, at least for Mn, Sr, and Ba. Therefore, there are some clear recommendations. Otoliths are growth structures that, in most cases, require extensive preparation prior to elemental analysis. Despite the effort involved in preparing otoliths for chemical analysis, which could also be used to generate estimates of otolith and somatic growth, many studies do not report any estimates of somatic or otolith growth and compare fish across relatively large ranges of size, ages and growth rates [but see (Darnaude et al., 2014; Bouchoucha et al., 2018)]. Our understanding of the factors influencing otolith elemental incorporation would be enhanced by the inclusion of somatic and/or otolith growth rates and consideration of body condition, whenever feasible, in both laboratory and field studies. This type of information could advance the understanding of factors influencing otolith chemistry. Additionally, other approaches to manipulate growth rates and condition, such as by manipulating activity levels, could help further disentangle the related aspects of temperature, growth, condition, and feeding rates and advance the understanding and utility of a powerful methodology in fisheries and ecological science.

DATA AVAILABILITY STATEMENT

The datasets generated for this study are available on request to the corresponding author.

ETHICS STATEMENT

Ethical review and approval was not required for the animal study because This experiment was conducted in NOAA's Alaska Fisheries Science Center Laboratory in Newport, Oregon. This research was carried out in accordance with all applicable institutional and national guidelines at the time that the study was conducted; all work followed American Fisheries Society policies on the Guidelines for Use of Fishes in Research (https://fisheries.org/docs/policy_useoffishes.pdf) and AVMA (American Veterinary Medical Association) Guidelines on Euthanasia (https://olaw.nih.gov/sites/default/files/Euthanasia2007.pdf). Fish were collected under permit CF-09-081 from the Alaska Department of Fish and Game. There was no formal ethics review of this study because NOAA National Marine Fisheries Service does not have an Institutional Animal Care and Use Committee (IACUC) or an ethics approval processes for research on fishes and, at the time of this study (2009–2010), OSU's IACUC did not provide review of research that was completed in US federal facilities.

AUTHOR CONTRIBUTIONS

JM and TH conceived of and executed the research, analyzed the data, and wrote the manuscript. TH led the laboratory experiment. JM completed the otolith and water analyses.

FUNDING

Experiment was supported North Pacific Research Board grant no. R0816.

ACKNOWLEDGMENTS

The laboratory experiment was performed with support from M. Ottmar, M. Spencer, S. Haines, and R. DiMaria. Thomas Murphy provided assistance with otolith preparation. We appreciate the comments of three reviewers on an earlier version of this manuscript.

SUPPLEMENTARY MATERIAL

The Supplementary Material for this article can be found online at: https://www.frontiersin.org/articles/10.3389/fmars.2020.00320/full#supplementary-material

Figure S1 | Scatter plot of D_{Me} and Hepatic Somatic Index (HSI) for all fish in the 2, 5, 9_low ration (9L), 9_high ration (9H), and 13°C treatments.

Figure S2 | Median, first, and third quartiles and outlying points for otolith Me:Ca (upper four graphs) and D_{Me} (lower four graphs) for each tank. Axis labels indicate the temperature followed by the tank number (e.g., 2.1 = 2°C treatment, tank 1).

Table S1 | Water chemistry during experiment. Values represent the mean based on samples collected from two tanks on each day. For Ba:Ca and Mn:Ca, all standard deviations were less than 0.005. In order to calculate partition coefficients (DMe), water values were averaged based on duration of experiment within each treatment. Values were averaged from 10 Dec 09 to 09 Jan 10 for the 9 and 13°C full ration treatments, from 10 Dec 09 to 01 Feb 10 for the 9_low °C restricted ration treatment, from 10 Dec 09 to 24 Feb 10 for the 5°C treatment, and from 10 Dec 09 to 25 Apr 10 for the 2°C treatment. "All" = 2, 5, 9_low, 9_high, and 13°C treatments.

Table S2 | Results of the one-way Analyses of Variance completed to evaluate the effect of treatment (A) on fish length, specific growth rate, otolith increment width, and hepatosomatic index and the effect of temperature (B) or ration (C) on partition coefficients (DMe).

REFERENCES

American Veterinary Medical Association (AVMA) (2007). *Guidelines on Euthanasia*. Available online at: https://olaw.nih.gov/sites/default/files/Euthanasia2007.pdf (accessed December 15, 2019).

Barnes, T. C., and Gillanders, B. M. (2013). Combined effects of extrinsic and intrinsic factors on otolith chemistry: implications for environmental reconstructions. *Can. J. Fish. Aquat. Sci.* 70, 1159–1166. doi: 10.1139/cjfas-2012-0442

Bath, G. E., Thorrold, S. R., Jones, C. M., Campana, S. E., McLaren, J. W., and Lam, J. W. H. (2000). Strontium and barium uptake in aragonitic otoliths of marine fish. *Geochim. Cosmochim. Acta* 64, 1705–1714. doi: 10.1016/S0016-7037(99)00419-6

Bouchoucha, M., Brach-Papa, C., Gonzalez, J.-L., Lenfant, P., and Darnaude, A. M. (2018). Growth, condition and metal concentration in juveniles of two *Diplodus* species in ports. *Mar. Poll. Bull.* 126, 31–42. doi: 10.1016/j.marpolbul.2017.10.086

Buckel, J. A., Sharack, B. L., and Zdanowicz, V. S. (2004). Effect of diet on otolith composition in *Pomatomus saltatrix*, an estuarine piscivore. *J. Fish Biol.* 64, 1469–1484. doi: 10.1111/j.0022-1112.2004.00393.x

Campana, S. E. (1983). Feeding periodicity and the production of daily growth increments in the otoliths of steelhead trout (*Salmo gairdneri*) and starry flounder (*Platichthys stellatus*). *Can. J. Zool.* 61, 1591–1597. doi: 10.1139/z83-214

Campana, S. E. (1999). Chemistry and composition of fish otoliths: pathways, mechanisms, and applications. *Mar. Ecol. Prog. Ser.* 188, 263–297. doi: 10.3354/meps188263

Chesney, E. J., McKee, B. M., Blanchard, T., and Chan, L. C. (1998). Chemistry of otoliths from juvenile menhaden *Brevoortia patronus*: evaluating strontium, strontium:calcium and strontium isotope ratios as environmental indicators. *Mar. Ecol. Prog. Ser.* 171, 261–273. doi: 10.3354/meps171261

Darnaude, A. M., Sturrock, A., Trueman, C. N., Mouillot, D., E. I. M. F., Campana, S. E., et al. (2014). Listening in on the past: what can otolith delta O-18 values really tell us about the environmental history of fishes? *PLOS ONE* 9:e114951. doi: 10.1371/journal.pone.0108539

De Choudens-Sánchez, V., and González, L. A. (2009). Calcite and aragonite precipitation under Controlled instantaneous supersaturation: elucidating the role of CaCO3 saturation state and Mg/Ca ratio on calcium carbonate polymorphism. *J. Sediment. Res.* 79, 363–376. doi: 10.2110/jsr.2009.043

DiMaria, R. A., Miller, J. A., and Hurst, T. P. (2010). Temperature and growth effects on otolith elemental chemistry of larval Pacific cod, *Gadus macrocephalus*. *Environ. Biol. Fish.* 89, 453–462. doi: 10.1007/s10641-010-9665-2

Dorval, E., Jones, C. M., Hannigan, R., and van Montfrans, J. (2007). Relating otolith chemistry to surface water chemistry in a coastal plain estuary. *Can. J. Fish. Aquat. Sci.* 64, 411–424. doi: 10.1139/f07-015

Doubleday, Z. A., Harris, H. H., Izzo, C., and Gillanders, B. M. (2014). Strontium randomly substituting for calcium in fish otolith aragonite. *Anal. Chem.* 86, 865–869. doi: 10.1021/ac4034278

Edeyer, A., de Pontual, H., Payan, P., Troadec, H., Severe, A., and Mayer-Gostan, N. (2000). Daily variations of the saccular endolymph and plasma compositions in the turbot *Psetta maxima*: relationship with the diurnal rhythm in otolith formation. *Mar. Ecol. Prog. Ser.* 192, 287–294. doi: 10.3354/meps192287

Elsdon, T. S., and Gillanders, B. M. (2002). Interactive effects of temperature and salinity on otolith chemistry: challenges for determining environmental histories of fish. *Can. J. Fish. Aquat. Sci.* 59, 1796–1808. doi: 10.1139/f02-154

Elsdon, T. S., and Gillanders, B. M. (2003). Relationship between water and otolith elemental concentrations in juvenile black bream *Acanthopagrus butcheri*. *Mar. Ecol. Prog. Ser.* 260, 263–272. doi: 10.3354/meps260263

Elsdon, T. S., and Gillanders, B. M. (2004). Fish otolith chemistry influenced by exposure to multiple environmental variables. *J. Exp. Mar. Biol. Ecol.* 313, 269–284. doi: 10.1016/j.jembe.2004.08.010

Gaetani, G. A., and Cohen, A. L. (2006). Element partitioning during precipitation of aragonite from seawater: a framework for understanding paleoproxies. *Geochim. Cosmochim. Acta* 70, 4617–4634. doi: 10.1016/j.gca.2006.07.008

Gaetani, G. A., Cohen, A. L., Wang, Z., and Crusius, J. (2011). Rayleigh-based, multi-element coral thermometry: A biomineralization approach to developing climate proxies. *Geochim. Cosmochim. Acta* 75, 1920–1932. doi: 10.1016/j.gca.2011.01.010

Gallahar, N. K., and Kingsford, M. J. (1996). Factors influencing Sr/Ca ratios in otoliths of *Girella elevata*: An experimental investigation. *J. Fish. Biol.* 48, 174–186. doi: 10.1111/j.1095-8649.1996.tb01111.x

Gauldie, R. W. (1996). Effects of temperature and vaterite replacement on the chemistry of metal ions in the otoliths of *Oncorhynchus tshawytscha*. *Can. J. Fish. Aquat. Sci.* 53, 2015–2026. doi: 10.1139/cjfas-53-9-2015

Gibson-Reinemer, D. K., Johnson, B. M., Martinez, P. J., Winkelman, D. L., Koenig, A. E., and Woodhead, J. D. (2009). Elemental signatures in otoliths of hatchery rainbow trout (*Oncorhynchus mykiss*): distinctiveness and utility for detecting origins and movement. *Can. J. Fish. Aquat. Sci.* 66, 513–524. doi: 10.1139/F09-015

Hoff, G. R., and Fuiman, L. A. (1995). Environmentally induced variation in elemental composition of red drum (*Sciaeops ocellatus*) otoliths. *Bull. Mar. Sci.* 56, 578–591.

Holcomb, M., Cohen, A. L., Gabitov, R. I., and Hutter, J. L. (2009). Compositional and morphological features of aragonite precipitated experimentally from seawater and biogenically by corals. *Geochim. Cosmochim. Acta* 73, 4166–4179. doi: 10.1016/j.gca.2009.04.015

Hurst, T. P., Laurel, B. J., and Ciannelli, L. (2010). Ontogenetic patterns and temperature-dependent growth rates in early life stages of Pacific cod (*Gadus macrocephalus*). *Fish Bull NOAA* 108, 382–392.

Hurst, T. P., Munch, S.B., and Lavelle, K. (2012). Thermal reaction norms for growth vary among cohorts of Pacific cod (*Gadus macrocephalus*). *Mar. Biol.* 159, 2173–2183. doi: 10.1007/s00227-012-2003-9

Izzo, C., Doubleday, Z. A., and Gillanders, B. M. (2016). Where do elements bind within the otoliths of fish? *Mar. Freshw. Res.* 67, 1072–1076. doi: 10.1071/MF15064

Izzo, C., Doubleday, Z. A., Woodcock, S. H., and Gillanders, B. M. (2015). Contribution of water chemistry and fish condition to otolith chemistry: comparisons across salinity environments. *J. Fish Biol.* 86, 1680–1698. doi: 10.1111/jfb.12672

Izzo, C., Reis-Santos, P., and Gillanders, B. M. (2018). Otolith chemistry does not just reflect environmental conditions: a meta-analytic evaluation. *Fish Fisher.* 19, 441–454. doi: 10.1111/faf.12264

Jones, C., and Brothers, E. B. (1987). Validation of the otolith increment aging technique for striped bass, *Morone saxatilis*, larvae reared under suboptimal feeding conditions. *Fish. Bull.* 85, 171–178.

Kalish, J. M. (1989). Otolith microchemistry: validation of the effects of physiology, age, and environment on otolith composition. *J. Exp.Mar. Biol.Ecol.* 132, 151–178.

Kalish, J. M. (1991). Determinants of otolith chemistry: seasonal variation in the composition of blood plasma, endolymph and otolith of the beared rock cod *Pseudophycis barbatus*. *Mar. Ecol. Prog. Ser.* 74, 137–159. doi: 10.3354/meps074137

Limburg, K. E., and Casini, M. (2018). Effect of marine hypoxia on Baltic Sea cod *Gadus morhua*: Evidence from otolith chemical proxies. *Front. Mar. Sci.* 5:482. doi: 10.3389/fmars.2018.00482

Limburg, K. E., Olson, C., Walther, Y., Dale, D., Slomp, C. P., and Høie, H. (2011). Tracking Baltic hypoxia and cod migration over millennia with natural tags. *Proc. Natl. Acad. Sci. U.S.A.* 108, E177–E182. doi: 10.1073/pnas.1100684108

Limburg, K. E., Walther, B. D., Lu, Z., Jackman, G., Mohan, J., Walther, Y., et al. (2015). In search of the dead zone: Use of otoliths for tracking fish exposure to hypoxia. *J. Mar. Sys.* 141, 167–178. doi: 10.1016/j.jmarsys.2014.02.014

Lopez, O., Zuddas, P., and Faivre, D. (2009). The influence of temperature and seawater composition on calcite crystal growth mechanisms and kinetics: Implications for Mg incorporation in calcite lattice. *Geochim. Cosmochim. Acta* 73, 337–347. doi: 10.1016/j.gca.2008.10.022

Marchitto, T. M., Bryan, S. P., Doss, W., McCulloch, M. T., and Montagna, P. (2018). A simple biomineralization model to explain Li, Mg, and Sr incorporation into aragonitic foraminifera and corals. *Earth Planet. Sc. Lett.* 481, 20–29. doi: 10.1016/j.epsl.2017.10.022

Marohn, L., Hilge, V., Zumholz, K., Klügel, A., Anders, H., and Hanel, R. (2011). Temperature dependency of element incorporation into European eel (*Anguilla anguilla*) otoliths. *Anal. Bioanal. Chem.* 399, 2175–2184. doi: 10.1007/s00216-010-4412-2

Martin, G. B., and Thorrold, S. R. (2005). Temperature and salinity effects on magnesium, manganese, and barium incorporation in otoliths of larval and early juvenile spot *Leiostomus xanthurus*. *Mar. Ecol. Prog. Ser.* 293, 223–232. doi: 10.3354/meps293223

Martin, G. B., Thorrold, S. R., and Jones, C. M. (2004). Temperature and salinity effects on strontium incorporation in otoliths of larval spot (*Leiostomus xanthurus*). *Can. J. Fish. Aquat. Sci.* 61, 34–42. doi: 10.1139/f03-143

Martin, G. B., and Wuenschel, M. J. (2006). Effect of temperature and salinity on otolith element incorporation in juvenile gray snapper *Lutjanus griseus*. *Mar. Ecol. Prog. Ser.* 324, 229–239. doi: 10.3354/meps324229

Melancon, S., Fryer, B. J., and Markham, J. L. (2009). Chemical analysis of endolymph and the growing otolith: Fractionation of metals in freshwater fish species. *Environ. Toxic. Chem.* 28, 1279–1287. doi: 10.1897/08-358.1

Menadakis, M., Maroulis, G., and Koutsoukos, P. G. (2008). Incorporation of Mg^{2+}, Sr^{2+}, Ba^{2+} and Zn^{2+} into aragonite and comparison with calcite. *J.Math. Chem.* 46:484. doi: 10.1007/s10910-008-9490-4

Miller, J. A. (2009). The effects of temperature and water concentration on the otolith incorporation of barium and manganese in black rockfish *Sebastes melanops*. *J. Fish. Biol.* 75, 39–60. doi: 10.1111/j.1095-8649.2009.02262.x

Miller, J. A. (2011). Effects of water temperature and barium concentration on otolith composition along a salinity gradient: implications for migratory history. *J. Exp. Mar. Biol. Ecol.* 405, 42–52. doi: 10.1016/j.jembe.2011.05.017

Miller, M. B., Clough, A. M., Batson, J. N., and Vachet, R. W. (2006). Transition metal binding to cod otolith proteins. *J. Exp. Mar. Biol. Ecol.* 329, 135–143. doi: 10.1016/j.jembe.2005.08.016

Mitsuguchi, T., Matsumoto, E., and Uchida, T. (2003). Mg/Ca and Sr/Ca ratios of Porites coral skeleton: Evaluation of the effect of skeletal growth rate. *Coral Reefs* 22, 381–388. doi: 10.1007/s00338-003-0326-1

Morse, J. W., and Bender, M. L. (1990). Partition coefficients in calcite: examination of factors influencing the validity of experimental results and their application to natural systems. *Chem. Geol.* 82, 265–277. doi: 10.1016/0009-2541(90)90085-L

Mosegaard, H., and Titus, R. (1987). "Daily growth rates of otoliths in yolk sac fry of two salmonid species at five different temperatures," in *Proceedings of the Fifth Conference of European Ichthyologists*, eds S. O. Kallender and B. Fernholm. Stockholm: Swedish Museum of Natural History, 221–227.

Mugiya, Y. (1984). Diurnal rhythm in otolith formation in the rainbow trout *Salmo gairdneri*: seasonal reversal of the rhythm in relation to plasma calcium concentration. *Comp. Biochem. Physiol.* 78A, 289–293. doi: 10.1016/0300-9629(84)90149-X

Mugiya, Y. (1987). Phase difference between calcification and organic matrix formation in the diurnal growth of otoliths in the Rainbow trout, *Salmo gairdneri*. *Fish. Bull.* 85, 395–401.

Narimatsu, Y., Hattori, T., Ueda, Y., Matsuzaka, H., and Shiogaki, M. (2007). Somatic growth and otolith microstructure of larval and juvenile Pacific cod *Gadus macrocephalus*. *Fish. Sci.* 73:1257–1264. doi: 10.1111/j.1444-2906.2007.01463.x

Payan, P., Borelli, G., Boeuf, G., and Mayer-Gostan, N. (1998). Relationship between otolith and somatic growth: consequence of starvation on acid-base balance in plasma and endolymph in the rainbow trout *Oncorhynchus mykiss*. *Fish Physiol. Biochem.* 19, 35–41. doi: 10.1023/A:1016064813517

Payan, P., Borelli, G., Priouzeau, F., De Pontual, H., Bœuf, G., and Mayer-Gostan, N. (2002). Otolith growth in trout *Oncorhynchus mykiss*: supply of $Ca2^{+}$ and $Sr2^{+}$ to the saccular endolymph. *J. Exp. Biol.* 205, 2687–2695.

Payan, P., De Pontual, H., Bœuf, G., and Mayer-Gostan, N. (2004a). Endolymph chemistry and otolith growth in fish. *Gen. Palaeont.* 3, 535–547. doi: 10.1016/j.crpv.2004.07.013

Payan, P., Edeyer, A., De Pontual, H., Borelli, G., Boeuf, G., and Mayer-Gostan, N. (1999). Chemical composition of saccular endolymph and otolith in fish inner ear: lack of spatial uniformity. *Am. J. Physiol.* 277, 123–131. doi: 10.1152/ajpregu.1999.277.1.R123

Payan, P., Pontual, H. D., Edeyer, A., Borelli, G., Boeuf, G., and Mayer-Gostan, N. (2004b). Effects of stress on plasma homeostasis, endolymph chemistry, and check formation during otolith growth in rainbow trout (*Oncorhynchus mykiss*). *Can. J. Fish. Aquat. Sci.* 61, 1247–1255. doi: 10.1139/f04-059

Radtke, R. L. (1989). Strontium-calcium concentration ratios in fish otoliths as environmental indicators. *Comp. Biochem. Physiol. A* 92, 189–193. doi: 10.1016/0300-9629(89)90151-5

Reis-Santos, P., Tanner, S. E., Elsdon, T. S., Cabral, H. N., and Gillanders, B. M. (2013). Effects of temperature, salinity and water composition on otolith elemental incorporation of *Dicentrarchus labrax*. *J. Exp. Mar. Biol. Ecol.* 446, 245–252. doi: 10.1016/j.jembe.2013.05.027

Sadovy, Y., and Severin, K. P. (1994). Elemental patterns in Red Hind (*Epinephelus guttatus*) otoliths from Bermuda and Puerto Rico reflect growth rate, not temperature. *Can. J. Fish. Aquat. Sci.* 51, 133–141. doi: 10.1139/f94-015

Schloesser, R. W., Rooker, J. R., Louchuoarn, P., Neilson, J. D., and Secor, D. H. (2009). Interdecadal variation in seawater delta C-13 and delta O-18 recorded in fish otoliths. *Limnol. Oceanogr.* 54, 1665–1668. doi: 10.4319/lo.2009.54.5.1665

Stanley, R. R. E., Bradbury, I. R., DiBacco, C., Snelgrove, P. V. R., Thorrold, S. R., and Killen, S. S. (2015). Environmentally mediated trends in otolith composition of juvenile Atlantic cod (*Gadus morhua*). *ICES J. Mar. Sci.* 72, 2350–2363. doi: 10.1093/icesjms/fsv070

Sturrock, A. M., Hunter, E., Milton, J. A., Johnson, R. C., Waring, C. P., Trueman, C. N., et al. (2015). Quantifying physiological influences on otolith microchemistry. *Methods Ecol. Evol.* 6, 806–816. doi: 10.1111/2041-210X.12381

Sturrock, A. M., Trueman, C. N., Milton, J. A., Waring, C. P., Cooper, M. J., and Hunter, E. (2014). Physiological influences can outweigh environmental signals in otolith microchemistry research. *Mar. Ecol. Prog. Ser.* 500, 245–264. doi: 10.3354/meps10699

Thomas, O. R. B., Ganio, K., Roberts, B. R., and Swearer, S. E. (2017). Trace element protein interactions in endolymph from the inner ear of fish: implications for environmental reconstructions using fish otolith chemistry. *Metallomics* 9, 239–249. doi: 10.1039/C6MT00189K

Thomas, O. R. B., and Swearer, S. E. (2019). Otolith biochemistry—A review. *Rev. Fish. Sci. Aquacul.* 27, 458–489. doi: 10.1080/23308249.2019.1627285

Townsend, D. W., Radtke, R. L., Corwin, S., and Libby, D. A. (1992). Strontium:calcium ratios in juvenile Atlantic herring *Clupea harengus* L. otoliths as a function of water temperature. *J. Exp. Mar. Biol.Ecol.* 160, 131–140. doi: 10.1016/0022-0981(92)90115-Q

Turner, S. M., and Limburg, K. E. (2015). Does daily growth affect the rate of manganese uptake in juvenile River Herring otoliths? *Trans. Amer. Fish. Soc.* 144, 873–881. doi: 10.1080/00028487.2015.1059888

Walsh, C. T., and Gillanders, B. M. (2018). Extrinsic factors affecting otolith chemistry – implications for interpreting migration patterns in a diadromous fish. *Environ. Biol. Fish.* 101, 905–916. doi: 10.1007/s10641-018-0746-y

Walther, B., Kingsford, M. J., O'Callaghan, M. D., and McCulloch, M. T. (2010). Interactive effects of ontogeny, food ration and temperature on elemental incorporation in otoliths of a coral reef fish. *Environ. Biol. Fish*. 89, 441–451. doi: 10.1007/s10641-010-9661-6

Webb, S. D., Woodcock, S. H., and Gillanders, B. M. (2012). Sources of otolith barium and strontium in estuarine fish and the influence of salinity and temperature. *Mar. Ecol. Prog. Ser.* 453, 189–199. doi: 10.3354/meps09653

Wendelaar Bonga, S. E. (1997). The stress response in fish. *Physiol. Rev*. 77, 591–625. doi: 10.1152/physrev.1997.77.3.591

Wright, P. J. (1991). The influence of metabolic rate on otolith increment width in Atlantic salmon parr, *Salmo salar* L. *J. Fish Biol.* 38, 929–933. doi: 10.1111/j.1095-8649.1991.tb03632.x

Wurster, C. M., and Patterson, W. P. (2001). Late Holocene climate change for the eastern interior United States: Evidence from high-resolution δ18O values of sagittal otoliths. *Palaeogeogr. Palaeoclimatol.* 170, 81–100. doi: 10.1016/S0031-0182(01)00229-2

Yamada, S. B., and Mulligan, T. J. (1982). Strontium marking of hatchery reared coho salmon *Oncorhynchus kisutch* identification of adults. *J. Fish Biol.* 20, 5–10. doi: 10.1111/j.1095-8649.1982.tb03889.x

Zhang, Z., and Runham, N. W. (1992). Effects of food ration and temperature level on the growth of *Oreochromis niloticus* (L.) and their otoliths. *J. Fish Biol*. 40, 341–349. doi: 10.1111/j.1095-8649.1992.tb02581.x

Disclaimer: Reference to trade names does not imply endorsement by the National Marine Fisheries Service. The findings in this paper are those of the authors an do not necessarily reflect the views of the National Marine Fisheries Service.

Conflict of Interest: The authors declare that the research was conducted in the absence of any commercial or financial relationships that could be construed as a potential conflict of interest.

Copyright © 2020 Miller and Hurst. This is an open-access article distributed under the terms of the Creative Commons Attribution License (CC BY). The use, distribution or reproduction in other forums is permitted, provided the original author(s) and the copyright owner(s) are credited and that the original publication in this journal is cited, in accordance with accepted academic practice. No use, distribution or reproduction is permitted which does not comply with these terms.

frontiers in Marine Science

ORIGINAL RESEARCH
published: 19 June 2020
doi: 10.3389/fmars.2020.00421

First Insights Into the Growth and Population Structure of *Cottoperca trigloides* (Perciformes, Bovichtidae) From the Southwestern Atlantic Ocean

María Eugenia Lattuca[1], Facundo Llompart[1,2], Esteban Avigliano[3], Marta Renzi[4], Ileana De Leva[4], Claudia Clementina Boy[1], Fabián Alberto Vanella[1], María Eugenia Barrantes[1], Daniel Alfredo Fernández[1,2] and Cristiano Queiroz de Albuquerque[5]*

[1] Laboratorio de Ecología, Fisiología y Evolución de Organismos Acuáticos, Centro Austral de Investigaciones Científicas (CADIC – CONICET), Ushuaia, Argentina, [2] Instituto de Ciencias Polares, Ambiente y Recursos Naturales (UNTDF – ICPA), Universidad Nacional de Tierra del Fuego, Ushuaia, Argentina, [3] Facultad de Ciencias Veterinarias – CONICET, Instituto de Investigaciones en Producción Animal (INPA, UBA – CONICET), Universidad de Buenos Aires, Buenos Aires, Argentina, [4] Instituto Nacional de Investigación y Desarrollo Pesquero (INIDEP), Mar del Plata, Argentina, [5] Departamento de Ciências Animais, Universidade Federal Rural do Semi-Arido (UFERSA), Mossoró, Brazil

OPEN ACCESS

Edited by:
Stelios Katsanevakis,
University of the Aegean, Greece

Reviewed by:
Jessica Miller,
Oregon State University,
United States
Audrey J. Geffen,
University of Bergen, Norway

***Correspondence:**
María Eugenia Lattuca
elattuca@gmail.com

Specialty section:
This article was submitted to Marine Ecosystem Ecology, a section of the journal Frontiers in Marine Science

Received: 20 December 2019
Accepted: 14 May 2020
Published: 19 June 2020

Citation:
Lattuca ME, Llompart F, Avigliano E, Renzi M, De Leva I, Boy CC, Vanella FA, Barrantes ME, Fernández DA and de Albuquerque CQ (2020) First Insights Into the Growth and Population Structure of Cottoperca trigloides (Perciformes, Bovichtidae) From the Southwestern Atlantic Ocean. Front. Mar. Sci. 7:421. doi: 10.3389/fmars.2020.00421

The aim of this work was to describe the growth of *Cottoperca trigloides*, a notothenioid species with a non-Antarctic distribution, and to test the existence of different nursery areas and fish stocks through changes in the otolith elemental composition. Fish were collected during spring 2009 over the Patagonia continental shelf, including the Marine Protected Area Namuncurá/Burdwood Bank, in the southwestern Atlantic Ocean. The age and growth analyses were performed by counting marks in *sagittae*, assuming an annual periodicity of their deposition, and identified 8-year classes (0+ to 7+). Given the size range of the fish, length-at-age data were fitted to the Gompertz growth model TL_t = 55.45 [exp ((exp) –0.32 (t – 1.89))], explaining more than 95% of the growth pattern. Moreover, the chemical composition of otolith core and edge areas was analyzed by laser ablation inductively coupled plasma mass spectrometry. The canonical analysis of principal coordinates successfully allocated 72.92% of the fish for the core and 91.67% for the edge area of the otolith, in three groups corresponding to "northern Patagonia shelf," "southern Patagonia shelf," and "Marine Protected Area Namuncurá/Burdwood Bank" areas, suggesting a high segregation among them over the Patagonian shelf. Thus, otolith elemental composition has proven to be an efficient approach to identify different nursery areas and stocks for the species. The present results provide new information on the growth and the population structure of *C. trigloides*, from a geographical area where information on this issue is still scarce, constituting an essential tool to develop conservation principles for the species.

Contribution INIDEP N° 2211

Keywords: age determination, *Cottoperca trigloides*, fish stocks, growth, MPA Namuncurá/Burdwood Bank, nursery areas, otolith chemistry, southwestern Atlantic Ocean

INTRODUCTION

Cottoperca trigloides (Forster, 1801) is the unique species of the family Bovichtidae (Balushkin, 2000; Eastman and Eakin[1], version December 30, 2019), the members of which are atypical notothenioids in having a largely non-Antarctic distribution (Eastman, 1993). This species has been reported from 41° to 54°S over the southeastern Pacific and the southwestern Atlantic Oceans (the Patagonian region of Chile and Argentina), including the Strait of Magellan, the Beagle Channel, the Burdwood Bank, the Staten Island, and the Malvinas/Falklands Islands (Lloris and Rucabado, 1991; Fernández et al., 2009). Although its bathymetric distribution was indicated between 10 and 270 m depth (Lloris and Rucabado, 1991), Laptikhovsky and Arkhipkin (2003) also pointed out that *C. trigloides* is commonly found between 150 and 400 m, in the outer shelf and slope around the Malvinas/Falklands Islands. According to the fishery statistics of these islands, the incidental catch of the species was 48.4 tons during 2018 (Falkland Islands Government [FIG], 2019). Despite its abundance and its quite remarkable bycatch during finfish and squid trawl fishing, data on its biology are still scarce. To date, it is known that *C. trigloides* is a benthic ambush predator, feeding mainly on fish, small crustaceans, and algae (Moreno and Jara, 1984; Matallanas, 1988; Lloris and Rucabado, 1991; Laptikhovsky and Arkhipkin, 2003). Arkhipkin et al. (2015) also described the spawning and early ontogeny of the species under captivity conditions, indicating that mature males and females attain 50–80 cm and 40–60 cm total length, respectively, and that the species has high fecundity and growth rates, enabling it to occupy large areas of the Patagonian Shelf. Additionally, studies performed in the Beagle Channel indicated that *C. trigloides* lives in association with the holdfast of *Macrocystis pyrifera* kelp forest (Vanella et al., 2007), in accordance with their low buoyancy (Fernández et al., 2012). In those ecosystems, Fernández et al. (2018) described an isometric growth for the species, without intersex differences in the slope for the length–weight relationships. Moreover, Fernández et al. (2009) determined the energy content of *C. trigloides*, obtaining the lowest value (21.82 kJ g^{-1} dry weight) among different notothenioid species. Although its physiology has not been studied in detail, as a temperate species, it is ideal for assessing the evolution and functional importance of biochemical adaptations to temperature (Giordano et al., 2008; Coppola et al., 2010). Much work has been done related to the biogeography (Balushkin, 2000; Colombo et al., 2015; Papetti et al., 2016) and morphology (Iwami, 2004; Eastman et al., 2014) of the notothenioid fish, as they were the main object of large-scale fisheries during the past three decades. Thus, at present there is an important stimulus to study the life history traits and the ecology of *C. trigloides* to protect and apply conservation principles to the species.

Otolith chemical composition has proven quite useful for managing and understanding the ecology of several marine and freshwater fish populations in recent years (Catalán et al., 2018; Radigan et al., 2018; Avigliano et al., 2019; Soeth et al., 2019). Otoliths are calcified structures, located in the inner ear of teleost fish, that are composed mainly of aragonite (calcium carbonate, ∼96%) deposited in an acellular matrix (Campana, 1999). Since the structure of fish otoliths is acellular and metabolically inert, once elements are incorporated from the endolymphatic fluid, their concentrations remain fixed over the life of the fish (Thomas et al., 2017; Thomas and Swearer, 2019). Thus, they can function as natural tags that provide information on life history and population structure of fish (Walther and Limburg, 2012; Tanner et al., 2016; Avigliano et al., 2018a). There are different mechanisms for the incorporation of trace elements in otoliths, such as calcium substitution, in which some divalent ions are incorporated in the substitution to calcium (Ca^{2+}) into the otolith carbonatic matrix, and random trapping of free ions (Thomas and Swearer, 2019). For the elements that substitute for Ca, there may be some proportion with its environmental availability, while for the elements that do not replace Ca, the relationships with the environment are less clear (Thomas et al., 2017; Thomas and Swearer, 2019).

By tracking changes in elemental concentrations over time in an individual fish or among fish captured from different locations, it is often possible to deduce much about their environmental history, such as the previous habitat uses, stock compositions, and nursery locations (Thresher, 1999; Brazner et al., 2004; Avigliano et al., 2018b; Soeth et al., 2019). In recent years, otolith chemical composition has been applied to the study of small pelagic (Mai et al., 2014; Carvalho et al., 2017) and demersal (Volpedo and Fernández Cirelli, 2006; Albuquerque et al., 2012; Avigliano et al., 2017a) fish in the southwestern Atlantic Ocean. Moreover, this technique resolved the population structure of some notothenioid species, such as the Patagonian toothfish *Dissostichus eleginoides* (Smitt, 1898) (Ashford et al., 2005, 2006), and the Scotia Sea icefish *Chaenocephalus aceratus* (Lönnberg, 1906) (Ashford et al., 2010) successfully. Previously, Radtke and Targett (1984) and Radtke et al. (1993) also employed otolith chemical analyses to characterize the environmental life history of two Antarctic fish, *Notothenia larseni* (Lönnberg, 1905) and *Pleuragramma antarcticum* (Boulenger, 1902).

In line with previous studies, we aimed to describe the growth of an extra-Antarctic notothenioid species, *C. trigloides*, and to test the existence of different nursery areas and fish stocks, corresponding to the "northern Patagonia shelf," "southern Patagonia shelf," and "Marine Protected Area (MPA) Namuncurá/Burdwood Bank" areas along the southwestern Atlantic Ocean, by using otolith chemistry. The present results represent the first data on the growth and the population structure of *C. trigloides*, from a geographical area where information on the subject is still scarce, constituting an essential tool to develop conservation strategies to the species.

MATERIALS AND METHODS

Ethics Statement

Cottoperca trigloides is not protected under wildlife conservation laws (local legislations, International Union for Conservation of Nature [IUCN], or Convention on International Trade in Endangered Species [CITES]). Individuals employed in this

[1]https://people.ohio.edu/eastman/

study were captured within the framework of the Pampa Azul interministerial initiative, promoted by the Ministerio de Ciencia, Tecnología e Innovación Productiva. As the Consejo Nacional de Investigaciones Cientificas y Técnicas (CONICET) does not possess formal Committees regarding the fish welfare and sampling protocols, fish handling during sampling was performed following guidelines of the ethical committee of the Universities Federation for Animal Welfare (UFAW) Handbook on the Care and Management of Laboratory Animals[2].

Fish Sampling and Processing

Fish were collected during November–December 2009 from the Oceanographic Vessel Puerto Deseado of the Consejo Nacional de Investigaciones Científicas y Técnicas (CONICET, Argentina) over the Patagonia continental shelf (PS) in the southwestern Atlantic Ocean (41°16′–55°03′S and 57°22′–68°15′W), including the Burdwood Bank (55°S, 59°W) (**Figure 1**). This latter area is a shallow seamount located in the northeastern portion of the Drake Passage. It has been recently declared a marine sanctuary, since it constitutes a highly productive ecosystem and an important migration destination for a wide variety of seabirds and marine mammals (Namuncurá Marine Protected Area; Schetjer et al., 2016).

Along the "northern Patagonia shelf" (NPS), "southern Patagonia shelf" (SPS), and "MPA Namuncurá/Burdwood Bank" (BB) areas, which were defined according to the circulation patterns observed over the PS, *C. trigloides* individuals were collected at 11 sampling stations employing a demersal bottom trawl pilot net (6 m total length, 25 mm mesh on the wings and 10 mm in the cod end, 0.6 m vertical opening and 1.8 m horizontal aperture). Hauls were performed during the day and night, with a target time of 15 min and a tow speed between 2 and 3.7 knots. Individuals captured in station nos. 1, 2, 3, 7, and 8 were assigned to the NPS group, individuals from station nos. 12, 13, 15, 16, and 18 composed the SPS group, and those from station 17 were included in the BB group. The sampling stations with no *C. trigloides* captures (4, 5, 6, 10, 14, 19, 20) were not included in the analyses. Fish were counted and identified following Gon and Heemstra (1990) and specific taxonomic articles. Individual *C. trigloides* were measured to total length (*TL*, ±0.1 mm) and sexed when possible, since gonads of some individuals were indistinguishable. The *sagittae* were extracted, cleaned mechanically with distilled water, and stored dry.

Moreover, a Seabird SBE 21 thermosalinograph was used to measure the sea surface temperature and salinity and an echo-sounder Monhaz was used to measure depth.

Age and Growth Analysis

The right otoliths of 141 *C. trigloides* individuals (84–510 mm *TL*) were embedded in crystal polyester resin and cut transversally through the core using a low-speed, diamond blade IsoMet™ LS saw. The number, width, and radius of each mark and otolith radius (*OR*) were recorded, along the longest axis of the transverse section, under an Olympus SZH10 stereomicroscope (10×) and an image analysis system (Otoli 32). The average percent error (APE, Beamish and Fournier, 1981) and the coefficient of variation (CV, Chang, 1982; Campana, 2001) were used to determine the precision level of age interpretations.

Because it was not possible to validate the periodicity of growth mark deposition in otoliths for *C. trigloides*, an annual periodicity was assumed according to the observations performed in other notothenioid species such as *Eleginops maclovinus* (Cuvier and Valenciennes, 1830) (Brickle et al., 2005; Licandeo et al., 2006) and *Patagonotothen ramsayi* (Regan, 1913) (Brickle et al., 2006).

After verifying linearity between *OR* and *TL*, the Fraser–Lee procedure (Campana, 1990) was used to back-calculate *TL* of each fish at past ages according to

$$TL_a = b + \left(TL - b\right)\ OR^{-1}\ OR_a$$

where TL_a and OR_a are the fish total length (cm) and otolith radius (μm) at some previous age *a*, *TL* and *OR* are the fish total length (cm) and otolith radius (μm) at capture, and *b* is the intercept of the linear regression between *OR* and *TL*.

Annual growth rates were calculated as

$$GR = \ TL_i - \ TL_{i-1}$$

where *GR* is the individual growth rate (cm year^{-1}), TL_i is the total length of fish back-calculated at age *i*, and TL_{i-1} is the total length of fish back-calculated at age *i* - 1.

Differences in *TL* and *GR* at previous ages were evaluated with one-way repeated measures analysis of variance (RM ANOVA) followed by pairwise multiple comparison procedures (Holm–Sidak test). Sphericity was previously assessed using the Mauchly test. The statistical decisions were based on α = 0.05 (Zar, 1984; Sokal and Rohlf, 2011).

Moreover, *TL* at first maturity was estimated following Froese and Binohlan (2000), who proposed the following equations:

Females: $\log TL_m = 0.9469 \log TL_\infty - 0.1162$

Males: $\log TL_m = 0.8915 \log TL_\infty - 0.1032$

where TL_m is the total length at maturity and TL_∞ is derived from

$$TL_\infty = 0.044 + 0.9841\ TL_{\max}$$

where TL_{max} is the maximum total length of the species. TL_{max} values used (80 cm for males and 60 cm for females) are those reported by Arkhipkin et al. (2015).

According to the size range of *C. trigloides* present in the samples and the low percent of mature individuals (7.2%) resulting from previous equations, the Gompertz function was chosen to model the growth of the species, as it is more appropriate in describing the growth of juvenile fish (Ricker, 1979). Thus, length-at-age data were fitted to the following equation:

$$TL_t = TL_\infty\ e\ \left[e^{-k\ (t-\mathrm{I})}\right]$$

where TL_t is the total length at age *t*, TL_8 represents the asymptotic total length, *k* is the growth rate, *t* is the age, and *I* is the age at the inflection point (Gompertz, 1825). Owing to the low number of individuals, no distinctions between sexes

[2]http://www.ufaw.org.uk

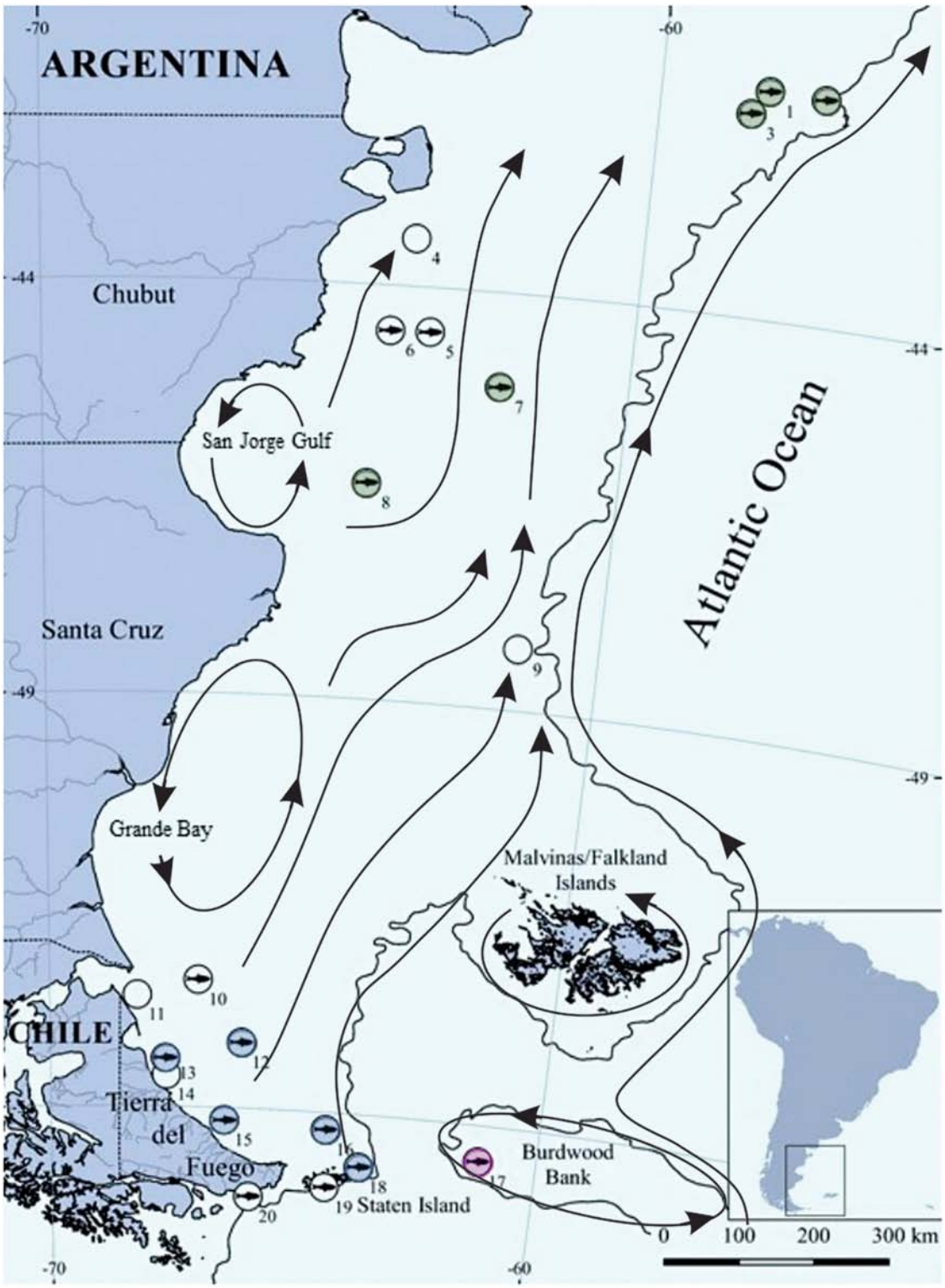

FIGURE 1 | Study area and sampling stations during November-December 2009 in the southwestern Atlantic Ocean. The solid black line represents the 200 m isobath, circles with a fish represent stations where *C. trigloides* was captured and empty circles represent stations where *C. trigloides* was not captured. Different colors indicate different geographic areas (NPS: northern Patagonia shelf, green; SPS: southern Patagonia shelf, blue; and BB: Burdwood Bank, pink). Stations without colors were not included in elemental analyses. Black arrows represent main currents over the PS according Palma et al. (2008).

or capture areas were made to fit the model. The estimates of the parameters of the model were performed using the program Growth II (Henderson and Seaby, 2006).

Elemental Analysis

Because the otolith material is continuously deposited and not reabsorbed (Campana, 1999; Takagi and Takahashi, 1999), the otolith core chemistry, which corresponds to the early stage of life, is a useful spawning or nursery area natural marker. On the other hand, the outer area composition, which represents the last time of life, is often used as a stock indicator (Campana, 2014; Avigliano et al., 2017b; Biolé et al., 2019). Thus, the chemical compositions of the otolith core and edge were analyzed separately to evaluate differences in the stocks and nursery structure of *C. trigloides* between NPS, SPS, and BB areas.

Transverse sections (400 μm) of the left otoliths (N_{total} = 48, N_{NPS} = 12, N_{SPS} = 30, N_{BB} = 6; 119–475 mm *TL*) were mounted onto glass slides with cyanoacrylic glue. Otolith surfaces were polished with silicon carbide paper (no. 8000), washed with Milli-Q water (resistivity of 18.2 mOhm cm^{-1}, Millipore, Bedford, MA, United States), and ultrasonically cleaned (3 min), followed by rinsing with Milli-Q water. The slides were then dried in a laminar flow cabinet before chemical analysis.

Elements Ca, Sr, Mg, Mn, Ba, and Pb were measured by laser ablation inductively coupled plasma mass spectrometry (LA-ICP-MS) in Pontificia Universidad Católica (Río de Janeiro, Brazil). Two radial line-scans were ablated separately in the otolith core and edge. These areas represent approximately the entire core area (nursery area indicator, 1338 ± 247 μm) and the last (stock indicator, 296 ± 74 μm) complete *annuli*. A Q-switched pulsed 266 nm Nd:YAG laser (LSX 100, CETAC Technologies Inc., Omaha, NE, United States) coupled to an ELAN 6000 ICPMS (PerkinElmer-SCIEX, Waltham, MA, United States) was used to analyze *C. trigloides* otoliths. The laser was set up with a scan speed of 20 μm/s, a pulse frequency of 20 Hz, and an energy output of 0.4–0.6 mJ per pulse. This setup resulted in a ∼25 μm crater width. Laser and ICP-MS were linked through a Teflon-coated tube, using argon as carrier gas (0.85 dm^3 min^{-1}). The ICP-MS power was set at 1500 W, with an outer and intermediate gas flow of 15 and 1.1 dm^3 min^{-1}, respectively. Before the analysis, the ICP-MS was optimized using the Daily Performance tool, with maximum analytic intensities and minimum interferences determined using oxides and double-charged ions. The samples were randomly analyzed to avoid systematic bias through the analytical session. Moreover, Ca was used as an internal standard to correct for the elemental fractionation caused by sensitivity drift, differences in ablation yield, and matrix effect (Jackson, 2008; Lin et al., 2016). Standardization to otolith Ca is used in otolith chemical analyses for reducing intersample variance because it is the major element and is relatively invariant (Campana et al., 1997). Furthermore, the reference material NIST1834 (National Institute of Standards and Technology, Gaithersburg, MD, United States), which was certified for Ba, Ca, Mg, and Sr (NIST, 1990), was measured as external standard 10 times among the 48 samples analyzed. The relative standard deviation (RSD,%) between the NIST1834 measurements was 2.4% for Ba, 4% for Sr, 7% for Mn, and 9.5% for Mg, which indicated acceptable repeatability and low drift throughout the analytical session. The values obtained in both the otoliths and NIST1834 were systematically above the limit of detection (LOD), which was calculated from the gas blank before laser ignition (Geffen et al., 2013) as the mean element:Ca ratio plus 3 standard deviations of the background. LODs were 0.058, 0.096, 0.278, and 0.042 for Ba:Ca, Mg:Ca, Mn:Ca, and Sr:Ca, respectively. Element counts per second (cps) were subtracted from the background level, and element:Ca ratios were then calculated for core and edge transects separately.

Otolith chemical composition was simplified and only the four most informative variables were retained (Ba:Ca, Mg:Ca, Mn:Ca, and Sr:Ca) and were log (×* 1000) transformed to balance their influence. The comparisons of these elemental ratios among geographic areas were made with one-way analysis of variance (ANOVA) or Kruskal–Wallis one-way analysis of variance on ranks (Kruskal–Wallis), followed by pairwise multiple comparison procedures (Tukey test or Dunn's test). The assumptions of normality and homoscedasticity were evaluated through Shapiro–Wilks and Levene tests, respectively. All statistical decisions were based on $\alpha = 0.05$ (Zar, 1984; Sokal and Rohlf, 2011). Moreover, as the growth rate can affect the incorporation of trace elements into the otolith, the effect of size on the elemental ration was tested using Spearman's rank-order correlation (Biolé et al., 2019).

In the following analyses, the existence of different nursery areas and stocks of *C. trigloides* between geographic areas along the southwestern Atlantic Ocean was tested. For each area of the otolith, a Euclidean distance matrix was constructed using the log-transformed elemental ratios. A one-way non-parametric permutational multivariate analysis of variance (PERMANOVA) was performed to determine whether significant differences exist in the chemical composition of fish grouped by geographical areas (NPS, SPS, and BB) for both the otolith core and edge. The responsible elements for the intragroup similarity were assessed through a percentage of similarity analysis (SIMPER). The resemblance matrix was further employed in a canonical analysis of principal coordinates (CAP) to visualize the spatial variability of the otolith chemical composition and to measure the degree of fish allocation success within the geographical groups. All the multivariate analyses were performed using the statistical package PRIMER v7 (Anderson et al., 2008; Clarke et al., 2014).

RESULTS

Environmental characteristics regarding depth, salinity, and temperature, of each sampling station over the PS in the southwestern Atlantic Ocean are shown in **Table 1**. Between 41° and 54°S, salinity values were quite similar and ranged from 32.5 (station 11) to 34.0 (station 17). On the other hand, temperature values were more variable, ranging between 5.43°C (station 17) and 12.50°C (station 4); this variability was associated not only with latitude but also with depth.

TABLE 1 | Location of sampling stations, environmental factors measured, and the number of *C. trigloides* captured in the southwestern Atlantic Ocean.

Sampling station	Latitude (S)	Longitude (W)	Depth (m)	Salinity	Temperature (°C)	*C. trigloides* (*n*)
1	41°16′12″	58°16′48″	78	33.5	8.14	1
2	41°17′24″	57°22′48″	123	33.6	5.70	2
3	41°33′36″	58°32′24″	137	33.6	6.9	6
4	43°25′29″	63°45′29″	76	33.5	12.5	0
5	44°32′24″	63°25′48″	83	33.6	7.25	1
6	44°33′00″	64°06′00″	86	33.6	7.19	1
7	45°08′24″	62°11′24″	85	33.7	6.31	3
8	46°23′59″	64°21′27″	113	33.1	9.64	5
9	48°15′41″	61°27′08″	175	33.6	7.78	0
10	52°27′55″	67°03′58″	96	33.1	6.66	1
11	52°39′29″	68°15′57″	71	32.5	6.97	0
12	53°12′38″	66°09′52″	103	33.0	7.09	21
13	53°25′09″	67°41′04″	54	32.6	6.34	11
14	53°37′13″	67°39′31″	46	32.6	7.56	0
15	54°09′08″	66°27′35″	65	32.7	6.88	24
16	54°12′33″	64°22′17″	121	33.7	5.86	8
17	54°26′05″	61°11′48″	97	34.0	5.43	11
18	54°37′57″	63°38′23″	88	33.2	6.32	33
19	54°54′08″	64°19′19″	145	33.2	6.34	3
20	55°03′44″	65°53′59″	125	32.9	6.74	10

Age and Growth Analysis

The age and growth analysis of the species was performed by counting annual marks in *sagittae*. These otoliths showed complex patterns of growth mark formation, making them difficult to read. However, the simple regression analysis (R^2 = 0.81, $p < 0.001$) showed an agreement between the two readers. Moreover, the values from both the APE (2.58%) and the CV (3.65%) indicated a good level of precision for readings. The count of annual marks allowed identifying 8-year classes, being the ages of individual *C. trigloides* ranging between 0+ and 7+. While the 0+ year class was the least represented (0.71%), the 1+ and 2+ year classes were dominant (22.70 and 31.21%, respectively). Furthermore, the ages of male individuals (20% of total capture) were between 1+ and 7+, and those of females (41% of total capture) between 1+ and 5+. The ages of the remaining unsexed individuals (39% of the capture) were between 1+ and 4+.

The relationship between *OR* and *TL* can be expressed as follows, $TL = 8.618 + 0.0135\ OR$ (R^2 = 0.807, $p < 0.001$). Mean back-calculated *TL* by sex are shown in **Table 2**. Sizes at previous ages were significantly different only for ages 3 (RM ANOVA, $F = 5.179$, $p = 0.009$) and 4 (RM ANOVA, $F = 6.711$, $p = 0.017$), with males larger than females and unsexed fish. The *GR* was individually estimated based on back-calculated *TL* (**Table 3**). Mean *GR* showed significantly larger values for males at previous ages 2 (RM ANOVA, $F = 7.238$, $p = 0.002$) and 3 (RM ANOVA, $F = 11.063$, $p = 0.003$).

Considering the TL_{max} values reported for males (50–80 cm) and females (40–60 cm) of *C. trigloides* (Arkhipkin et al., 2015) and following Froese and Binohlan (2000), the TL_{max} of males and females of the species was estimated at 40.3 and 38.2 cm, respectively. These values indicated that few mature individuals (8 males and 2 females) were present in the total capture and that most of the fish were juveniles. Therefore, pooled length-at-age data were used to fit the Gompertz growth model for *C. trigloides* from the southwestern Atlantic Ocean (**Figure 2**). The estimated parameters and their 95% confidence intervals are: TL_8 = 52.85 (52.13–53.57), k = 0.33 (0.03–0.63), and I = 2.04 (-0.35 to 4.43). Sample sizes did not allow growth comparison between sexes or among capture areas.

TABLE 2 | Back-calculated total length (*TL*, mean ± standard deviation) for past ages of *C. trigloides* from the southwestern Atlantic Ocean.

Past ages (years)	Back-calculated *TL* (cm)		
	Unsexed	Males	Females
1	8.77 ± 2.92[a]	9.35 ± 2.87[a]	9.39 ± 3.07[a]
2	16.52 ± 3.33[a]	18.38 ± 3.60[a]	17.47 ± 3.29[a]
3	22.16 ± 3.96[a]	25.94 ± 4.05[b]	23.50 ± 3.88[a]
4		32.13 ± 4.88[a]	29.10 ± 4.25[b]
5		38.11 ± 4.54	
6		42.77 ± 3.28	

Different letters indicate significant differences between sexes.

Elemental Analysis

No significant relationships were detected between the four elemental ratios in the otolith core or edge and fish size (Spearman's correlation, $0.0343 < r_S < 0.284$; $0.169 < p < 0.816$); therefore, it was not necessary to make any correction on the original variables.

Comparisons of element:Ca ratios at the otolith core and edge for the different geographic areas are shown in **Figure 3**. For the otolith core, significant differences in Ba:Ca (Kruskal–Wallis,

TABLE 3 | Annual growth rates (*GR*, mean ± standard deviation) for past ages of *C. trigloides* from the southwestern Atlantic Ocean.

Past ages (years)	GR (cm year^{-1})		
	Unsexed	Males	Females
1	7.74 ± 2.78[a]	9.02 ± 2.91[a]	8.11 ± 3.14[a]
2	4.76 ± 2.40[a]	7.48 ± 2.15[b]	5.58 ± 2.13[a]
3		6.35 ± 1.95[a]	4.54 ± 1.60[b]
4		4.47 ± 1.75	
5		2.73 ± 0.73	

Different letters indicate significant differences between sexes.

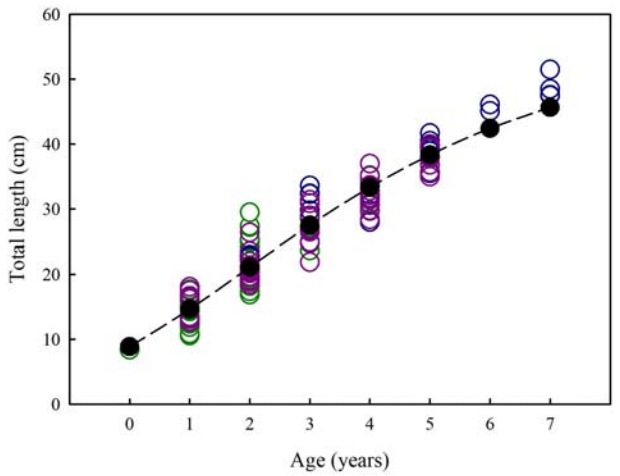

FIGURE 2 | Length-at-age data (empty circles) of *C. trigloides* from the southwestern Atlantic Ocean fitted to the Gompertz (dashed line, filled black circles) growth models. Different colors indicate different sexes: males (blue), females (pink), and unsexed (green).

H = 10.094, p = 0.006) and Mn:Ca ratios were found (Kruskal–Wallis, H = 21.407, p = 0.001). Fish from BB showed lower values as compared to NPS and SPS (Dunn's tests, $p < 0.05$). No significant differences in Mg:Ca (Kruskal–Wallis, H = 3.615, p = 0.164) and Sr:Ca (Kruskal–Wallis, H = 2.737, p = 0.254) ratios were found among geographic areas. For the otolith edge, Ba:Ca (Kruskal–Wallis, H = 7.954, p = 0.019) and Sr:Ca (ANOVA, F = 5.948, p = 0.005) ratios differed significantly, and multiple comparison tests showed that values registered in BB were higher than those of NPS and SPS (Ba:Ca, Dunn's test, $p < 0.05$; Sr:Ca: Tukey test, $p < 0.05$). The Mn:Ca (Kruskal–Wallis, H = 2.180, p = 0.336) and Mg:Ca (Kruskal–Wallis, H = 5.473, p = 0.065) ratios did not differ among geographic areas.

Moreover, the concentration of the four element:Ca ratios among all areas were statistically different for the core (PERMANOVA, BB vs. SPS, p = 0.0007; BB vs. NPS, p = 0.0003 and SPS vs. NPS, p = 0.0005) and edge (PERMANOVA, BB vs. SPS, p = 0.0001; BB vs. NPS, p = 0.0002 and SPS vs. NPS, p = 0.0001) areas. Thus, these analyses proved the existence of three different groups of *C. trigloides* individuals that corresponded to NPS, SPS, and BB areas. In addition, for both otolith areas, the SIMPER analyses indicated that Mn:Ca, Mg:Ca, and Ba:Ca ratios were the element:Ca ratios that most accounted for the intragroup similarity of the three major groups of *C. trigloides* individuals identified (**Table 4**). Although the variabilities of the chemical composition (four element:Ca ratios) in the otolith core and the edge area were analyzed separately, they generated similar spatial arrangements (**Figures 4**, **5**). The CAP analyses, constrained by geographical arrangement, was able to successfully allocate a 72.92% of the fish for the core area (NPS: 84.62%, SPS: 65.52%, and BB: 83.33%) and 91.67% for the edge area of the otolith (NPS: 100%, SPS: 86.67%, and BB: 100%).

DISCUSSION

Age and Growth Analysis

The present study describes, for the first time, the age and growth of *C. trigloides* from the southwestern Atlantic Ocean. Although their *sagittae* showed a complex pattern of growth mark formation, age estimates were precise enough, suggesting that these otoliths were appropriate structures for the age estimation of the species. According to the available information in the literature related to the growth of different notothenioid species, an annual growth mark deposition was assumed on these otoliths (Brickle et al., 2005, 2006; Licandeo et al., 2006). This fact was due to the absence of the necessary samples to verify the periodicity of mark formation in the present samples, given that the sampling program performed included many stations but in a limited period.

Cottoperca trigloides captured between 41° and 54°S of the southwestern Atlantic Ocean, with sizes ranging from 8.4 to 51.5 cm *TL*, belonged to 8-year classes, and 92.8% of them were juveniles. In this regard, Lobao-Tello and Hüne (2012) mentioned that *C. trigloides* less than 55 cm *TL* are the most frequent individuals in wild populations, in agreement with the size range registered by Vanella et al. (2007) and Fernández et al. (2012, 2018). The lack of older fish in the capture restricted the ages to a narrow range that is functionally linear and makes it difficult to fit a non-linear function, especially those with a horizontal asymptote. In consequence, the Gompertz growth function was fitted, being more appropriate for this type of data. This model described the growth of the species adequately, with an estimated $TL\infty$ (52.85 cm) quite similar to that of the larger fish (51.5 cm) registered in the samples and a large k value (0.33) that reflected the typically fast growth observed in juvenile fish. Moreover, the back-calculation of *TL* at previous ages revealed some growth differences related to sex. *Cottoperca trigloides* males attained larger *TL* than females and exhibited faster growth rates since the age of 2 years. Given that the growth of some notothenioid fish from the sub-Antarctic area has been described through the von Bertalanffy growth model (Brickle et al., 2005, 2006; Licandeo et al., 2006), it was not possible to make interspecific comparisons of the growth performance. Nevertheless, Brickle et al. (2006) reported that *P. ramsayi* is a relatively slow-growing fish, with a maximum age of 14 years, and that males have lower growth rates and larger *TL* than females. For the same geographic area, Brickle et al. (2005) described the growth of *E. maclovinus* and characterized it as a short-lived

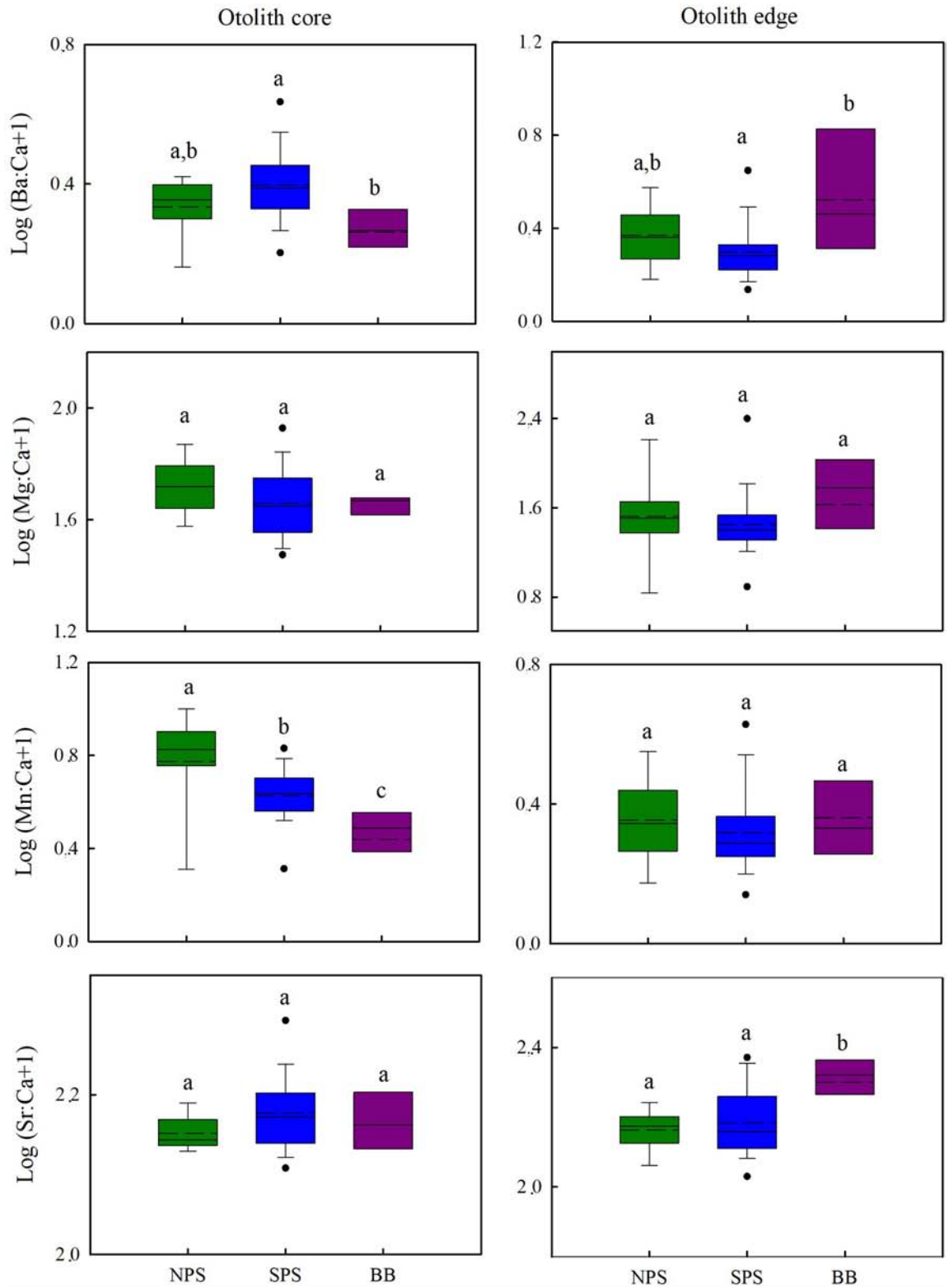

FIGURE 3 | Box plots showing the mean (dashed line), the median (solid line) and 25th and 75th percentiles of Ba:Ca, Mg:Ca, Mn:Ca, and Sr:Ca ratios for otolith core and edge areas of *C. trigloides* from the southwestern Atlantic Ocean. Different letters indicate significant differences among geographic areas. BB, Burdwood Bank; NPS, northern Patagonia shelf; SPS, southern Patagonia shelf.

TABLE 4 | SIMPER analyses for the three groups of *C. trigloides* individuals identifying the most relevant element:Ca ratios responsible for the grouping for the core and edge areas of the otolith.

Groups	Element:Ca ratios	Average value	Contribution%	Cumulative%	Average squared distance
Otolith core					
NPS	Sr:Ca	2.15	1.52	1.52	0.03
	Ba:Ca	0.36	8.00	9.52	
	Mg:Ca	1.72	30.96	40.48	
	Mn:Ca	0.82	59.52	100.00	
SPS	Sr:Ca	2.18	6.07	6.07	0.04
	Mn:Ca	0.64	24.61	30.68	
	Ba:Ca	0.41	28.86	59.53	
	Mg:Ca	1.66	40.47	100.00	
BB	Mg:Ca	1.66	7.12	7.12	0.01
	Sr:Ca	2.16	8.80	15.93	
	Ba:Ca	0.29	39.79	55.72	
	Mn:Ca	0.49	44.28	100.00	
Otolith edge					
NPS	Sr:Ca	2.07	10.47	10.47	0.04
	Mn:Ca	0.36	24.31	34.78	
	Mg:Ca	1.20	31.70	66.48	
	Ba:Ca	0.35	33.52	100.00	
SPS	Sr:Ca	2.18	15.27	15.27	0.06
	Ba:Ca	0.29	19.74	35.01	
	Mn:Ca	0.33	25.35	60.37	
	Mg:Ca	1.42	39.63	100.00	
BB	Sr:Ca	2.34	1.44	1.44	0.12
	Mn:Ca	0.42	18.52	19.96	
	Mg:Ca	1.92	28.92	48.88	
	Ba:Ca	0.63	51.12	100.00	

BB, Burdwood Bank; NPS, northern Patagonia shelf; SPS, southern Patagonia shelf.

species, attaining a maximum age of 11 years, with an average growth rate of 10.2 cm year^{-1} for the first 6 years. In the central-southern Chilean coasts, Licandeo et al. (2006) found that the same species reached smaller sizes with a slower growth pattern. According to the maximum ages registered in other notothenioids from the same geographic area and the TL_{max} of *C. trigloides* (∼80 cm) registered by Lobao-Tello and Hüne (2012) and Arkhipkin et al. (2015), it is likely that older *C. trigloides* individuals will be found in Patagonian populations. A greater sample, encompassing a larger age range, would allow us to describe the growth of the species by applying the von Bertalanffy growth function and hence to support the intersex differences obtained from the back-calculated sizes. Moreover, the estimated parameters will allow comparison of the growth of notothenioids with different sizes through the growth performance index (Pauly and Munro, 1984). About it, Kock and Everson (1998) and La Mesa and Vacchi (2001) found that the growth performances of sub-Antarctic notothenioid species appear to be higher than those estimated for commercially harvested species from the seasonal pack-ice and the high Antarctic zones.

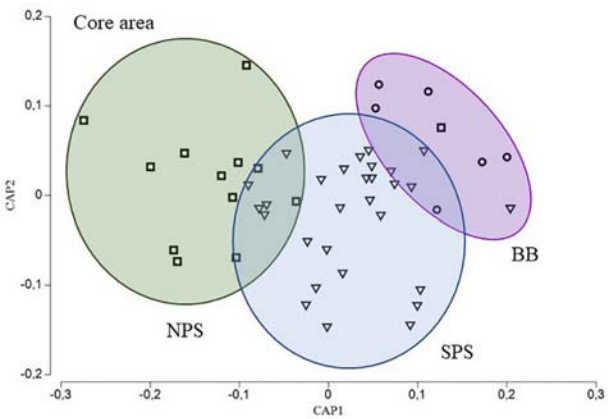

FIGURE 4 | CAP ordination diagram for *C. trigloides* based on the otolith chemical composition (Ba:Ca, Mg:Ca, Mn:Ca, and Sr:Ca) for the otolith core area. Geographical areas: northern Patagonia shelf (NPS, squares), southern Patagonia shelf (SPS, triangles), and Burdwood Bank (BB, circles).

Elemental Analysis

In this study, the analysis of the chemical composition in *C. trigloides* otolith edges was an efficient approach to discriminate among NPS, SPS, and BB areas, which suggests the possible existence of different stocks. Also, core analysis revealed marked segregation during the early stages of life for the

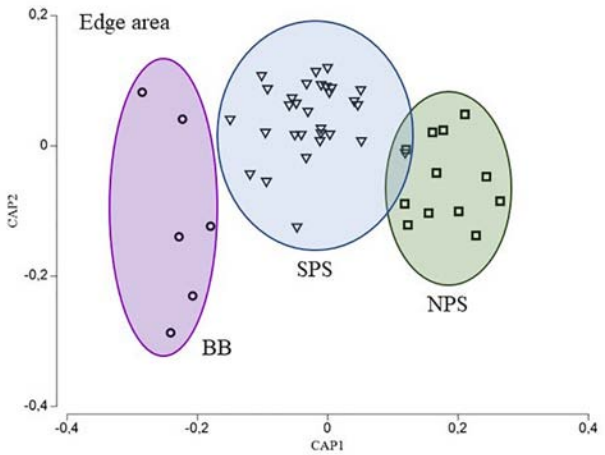

FIGURE 5 | CAP ordination diagram for *C. trigloides* based on the otolith chemical composition (Ba:Ca, Mg:Ca, Mn:Ca, and Sr:Ca) for the otolith edge area. Geographical areas: northern Patagonia shelf (NPS, squares), southern Patagonia shelf (SPS, triangles), and Burdwood Bank (BB, circles).

sampling sites, suggesting the existence of different nursery areas for NPS, SPS, and BB.

The similarities within these groups, identified throughout the ontogeny of *C. trigloides*, were mainly due to Mn:Ca, Mg:Ca, and Ba:Ca ratios. Factors influencing the incorporation of trace elements into otolith calcium carbonate matrix are element and species specific, and can be related to environmental variables (Elsdon and Gillanders, 2003; Brown and Severin, 2009; Avigliano et al., 2019), genetics (Clarke et al., 2011), physiology (Sturrock et al., 2014, 2015), growth rate, and ontogeny (Walther et al., 2010), among others.

For instance, the otolith Sr:Ca ratio is usually positively correlated with salinity, while otolith Ba:Ca shows the opposite pattern (Martin and Thorrold, 2005; Brown and Severin, 2009; Avigliano et al., 2018b). Thus, these ratios have been used as habitat indicators in environments with salinity gradients, especially in diadromous fish (Albuquerque et al., 2010; Mai et al., 2014; Avigliano et al., 2017b). However, in several marine systems, where the salinity is relatively homogeneous, as observed in this study, otolith Sr:Ca and Ba:Ca can vary with other factors, such as temperature, water composition (mainly Ba), genetics, ontogeny, and diet (Miller, 2009; DiMaria et al., 2010; Walther et al., 2010; Clarke et al., 2011). Specifically, Miller (2009) found a positive relationship between temperature and water concentration on the otolith incorporation of Ba:Ca in juvenile black rockfish *Sebastes melanops* (Girard, 1856) under experimental conditions. Walther et al. (2010) found interactive effects between temperature, ontogeny (stage of the life history), and food quantity with otolith Ba:Ca, and significant interactions between stage and food with Sr:Ca in the coral reef fish *Acanthochromis polyacanthus* (Bleeker, 1855). Moreover, DiMaria et al. (2010) described a negative relationship between Sr:Ca and Ba:Ca with temperature, and no relationship between Mg:Ca and this environmental factor, in the Pacific cod *Gadus macrocephalus* (Tilesius, 1810). For that species, they suggested that the kinetic effects could be more important in the incorporation of Sr and Ba while metabolic effects would have a greater effect on the Mg incorporation. For the pelagic-neritic fish *Menidia menidia* (Linnaeus, 1766), a significant temperature effect on both Sr:Ca and Ba:Ca was reported (Clarke et al., 2011). Nevertheless, it turned out to be complex, not linear, and there was also an interaction with genetics (Clarke et al., 2011).

In addition, the coastal waters are richer in Ba, due to the influence of water and continental sediments (Wolgemuth and Broecker, 1970). Unlike what happens with Sr, the levels of Ba in the ocean are not homogeneous and can vary both horizontally and vertically, especially in the Atlantic Ocean (Wolgemuth and Broecker, 1970). A Ba-enrichment was also reported in deep water, which reflects the uptake of Ba by the particles in the surface water and the subsequent release into deep waters (Wolgemuth and Broecker, 1970).

Concerning Mn:Ca, a relationship with environmental concentration was found in some species (Dorval et al., 2007; Mohan et al., 2012), while in others, it was not (Walther and Thorrold, 2008; Miller, 2009). It has been reported that the concentration of dissolved oxygen is negatively associated with Mn:Ca in marine species such as the Atlantic cod *Gadus morhua* (Linnaeus, 1758), the European flounder *Platichthys flesus* (Linnaeus, 1758), the winter flounder *Pseudopleuronectes americanus* (Walbaum, 1792), and the Atlantic croaker *Micropogonias undulatus* (Linnaeus, 1766) (Mohan et al., 2014). The hypoxic or anoxic environments that are often associated with otolith Mn peaks are typically related to high depths (Limburg et al., 2015). This ratio also seems to be strongly associated with ontogenetic changes because a peak has been found in the otolith core of several marine species such as *Dascyllus marginatus* (Rüppell, 1829) (Ben-Tzvi et al., 2007), *Sicydium punctatum* (Perugia, 1896), and *Sillaginodes punctatus* (Cuvier, 1829) (Rogers et al., 2019).

In the present study, most of the sampling stations were located far from the coast, and only two sites with *C. trigloides* captures (13 and 15) could be associated with fresher sub-Antarctic waters (advected from Chile and entering the PS via Magellan and Le Maire Straits) around Tierra del Fuego Island. Nevertheless, salinity was relatively constant among sampling sites; therefore, the otolith Ba:Ca variation would not seem to be related to the proximity of continental water bodies. On the other hand, the heterogeneity in the bathymetry of the study area (Piola et al., 2018) could affect the concentration or bioavailability of element:Ca ratios (mainly Sr:Ca, Ba:Ca, and Mn:Ca) in water (Wolgemuth and Broecker, 1970; Limburg et al., 2015), and thus on their incorporation into the otolith, which should be particularly studied. Over the PS, the temperature ranged up to 9.97°C between sampling stations and was more related to the depth than to latitude. Thus, we cannot rule out the potential effect of depth or some physicochemical parameters (i.e., temperature) on the element:Ca ratios responsible for the grouping.

Oceanographic phenomena could create barriers for fish populations and contribute to segregation, which could be reflected in the composition of otoliths (Cadrin et al., 2013;

Wilson et al., 2018). Thus, we proposed that the circulation pattern in the PS and Burdwood Bank could also explain the multivariate differences found among areas. Numerical simulations suggested that the mean circulation over the PS consists of a broad northeastward flow that intensifies toward the outer shelf, with anticyclonic gyres and relatively weak poleward coastal currents within the Grande Bay and San Jorge Gulf (Palma et al., 2008; Combes and Matano, 2014; Piola et al., 2018). This circulation pattern may be the physical feature involved in maintaining the integrity of NPS and SPS nursery areas and fish stocks. A similar association between the existence of a geographically stable larval retention area for *Sprattus fueguensis* (Jenyns, 1842) and the anticyclonic current circulation and sinking of shelf waters in southern Patagonia was also indicated by Sánchez et al. (1995). Regarding BB, Matano et al. (2019) suggested that it is an active center for the obduction of deep, fertile waters to the surface layers of the Drake Passage. This phenomenon, which includes upwelling and mixing, is primarily driven by tides and strengthened by winter convection. According to numerical models, the resulting circulation patterns over the BB consists of a broad anticyclonic flow around the bank's rim and anticyclonic vortices on top of the interior seamounts that increase the retention of fluid parcels. Therefore, it could be contributing to the retention of *C. trigloides* individuals within the BB area. Moreover, considering that it is species living on or near the bottom, with adult males being territorial (Arkhipkin et al., 2015), low connectivity of individuals among different geographic areas could be expected.

Finally, the objective of this study was not to reveal the factors that influence the incorporation of elements into the *C. trigloides* otolith; however, this type of information could contribute to revealing the population structure with greater depth. In this sense, it is recommended to evaluate the relationship between different endogenous and exogenous factors in the incorporation of different elements. Moreover, future studies could incorporate other markers such as Li:Ca, Cu:Ca, Rb:Ca, Zn:Ca, and other methods such as genetics or otolith stable isotopes, which could also contribute to a better understanding of the observed differences over the PS.

CONCLUSION

This is the first time that the growth of *C. trigloides* has been described by using the Gompertz model, with males attaining larger sizes at faster growth rates. Moreover, the chemical analyses showed high segregation among the studied groups along the southwestern Atlantic Ocean, suggesting the presence of different stocks and nursery areas. The information obtained regarding the growth and population structure of *C. trigloides* could provide new information, constituting an essential tool to develop conservation principles for the species.

DATA AVAILABILITY STATEMENT

The datasets generated for this study are available on request to the corresponding author.

ETHICS STATEMENT

As the Consejo Nacional de Investigaciones Cientificas y Técnicas (CONICET) does not possess formal committees regarding the fish welfare and sampling protocols, fish handling during sampling was performed following guidelines of the Ethical Committee of the UFAW Handbook on the Care and Management of Laboratory Animals (http://www.ufaw.org.uk).

AUTHOR CONTRIBUTIONS

ML conceived and wrote the manuscript, with contributions from MB, and read the otoliths. FL and EA analyzed the data with contributions from ML. MR read the otoliths and contributed to age and growth analyses. ID prepared the otoliths for biochemical analyses. CB, FV, and DF participated in the research cruise and collected the fish samples. CA conducted the biochemical analyses. All authors contributed to the article and approved the submitted version.

FUNDING

This work was supported by the Consejo Nacional de Investigaciones Científicas y Técnicas (grant numbers PIP 0321, PIP 0440, and PUE 2016 - CADIC).

ACKNOWLEDGMENTS

The authors wish to thank S. Rimbau, D. Aureliano, and the crew of the Oceanographic Vessel Puerto Deseado for their technical assistance and Dr. Frank Sola for his assistance with the English language editing of the manuscript. Dr. Mario La Mesa and Daniel Brown are also acknowledged for their invaluable advice on the age and growth analyses.

REFERENCES

Albuquerque, C. Q., Miekeley, N., and Muelbert, J. H. (2010). Whitemouth croaker, *Micropogonias furnieri*, trapped in a freshwater coastal lagoon: A natural comparison of freshwater and marine influences on otolith chemistry. *Neotrop. Ichthyol.* 8, 311–320. doi: 10.1590/S1679-62252010000200009

Albuquerque, C. Q., Miekeley, N., Muelbert, J. H., Walther, B. D., and Jaureguizar, A. J. (2012). Estuarine dependency in a marine fish evaluated with otolith chemistry. *Mar. Biol.* 159, 2229–2239. doi: 10.1007/s00227-012-2007-5

Anderson, M. J., Gorley, R. N., and Clarke, K. R. (2008). *PERMANOVA+ for PRIMER: Guide to Software and Statistical Methods*. Plymouth: PRIMER-E.

Arkhipkin, A., Boucher, E., and Howes, P. N. (2015). Spawning and early ontogenesis in channel bull blenny *Cottoperca gobio* (Notothenioidei,

Perciformes) caught off the Falkland Islands and maintained in captivity. *Polar Biol.* 38, 251–259. doi: 10.1007/s00300-014-1582-y

Ashford, J. R., Arkhipkin, A. I., and Jones, C. M. (2006). Can the chemistry of otolith nuclei determine population structure of Patagonian toothfish *Dissostichus eleginoides*? *J. Fish Biol.* 69, 708–721. doi: 10.1111/j.1095-8649.2006.01144.x

Ashford, J. R., Jones, C. M., Hofmann, E., Everson, I., Moreno, C., Duhamel, G., et al. (2005). Can otolith elemental signatures record the capture site of patagonian toothfish (*Dissostichus eleginoides*), a fully marine fish in the Southern Ocean? *Can. J. Fish. Aquat. Sci.* 62, 2832–2840. doi: 10.1139/f05-191

Ashford, J. R., La Mesa, M., Fach, B., Jones, C., and Everson, I. (2010). Testing early life connectivity using otolith chemistry and particle-tracking simulations. *Can. J. Fish. Aquat. Sci.* 67, 1303–1315. doi: 10.1139/F10-065

Avigliano, E., Leisen, M., Romero, R., Carvalho, B., Velasco, G., Vianna, M., et al. (2017a). Fluvio-marine travelers from South America: cyclic amphidromy and freshwater residency, typical behaviors in *Genidens barbus* inferred by otolith chemistry. *Fish. Res.* 193, 184–194. doi: 10.1016/j.fishres.2017.04.011

Avigliano, E., Maichak de Carvalho, B., Leisen, M., Romero, R., Velasco, G., Vianna, M., et al. (2017b). Otolith edge fingerprints as an approach for stock identification of *Genidens barbus*. *Estuar. Coast. Shelf Sci.* 194, 92–96. doi: 10.1016/j.ecss.2017.06.008

Avigliano, E., Maichak de Carvalho, B., Miller, N., Córdoba Gironde, S., Tombari, A., Limburg, K., et al. (2019). Fin spines chemistry as a non-lethal alternative to otoliths for habitat and stock discrimination: comparison between structures for an endangered catfish species. *Mar. Ecol. Prog. Ser.* 614, 147–157. doi: 10.3354/meps12895

Avigliano, E., Miller, N., and Volpedo, A. V. (2018a). Silversides (*Odontesthes bonariensis*) reside within freshwater and estuarine habitats, not marine environments. *Estuar. Coast. Shelf. Sci.* 205, 123–130. doi: 10.1016/j.ecss.2018.03.014

Avigliano, E., Pisonero, J., Dománico, A., Silva, N., Sánchez, S., and Volpedo, A. V. (2018b). Spatial segregation and connectivity in young and adult stages of *Megaleporinus obtusidens* inferred from otolith elemental signatures: implications for managment. *Fish. Res.* 204, 239–244. doi: 10.1016/j.fishres.2018.03.007

Balushkin, A. V. (2000). Morphology, classification, and evolution of notothenioid fishes of the Southern Ocean (Notothenioidei, Perciformes). *J. Ichthyol.* 40, 74–109.

Beamish, R. J., and Fournier, D. A. (1981). A method for comparing the precision of a set of age determinations. *Can. J. Fish. Aquat. Sci.* 38, 982–983. doi: 10.1139/f81-132

Ben-Tzvi, O., Abelson, A., Gaines, S. D., Sheehy, M. S., Paradis, G. L., and Kiflawi, M. (2007). The inclusion of sub-detection limit LA-ICPMS data, in the analysis of otolith microchemistry, by use of a palindrome sequence analysis (PaSA). *Limnol. Oceanogr. Methods* 95, 97–105. doi: 10.4319/lom.2007.5.97

Biolé, F. G., Thompson, G. A., Vargas, C. V., Leisen, M., Barra, F., Volpedo, A. V., et al. (2019). Fish stocks of *Urophycis brasiliensis* revealed by otolith fingerprint and shape in the Southwestern Atlantic Ocean. *Estuar. Coast. Shelf Sci.* 229:106406. doi: 10.1016/j.ecss.2019.106406

Brazner, J. C., Campana, S. E., Tanner, D. K., and Schram, S. T. (2004). Reconstructing habitat use and wetland nursery origin of yellow perch from Lake Superior using otolith elemental analysis. *J. Great Lakes Res.* 30, 492–507. doi: 10.1016/S0380-1330(04)70365-2

Brickle, P., Arkhipkin, I., and Shcherbich, Z. N. (2005). Age and growth in a temperate euryhaline notothenioid, *Eleginops maclovinus* from the Falklands Islands. *J. Mar. Biol. Ass. U.K.* 85, 1217–1221. doi: 10.1017/S0025315405012348

Brickle, P., Arkhipkin, I., and Shcherbich, Z. N. (2006). Age and growth of a sub-Antarctic notothenioid, *Patagonotothen ramsayi* (Regan 1913), from Falklands Islands. *Polar Biol.* 29, 633–639. doi: 10.1007/s00300-005-0099-9

Brown, R. J., and Severin, K. P. (2009). Otolith chemistry analyses indicate that water Sr:Ca is the primary factor influencing otolith Sr:Ca for freshwater and diadromous fish but not for marine fish. *Can. J. Fish. Aquat. Sci.* 66, 1790–1808. doi: 10.1139/F09-112

Cadrin, S. X., Karr, L. A., and Mariani, S. (2013). "Stock identification methods: an overview," in *Stock Identification Methods. Applications in Fishery Science*, eds S. X. Cadrin, L. A. Kerr, and S. Mariani (Woods Hole, MA: Academic Press), 3–6. doi: 10.1016/b978-012154351-8/50002-2

Campana, S. E. (1990). How reliable are growth back-calculations based on otoliths? *Can. J. Fish. Aquat. Sci.* 47, 2219–2227. doi: 10.1139/f90-246

Campana, S. E. (1999). Chemistry and composition of fish otoliths: pathways, mechanisms and applications. *Mar. Ecol. Prog. Ser.* 188, 263–297. doi: 10.3354/meps188263

Campana, S. E. (2001). Accuracy, precision and quality control in age determination, including a review of the use and abuse of age validation methods. *J. Fish Biol.* 59, 197–242. doi: 10.1111/j.1095-8649.2001.tb00127.x

Campana, S. E. (2014). "Otolith elemental as a natural marker of fish stocks," in *Stock Identification Methods: Applications in Fishery*, eds S. X. Cadrin, L. A. Kerr, and S. Mariani (Amsterdam: Elsevier), 227–245. doi: 10.1017/S002531541900016X

Campana, S. E., Thorrold, S. R., Jones, C. M., Gunther, D., Tubrett, M., Longerich, H., et al. (1997). Comparison of accuracy, precision and sensitivity in elemental assays of fish otoliths using the electron microprobe, proton-induced X-ray emission, and laser ablation inductively coupled plasma mass spectrometry. *Can. J. Fish. Aquat. Sci.* 54, 2068–2079. doi: 10.1139/cjfas-54-9-2068

Carvalho, B. M., Volpedo, A. V., Vaz-dos-Santos, A. M., and Spach, H. L. (2017). Use of otolith microchemistry as habitat indicator of Anchoa tricolor (Spix & Agassiz, 1829) in a subtropical estuary. *Lat. Am. J. Aquat. Res.* 45, 457–465. doi: 10.3856/vol45-issue2-fulltext-20

Catalán, I. A., Alós, J., Díaz-Gil, C., Pérez-Mayol, S., Basterretxea, G., Morales-Nin, B., et al. (2018). Potential fishing-related effects on fish life history revealed by otolith microchemistry. *Fish. Res.* 199, 186–195. doi: 10.1016/j.fishres.2017.11.008

Chang, W. Y. B. (1982). A statistical method for evaluating the reproducibility of age determination. *Can. J. Fish. Aquat. Sci.* 39, 1208–1210. doi: 10.1139/f82-158

Clarke, K. R., Gorley, R. N., Somerfield, P. J., and Warwick, R. M. (2014). *Change in Marine Communities: An Approach to Statistical Analysis and Interpretation*, 3rd Edn. Plymouth: PRIMER-E.

Clarke, L. M., Conover, D. O., and Thorrold, S. R. (2011). Population differences in otolith chemistry have a genetic basis in Menidia menidia. *Can. J. Fish. Aquat. Sci.* 68, 105–114. doi: 10.1139/F10-147

Colombo, M., Damerau, M., Hanel, R., Salzburger, W., and Matschiner, M. (2015). Diversity and disparity through time in the adaptive radiation of Antarctic notothenioid fishes. *J. Evol. Biol.* 28, 376–394. doi: 10.1111/jeb.12570

Combes, V., and Matano, R. P. (2014). A two-way nested simulation of the oceanic circulation in the Southwestern Atlantic. *J. Geophys. Res. Oceans* 119, 731–756. doi: 10.1002/2013jc009498

Coppola, D., Giordano, D., Vergara, A., Mazzarella, L., di Prisco, G., Verde, C., et al. (2010). The hemoglobins of sub-Antarctic fishes of the suborder Notothenioidei. *Polar Sci.* 4, 295–308. doi: 10.1016/j.polar.2010.04.007

DiMaria, R. A., Miller, J. A., and Hurst, T. P. (2010). Temperature and growth effects on otolith elemental chemistry of larval Pacific cod, *Gadus macrocephalus*. *Environ. Biol. Fish* 89, 453–462. doi: 10.1007/s10641-010-9665-2

Dorval, E., Jones, C. M., Hannigan, R., and Montfrans, J. V. (2007). Relating otolith chemistry to surface water chemistry in a coastal plain estuary. *Can. J. Fish. Aquat. Sci.* 64, 411–424. doi: 10.1139/f07-015

Eastman, J. T. (1993). *Antarctic Fish Biology: Evolution in a Unique Environment*. San Diego, CA: Academic Press.

Eastman, J. T., Witmer, L. M., Ridgely, R. C., and Kuhn, K. L. (2014). Divergence in skeletal mass and bone morphology in Antarctic notothenioid fishes. *J. Morphol.* 275, 841–861. doi: 10.1002/jmor.20258

Elsdon, T. S., and Gillanders, B. M. (2003). Relationship between water and otolith elemental concentrations in juvenile black bream *Acanthopagrus butcheri*. *Mar. Ecol. Prog. Ser.* 260, 263–272. doi: 10.3354/meps260263

Falkland Islands Government [FIG] (2019). *Fisheries Department Fisheries Statistics, 23*. Stanley: FIG Fisheries Department.

Fernández, D. A., Bruno, D. O., and Llompart, F. M. (2018). Length–weight relationship of six notothenioid species from sub-Antarctic waters (Beagle Channel, Argentina). *J. Appl. Ichthyol.* 35, 597–599. doi: 10.1111/jai.13833

Fernández, D. A., Ceballos, S. G., Malanga, G., Boy, C. C., and Vanella, F. A. (2012). Buoyancy of sub-Antarctic notothenioids including the sister lineage of all other notothenioids (Bovichtidae). *Polar Biol.* 35, 99–106. doi: 10.1007/s00300-011-1037-7

Fernández, D. A., Lattuca, M. E., Boy, C. C., Pérez, A. F., Cevallos, S. G., Vanella, F. A., et al. (2009). Total energy content and energy densities of the main tissues

of Sub-Antarctic fishes from the Beagle Channel. *Fish Physiol. Biochem.* 35, 181–188. doi: 10.1007/s10695-008-9234-1

Froese, R., and Binohlan, C. (2000). Empirical relationships to estimate asymptotic length, length at first maturity and length at maximum yield per recruit in fishes, with a simple method to evaluate length frequency data. *J. Fish Biol.* 56, 758–773. doi: 10.1006/jfbi.1999.1194

Geffen, A. J., Morales-Nin, B., Pérez-Mayol, S., Cantarero-Roldán, A. M., Skadal, J., and Tovar-Sánchez, A. (2013). Chemical analysis of otoliths: cross validation between techniques and laboratories. *Fish. Res.* 143, 67–80. doi: 10.1016/j.fishres.2013.01.005

Giordano, D., Boechi, L., Vergara, A., Martí, M. A., Samuni, U., Dantsker, D., et al. (2008). The hemoglobins of the sub-Antarctic fish *Cottoperca gobio*, a phyletically basal species - oxygen-binding equilibria, kinetics and molecular dynamics. *FEBS J.* 276, 2266–2277. doi: 10.1111/j.1742-4658.2009.06954.x

Gompertz, B. (1825). On the nature of the function expressive of the law of human mortality, and on a new mode of determining the value of life contingencies. *Phil. Trans. R. Soc. Lond.* 115, 513–583. doi: 10.1098/rstl.1825.0026

Gon, O., and Heemstra, P. C. (1990). *Fishes of the Southern Ocean*. Grahamstown: J. L. B. Smith Institute of Ichthyology.

Henderson, P. A., and Seaby, R. M. (2006). *Growth II*. Lymington: Pisces Conservation Ltd.

Iwami, T. (2004). Comparative morphology of the adductor mandibulae musculature of notothenioid fishes (Pisces. Perciformes). *Antarct. Sci.* 16, 17–21. doi: 10.1017/S0954102004001762

Jackson, S. (2008). Calibration strategies for elemental analysis by LA-ICP-MS" in Mineralogical Association of Canada Short Course. *Vancouver* 40, 169–188.

Kock, K.-H., and Everson, I. (1998). "Age, growth and maximum size of Antarctic notothenioid fish – Revisited," in *Fishes of Antarctica. A biological review*, eds G. di Prisco, E. Pisano, and A. Clarke (Italy: Springer-Verlag), 29–40. doi: 10.1007/978-88-470-2157-0_2

La Mesa, M., and Vacchi, M. (2001). Age and growth of high Antarctic notothenioid fish. *Antart. Sci.* 13, 227–235. doi: 10.1017/s0954102001000335

Laptikhovsky, V. V., and Arkhipkin, A. I. (2003). An impact of seasonal squid migrations and fishing on the feeding spectra of subantarctic notothenioids Patagonotothen ramsayi and *Cottoperca gobio* around the Falkland Islands. *J. Appl. Ichthyol.* 19, 35–39. doi: 10.1046/j.1439-0426.2003.00340.x

Licandeo, R. R., Barrientos, C. A., and González, M. T. (2006). Age, growth rates, sex change and feeding habits of notothenioid fish *Eleginops maclovinus* from the central-southern Chilean coast. *Environ. Biol. Fish.* 77, 51–61. doi: 10.1007/s10641-006-9054-z

Limburg, K. E., Walther, B. D., Lu, Z., Jackman, G., Mohan, J., Walther, Y., et al. (2015). In search of the dead zone: Use of otoliths for tracking fish exposure to hypoxia. *J. Mar. Syst.* 141, 167–178. doi: 10.1016/j.jmarsys.2014.02.014

Lin, J., Liu, Y., Yang, Y., and Hu, Z. (2016). Calibration and correction of LA-ICP-MS and LA-MC-ICP-MS analyses for element contents and isotopic ratios. *Solid Earth Sci.* 1, 5–27. doi: 10.1016/j.sesci.2016.04.002

Lloris, D., and Rucabado, J. (1991). Ictiofauna del Canal Beagle (Tierra de Fuego), aspectos ecológicos y análisis biogeográfico. *Publicación Especial del Instituto Español de Oceanografía* 8:182.

Lobao-Tello, P. R., and Hüne, M. (2012). *Peces del Sur de Chile*. Santiago, CA: Fundación Ictiológica.

Mai, A. C. G., Condini, M. V., Albuquerque, C. Q., Loebmann, D., Saint'Pierre, T. D., Miekeley, N., et al. (2014). High plasticity in habitat use of *Lycengraulis grossidens* (Clupeiformes. Engraulididae). *Est. Coast. Shelf. Sci.* 141, 17–25. doi: 10.1016/j.ecss.2014.01.014

Martin, G. B., and Thorrold, S. R. (2005). Temperature and salinity effects on magnesium, manganese, and barium incorporation in otoliths of larval and early juvenile spot *Leiostomus xanthurus*. *Mar. Ecol. Prog. Ser.* 293, 223–232. doi: 10.3354/meps293223

Matallanas, J. (1988). Datos morfológicos y morfométricos del tracto alimentario de peces del Canal de Beagle. *Misc. Zool.* 12, 237–243.

Matano, R. P., Palma, E. D., and Combes, V. (2019). The Burdwood Bank circulation. *J. Geophys. Res. Oceans* 124, 6904–6926. doi: 10.1029/2019JC015001

Miller, J. A. (2009). The effects of temperature and water concentration on the otolith incorporation of barium and manganese in black rockfish *Sebastes melanops*. *J. Fish Biol.* 75, 39–60. doi: 10.1111/j.1095-8649.2009.02262.x

Mohan, J., Rahman, M. S., Thomas, P., and Walther, B. (2014). Influence of constant and periodic experimental hypoxic stress on Atlantic croaker otolith chemistry. *Aquat. Biol.* 1, 1–11. doi: 10.3354/ab00542

Mohan, J. A., Rulifson, R. A., Reide Corbett, D., and Halden, N. M. (2012). Validation of oligohaline elemental otolith signatures of striped bass by use of in situ caging experiments and water chemistry. *Mar. Coast. Fish.* 4, 57–70. doi: 10.1080/19425120.2012.656533

Moreno, C. A., and Jara, H. F. (1984). Ecological studies on fish fauna associated with Macrocystis pyrifera belts in the south of Fueguian Islands. *Chile. Mar. Ecol. Progr. Ser.* 15, 99–107. doi: 10.3354/meps015099

NIST (1990). *Certificate Analysis. Standard Reference Material NIST*1834. Gaithersburg: National Institute of Standards and Technology.

Palma, E. D., Matano, R. P., and Piola, A. R. (2008). A numerical study of the southwestern Atlantic shelf circulation: stratified ocean response to local and offshore forcing. *J. Geophys. Res. Oceans* 113:C11010. doi: 10.1029/2007JC004720

Papetti, C., Windisch, H. S., La Mesa, M., Lucassen, M., Marshall, C., and Lamare, M. D. (2016). Non-Antarctic notothenioids: Past phylogenetic history and contemporary phylogeographic implications in the face of environmental changes. *Mar. Genom.* 25, 1–9. doi: 10.1016/j.margen.2015.11.007

Pauly, D., and Munro, J. L. (1984). Once more on the comparison of growth in fishes and invertebrates. *Fishbyte* 2:21.

Piola, A. R., Palma, E. D., Bianchi, A. A., Castro, M., Dottori, M., Guerrero, R. A., et al. (2018). "Physical oceanography of the SW Atlantic Shelf: a review," in *Plankton Ecology of the Southwestern Atlantic*, eds M. S. Hoffmeyer, M. E. Sabatini, F. P. Brandini, D. L. Calliari, and N. H. Santinelli (Cham: Springer International Publishing AG), 37–56. doi: 10.1007/978-3-319-77869-3_2

Radigan, W. J., Carlson, A. K., Fincel, M. J., and Graeb, B. D. S. (2018). Otolith chemistry as a fisheries management tool after flooding: The case of Missouri River gizzard shad. *River Res. Appl.* 34, 270–278. doi: 10.1002/rra.3247

Radtke, R., Hubold, G., Folsom, S., and Lenz, P. (1993). Otolith structural and chemical analyses: the key to resolving age and growth of the Antarctic silverfish, *Pleuragramma antarcticum*. *Antarct. Sci.* 5, 51–62. doi: 10.1017/S0954102093000082

Radtke, R. L., and Targett, T. E. (1984). Rhythmic structural and chemical patterns in otoliths of the Antarctic fish *Notothenia larseni*: Their application to age determination. *Polar Biol.* 3, 203–210. doi: 10.1007/bf00292624

Ricker, W. (1979). "Growth rates and models," in *Fish Physiology. Volume VIII; Bioenergetics and Growth*, eds W. Hoar, D. Randall, and J. Brett (New York, NY: Academic Press), 677–743. doi: 10.1016/S1546-5098(08)60034-5

Rogers, T. A., Fowler, A. J., Steer, M. A., and Gillanders, B. M. (2019). Discriminating natal source populations of a temperate marine fish using larval otolith chemistry. *Front. Mar. Sci.* 6:711. doi: 10.3389/fmars.2019.00711

Sánchez, R. P., Remeslo, A., Madirolas, A., and Ciechomski, J. D. (1995). Distribution and abundance of post-larvae and juveniles of the Patagonian sprat, Sprattus fueguensis, and related hydrographic conditions. *Fish. Res.* 23, 47–81. doi: 10.1016/0165-7836(94)00339-x

Schetjer, L., Rimondino, C., Chiesa, I., Astarloa, J., Doti, B., Elias, R., et al. (2016). Namuncurá marine protected area: An oceanic hotspot of benthic biodiversity at Burdwood Bank. Argentina. *Polar Biol.* 39, 2372–2386. doi: 10.1007/s00300-016-1913-2

Soeth, M., Spach, H. L., Daros, F. A., Adelir-Alves, J., de Almeida, A. C. O., and Correia, A. T. (2019). Stock structure of Atlantic spadefish *Chaetodipterus faber* from Southwest Atlantic Ocean inferred from otolith elemental and shape signatures. *Fish. Res.* 211, 81–90. doi: 10.1016/j.fishres.2018.11.003

Sokal, R. R., and Rohlf, F. J. (2011). *Biometry: The Principles and Practice of Statistics in Biological Research*, 2nd Edn. New York, NY: W. H. Freeman, doi: 10.2307/2343822

Sturrock, A. M., Hunter, E., Milton, J. A., Johnson, R. C., Waring, C. P., and Trueman, C. N. (2015). Quantifying physiological influences on otolith microchemistry. *Methods Ecol. Evol.* 6, 806–816. doi: 10.1111/2041-210X.12381

Sturrock, A. M., Trueman, C. N., Milton, J. A., Waring, C. P., Cooper, M. J., and Hunter, E. (2014). Physiological influences can outweigh environmental signals in otolith microchemistry research. *Mar. Ecol. Prog. Ser.* 500, 245–264. doi: 10.3354/meps10699

Takagi, Y., and Takahashi, A. (1999). Characterization of otolith soluble-matrix producing cells in the saccular epithelium of rainbow trout (*Oncorhynchus*

mykiss) inner ear. *Anat. Rec.* 254, 322–329. doi: 10.1002/(SICI)1097-0185(19990301)254:3<322::AID-AR2<3.0.CO;2-Q

Tanner, S. E., Reis-Santos, P., and Cabral, H. N. (2016). Otolith chemistry in stock delineation: A brief overview, current challenges and future prospects. *Fish. Res.* 173, 206–213. doi: 10.1016/j.fishres.2015.07.019

Thomas, O. R. B., Ganio, K., Roberts, B. R., and Swearer, S. E. (2017). Trace element-protein interactions in endolymph from the inner ear of fish: implications for environmental reconstructions using fish otolith chemistry. *Metallomics* 9, 239–224. doi: 10.1039/c6mt00189k

Thomas, O. R. B., and Swearer, S. E. (2019). Otolith biochemistry - a review. *Rev. Fish. Sci. Aquac.* 27, 458–489. doi: 10.1080/23308249.2019.1627285

Thresher, R. E. (1999). Elemental composition of otoliths as a stock delineator in fishes. *Fish. Res.* 43, 165–204. doi: 10.1016/S0165-7836(99)00072-7

Vanella, F. A., Fernaìndez, D. A., Romero, M. C., and Calvo, J. (2007). Changes in the fish fauna associated with a sub-Antarctic *Macrocystis pyrifera* kelp forest in response to canopy removal. *Polar Biol.* 30, 449–457. doi: 10.1007/s00300-006-0202-x

Volpedo, A., and Fernández Cirelli, A. (2006). Otolith chemical composition as a useful tool for sciaenids stock discrimination in Southwestern Atlantic. *Sci. Mar.* 70, 325–334. doi: 10.3989/scimar.2006.70n2325

Walther, B. D., Kingsford, M. J., O'Callaghan, M. D., and McCulloch, M. T. (2010). Interactive effects of ontogeny, food ration and temperature on elemental incorporation in otoliths of a coral reef fish. *Environ. Biol. Fish* 89, 441–451. doi: 10.1007/s10641-010-9661-6

Walther, B. D., and Limburg, K. E. (2012). The use of otolith chemistry to characterize diadromous migrations. *J. Fish Biol.* 81, 796–825. doi: 10.1111/j.1095-8649.2012.03371.x

Walther, B. D., and Thorrold, S. R. (2008). Continental-scale variation in otolith geochemistry of juvenile American shad (*Alosa sapidissima*). *Can. J. Fish. Aquat. Sci.* 65, 2623–2635. doi: 10.1139/F08-164

Wilson, M. T., Dougherty, A., Matta, M. E., Mier, K. L., and Miller, J. A. (2018). Otolith chemistry of juvenile walleye pollock *Gadus chalcogrammus* in relation to regional hydrography: evidence of spatially split cohorts. *Mar. Ecol. Prog. Ser.* 588, 163–178. doi: 10.3354/meps12425

Wolgemuth, K., and Broecker, W. S. (1970). Barium in seawater. *Earth Planet. Sci. Lett.* 8, 372–378. doi: 10.1016/0012-821X(70)90110-X

Zar, J. H. (1984). *Biostatistical Analysis*. New Jersey: Prentice-Hall International Editions.

Conflict of Interest: The authors declare that the research was conducted in the absence of any commercial or financial relationships that could be construed as a potential conflict of interest.

Copyright © 2020 Lattuca, Llompart, Avigliano, Renzi, De Leva, Boy, Vanella, Barrantes, Fernández and de Albuquerque. This is an open-access article distributed under the terms of the Creative Commons Attribution License (CC BY). The use, distribution or reproduction in other forums is permitted, provided the original author(s) and the copyright owner(s) are credited and that the original publication in this journal is cited, in accordance with accepted academic practice. No use, distribution or reproduction is permitted which does not comply with these terms.

frontiers in Marine Science

BRIEF RESEARCH REPORT
published: 26 June 2020
doi: 10.3389/fmars.2020.00417

Cryptic Lives of Conspicuous Animals: Otolith Chemistry Chronicles Life Histories of Coastal Lagoon Fishes

Frederick Feyrer[1], Matthew Young[1], Darren Fong[2], Karin Limburg[3] and Rachel Johnson[4,5]*

[1] California Water Science Center, U.S. Geological Survey, Sacramento, CA, United States, [2] Golden Gate National Recreation Area, National Park Service, San Francisco, CA, United States, [3] College of Environmental Science and Forestry, State University of New York, Syracuse, NY, United States, [4] Fisheries Ecology Division, Southwest Fisheries Science Center, National Oceanic and Atmospheric Administration Fisheries, Santa Cruz, CA, United States, [5] Center for Watershed Sciences, University of California, Davis, Davis, CA, United States

Bar-built coastal lagoons are dynamic ecosystems at the land-sea interface that are important habitats for a variety of species. This study examined the habitat ecology of two lagoon species, the endangered Tidewater Goby (*Eucyclogobius newberryi*) and the Prickly Sculpin (*Cottus asper*) by reconstructing individual life histories from patterns in the concentration of the element Sr (as ratioed to Ca; Sr:Ca) in otoliths. Specific objectives were to (1) elucidate any movements of individual fishes among three primary habitat components of typical bar-built lagoon systems: coastal ocean, brackish lagoon, and freshwater watershed streams, and (2) determine if either species exhibited a consistent life history as defined by a stereotypical otolith Sr:Ca chronology, which could be indicative of a consistent range of salinity or temperature occupied through ontogeny. Results suggested that Tidewater Goby was a lagoon resident and that Prickly Sculpin exhibited migrations between lagoon and watershed stream habitats. There was no strong evidence in either species of ocean occupancy or of a stereotypical Sr:Ca chronology, the latter suggesting the full range of available lagoon habitat in terms of salinity and temperature was likely utilized at all life stages. These findings add to the body of evidence that bar-built lagoons are not isolated habitats, and holistic management of these habitats with adjoining watershed and marine environments could increase habitat connectivity across the landscape, with potential benefits to fishes.

Keywords: otolith, strontium, synchrotron, Tidewater Goby (*Eucyclogobius newberryi*), Prickly Sculpin (*Cottus asper*), amphidromy, bar-built estuary, Rodeo Lagoon

OPEN ACCESS

Edited by:
Alejandra Vanina Volpedo, University of Buenos Aires, Argentina

Reviewed by:
Stephen E. Swearer, University of Melbourne, Australia
Jed Ian Macdonald, Pacific Community (SPC), New Caledonia

****Correspondence:***
Frederick Feyrer
ffeyrer@usgs.gov

Specialty section:
This article was submitted to Marine Ecosystem Ecology, a section of the journal Frontiers in Marine Science

Received: *24 January 2020*
Accepted: *12 May 2020*
Published: *26 June 2020*

Citation:
Feyrer F, Young M, Fong D, Limburg K and Johnson R (2020) Cryptic Lives of Conspicuous Animals: Otolith Chemistry Chronicles Life Histories of Coastal Lagoon Fishes. Front. Mar. Sci. 7:417. doi: 10.3389/fmars.2020.00417

INTRODUCTION

Coastal lagoons are dynamic ecosystems at the land-sea interface that are important habitats for a variety of species (Barnes, 1980; Yáñez-Arancibia, 1985; Pérez-Ruzafa et al., 2019). They can be generally characterized as relatively small, shallow habitats typically connected to the ocean by a small inlet and exhibit a broad range of physical habitat and water quality conditions (Kjerfve, 1994). Bar-built lagoons represent a special form of the habitat in which the inlet is open to the

ocean only episodically in response to a combination of factors driven primarily by wave energy from the ocean and flow dynamics from the watershed (Fong and Kennison, 2010; Behrens et al., 2013; Mcsweeney et al., 2014). Bar-built lagoons are common features along coastlines worldwide, including North and South America, Australia, New Zealand, and South Africa (e.g., Bell et al., 2001; Smakhtin, 2004; Mouillot et al., 2005; Haines et al., 2006; Hume et al., 2016).

The spatio-temporal dynamism of bar-built lagoons provides a variety of habitat functions for fishes, which can be broadly characterized as either temporary habitat for transient species or permanent habitat for resident species (Yáñez-Arancibia et al., 1994). In many cases, especially in CA, United States, where bar-built estuaries represent ∼50% of the region's inland-coastal confluences (Heady et al., 2015; Clark and O'Connor, 2019), lagoon fish faunas are dominated by small-bodied demersal species (Monaco et al., 1990; Allen et al., 2006). Quantifying the habitat and movements of small, demersal fishes is a challenge in marine science and presents obstacles to fully understanding the ecology of coastal lagoons and their biota. An increasingly popular tool to address the challenge of tracking fish among aquatic ecosystems and elucidating coastal dispersal/migration is the application of otolith chemistry as a natural marker of fish life history (Elsdon et al., 2008; Walther and Limburg, 2012; Shao et al., 2018).

Otolith chemistry markers are an effective tool for reconstructing fish life histories, in part, because otolith elemental strontium (Sr) is positively correlated with Sr concentration in water and its salinity (Campana, 1999; Bath et al., 2000). While it is recognized that temperature and physiology can play a role in controlling otolith chemistry (Elsdon and Gillanders, 2004, 2002; Sturrock et al., 2015), it has been shown that approximately 80% of otolith Sr content is derived from the surrounding water for both freshwater and marine species (Farrell and Campana, 1996; Walther and Thorrold, 2009).

The objective of this study was to elucidate the habitat ecology of two fish species common to bar-built lagoons in CA, United States, using the chemical composition of their otoliths: the small-bodied, demersal fishes Tidewater Goby (*Eucyclogobius newberryi*) and Prickly Sculpin (*Cottus asper*). Otolith chemistry was an appropriate tool for this study because behavior and movement of Tidewater Gobies and Prickly Sculpins cannot be directly observed efficiently via traditional technologies. Tidewater gobies are generally considered lagoon residents but are thought to disperse among coastal lagoons via the Pacific Ocean (Lafferty et al., 1999a,b). Tidewater gobies are broadly distributed in lagoons but there is no knowledge of the movements of individuals across habitats or if the species exhibits a consistent life history in terms of salinity or temperature occupied through ontogeny (Swift et al., 1989; Swenson, 1999; Chamberlain, 2006). Prickly sculpins are thought to exhibit a range of life history strategies that could include lagoon residency or migrations between coastal estuaries and watershed streams. While amphidromy has been suggested in some *Cottus* species (Goto and Arai, 2006; Dennenmoser et al., 2014), similar movements have only been inferred in coastal California populations of Prickly Sculpin indirectly based on inferences from size distributions across space (Brown et al., 1995; Moyle, 2002).

This study uses otolith chemistry to contribute new empirical information on movement patterns and habitat use for both species. Specifically, otolith chemistry was applied to (1) elucidate movements of individual Tidewater Gobies or Prickly Sculpins among three primary habitat components of typical bar-built lagoon systems: coastal ocean, brackish lagoon, and freshwater watershed streams, and (2) determine if either species exhibited a consistent life history as defined by a stereotypical otolith Sr chronology, which could be indicative of a consistent range of salinities or temperatures occupied through ontogeny. This information would be useful for conservation and management as it would provide greater knowledge of the habitat needs and life histories of coastal lagoon fishes, many of which, including the Tidewater Goby, are imperiled.

MATERIALS AND METHODS

Study System

Rodeo Lagoon has similar characteristics to many of the bar-built lagoons along the northeastern Pacific. It is located within the Marin Headlands of the Golden Gate National Recreation Area, CA, United States, and is a key component of the United Nations Educational, Scientific, and Cultural Organization's (UNESCO) Golden Gate Biosphere Reserve[1]. There are four key aquatic habitats comprising the system: Pacific Ocean, Rodeo Lagoon, Rodeo Lake, and watershed streams (**Figure 1**). Rodeo Lagoon is a relatively small (15.2 ha), shallow (1–2 m in depth) brackish coastal lagoon that is intermittently (∼30 days per year) connected to the Pacific Ocean when a sand bar at its seaward end breaches in response to sand erosion from high water levels in the lagoon and strong wave action from the Pacific Ocean. A weir and associated vehicle bridge have isolated the landward, eastern tip of Rodeo Lagoon to form Rodeo Lake. Connectivity between Rodeo Lagoon and Rodeo Lake is primarily limited to wet seasons when there is enough freshwater inflow from the watershed to overtop the ∼1.5 m weir. Freshwater inflow originates primarily from Gerbode and Rodeo Creeks, which drain the relatively small (∼777 ha) Rodeo Valley watershed.

Rodeo Lagoon is considered hypereutrophic and characterized by extremely high productivity, spatio-temporal variability in stratification, large fluctuations in dissolved oxygen concentration, and limited water circulation (Cousins et al., 2010; Drake et al., 2010). Salinity varies spatially and seasonally in Rodeo Lagoon. Salinity in the seaward end of Rodeo Lagoon can temporarily match local seawater [∼28 practical salinity units (PSU)] during breaches. For the time period of approximately 1 year leading up to the collection of fishes in our study, there were at least 5 instances of wave overwash from the Pacific Ocean into the Rodeo Lagoon and 3 instances of a breach with full connectivity (totaling 32 days). When the lagoon is isolated from the ocean, salinity typically ranges from approximately 0–10 PSU

[1]http://www.unesco.org/mabdb/br/brdir/directory/biores.asp?mode=all&code=USA+42

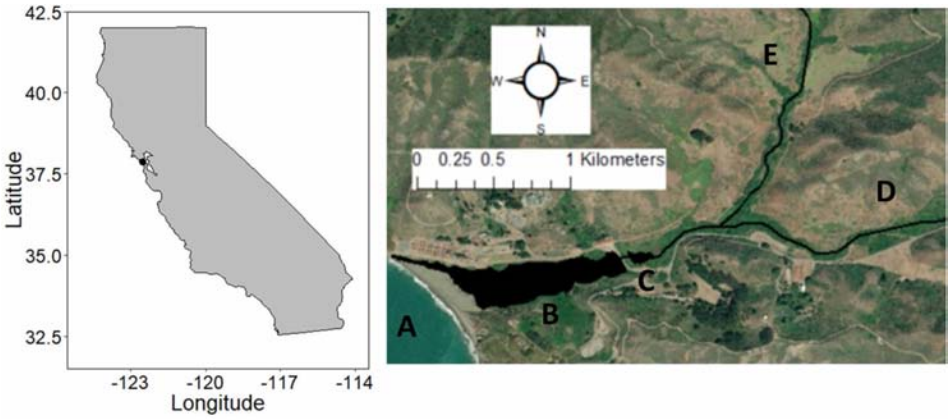

FIGURE 1 | Map of the study area. A = Pacific Ocean. B = Rodeo Lagoon. C = Rodeo Lake. D = Rodeo Creek. E = Gerbode Creek. Imagery source: Esri: DigitalGlobe, GeoEye, EarthStar Geographics, CNES/Airbus DS, USDS, USGS, AeroGRID, IGN, and the GIS User community.

spatially (horizontally and vertically) and temporally (seasonally) in response to freshwater inflow from the watershed. Rodeo Lake and the watershed streams are perennially freshwater with a salinity of 0 PSU. Water temperature ranges seasonally from approximately 8–20°C in Rodeo Lagoon and Rodeo Lake.

Water Chemistry

Baseline Sr and Ca concentrations in the system were determined from discrete water samples collected from the Pacific Ocean, Rodeo Lake, and Rodeo Lagoon. Rodeo Lake was assumed to be a surrogate for the watershed streams since it is directly fed by them and all are freshwater. A total of 17 water samples was collected in April, May, and August 2016. Samples were collected with sterile containers and passed through 0.45 μm filters into acid-washed polyethylene containers. Concentrations of Sr and Ca were measured at the U.S. Geological Survey's National Water Quality Laboratory in Reston, VA, United States. Ambient salinity and temperature conditions associated with each water sample were measured at the time of collection with a handheld YSI EXO2 sonde (Yellow Springs Instruments, Yellow Springs, OH, United States). One-way analysis of variance with Tukey's pairwise comparisons was used to test for differences in Sr:Ca among Pacific Ocean, Rodeo Lagoon, and Rodeo Lake.

Study Species

Tidewater Goby and Prickly Sculpin are sympatric and relatively abundant in Rodeo Lagoon. Prickly Sculpin also occupies Rodeo Lake and the watershed streams. The two species, along with Threespine Stickleback (*Gasterosteus aculeatus*), are the dominant fishes of Rodeo Lagoon as determined from annual fish surveys conducted by the National Park Service (Fong, unpublished data). Tidewater Gobies and Prickly Sculpins are readily collected in beach seine samples and can often be visually observed in shallow water under suitable viewing conditions. Despite its abundance in Rodeo Lagoon, Tidewater Goby is listed as endangered under the U.S. Endangered Species Act. Primary threats to the species across its range include the alteration and loss of coastal lagoons, which are its sole habitat (U.S. Fish and Wildlife Service [USFWS], 2005). In contrast, Prickly Sculpin is a common species broadly distributed in streams, lakes, and estuaries across ∼5,000 km of eastern Pacific coastline, including inland California (Krejsa, 1967; Moyle, 2002). Tidewater Gobies grow to approximately 5 cm and reach 1 year of age while Prickly Sculpins grow to approximately 10 cm and reach 3 years of age. Both species have pelagic larvae and are omnivorous as juvenile and adults feeding primarily on a variety of micro- and macro-crustaceans and insects (Swenson and McCray, 1996; Moyle, 2002; Feyrer et al., 2003; Spies et al., 2014).

Individual Tidewater Gobies and Prickly Sculpins examined in this study were collected freshly dead from around the perimeter of Rodeo Lagoon following a hypoxia-induced fish kill that occurred on 08 August 2016. Additional Prickly Sculpins were collected on 12 April 2016 from Rodeo Lagoon using a beach seine and from Rodeo Creek using a minnow trap. In total, 14 Tidewater Gobies (mean standard length = 40 mm, standard deviation = 2) and 10 Prickly Sculpins (mean standard length = 62 mm, standard deviation = 12) were examined (**Table 1**).

Otolith Preparation and Analysis

Sagittae otoliths were extracted from Tidewater Gobies and Prickly Sculpins. A single otolith from each individual was cleaned and embedded in West Systems 105 epoxy resin and sectioned in the transverse plane for Tidewater Goby and the frontal plane for Prickly Sculpin using a low speed diamond saw. Otoliths were polished to reveal the growth plane and a smooth surface from core to edge using 1500 grit sandpaper and 3 μm lapping film. Finished preparations were cleaned by sonicating in deionized water and wiped with ethanol prior to elemental measurements.

Chemical composition of otoliths was measured at Cornell University's High Energy Synchrotron Source (CHESS; Cornell University, Ithaca, NY, United States) using scanning X-ray fluorescence microscopy (SXFM) on the F3 beamline per established techniques (Limburg et al., 2007). This

TABLE 1 | Sources of otoliths examined in this study.

Species	ID code	Capture location	Capture date	Standard length (mm)
Tidewater Goby (*Eucyclogobius newberryi*)	6	Rodeo Lagoon	8/16/2016	38
Tidewater Goby (*Eucyclogobius newberryi*)	11	Rodeo Lagoon	8/16/2016	40
Tidewater Goby (*Eucyclogobius newberryi*)	12	Rodeo Lagoon	8/16/2016	39
Tidewater Goby (*Eucyclogobius newberryi*)	13	Rodeo Lagoon	8/16/2016	41
Tidewater Goby (*Eucyclogobius newberryi*)	14	Rodeo Lagoon	8/16/2016	42
Tidewater Goby (*Eucyclogobius newberryi*)	18	Rodeo Lagoon	8/16/2016	37
Tidewater Goby (*Eucyclogobius newberryi*)	22	Rodeo Lagoon	8/16/2016	40
Tidewater Goby (*Eucyclogobius newberryi*)	25	Rodeo Lagoon	8/16/2016	41
Tidewater Goby (*Eucyclogobius newberryi*)	27	Rodeo Lagoon	8/16/2016	42
Tidewater Goby (*Eucyclogobius newberryi*)	28	Rodeo Lagoon	8/16/2016	41
Tidewater Goby (*Eucyclogobius newberryi*)	37	Rodeo Lagoon	8/16/2016	40
Tidewater Goby (*Eucyclogobius newberryi*)	173	Rodeo Lagoon	8/16/2016	38
Tidewater Goby (*Eucyclogobius newberryi*)	175	Rodeo Lagoon	8/16/2016	38
Tidewater Goby (*Eucyclogobius newberryi*)	176	Rodeo Lagoon	8/16/2016	36
Prickly Sculpin (*Cottus asper*)	59	Rodeo Lagoon	8/15/2016	54
Prickly Sculpin (*Cottus asper*)	60	Rodeo Lagoon	8/15/2016	49
Prickly Sculpin (*Cottus asper*)	63	Rodeo Lagoon	8/15/2016	64
Prickly Sculpin (*Cottus asper*)	65	Rodeo Lagoon	8/15/2016	78
Prickly Sculpin (*Cottus asper*)	66	Rodeo Creek	4/12/2016	58
Prickly Sculpin (*Cottus asper*)	69	Rodeo Creek	4/12/2016	89
Prickly Sculpin (*Cottus asper*)	72	Rodeo Lagoon	4/12/2016	62
Prickly Sculpin (*Cottus asper*)	74	Rodeo Lagoon	4/12/2016	58
Prickly Sculpin (*Cottus asper*)	75	Rodeo Lagoon	4/12/2016	53
Prickly Sculpin (*Cottus asper*)	78	Rodeo Lagoon	4/12/2016	56

instrument allows for two-dimensional spatial mapping of elemental concentrations across the full otolith surface using a non-destructive technique with minimal interferences among elements. Briefly, a multi-layer monochromater (0.6% bandwidth) produced an X-ray with 16 KeV energy focused on the otolith with a single glass capillary necessary to achieve 5–20 μm spot resolution over the entire otolith. The photon flux was about 0.5×10^{11} counts per second and a florescence spectrum integrated for 1 s. Fluorescence spectra were calibrated using an in-house otolith pellet previously described (Limburg et al., 2007, 2011).

Distributions of absolute concentrations (ppm) of Sr and Ca were processed with PyMCA (Sole et al., 2007). Commercial geographic information system software (ArcMap v10.5, ESRI, Redlands, CA, United States) was used to process elemental maps of the otolith surfaces and analyze spatial patterns following established practices (Limburg et al., 2007). Sr and Ca concentrations along linear transects across otolith surfaces were extracted from the elemental maps using tools available in ArcMap. Transects were made along the primary growth axis of each otolith from core to edge (**Figure 2**). Discrete values of Sr and Ca concentration were captured approximately every 1 μm along the transects to generate a chronological time series of data for each individual from approximately birth to death. Sr was ratioed to Ca (Sr:Ca) for data analyses and interpretation. Individual chronologies were visually inspected for patterns. Additionally, hierarchical time series cluster analysis was used to test for similarities in chronologies among individuals of each species. Analyses were implemented in the "dtwclust" package in the R statistical computing environment (Sardá-Espinosa, 2019a,b). Cluster validity indices were calculated to objectively determine the appropriate number of clusters.

RESULTS

Water Chemistry

The 17 water samples examined in this study spanned the full range of salinity that fish could have potentially

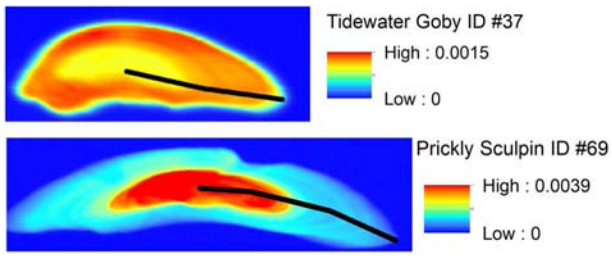

FIGURE 2 | Spatial distribution of Sr concentration (ppm) in example otoliths from a Tidewater Goby (frontal section) and Prickly Sculpin (transverse section). Lines on each otolith represent the growth plane where Sr:Ca chronologies were obtained. Note that images are not on the same scale: line lengths are 773 μm on the Tidewater Goby otolith and 2,683 μm on the Prickly Sculpin otolith.

TABLE 2 | Sources and details of water samples examined in this study.

Habitat	Date	Lat.	Lon.	Temp. (°C)	Salinity (PSU)	Sr (ppm)	Ca (ppm)	Sr:Ca
Pacific Ocean	4/12/2016	37.830	−122.537	13	27.9	7,568	369,000	0.0205
Pacific Ocean	8/16/2016	37.830	−122.537	18	29.3	7,542	381,300	0.0198
Rodeo Lagoon	4/11/2016	37.831	−122.528	18	2.3	520	32,500	0.0160
Rodeo Lagoon	4/11/2016	37.830	−122.534	16	2.5	508	31,270	0.0163
Rodeo Lagoon	4/11/2016	37.830	−122.534	17	16.8	4,466	218,000	0.0205
Rodeo Lagoon	5/17/2016	37.831	−122.528	–	0.9	1,005	64,560	0.0156
Rodeo Lagoon	5/17/2016	37.831	−122.528	–	4.4	992	60,570	0.0164
Rodeo Lagoon	5/17/2016	37.830	−122.534	–	4.4	1,019	63,330	0.0161
Rodeo Lagoon	5/17/2016	37.830	−122.534	20	4.5	1,022	60,750	0.0168
Rodeo Lagoon	8/15/2016	37.831	−122.528	14	6.8	1,535	84,030	0.0183
Rodeo Lagoon	8/15/2016	37.831	−122.528	17	6.8	1,471	83,910	0.0175
Rodeo Lagoon	8/15/2016	37.830	−122.534	16	6.8	1,463	83,880	0.0174
Rodeo Lagoon	8/15/2016	37.830	−122.534	19	6.8	1,526	83,610	0.0183
Rodeo Lagoon	8/16/2016	37.830	−122.534	18	6.8	1,492	83,830	0.0178
Rodeo Lake	4/12/2016	37.832	−122.525	14	0.1	56	8,346	0.0067
Rodeo Lake	5/17/2016	37.832	−122.525	19	0.1	70	10,400	0.0067
Rodeo Lake	8/15/2016	37.832	−122.525	13	0.1	92	12,160	0.0076

encountered (0–28 PSU) and a wide temperature range (12–20°C) (**Table 2**). Absolute Sr concentrations ranged from 56 to 7,568 ppm (mean = 1902, standard deviation = 2350). Absolute Ca concentrations ranged from 8,346 to 381,300 ppm (mean = 101,849, standard deviation = 113,407). Sr:Ca values ranged from 0.0067 to 0.0205 (mean = 0.0157, standard deviation = 0.0044). The relation between Sr:Ca and salinity was exponentially asymptotic in that Sr:Ca values increased rapidly with salinity up to about 8 PSU and then remained relatively flat thereafter (**Figure 3**). Sr:Ca values were statistically unique among habitat types ($P < 0.001$) with values highest in the Pacific Ocean (mean = 0.0201, standard deviation = 0.0005), intermediate in Rodeo Lagoon (mean = 0.01724, standard deviation = 0.0013), and lowest in Rodeo Lake (mean = 0.0070, standard deviation = 0.0005).

Otolith Chemistry

A Sr:Ca salinity and otolith relationship was developed using salinity and Sr:Ca measured in water across habitats and Sr:Ca values measured in otoliths associated with capture locations for individuals. It was posited that 0.002 was a conservative breakpoint value of otolith Sr:Ca that distinguished occupancy in Rodeo Lagoon (>0.002) versus upstream habitats such as Rodeo Lake and watershed streams (<0.002) for both species. This value was based on a weight of evidence that included corresponding salinity and Sr:Ca water measurements across the habitats and Sr:Ca otolith values at capture locations for individuals. There was further support for this freshwater-lagoon cut-off given that none of the Tidewater Gobies had Sr:Ca values < 0.002 and that they have never been documented in upstream habitats. The Sr:Ca values comprising Tidewater Goby otolith chronologies ranged from 0.0024 to 0.0066 (mean = 0.0043, standard deviation = 0.0009) while the Sr:Ca values comprising Prickly Sculpin otolith chronologies ranged from 0.0008 to 0.0113 (mean = 0.0058, standard deviation = 0.0019) (**Figure 4**).

The range of Sr:Ca values exhibited in Tidewater Goby otoliths were consistent with all individuals having solely inhabited Rodeo Lagoon (**Figure 4**). In contrast, the range of Sr:Ca values exhibited in Prickly Sculpin otoliths demonstrated movement between Rodeo Lagoon and the watershed streams (**Figure 4**). Specifically, the chronologies of two Prickly Sculpins that were captured in Rodeo Creek suggested they had been born in Rodeo

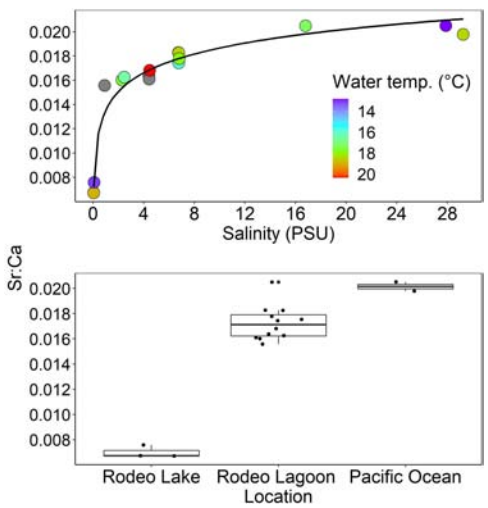

FIGURE 3 | Upper: Relation between salinity and Sr:Ca in the Rodeo Lagoon system. The line is an exponential curve fitted to the data. Water temperature values were measured at the time of water sample collection; dark gray points do not have corresponding temperature data. **Lower:** Boxplot representation of the same Sr:Ca data aggregated according to samples collected in Pacific Ocean, Rodeo Lagoon, and Rodeo Lake. Jitter was imposed on the data points in the lower plot to avoid superimposition. Box plot shows the median, 25th and 75th percentile and upper and lower values of 1.5* (inter quartile range).

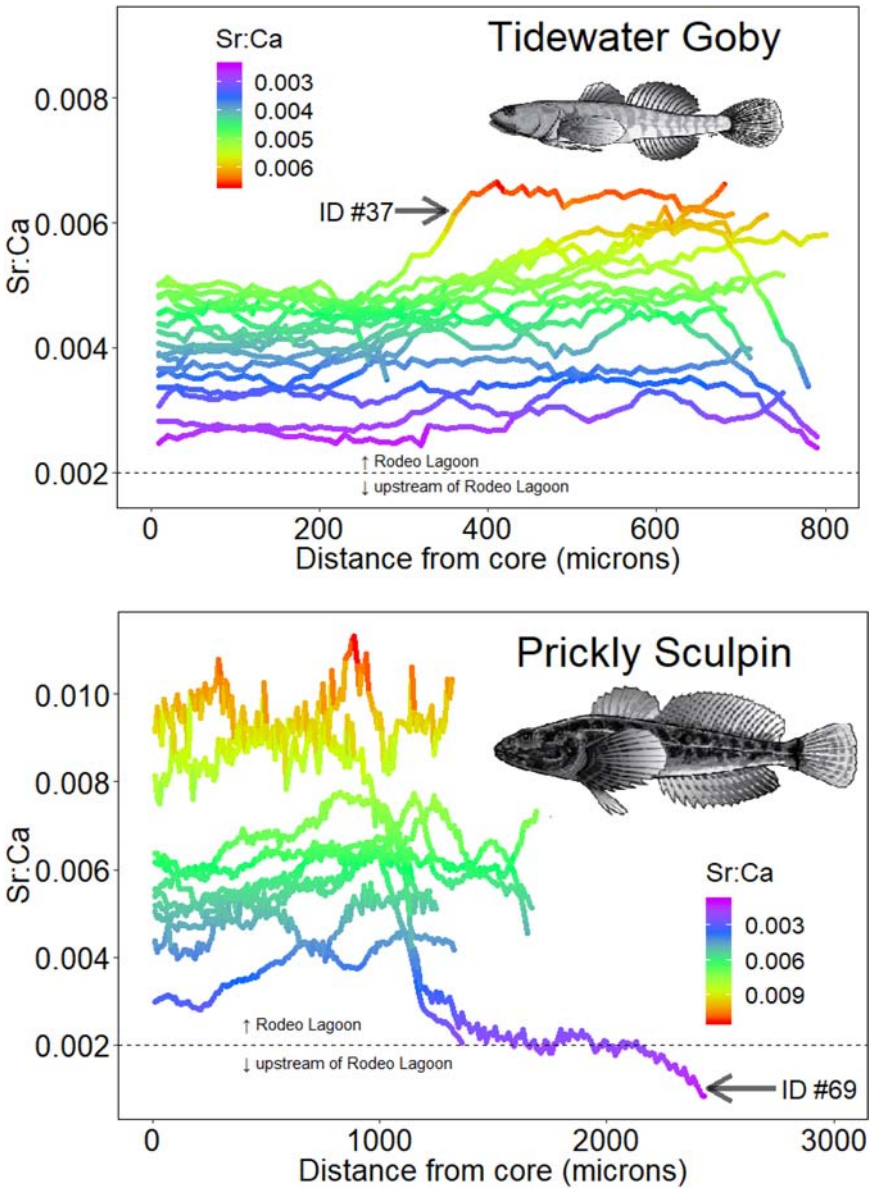

FIGURE 4 | Otolith Sr:Ca chronologies of Tidewater Gobies **(upper panel)** and Prickly Sculpins **(lower panel)**. The horizontal dashed lines show the Sr:Ca value distinguishing Rodeo Lagoon from upstream habitats. For illustrative purposes, otoliths of the noted individuals are shown in **Figure 2**. The two Prickly Sculpin with ending Sr:Ca values at or below 0.002 were the individuals that were collected from Rodeo Creek upstream of Rodeo Lagoon.

Lagoon. While we cannot discount possible marine habitat use given the limited resolution of Sr:Ca to resolve brackish from fully marine habitats, we would have expected higher Sr:Ca values in otoliths if individuals had occupied the Pacific Ocean given the water values were statistically higher in the Pacific Ocean compared to Rodeo Lagoon (**Figure 3**). We did not find any strong evidence that any individuals of either species occupied the Pacific Ocean.

Hierarchical time series cluster analysis and cluster validation indices suggested little similarity in Sr:Ca chronologies among individuals of each species, indicating that there was no consistent life history in either species (**Supplementary Material**). Specifically, eighty-six percent (12 of 14) of individual Tidewater Gobies and eighty percent (8 of 10) of individual Prickly Sculpins exhibited unique chronologies, thereby providing no evidence of a stereotypical otolith Sr:Ca chronology in either species.

DISCUSSION

This study demonstrated the utility of otolith chemistry as a tool to generate habitat and life history information on fishes that would have otherwise been costly and challenging to

obtain. In this case, reconstructing habitat use of individual fishes with otolith chemistry was possible because of sufficient variation in aqueous Sr:Ca among key habitat components of the Rodeo Lagoon system. This facilitated observations that sampled Tidewater Gobies were resident to Rodeo Lagoon and that some Prickly Sculpins exhibited migration from Rodeo Lagoon upstream into watershed streams.

The relatively small number of individuals examined was unavoidable given the endangered status of Tidewater Goby. Nonetheless, this study took advantage of a rare opportunity to examine an endangered species and generate missing and direct empirical information on the habitat and movements of coastal lagoon fishes. It is also important to note that while this study provides information on the range of habitat and behaviors possible, behaviors may vary in other systems in response to unique hydrology and associated physico-chemical properties.

The absence of stereotypical Sr:Ca chronologies in Tidewater Goby and Prickly Sculpin suggests individuals used a diversity of microhabitats and exhibited variable movement patterns and/or that individuals experienced a range of different physio-chemical habitat conditions expressed by the dynamic nature of the lagoon. The range of Sr:Ca values exhibited within and between each species suggested that the full range of salinity and temperature within Rodeo Lagoon was likely occupied across all life stages. What remains unclear is if a specific range of temperature or salinity provides fitness benefits to either species. This could potentially be resolved with studies that integrate health indicators with other otolith chemistry markers, such as oxygen isotopes ($\delta^{18}O$) that could potentially provide a higher level of resolution of salinities or temperatures occupied by individuals (Walther and Limburg, 2012; Willmes et al., 2019).

The information generated by this study has important implications for the conservation and management of bar-built lagoons and their biota. Foremost, these findings add to the body of evidence that bar-built lagoons are not isolated habitats, and holistic management of these habitats with adjoining watershed and marine environments could increase habitat connectivity across the landscape, with potential benefits to fishes. Ecosystem-level management of bar-built lagoon systems would benefit a diverse suite of fishes. In addition to the species examined in this study, bar-built lagoons are important habitats that provide consequential fitness benefits for anadromous salmonids, many of which are protected under the U.S. Endangered Species Act (e.g., Shapovalov and Taft, 1954; Bond et al., 2008; Hayes et al., 2008). Additionally, it has been demonstrated that artificial manipulation of connectivity between bar-built lagoons and the ocean can cause devastating fish kills (Swift et al., 2018). Specific to the study system, modification or removal of the weir that forms Rodeo Lake would potentially increase the amount of habitat area available to support the endangered Tidewater Goby and remove a passage barrier that would potentially benefit highly mobile anadromous and amphidromous species if the reclaimed habitat is suitable (Hale et al., 2016).

DATA AVAILABILITY STATEMENT

Data generated for this study are available from the U.S. Geological Survey's ScienceBase catalog (Steinke and Feyrer, 2020; https://doi.org/10.5066/P9PZMELL).

ETHICS STATEMENT

Samples examined in this study were collected with authority granted in U.S. National Park Service Scientific Research and Collecting Permit GOGA-2016-SCI-0005 and U.S. Fish and Wildlife Service Permit #TE036499-8.

AUTHOR CONTRIBUTIONS

RJ, FF, and KL analyzed the samples. FF analyzed the data and prepared the figures. All authors contributed to writing the manuscript and design of the study.

FUNDING

Funding was provided by the U.S. Geological Survey-National Park Service Water Quality Partnership. The Cornell High Energy Synchrotron Source was supported by the National Science Foundation under award DMR-1332208.

ACKNOWLEDGMENTS

We extend our appreciation to O. Patton and D. Ayers for assistance with field work, to T. Kraus and E. Stumpner for processing water samples, to G. Whitman for preparing and processing otoliths, to R. Huang for assistance at the Cornell High Energy Synchrotron Source, to E. Gusto for creating the fish illustrations, and to V. Larwood for assistance creating the map. Any use of trade, firm, or product names is for descriptive purposes only and does not imply endorsement by the U.S. Government.

SUPPLEMENTARY MATERIAL

The Supplementary Material for this article can be found online at: https://www.frontiersin.org/articles/10.3389/fmars.2020.00417/full#supplementary-material

REFERENCES

Allen, L. G., Yoklavich, M. M., Cailliet, G. M., and Horn, M. H. (2006). "Bays and estuaries," in *The Ecology of Marine Fishes: California and Adjacent Waters*, eds L. G. Allen and M. H. Horn (Berkeley, CA: University of California Press), 119–148.

Barnes, R. S. K. (1980). *Coastal Lagoons*. Cambridge: Cambridge University Press.

Bath, G. E., Thorrold, S. R., Jones, C. M., Campana, S. E., McLaren, J. W., and Lam, J. W. H. (2000). Strontium and barium uptake in aragonitic otoliths of marine fish. *Geochim. Cosmochim. Acta* 64, 1705–1714. doi: 10.1016/s0016-7037(99)00419-6

Behrens, D. K., Bombardellia, F. A., Largier, J. L., and Twohy, E. (2013). Episodic closure of the tidal inlet at the mouth of the Russian River — A small bar-built estuary in California. *Geomorphology* 189, 66–80. doi: 10.1016/j.geomorph.2013.01.017

Bell, K. N. I., Cowley, P. D., and Whitfield, A. K. (2001). Seasonality in frequency of marine access to an intermittently open estuary. *Estuar. Coast. Shelf Sci.* 52, 327–337. doi: 10.1006/ecss.2000.0709

Bond, M. H., Hayes, S. A., Hanson, C. V., and MacFarlane, R. B. (2008). Marine survival of steelhead (*Oncorhynchus mykiss*) enhanced by a seasonally closed estuary. *Can. J. Fish. Aquat. Sci.* 65, 2242–2252. doi: 10.1139/f08-131

Brown, L. R., Matern, S. A., and Moyle, P. B. (1995). Comparative ecology of prickly sculpin, Cottus asper, and coastrange sculpin, *C. aleuticus*, in the Eel River, California. *Environ. Biol. Fish.* 42, 329–343. doi: 10.1007/BF00001462

Campana, S. E. (1999). Chemistry and composition of fish otoliths: pathways, mechanisms and applications. *Mar. Ecol. Prog. Ser.* 188, 263–297. doi: 10.3354/meps188263

Chamberlain, C. D. (2006). *Environmental Variables of Northern California Lagoons and Estuaries and the Distribution of Tidewater Goby (Eucyclogobius newberryi)*. Arcata Technical Report TR 2006–2004. Washington, DC: U.S. Fish and Wildlife Service.

Clark, R., and O'Connor, K. (2019). A systematic survey of bar-built estuaries along the California coast. *Estuar. Coast. Shelf Sci.* 226:106285. doi: 10.1016/j.ecss.2019.106285

Cousins, M., Stacey, M. T., and Drake, J. L. (2010). Effects of seasonal stratification on turbulent mixing in a hypereutrophic coastal lagoon. *Limnol. Ocean* 55, 172–186. doi: 10.4319/lo.2010.55.1.0172

Dennenmoser, S., Rogers, S. M., and Varnosi, S. M. (2014). Genetic population structure in prickly sculpin (*Cottus asper*) reflects isolation-by-environment between two life-history ecotypes. *Biol. J. Linn. Soc.* 113, 943–957. doi: 10.1111/bij.12384

Drake, J. L., Carpenter, E. J., Cousins, M., Nelson, K. L., Guido-Zarate, A., and Loftin, K. (2010). Effects of light and nutrients on seasonal phytoplankton succession in a temperate eutrophic coastal lagoon. *Hydrobiologia* 654, 177–192. doi: 10.1007/s10750-010-0380-y

Elsdon, T., and Gillanders, B. (2002). Interactive effects of temperature and salinity on otolith chemistry: challenges for determining environmental histories of fish. *Can. J. Fish. Aquat. Sci.* 59, 1796–1808. doi: 10.1139/f02-154

Elsdon, T., and Gillanders, B. (2004). Fish otolith chemistry influenced by exposure to multiple environmental variables. *J. Exp. Mar. Biol. Ecol.* 313, 269–284. doi: 10.1016/j.jembe.2004.08.010

Elsdon, T. S., Wells, B. K., Campana, S. E., Gillanders, B. M., Jones, C. M., Limburg, K. E., et al. (2008). Otolith chemistry to describe movements and life history parameters of fishes: hypotheses, assumptions, limitations and inferences. *Ocean Mar. Biol.* 46, 297–330. doi: 10.1201/9781420065756.ch7

Farrell, J., and Campana, S. E. (1996). Regulation of calcium and strontium deposition on the otoliths of juvenile tilapia. *Oreochromis niloticus*. Comp. Biochem. Physiol. 115, 103–109. doi: 10.1016/0300-9629(96)00015-1

Feyrer, F., Herbold, B., Matern, S. A., and Moyle, P. B. (2003). Dietary shifts in a stressed fish assemblage. *Environ. Biol. Fish.* 67, 277–288. doi: 10.1023/A:1025839132274

Fong, P., and Kennison, R. L. (2010). "Phase shifts, alternative stable states, and the status of southern California lagoons," in *Coastal Lagoons; Critical Habitats of Environmental Change*, eds M. J. Kennish and H. W. Paerl (Boca Raton, FL: CRC Press), 227–251. doi: 10.1201/ebk1420088304-c10

Goto, A., and Arai, T. (2006). Diverse migratory histories of Japanese *Trachidermus* and *Cottus* species (*Cottidae*) as inferred from otolith microchemistry. *J. Fish Biol.* 68, 1731–1741. doi: 10.1111/j.1095-8649.2006.01040.x

Haines, P. E., Tomlinson, R. B., and Thom, B. G. (2006). Morphometric assessment of intermittently open/closed coastal lagoons in New South Wales. *Australia. Estuar. Coast Shelf Sci.* 67, 321–332. doi: 10.1016/j.ecss.2005.12.001

Hale, R., Morrongiello, J. R., and Swearer, S. E. (2016). Evolutionary traps and range shifts in a rapidly changing world. *Biol. Lett.* 12:20160003. doi: 10.1098/rsbl.2016.0003

Hayes, S. A., Bond, M. H., Hanson, C. V., Fruend, E. V., Smith, J. J., Anderson, E. C., et al. (2008). Steelhead growth in a Small central California watershed: upstream and estuarine rearing patterns. *Trans. Amer. Fish. Soc.* 137, 114–128. doi: 10.1577/t07-043.1

Heady, W. N., Clark, R. P., O'Connor, K., Clark, C., Endris, C., Ryan, S., et al. (2015). Assessing California's bar-built estuaries using the California rapid assessment method. *Ecol. Ind.* 58, 300–310. doi: 10.1016/j.ecolind.2015.05.062

Hume, T., Gerbeaux, P., Hart, D., Kettles, H., and Neale, D. (2016). *A Classification of New Zealand's Coastal Hydrosystems*. New Zealand Technical Report, Report No. HAM2016-062. Auckland: National Institute of Water & Atmospheric Research Ltd. .

Kjerfve, B. (1994). "Coastal lagoons," in *Coastal Lagoon Processes*, ed. B. Kjerfve (Amsterdam: Elsevier Oceanographic Series), 1–8. doi: 10.1016/s0422-9894(08)70006-0

Krejsa, R. J. (1967). The systematics of the prickly sculpin, cottus asper richardson, a polytypic species. Part I. Synonymy, nomenclatural history, and distribution. *Pacific Sci.* 21, 241–251. doi: 10.1093/jhered/esw045

Lafferty, K. D., Swift, C. C., and Ambrose, R. F. (1999a). Extirpation and recolonization in a metapopulation of an endangered fish, the tidewater goby. *Conserv. Biol.* 13, 1447–1453. doi: 10.1046/j.1523-1739.1999.98016.x

Lafferty, K. D., Swift, C. C., and Ambrose, R. F. (1999b). Postflood persistence and recolonization of endangered tidewater goby populations. *North Am. J. Fish. Manag.* 19, 618–622. doi: 10.1577/1548-8675(1999)019<0618:pparoe>2.0.co;2

Limburg, K. E., Huang, R., and Bilderback, D. H. (2007). Fish otolith trace element maps: new approaches with synchrotron microbeam x-ray fluorescence. *X Ray Spectrometry* 36, 336–342. doi: 10.1002/xrs.980

Limburg, K. E., Olson, C., Walther, Y., Dale, D., Slomp, C., and Høie, H. (2011). Tracking Baltic hypoxia and cod migration over millennia with natural tags. *Proc. Natl. Acad. Sci. U.S.A.* 108, E177–E182. doi: 10.1073/pnas.1100684108

Mcsweeney, S. L., Kennedy, D. M., and Rutherfurd, I. D. (2014). "Classification of intermittently closed and open coastal lakes and lagoons in Victoria, Australia," in *Proceedings of the 7th Australian Stream Management Conference*, Townsville, QLD, 1–8.

Monaco, M. E., Emmett, R. L., Nelson, D. M., and Hinton, S. A. (1990). *Distribution and Abundance of Fishes and Invertebrates in West Coast Estuaries Volume I: Data summaries*. ELMR Rp. No. 4. Silver Spring, MD: NOAA/NOS Strategic Environmental Assessments Division, 322.

Mouillot, D., Gaillard, S., Aliaume, C., Verlaque, M., Belsher, T., Troussellier, M., et al. (2005). Ability of taxonomic diversity indices to discriminate coastal lagoon environments based on macrophyte communities. *Ecol. Indicat.* 5, 1–17. doi: 10.1016/j.ecolind.2004.04.004

Moyle, P. B. (2002). *Inland fishes of California. Revised and expanded*. Berkeley, CA: University of California Press.

Pérez-Ruzafa, A., Mompeán, M. C., and Marcos, C. (2019). Hydrographic, geomorphologic and fish assemblage relationships in coastal lagoons. *Hydrobiologia* 577, 107–125. doi: 10.1007/s10750-006-0421-428

Sardá-Espinosa, A. (2019a). Dtwclust: Time Series Clustering Along With Optimizations for the Dynamic Time Warping Distance. R Package Version 5.5.6. Avaliable online at: https://cran.r-project.org/web/packages/dtwclust/index.html

Sardá-Espinosa, A. (2019b). Time-series clustering in R using the dtwclust package. *R J.* 11, 22–43. doi: 10.32614/RJ-2019-023

Shao, Y., Farkas, J., Holmden, C., Mosley, L., Kell-Duivestein, I., Izzo, C., et al. (2018). Calcium and strontium isotope systematics in the lagoon-estuarine environments of South Australia: implications for water source mixing, carbonate fluxes and fish migration. *Geochim. Cosmochim. Acta* 239, 90–108. doi: 10.1016/j.gca.2018.07.036

Shapovalov, L., and Taft, A. C. (1954). The life histories of the steelhead rainbow trout (*Salmo gairdneri gairdneri*) and silver salmon (*Oncorhynchus kisutch*) with special reference to Waddell Creek, California, and recommendations regarding their management. *Calif. Dep. Fish Game Fish Bull.* 98:375.

Smakhtin, V. U. (2004). Simulating the hydrology and mouth conditions of small, temporarily closed/open estuaries. *Wetlands* 24, 123–132. doi: 10.1672/0277-5212(2004)024[0123:sthamc]2.0.co;2

Sole, V. A., Papillon, E., Cotte, M., Walter, P., and Susini, J. (2007). A multiplatform code for the analysis of 477 energy-dispersive X-ray fluorescence spectra. *Spectroc. Acta Pt. B Atom. Spectr.* 62, 63–68. doi: 10.1016/j.sab.2006.12.002

Spies, B. T., Tarango, B. C., and Steele, M. A. (2014). Larval Duration, Settlement, and Larval Growth Rates of the Endangered Tidewater Goby (*Eucyclogobius*

newberryi) and the Arrow Goby (*Clevelandia ios*) (*Pisces*, *Teleostei*). *Bull. Soc. Calif. Acad. Sci.* 113, 165–175. doi: 10.3160/0038-3872-113.3.165

Steinke, D., and Feyrer, F. (2020). *Otolith chemistry of fishes in Rodeo Lagoon, Marin County, California, 2016*. Reston, VA: U.S. Geological Survey Data Release.

Sturrock, A. M., Hunter, E., Milton, J. A., Johnson, R. C., Waring, C. P., and Trueman, C. N. (2015). Quantifying physiological influences on otolith microchemistry. *Methods Ecol. Evol.* 6, 806–816. doi: 10.1111/2041-210X.12381

Swenson, R. O. (1999). The ecology, behavior, and conservation of the tidewater goby, *Eucyclogobius newberryi*. *Environ. Biol. Fish.* 55, 99–114. doi: 10.1023/A:1007478207892

Swenson, R. O., and McCray, A. T. (1996). Feeding ecology of the tidewater goby. *Trans. Am. Fish. Soc.* 125, 956–970. doi: 10.1577/1548-8659(1996)125<0956:feottg>2.3.co;2

Swift, C. C., Mulder, J., Dellith, C., and Kittleson, K. (2018). Mortality of native and non-native fishes during artificial breaching of coastal lagoons in southern and central California. *Southern Calif. Acad. Sci.* 117, 157–168. doi: 10.3160/1767.1

Swift, C. C., Nelson, J. L., Maslow, C., and Stein, T. (1989). Biology and distribution of the tidewater goby, *Eucyclogobius newberryi* (*Pisces*: *Gobiidae*) of California. *Contrib. Sci.* 404, 1–19.

U.S. Fish and Wildlife Service [USFWS] (2005). *Recovery plan for the tidewater goby (Eucyclogobius newberryi)*. Portland, OR: Pacific Region, U.S. Fish and Wildlife Service, 199.

Walther, B. D., and Limburg, K. (2012). The use of otolith chemistry to characterize diadromous migrations. *J. Fish Biol.* 81, 796–825. doi: 10.1111/j.1095-8649.2012.03371.x

Walther, B. D., and Thorrold, S. R. (2009). Inter-annual variability in isotope and elemental ratios recorded in otoliths of an anadromous fish. *J. Geochem. Explor.* 102, 181–186. doi: 10.1016/j.gexplo.2008.10.001

Willmes, M., Lewis, L. S., Davis, B. E., Loiselle, L., James, H. F., Denney, C., et al. (2019). Calibrating temperature reconstructions from fish otolith oxygen isotope analysis for California's critically endangered Delta Smelt. *Rapid Commun. Mass Spectrom.* 33, 1207–1220. doi: 10.1002/rcm.8464

Yáñez-Arancibia, A. (ed.) (1985). *Fish Community Ecology in Estuaries, and Coastal Lagoons: Towards an Ecosystem Integration*. Mexico: UNAM Press.

Yáñez-Arancibia, A., Lara-Domínguez, A. L., and Pauly, Y. (1994). "Coastal lagoons as fish habitats," in *Coastal Lagoon Processes*, ed. K. Kjerfve (Amsterdam: Elsevier), 363–376. doi: 10.1016/s0422-9894(08)70017-5

Conflict of Interest: The authors declare that the research was conducted in the absence of any commercial or financial relationships that could be construed as a potential conflict of interest.

Copyright © 2020 Feyrer, Young, Fong, Limburg and Johnson. This is an open-access article distributed under the terms of the Creative Commons Attribution License (CC BY). The use, distribution or reproduction in other forums is permitted, provided the original author(s) and the copyright owner(s) are credited and that the original publication in this journal is cited, in accordance with accepted academic practice. No use, distribution or reproduction is permitted which does not comply with these terms.

frontiers in Marine Science

ORIGINAL RESEARCH
published: 03 July 2020
doi: 10.3389/fmars.2020.00529

Comparison of Otolith Microstructure of Herring Larvae and Sibling Adults Reared Under Identical Early Life Conditions

Susanne Tonheim[1,2], Aril Slotte[2], Leif Andersson[3,4,5], Arild Folkvord[1,2] and Florian Berg[1,2]**

[1] Department of Biological Sciences, University of Bergen, Bergen, Norway, [2] Institute of Marine Research (IMR), Bergen, Norway, [3] Science for Life Laboratory, Department of Medical Biochemistry and Microbiology, Uppsala University, Uppsala, Sweden, [4] Department of Animal Breeding and Genetics, Swedish University of Agricultural Sciences, Uppsala, Sweden, [5] Department of Veterinary Integrative Biosciences, Texas A&M University, College Station, TX, United States

OPEN ACCESS

Edited by:
Benjamin D. Walther,
Texas A&M University Corpus Christi,
United States

Reviewed by:
Dorothee Moll,
Thünen-Institut, Germany
Paul Kotterba,
University of Rostock, Germany

***Correspondence:**
Susanne Tonheim
susanne.tonheim@hi.no
Florian Berg
florian.berg@hi.no

Specialty section:
This article was submitted to
Marine Ecosystem Ecology,
a section of the journal
Frontiers in Marine Science

Received: 30 January 2020
Accepted: 10 June 2020
Published: 03 July 2020

Citation:
Tonheim S, Slotte A, Andersson L, Folkvord A and Berg F (2020) Comparison of Otolith Microstructure of Herring Larvae and Sibling Adults Reared Under Identical Early Life Conditions. Front. Mar. Sci. 7:529. doi: 10.3389/fmars.2020.00529

Atlantic herring (*Clupea harengus*) is a euryhaline species, occupying fully marine habitats (35 psu) in the North Atlantic, as well as brackish waters (<20 psu) such as in the adjacent Baltic Sea. We co-reared Atlantic purebreds and Atlantic/Baltic F1 hybrids in two salinity regimes (16 and 35 psu) in a common garden experiment for 3 years until their first maturity. This setup enabled for the first time a direct comparison between adults and their larval siblings at respective salinity regimes in terms of larval growth indicated by otolith microstructure. We validated that otolith microstructure analysis of adult otoliths is reflecting the experienced otolith growth during the larval stage. No major selection in terms of otolith growth had taken place during the juvenile stage, except for one experimental group. Surviving adult Atlantic purebreds reared at 16 psu had higher otolith growth compared to their larval stages. The validation that otolith microstructure analyses of adult herring can reliably be extracted and used to examine larval growth even after several years adds strong support for further use of such analyses. Among the parental generation, Baltic herring had a faster initial otolith growth than Atlantic herring. The growth of their laboratory-reared F1 progeny was intermediate compared to their parents. In general, larval growth of both Atlantic purebreds and Atlantic/Baltic hybrids reared in 16 psu was significantly larger than for those herring reared at 35 psu. There was no significant difference in larval growth between Atlantic purebreds and Atlantic/Baltic hybrids reared at 35 psu, but hybrid larval growth was significantly higher compared to larval growth of Atlantic purebreds at 16 psu. This was not reflected at the adult stage where purebreds were ultimately larger than hybrids (Berg et al., 2018). This indicates the influence and importance of environmental and genetic factors throughout the life of Atlantic herring, along with genetic contributions to phenotypic variability.

Keywords: population structure, otolith microstructure, common garden, population discrimination, salinity, phenotypic plasticity

INTRODUCTION

Phenotypic characteristics of marine fish are the result of the interaction between their genotype and the prevailing environmental conditions (Swain and Foote, 1999; Mitchell-Olds et al., 2007; Barrett and Hoekstra, 2011). Non-genetic changes of phenotypes in response to environmental factors is known as phenotypic plasticity (Via et al., 1995). Otoliths are amenable structures to study the extent of phenotypic plasticity since they allow for estimation of age and growth of individual fish (Campana and Thorrold, 2001). Pannella (1971) initially hypothesized that otolith growth occurs by daily increments which was later confirmed for a variety of species (Brothers et al., 1976; Rey et al., 2016; Gibb et al., 2020). The formation of daily increments was also validated for several life stages from larvae to adults (Panfili and Tomas, 2001; Cermeño et al., 2003). These daily increments are the baseline for otolith microstructure analysis being the most applied approach in otolith science (Campana, 2005). Further, otolith chemistry studies validated that the information stored during the larval stage can be still detected in adult otoliths (Gillanders, 2002; Reis-Santos et al., 2013; Rogers et al., 2019). It is, therefore, justifiable to assume that the observed microstructure of adult otoliths still reflects the larval daily growth even after several years of living. In theory, the larval otolith microstructure should not alter in adult otoliths, but the accuracy of daily increment measurements from adult otoliths might be limited (Campana and Jones, 1992). So far, no studies have directly compared if the microstructure formed at early life stages remains reliably measurable and unaltered for analyses in the otoliths from adult life stages. All studies using adult otoliths to investigate the early life history of fish assume that the otolith microstructure reflects the growth pattern experienced at the larval stage.

In general, the growth of otoliths, both on daily or yearly level, is affected by factors like temperature (Folkvord et al., 2004), photoperiod (Mugiya, 1987), or prey density (Johannessen et al., 2000). Otolith microstructure analyses are commonly used for reconstructing individual daily growth patterns during the larval and juvenile stage of fish (Baumann et al., 2006; Gagliano et al., 2007) as well as for adults (Morrongiello and Thresher, 2015). Individual back-calculation of ages using the otolith microstructure is only applicable for young-of-year fish before the onset of the winter ring formation in most temperate species (Pringle and Baumann, 2019). Further, the otolith microstructure can be used to link larval growth to recent environmental histories (Bailey and Heath, 2001; Baumann et al., 2003) or to infer dispersal pathways (Kokita and Omori, 1999; Brophy and King, 2007). In cases of sufficiently distinct spawning areas or seasons, the fidelity and integrity of adult populations can be assessed by otolith microstructure (Husebø et al., 2005; Brophy et al., 2006).

Given this knowledge gap and missing evaluation of using adult otoliths to examine larval growth, our main objective was to conduct such an evaluation based on otoliths from full-siblings, sampled as larvae or adults, that had experienced the same early-life environmental conditions. Such an evaluation is needed to strengthen the support of studies conducting otolith microstructure analysis on adult otoliths. We used offspring of Atlantic herring (*Clupea harengus*) that were reared in a common garden experiment for 3 years (Berg et al., 2018). This long-time experimental design thus enabled a direct comparison of larval growth between the adults and their larval siblings from the same generation. We hypothesized that otolith microstructure of larvae and adults reared under common garden conditions should be the same.

Further, common garden experiments give a unique possibility to investigate the influence of environmental factors based on the rearing of offspring from different populations under identical environmental conditions. In this case, Atlantic herring was used due to its phenotypic plasticity (Geffen, 2009) as well as complex population structure (Iles and Sinclair, 1982). Especially for herring, otolith microstructure analysis is essential because it is used in stock assessment to identify spring, autumn, and winter spawning herring (Mosegaard and Madsen, 1996; Clausen et al., 2007). Two of the most distinct herring populations are probably Norwegian spring spawners (NSS) and central Baltic (CB) spring spawners (henceforth denoted as Atlantic and Baltic, respectively), differing both phenotypically (Gröhsler et al., 2013; Berg et al., 2017), and genetically (Martinez Barrio et al., 2016; Pettersson et al., 2019), as well as in ambient environmental conditions (fully marine vs. brackish conditions). Therefore, herring in the central Baltic are often specified as a subspecies *Clupea harengus membras*. Salinity is an environmental factor that is mostly neglected when applying otolith microstructure analysis but linked to a large proportion of the genetic differences among herring populations (Lamichhaney et al., 2012; Martinez Barrio et al., 2016). We conducted a case study, where we focused on the effect of salinity and genetics on phenotypic traits. We used Atlantic and Baltic purebreds as well as Atlantic/Baltic hybrids were reared under controlled conditions with fixed salinities of either 6, 16, or 35 psu (Berg et al., 2018, 2020a). For this case study, we first hypothesized that salinity influences the somatic growth and otolith microstructure and secondly that Atlantic/Baltic hybrids may benefit from the combination of genes displaying highest somatic and otolith growth (i.e., hybrid vigor). The second hypothesis is based on previous crossing experiments with seasonal light regimes (Folkvord et al., 2009), where hybrids outperformed purebred larvae of autumn spawners at both spring and autumn light regimes.

MATERIALS AND METHODS

Population Samples and Larval Rearing

Wild spring spawning Atlantic herring (*Clupea harengus*) were used as parental fish to produce first (F1) generation filial herring used in this study. The parental herring populations originated from two different environments: one fully marine environment (35 psu) along the south-western Norwegian coast adjacent to the Atlantic Ocean and one brackish environment (6 psu) in the central Baltic Sea. Norwegian spring spawning-herring were caught approximately 26 km west of Bergen, Norway (60°34′11.2″N 5°0′18.9″E). Central Baltic herring were caught at Hästskär approximately 80 km North of Uppsala,

Sweden (60°38′52.0″N 17°48′44.2″E). Both parental populations were caught 21st of May 2013 by gillnets. After net retrieval, euthanized herring were transported to the lab facilities in Bergen for the fertilization experiments. A short summary of the experimental setup will be presented, however, for a detailed experiment description see Berg et al. (2018) and Berg et al. (2019).

For this case study, one single Atlantic female was crossed with one single Atlantic male to produce Atlantic purebred herring (**Table 1**). Further, one Baltic female was crossed with one Baltic male to produce Baltic purebred herring. The same Atlantic female was also crossed with the same Baltic male producing Atlantic/Baltic F1 hybrids. The rationale of the experimental setup (e.g., the use of single parental crossing) used for this case study will be further elaborated in section "Discussion." The original plan was to co-rear the F1 progeny, consisting of Atlantic purebreds, Baltic purebreds, and Atlantic/Baltic hybrids, in a common garden experiment using three different salinities (6, 16, and 35 psu) with a water temperature of ∼9°C (see Berg et al. (2018) for details of minimal seasonal fluctuations) and natural light regime corresponding to the light regime at the sampling locations of the parental herring populations (60°N). These salinity regimes were chosen to simulate the original salinities found in Atlantic water (35 psu) and central Baltic water (6 psu) in addition to an intermediate salinity regime of 16 psu. However, due to limited numbers of larvae, we had to adjust the initial experimental setup. Another Atlantic crossing between an additional Atlantic female and male was conducted to produce extra Atlantic purebred larvae to supplement the number of larvae in one of the tanks (Tank 1, 6 psu, see **Table 1**). Atlantic purebreds and Atlantic/Baltic hybrids were co-reared (approx. ratio 2 hybrids to 1 purebred) at salinities 16 and 35 with two replicates per salinity (**Table 1**). Baltic purebreds could solely be reared in a single tank at 16 psu (**Table 1**) because the fertilization success and incubation salinity were too low to supply more larvae. We chose 16 psu for the Baltic purebreds instead of 6 psu because of lacking experiences with rearing of herring at lower salinities. The survival of both Baltic purebreds and larvae at 6 psu was low. Consequently, the 6 psu group was terminated after 4 months and the purebred Baltic group after 24 months. Herring juveniles at 16 and 35 psu were reared until maturity 3 years later. Larvae were fed ad libitum with live feed consisting of algae (*Rhodomonas* and *Isochrysis* spp.), rotifers (*Brachionus* spp.), and natural zooplankton and later *Artemia* spp. After 3 months the herring were given dry feed.

Weekly samples of 10 larvae from each of the different tanks were routinely taken throughout the larval period (approximately 3 months). The number of 10 larvae was based on prior experienced variability in somatic traits between individuals of replicate units (2 × 10, i.e., 20 per treatment), and the considerations regarding animal welfare to reduce the number of animals used for experimentation. In addition, two main samples were conducted 57 and 71 days post hatching (DPH), respectively. Directly after sampling, the standard length of larvae was measured. Further, the larvae were then dried at 55°C for 24 h before measuring the dry weight. Further, routine samples were taken throughout the whole period from the juvenile to the adult stage. Standard length, sex, weight, and maturity stage were determined alongside with otolith extraction for each individual fish. Sampled herring were post-mortem identified as Atlantic purebreds or Atlantic/Baltic hybrids by genotyping a diagnostic SNP using a Custom TagMan® Assay Design Tool (Berg et al., 2018). Somatic parameters of F1 adults are presented in Berg et al. (2018). A bacterial infection was discovered in the 35 psu salinity tank only, 590 DPH. The infection was caused by *Tenacibaculum* spp. and the herring were put under an antibiotic treatment. Sick and weakened fish were selectively excluded from the experiment. The growth of surviving fish was not influenced by the antibiotic treatment based on a comparison of growth rates before and after the treatment. After 3 years we thus had four experimental groups in the F1 progeny that were followed from larval life stages to adult life stages: Atlantic purebreds reared at 16 psu, Atlantic/Baltic hybrids reared at 16 psu, Atlantic purebreds reared at 35 psu and Atlantic/Baltic hybrids reared at 35 psu (Berg et al., 2019).

TABLE 1 | Overview of parents used for producing the F1 progeny.

Tank nr.	Crosses	Salinity (psu)	Hybrids	Purebreds
1	AF31 × BM19 + AF31 × AM33+ AF29 × AM27	6	238	353 + 225
2	AF31 × BM19 + AF31 × AM33	35	653	350
3	AF31 × BM19 + AF31 × AM33	16	664	350
6	AF31 × BM19 + AF31 × AM33	16	647	350
7	AF31 × BM19 + AF31 × AM33	35	650	346
9	BF21 × BM19	16	–	550
10	AF31 × BM19 + AF31 × AM33	6	651	277

AF, Atlantic female; AM, Atlantic male; BF, Baltic female; BM, Baltic male. Initial numbers of F1 larvae are presented per tank and cross. Note that in Tank 1 an additional cross was used.

Otolith Extraction and Analysis

Larval Herring Otolith Extraction

The selected larvae used in this study (**Table 2**) were rehydrated before dissection of both sagittal otoliths. Otoliths were mounted on microscope glass slides using QuickStick 135 Mounting Wax, with the proximal (convex side) facing up. Multiple images were taken with 40× magnification with a Nikon camera (camera: DS-Fi2, control unit: DS-U3) attached to an Olympus BX microscope for further microstructure analysis of each otolith. In total, 59 and 86 pairs of otoliths from the two main larval samplings were used for otolith microstructure analysis. Additional 7 individual otoliths from extra samplings (50 and 64 DPH) were specifically chosen to ensure sufficient numbers of Atlantic purebred larvae and to improve the unbalanced group sizes (**Table 2**).

Adult Herring Otolith Extraction

Only otoliths from 3-year-old adult F1 herring, sampled 1098, 1106, and 1120 DPH, were used within this study. In addition,

TABLE 2 | Overview of number of F1 progeny larvae (50–71 days post hatching = DPH) and adults (1098-1120 DPH) used for otolith microstructure analysis from various sampling dates and different salinities.

Days post hatching	Atlantic purebreds			Atlantic/Baltic hybrids			Baltic purebreds
	6 psu	16 psu	35 psu	6 psu	16 psu	35 psu	16 psu
50	–	3	–	–	–	–	–
57	3	1	9	6	19	11	10
64	–	4	–	–	–	–	–
71	–	3	10	–	27	31	15
1,098	–	5	7	–	6	13	–
1,106	–	8	6	–	7	6	–
1,120	–	4	7	–	7	1	–
Total larvae	3	11	19	6	46	42	25
Total adults	–	17	20	–	20	20	–

A total of 152 larvae and 77 adults was used.

otoliths from the parental populations were included in the otolith microstructure analysis. One otolith from each individual was mounted on glass slides using Crystalbond with the sulcus acusticus facing up. The otoliths were further ground (grit 600 grinding paper) and polished (grit 1200 grinding paper). The slides were thereafter reheated, and the otoliths flipped, so the distal side was facing up. The process of grinding and polishing was repeated on the distal side of the otolith until the core and the microstructure of the otolith appeared clear and visible when using a Leica DMLB light microscope with a 20× magnification. A series of pictures was taken for each otolith with a Nikon camera (same as above) attached to the light microscope for microstructure analysis. A total of 97 wild Atlantic herring and 48 wild Baltic herring were sampled from gillnet samples from 2013, and 17 otoliths were analyzed from each parental population. In total 202 adult F1 herring were randomly collected across the two salinity regimes at three different sampling days in 2016. For each of the four experimental groups (Atlantic purebreds at 16 or 35 psu, Atlantic/Baltic hybrids at 16 or 35 psu), 20 otoliths of adult F1 herring were analyzed (**Table 2**). However, the total number of Atlantic purebreds at 16 psu was limited to 17 individuals.

Otolith Microstructure Analysis

The otolith microstructure analysis was carried out on calibrated digital images. For larvae otoliths, the otolith microstructure along the longest possible radius of the otolith was used. Daily increments were measured from the core to the outer edge using ImageJ version 1.46r (National Institutes of Health, United States). The first visible increment termed the "first check" (Folkvord et al., 2004), while the next annotation was the first pronounced and (presumed) daily increment. The widths of all the increments, from the first daily increment (excluding the first check) toward the outer margin were measured. For adult otoliths, the Caliper function in Image-Pro Plus® version 7.0 (Media Cybernetics, United States) was used to automatically detect the daily increments. Otolith annotations were individually verified, and additional or missing increments were manually removed or added, respectively, to avoid any misinterpretation. Only increments with a minimum distance of 20 μm from the core were used for the analyses because former increments are not necessarily daily or easily discernible (Geffen, 1982; Campana et al., 1987; Fox et al., 2003). For larvae, all increments until the edge of the otolith were measured. In combination with the exact known age of larvae, we could assign each increment to a given day and could, therefore, back-calculate the age of the otolith at a specific distance from the core. Such an exact back-calculation of the age based on the number of increments was not possible for adult otoliths because only a part of the otolith increments (approximately up to 150–200 μm from the core) were measured. Therefore, distance from otolith core was chosen for this comparison of otoliths from larvae and adults.

Statistical Analysis

All statistical analyses and plotting were conducted in the R software (R Core Team, 2019). For all tests, we used $p < 0.05$ as the level of significance. The best-fitting model explaining the data was selected based on the Akaike information criterion (AIC). The model with the lowest AIC was chosen, in case the AIC difference was <2 the simpler model was selected.

For the F1 progeny, both for larvae and adults, only Atlantic purebreds and Atlantic/Baltic hybrids from 16 and 35 psu were used for statistical analysis. These groups were also the only ones available at adult stages after 3 years. Other groups (herring reared at 6 psu and Baltic purebreds at 16 psu) were excluded from statistical testing due to low sample size and lacking coverage across life stages and are only included in graphs for visual comparison.

The somatic growth measurements weight, length (total length for adults and standard length for larvae), and otolith radius were generally log-transformed, both for the parental and F1 progeny, while we used the untransformed standard length for the growth estimates of F1 larvae. We used simple linear models for the estimation of somatic growth. The final model explaining the somatic growth of the parental population was:

$$\mathbf{Log\,(Weight) = \alpha + \beta_1 \times Log\,(TL) + \beta_2 \times Pop + \beta_3 \times Log\,(TL) \times Pop} \quad (1)$$

where weight is the wet weight, TL the total length, and Pop the population (Atlantic vs. Baltic). The growth of F1 larvae was best fitted by the following model:

$$\mathbf{SL = \alpha + \beta_1 \times Age + \beta_2 \times Sal + \beta_3 \times Age \times Sal} \quad (2)$$

where SL is the standard length of larvae, Age the age in days post hatching, and Sal the rearing salinity. All larvae sampled were included in this model, but not all of them were genetically identified. Therefore, only salinity was added as a covariate.

For the following analyses, only larvae included for the otolith microstructure were used. All these larvae were genetically identified and genetics (Atlantic purebreds vs. Atlantic/Baltic hybrids) was included as a factor in the initial models.

$$\mathbf{Log\,(DW) = \alpha + \beta_1 \times Log\,(SL) + \beta_2 \times Gen + \beta_3 \times Sal + \beta_4 \times Log\,(SL) \times Gen} \quad (3)$$

$$\mathbf{Log\,(OR) = \alpha + \beta_1 \times Log\,(DW) + \beta_2 \times Gen + \beta_3 \times Sal} \quad (4)$$

where DW is the dry weight, Gen the genetics of the larvae (Atlantic purebred and Atlantic/Baltic hybrid), and OR the otolith radius of each larval otolith.

For the otolith microstructure, we used linear mixed-effects models. First, the optimal structure of the random effects was tested using likelihood estimations (REML) (Zuur et al., 2009). The fixed effects structure was selected based on AIC. All mixed-effects models were fitted using the "lme" function within the "nlme" R-package (Pinheiro and Bates, 2000).

For all models on the otolith microstructure, both for the parental and F1 progeny, we used only increments between 30 and 100 μm distance from the core of an otolith. The distance from the core was also log-transformed for all models on the otolith microstructure to accomplish overall linearity in the increment width vs. otolith size relationship. For each model, the first observation j = 1 was the first increment after a distance >30 μm of the individual otolith i and the last observation was the last increment before a distance <100 μm. The term a_i is the random intercept for the individual otolith i. The final models describing best the otolith growth for the parental generation was:

$$\mathbf{Width_{ij} = \alpha + \beta_1 \times Dis_{ij} + \beta_2 \times Pop_i + \beta_3 \times Dis_{ij} \times Pop_i + a_i} \quad (5)$$

for the F1 progeny, both for larvae and adults:

$$\mathbf{Width_{ij} = \alpha + \beta_1 \times Dis_{ij} + \beta_2 \times Sal_i + \beta_3 \times Gen_i + \beta_4 \times Dis_{ij} \times Sal_i + a_i} \quad (6)$$

where Width is the width between the increment j and the next increment, Dis the log-transformed distance from the core to the increment j, Pop the parental population (Atlantic vs. Baltic), Sal the rearing salinity (16 vs. 35 psu), and Gen the genetics of the F1 progeny (Atlantic purebreds vs. Atlantic/Baltic hybrids). The population, salinity, and genetics were categorical variables.

The last models we used were to compare if larvae and adults of the F1 progeny had similar daily otolith growth. This analysis was conducted for hybrids and purebreds separately to identify potential growth-dependent selection within each group. The following model was selected based on the lowest AIC for hybrids:

$$\mathbf{Width_{ij} = \alpha + \beta_1 \times Dis_{ij} + \beta_2 \times Sal_i + \beta_3 \times Generation_i + \beta_4 \times Dis_{ij} \times Sal_i + a_i} \quad (7)$$

and for purebreds:

$$\mathbf{Width_{ij} = \alpha + \beta_1 \times Dis_{ij} + \beta_2 \times Sal_i + \beta_3 \times Generation_i + \beta_4 \times Sal_i \times Generation_i + a_i} \quad (8)$$

In case significant statistical interactions were noted, Tukey contrasts were performed on combined groups using the multcomp package in R (Hothorn et al., 2008), to evaluate overall differences of main factors. Further, we estimated the ratio between hybrids and purebreds as a proxy for growth-independent mortality during the larval stage (<80 DPH). The ratio between hybrids and purebreds for juvenile and adult fish (>180 DPH) has been previously published by Berg et al. (2019).

RESULTS

Parental Populations

Somatic Parameters

The mean total length and weight of Atlantic herring (N = 97) was 32.2 ± 1.9 cm (mean ± standard deviation) and 273.0 ± 44.7 g, respectively, while it was 20.2 ± 1.0 cm and 55.5 ± 9.7 g for Baltic herring (N = 48) (**Figure 1**).

Otolith Microstructure

Both populations had a steady increase in increment widths with increasing distance from the core. The Baltic parental population had wider increments in the beginning, but the increase in daily otolith growth was lower compared to the Atlantic parental population (ANOVA, $F_{1,897}$ = 9,51, p < 0.01; **Figure 2** and **Supplementary Table S8**). After 100 μm the increments of both populations followed different trajectories, whereas the otolith growth of Baltic herring continued increasing, even though to a lower extent than previously, the otolith growth of Atlantic herring was decreasing (**Figure 2**).

Comparisons of F1 Larvae and Adults

Otolith Microstructure

Comparing the daily otolith growth of F1 larvae with their sibling F1 adults indicate no difference between the stages for all groups (Tukey tests, p > 0.05), except Atlantic purebreds reared at 16 psu (Tukey tests, p < 0.05, **Figure 3** and **Supplementary Tables S1**, **S2**). In Atlantic purebreds from 16 psu, the daily increments of adults were wider than for larvae (ANOVA, $F_{1,63}$ = 7.06, p = 0.01). Generally, the increment widths increased from somewhat over 1.5 μm near the core (∼25 μm) to width of 3 μm or more further outside from the core (∼100 μm).

Hybrid to Purebred Ratio

Initially, the hybrid to purebred ratio of F1 herring was near 2:1 in the 16 and 35 psu salinity regimes. The overall ratio did not change at 35 psu (**Table 3**). During the early larval phase, hybrid survival at 16 psu was higher than for purebreds, as the overall ratio had changed drastically (11.5:1). The survival at 16 psu from the larval phase to adult phase was higher for purebreds indicated by a decreasing ratio (4.3:1). The survival of purebreds and hybrids at 35 psu was similar as indicated by the constant ratios during the entire experiment (for details see Berg et al., 2019).

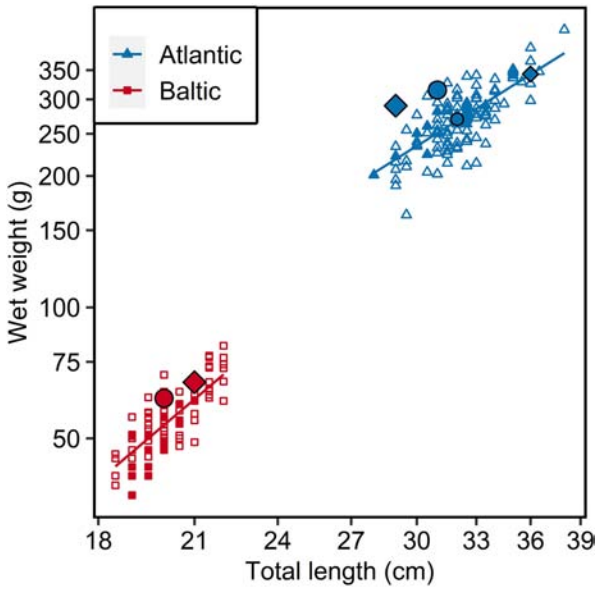

FIGURE 1 | Length-weight relationship of Atlantic (N = 97) and Baltic (N = 48) parental herring. Filled points represent individuals used for otoliths analysis (17 individuals from each parental population), largest points represent main parental fish (Diamond = female; circle = male) used in crossing, medium sized points represent additional parents used for 6 psu group in tank 1. Fitted lines represent regressions from statistical model on logarithmic values.

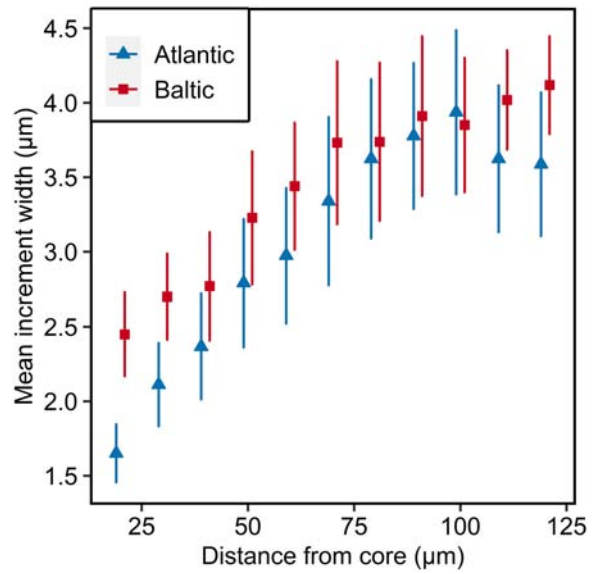

FIGURE 2 | Otolith microstructure of parental Atlantic (blue) and Baltic (red) populations. Mean increment width ± 95% confidence intervals are given for each 10 µm interval. Data points are offset for visual clarity.

F1 Larvae

Somatic Parameters

F1 larvae showed an expected increase in standard length with increasing age at all three salinity regimes (6, 16, and 35 psu; **Figure 4**), including the purebred Baltic larvae reared at 16 psu. The initial size at hatching of Baltic purebreds was smaller compared to offspring from the Atlantic females. Atlantic purebred and Atlantic/Baltic hybrid F1 larvae co-reared at 16 psu grew faster in length than purebreds and hybrids co-reared at 35 psu (ANOVA, $F_{1,390} = 23.66$, $p < .001$; **Supplementary Table S3**).

The dry weights of larvae increased allometrically with standard length. Independent of the salinity, the weight of Atlantic/Baltic hybrids increased faster with increasing length than for Atlantic purebreds (ANOVA, $F_{1,81} = 26.77$, $p < 0.0001$: **Supplementary Table S4**). Also, herring at 35 psu were generally heavier than herring at 16 psu in respective genetic groups (Tukey test, $p < 0.05$). Herring at 6 psu were even lighter at length than those at 16 psu (**Figure 5A**).

A similar trend was observed comparing the otolith radius and dry weight of F1 larvae. Purebreds and hybrids at 35 psu had larger otolith radii compared to purebreds and hybrids reared at 16 psu (ANOVA, $F_{1,82} = 42.87$, $p < 0.001$; **Figure 5B**, **Supplementary Table S5**). There were no differences between purebreds and hybrids within each salinity (ANOVA, $F_{1,82} = 2.30$, $p = 0.13$; **Supplementary Table S5**).

Otolith Microstructure

The otolith microstructure analysis of all larval salinity groups showed generally a positive relationship with increasing increment widths with increasing distance from core up to 100 µm (**Figure 6**). The statistical model included an interaction between distance from core, salinity, and genetics (ANOVA, $F_{1,3093} = 9.59$, $p = 0.002$; **Supplementary Table S6**). The daily otolith growth did not differ between Atlantic purebreds at 16 and 35 psu (Tukey test, $p > 0.05$), while it was higher at 16 psu than 35 psu for hybrids (Tukey test, $p < 0.05$). The hybrids at 35 psu had similar otolith growth as the purebred groups (Tukey test, $p > 0.05$). Baltic purebred larvae reared at 16 psu had a similar daily otolith growth as hybrids. Atlantic purebreds and Atlantic/Baltic hybrids co-reared at 6 psu had the lowest daily otolith growth (narrowest increments) of all groups (**Figure 6**).

F1 Adults

Otolith Microstructure

The otolith microstructure analysis of the F1 adults showed generally an increasing trend in increment widths up to 100 µm where the increment widths of F1 adults at 16 psu increased faster compared to F1 adults at 35 psu (ANOVA,

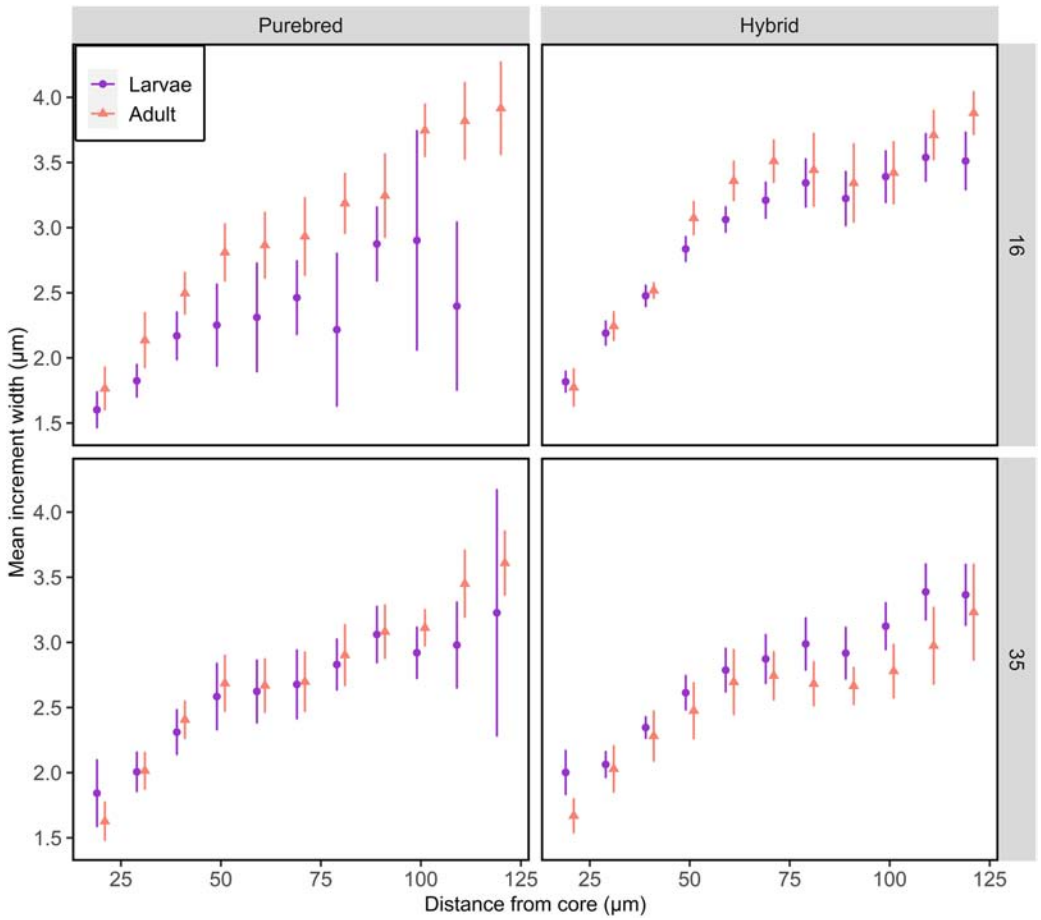

FIGURE 3 | Otolith growth of F1 larvae and adult purebred and hybrid herring reared at salinity of 16 or 35 psu. Mean increment width ± 95% confidence intervals are given for each 10 µm interval. Data points are offset for visual clarity.

TABLE 3 | Overview of the ratio between Atlantic purebreds and Atlantic/Baltic hybrids during the larval stage and as adults.

	Salinity 6			Salinity 16			Salinity 35		
Genetics	**Hybrid**	**Purebred**	**Ratio**	**Hybrid**	**Purebred**	**Ratio**	**Hybrid**	**Purebred**	**Ratio**
F1 larvae	6	3	2.0	46	4	11.5	42	19	2.2
F1 adults	–	–	–	73	17	4.3	72	40	1.9

Only larvae collected during the main two samplings (57 and 71 days post hatching) were included.

$F_{1,2246} = 48.11$, $p < 0.0001$; **Figure 3**, **Supplementary Figure S1** and **Supplementary Table S7**). Also, the otolith growth was higher in 16 than 35 psu for hybrids, but not for purebreds (ANOVA, $F_{1,73} = 6.08$, $p = 0.016$; **Supplementary Table S7**). The somatic growth of F1 adults has been previously described in Berg et al. (2018).

DISCUSSION

This is, to our knowledge, the first study contrasting the otolith microstructure of Atlantic herring (*Clupea harengus*) larvae and full sibling adults originating from identical larval environments. We evaluated and validated that microstructure analysis of adult otoliths is reflecting otolith growth during the larval stage based on Atlantic purebreds and Atlantic/Baltic hybrids co-reared at different salinities over several years. This validation is beneficial for further otolith microstructure analyses, strengthening the validity of their results. However, growth-dependent selection during the development from larvae to adults might produce biases when using adult otoliths to estimate larval growth. Besides the validation of the methods, we demonstrated in a case study that herring had higher otolith growth under intermediate salinity conditions (16 psu) independent of their genetic background. This demonstrates the plasticity of herring and the importance of salinity. In

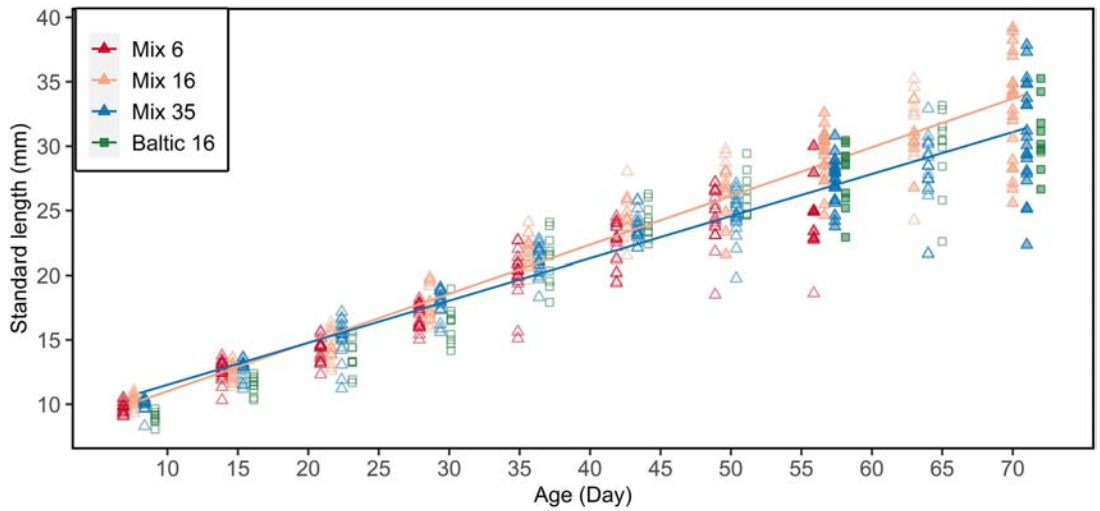

FIGURE 4 | Standard length-at-age relationship for all sampled F1 larvae. Filled symbols indicate larvae used for the otolith microstructure analysis (at age 57 and 71 for all tanks, and age 50 and 64 solely for 16 psu). Atlantic purebreds and Atlantic/Baltic hybrids were co-reared (mix) at 6, 16, or 35 psu. Baltic purebreds were separately reared at 16 psu. Lines indicate linear regression for salinity 16 (excluding Baltic purebreds) and 35 psu. Data points are jittered to reduce overlap of data points.

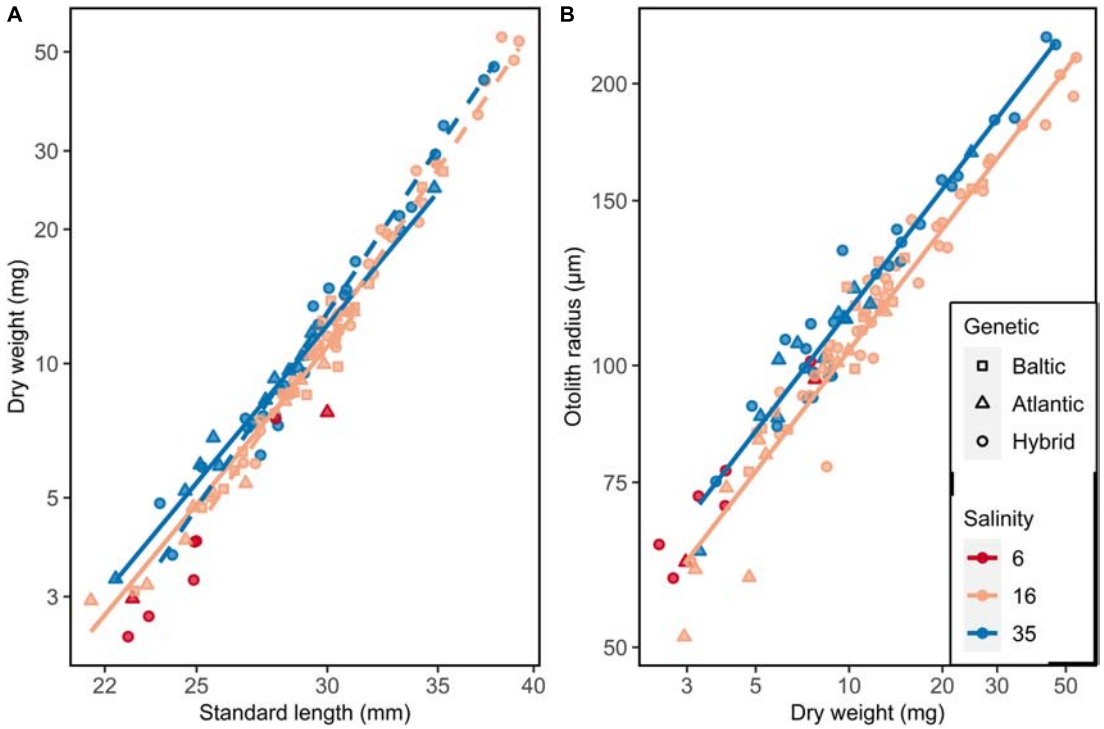

FIGURE 5 | Somatic growth of F1 larvae used for otolith microstructure analysis. **(A)** Length-weight relationship and **(B)** Dry weight-otolith radius. Lines represent linear models: **(A)** Solid line = Atlantic purebred, dashed line = Atlantic/Baltic hybrids; **(B)** no significant differences between genetic groups.

addition, to the documentation of growth-dependent selection and general growth trajectories, this experiment indicated different survival rates during the larval stage which is also supported by Berg et al. (2019) for the juvenile and adult stages. Finally, this study shows the strength of a common garden experiment with several closed and well-defined groups.

There is no doubt that the otolith microstructure, more specifically the increment width pattern, to a certain extent reflects daily growth patterns during the larval stage, but

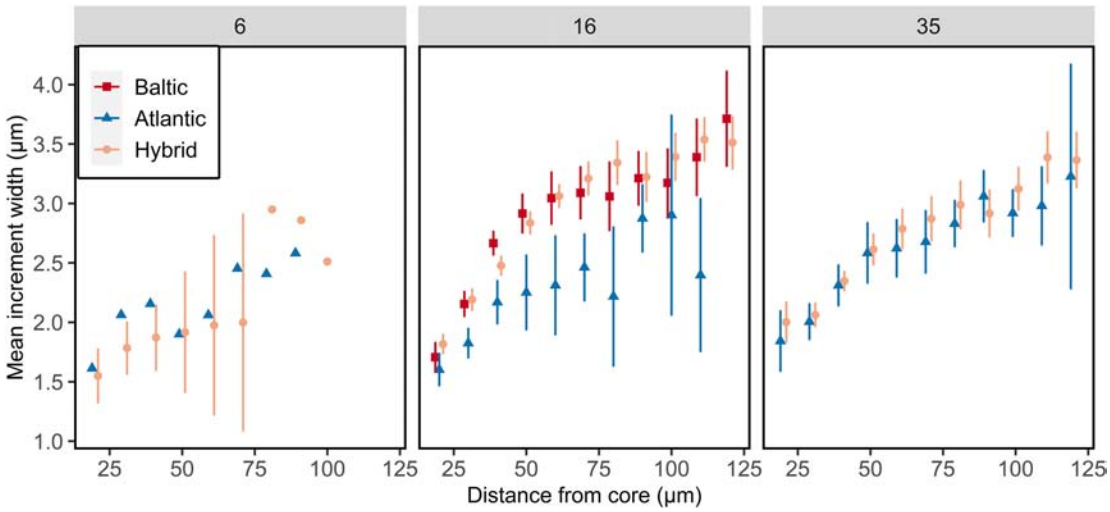

FIGURE 6 | Otolith growth of F1 larvae reared at salinity of 6, 16, or 35 psu. Mean increment width ± 95% confidence intervals are given for each 10 µm interval. Data points are offset for visual clarity. Confidence intervals are only displayed for $n > 5$.

in most cases, these patterns are extracted from otoliths of larvae. Within this study, we validated that the microstructure revealed from adult otoliths did not differ from the otolith microstructure of larvae in absence of selective mortality. High accuracy and precision are needed when conducting otolith microstructure analysis and small deviations can lead to inconclusive results (Campana, 2001). Preparing adult otoliths for microstructure analysis is challenging since large amounts of material must be removed (Campana and Jones, 1992; Brophy, 2014), whereas larval otoliths need little or no preparation as in this study. In some species, time-consuming thin sectioning of adult otoliths is recommended to obtain clear increment patterns (e.g., Tomás and Panfili, 2000). Still, the choice of sectioning plane, as will over- or under-grinding of adult otoliths, may inaccurately align the mid-core area, resulting in inaccurate appearance of increment numbers and widths. Thus, the shape of the adult otoliths may to a variable extent be amenable to accurate microincrement estimation due to their thickness and need for extensive grinding or sectioning. Adult herring otoliths, like for most clupeid fish, increasingly attain a relatively thin and compressed form along the medial-distal axis past metamorphosis (Härkönen, 1986; Berg et al., 2018) making them well suited for studies of otolith microstructure.

The results of selection and mortality studies based on microstructure analyses (see Sponaugle (2010) and references therein for examples) will be strengthened by this validation because they use the survivors, mostly adults to contrast against individuals from earlier stages. If there would be differences between the otolith microstructure of larvae and adults without selective mortality, this could lead to false interpretations. For Atlantic herring, most selection studies have concentrated on juvenile fish (Stenevik et al., 1996; Slotte et al., 2019). However, our results allow for new studies on the selection of Atlantic herring in the wild using adults. Year class strength of herring, especially the Norwegian spring-spawning herring, is highly variable and not predictable. Selection studies comparing otolith growth of larvae and survivors (adults) on for example strong and weak year classes might reveal new insights on the recruitment dynamics of herring. Further, this validation strengthens other studies where conclusions are drawn from microstructure analysis of adult otoliths which have management (Clausen et al., 2007) or ecological (Berg et al., 2020b) implications.

Despite the methodological validation, there are some limitations when applying this approach to wild-caught adult herring which should be considered. Within our experiment, we observed growth-dependent selection for one of our experimental groups (Atlantic purebreds reared at 16 psu), even without strain-selective mortality. A significant fraction of purebreds was possibly not able to adapt fully to their new salinity environment and consequently only the fittest and faster growing offspring survived. A typical mechanism that could explain this growth-dependent selection in experiments is cannibalism (Puvanendran et al., 2008; Folkvord et al., 2010). Although intra-cohort cannibalism on rare occasions has been reported in late larval and early juvenile herring (e.g., Wespestad and Moksness, 1990). Atlantic purebreds were, in general, suffering during the larval phase in 16 psu as indicated by the hybrid to purebred ratio. Therefore, it is most likely that surviving adult purebreds had the highest capability, potentially trough higher growth, to cope with their non-native salinity. Such a selection during the development from larvae to adults might produce biases when estimating larval growth based on adult otoliths (Pringle and Baumann, 2019). In the wild, natural selection will probably account for even larger differences and should not be neglected. Further, different environmental conditions, like salinity in this case study, could have strong effects on the otolith microstructure. Additional analysis, such as otolith microchemistry (Moll et al., 2019), in combination with otolith microstructure, can be applied, e.g., to investigate the migration

dynamics of herring in the transition zone, as is the case between the Atlantic and Baltic Sea where a strong salinity gradient exists.

A further aspect of this study is the use of a small number of parental herring (n = 3 for main study, n = 6 in total) resulting in a narrow genetic baseline. By using only one female as parental female for Atlantic purebreds and Atlantic/Baltic hybrids, non-environmental maternal effects were purposely and effectively minimized. This setup was considered beneficial when evaluating and validating the otolith microstructure analysis of larvae and adult siblings. It should be noted that Atlantic and Baltic herring show very strong genetic differentiation at hundreds of loci underlying ecological adaptation (Pettersson et al., 2019). Therefore, a single random Atlantic herring and a single Baltic herring are expected to show genotype differences at the majority of these loci. However, we cannot, even if our results are clear and significant, formally differentiate between individual and population-specific effects, which makes a transfer of the findings to the entire populations somewhat uncertain. Also, the observed differences in otolith growth trajectories could be a result of paternal effects rather than environmental effects (Bang et al., 2006; Poirier et al., 2017). Still, the findings serve as a good basis for further refined hypotheses and experiments on herring dealing with population-specific responses to different salinity conditions.

For the parental populations, phenotypic differences in terms of body length and growth have been previously described and related to lower temperatures in the central Baltic (Brunel and Dickey-Collas, 2010; Gröhsler et al., 2013). This is supported by our findings, where all the mature adult Baltic herring are much smaller, even though marginally older than the mature Atlantic herring used in this study. Consequently, age effects can be considered minor and other factors must be driving these differences. However, a direct or indirect impact of salinity on the smaller sizes of central Baltic herring cannot be excluded as being demonstrated for other clupeids (Palkovacs et al., 2007; Palkovacs and Post, 2009). Although the central Baltic is in general colder [see S5 Figure in Berg et al. (2018)], spawning locations are typically on vegetation in coastal areas (Aneer, 1989; Rajasilta et al., 1989) where the ambient water temperature is more susceptible to sudden temperature increase. Local coastal spawning areas might thus have higher temperatures explaining the contrasting results of initially higher otolith growth of Baltic herring than for Atlantic herring during the larval phase. Due to the general lower temperature in the central Baltic and the strong effect of temperature on the otolith growth (Folkvord et al., 2004) one would expect lower larval otolith growth for Baltic herring. Usually, herring at lower temperatures have a smaller growth coefficient (Brunel and Dickey-Collas, 2010). Also at later life stages, the conditions within the central and northern Baltic are less favorable and consequently restricting the growth of adult herring resulting in smaller total length (Gröhsler et al., 2013). In general, the prey density within the Baltic (Flinkman et al., 1998; Möllmann et al., 2000) is approximately 10-times lower compared with the density of the Atlantic (Dalpadado et al., 2000; Gislason and Astthorsson, 2002). Another explanation for the better larval otolith growth can be natural selection of the best fit individuals. Assuming the Baltic conditions are marginal, only the strongest and best-adapted individuals actually survive the larval period. A direct comparison of adult otolith microstructure and those of wild larvae is needed to justify and strengthen this explanation. One adaptation to the marginal conditions of the Baltic is a mutation on rhodopsin allowing Baltic herring to cope with lower water clarity conditions (Hill et al., 2019). The benefit of improved vision is expected to be of special importance during the early stages in fish since they are strongly affected by turbidity and reduced water clarity (Utne-Palm, 2004). This may also be one of the reasons for the relatively good larval growth performance of Baltic herring larvae compared to Atlantic herring larvae. In addition to the effects of visibility, reduced water oxygen content (Pauly and Cheung, 2018), salinity (Berg et al., 2018), limited availability of suitably sized plankton for the larger herring may reduce the growth and maximum size of Baltic herring (Möllmann et al., 2005). Further, there is a tendency that adult Baltic populations migrate into habitats with higher salinities for feeding, e.g., from the western Baltic into the Skagerrak (Clausen et al., 2015) or from the central Baltic into the western Baltic (Gröhsler et al., 2015). Whether this migration is due to direct salinity effect on herring or is due to better feeding conditions needs to be investigated. Within this study, however, we demonstrated the potential of Baltic purebred herring reared under optimal environmental conditions (16 psu, water temperature of approximately 9°C, fed *ad libitum*, and clear visibility) to attain higher growth rates than the parental fish and they obtained a size of 18.5 cm and weight of 52.0 g after 2 years (unpubl. results). This indicates the potential phenotypic plasticity in growth of Baltic herring when provided alternative and more beneficial environmental conditions. However, we cannot exclude that the growth of Baltic purebreds might be even higher when reared under laboratory conditions at their original salinity of 6 psu.

Given the common garden design, we could contrast the otolith growth under salinity conditions typical for the Atlantic Ocean (35 psu) and Baltic Sea (6 & 16 psu). Our results indicate that salinity can act as a major factor influencing the somatic and otolith growth of herring. In general, highest otolith and somatic growth were observed for larvae at 16 psu which is in accordance with other studies showing the positive effect of intermediate salinities on the growth (Boeuf and Payan, 2001), oxygen consumption (Berg et al., 2020a), or fertilization (Berg et al., 2019). The studies concluded that osmoregulation is less resource demanding at intermediate salinities allowing for larger growth. Caution is needed interpreting the results for larvae reared in 6 psu due to the low sample size (3 and 6 for purebreds and hybrids, respectively). Following our results, there is a tendency that both Atlantic purebred and Atlantic/Baltic hybrid larvae had the lowest otolith growth at 6 psu. Further studies including a comparison of Baltic purebreds reared at 6 psu are needed to draw any general conclusion, e.g., that herring with Atlantic genes might not be well adapted to low salinities or if this is an artifact regarding low survival of certain types of zooplankton at 6 psu. Besides the effect of salinity on otolith growth, the findings in this study demonstrate a changing mortality of genetic groups in

the intermediate salinity. The ratio of hybrids to purebreds at 16 psu had drastically increased during the larval stage followed by a steady decrease during the juvenile and adults stage as indicated by Berg et al. (2019) to a level higher than the original 2:1 ratio. Similar results were observed for hybrid spring x autumn spawned herring larvae by Folkvord et al. (2009), with hybrids also outperforming purebred larvae under their original light regime conditions. The reasons for the reverse selection of purebreds vs. hybrids from the larval stage to the adult stage in the 16 psu group in this experiment remains unresolved, however, it could possibly be linked to past selection of superior purebred offspring during the larval stage. A consequence of this mortality was an unbalanced group size between Atlantic purebreds and Atlantic/Baltic hybrids at 16 psu which was counteracted by additional analyses of purebreds from extra sampling dates.

In conclusion, this study validates that otolith microstructure analysis of adults reflects the experienced otolith growth during the larval stages. Otolith microstructure analyses have been widely used for many years, but this is the first evaluation that the larval otolith growth can be analyzed in sibling groups after several years. This evaluation will be beneficial for future studies investigating the patterns of selection based on otolith microstructure analysis. Further, we demonstrated the importance of the environmental factor salinity along with genetic contributions to phenotypic variability and plasticity in herring. Similar common garden experiments with multiple parents are needed to verify our findings and conclusion that genetics affect key life-history traits as well as the ability of herring to adapt to different salinity environments at the population level.

DATA AVAILABILITY STATEMENT

The datasets generated for this study are available on request to the corresponding author.

ETHICS STATEMENT

The animal study was reviewed and approved by Norwegian national animal Ethics Committee (Forsøksdyrutvalget-FOTS ID-5072).

AUTHOR CONTRIBUTIONS

AF conceived and designed the study with contributions from LA, AS, and FB. ST performed the otolith analysis. ST and FB performed the statistical analysis. ST wrote the first draft of the manuscript. FB wrote sections of the manuscript. All authors contributed to manuscript revision, read and approved the submitted version.

FUNDING

This work was funded by the RCN project 254774 (GENSINC).

ACKNOWLEDGMENTS

We are grateful to Christel Krossøy, Frank Midtøy, Heikki Savolainen, and Julie Skadal from the UiB for their efforts in sampling the data material. We also acknowledge two reviewers for their input and comments having a considerable contribution to improvements of the manuscript.

SUPPLEMENTARY MATERIAL

The Supplementary Material for this article can be found online at: https://www.frontiersin.org/articles/10.3389/fmars.2020.00529/full#supplementary-material

REFERENCES

Aneer, G. (1989). Herring (*Clupea harengus L.*) spawning and spawning ground characteristics in the Baltic Sea. *Fish. Res.* 8, 169–195. doi: 10.1016/0165-7836(89)90030-1

Bailey, M. C., and Heath, M. R. (2001). Spatial variability in the growth rate of blue whiting (*Micromesistius poutassou*) larvae at the shelf edge west of the UK. *Fish. Res.* 50, 73–87. doi: 10.1016/s0165-7836(00)00243-5

Bang, A., Grønkjær, P., Clemmesen, C., and Høie, H. (2006). Parental effects on early life history traits of Atlantic herring (*Clupea harengus L.*) larvae. *J. Exp. Mar. Biol. Ecol.* 334, 51–63. doi: 10.1016/j.jembe.2006.01.003

Barrett, R. D. H., and Hoekstra, H. E. (2011). Molecular spandrels: tests of adaptation at the genetic level. *Nat. Rev. Genet.* 12, 767–780. doi: 10.1038/nrg3015

Baumann, H., Gröhsler, T., Kornilovs, G., Makarchouk, A., Feldmann, V., and Temming, A. (2006). Temperature-induced regional and temporal growth differences in Baltic young-of-the-year sprat *Sprattus sprattus*. *Mar. Ecol. Prog. Ser.* 317, 225–236. doi: 10.3354/meps317225

Baumann, H., Pepin, P., Davidson, F. J. M., Mowbray, F., Schnack, D., and Dower, J. F. (2003). Reconstruction of environmental histories to investigate patterns of larval radiated shanny (*Ulvaria subbifurcata*) growth and selective survival in a large bay of Newfoundland. *ICES J. Mar. Sci.* 60, 243–258. doi: 10.1016/s1054-3139(03)00019-5

Berg, F., Almeland, O. W., Skadal, J., Slotte, A., Andersson, L., and Folkvord, A. (2018). Genetic factors have a major effect on growth, number of vertebrae and otolith shape in Atlantic herring (*Clupea harengus*). *PLoS One* 13:e0190995. doi: 10.1371/journal.pone.0190995

Berg, F., Andersson, L., and Folkvord, A. (2020a). Respiration rates of herring larvae at different salinities and effects of previous environmental history. *Mar. Ecol. Prog. Ser.* (inpress), doi: 10.3354/meps13318

Berg, F., Østgaard, H. D., Slotte, A., Andersson, L., and Folkvord, A. (2020b). A combination of genetic and phenotypic characterization of spring- and autumn-spawning herring suggests gene flow between populations. *ICES J. Mar. Sci.* (inpress), doi: 10.1093/icesjms/fsaa046

Berg, F., Slotte, A., Andersson, L., and Folkvord, A. (2019). Genetic origin and salinity history influence reproductive success of Atlantic herring. *Mar. Ecol. Prog. Ser.* 61, 81–94. doi: 10.3354/meps12680

Berg, F., Slotte, A., Johannessen, A., Kvamme, C., Clausen, L. A. W., and Nash, R. D. M. (2017). Comparative biology and population mixing among local, coastal and offshore Atlantic herring (Clupea harengus) in the North Sea, Skagerrak, Kattegat and western Baltic. *PLoS One* 12:e0187374. doi: 10.1371/journal.pone.0187374

Boeuf, G., and Payan, P. (2001). How should salinity influence fish growth? *Comp. Biochem. Physiol. Part C* 130, 411–423. doi: 10.1016/S1532-0456(01)00268-X

Brophy, D. (2014). "Chapter eight - Analysis of growth marks in calcified structures: insights into stock structure and migration pathways," in *Stock*

Identification Methods (Second edition), eds S. X. Cadrin, L. A. Karr, and S. Mariani (San Diego: Academic Press), 141–170. doi: 10.1016/b978-0-12-397003-9.00008-4

Brophy, D., Danilowicz, B. S., and King, P. A. (2006). Spawning season fidelity in sympatric populations of Atlantic herring (*Clupea harengus*). *Can. J. Fish. Aquat. Sci.* 63, 607–616. doi: 10.1139/f05-235

Brophy, D., and King, P. A. (2007). Larval otolith growth histories show evidence of stock structure in Northeast Atlantic blue whiting (*Micromesistius poutassou*). *ICES J. Mar. Sci.* 64, 1136–1144. doi: 10.1093/icesjms/fsm080

Brothers, E. B., Mathews, C. P., and Lasker, R. (1976). Daily growth increments in otoliths from larval and adult fishes. *Fish. Bull.* 74, 1–8. doi: 10.1006/jfbi.1993.1006

Brunel, T., and Dickey-Collas, M. (2010). Effects of temperature and population density on von Bertalanffy growth parameters in Atlantic herring: a macro-ecological analysis. *Mar. Ecol. Prog. Ser.* 405, 15–28. doi: 10.3354/meps08491

Campana, S. E. (2001). Accuracy, precision and quality control in age determination, including a review of the use and abuse of age validation methods. *J. Fish Biol.* 59, 197–242. doi: 10.1111/j.1095-8649.2001.tb00127.x

Campana, S. E. (2005). Otolith science entering the 21st century. *Mar. Freshwater Res.* 56, 485–495. doi: 10.1071/mf04147

Campana, S. E., Gagné, J. A., and Munro, J. (1987). Otolith microstructure of larval herring (*Clupea harengus*): image or reality? *Can. J. Fish. Aquat. Sci.* 44, 1922–1929. doi: 10.1139/f87-236

Campana, S. E., and Jones, C. M. (1992). "Analysis of otolith microstructure data," in *Otolith Microstructure Examination and Analysis*, eds D. K. Stevenson and S. E. Campana (Ottawa, ON: Canadian Special Publication of Fisheries and Aquatic Sciences), 73–100.

Campana, S. E., and Thorrold, S. R. (2001). Otoliths, increments, and elements: keys to a comprehensive understanding of fish populations? *Can. J. Fish. Aquat. Sci.* 58, 30–38. doi: 10.1139/f00-177

Cermeño, P., Uriarte, A., De Murguía, A. M., and Morales-Nin, B. (2003). Validation of daily increment formation in otoliths of juvenile and adult European anchovy. *J. Fish Biol.* 62, 679–691. doi: 10.1046/j.1095-8649.2003.00056.x

Clausen, L. A. W., Bekkevold, D., Hatfield, E. M. C., and Mosegaard, H. (2007). Application and validation of otolith microstructure as a stock identification method in mixed Atlantic herring (*Clupea harengus*) stocks in the North Sea and western Baltic. *ICES J. Mar. Sci.* 64, 377–385. doi: 10.1093/icesjms/fsl036

Clausen, L. A. W., Stæhr, K. J., Rindorf, A., and Mosegaard, H. (2015). Effect of spatial differences in growth on distribution of seasonally co-occurring herring *Clupea harengus* stocks. *J. Fish Biol.* 86, 228–247. doi: 10.1111/jfb.12571

Dalpadado, P., Ellertsen, B., Melle, W., and Dommasnes, A. (2000). Food and feeding conditions of Norwegian spring-spawning herring (Clupea harengus) through its feeding migrations. *ICES J. Mar. Sci.* 57, 843–857. doi: 10.1006/jmsc.2000.0573

Flinkman, J., Aro, E., Vuorinen, I., and Viitasalo, M. (1998). Changes in northern Baltic zooplankton and herring nutrition from 1980s to 1990s: top-down and bottom-up processes at work. *Mar. Ecol. Prog. Ser.* 165, 127–136. doi: 10.3354/meps165127

Folkvord, A., Høie, H., Johannessen, A., and Solbakken, T. (2009). Effects of prey concentration, light regime, and parental origin on growth and survival of herring larvae under controlled experimental conditions. *ICES J. Mar. Sci.* 66, 1702–1709. doi: 10.1093/icesjms/fsp072

Folkvord, A., Johannessen, A., and Moksness, E. (2004). Temperature-dependent otolith growth in Norwegian spring-spawning herring (*Clupea harengus* L.) larvae. *Sarsia* 89, 297–310. doi: 10.1080/00364820410002532

Folkvord, A., Koedijk, R. M., Lokøy, V., and Imsland, A. K. (2010). Timing and selectivity of mortality in reared Atlantic cod revealed by otolith analysis. *Environ. Biol. Fishes* 89, 513–519. doi: 10.1007/s10641-010-9699-5

Fox, C. J., Folkvord, A., and Geffen, A. J. (2003). Otolith micro-increment formation in herring *Clupea harengus* larvae in relation to growth rate. *Mar. Ecol. Prog. Ser.* 264, 83–94. doi: 10.3354/meps264083

Gagliano, M., McCormick, M. I., and Meekan, M. G. (2007). Survival against the odds: ontogenetic changes in selective pressure mediate growth-mortality trade-offs in a marine fish. *Proc. R. Soc. B* 274, 1575–1582. doi: 10.1098/rspb.2007.0242

Geffen, A. J. (1982). Otolith ring deposition in relation to growth rate in herring (*Clupea harengus*) and turbot (*Scophthalmus maximus*) larvae. *Mar. Biol.* 71, 317–326. doi: 10.1007/bf00397048

Geffen, A. J. (2009). Advances in herring biology: from simple to complex, coping with plasticity and adaptability. *ICES J. Mar. Sci.* 66, 1688–1695. doi: 10.1093/icesjms/fsp028

Gibb, F. M., Régnier, T., and Wright, P. J. (2020). Inferring early larval traits from otolith microstructure in the sandeel. *J. Sea Res.* 158, 101872. doi: 10.1016/j.seares.2020.101872

Gillanders, B. M. (2002). Connectivity between juvenile and adult fish populations: do adults remain near their recruitment estuaries? *Mar. Ecol. Prog. Ser.* 240, 215–223. doi: 10.3354/meps240215

Gislason, A., and Astthorsson, O. S. (2002). The food of Norwegian spring-spawning herring in the western Norwegian Sea in relation to the annual cycle of zooplankton. *Sarsia* 87, 236–247. doi: 10.1080/00364820260294860

Gröhsler, T., Oeberst, R., Schaber, M., Larson, N., and Kornilovs, G. (2013). Discrimination of western Baltic spring-spawning and central Baltic herring (*Clupea harengus L.*) based on growth vs. natural tag information. *ICES J. Mar. Sci.* 70, 1108–1117. doi: 10.1093/icesjms/fst064

Gröhsler, T., Schaber, M., Larson, N., and Oeberst, R. (2015). Separating two herring stocks from growth data: long-term changes in survey indices for Western Baltic Spring Spawning Herring (*Clupea harengus*) after application of a stock separation function. *J. Appl. Ichthyol.* 32, 40–45. doi: 10.1111/jai.12924

Härkönen, T. (1986). *Guide to the Otoliths of the Bony Fishes of the Northeast Atlantic*. Hellerup: Danbiu ApS.

Hill, J., Enbody, E. D., Pettersson, M. E., Sprehn, C. G., Bekkevold, D., Folkvord, A., et al. (2019). Recurrent convergent evolution at amino acid residue 261 in fish rhodopsin. *Proc. Natl. Acad. Sci. U.S.A.* 116, 18473–18478. doi: 10.1073/pnas.1908332116

Hothorn, T., Bretz, F., and Westfall, P. (2008). Simultaneous inference in general parametric models. *Biometric. J.* 50, 346–363. doi: 10.1002/bimj.200810425

Husebø, Å, Slotte, A., Clausen, L. A. W., and Mosegaard, H. (2005). Mixing of populations or year class twinning in Norwegian spring spawning herring? *Mar. Freshw. Res.* 56, 763–772. doi: 10.1071/mf04170

Iles, T. D., and Sinclair, M. (1982). Atlantic herring: stock discreteness and abundance. *Science* 215, 627–633. doi: 10.1126/science.215.4533.627

Johannessen, A., Blom, G., and Folkvord, A. (2000). Differences in growth pattern between spring and autumn spawned herring (*Clupea harengus L.*) larvae. *Sarsia* 85, 461–466. doi: 10.1080/00364827.2000.10414595

Kokita, T., and Omori, M. (1999). Long distance dispersal of larval and juvenile rockfish, Sebastes thompsoni, with drifting seaweed in the Tohoku area, northwest Pacific, estimated by analysis of otolith microstructure. *Bull. Mar. Sci.* 65, 105–118.

Lamichhaney, S., Martinez Barrio, A., Rafati, N., Sundström, G., Rubin, C.-J., Gilbert, E. R., et al. (2012). Population-scale sequencing reveals genetic differentiation due to local adaptation in Atlantic herring. *Proc. Natl. Acad. Sci. U.S.A.* 109, 19345–19350. doi: 10.1073/pnas.1216128109

Martinez Barrio, A., Lamichhaney, S., Fan, G., Rafati, N., Pettersson, M., Zhang, H., et al. (2016). The genetic basis for ecological adaptation of the Atlantic herring revealed by genome sequencing. *eLife* 5:e12081. doi: 10.7554/eLife.12081

Mitchell-Olds, T., Willis, J. H., and Goldstein, D. B. (2007). Which evolutionary processes influence natural genetic variation for phenotypic traits? *Nat. Rev. Genet.* 8, 845–856. doi: 10.1038/nrg2207

Moll, D., Kotterba, P., Jochum, K. P., von Nordheim, L., and Polte, P. (2019). Elemental inventory in fish otoliths reflects natal origin of Atlantic herring (*Clupea harengus*) from Baltic Sea juvenile areas. *Front. Mar. Sci.* 6:191. doi: 10.3389/fmars.2019.00191

Möllmann, C., Kornilovs, G., Fetter, M., and Köster, F. W. (2005). Climate, zooplankton, and pelagic fish growth in the central Baltic Sea. *ICES J. Mar. Sci.* 62, 1270–1280. doi: 10.1016/j.icesjms.2005.04.021

Möllmann, C., Kornilovs, G., and Sidrevics, L. (2000). Long-term dynamics of main mesozooplankton species in the central Baltic Sea. *J. Plankton Res.* 22, 2015–2038. doi: 10.1093/plankt/22.11.2015

Morrongiello, J. R., and Thresher, R. E. (2015). A statistical framework to explore ontogenetic growth variation among individuals and populations: a marine fish example. *Ecol. Monog.* 85, 93–115. doi: 10.1890/13-2355.1

Mosegaard, H., and Madsen, K. P. (1996). Discrimination of mixed herring stocks in the North Sea using vertebral counts and otolith microstructure. *ICES C.M. 1996/H* 17, 1–8.

Mugiya, Y. (1987). Effects of photoperiods on the formation of otolith increments in the embryonic and larval rainbow trout Salmo gairdneri. *Nippon Suisan Gakkaishi* 53, 1979–1984. doi: 10.2331/suisan.53.1979

Palkovacs, E. P., Dion, K. B., Post, D. M., and Caccone, A. (2007). Independent evolutionary origins of landlocked alewife populations and rapid parallel evolution of phenotypic traits. *Mol. Ecol.* 17, 582–597. doi: 10.1111/j.1365-294x.2007.03593.x

Palkovacs, E. P., and Post, D. M. (2009). Experimental evidence that phenotypic divergence in predators drives community divergence in prey. *Ecology* 90, 300–305. doi: 10.1890/08-1673.1

Panfili, J., and Tomas, J. (2001). Validation of age estimation and back-calculation of fish length based on otolith microstructures in tilapias (Pisces, Cichlidae). *Fish. Bull.* 99, 139–150.

Pannella, G. (1971). Fish otoliths: daily growth layers and periodical patterns. *Science* 173, 1124–1127. doi: 10.1126/science.173.4002.1124

Pauly, D., and Cheung, W. W. L. (2018). Sound physiological knowledge and principles in modeling shrinking of fishes under climate change. *Glob. Change Biol.* 24, e15–e26. doi: 10.1111/gcb.13831

Pettersson, M. E., Rochus, C. M., Han, F., Chen, J., Hill, J., Wallerman, O., et al. (2019). A chromosome-level assembly of the Atlantic herring genome—detection of a supergene and other signals of selection. *Genome Res.* 1919–1928. doi: 10.1101/gr.253435.119

Pinheiro, J. C., and Bates, D. M. (2000). *Mixed-Effects Models in S and S-PLUS*. New York, NY: Springer.

Poirier, M., Listmann, L., and Roth, O. (2017). Selection by higher-order effects of salinity and bacteria on early life-stages of Western Baltic spring-spawning herring. *Evol. Appl.* 10, 603–615. doi: 10.1111/eva.12477

Pringle, J. W., and Baumann, H. (2019). Otolith-based growth reconstructions in young-of-year Atlantic silversides Menidia menidia and their implications for sex-selective survival. *Mar. Ecol. Prog. Series* 632, 193–204. doi: 10.3354/meps13174

Puvanendran, V., Laurel, B., and Brown, J. (2008). Cannibalism of Atlantic cod Gadus morhua larvae and juveniles on first-week larvae. *Aquat. Biol.* 2, 113–118. doi: 10.3354/ab00044

R Core Team (2019). *R: A Language and Environment for Statistical Computing (version 3.6.1)*. Vienna: R Foundation for Statistical Computing.

Rajasilta, M., Eklund, J., Kääriä, J., and Ranta-Aho, K. (1989). The deposition and mortality of the eggs of the Baltic herring Clupea harengus membras L., on different substrates in the south-west archipelago of Finland. *J. Fish Biol.* 34, 417–427. doi: 10.1111/j.1095-8649.1989.tb03324.x

Reis-Santos, P., Tanner, S. E., Vasconcelos, R. P., Elsdon, T. S., Cabral, H. N., and Gillanders, B. M. (2013). Connectivity between estuarine and coastal fish populations: contributions of estuaries are not consistent over time. *Mar. Ecol. Prog. Ser.* 491, 177–186. doi: 10.3354/meps10458

Rey, J., Fernández-Peralta, L., García, A., Nava, E., Clemente, M. C., Otero, P., et al. (2016). Otolith microstructure analysis reveals differentiated growth histories in sympatric black hakes (*Merluccius polli* and *Merluccius senegalensis*). *Fish. Res.* 179, 280–290. doi: 10.1016/j.fishres.2016.03.020

Rogers, T. A., Fowler, A. J., Steer, M. A., and Gillanders, B. M. (2019). Spatial connectivity during the early life history of a temperate marine fish inferred from otolith microstructure and geochemistry. *Estuar. Coast. Shelf Sci.* 227:106342. doi: 10.1016/j.ecss.2019.106342

Slotte, A., Husebø, Å, Berg, F., Stenvik, E. K., Vikebø, F., Folkvord, A., et al. (2019). Earlier hatching and slower growth, a key to survival in the early life history of Norwegian spring spawning herring. *Mar. Ecol. Prog. Ser.* 617-618, 25–39. doi: 10.3354/meps12682

Sponaugle, S. (2010). Otolith microstructure reveals ecological and oceanographic processes important to ecosystem-based management. *Environ. Biol. Fishes* 89, 221–238. doi: 10.1007/s10641-010-9676-z

Stenevik, E. K., Fossum, P., Johannessen, A., and Folkvord, A. (1996). Identification of Norwegian spring spawning herring (*Clupea harengus L.*) larvae from spawning grounds off Western Norway applying otolith microstructure analysis. *Sarsia* 80, 285–292. doi: 10.1080/00364827.1996.10413602

Swain, D. P., and Foote, C. J. (1999). Stocks and chameleons: the use of phenotypic variation in stock identification. *Fish. Res.* 43, 113–128. doi: 10.1016/S0165-7836(99)00069-7

Tomás, J., and Panfili, J. (2000). Otolith microstructure examination and growth patterns of *Vinciguerria nimbaria* (Photichthyidae) in the tropical Atlantic Ocean. *Fish. Res.* 46, 131–145. doi: 10.1016/s0165-7836(00)00140-5

Utne-Palm, A. C. (2004). Effects of larvae ontogeny, turbidity, and turbulence on prey attack rate and swimming activity of Atlantic herring larvae. *J. Exp. Mar. Biol. Ecol.* 310, 147–161. doi: 10.1016/j.jembe.2004.04.005

Via, S., Gomulkiewicz, R., De Jong, G., Scheiner, S. M., Schlichting, C. D., and Van Tienderen, P. H. (1995). Adaptive phenotypic plasticity: consensus and controversy. *Trends Ecol. Evol.* 10, 212–217. doi: 10.1016/S0169-5347(00)89061-8

Wespestad, V. G., and Moksness, E. (1990). Observations on growth and survival during the early life history of Pacific herring *Clupea pallasii* from Bristol Bay, Alaska, in a marine mesocosm. *Fish. Bull.* 88, 191–200.

Zuur, A., Ieno, E. N., Walker, N., Saveliev, A. A., and Smith, G. M. (2009). *Mixed Effects Models and Extensions in Ecology with R*. New York, NY: Springer.

Conflict of Interest: The authors declare that the research was conducted in the absence of any commercial or financial relationships that could be construed as a potential conflict of interest.

Copyright © 2020 Tonheim, Slotte, Andersson, Folkvord and Berg. This is an open-access article distributed under the terms of the Creative Commons Attribution License (CC BY). The use, distribution or reproduction in other forums is permitted, provided the original author(s) and the copyright owner(s) are credited and that the original publication in this journal is cited, in accordance with accepted academic practice. No use, distribution or reproduction is permitted which does not comply with these terms.

Advantages of publishing in Frontiers

OPEN ACCESS
Articles are free to read for greatest visibility and readership

FAST PUBLICATION
Around 90 days from submission to decision

HIGH QUALITY PEER-REVIEW
Rigorous, collaborative, and constructive peer-review

TRANSPARENT PEER-REVIEW
Editors and reviewers acknowledged by name on published articles

Frontiers
Avenue du Tribunal-Fédéral 34
1005 Lausanne | Switzerland

Visit us: www.frontiersin.org
Contact us: info@frontiersin.org | +41 21 510 17 00

REPRODUCIBILITY OF RESEARCH
Support open data and methods to enhance research reproducibility

DIGITAL PUBLISHING
Articles designed for optimal readership across devices

FOLLOW US
@frontiersin

IMPACT METRICS
Advanced article metrics track visibility across digital media

EXTENSIVE PROMOTION
Marketing and promotion of impactful research

LOOP RESEARCH NETWORK
Our network increases your article's readership